Crust and upper mantle structure in the region of Barbados and the Lesser Antilles

Graham K. Westbrook

Earth and Ocean seem

To sleep in one another's arms, and dream

of waves, flowers, clouds, woods, rocks, and all that we

Read in their smiles, and call reality.

Epipsychidion - P. B. Shelley

The Morning Watch, HMS HECLA, east of Barbados, 1971

CRUST AND UPPER MANTLE STRUCTURE IN THE REGION OF BARBADOS AND THE LESSER ANTILLES

by

Graham K. Westbrook

A thesis submitted for the Degree of Doctor of Philosophy

in the University of Durham

Graduate Society

October 1973

ABSTRACT

The Lesser Antilles form one of only two island arcs that occur in the Atlantic Ocean. Bathymetric, gravity, magnetic, and seismic reflection data were collected by HMS HECLA during 1971 in an area bounded by latitudes 12° 54' N and 13° 54' N, and longitudes 57° W and 61° 10' W, including the islands of St. Lucia, St. Vincent, and Barbados. These data are reduced and interpreted in conjunction with seismic refraction data from an experiment run in 1972 and data from other published and unpublished sources.

The structure of the upper sedimentary layers is derived from the seismic reflection records. The crustal structure is modelled two dimensionally using a non-linear optimisation technique to fit the observed gravity and seismic refraction data. The island arc and the Barbados Ridge are examined in detail, and the nature of a ridge running eastward from St. Lucia into the Atlantic Ocean basin is investigated. Magnetic anomalies are treated by direct modelling, magnetic to gravity transformation, and analysis of the power spectrum.

The seismicity of the eastern Caribbean is considered with respect to possible plate motions, and maps of focal depth and energy release are presented. The mechanism and causes of subduction beneath the Lesser Antilles are discussed. The possible gravity anomaly caused by subducted lithosphere is estimated and its effect on the determination of the crustal structure examined. The influence of the relative motions between the North and South American plates on the development of the Caribbean and the Lesser Antilles is studied. Some ideas on the origin and growth of the Barbados Ridge and the island

arc are put forward.

Geophysical data profiles, and computer programs for reduction and interpretation of data are presented in appendices.

ACKNOWLEDGEMENTS

My thanks are due to Professor M.H.P. Bott for his supervision and provision of departmental facilities. I would also thank Dr. G. Peter for his cooperation in the Lesser Antilles Seismic Project and provision of much useful data and information; Dr. J. Tomblin for much information on earthquakes in the Caribbean; Dr. B. Bassinger for providing photographs of airgun reflection records; Mr. C. Boynton for the early results from L.A.S.P.; Mr. J. Fisher for his assistance with data collection; Mr. P. Kearey for providing geophysical data from west of the Lesser Antilles; Mr. B. Lander for assistance with paper tape translating programs; Mr. A. G. McKay for providing a wide angle reflection program and data, and his good natured assistance with data collection; Mr. J. H. Peacock for his endeavours with the air gun profiling system; Dr. J. Sunderland for his organisation of shooting and provision of shot times from L.A.S.P.; Mr. K. Wills for discussion and information on the petrological aspects of the island arc.

I gratefully acknowledge the Captain, officers and crew of HMS HECLA, and in particular Lieutenant Commander J. Connolly the ship's scientific officer, for their considerable contribution in data collection. The Captain,officers, and crew of the NOAA Ocean Survey Ship DISCOVERER were extremely cooperative in establishing the hydrophone stations for L.A.S.P. The computations necessary for this work were carried out on the NUMAC IBM 360/67 computer, and the staff of the Durham University Computer Unit are thanked for their assistance. Daphne Westbrook accommodated an irascible thesis writer, and a large

amount of paper and books. She is thanked for her efforts.

The work for this thesis was carried out whilst in receipt of a Natural Environment Research Council Research Studentship.

Much is owed to conversations with colleagues, and the general environment created by their presence.

CONTENTS

LIST OF FIGURES

Chapter 1

Introduction

In 1971 and 1972 the Department of Geological Sciences, University of Durham, in conjunction with the Hydrographic Branch of the Royal Navy carried out geophysical surveys in the area of the Lesser Antilles aboard HMS HECLA as part of the international CICAR project (Co-operative Investigation of the Caribbean and Adjacent Regions) (fig. 1.1). During the first survey period, from April to August 1971, gravity, magnetic, and seismic reflection profiles were obtained along mostly east-west lines in a rectangular area crossing the island arc between latitudes 12° 55' N and 13° 55' N, extending to longitude 57° W in the east and longitude 64° 30' W in the west. The survey in 1972 was in two parts. The first part was a seismic refraction experiment in which HMS HECLA acted as shooting ship, and receiving stations were situated on all the major islands and on the NOAA Ocean Survey Ship DISCOVERER. This last being a hydrophone system operated by the writer. Shot lines were run across the area, along the island arc and along the Aves Swell. The second part of the 1972 cruise was a gravity and magnetic survey of the Aves Swell.

This thesis is principally concerned with the interpretation of gravity, magnetic, and seismic reflection data collected between and east of St. Vincent and St. Lucia, and also the seismic refraction line running eastward from St. Vincent through Barbados to the Atlantic Ocean basin.* In addition to the detailed interpretation of the collected data a study is made of the tectonic system of the Caribbean

* A short account of the interpretation of the Barbados Ridge area is given in Westbrook, Bott and Peacock (1973)

1.1 Summary map of geophysical surveys in the Lesser Antilles carried out by Durham University in HMS HECLA.

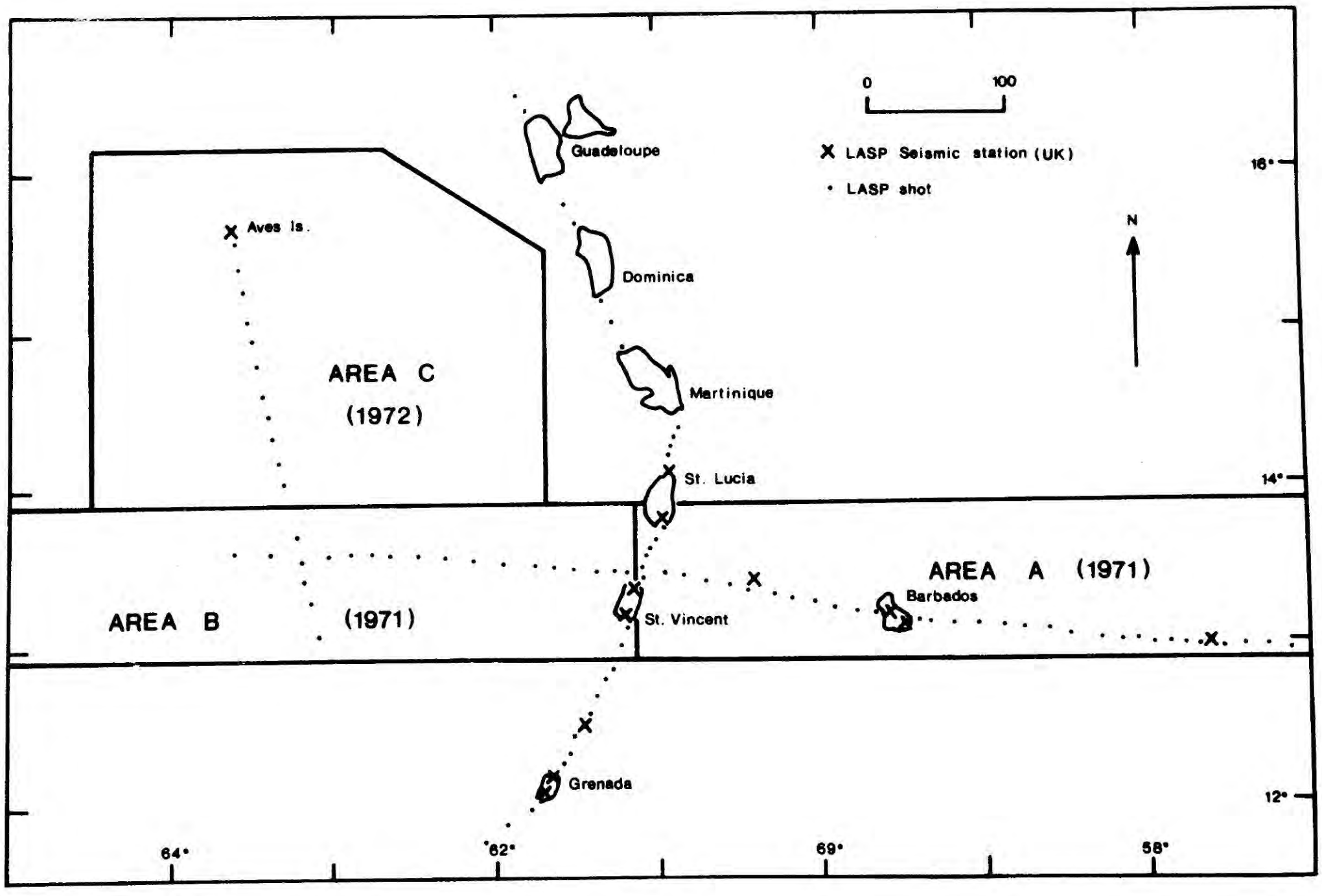
0
100
X LASP Seismic station (UK)
• LASP shot
N
Guadeloupe
Dominica
Martinique
St. Lucia
St. Vincent
Grenada
Barbados
Aves Is.
AREA C
(1972)
AREA B
(1971)
AREA A (1971)
16°
14°
12°
64°
62°
60°
58°

(in chapters 6 & 7) and the significance of area is considered in the light of more general hypotheses for subduction zones. Data west of the Lesser Antilles has been interpreted by P. Keary (thesis to be submitted 1973) and an analysis of the refraction experiment is being made by C. Boynton.

The reduction and interpretation of data was accomplished with the use of an IBM 360/67 computer and a large part of the work for this thesis was entailed in writing programs for it. In general, the formulae and computational techniques used are well documented and are, therefore, given only brief mention in the text, which is mainly concerned with the interpretation and results. Details of the theoretical basis and manner of operation of the programs are given in appendices, together with their listings.

Geological Introduction

The Caribbean area (fig 1.2) has long been of great interest to geologists and geophysicists, mainly because of its complexity, which results from the close juxtaposition of many major structures. Outstanding among them is the island arc and trench system which forms the eastern margin of the Caribbean and is of especial interest in that, with the exception of the Scotia Arc in the South Atlantic, it is the only feature of this type occurring in the Atlantic.

The Lesser Antilles (fig 1.3) are a chain of Tertiary volcanic islands currently active, and behind them at a distance of 250 km to the west lies a ridge of uncertain origin, the Aves Swell. Beyond the Aves Swell is the Venezuelan Basin, one of the two main basins forming the

1.2 Major bathymetric features of the Caribbean region. Contours of the bathymetry and topography of the adjacent land are at 1 km intervals and are taken from Nederlands Hydrographic Office Plotting sheet of Caribbean and adjacent areas, 1967.

Caribbean Bathymetry

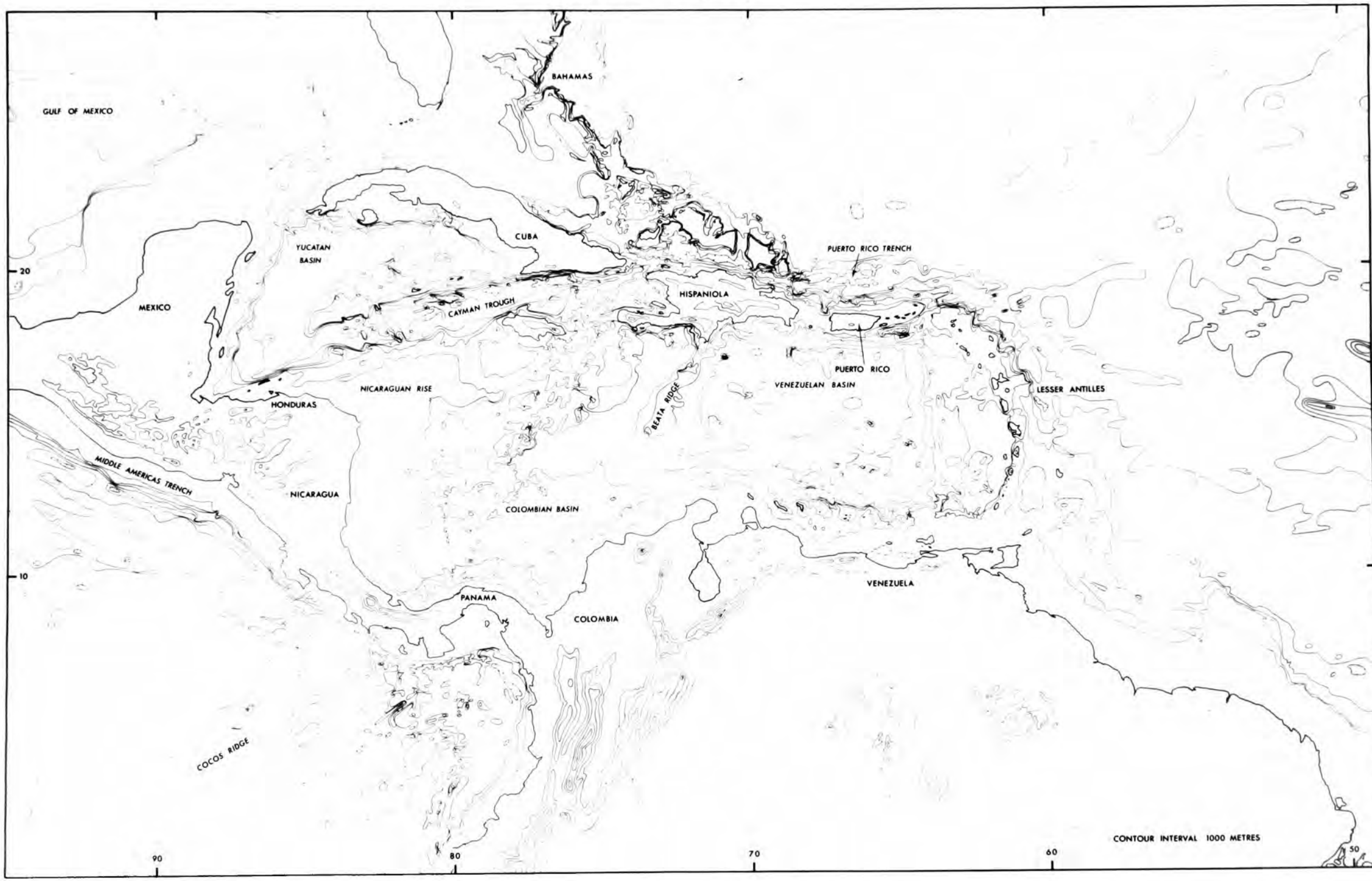

Caribbean, and between it and the Lesser Antilles lies the Grenada Trough Forming the northern margin of the Caribbean are the Greater Antilles, and the southern margin is bounded by Colombia and Venezuela on the northern coast of South America.

The large negative free air gravity anomaly associated with the trench was first discovered off Puerto Rico by Vening-Meinesz in 1926 and subsequently investigated by him and Hess during the 1930s. The Antilles were one of the first areas to which the tectogene concept of Vening-Meinesz and Kuenen was applied (Hess, 1938). More recent gravity work, including that undertaken by Durham University and the Royal Navy in 1971 and 1972, has given a very good coverage of the gravity field in the eastern Caribbean. Fig. 1.4 shows a free air gravity anomaly map compiled from data east of the Lesser Antilles. The negative anomaly, situated over the Puerto Rico Trench in the north, curves around the outside of the Lesser Antilles running southward until it curves inland east of Trinidad. In the north of the Lesser Antilles it does not follow the eastern extension of the Puerto Rico Trench, but runs between it and the arc, and in the southern part runs next to the sedimentary Barbados Ridge.

Venezuelan Basin

This major basin forms about half the area of the Caribbean and is fairly flat bottomed with an average depth of about 4500 m. Seismic refraction and reflection (summarised by Edgar, Ewing and Hennion, 1971) with recent JOIDES drill hole results (Edgar, Saunders and others, 1972) have delineated the crustal structure in some detail. Seismic reflection showed that a thin layer of Quaternary turbidites overlies two acoustically transparent layers, the 'Carib Beds' which

1.3 Bathymetry and geology of the Lesser Antilles area. Bathymetric contours, at 0.5 km intervals are taken from an unpublished United States Government chart and unpublished data collected by NOAA, Miami (G. Peter, personal communication). Geology of the Lesser Antilles is from Martin-Kaye (1969), and that of Venezuela and Trinidad is from Gansser (1973).

Lesser Antilles Bathymetry & Geology

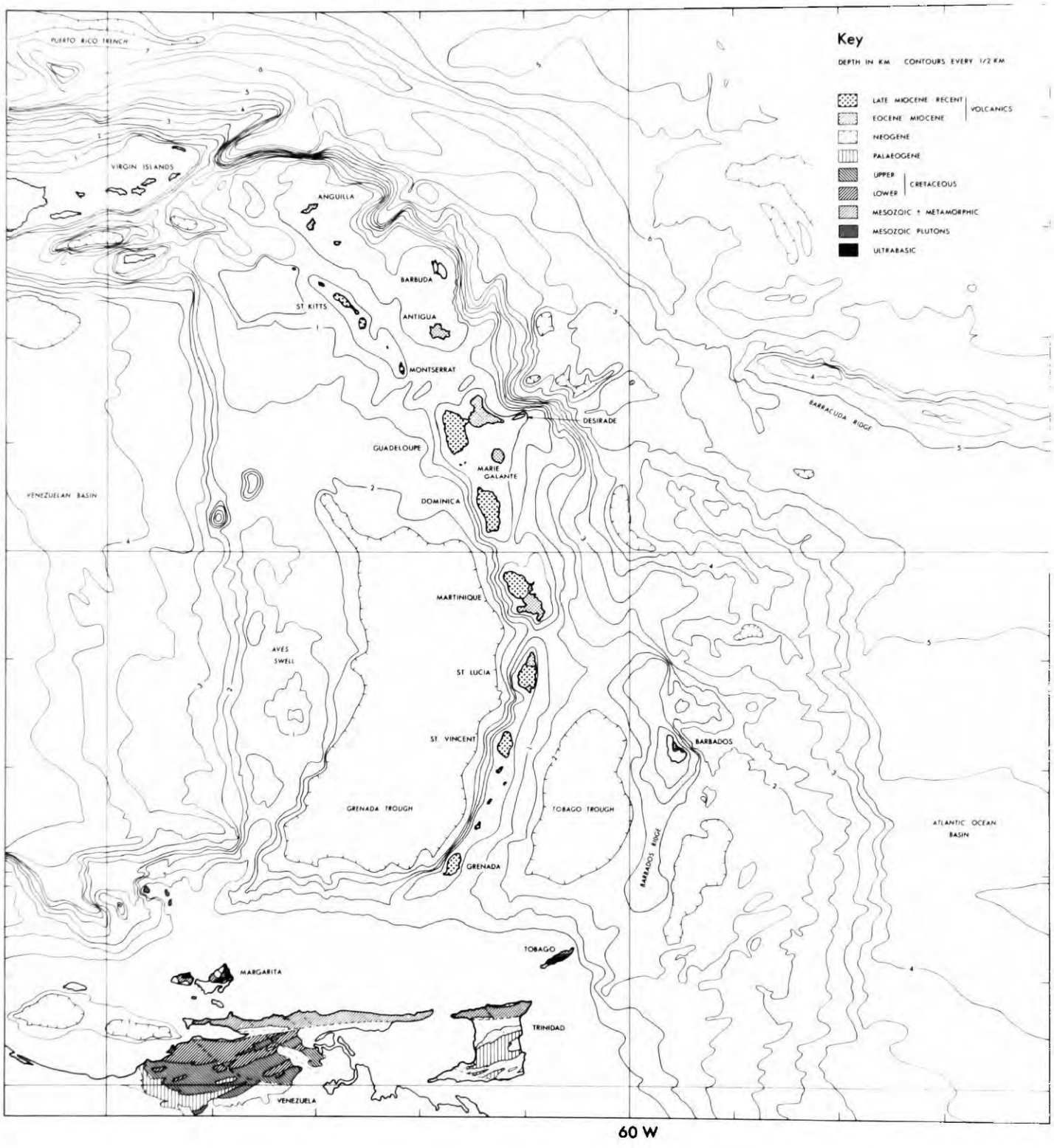

are separated by a strong reflector A" and underlain by another reflector B". Both these reflectors are smooth and continuous. Seismic refraction showed that below these sediments is a layer about 1.5 km thick in which the velocity varies between 3.2 and 5.5 km s^{-1}. Under this a layer of velocity 6.3 km s^{-1} and thickness 2.5 km overlies a layer of velocity 7.3 km s^{-1} and thickness 4.5 km. The lowest layer overlies the Moho which is at a depth of just under 15 km underlain by material of velocity 8.1 km s^{-1}. The JOIDES results showed that reflector A" is a group of Eocene chert bands a few cm thick and dolerite and basalt were found overlain by Cretaceous sediments of the Coniacian stage at the level of B" (Elsewhere in the Caribbean, Campanian and Santonian ages were determined).

Greater Antilles

These islands are composed mainly of geosynclinal sediments dating from the Jurassic to the early Tertiary (in Cuba Palaeozoic rocks may be present) and volcanics of Cretaceous to Mid Eocene age. Typical associations are cherts, spilites and serpentinites and there are volcanic products of calc-alkaline type, andesites, dacites and pyroclasts. Khudoley and Meyerhoff (1971) consider that by mid Eocene times the Greater Antilles had reached their present configuration. Sediments of later Tertiary age are not of geosynclinal type, and those of the Miocene are mainly limestones. Major unconformities are present in the Turonian, at the beginning of the late Eocene, and at the beginning of the late Miocene. The Greater Antilles emerged above sea level in the late Miocene. The age of the Puerto Rico Trench is either post mid-Eocene (Monroe, 1968), or post Miocene if the

1.4 Free-air gravity anomaly map of the area east of the Lesser Antilles. Data sources are the 1971 HECLA survey; G. Laving (1971); NOAA data provided by L. Dorman and G. Peter; Masson Smith, Andrew and Robson, (1970).

FREE AIR GRAVITY ANOMALY EAST OF THE LESSER ANTILLES

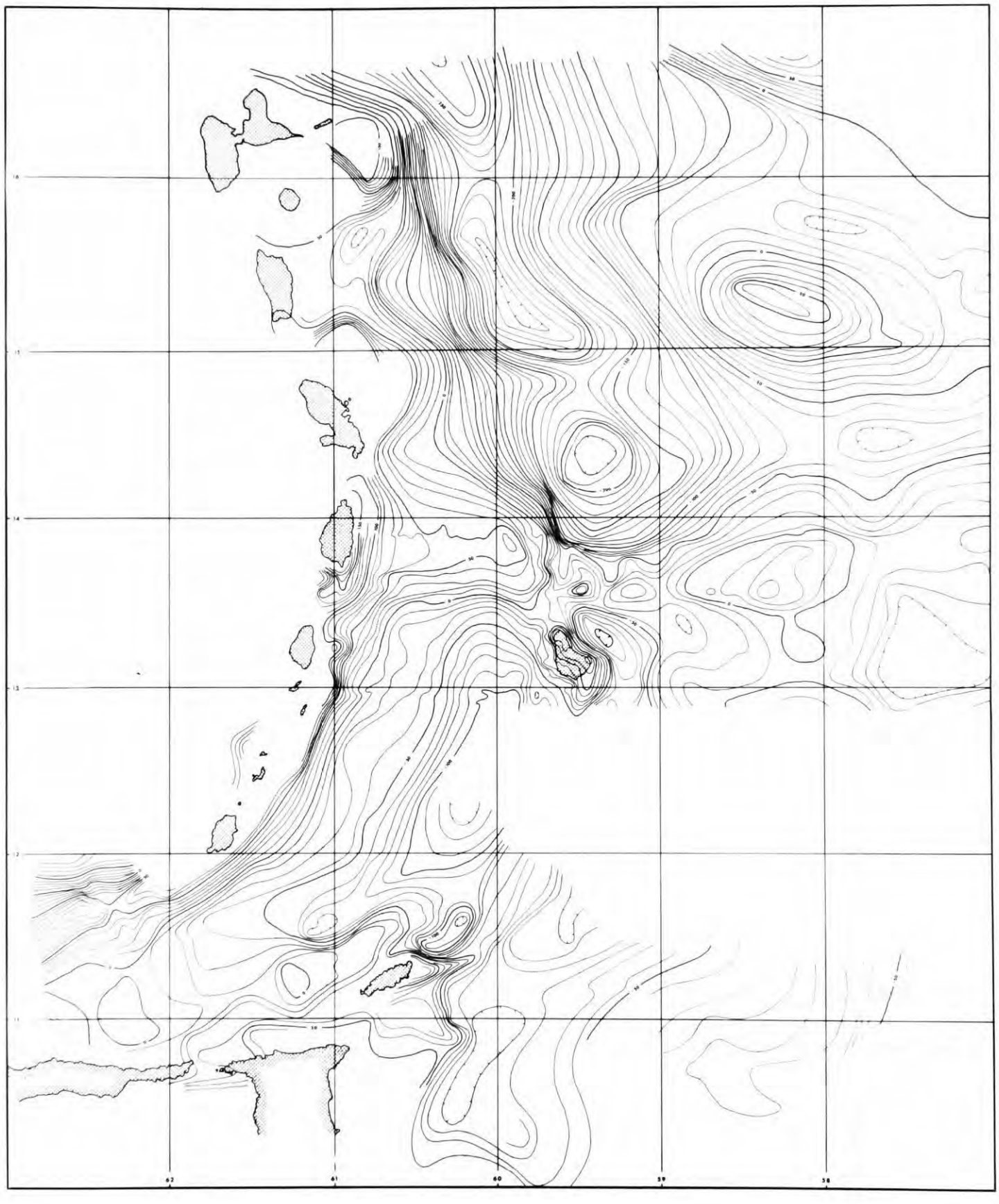

acoustically transparent layer in the trench is older than the trench (R.L. Chase, page 156 of Khudoley and Meyerhoff, 1968). Although they are apparently continuous with the Lesser Antilles, the Greater Antilles are thought by many authors to be unrelated to them genetically.

Aves Swell

This ridge has an average depth of 1 to 2 km, but locally seamounts rise higher, and one emerges above sea level to form Aves Island on the northern part of the Swell. The slope of the ridge on its western side is remarkably straight, and on the eastern side it tends to follow the curvature of the Lesser Antilles. A wide variety of rock types have been dredged from the Aves Swell. The major types are granites, andesites, basalts, volcanic conglomerates and breccias, with minor dacites, tuffs and limestones (Nagle, 1971). Granites from the ridge have yielded isotopic dates of 89 to 57 my and two diabases have given ages of 57 and 60 my (Fox, Schreiber and Heezen, 1971). The suite of rocks collected favours the possibility that the Aves Swell was once an island arc, though it may have been modified subsequently. There is much evidence for vertical movement of the Aves Swell, including a subaerial unconformity found in hole 148 of JOIDES Leg XV.

Grenada Trough

Lying between the Aves Swell and the Lesser Antilles, this small basin has a remarkably flat floor at a depth of about 2600 metres, and contains a considerable thickness of sediment. The sediment is about

7 km thick and the underlying crust is similar to that of the Venezuelan Basin, with a layer of velocity 6.2 km s^{-1} underlain by a layer of velocity 7.4 km s^{-1} (Officer and others, 1959). The Moho was not detected.

Venezuela and Trinidad

South of the Lesser Antilles lie Venezuela and Trinidad on the northern edge of the South American continent. Forming the northern coastline of these countries is a small mountain range composed of metamorphosed Mesozoic rocks. South of this range lie a series of Cretaceous and Tertiary sediments which exhibit some folding and extensive overthrusting towards the south (Barr and Saunders, 1968). The southern boundary of the Coast Ranges is formed by a long easterly trending fault (El Pilar) and the northern boundary appears to be similarly faulted (Bassinger and others, 1971). On the continental shelf north of Venezuela and Trinidad the islands of Margarita and Tobago are composed of Mesozoic metamorphics with ultrabasic rocks and Mesozoic plutons. On Margarita eclogitic amphibolites occur (Maresch, 1973). Diorites dredged from the continental shelf have isotopic ages of about 80 my (Peter, 1971). At Carupano on the north coast of Venezuela 20 small dacite plugs occur. Gansser, 1973). These lie along strike from the Lesser Antilles, and dated isotopically at 5 my these may be the most southerly expression of the Late Miocene to Recent vulcanism of the Lesser Antilles.

Lesser Antilles

The Lesser Antilles are a chain of volcanic islands composed predominantly of the products of calc-alkaline vulcanicity. The main constituent rock types are basaltic andesites, andesites, forming flows and sills; tuffs and ashes, many of them water lain; intrusive dacitic domes and viscous flows; and intrusive diorites. There are, in fact, two island arcs which become superimposed south of Martinique. In the north of the chain the more recent, currently active, arc is the more westerly and runs through the islands of Montserrat, St. Kitts and Saba. These volcanics are dated stratigraphically as being not earlier than late Miocene, and radiometric dates no older than 7.2 my bp have been determined from them (Briden, unpublished data). The older arc, which in the north runs through the islands of Marie Galante, Antigua and Anguilla, contains no evidence of Miocene or later vulcanism. Lower Miocene and Oligocene sediments, mainly limestones, rest on the bevelled surfaces of older volcanics mostly of Eocene age. At the southern end of the arc, on Grenada, volcanics of the recent volcanic episode overlie the folded Tufton Hall Formation which is Upper Eocene flysch containing tuffs of the earlier volcanic episode.

On Desirade a late Jurassic date has been obtained for an intrusive trondheimite, and associated spilites and keratophyres have yielded dates ranging from 98.6 my bp to 43.4 my bp (Fink and others, 1971). As will be shown in chapter 7, the Atlantic Ocean floor in the region of the Lesser Antilles dates from the earliest period of seafloor spreading in the North Atlantic, and it seems likely that the rocks on Desirade are an uplifted portion of the seafloor existing in the area before the island arc was formed. The age of the Caribbean basin,

at a little over 80 my bp, precludes the possibility of these rocks being the product of an island arc since the Caribbean Plate must have been in existence before island arcs could be formed on its margins.

A general observation on the Lesser Antilles is that the bathymetry shows that the volume of material above the average level of the ocean floor is much greater in the north of the arc. Maybe this is a result of greater vulcanicity in the north, or possibly the incorporation of some material from the Greater Antilles when the arc first formed.

All the Lesser Antilles show evidence of Pleistocene to Recent uplift and the following estimates (from Martin-Kaye, 1969) are based on the amount of uplift of Pleistocene limestones. St. Eustatius, 1000 ft: St. Kitts, 1150 ft: Dominica, 500 ft: St. Lucia, 250 ft: St. Vincent, 1000 ft?: Grenada, 200 ft: Barbuda, 200 ft.

St. Lucia

The rocks exposed on this are mainly volcanic products of the newer arc. Older material, tuffs and agglomerates with limestone lenses, outcrops in the north and extreme south of the island. In the Soufriere district there is fumarolic activity, and nearby, two dacite plugs form the Gros and Petit Pitons. Geochemical sampling reveals (Arculus, Holland, Tomblin, personal communications) that St. Lucia has an anomalously high percentage of acidic rocks compared with the other islands in the arc.

St. Vincent

Only volcanic rocks of the late Miocene to Recent period outcrop on this island, but metasedimentary blocks ejected from the Soufriere volcano are thought to be of an earlier age. Many of the tuffs and ashes show evidence of waterlain deposition. The Soufriere volcano erupted catastrophically in 1902, and more recently, in the autumn of 1971, a dome rose above the surface of the boiling crater lake, accompanied by many earth tremors (Tomblin and others, 1972).

Barbados

Barbados lies 160 km east of the Lesser Antilles and is composed entirely of sedimentary rocks. The rocks are all of Tertiary age, but there may be some exotic blocks of Cretaceous. Shown in fig. 1.5 is the stratigraphic table of Saunders (1968) and, although there have been variations by other authors on the nomenclature of some beds (Baadsgard, 1960) and the extent of Oligocene rocks, it is his scheme that is followed in discussion of Bajan rocks in this thesis.

The Lower Scotland Formation consists of flysch deposits, most probably laid down in a deep water environment by turbidity currents. The upper part of the formation, containing conglomerates, grits, sands and silts, may have been deposited in somewhat shallower conditions. Fauna and detrital metamorphic minerals found in these rocks indicate derivation from the north coast of South America (Senn, 1940). The Scotland Formation is very strongly disturbed. The surface exposure shows a marked northeast-southwest strike trend and the rocks are quite clearly multiply folded with much overturning of beds. The exploration

Recent — Pliocene	**Coral Rock Formation**		Mainly algal and coral reef limestones with consolidated reef detritus — **Up to 300 ft.**
Miocene	**Conset Marl**		Foraminiferal marls; greenish or cream coloured, glauconitic in parts — **Estimated 1500-2000 ft.**
	Bissex Hill Formation		**Algal and foraminiferal limestones and foraminiferal marls — Estimated 100 ft.**
Oligocene	**Oceanic Formation**	**Codrington College Member**	**Foraminiferal marl — 400 ft.**
		Bath Member	**Foraminiferal and radiolarian marls with some volcanic ash beds towards bottom — 300 ft.**
		Mt. Hillaby Member	**Foraminiferal and radiolarian marls with volcanic ash beds — 1000 ft.**
	Joes River Formation		**Slickensided shales with pebbles and boulders — 1000 ft.**
Eocene	**Scotland Formation**	**Mt. All Member**	**Sands with silty and sandy shales — 700 ft.**
		Chalky Mt. Member	**Conglomerates, grits, sands and silts — Max. 660 ft.**
		Murphy's Member	**Gritty sands and silts — 250-300 ft.**
		Morgan Lewis Member	**Shales with rare sands — 1500 ft.**
		Walkers Member	**Interbedded sandstones and shales — 1500 ft.**
L. Eocene, Paleocene Cretaceous	**(Blocks)**		**Blocks of fossiliferous limestones, argillites, etc. mainly found in Joes River Formation and in Chalky Mt. conglomerate.**

figure 1.5

Stratigraphic Table : Barbados. From Saunders (1968).

boreholes of oil companies (there is oil in the Scotland Formation) reveal many overturned and repeated sequences down to a depth of 4595 m (Baadsgard, 1960). These indicate that there are at least three superimposed sheets containing the same sequence of formations. The rocks are so highly disturbed that correlation between close boreholes is not possible. Baadsgard invoked large scale sheet displacement further disturbed by high angle reverse, normal and wrench faults to account for the situation. The regular tight folding of some areas is of a tectonic origin, but this is superimposed on features such as slumping, gravity folding etc., contemporaneous with deposition. The resulting structure is so complex that an accurate description of it has not yet been obtained, and more accurate dating of the rocks is needed before this could be attempted.

The Joes River Formation, which structurally overlies the Scotland Formation, consists of slickensided clays and silts with included pebbles and boulders, and contain hydrocarbons in the form of tar and manjak. Baadsgard interpreted the formation as a shear zone breccia, but other authors have interpreted it as the product of a mud volcano (Senn, 1940); mud vents from anticlines extruding flows onto the seafloor. Hess considered it to be the result of submarine landsliding into a trench.

Lying with strong unconformity on the older beds is the Oceanic Formation, extending in age from the upper part of the Eocene to Lower Miocene. The formation comprises radiolarian earths and calcareous foraminiferal marls, and a thickness of 1500 m has been penetrated in a borehole. The lower part of the formation is strongly radiolarian,

with many ash beds in the Eocene part of it. The upper part is mainly foramniferal. Senn considered these rocks to have been formed at a depth of 5500 m, whereas Beckmann (1953) from a study of benthonic fauna thought 1000 to 1500 m to be more likely. Saunders (1968) wondered whether "the presence of silica rich water associated with volcanic eruptions and the absence of a source of appreciable terrigenous material might allow "radiolarian earths" to be formed at shallower depths than they normally occupy today."

Overlying the Oceanics are two Miocene formations; the Bissex Hill Formation, algal and foraminiferal limestones with foraminiferal marls; and the Conset Marl, foraminiferal and glauconitic in parts, unconformable on the Oceanics.

Covering most of Barbados is the Coral Rock which is up to 100 m thick and was formed as a series of fringing reefs about an emergent island. Some of the oldest terraces in the centre of the island have been isotopically dated using the thorium 230 method (Ku, 1968) and gave a maximum age of 215000 y.

Barbados Ridge

Barbados is the highest point on a north-south trending ridge which extends from just northeast of Tobago in the south to east of Martinique in the north. Although some authors differ on the point (Bassinger and others, 1971), there does not seem to be any continuity between the ridge and structural trends on the continental shelf. About 35 km north of Barbados dredge samples of flysch rocks similar to those of the Scotland Formation have been collected from the ridge crest

(Hurley, 1966). Just to the south of Barbados, Hurley also dredged manganese nodules embedded in a lithified limestone suspected to be a facies of the upper Oceanic or Bissex Hill formations. Between Barbados and Tobago several core samples (longest: 12.07 m) have been taken from the uppermost sediments (Ramsay, 1968). These cores all contained Quaternary lutites, except one which contained Upper Miocene foraminiferal lutites. All the cores contained reworked Eocene nannofossils.

Atlantic Ocean floor east of the Lesser Antilles

The area has been investigated by several workers in the past few years, and a number of seimic reflection records have been collected from it (Collette and others, 1969; Kane 9 Cruise, Chase and Bunce, 1969). These show that the sediments, which overlie an acoustic basement of irregular topography, thicken towards the south and towards the west. Turbidites from South America contribute greatly to the thickness in the south where the acoustic basement is not detected and penetration is greater than two seconds reflection time.

A JOIDES hole (Hole 27 of Leg IV, Bader and others, 1970) drilled south of Barracuda Ridge showed typical deep sea clays to a depth of 400 m below the sea floor. At depths of 67 and 70 m two sandy silt turbidites of Pliocene age appear to be responsible for the strong reflector which had been previously assumed to be Horizon A. At sites 23 and 24, further east, the "Horizon A" reflector was due to Middle Miocene turbites. Nowhere in this area were the Eocene chert bands,

which form Horizon A in the North Atlantic, found by JOIDES. These results emphasise the difficulties and errors inherent in the identification of reflecting horizons by extrapolation from areas where they have been identified previously. A lower reflector at site 27 which might in other circumstances have been correlated with Horizon Beta, seemed to result from thin turbidites of Miocene age. At 455 to 475 m depth, radiolarian rich calcareous sediments strikingly similar in lithology and age (Upper Eocene) to the lower part of the Oceanic Formation of Barbados were discovered. A hard calcareous claystone or impure limestone found at the base of these sediments may be the acoustic basement. This bed has dips of 24^{o} and may be unconformable with the upper Oceanic correlatives. It is possible, however, that an unconformity may exist several metres below this rock and form the acoustic basement.

Seismic refraction (Ewing and others, 1957) found a total sediment thickness of nearly 3 km (main layer of velocity 2.2 km s^{-1}) in the region east of the Lesser Antilles, overlying a crust which is of a normal oceanic type, with the exception that Layer 2 velocities were not detected.

Chapter 2

Collection and reduction of bathymetric, gravity and magnetic data

Navigation

The principal navigational aid for the gravity, magnetic and seismic reflection survey of 1971 was the Decca Lambda System. This is a radio navigational system using phase comparisons to determine the range of the ship from two radio stations at known positions. It is similar to the commercial Decca system except that the master station instead of being situated at a permanent station on land, is carried on the ship. The chart drawn up for navigation in the chosen area consists of two sets of concentric circles (lanes) about the two slave stations rather than the hyperbolic pattern of the normal Decca system. The ship is always at the effective baseline of the system, and because of this it is generally more accurate than normal Decca, with an accuracy in range from a slave station of about 10 m. The positions of the slave stations for the survey were at the southern tip of St. Lucia and the northern point of Tobago, which gave a good cut between the concentric lane circles drawn about them in most of the area.

The Lambda system, though very accurate, has a tendency to 'jump' lanes, especially around dawn and dusk. To check for this and to act as a back-up system, a satellite navigator was used. In the vicinity of St. Vincent, where the cut between the Lambda lines was poor, an Alpine radar transponder, situated at a trig. point near Soufriere, was used in conjunction with a precision ranging attachment

2.1 Track chart of HMS HECLA for 1971 survey, east of the Lesser Antilles. Shows days on which the lines were run and type of data collected.

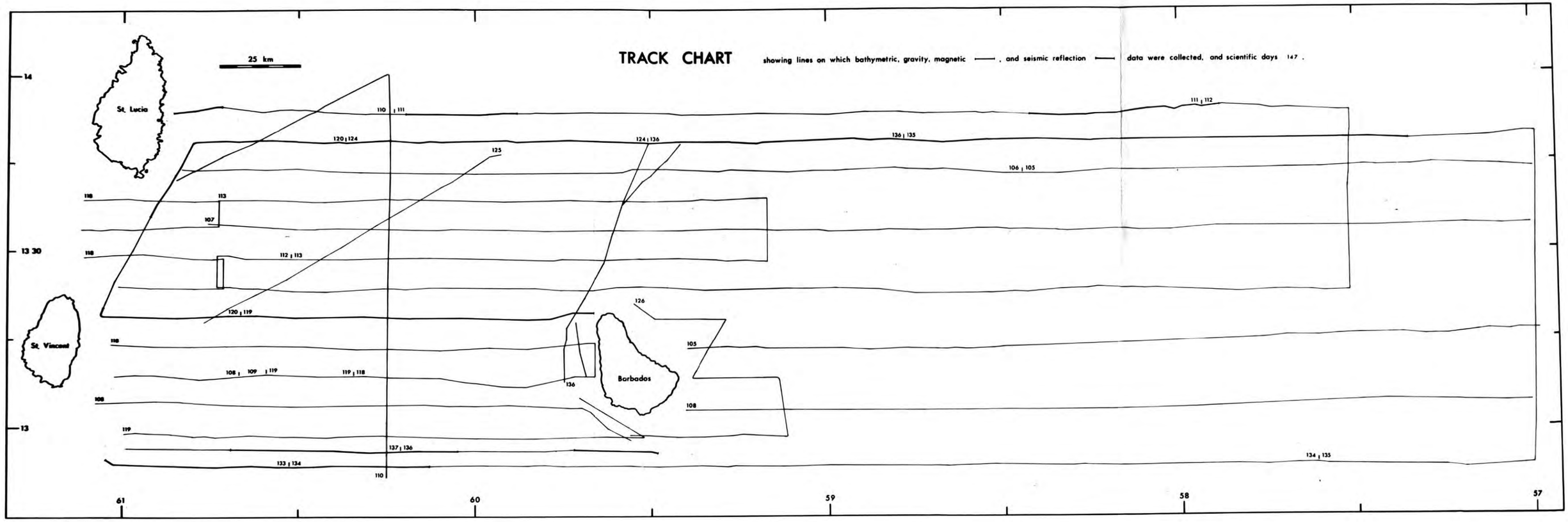
TRACK CHART
showing lines on which bathymetric, gravity, magnetic ——, and seismic reflection ⊢⊣ data were collected, and scientific days 147 .
25 km
St. Lucia
St. Vincent
Barbados
14
13 30
13
61
60
59
58
57
110 | 111
111 | 112
120 | 124
124 | 136
136 | 135
125
106 | 105
118
113
107
112 | 113
120 | 119
126
105
108 | 109 | 119
119 | 118
136
108
119
137 | 136
133 | 134
134 | 135
110

on the radar.

Fixes were taken every ten minutes and plotted on to plastic fix-plot charts layed over the Lambda grid. If later, satellite or some other navigational aid indicated that a lane shift had occurred unnoticed, the time of the shift was investigated and the fixes replotted from that time. The ship's speed on lines of only gravity and magnetic measurements was 10.5 knots . The charts are the prime source navigational data, because although the Lambda positions were logged automatically on paper tape, the tapes were not corrected for lane shifts or areas were navigation was not only by Lambda.

A permatrace copy of the fix-plot charts was made by the writer in the ship, and the positions used for data analysis were taken from this. The scale of this chart is 1:200000 and the positions were picked to the nearest twentieth of a minute of a latitude or longitude. A track chart compiled from the fix-plot chart is shown in fig. 2.1. This and all other survey charts are plotted on a Universal Transverse Mercator Projection about a central meridian at 59°W (Clark's 1866 figure of the Earth). Full details of navigation are given in HMS HECLA "Return of geodetic data - Approaches to the Windward Isles. 1971".

Bathymetry

Depths to the seabed were obtained using a Kelvin Hughes precision depth recorder. The transducer for the system was in a 'fish' towed alongside on a boom. The bathymetry shown in fig. 2.2 is drawn from uncorrected depths obtained using a sounding velocity of

2.2 Bathymetry; uncorrected depths for a sounding velocity of 1500 metres per second.

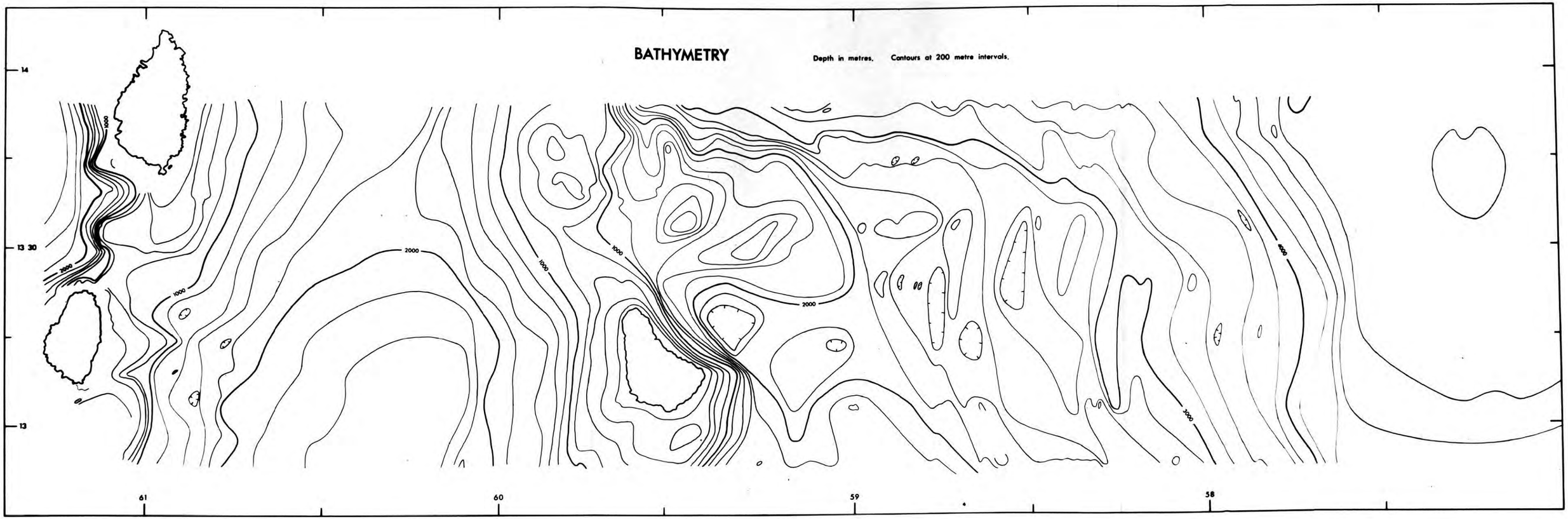
BATHYMETRY
Depth in metres. Contours at 200 metre intervals.
14
13 30
13
61
60
59
58
1000
2000
1000
1000
2000
3000
4000

1500 m s^{-1} and picked at two minute intervals, or less, from the continuous records.

Gravity

Variations in gravitational attraction were measured with Askania Sea Gravimeter Gss-2 no. 18, operated in manual mode. The gravity measured was reduced to a free-air anomaly by the ship's scientific officer, Lt. Cdr. J. Conolly, using a standard computer program, Mangra Mk 3. This anomaly was not corrected for gravimeter drift or meter height. The Eotvos correction was calculated from the course and speed averaged over three successives fixes (30 minutes). The distances between fixes are given to the nearest tenth of a nautical mile and if they are systematically over or under estimated, errors approaching 4.5 mgal could be introduced.

A small computer taken on the survey to calculate the errors due to the cross coupling effect was found to be incompatible with the gravimeter, even though it had been supplied specifically for that type of meter by the manufacturers. Hence no quantitative estimate of the errors due to the cross coupling effect was obtained. Weather conditions, however, were very favourable during the survey, and it is unlikely that cross coupling had any large effect. The line showing the worst crossover errors (7.0, 7.2 and 8.5 mgal) may have been one on which cross coupling had a significant effect.

Gravity ties to base stations established by Masson Smith and Andrew (1965) were made using a Worden gravimeter, and details of these are given in appendix 2.1. The gravimeter drift obtained from these

2.3 Gravimeter drift; B = Bridgetown, Barbados; C = Castries, St. Lucia; K = Kingstown, St. Vincent.

2.4 Gravity crossover errors. North-south lines minus east-west lines. Mean is not significantly different from zero. The standard error is 3.4 mgal, or 2.7 mgal if the data shown with opposite diagonal ornament is ommitted.

Gravimeter Drift

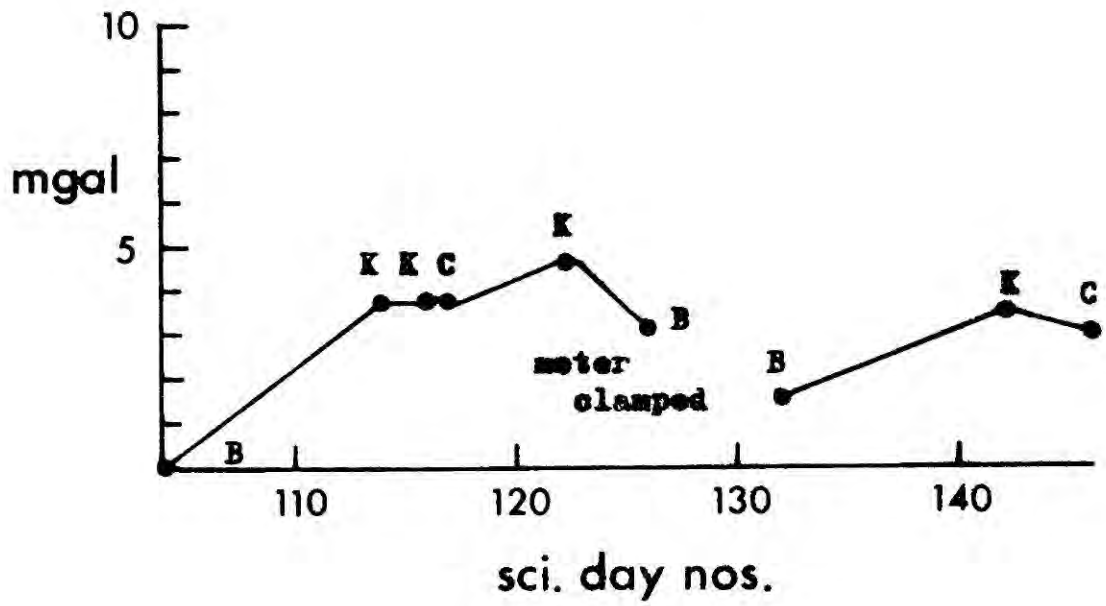

Crossover Errors

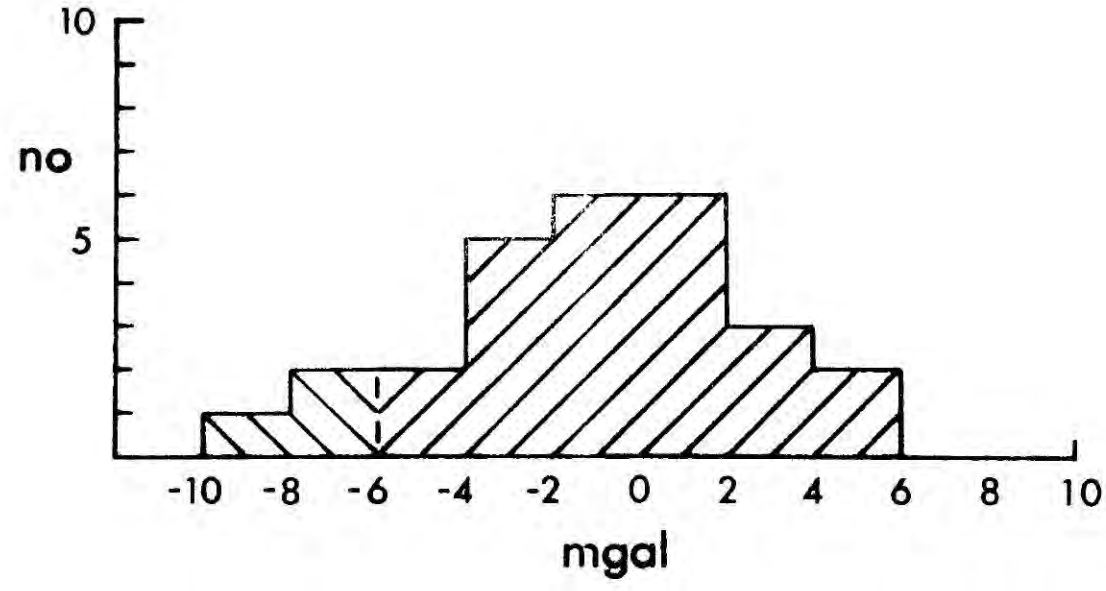

ties is shown in fig. 2.3.

Gravity data were taken from the survey in paper tape form, accompanied by the printouts of the Mangra Mk 3 program. These data were translated and put on punch cards (program C2.1). The cards were edited to remove or correct errors in the data. Following this the gravity data were incorporated with the navigational and bathymetric data, and corrected for meter height and drift (program C2.2). The free-air gravity map produced is shown in fig 2.5.

A histogram of the crossover errors (difference in gravity value between north-south lines and east-west lines where they cross) is shown in fig. 2.4. The block shaded in an opposite manner to the rest of the diagram represents the crossover values on the short north-south line at 57° $30'$ W, where cross coupling errors may be significant. With this line included the mean error is -1.1 mgal and the standard error of the distribution is 3.4 mgal, with it excluded the mean error is -0.27 mgal and the standard error is 2.7 mgal. Neither of the means is significantly different from zero (Student t test at 95% confidence).

To estimate the probable magnitude of errors arising from the measurement and reduction of the gravity data, free-air anomaly values were low pass filtered (program C2.3) using as a cutoff frequency that produced by a line mass at 2 km depth. This is higher than expected from any natural source, because the water depth is usually greater than 2 km. The residual short wavelength anomalies obtained were no greater than 3 mgal and generally far less.

Bouguer anomalies were derived from the free-air gravity and

2.5 Free-air gravity anomaly map.

FREE AIR GRAVITY ANOMALY

in milligals. Contours every 10 mgal.

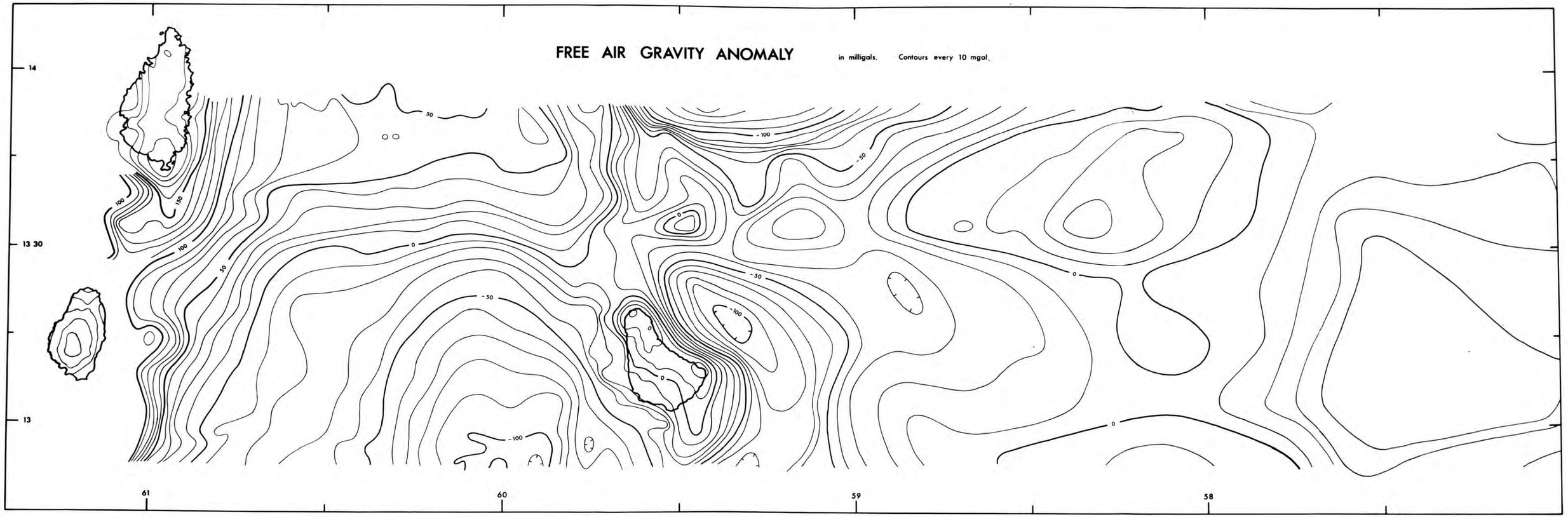

bathymetric data using a modified version of GRAVN (A Durham computer program, M.H.P. Bott, 1968) to calculate the effect of the bathymetric relief along each line. Two maps were produced; one (fig. 2.6) for a density of 2.0 gm cm^{-3}, which is the density of sediments on Barbados determined by Masson Smith and Andrew (1965); the other (fig. 2.7) for a density of 2.67 gm cm^{-3}, which is the most commonly assumed average crustal velocity. Comparison of Bouguer anomalies for many densities over topographic features of a sedimentary nature indicates that 2.1 gm cm^{-3} is probably the average sedimentary density (Nettleton's Method).

Magnetics

Values of the total intensity of the magnetic field, to the nearest gamma, were obtained using a Barringer Research Associates marine proton magnetometer, and logged every minute on paper tape and teleprinter paper by HMS HECLA's automatic data logging system. The magnetic values were extracted from the tape (program C2.4) at the 10 minute fix times, for most of the survey area, and at 1 minute intervals in the region of the island arc, where the wavelengths of the anomalies are shorter. Fig. 2.8 is the map of the measured magnetic field.

To obtain the magnetic anomaly, the International Geomagnetic Reference Field (I.G.R.F) (1965 epoch, I.A.G.A, 1969) was subtracted from the measured values using the Cambridge program REGMAG. When this was done initially it was found that differences at crossovers were in some cases unacceptably large, being as much as 60 gammas. This was

2.6 Bouguer gravity anomaly map. Correction density is 2.0 gm cm $^{-3}$.

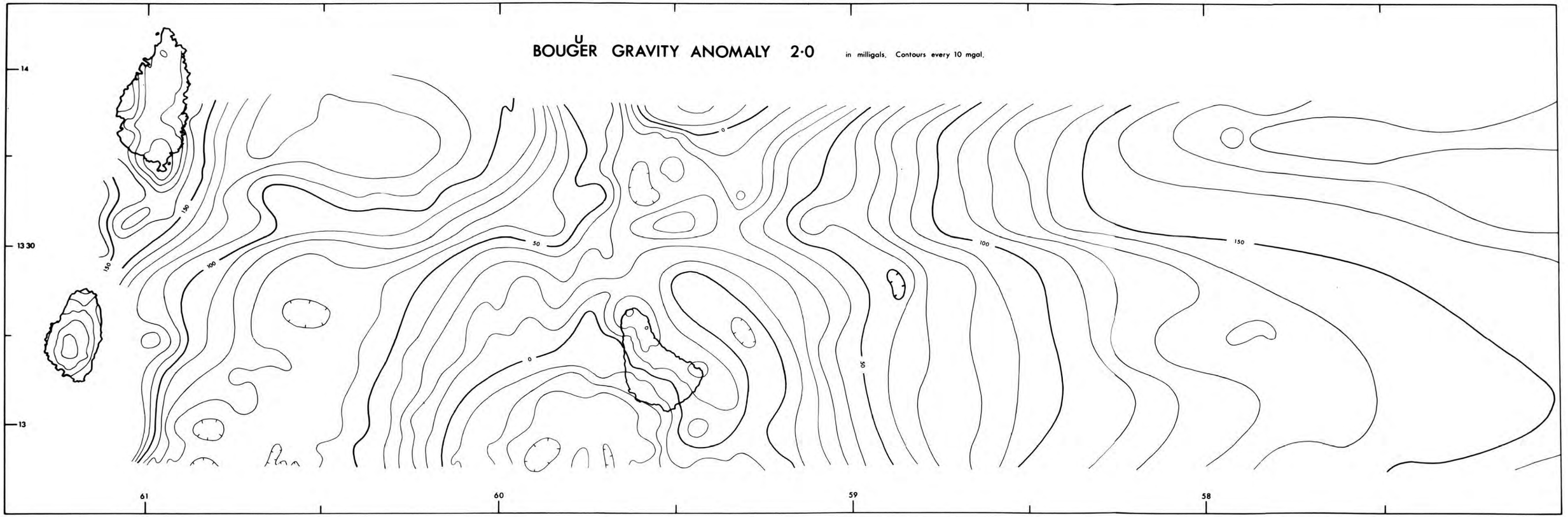
BOUGUER GRAVITY ANOMALY 2·0
in milligals. Contours every 10 mgal.
14
13 30
13
61
60
59
58
150
100
50
0
50
100
150

2.7 Bouguer gravity anomaly map. Correction density is 2.67 gm cm^{-3}.

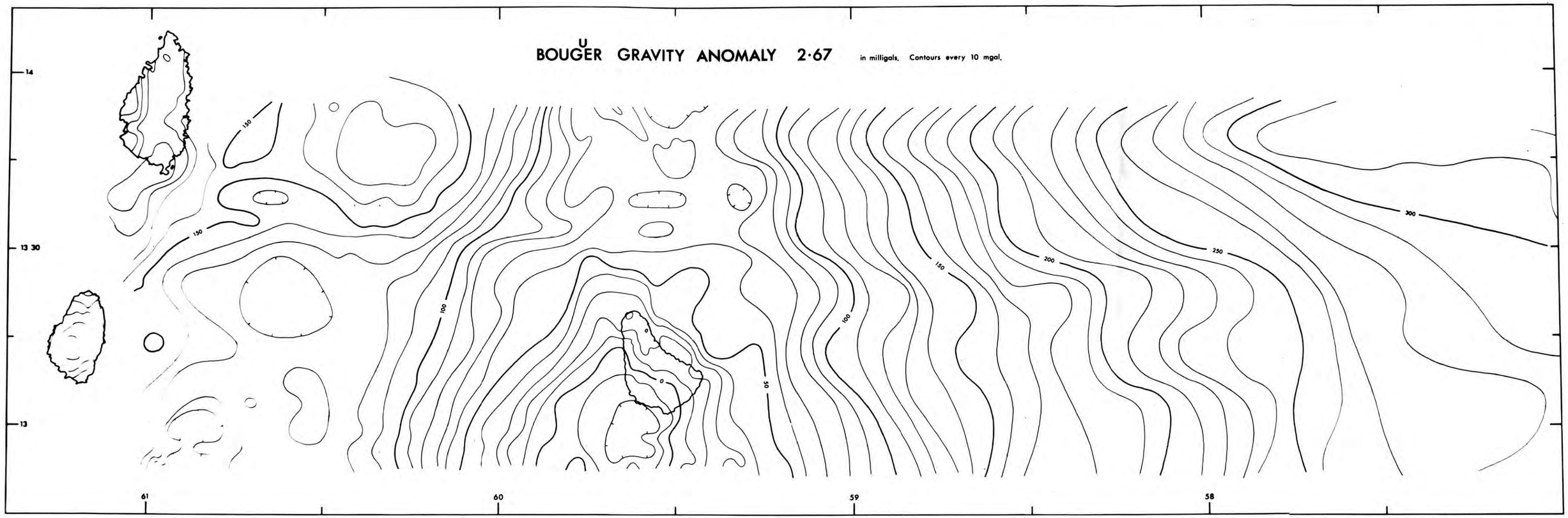
BOUGUER GRAVITY ANOMALY 2·67 in milligals. Contours every 10 mgal.
14
13 30
13
61
60
59
58
150
150
100
0
0
50
100
150
200
250
300

suspected to be due to diurnal and solar storm effects, and accordingly magnetograms for the period covered by the survey were obtained from the nearest geomagnetic observatories, San Juan, Puerto Rico, and Paramaribo, Surinam. On certain days the magnetograms show disturbances of considerable amplitude. These disturbances were corrected for by subtracting from the measure magnetic values the expected values obtained from the magnetograms, using a weighted mean based on distance from the station.

The observatories are separated in longitude so between them there is a phase shift in the diurnal part of the disturbance. Roden and Mason (1965) have considered this problem, and tried separating the diurnal and storm effect, and correcting the measured values accordingly. By comparing the synthesised variation with the actual measured variation at an intermediate position, they found that a weighted average technique was equally good, if not better in some cases. Interpolation of the field variation between the two observatories with respect to latitude would seem, initially, to be best accomplished by relating it to the variation in amplitude of the horizontal and vertical components of the diurnal field (Matsushita, 1967) predicted from world wide data. The phase of the horizontal component at San Juan, however, is not always the same as that at Paramaribo. Because of this and the absence of a predicted field for the storm variations, a straightforward empirical correction was used. It might not give a completely accurate expression of the variation in the field, but is least likely to introduce artificial errors.

The magnetograms were digitised using a DMAC table and from them

2.8 Map of the measured total intensity magnetic field.

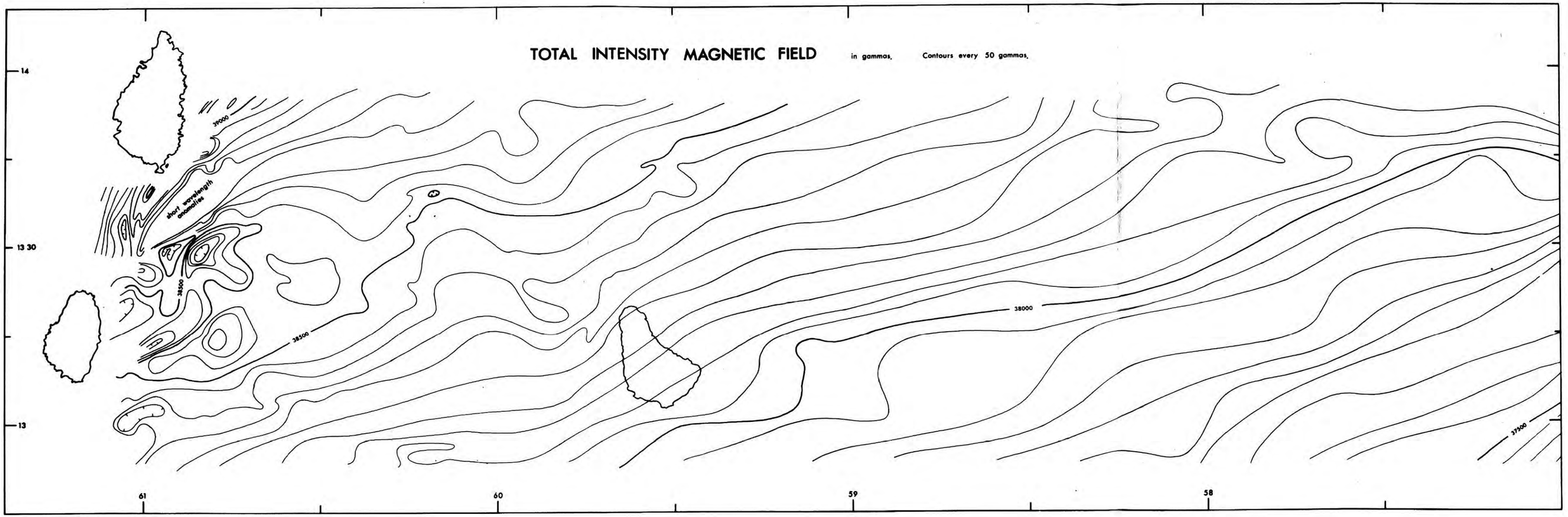
TOTAL INTENSITY MAGNETIC FIELD in gammas. Contours every 50 gammas.
14
13 30
13
61
60
59
58
39000
short wavelength anomalies
38500
38500
38000
37500

2.9 Total intensity magnetic anomaly map. IGRF and solar magnetic effects have been removed.

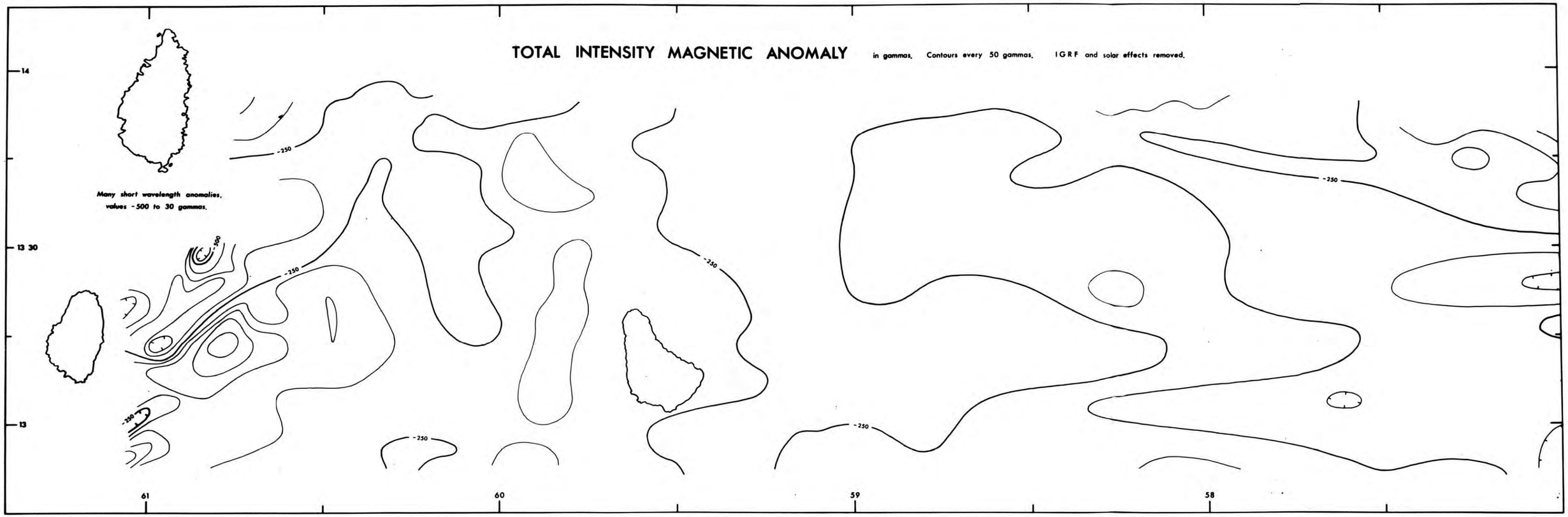
TOTAL INTENSITY MAGNETIC ANOMALY in gammas. Contours every 50 gammas. IGRF and solar effects removed.
Many short wavelength anomalies, values -500 to 30 gammas.
-250
-500
14
13 30
13
61
60
59
58

values at ten minute intervals were produced (C2.5), given with respect to a base value which was the average value on a quiet day (110), adjusted for secular variation. The measured magnetic values were combined with the other data, and reduced to a total field magnetic anomaly by removal of the IGRF and correction for magnetic disturbances, using the programs described in appendix C2.6. The total intensity magnetic anomaly map is shown in fig. 2.9. The average value of the anomaly is about-230 gammas. The negative value of the anomaly is common in the eastern Caribbean (Kearey, Peter, 1971) and reflects an inconsistency in the IGRF.

Correction for solar magnetic disturbances improved the crossover errors considerably, and a histogram of the magnetic crossovers is shown in fig. 2.10. The mean is 12.5 gammas and the standard error is 11.3 gammas. The mean is significantly different from zero at greater than 99.9% confidence, and shows that values measured on north-south lines are consistently higher than those on east-west lines. This suggests that the magnetometer was too close to the ship, as one expects reinforcement of the field when the ship is north or south of the magnetometer and diminution when it is east or west of the magnetometer. The streaming of the magnetometer was carried out by the ship's crew, and the distance that it was towed astern was reported to be greater than two ship's lengths.

In any future investigation near the Antilles it would be prudent to set up a magnetometer station on one of the islands in, or near to, the survey area, to monitor diurnal and magnetic storm disturbances of the Earth's field.

2.10 Magnetics crossover errors. North-south lines minus east-west lines. The mean value is 12.5 gammas and is significantly different from zero at 99.9% confidence. The standard error is 11.3 gammas.

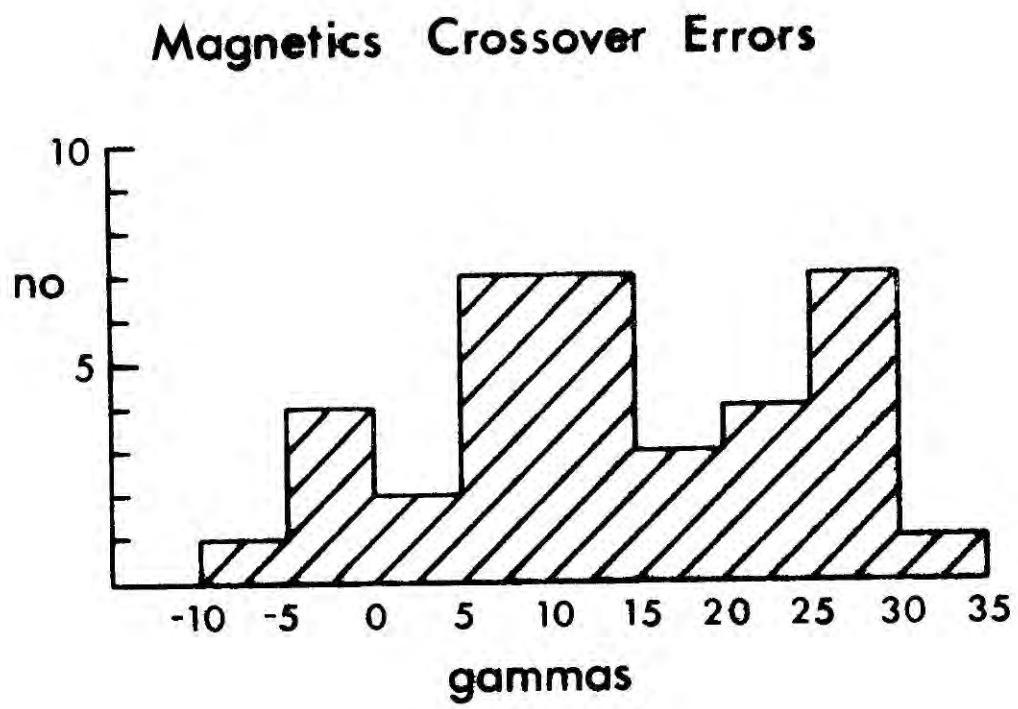
Magnetics Crossover Errors
10
no
5
-10
-5
0
5
10
15
20
25
30
35
gammas

Chapter 3

Seismic reflection and refraction

Seismic Reflection

Vertical incidence reflection profiles

Seismic reflection profiles were obtained on the lines indicated in fig. 2.1. The sound source used for the profiling was one or two air guns of 174.5 cm^3 capacity, designed and built at Durham University under the supervision of Mr. J. H. Peacock. Two guns were mounted on a frame which was towed at a depth of 10 m from the after davit on the ship's quarterdeck. The towing speed was 6 knots. The maximum operating pressure of the guns is 4000 psi, but because of compressor difficulties they were normally operated at 3000 to 3500 psi, and for the same reason, usually only one gun was run at a time. The firing period for the guns was 21 s.

Reflected arrivals were received by a Flexotir array streamed astern at a depth of 10 m. The array was made up of two 60 m long active sections, separated by an inactive section 40 m long, preceded by an inactive header section 100 m long and followed by another inactive section 40 m long. The whole was towed on a 150 m long cable, and the tail was attached to a marker buoy by 50 m of rope. The array was handled using the stern capstan, suitably enlarged by the addition of wooden blocks and wedges held on by thin steel bands. The arrangement of the active sections was such that the records from them could be common depth point stacked.

Signals from the active sections of the array were recorded

unfiltered on separate tracks on a magnetic tape, together with a time code, the gun firing sequence, and data on gun pressure, gun depth and array depth. Concurrent with the recording on magnetic tape, a filtered signal from one active section was played out on Linagraph direct print paper by a variable area recorder.

When the magnetic tape was replayed through the variable area recorder in the laboratory, the horizontal scale was halved to give more condensed records. The two channels were replayed separately, and also replayed summed, which gave better records from the deep water areas. The records were bandpass filtered, usually between 20 Hz and 60 Hz, but some narrower bands were tried, in order to enhance some of the deeper reflectors.

The positions of the reflectors on the clearest examples of the records were digitised using the DMAC table, and redrawn to a uniform reduced scale by the program described in appendix C3.1. The line dawings of the reflection records produced by this method are presented in chapter 4.

Wide angle reflection

Several attempts were made at obtaining the velocity layering of the sediments by measuring the wide angle reflections from the airguns, using sonobuoys. The technique is described by Le Pichon, Ewing and Houtz (1968). The attempts were mostly unsuccessful, because contact with the sonobuoy was lost soon after it had been dropped overboard. The reasons for this were that there was an open circuit in the lead to the aerial and that the receiver overheated. One good record showing five sub-bottom reflectors, was obtained from the Tobago Trough.

The Tobago Trough record was analysed, using two computer programs. One is an adaption by A.G. McKay of a program by X. Le Pichon, which uses a modified T^2/X^2 solution (Le Pichon, Ewing and Houtz, 1968). The other is an iterative method which models the seismic structure and obtains the optimum fit of the calculated reflection times to the observed reflection times, using a non-linear optimisation routine ("MINUIT", James and Roos, 1969). The variable parameters were the depth and dip of each reflector and the velocity of sound in the immediately overlying layer. The program is described in appendix C3.2. Data was entered in to both programs by digitising the playouts from the variable area recorder.

The relative performances of these programs were compared initially on several wide angle reflection records obtained by Durham University in the North Atlantic, and there was close agreement between the results. The advantages of the optimisation program are that the velocities obtained for the lower layers are not so badly affected by a poor determination for an overlying layer and the parameters may be fixed to values obtained by other methods, such as seismic refraction.

Sediment velocities in the Tobago Trough, from wide angle reflection.

Le Pichon Program				Optimisation Program			
Velocity	Thickness	Dip	SE of fit	Velocity	Thickness	Dip	SE of fit
1.52	2.54	0.0	0.135	1.50	2.52	0.0	0.012
2.14	0.268	0.0	0.038	1.54	0.19	0.0	0.019
1.65	0.225	0.0	0.005	1.55	0.22	0.0	0.019
1.59	0.429	0.0	0.042	1.90	0.48	1.1E	0.013
2.35	0.437	0.0	0.006	2.49	0.47	1.0E	0.009
2.48	0.305	0.0	0.016	2.51	0.34	0.0	0.022

Difficulty was encountered in determining a reasonable value for the velocity of the uppermost sediment layer. When the Le Pichon program was run the first time on the data a velocity of 1.45 km s^{-1} was obtained for the top sediment layer (other layer velocities in that run were 1.58, 1.88, 2.42 and 2.48). This was thought to be too low, being below the lowest values actually measured in deep sea sediments (Horn and others, 1968). The data were digitised again, taking more care over the 'picks' for the second reflector, and the results given above were obtained. In these the velocity in the top layer is unreasonably high, but the standard error for the water layer is lower than in the previous run. Velocities obtained by the optimisation program for the top sediment layer were all too low, and that given above was obtained by imposing the condition that the velocity must be greater than 1.5 km s^{-1}. No velocity inversions were produced by the optimisation program. The difficulty may arise from there being several reflectors of a semi-continuous nature, rather than one continuous reflector. The vertical incidence reflection profile lends some support to this view.

Seismic Refraction

As part of the Lesser Antilles Seismic Project (LASP) the NOAA Ocean Survey Ship DISCOVERER, acting as a receiving ship, occupied two positions (h1 and h2, fig. 3.1) on a line of shot points extending eastward from St. Vincent to the Atlantic Ocean. Given below is a description of the hydrophone system used on DISCOVERER and the results obtained from it. Full details are given in the logbook. The technique is similar to that described by Shor (1963).

3.1 Summary map of seismic refraction work in the area. Small dots indicate shot points. Their numbers are shown occasionally. Large dots are receiving stations C is Cole's Cave; P is St. Phillips; L is St. Lucia; V is St. Vincent; h1 and h2 are the hydrophone positions occupied by DISCOVERER. Also shown are the refraction lines of Ewing and others (1959), marked by an e, and a line from Worzel and Ewing (1948), b. Depth contours, in fathoms are from Hess (1966).

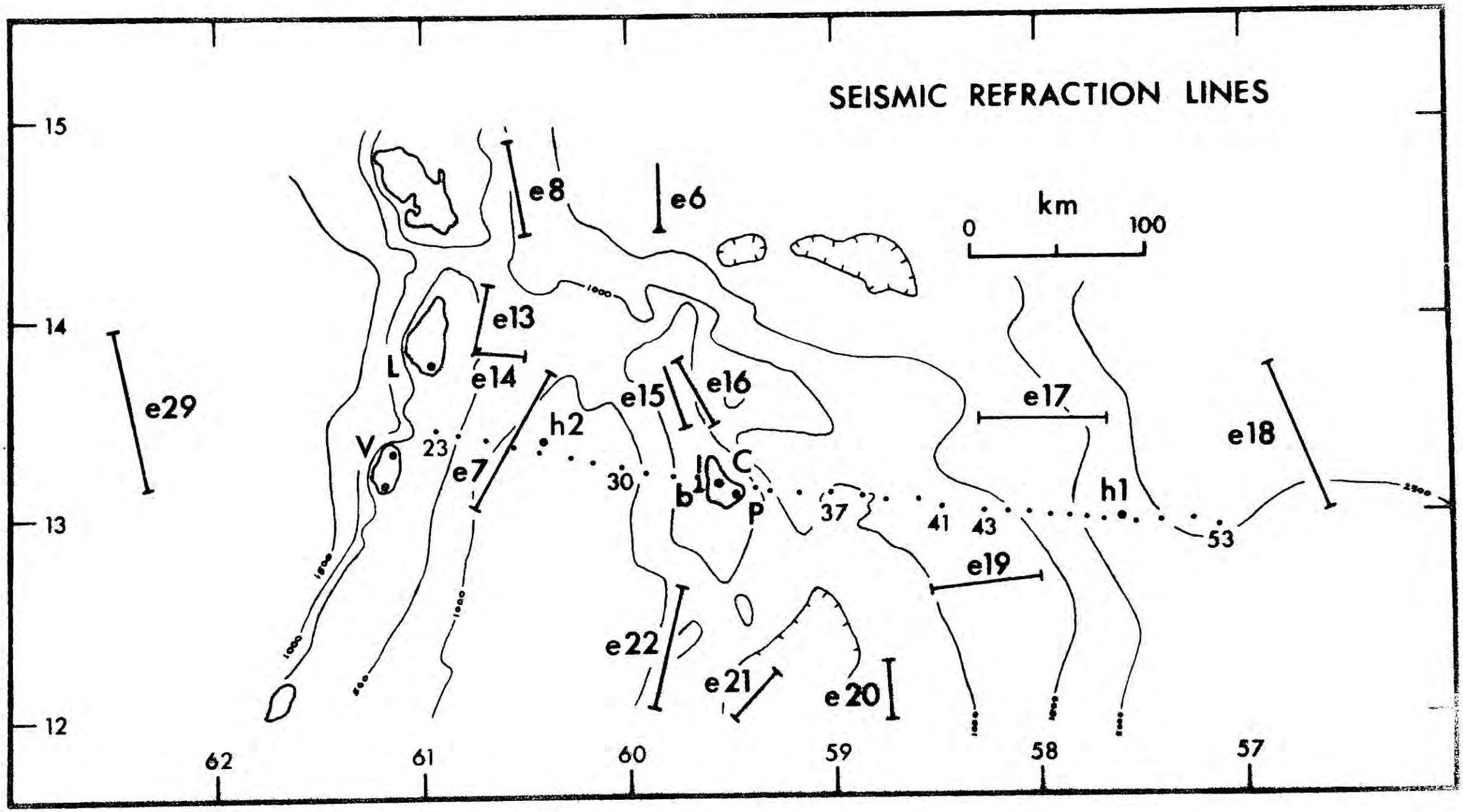
SEISMIC REFRACTION LINES
km
0
100
15
14
13
12
62
61
60
59
58
57
e29
e8
e6
e13
e14
e15
e16
e17
e18
e19
e20
e21
e22
e7
h2
h1
L
V
C
P
b
1000
1500
2000
2500
23
30
37
41
43
53

Equipment

Two Clevite (Type CS-1331LAF) hydrophones and pre-amp. modules, with a flat range frequency response of 2 Hz to 10 kHz, acted as detectors. The signals from these were passed through two separate amplifiers and recorded on separate tracks of a 4 track magnetic tape by an FM tape recorder. Recorded on a third track was the output from a digital clock, giving the time to tenths of a second, and on the fourth track were W.W.V., broadcasts from the shooting ship and identification by voice of the shot number and time. The tape speed was 3.75 inches per second. The noise on the hydrophones was monitored using an oscilloscope and an A.C. microvoltmeter (frequency range 1 Hz - 3 MHz). A block diagram of the system is shown in fig. 3.2.

The hydrophones were suspended in the water at depths of 30m and 60 m, a distance of 500 m from the ship (maximum). The method of suspension (fig. 3.2) was as follows. A nylon rope, with a heavy lead sinker at one end, was attached to a large buoy. Fixed to the rope were the cables to the hydrophones leading off at 30 m and 60 m to neutrally buoyant sections, suspended by spherical fishing floats, at the end of which were the hydrophones. The spacing of floats on the neutrally buoyant sections was designed to reduce the amount of wave movement transmitted to the hydrophones from the vertical rope beneath the buoy. The weight borne by each float if it is in equilibrium is equal to the weight of half the loop of cable either side plus the balancing weight attached to it. If one float moves up or down, the amount of cable supported by the adjacent buoy is altered, causing it to move also.

3.2 Diagram showing the listening configuration of DISCOVERER, to scale, with the detail of the hydrophone suspension system, and a block diagram of the equipment.

Discoverer
Hydrophone Station

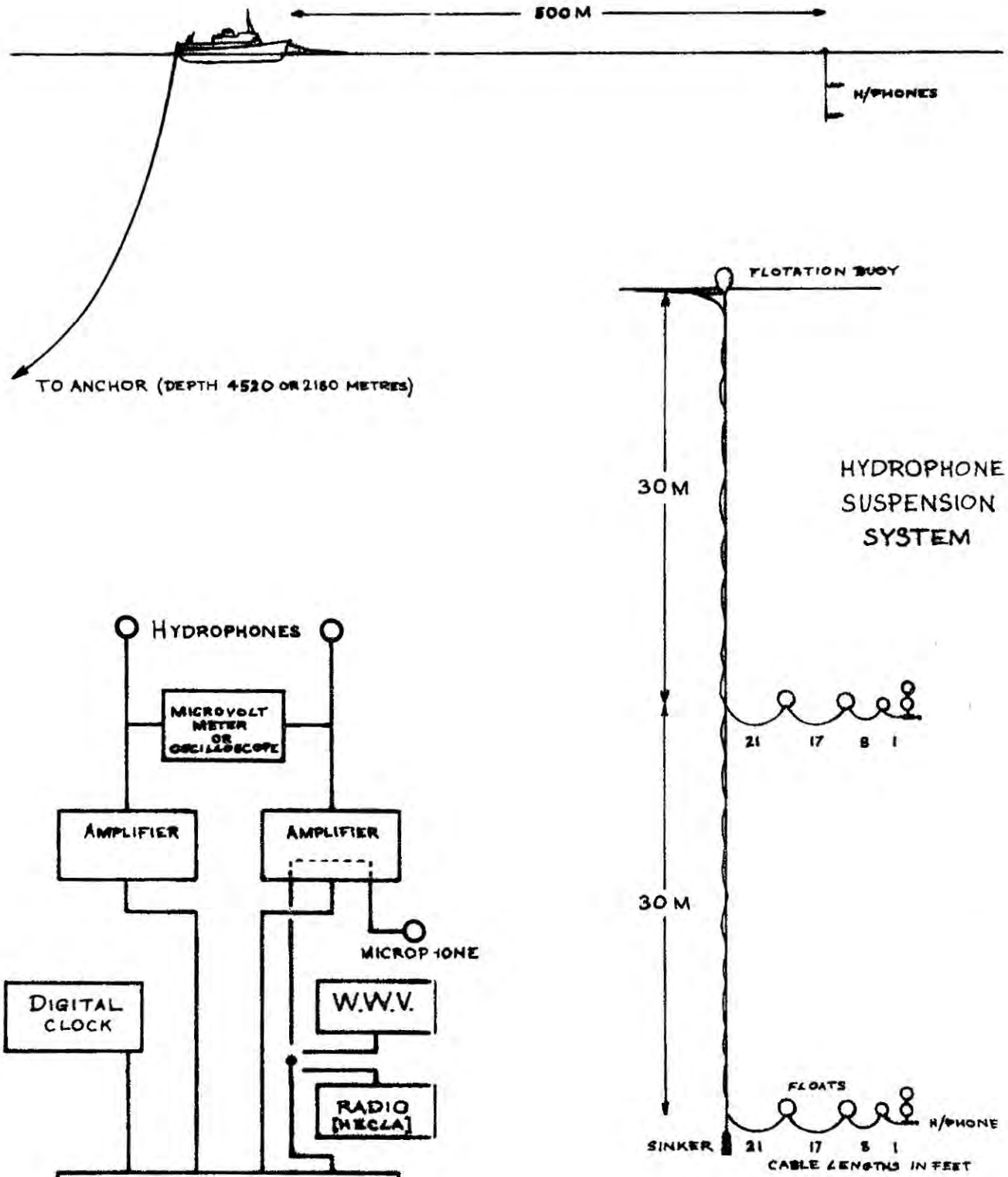

HYDROPHONE SUSPENSION SYSTEM

EQUIPMENT LAYOUT

By successively decreasing the lengths of the cable loops the amount of movement passed along is decreased, provided that the amplitude of movement does not take the cable out of a catenary situation.

The buoyancy of the neutral sections was adjusted in the water before leaving harbour. Sufficient weights were added to each float to make the whole system very slightly negatively buoyant, with the floats level with each other. In this condition the section will not sink, because as the floats descend more of the weight of the first cable loop is put on the standing rope until equilibrium is achieved.

Connecting the hydrophone suspension system to the ship was a buoyant armoured cable 200 m long, joined to 300 m of armoured towing cable (loaned by NOAA, Miami) floated by small expanded polystyrene floats fastened every 1.3 m along it.

Operation

The seismic experiment was run at night so that cultural noise at the land stations would be at a minimum. Radio broadcasts from the shooting ship, HMS HECLA, were received throughout the experiment, and from them operation of the hydrophone system was synchronised with shooting.

At both the positions occupied by DISCOVERER, she anchored by the stern, in 4520 and 2180 metres of water, using a Danforth anchor connected by a short length of chain to the deep sea core cable. The hydrophones were payed out from the bow of the ship. Attached to the last part of the hydrophone cable was 100 m of polypropylene buoyant

rope for putting slack in the system when required. This rope was hauled in after the arrivals from a shot had been received and if the noise on the hydrophones, due to drag through the water, was high when the next shot was due, the rope was released a few seconds before the shot was expected to detonate. The free movement obtained by allowing the hydrophones to move with the water, reduced the noise considerably. Occasionally the drift of the system and the ship was such that slacking was not required. While the ship was at anchor, only the ship's service generator was running and consequently general noise from the ship was low.

At each receiving position several good fixes were obtained from the satellite navigator, and so the position of the hydrophones was well determined with an accuracy of better than 0.4 km, allowing for some drift from their expected position relative to the ship.

Results

West of hydrophone position h1, arrivals were detected from shots up to no. 37, which was the most westerly shot fired while DISCOVERER was at h1. Detonation times for the shots were provided by J. Sunderland. The travel time graph plotted from these arrivals is shown in fig. 3.3. The positions of the shots were determined by the shooting ship, using taut wire measuring gear in conjunction with satellite navigation, and radar near land. Preliminary analysis found that the ranges calculated from the given positions (using program Distaz, C3.3) did not correspond to the ranges indicated by the times of arrival of the water wave. The shot positions were

3.3 Travel time graph for the hydrophone position h1. Numbers against the arrivals indicate the shot identification numbers.

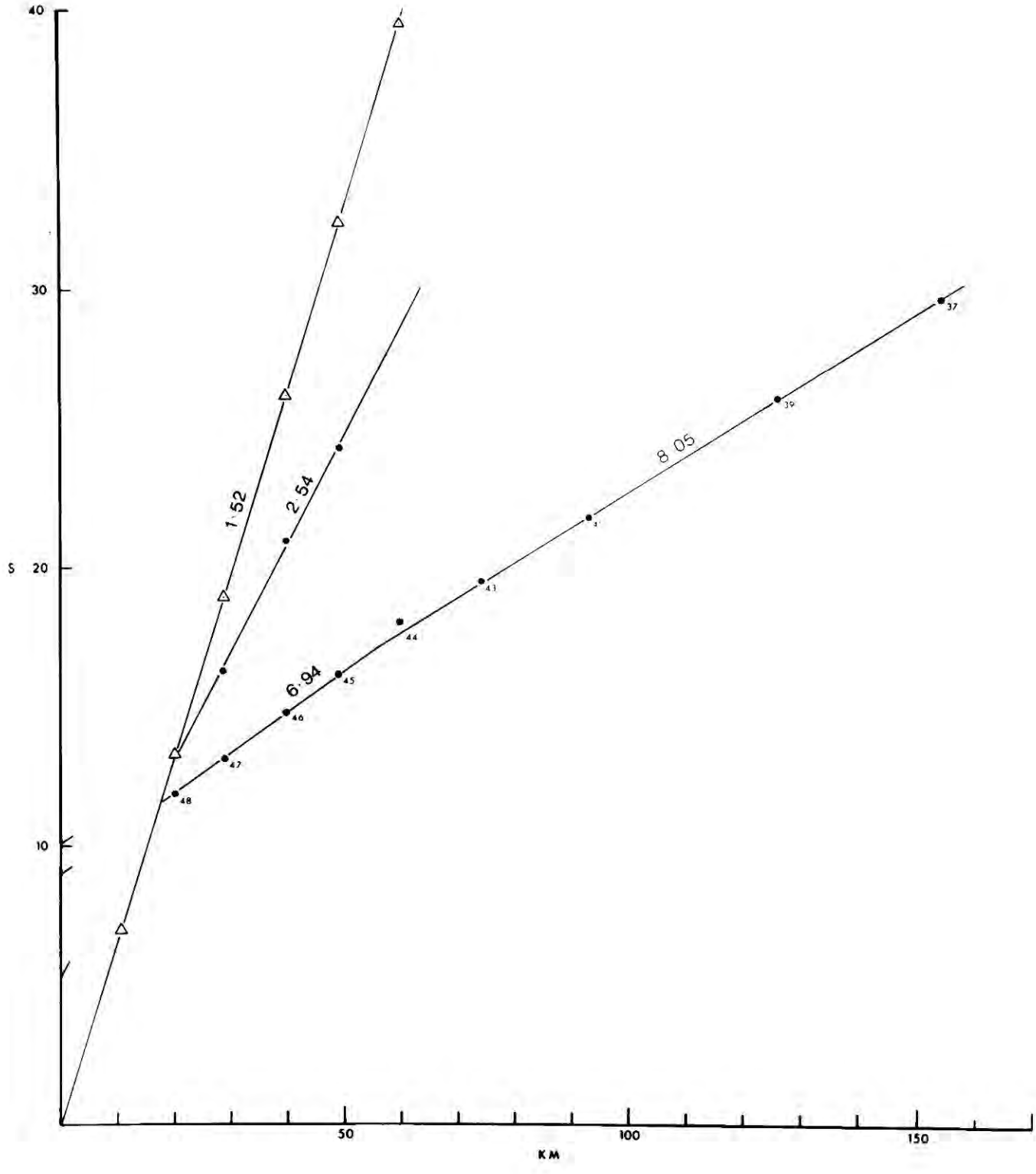

Hydrophone 1

adjusted along the ship's track to give the ranges indicated by the water wave arrival times. Beyond the point where the amplitude of the direct water wave was too small to be easily distinguished, the shot positions were adjusted by comparing the bathymetry recorded by the shooting ship with that measured in the survey the previous year, when the positions were given by Lambda. The direct water wave is a short high frequency arrival which precedes the long train of large amplitude waves, which are a combination of channel waves, refractions through the water and reflection from the bottom (Tucker and Gazey, 1966). Fig. 3.4 is an example of the records obtained showing the principal arrivals. Following the direct water wave is another similar arrival which may be a bubble pulse.

Velocities were determined from the arrival times and corrected for effects due to bathymetry by the program described in appendix C3.6. The value used for the sediment in the bathymetry correction was 2.44 km s^{-1}. Before correction, the apparent velocities observed at h1 were 8.05, 6.94 and 2.54 km s^{-1}. After correction the following velocities were obtained.

7.79 $\pm$ 0.19 km s^{-1} intercept 10.19 $\pm$ 0.37s s.e. of fit 0.20 s

6.61 $\pm$ 0.06 km s^{-1} intercept 9.04 $\pm$ 0.05 s " " " 0.03 s

2.45 $\pm$ 0.09 km s^{-1} intercept 5.02 $\pm$ 0.060 s " " " 0.22 s

At the two receiving stations on Barbados, operated by personnel from the Department of Geology at Leicester University, St. Phillip's and Cole's Cave, no velocities greater than 3.9 km s^{-1} were determined and correlatable arrivals were not observed east of shot 37. Consequently a reversed profile was not obtained east of Barbados.

3.4 Example of a record from the hydrophone station. Arrivals from shot 46. 1st arrival from oceanic Layer 3, (L3), followed by emergent Moho arrival (M). 2nd clear arrival from 2.45 km s^{-1} sediment layer (sed). Short direct water wave arrival (d.w.) is followed by a long train of water transmitted refractions and reflections.

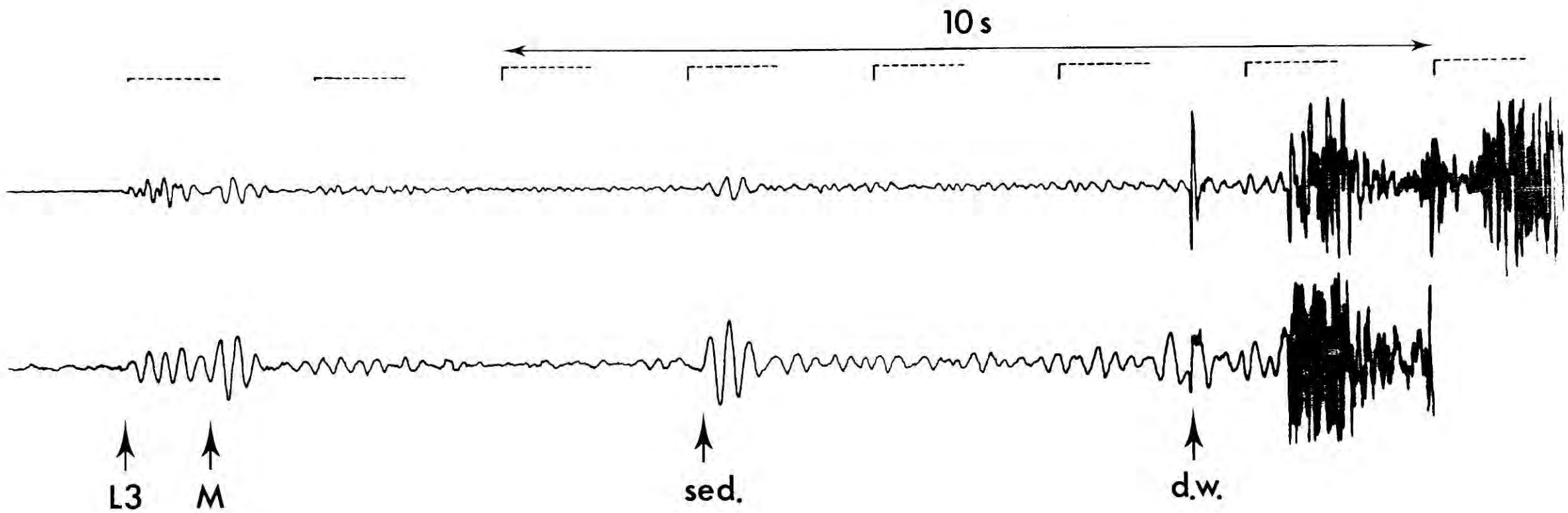

Record of shot 46 at hydrophone station 1

There are several reasons why the results from Barbados were poor. Many of the shots were not recorded, because of various accidents. Sea noise from the coast was quite high, and at the station where most shots were recorded, the signal was passed through a low cut filter with a cutoff frequency at 3Hz. This is in the range of the expected signal frequency and the destructive effect of the filter on the arrivals can be seen clearly as the range from the station increases. Lastly, the great thickness of sediment below Barbados and the very complicated nature of the structure may absorb and diffract the arrivals from the basement sufficiently to reduce their amplitude below that of the noise.

Other, shorter, reversed seismic refraction measurements have been made nearby by Ewing and others (1959) (fig 3.1). These obtained lower crustal layer velocities of 6.64 to 6.77 km s^{-1} and sub-Moho velocities of 8.09 to 8.32 km s^{-1}, and established that the crust dips gently to the west. Additional thicknesses of 2.44 km s^{-1} or 4.0 km s^{-1} layers were fed into the program (C3.4) to find what dip of the crust along the line of shots would give the velocities observed by Ewing and others (1959). The results obtained are shown below.

dip	0^o	1^o	2^o	2.25^o	overlying layer
Apparent velocity	7.79	8.02		8.33	4.0 km s^{-1}
"	6.61	6.77	6.94		4.0
"	6.61	6.92	7.26		2.44

From other seismic refraction data it seems certain that the dip of the crust in the region of shots giving Moho arrivals is due mainly to variation in thickness of a 4.0 km s^{-1} layer. Further east it is

3.5 Travel time graph for the hydrophone position h2. Small figures indicate the shot numbers.

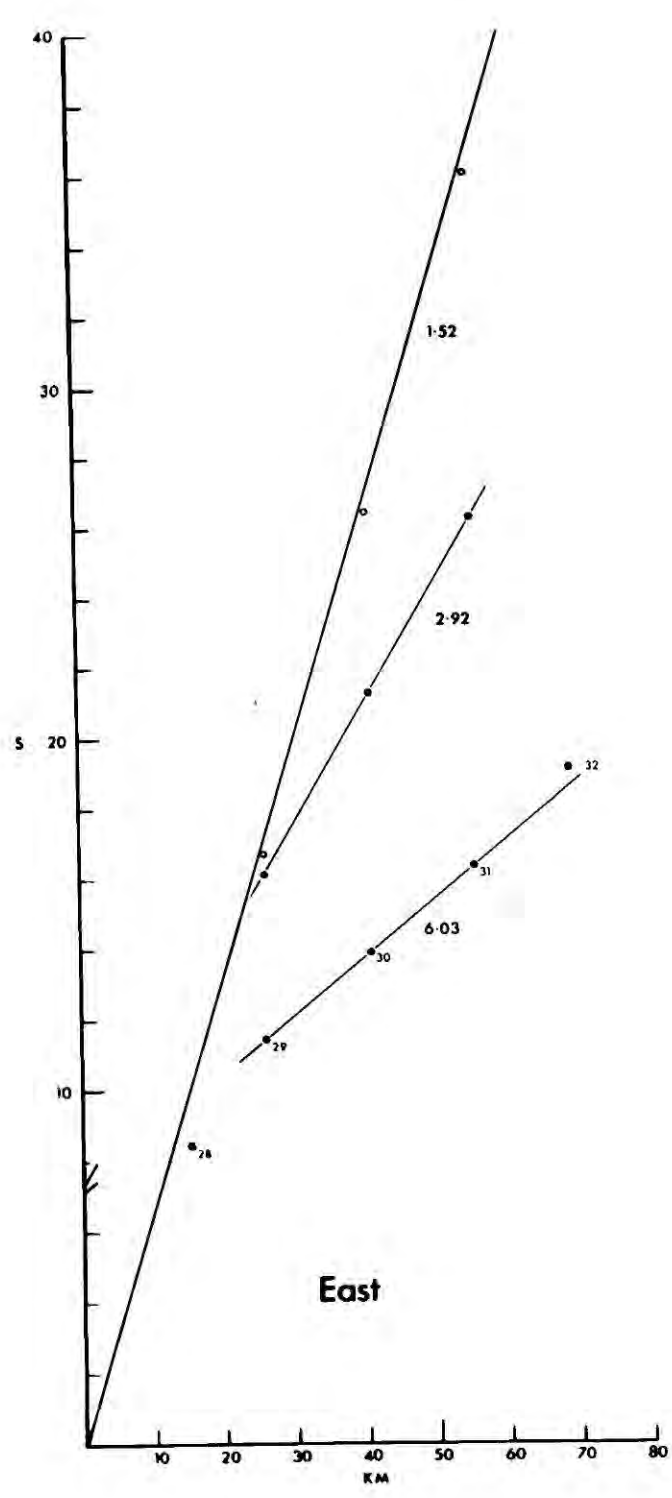

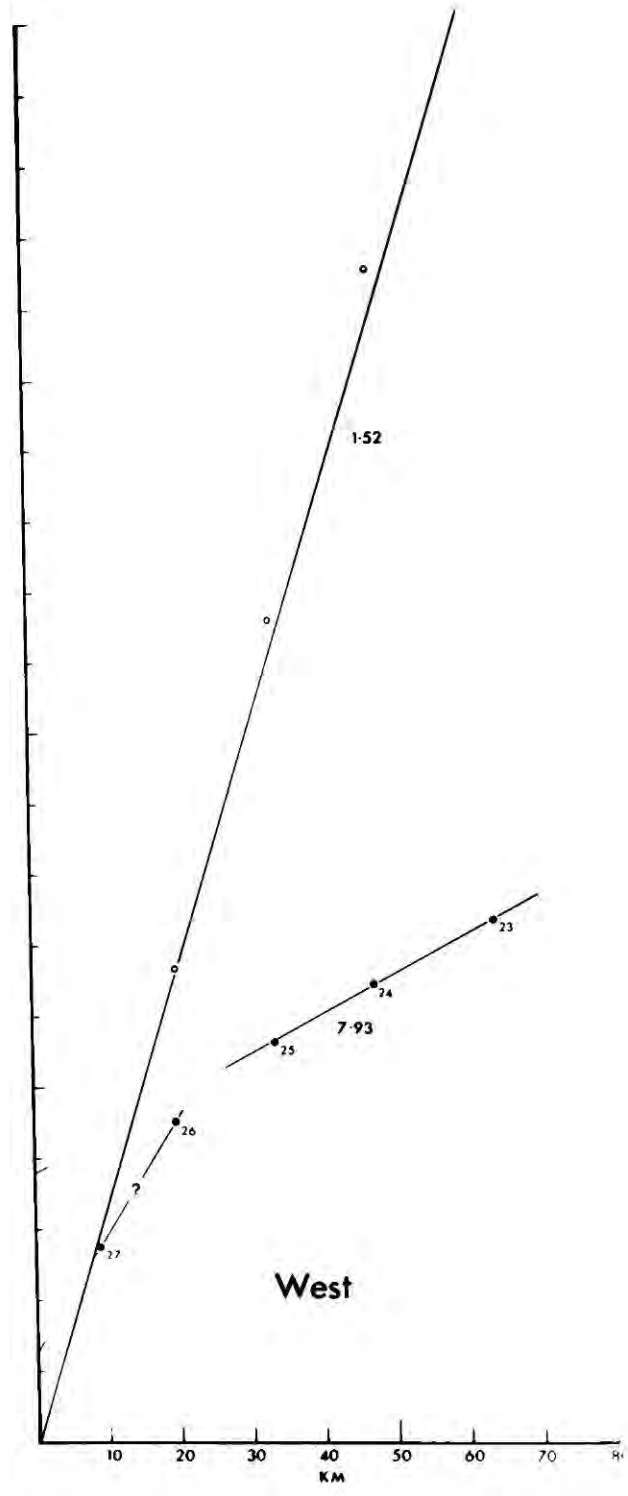

Hydrophone 2

uncertain which layer gives the dip. It is possible that the 4.0 layer is not present. Neither this experiment or the refraction work of Ewing and others (1959) detected a layer with a velocity of about 5.0 km s^{-1} (Layer 2). This may be because the layer is thin in comparison to the overlying sediments and hence gives no first arrivals between those from the sediments and those from Layer 3. The velocity layering obtained below h1 is given below.

	velocity	thickness	depth
water	1.5	4.463	= depth below lowest h/phone
sediment (assumed)	1.7	0.376	4.463
refractor 1	2.45	3.681	4.838
refractor 2	6.73	6.571	8.519
refractor 3	8.02		15.090

On the second night of the experiment, DISCOVERER occupied a position midway across the Tobago Trough (h2). The travel time graphs obtained are shown in fig. 3.5. Arrivals from the Tobago Trough were also received at the Barbados stations, but the maximum range was not very great. Travel time graphs are shown in fig. 3.5.

The shot positions given by the shooting ship do not produce ranges corresponding to those obtained from the water wave, and differ by up to 2.5 km. Generally, east of h2 water wave ranges are less than predicted, west of h2 they are greater. It might appear from this that the hydrophone position is incorrect and should be further east. The position is, however, determined from five satellite fixes and the water wave ranges seem to be correct for the closest shots. The ship did not vary in position by more than 0.2 km in an east-west direction

3.6 Travel time graphs from the seismic receiving stations at St. Phillip's and Cole's Cave, Barbados. Small figures indicate the shot numbers.

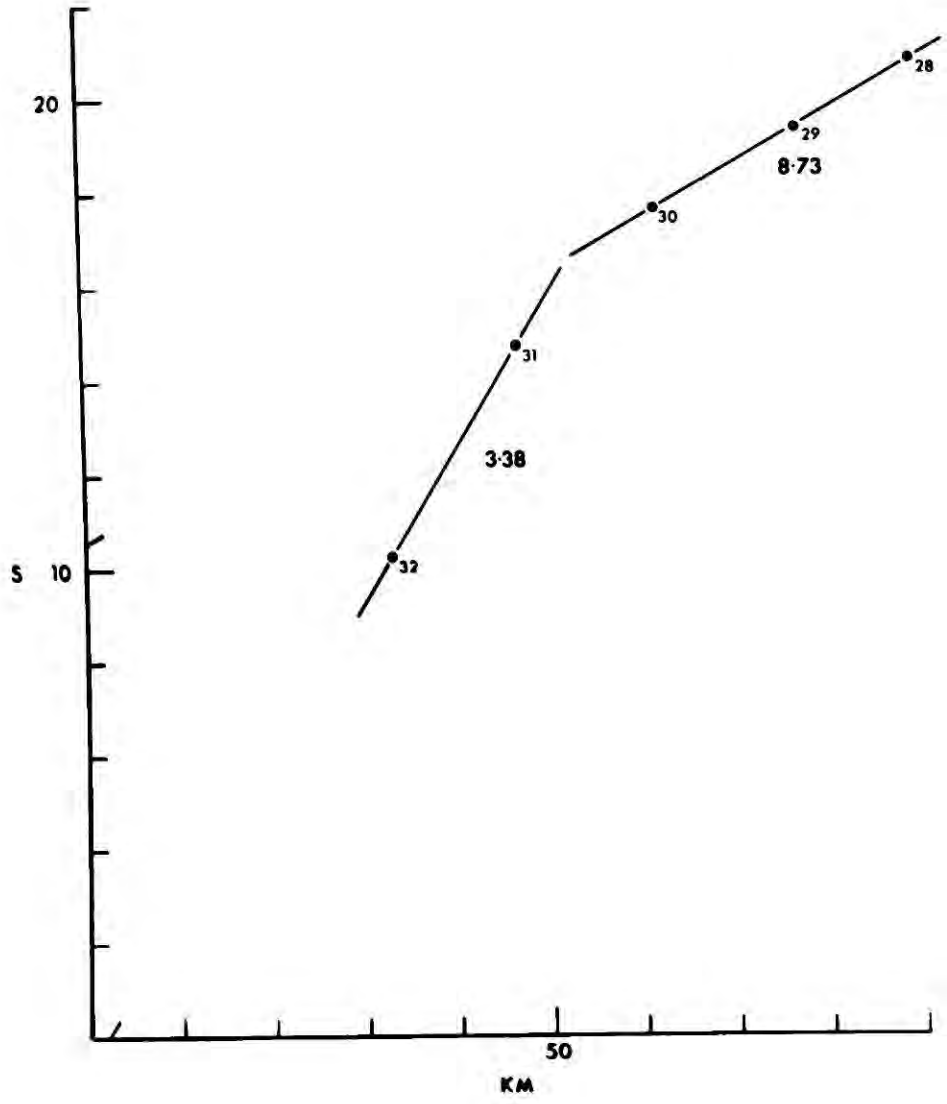

St. Phillip's

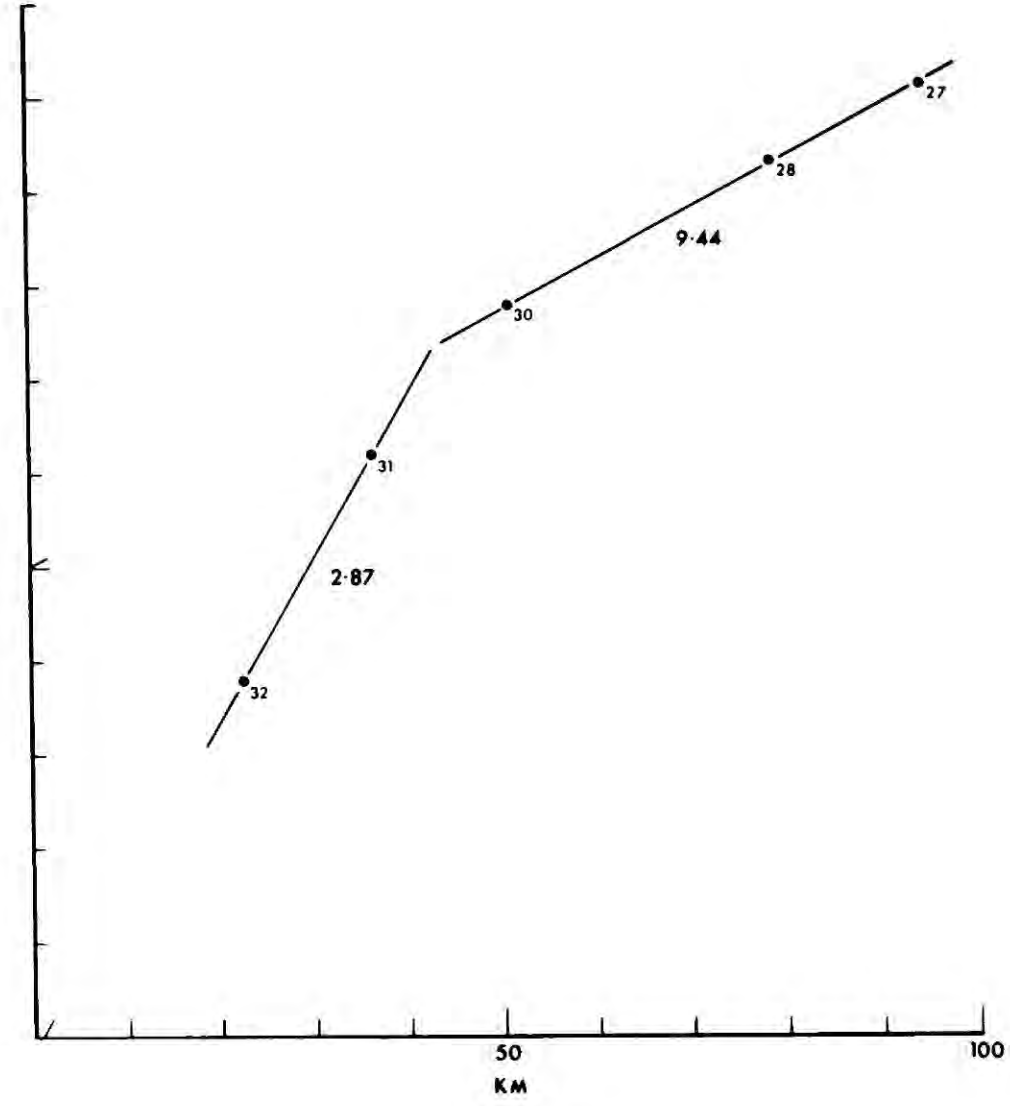

Cole's Cave

during the night and the error in the hydrophone position with respect to the ship is unlikely to be more than 0.4 km. An eastward shift of the hydrophone position would improve matters, but a systematic error in the shot positions still remains.

Velocities were calculated using both the ranges from the water wave arrival times and those determined from the given shot positions. A comparison is given below.

	shot position range		water wave range	
	velocity	intercept	velocity	intercept
east of h2	5.76 ± 0.08	6.81 ± 0.10	5.73 ± 0.05	6.90 ± 0.06
west of h2	7.22 ± 0.13	6.70 ± 0.12	7.87 ± 0.07	6.89 ± 0.06

The velocities were calculated and corrected for sea bed topography as for h1. The refraction data of Ewing and others (1959) and this analysis indicates that 3.0 km s^{-1} is the best overall velocity for the topographic correction.

The shot positions were not adjusted from those given by the shooting ship for the velocities calculated from the arrivals at the land stations, and the velocities used from h2 in reversing the profiles were also those from the given shot positions. The corrected velocities calculated from the arrivals at the St. Phillip's and Cole's Cave stations are given below.

St. Phillip's:

Velocity 8.98 ± 0.3 intercept 10.05 ± 0.29 se of fit 0.66

Cole's Cave:

Velocity 9.54 ± 0.05 intercept 9.41 ± 0.04 se of fit 0.16

The apparent velocities measured at h2 were combined with those from Barbados and those from St. Vincent and St. Lucia (C. Boynton, personal communication) to give reversed lines and the true velocity and dip of the basement. The dip and, to a small extent the velocity are dependent on the average velocity of the overlying layer, the variation in thickness of which gives the dip of the refractor. Given below is a summary of reversed line calculations using three likely velocities for the overlying layer.

h2	to	St. Vincent and St. Lucia			
Apparent velocity	7.22	5.59		5.64	
Intercept	6.7	1.86		1.77	
velocity in overlying layer		velocity	dip	velocity	dip
3.0		6.27	3.95°	6.31	3.8°
3.5		6.26	4.90°	6.305	4.70°
4.0		6.25	6.02°	6.30	5.77°

h2	to	St. Phillip's and Cole's Cave			
Apparent velocity	5.76	8.98		9.54	
Intercept time	6.81	10.05		9.41	
velocity in overlying layer		velocity	dip	velocity	dip
3.0		6.98	5.93°	7.14	6.34°
3.5		6.96	7.76°	7.12	8.13°
4.0		6.94	8.78°	7.10	9.42°

Cole's Cave is closer in line with the shots that St. Phillip's and the velocity and dip derived from its data are the most accurate.

The velocity west of h2 must be regarded as a minimum value. Firstly because the water wave ranges give a higher velocity than that used, and secondly, because the St. Vincent and St. Lucia stations are some way off the line of the shots. The velocity layering below h2 is given below. Estimates of the thicknesses of the 1.7 and the 2.5 or 3.0 km s^{-1} layers were obtained from the seismic reflection profiles and line 7 of the refraction work of Ewing and others (1959).

Seismic structure at h2

velocity	thickness	
1.5	2.12	water
1.7	0.95	
2.5 or 3.0	1.75 or 2.1	
4.0	4.151 or 4.267	

depth to basement (6.3 to 7.1 km s^{-1}) = 8.971 or 9.437

Several of the early arrivals yielded velocities likely to be from sediments. East of St. Phillip's three arrivals give a well determined velocity of 3.57 km s^{-1}. West of Barbados shots 32 and 31 give velocities of 3.38 km s^{-1} and 3.19 km s^{-1} at St. Phillip's and Cole's Cave respectively. A velocity of 2.82 km s^{-1} was given by second arrivals east of h2 and the intercept time was greater than that for the first arrivals from the basement (7.0 layer). This precludes the arrivals from being headwaves. It was thought that they might be reflections from the basement, but trial calculations indicated that the arrival times were still too great for even this. The velocities discussed above are those obtained after correction for bathymetry.

Chapter 4

Crustal structure

The Sedimentary Layer

Most of the information regarding the sedimentary structure of the area has been obtained from seismic reflection profiles (fig. 4.1). As well as the profiles collected by HMS HECLA in 1971 (H1 to H4), additional coverage was obtained from the 1970 and 1972 cruises of the NOAA ship DISCOVERER. Photographs of the 1970 records were obtained from B. Bassinger, and line drawings from the digtised records (D4 to D7) are shown in figs. 4.2 and 4.3, together with digitised line drawings of tracings taken from the original records in DISCOVERER in 1972 (D1 to D3). Other sources are profiles made by Bunce and others (1969) (B1 to B4), a profile made by Collette and others (1969) in HMS VIDAL (C), and a profile made by USNS KANE (1968) (K).

The horizontal scales on the diagram showing profiles and crustal models are given as kilometres west of Longitude 62^{o} W for west-east profiles, and north of latitude 12^{o}N for south-north profiles.

The velocities of sound in the sediments have been determined mainly by seismic refraction experiments (Ewing and others, 1957), with some information from wide angle reflection. Gravity and magnetic anomalies in some places indicate structures within the sediments as well as the nature of the sediment/basement interface.

For the purpose of description and analysis the area is divided into four provinces, which are the Tobago Trough, the Barbados Ridge, the Barbados Slope east of the ridge, and the Atlantic Ocean floor.

4.1 Seismic reflection lines in the general area of Barbados. H - HMS HECLA (W - wide angle reflection run). D - DISCOVERER (Pecked lines show lines run in 1971, but not displayed). K - KANE 9. B - CHAIN (Bunce and others, 1971. V - HMS VIDAL (Collette and others, 1969). o h position of dredge samples taken by Hurley (1966). o r position of Miocene core sample taken by Ramsay (1968). The bathymetry is in fathoms and is taken from Hess (1969).

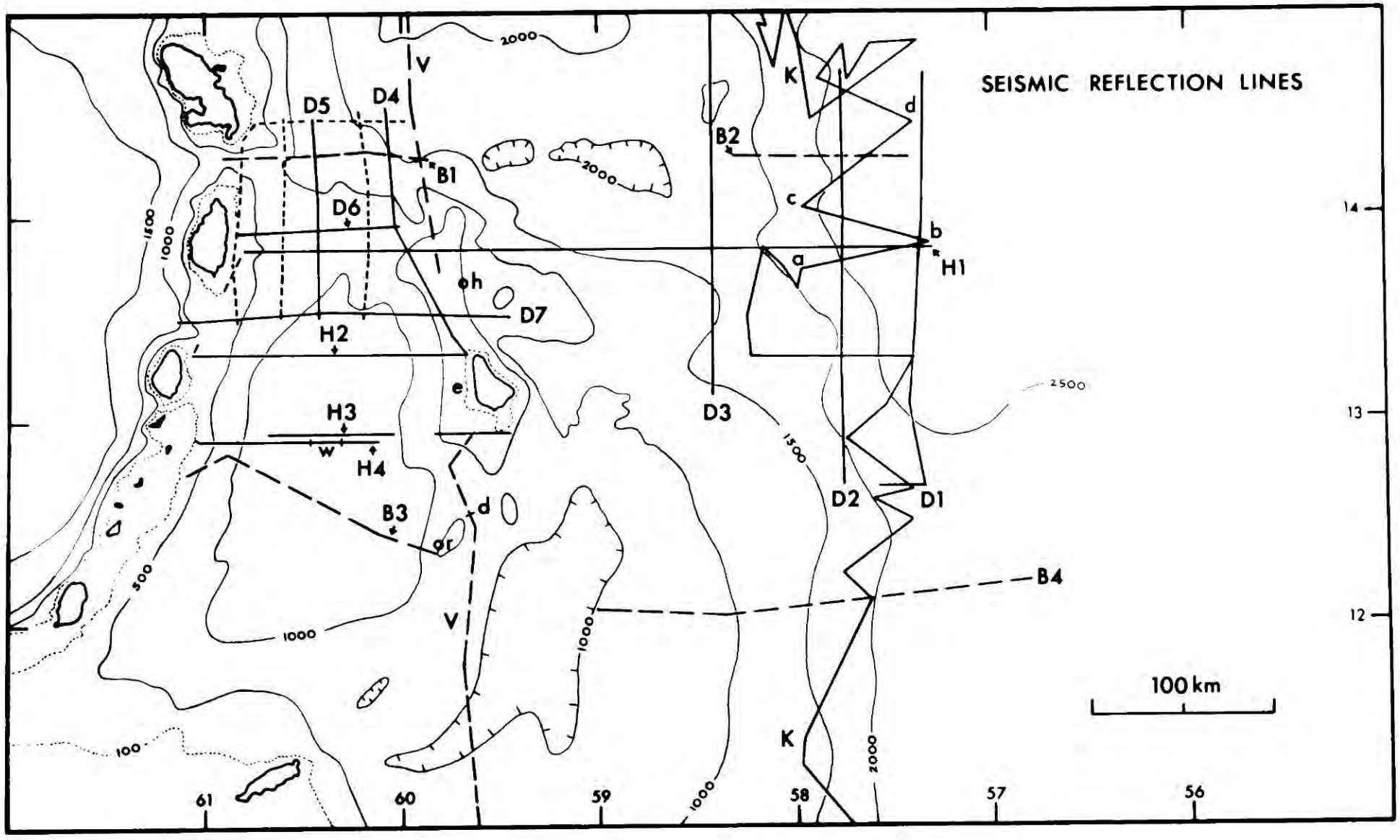
SEISMIC REFLECTION LINES
2000
V
D5
D4
B1
D6
1500
1000
h
D7
H2
e
H3
W
H4
B3
d
r
500
1000
100
V
1000
K
d
B2
c
b
a
H1
2500
1500
D3
D2
D1
B4
K
2000
100 km
14
13
12
61
60
59
58
57
56

The Tobago Trough

This smooth bottomed basin occupies a position between the Lesser Antilles and the Barbados Ridge. It terminates against the South American continental shelf in the south, and a gentle east-west rise east of St. Lucia is taken as its northern margin. Profiles across the trough (figs. 4.2 & 4.4) show a smooth sea bed in the centre underlain by regularly bedded reflecting horizons which become more disturbed at the margins of the trough, where they bow upwards.

The maximum penetration obtained through the sediments is 3 seconds reflection time, and this was obtained on lines H3 and H4 by HMS HECLA (fig. 4.2). The central portions of these lines give the best section of the sediments. Combining the refraction results of Ewing and others (1957) with the wide angle reflection and the reflection profiles the following generalised description of the sedimentary sequence in the centre of the trough is obtained.

	velocity	thickness
Layer A	1.55	0.4
Layer B	1.9	0.5
Layer C	2.2-2.6	0.8
Layer D	2.9-3.4	2.0-3.0
Layer E	3.8-4.3	2.0-5.0
	km s^{-1}	km

The depths to layers obtained by seismic refraction correspond well with the reflectors seen on the reflection records. In the seismic refraction work of Ewing and others (1957) Layers A and B were given an assumed velocity of 1.7 km s^{-1} to satisfy the discrepancy between the depth to the seabed and the depth to the top refractor.

4.2 Reflection profiles across the Tobago Trough. The vertical exaggeration of the bathymetry is 10:1. The layered sequence marked by colour is fully represented from A to E on line H4. The reflectors in red on the west side of H2 are probably of volcanoclastic origin. The horizontal scale is given in kilometres west of longitude 62°W.

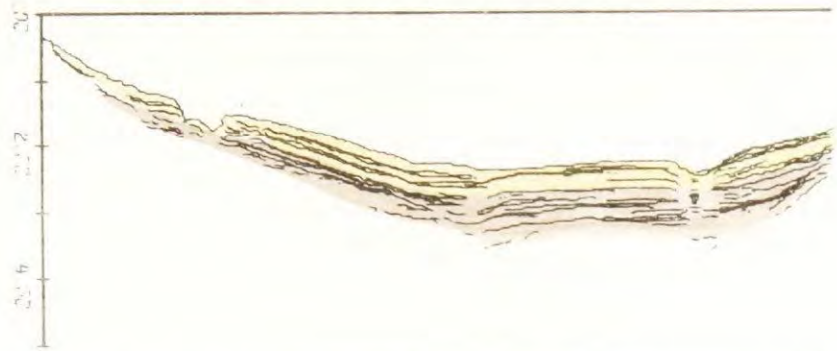

D6 13° 57′N

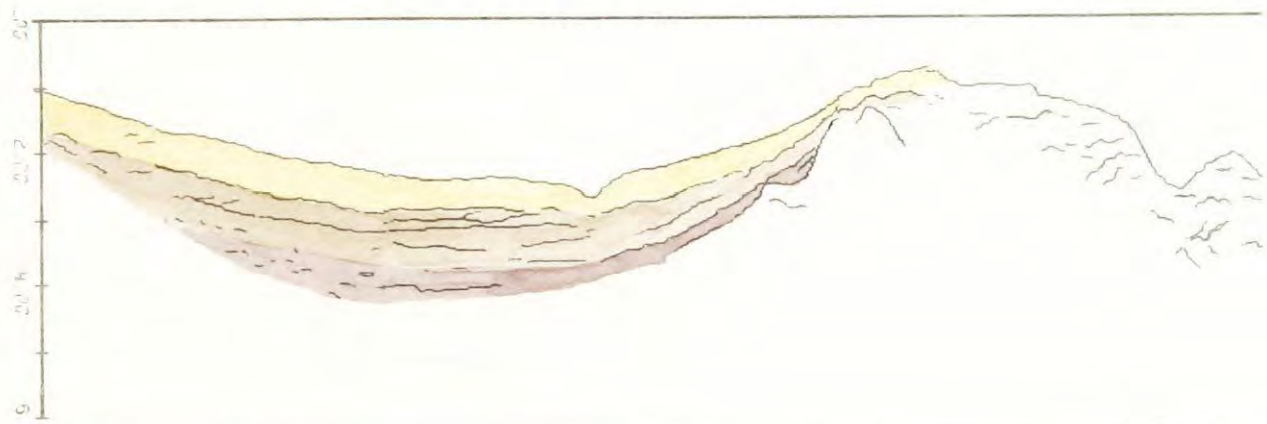

H1 13° 49′N

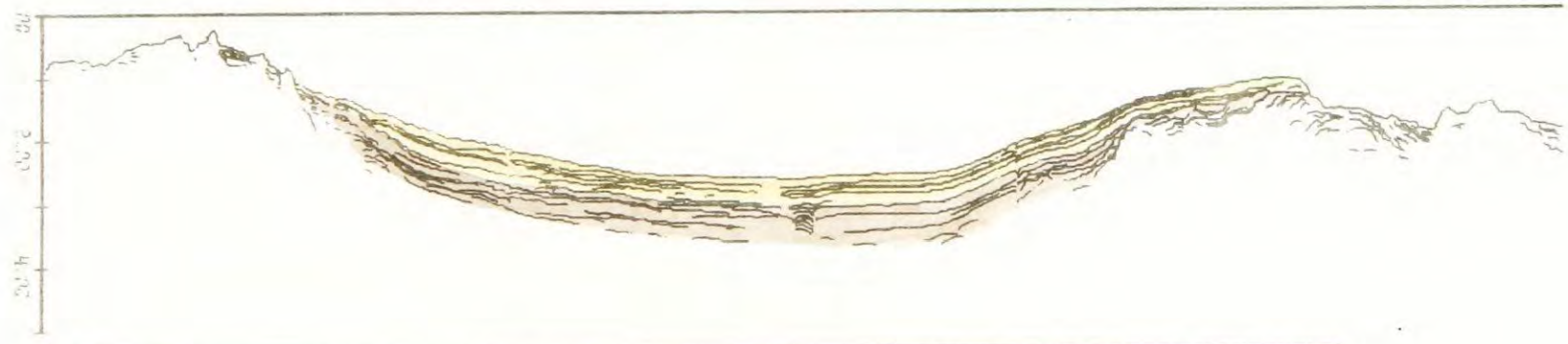

D7 13° 31′N

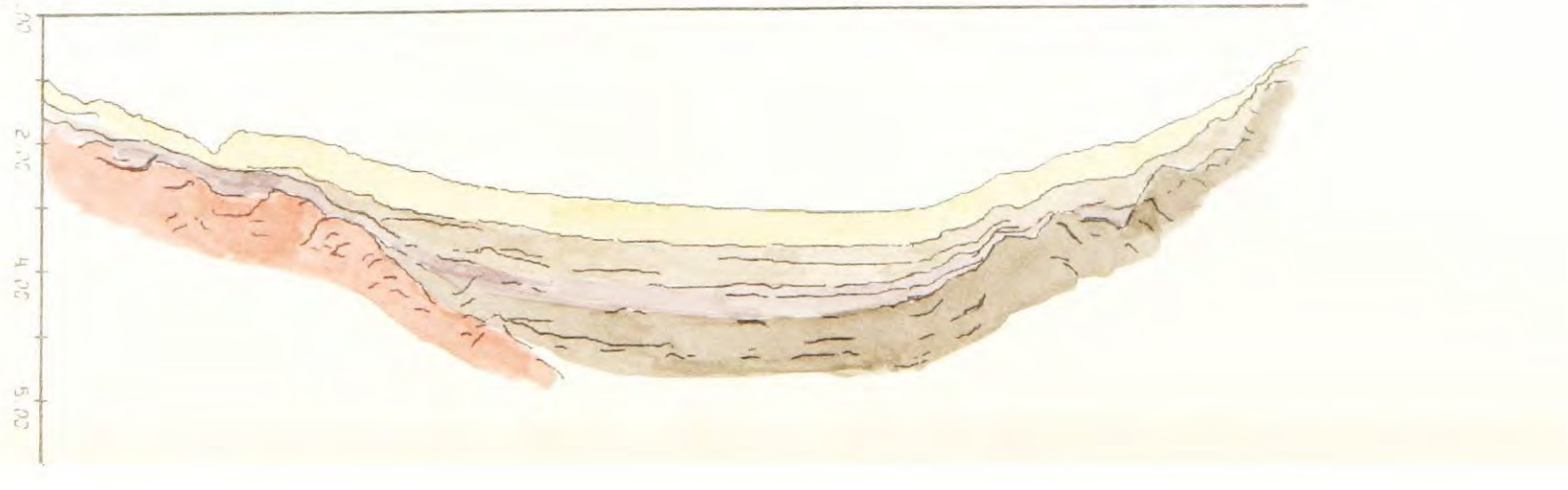

H2 13° 18′N

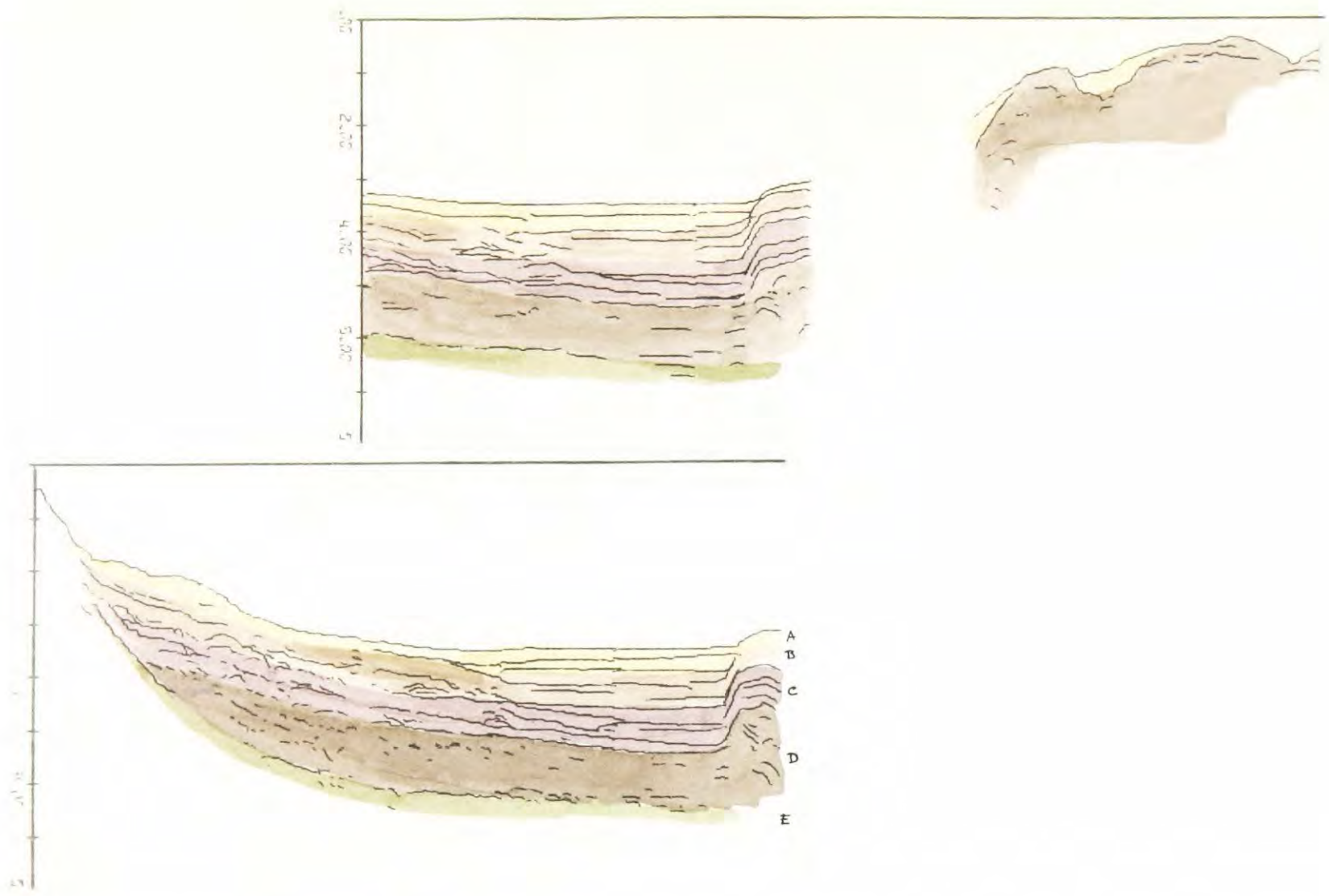
H3 12°56·6′N
H4 12°54′N
A
B
C
D
E
100
150
200
250
300
km
61°W
60·5°W
60°W
59·5°W

The top two layers have prominent regular bedding which is shown clearly on profile D6 and D7 (fig. 4.2). The air gun system on DISCOVERER gave a better definition than that on HECLA, but had smaller penetration. From the DISCOVERER records it can be seen that the reflectors in Layer A have greater continuity than those in Layer B. The reflectors of B, however, have greater reflectivity, so that the two layers are similar but easily distinguishable. This distinction is more marked closer to the volcanic arc than further east near the Barbados Ridge.

In the north of the trough layers A and B conform in shape to the bathymetry, thinning towards the margins of the trough. Further south flat lying reflectors in the centre of the trough unconformably overlie a series of reflectors which dip gently eastward (B3 fig. 4.4). Direct analogy with the northern profiles indicates that Layers A and B are part of the underlying sequence, because this sequence bends upward at the margins of the trough as do A and B further north. The overlying sequence of flat reflectors extends as far north as line H3, but the thickness there is much less than on B3 and the deposit is less extensive. This layer is, however, included in the wide angle reflection determination and consequently Layer A may have a higher velocity than given above or be thinner. This emphasises the difficulty of identifying layers by their velocity alone. A layer which is isochronous and is partly overlain by later sediments may have a higher velocity where it is overlain than where it is still at the surface. The flat lying sediments in the central part of the trough which are unconformable with Layer A are hence forward referred to as Layer A*. This most recent layer is prominent on a reflection profile made in the southeast of the trough by Bassinger and others (1971).

4.3 Reflection profiles running in a northerly direction across the area, from the Atlantic Ocean (D1) to the East St. Lucia Ridge (D5). Vertical exaggeration of bathymetry is 10:1. The horizontal scale is given in kilometres north of latitude 12°N.

12·5° 13°N 13·5° 14°N 14·5° 15°N 15·5°

South-North Reflection Lines

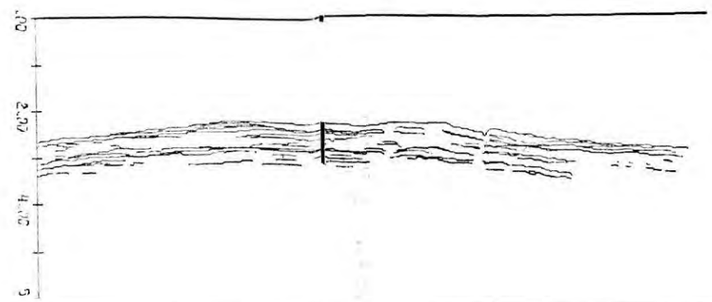

D5
60° 27′W

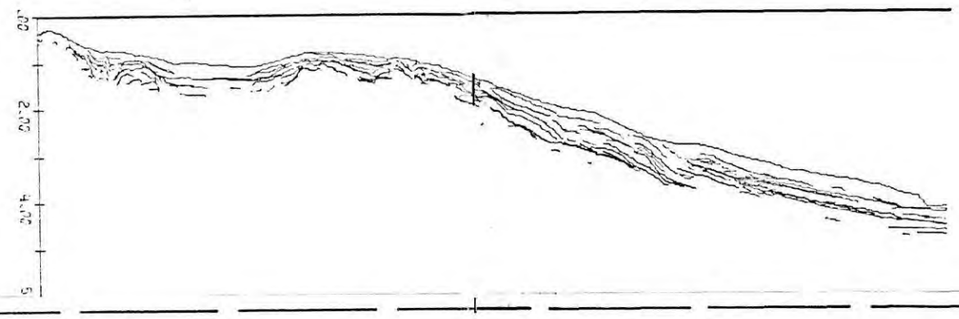

D4
60° W

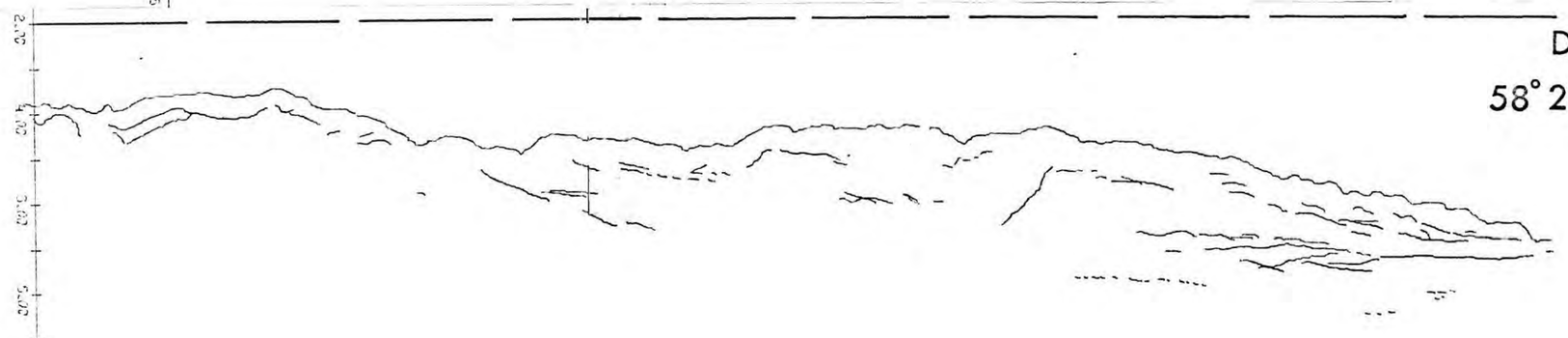

D3
58° 23′W

D2
57° 44′W

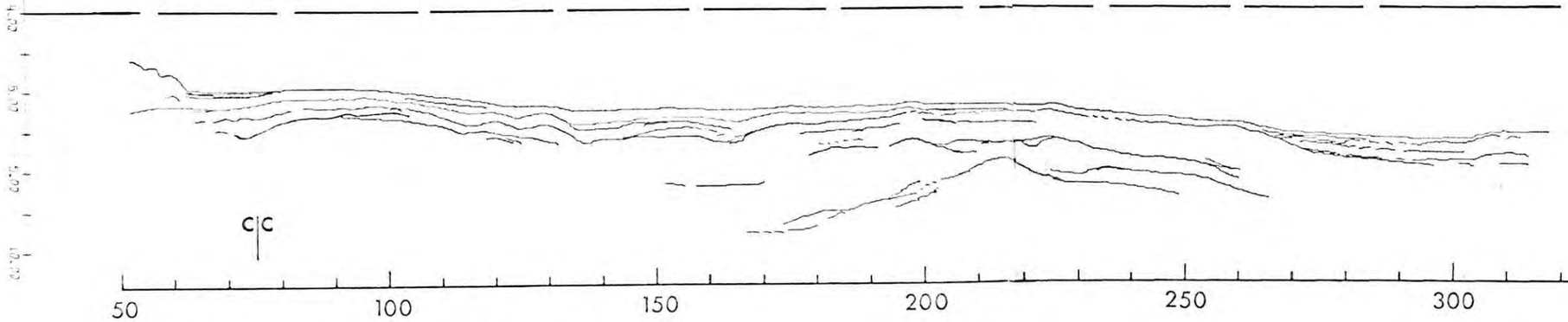

D1
57° 22′W

C C

50 100 150 200 250 300 350 400

Layer C (average velocity 2.5 km s^{-1}) is the lowest layer in which many continuous reflectors are observed, and apart from the velocity difference observed in the wide angle reflection run there seems to be no large difference in character between B and C. It is possible that there is a fairly continuous increase in velocity through B and C. The layered structure of Layers A, B and C, particularly A and A*, suggests that they are mainly turbidites and a few cores taken from the suppermost layer in the trough did contain turbidite sediments (Keller and others, 1971).

Layer D does not contain any very continuous horizons, and there appears to be a marked break between it and the overlying sediments. This is seen clearly on the western flank of the Barbados Ridge, where the top of D is a rough surface over which the later sediments are lain. Beneath this surface are discontinuous reflectors, many of which dip to the east.

Layer E lies below the deepest reflector seen on profiles H2, H3, and H4, and from refraction line E7 a velocity of 4.0 km s^{-1} was determined for it. The top of this layer is not seen in the east of the trough but in the west it slopes gently upward to within 0.7 km of the seabed and forms the base of the sedimentary basin in which the later sediments were deposited, overlapping on this surface towards the west.

Sediment cores collected from the trough by Keller and others (1971) indicate that on the western side of it the sand content is high, as much as 75%, and that in its centre clay and silt size materials are predominant. The central sediments are relatively

4.4 Reflection profiles across the Tobago Trough and the Barbados Slope by Bunce and others (1971).

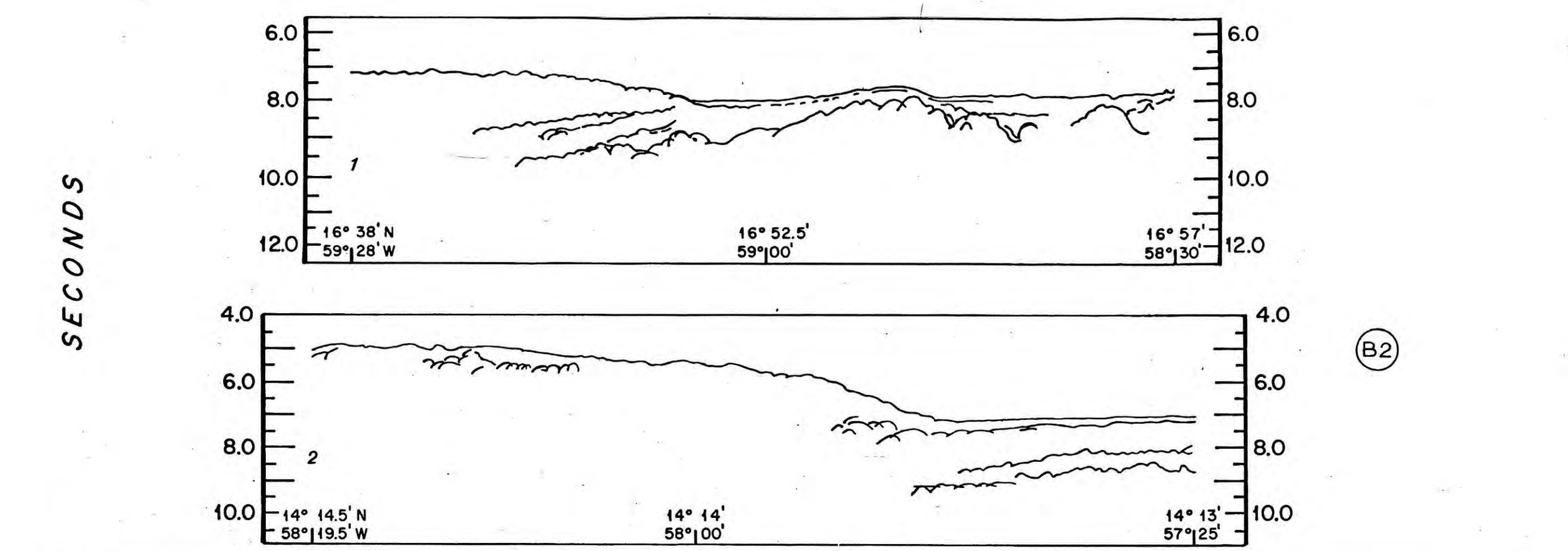

Plate VII. Continuous seismic profiles: (1) southeastern extension of Puerto Rico Trench; (2) Barbados Ridge north of Barbados; (3) Barbados Ridge southeast of Barbados

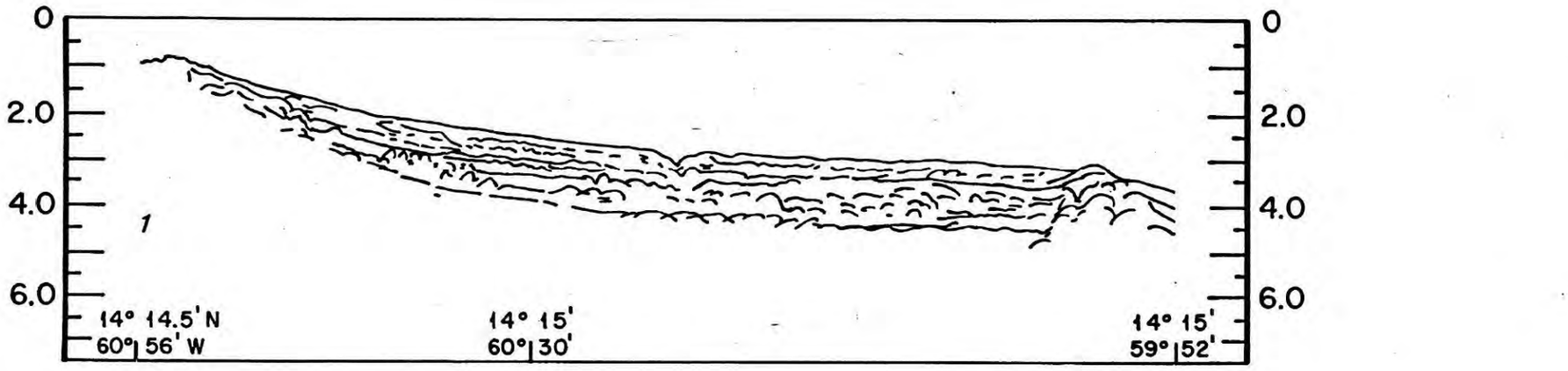

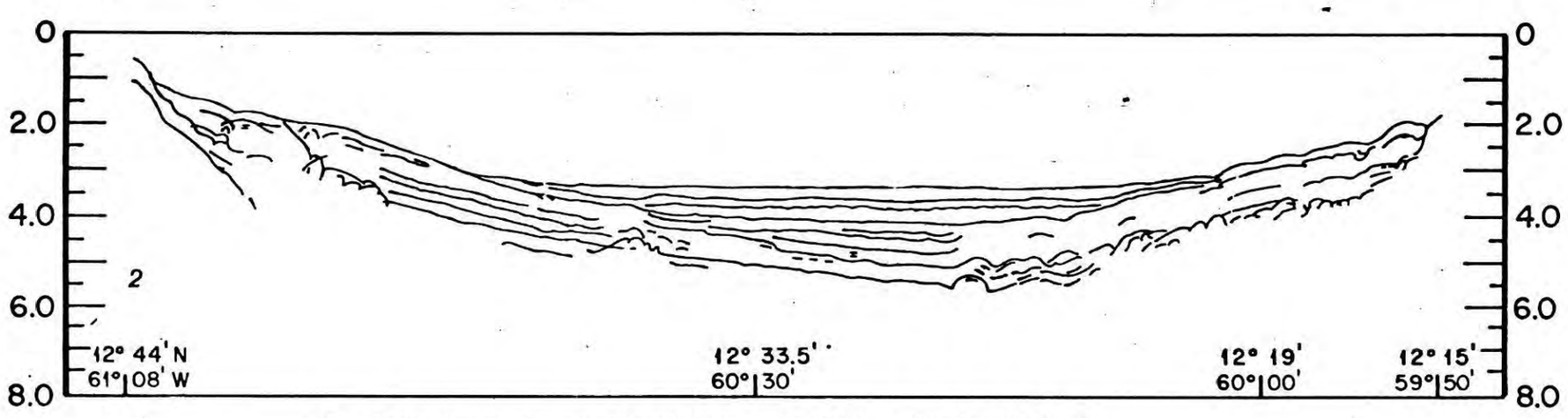

Plate V. Continuous seismic profiles: (1) basin north of Tobago Trough; (2) Tobago Trough.

homogeneous with few graded beds, whereas those from the western margin contain numerous layers of coarse and fine material. Keller's study of the cores revealed that much of the clay and silt size fraction comes from the Amazon and Orinico rivers, and the northern margin of Venezuela and Trinidad. Most of the sand size materials comes from the island arc with a contribution in the south of the trough from Venezuela.

The sediment structure of the western margin of the trough is much less uniform than the centre, showing possible slumps and ash flows. On lines D6 and H2 canyons can be seen to cut into the uppermost layer. That on line D6 leads northeastwards from St. Lucia and shows slump structures within it. The canyon seen on line H2 leads southeastwards.

On western side of line H2 there is a subsurface rise containing disturbed reflectors. Associated with this rise is a small local gravity high and an increase in amplitude of the magnetic anomaly coupled with a decrease in wavelength (fig. 4.5). It is possible that this rise is a pronounced series of pyroclastic deposits and lavas.

Tectonic disturbances of the Tobago Trough.

The basinal shape of the trough is partly due to deposition against the western side of the trough of erosional and volcanic products from the island arc as the arc was built up, but its form is mainly due to earth movements on the eastern side of the trough. The effect of these movements is most noticeable on the western flank of the Barbados Ridge. On profiles H1 and D7 the upper layers of sediment can be seen to extend to the highest part of the ridge, and if they were

4.5 Comparisons of the Bouguer gravity anomalies (2.0 gm cm^{-3}) (b) and the total field magnetic anomalies with the seismic reflection profiles on lines H1, H2 and H3 (from top to bottom). Compare with fig. 4.2.

H1

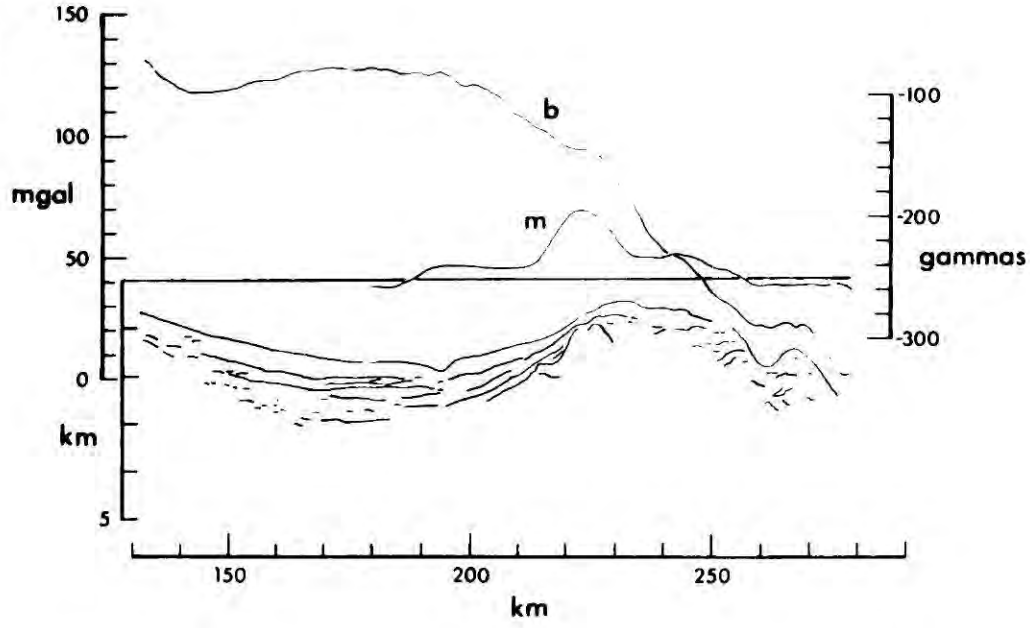

H2

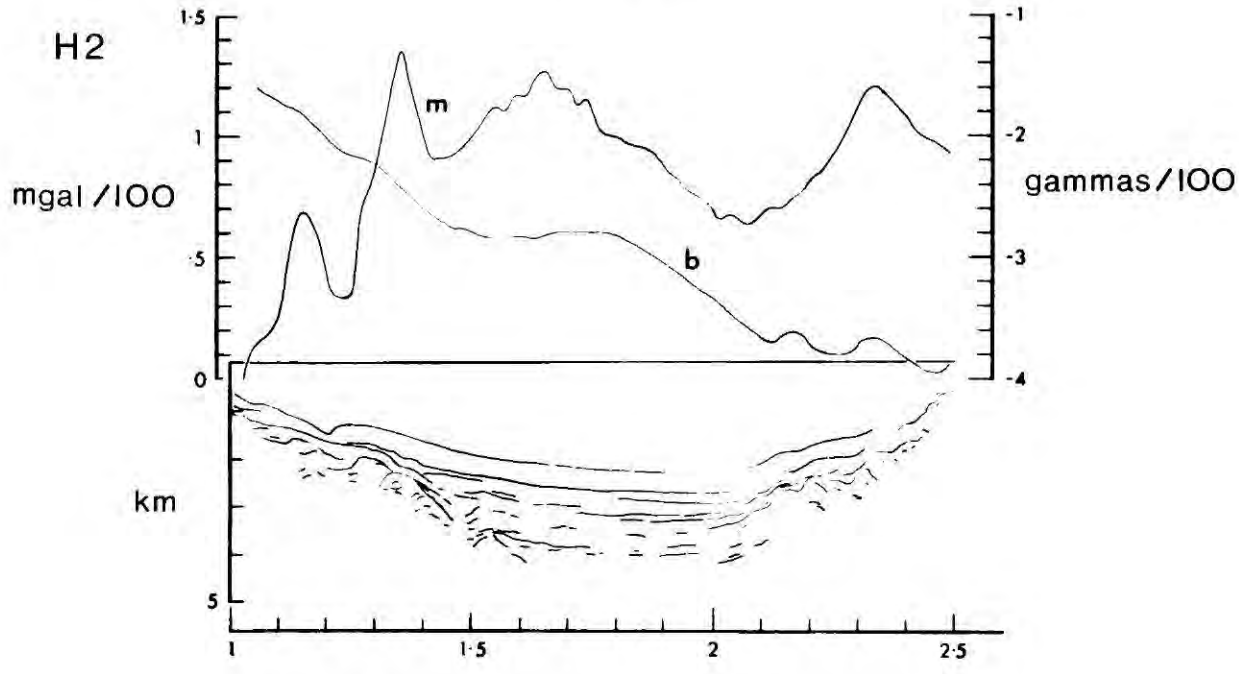

mgal/100

H3

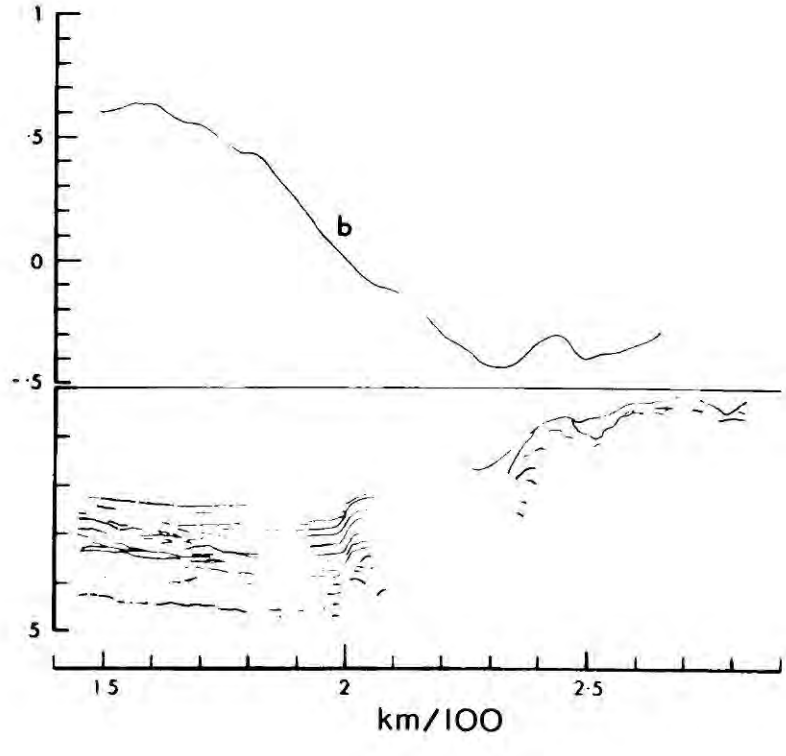

originally deposited at the same level as those in the centre of the trough the Barbados Ridge has been uplifted 1.5 to 2.0 km relatively. The sediment layers on the ridge are gently inclined to the seabed and outcrop on it. Hence the seabed is an erosional surface and so the estimates of uplift must be minimum values. The ridge was probably rising during the deposition of sediments in the trough, because the sediments thin towards the crest of the ridge.

During the uplift of the Barbados Ridge there was differential movement on its western flank causing the warping of upper sedimentary layers (A, B & C). The top of layer D wasthe surface on which the sediments were laid down prior to the uplift of the ridge, and it appears to have had a slightly irregular topography in the region of the ridge which has been accentuated by the deformation associated with the uplift. The effect of the density contrast at this irregular surface is the production of local short wavelength gravity anomalies which can be observed on the profiles shown in fig. 4.5. Layer D had undergone some tectonic disturbance prior to the deposition of layers A, B and C since the erosion surface which is the top of D truncates many of the dipping reflectors within it.

On lines H3 and H4 the edge of the deformed region caused by the uplift of the Barbados Ridge is distinct, with flat lying sediments bent suddenly upward (fig. 4.6). On first examination it seemed possible that there was a fault associated with this feature, and to ascertain the nature of it a two dimensional migration was carried out on the reflection record at this point using a graphical method (Grant and West, 1965). In order to effect this a series of wavefront curves and curves of maximum convexivity were drawn to match the

4.6 Sample of an air gun reflection record from the Tobago Trough on line H3 showing the reflectors disturbed at the foot of the slope from the Barbados Ridge.

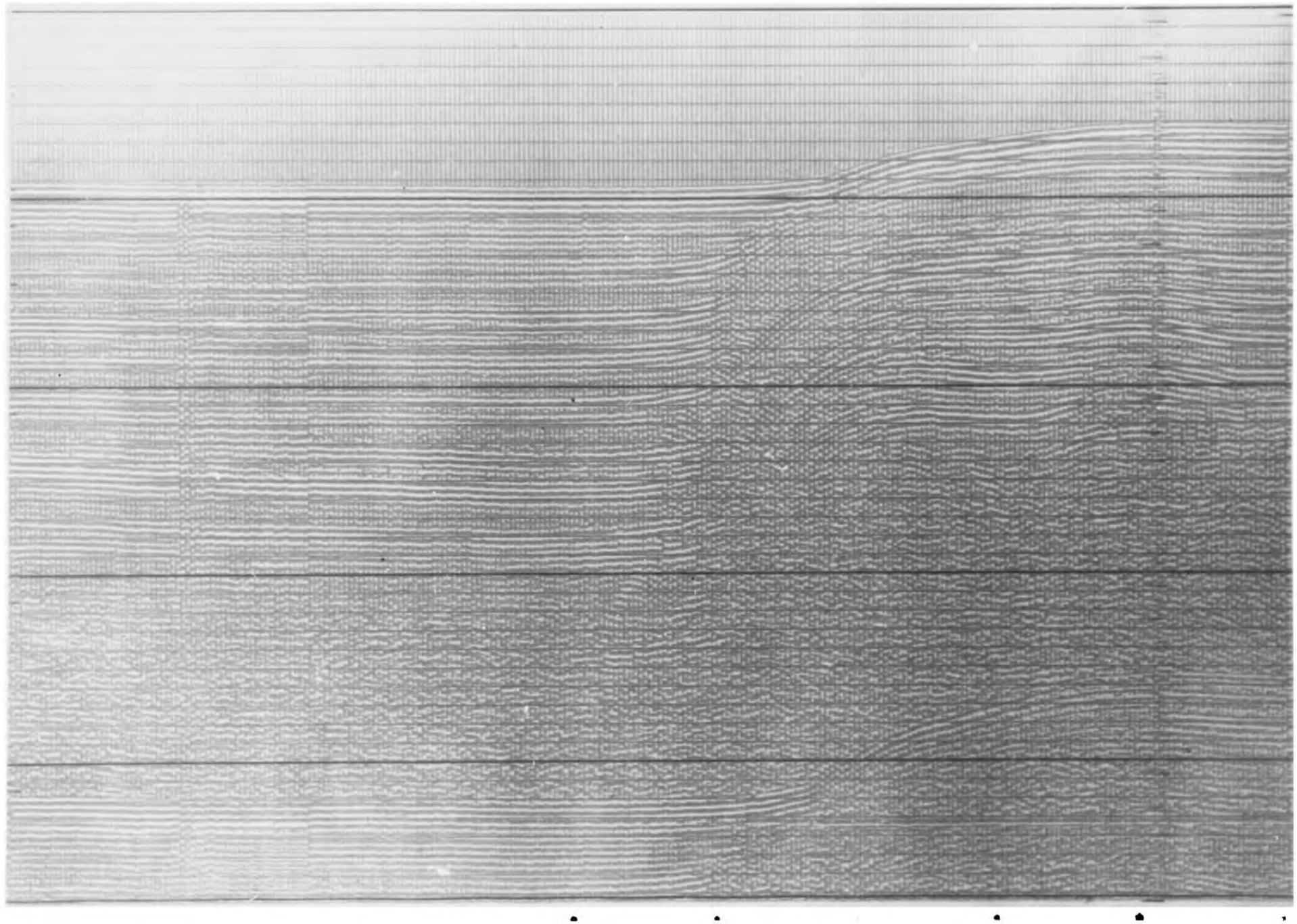
3·5
(S)
6·5

4.7 Migration of the reflectors shown in fig. 4.6. Dashed lines show the apparent reflector position. Solid lines show the migrated positions. The reflectors are shown to be warped but not faulted.

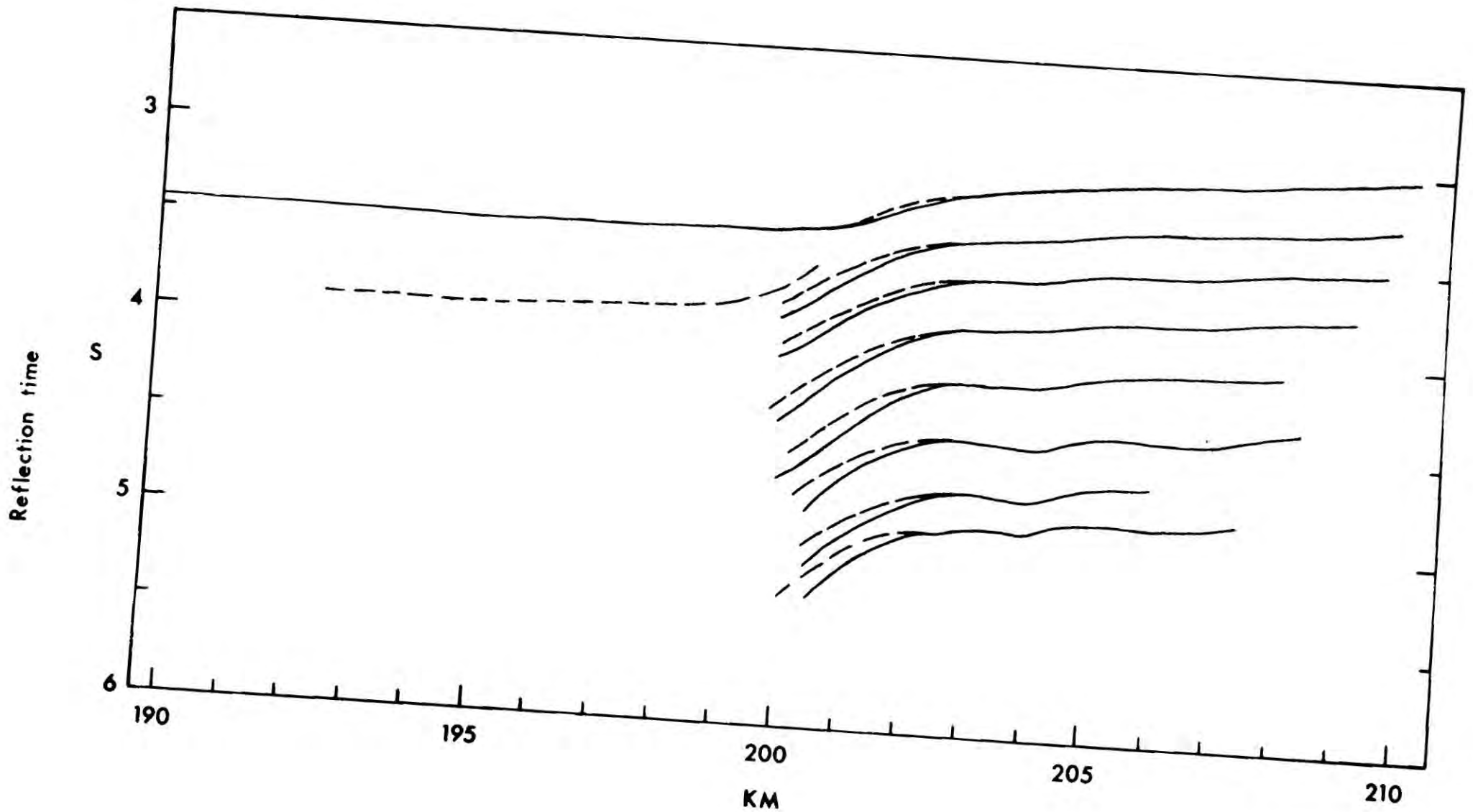
3
4
S
5
6
Reflection time
190
195
200
205
210
KM

variable area records using the computer graph plotter. The maximum convexivity graphs were used to test apparent slopes and reflection points on other parts of the records. Fig. 4.7 shows a tracing of the reflectors and their migrated positions. From this it can be seen that a fault does not exist in the upper sedimentary layers, but it is possible that one exists below in the more competent sediments.

In addition to the features arising from the uplift of the Barbados Ridge, it is evident that some characteristics of the trough are due to the relative uplift of the island arc. The principal consequence of this uplift is the sequence of dipping reflectors seen on the southerly profiles, which are overlain in the centre of the trough by A*. Also some of the upward turn of the sedimentary layering on the west side of the trough may be the result of the uplift of the islands as well as differential deposition.

The sediments in the north of the Tobago Trough bow gently over a rise extending eastward from St. Lucia to the Barbados Ridge Crossing the rise, running NNE, is a linear depression which can be seen clearly on lines D6 and H1, and is present at the extreme northern end of D4. Beneath the surface depression the sediments are disturbed and appear to have subsided. On line D7 it is only from these disturbed layers that the feature can be identified, because the depression in the seabed is not present there. The feature is not seen on H2, which is the next profile to the south. The form of subsidence seen on line D7 is that of downward warping of the layers either side of a central, comparatively unaffected, block. It is not obvious to the writer what process can have lead to the formation this feature. One interpretation (Bassinger and Keller, 1971) is that the feature is a fault or underlain by a fault. There

There does not, however, appear to be any vertical displacement of the beds either side of the feature, and so a strike slip fault would have to be invoked. The termination of the feature south of D7 and the lack of any obvious break in the layering casts doubt on a strike slip fault also. The feature may possibly be an incipient graben structure, with two rifts, formed by tensional conditions arising from uplift of the St. Lucia East Ridge.

The valley like depression could have been eroded by bottom currents moving northward out of the Tobago Trough, and acted as an exit channel for them. The greater depth of the subsidence feature on line D7 is the reason why it is not eroded there. Line H1, which runs along the crest of St. Lucia East Ridge is the one on which the feature shows most erosion. The course of the channel can be seen clearly on the bathymetric chart (fig. 2.2), picked out by the 1800 m contour.

The Barbados Ridge

Seismic reflection profiles crossing the ridge are H1, D7 and H3 (fig. 4.2) and lines along the ridge are D4 (fig. 4.3) and V (fig. 4.8). On the ridge stratified sediments of varying thickness overlie an irregular surface which is underlain by material with a disturbed internal structure or one that produces no discernible reflectors. The overlying material is formed of Layers A and B, and there is a strong contrast in density between it and the underlying rocks which gives rise to small gravity anomalies. An example of a gravity anomaly caused by the shape of the interface between the two rock groups is on line H3 (fig. 4.5), where a small outcropping ridge

4.8 Reflection profiles V (top) obtained by Collette and others (1969), and K (bottom) obtained on the KANE 9 Cruise (Lowrie and Escowitz, 1970).

60° WEST SECTION

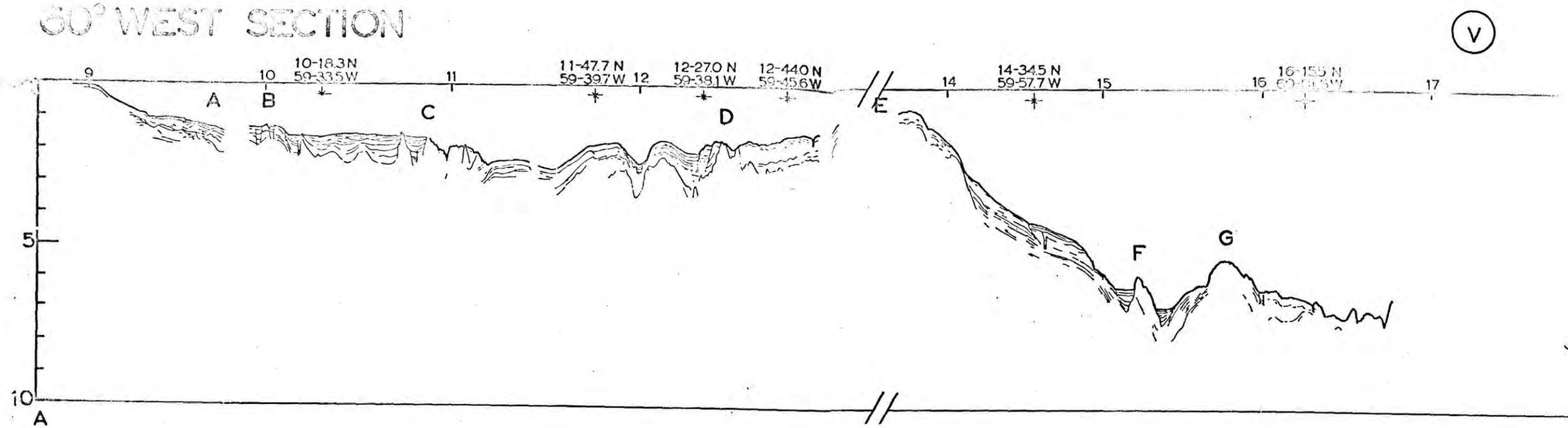

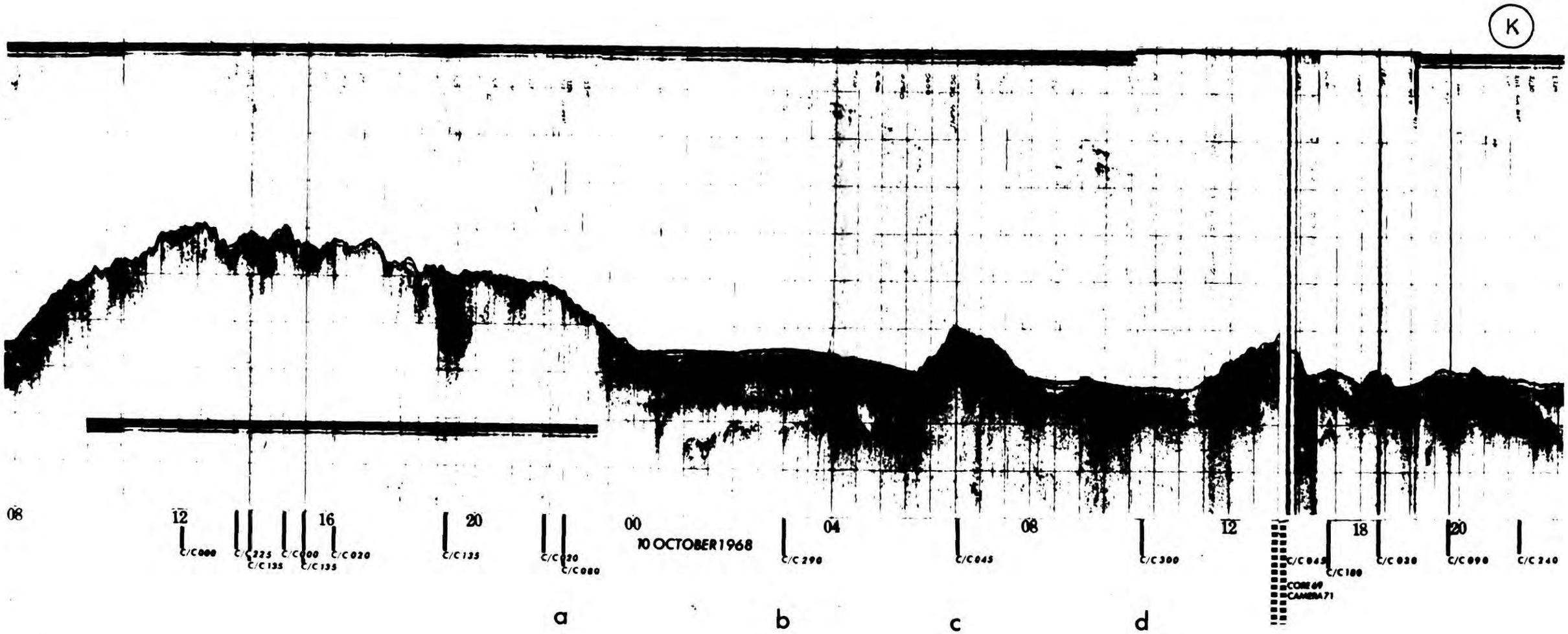

of the higher density sediment is separated by a small trough of lower density sediment from the main outcrop of higher density sediment at the crest of the Barbados Ridge. The amplitude of the anomaly is about 10 mgal.

On line H1 a magnetic anomaly of 40 gammas amplitude is apparently associated with a rise of the sediment underlying layers A and B (fig. 4.5). The anomaly is also seen on two lines to the south of H1 on which only gravity and magnetic data were collected. Coincident with the magnetic anomaly is a short wavelength positive gravity anomaly. A two dimensional magnetic body with induced magnetisation and its top surfaces were fixed at the shape given by the reflection profile gives a similar anomaly if the magnetic susceptibility is 0.0013. This is rather high for sedimentary rocks, but seismic refraction and gravity data exclude the possibility of a volcanic basement ridge. The Upper Scotland Formation of Barbados does contain iron oxide minerals which form concretions and stain the rocks with rust. These minerals when metamorphosed at chlorite grade in pelitic and semi-pelitic rocks will alter to magnetite (Turner, 1968). It is possible therefore that the cause of the magnetic anomaly could be an uplifted segment of metasediment from deeper in the sediment pile beneath the Barbados Ridge. The smoothness of the observed anomaly compared with the calculated anomaly suggests that the source is deeper than the surface of the rise seen on the reflection record, but its wavelength limits its maximum depth to about 5 or 6 km. A body of the same shape but 2 km deeper than the reflector surface, with a susceptibility of 0.0018 gave a good fit to the observed anomaly.

Seismic refraction work on the Barbados Ridge (Ewing and others,

1957) indicates a top layer of low velocity (1.7 km s^{-1}) and varying thickness (1.07 km on E22 to 0.2 km on E16) which conforms well to the upper stratified layers (A & B) seen on the reflection records. On the northern part of the ridge the upper layers are underlain by one of velocity 2.22 to 2.75 km s^{-1} and below this is a layer of velocity 3.2 - 3.4 km s^{-1} which rests on one of velocity 4.0 - 4.3 km s^{-1}. As the reflection records show, the structure is very variable, which limits the usefulness of the refraction method. The method does, however, broadly differentiate between the main sedimentary groups, although the effect of depth and varying states of lithification must be considered. As a generalisation it seems that rocks of velocity 2.0 km s^{-1} or less are stratified sediments of layers A, B and possibly C. Rocks of velocity 3.0 km s^{-1} and above belong to the Scotland and Oceanic Formation of Barbados. Hurley (1966) dredged rocks similar to those of the Scotland Formation from a point on the ridge north of Barbados (marked h on fig 4.1). At that point on the seabed the Scotland Formation has a seismic velocity of 2.2 km s^{-1}, and gives a characteristic reflection record of many discontinuous, often contorted, reflectors.

Just south of Barbados, Hurley (1966) dredged limestones containing manganese nodules which he thought likely to be a facies of the Upper Oceanic or Bissex Hill Formations. Line H3 shows a few sub-horizontal and not very well defined reflectors occurring in the rock which forms the ridge crest and occurs beneath a small basin of low density sediment on the western slope of the ridge. The single Miocene core collected by Ramsay (1968) came from a point (r fig. 4.1) close to D on line V (fig. 4.8) and the east end of B3 (fig. 4.4), where the layer below the stratified sediments crops out. This evidence suggests that the Oceanic and Bissex Hill Formations forms the basement

to the uppermost stratified sediments (A & B) on the ridge south of Barbados. The refraction velocity obtained on line E22 for the rock below the uppermost layer was 3.97 km s^{-1}, and line E21, nearby, gives 3.81 km s^{-1}. These are quite acceptable values for lithified limestone but the thicknesses obtained by refraction, of 2.55 and 4.7 km, are greater than expected from Barbados where the maximum thickness of Oceanics is 1.5 km. It is probable that included in the thickness values found by seismic refraction are some Scotland Formation sediments, the boundary between the Oceanic and Scotland sediments not having been observed.

The deepest refractors of lines E22 and E21 (Ewing and others, 1957) gave velocities of 4.9 and 5.3 km s^{-1} respectively at depths of 4.4 to 10.4 km. The refractor dips away from the ridge to the east. Although the velocities are similar to those of oceanic Layer 2, it is unlikely that Layer 2 is the refractor in this case. The gravity anomaly excludes this, because interpretation of it reveals that the igneous basement is depressed below the ridge (see p.72). It is possible that the 4.9 - 5.3 km s^{-1} layer is made up of metamorphic rocks (metasediments). If these are autochthonous, and possibly once depresed 5 to 10 km below their present depth, then they are likely to be of the zeolite facies or the prehnite-pumpellyite metagraywacke facies (Turner, 1968). Further depression might have put them in the greenschist or glaucophane-lawsonite schist facies, depending on the temperature gradient. The 4.9 - 5.3 layer has not been detected beneath Barbados, and the deepest borehole, of 4.6 km depth, contains no metamorphic rocks (Baadsgard, 1960).

Tectonic structures of the Barbados Ridge.

Both north and south of Barbados the uppermost sediments are draped over rises in the lower sediments, giving the impression of occasional anticlines and synclines. These structures can be seen on the southern part of D4 and on V around lat. 12° N. (figs. 4.3 and 4.8). They are observable on many east-west lines as noted above. Similar features were described by Bassinger and others (1971) at the southern end of the Barbados Ridge, who attempted to correlate these structures along the ridge and onto the continental shelf. However the only features which can be shown to cross more than one of their profiles are the crestal part of the ridge and a shallow trough east of it. Their profiles show clearly that the upper stratified sediments (A & B) are unconformable to the underlying sediments which outcrop locally along the crest of the Barbados Ridge.

The synclinal and anticlinal like features seen in figs. 4.3, 4.4, 4.8 and the profiles of Bassinger and others (1971), are probably not true fold features. There is no evidence of secondary folding in the stratified sediments and the shape of the large "folds" is controlled entirely by the form of the underlying sediment. The upper sediment layers are warped locally by differential movement of the underlying material, probably along faults. As well as the overall uplift which forms the ridge, there are many local vertical movements along it. The average trend of major fold axes in the Scotland Formation on Barbados is 065° and the largest folds have a wavelength of about 2 km. Features of this size would not show their shape on a reflection record, but would show as a series of irregular and intermittent reflectors. There are gentle folds in the Oceanic Formation

and their overall structure on Barbados is one of gentle doming about the centre of the island (Daviess, 1971).

The ridge north of latitude 13.8°N slopes down to the north at about 1.5° and the 1 km thickness of stratified sediments shows discontinuities and deformations which are suggestive of gravity sliding.

Taken overall, the Barbados Ridge is an uplifted rise of older sediments, over which younger sediments are draped, and along which a series of smaller uplifted blocks locally deform the younger sediments into anticlinal, synclinal, periclinal and basinal structures. The longest of these appears to be that which gives rise to the magnetic anomaly north of Barbados, and it is only 18 km long.

The Atlantic Ocean floor

Seismic reflection profiles across the floor of the Atlantic east of the Lesser Antilles are described by Collette and others (1969), and others are displayed in the Kane 9 Cruise Volume (1969). A JOIDES hole (27) has been drilled at 15° 51.39' N and 56° 52.76' W, south of the Barracuda Ridge (Bader and others, 1970). At this drill site there are three reflectors. The uppermost, at 0.08 s reflection time from the seabed, correlates with two turbidite layers of Pleistocene age at 67 to 70 metres depth. The second reflector at 0.28 s correlates with thin turbidites of Miocene age at 236 and 248 metres. The bottom reflector, which forms a rough basement surface at 0.53 s, correlates with a hard clayey limestone at 437 m, or possibly with an unconformity just below it not penetrated by the borehole. The topography of the acoustic basement has a relief of 0.5 s and the

bedding measured in the hard limestone dipped at 24°. This limestone and the overlying 20 m of sediment are very similar in lithology and faunal content to the Oceanic Formation of Barbados. The seismic velocities in the layers overlying the top two reflectors are 1.71 and 1.74 km s^{-1}. The velocity in the layer between the second reflector and the basement is 1.85 km s^{-1}.

The acoustic basement appears to outcrop on the sou thern flank of the Barracuda Ridge. The thickness of sediments increases markedly away from the drill site to the south and west, particularly in the upper finely layered sediments of Pleistocene age. This thickening to the south and west is substantiated by the reflection profiles of Collette and others (1969), Bunce and others (1971), and Peter (personal communication).

To the east of the Lesser Antilles, at the base of the slope from the Barbados Ridge, reflection profiles H1, B2, B3, D1 and K (figs. 4.9, 4.4, 4.3, 4.8) show comparatively flat lying reflectors to about two seconds penetration below the seabed. The upper half second shows considerable stratification, but apart from these upper layers there are two main reflectors. These are seen at 0.9 and 2.0 s on the eastern end of H1, and between a and b on K. Profiles H1 and K are almost coincident there and the great similarity between the two independently collected records gives one confidence in the existence of the features observed.

The lowest reflector has an irregular topography and is approximately at the depth to basement, of 2.24 km below the seabed, found at the north end of refraction line E18 (fig. 3.1). Lines H1 and K (a to b) run just to the south of the crest of a basement ridge

4.9 Reflection profile H1. Rose diagram indicates dips of reflectors in sediment of velocity 2.0 km s^{-1}.

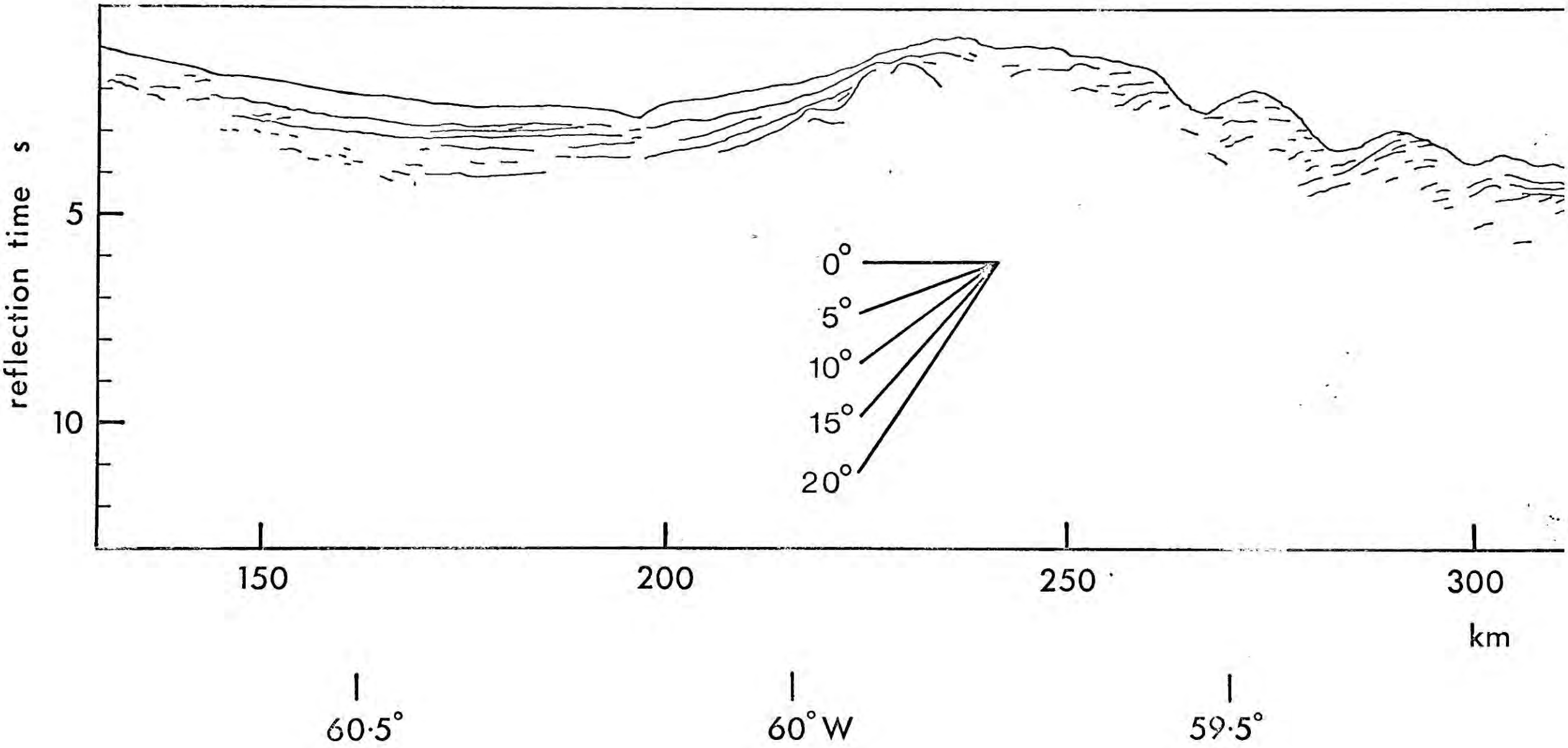
reflection time s
5
10
0°
5°
10°
15°
20°
150
200
250
300
km
60·5°
60° W
59·5°

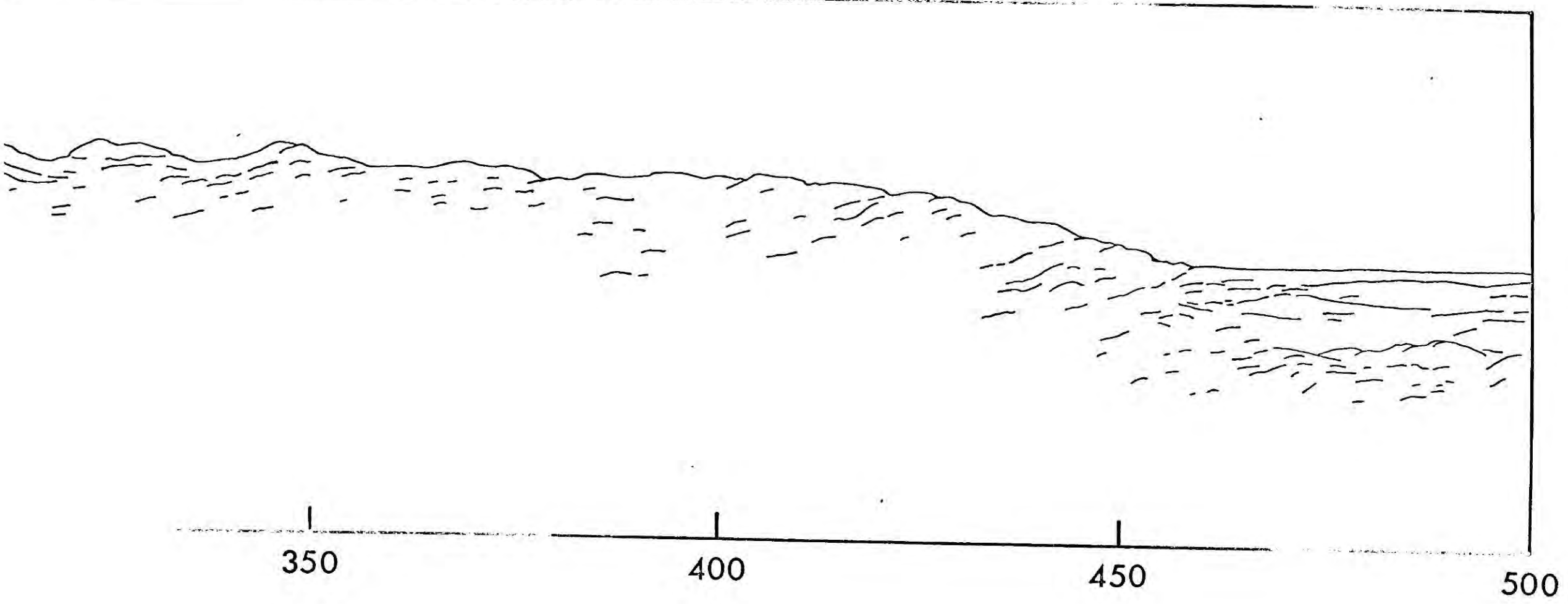
350
400
450
500
59° W
58·5°
58° W
57·5°

which can be seen on profiles D1 and D2 (fig. 4.3). The basement deepens to the south, by at least 1.8 s, and it also dips slightly to the west (a depth increase of 0.3 s in 20 km, which is a dip of about 1^{o}). These observations are compatible with the basement depths of 4.05 km, obtained at h1, and 3.1 km, obtained at the southern end of E18, 115 km further east. The depths to basement given above are to the refractor of seismic velocity 6.6 - 6.8 km s^{-1} (oceanic Layer 3) which, by analogy with the observed oceanic crustal structure elsewhere must be overlain by basalts of Layer 2, first arrivals from which were apparently not detected on the refraction lines in this area. Layer 2 is probably about 1 km thick and this means that the basement to the sediments is 0.25 km shallower at the refraction stations than given above.

On line H1 there are what appear to be several discontinuous reflectors below the hummocky reflector which on other profiles is the acoustic basement. This taken by itself would throw doubt on the identification of the reflector as the top of Layer 2, but the refraction data seems to establish this beyond reasonable doubt. This raises the question of the nature of the discontinuous reflectors. Possible explanations are that they are patches of coherent noise, side reflections from the basement topography to the side of the line (the presence of the east-west basement ridge may be a factor in this), or reflectors in an interbedded lava/sediment sequence.

The reflector at 0.9 s has an undulating surface which is not as rough as the basement. The reflector gets deeper to the south. The separation between it and the basement is variable, being only 0.5 s over the ridge seen on D1 and 1.5 s on the flank of the ridge, 30 km

to the south. Further south the separation is about 1.2 s, and about 1 s separation is seen between the deepest reflector and the next overlying layer on B4. The lowest reflector on B4 is, however, rather flat and is only at 2 s penetration, whereas the depths obtained at h1 and E18 combined with the deepening trend seen on D1 leads one to expect the basement at 3 to 4 s. The bottom reflector on B4 is, therefore, much more likely to be the second reflector (0.9 s) seen on H1 and K. The second reflector is seen on B2 at 0.6 s above the basement. This second reflector may well be the acoustic basement seen at JOIDES site 27 and identified as the Oceanic Formation of Barbados. The reflector is more irregular at the drill site than it is further south, which could be a consequence of deformation associated with the uplift of the Barracuda Ridge. The amount of thickening of the sediments to the south and west of the drill site also increases the likelihood that the reflector seen at 0.9 s on H1 (the second reflector) is the reflector seen at 0.53 s at hole 27.

The upper stratified sediments are of Pliocene to Recent age, which can be shown by straight forward extrapolation from sediment structure observed at the JOIDES drill site. The youngest sedimentary feature is a small wedge shaped basin, 0.2 s thick, at the base of the Barbados Slope, which is shown well on line D1 west of the course change. The sediments in this small deposit may be derived from the slope. The upper stratified sediments are only 0.2 s thick over the east-west ridge seen on D1 and D2, but further south they are 0.7 to 0.8 s thick.

The Barbados Slope

This is the region between the crest of the Barbados Ridge and the position where the seabed becomes level on the Atlantic Ocean Floor. It has an irregular topography consisting of many minor ridges and valleys. In the survey area (fig. 2.2) there appears to be a pronounced trend of these features parallel to the Barbados Ridge. This is partly a function of survey line spacing and direction, and the north-south lines also show much minor relief, but there is a definite overall trend parallel to the ridge.

Reflection profiles covering the area of the Barbados Slope are H1 (fig. 4.9), B2 and B4 (fig. 4.4), K (fig. 4.8), and D2 and D3 (fig. 4.3). In this region reflecting horizons are much disturbed and do not appear very far below the seabed. The amount of energy reflected from the sediments is great, but the coherence of the reflectors is low, and they could be described as acoustically opaque.

The uppermost layer is of variable thickness (0.5 s average), and overlies an irregular reflecting horizon, or horizons, the shape of which does not usually match that of the topography of the seabed. This overlying layer is not always well shown on profile H1, mainly because the top 0.3 s is obscured by the signal of the bottom reflection. It is shown best on lines B2, B4, D2 and D3, and on the photographs of records given in Chase and Bunce (1969). The layer does not usually contain reflectors within it except in some of the deeper pockets, such as that at long. 58° 45' W on B4. The profiles of Bassinger and others (1971) indicate that there is a considerable accumulation of the overlying layer in a shallow basin

east of the Barbados Ridge, and immediately to the east of Barbados itself there is a flat bottomed basin which the gravity anomaly indicates is filled by sediments of a density less than 2.1 gm cm^{-3}. The anomaly caused by this basin is a pronounced feature on the Bouguer anomaly map with a correction density of 2.0 gm cm^{-3} (fig. 2.6). The overlying layer is absent in places and is unconformable with the underlying sediments. A minor unconformity can be seen at 320 km (west of $62^{o}W$) on profile H1.

The underlying sediments have an irregular top surface and contain many reflectors dipping to the west, which are seen best on profile H1. These dipping reflectors commence close to the break of slope at the eastern edge of slope and continue through to the Barbados Ridge crest. The amount of dip varies, and the maximum value of 7^{o} is seen at 280 km, but normally the dip is 5^{o} or under (assuming a sediment velocity of 2.0 km s^{-1}) On one playback of the reflection record along H1 the dipping reflectors were longer, more numerous, and more pronounced than shown in fig. 4.9. Since this record was obtained modifications were made to the playback equipment, and the record was found to be unrepeatable even though numerous filter settings were tried. How this anomalous record was obtained is still unknown. When on-line digital filtering facilities become available at Durham University, and more sophisticated filters and common depth point stacking are applied to the record it is hoped that this enigma will be resolved. Chase and Bunce (1969) recognised reflectors which dip at 30^{o} to the west and lead from the declivites between the rounded highs on the irregular first sub-bottom reflector. These they interpreted as thrust faults formed as a result of underthrusting of the seafloor beneath the sediments, making a comparison with the well

known sand-box experiment of Hubbert (1951). As will be discussed in chapter 8, this experiment is not a particularly good analogy here, and it does seem that Chase and Bunce in trying to prove their case have been over optimistic in their interpretation of these dipping reflectors. Brief analysis of their shape and attitude leads one to think that they might be reflection hyperbolae from sloping faces in the irregular top reflector. The asymptote to a reflection hyperbola from a point at the depth considered dips at 40^{o} The dip produced from a convex surface will be less. Also a fault may not be a good reflector unless rocks of differing density and seismic velocity were separated by the fault. Although this is possible, there is no evidence to show that it is likely.

Seismic refraction lines across the slope found several velocities likely to be from sedimentary rocks. Lines E17 and E19 show a layer of velocity 2.58 and 2.41 km s^{-1} underlying a variable thickness (0.54 to 2.38 km) of a layer of assumed velocity 1.7 km s^{-1} which is the overlying layer identified on the reflection records. At the western end of E19 an apparent surface velocity of 1.91 km s^{-1} was obtained. The sediment velocity obtained at station h1 of LASP was 2.45 km s^{-1}. At the eastern side of the slope the "2.5" layer appears to lie directly on oceanic basement. Further west (E19) it overlies a layer of velocity 4.31 km s^{-1}. Both lower sedimentary layers thicken towards the west. The thickness of the "2.5" layer ranges from 2.6 to 6.2 km, and that of the 4.3 km s^{-1} layer varies between 3.1 and 3.9 km.

According to plate tectonic hypotheses, the Atlantic Ocean floor is being thrust beneath the sediment pile on which Barbados is

situated, deforming the sediments in the process. As mentioned above, Chase and Bunce (1969) claimed to have found thrusts associated with this deformation. The tectonics of this are treated more fully in chapter 8, but it is apt here to consider what sedimentary features are likely to be related to any under thrusting-process. The shape of the slope is significant in this respect. The rough nature of the bottom topography and sub-bottom reflectors is itself suggestive of tectonic activity. The final curve of the slope down to the ocean floor is convex and cannot be attributed to the normal sedimentary processes of erosion and deposition which would tend to give it a concave profile. It resembles the toe of an enormous earth slip, and this may be a good analogy except that instead of the upper material moving over that beneath, it is the material underneath that is moving. If this analogy is correct, then active deformation of the sediments is only taking place in the first 40 or 50 km of the slope, where it retains its convex shape. It seems that in the first 50 km the sediments are uplifted and tilted back to the west, giving rise to the series of dipping reflectors seen on H1. The north-south profiles, D2 and D3, show some dipping reflectors, but the angle and direction of dip varies, and most seem to be associated with the sloping down of sediments towards the north of the pile.

Fig. 4.10 shows a photograph of the reflection record on H1 at the foot of the slope. It can be seen that the reflectors dip slightly to the west even where they are below the flat ocean bottom, but that where the slope begins the layers dip more strongly and that it is the upper layers which are affected first. The lower layers extend a little way below the foot of the slope without any disturbance.

4.10 Portion of the air gun record on Profile H1 showing the junction of the base of the Barbados Slope and the Atlantic Ocean floor. Reflectors in the Atlantic are nearly horizontal. Reflectors below the slope dip gently to the west. Some of the reflectors have been artificially emphasised to bring out the structure.

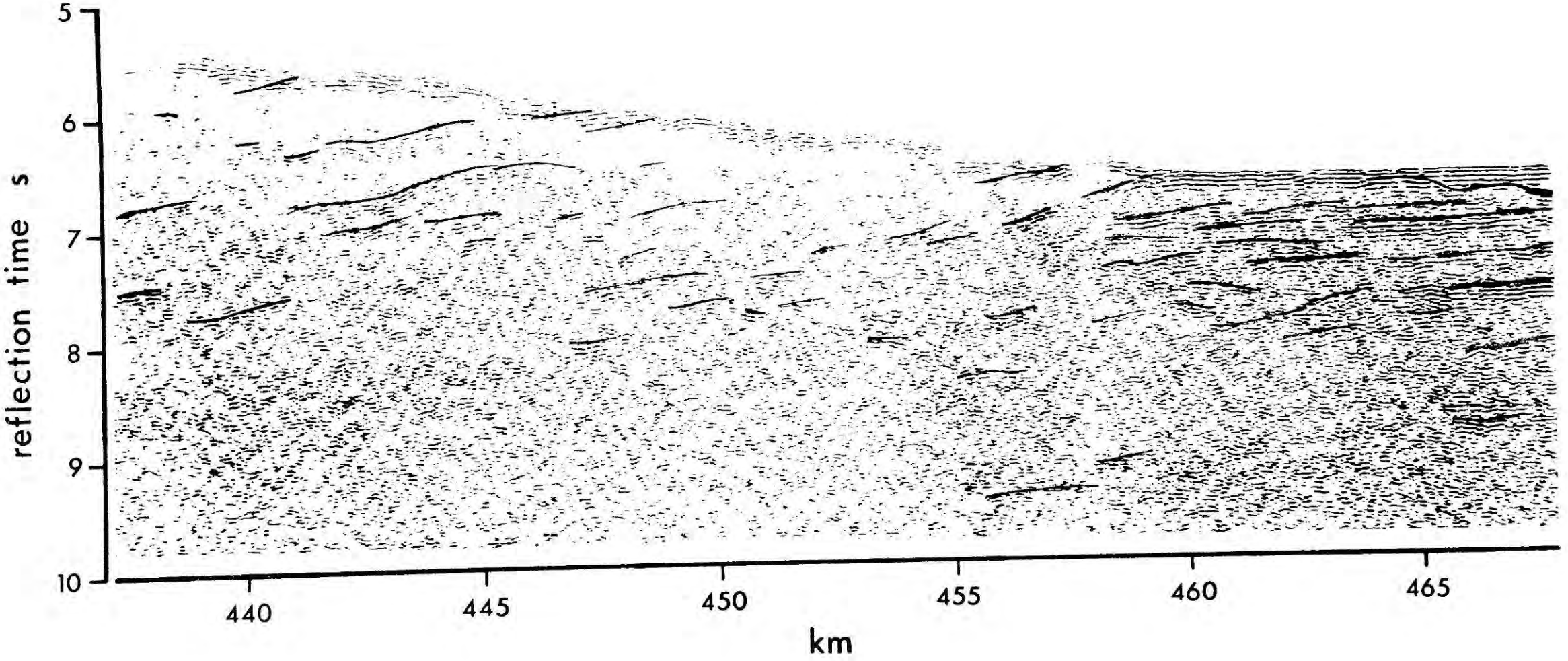
reflection time s
5
6
7
8
9
10
440
445
450
455
460
465
km

Correlation of seismically defined layers with rock formations.

The probable nature of rocks overlying reflectors in the Atlantic Ocean floor has already been discussed in some detail.

The correlation of the apparent layers in the Barbados Slope with formations of known ages poses a problem. At the crest of the Barbados Ridge north of Barbados, the sediment containing dipping reflectors seems to be well established from dredge samples as part of the Scotland Formation. At the eastern side of the slope, the Scotland Formation, if present,must be at the base of the sediment pile. So, many of the dipping reflectors are in rocks of a younger age than the Scotland Formation. The "2.5" layer, however, extends continuously from the Barbados Ridge to the Atlantic Ocean floor and must therefore be diachronous. The layers defined by the refraction method must be principally the result of compaction, although it is likely that the boundary between the "2.5"and 4.31 km s^{-1} layers represents some discontinuity in the structure and history of the sedimentary pile.

Much of the overlying layer in the Barbados Slope region must by young in age, especially those parts which fill minor troughs on the slope and those on the eastern edge of it. The profiles of Bassinger show that the sediments filling the basin east of the Barbados Ridge unconformably overlie those draped over the ridge, which means that they are of the same age as A* in the Tobago Trough. At some places on the slope the overlying layer is presently being eroded and it seems that much of the overlying layer is older than A*.

Turbidite deposits are mainly derived from the continental shelf of South America and turbidity flows will not be able to climb the

slope once they are on the ocean floor. Any flows emerging onto the slope will either be trapped in the small troughs or descend by the most direct route to the ocean floor. Most of the erosional products from Barbados and the ridge will be swept into the Tobago Trough by the strong westward moving ocean current, except immediately to the east of Barbados. A large proportion of the overlying sediment layer on the slope, except for the trough fills, is likely, therefore to have been deposited before the slope was uplifted substantially. The unconformity at 320 km on H1 may be between the Oceanics and the Scotland Formation, but it is just as likely to be younger.

Higgins (1959) compared seismic velocity data from boreholes in Trinidad with seismic refraction results (mainly Ewing and others, 1957) from the adjacent sea area. He suggested that the 2.2 - 2.6 km s^{-1} layer (layer C of the Tobago Trough) corresponds to Plio-Miocene rocks, that the 2.9 - 3.43 km s^{-1} layer (D) corresponds to Oligocene-Eocene rocks, and that the 4.9 - 5.33 km s^{-1} layer corresponds to the metamorphics of the North Range of Trinidad which are mostly phyllites, quartzites and limestones of lower greenschist facies metamorpism. The stratified sediments of layers A to C overlie the Miocene rocks of Barbados and are therefore of late Miocene to Recent age. Layer A* is almost certainly Quaternary and it is likely that some of Layer A is Quaternary also. Higgins did not put forward any correlation for the 3.8 - 4.0 km s^{-1} layer (E), but it is possibly of early Tertiary age and composed mainly of Scotland Formation sediments, as must be most of layer D.

It seems that Cretaceous rocks do not occur in the top few kilometres of sediment, but the ocean crust (see Chapter 7) is old

enough for them to be present somewhere in the sequence, and they may now be metamorphosed to some extent and form the 4.9 - 5.33 layer which rises under the Barbados Ridge towards the continental shelf. Metamorphism of sufficiently high grade could have been achieved by burial in the trench, which the Barbados Ridge now covers, to a depth of 15 km. Deformation would aid the development of lower greenschist facies rocks (Turner, 1968).

As has already been remarked on above, the correlation between layering determined seismically and rock formations is a far from straightforward process when borehole data is sparse, and especially when it can be seen that some layers defined by seismic refraction are diachronous. A layer defined by seismic reflection may vary its seismic velocity according to its depth and its lithology may also vary along it. Some of the layers in the Tobago Trough vary from sands rich in volcanic products on the western margin to fine silts and clays on the eastern margin. The structural relations between layers and outcrops of known age and lithology are of great importance in determining the nature and ages of the layers.

The Basement

The basement in this region is either oceanic or derived from the volcanic island arc. In either case it is composed of basic igneous rocks, and is therefore magnetic, which means that analysis of magnetics as well as gravity and seismic data will aid the elucidation of the basement structure. Except for the Atlantic Ocean Floor, the seismic reflection method has not penetrated to the basement, but seismic refraction exper iments have detected it in many areas. The

results of the magnetic analysis will be dealt with first, followed by the combined interpretation of gravity, magnetic and seismic evidence.

Direct magnetic interpretation

The most intense magnetic anomalies in the area occur in the region of the island arc. East of the arc the anomalies are of smaller amplitude (<100 gammas) and longer wavelength (50 to 100 km). On the western flank of the Barbados Ridge (fig. 2.9) there is a north-south trending positive anomaly with a wavelength of about 90 km. Magnetic profiles across this anomaly are shown in fig. 4.11 and the alignment of anomalies is more clear from the profiles than from the map. The trend is slightly east of north, and on some lines anomalies of shorter wavelength are present. Those occurring on lines at latitudes 13° 39', 13° 44', and 13° 49' N were discussed above in the context of the structure of the sediments composing the Barbados Ridge, and are thought to be caused by a magnetic body of sedimentary origin at a depth of about 4 km. The shorter wavelength anomalies at latitudes 13° 14' and 13° 19' N may have a similar cause.

The long wavelength anomaly may be produced by magnetic rocks within the Barbados Ridge, but there is another possibility, which is that the anomaly is caused by the shape of the basement. The seismic refraction results indicate that the basement dips from the east and the west below the Barbados Ridge and this is corroborated by the gravity anomaly.

The structure of the magnetic basement was modelled using a two dimensional model. The positions of the corners of the faces and the angle of magnetisation in the plane of the profile were found by

4.11 Magnetic anomaly profiles across the Barbados Ridge and east Tobago Trough. Upper part shows the anomalies superimposed. The lower part shows the anomalies spaced proportionally to the line spacing.

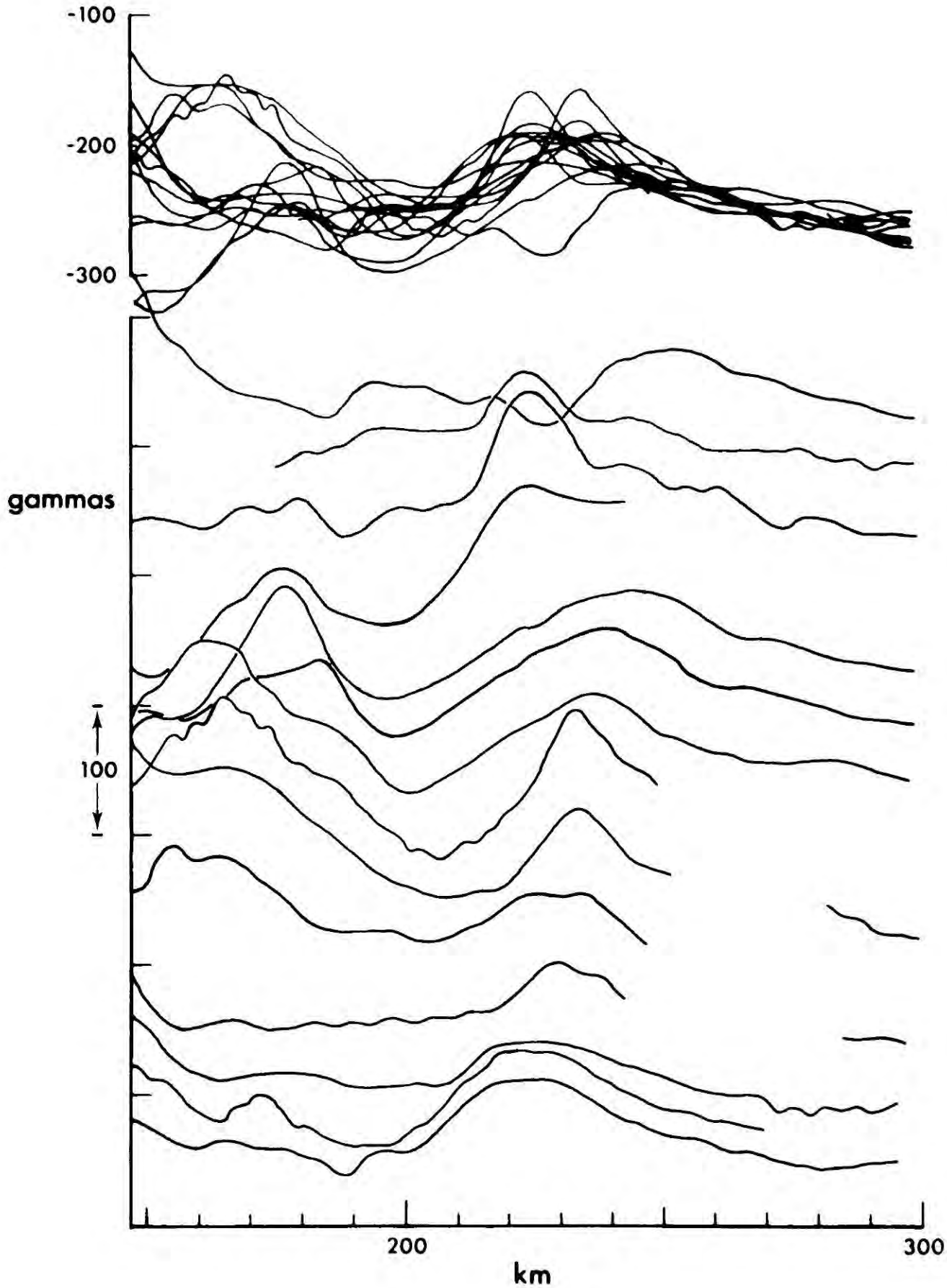
-100
-200
-300
gammas
100
200
300
km

non-linear optimisation. This method finds the minimum of a function, which in this case was the variance of the difference between the observed magnetic anomaly and the computed values. The magnetisation and the background value of the magnetic field were obtained by linear regression of the computed values on the observed values of the anomaly. The computations were carried out by the subroutine OPTIMAG with the MINUIT optimisation program (see appendices 4.1 & 4.2).

Two types of models were used. One was a simple interface between magnetic basement and non-magnetic cover. The other was a layer of constant thickness at the top surface of the basement. This latter is the situation which approximates most closely to that of oceanic crust, where the upper part of layer 2 is most strongly magnetised, and produces the linear anomalies due to remanent magnetisation reversals characteristic of ocean basins. Talwani, Windisch and Langseth (1971), from a detailed study of the Reykjanes Ridge crest, calculated this layer to be 0.4 km thick. Vine and Moores (1972) have examined the magnetic properties of rocks from the Troodos Massif of Cyprus which are thought to be part of an uplifted segment of oceanic crust, and considered that the probable thickness of the highly magnetised layer is 0.5 to 1.0 km, and consists entirely of pillow lavas, whereas the rest of layer 2 also contains dykes. In the model used here the magnetised layer was taken to be 0.4 km thick.

The starting shapes for the models were estimated from the seismic refraction data and bounds were placed on the movement of the body points to keep them within the limits imposed by the seismic refraction results. At the start of each optimisation sequence, the shape of the

4.12 The magnetised body model derived to fit the magnetic anomaly on the east flank of the Barbados Ridge at latitude 12° 54' N. The model is an interface between magnetised and nonmagnetised rock. The angle of dip of the magnetisation vector is -32.5°. S is the standard error. C is the correlation coefficient. B is the value of the background to the anomaly. Dots are the observed values. The continuous curve is the calculated anomaly.

4.13 The magnetic anomaly on the line at latitude 12° 54' N modelled by a magnetised layer 0.4 km thick. The dip of the magnetisation is -26.4°.

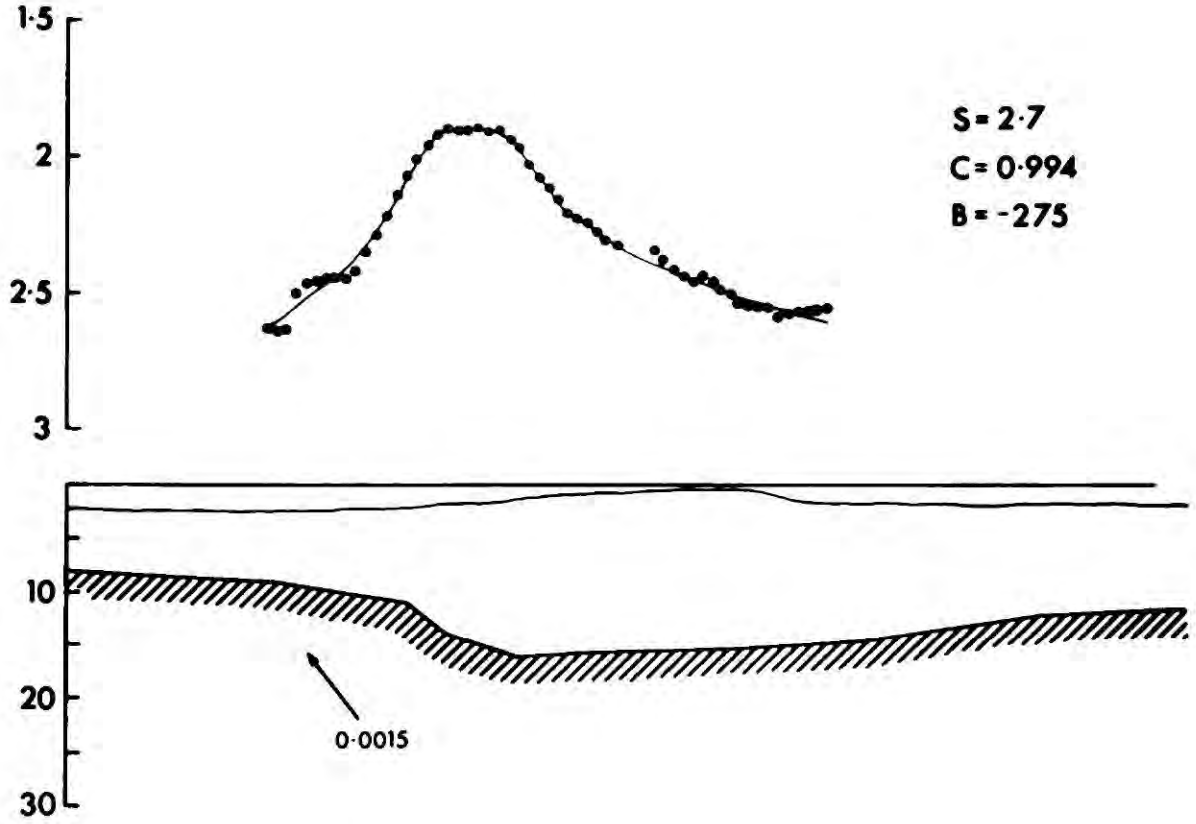
1·5
2
2·5
3
S = 2·7
C = 0·994
B = -275
10
20
30
0·0015
1·5
2
gammas/100
2·5
3
S = 2·0
C = 0·997
B = -242
10
km
20
30
0·081
0·4
150
200
250
300
350
km

body was held while the angle of magnetisation in the plane of the profile was varied to obtain the best fit with the initial shape estimated from the seismic data.

Models of the magnetic basement shape are shown in figs. 4.12, 4.13, 4.14 and 4.15. The layer models produce better fits to the anomaly than the interface models, and also have shapes which are more compatible with the seismic and gravity data, producing the anomalies from a smoother form than the interface models, which have a more angular shape. The interface model was used to give the shape of the top of the basement layer in gravity models of the Barbados Ridge area, and was found to be quite compatible.

The values of magnetisation obtained for the layer model are of the right order of magnitude for the top of oceanic layer 2 (Vine and Moores, 1972), but are a little high, which suggests that the layer may be thicker than 0.4 km. The magnetisation obtained for the profile at 12^{o} 54' N, using a layer 0.4 km thick, was 0.081 emu cm^{-3}, and that obtained for a layer 1.0 km thick was 0.034 emu cm^{-3}. The angle of dip of the magnetisation vector is not far from horizontal and is very different from that expected from induced magnetisation, which would be 80^{o} when projected in the plane of the profiles. If the model is valid, then the magnetisation must be mainly remanent. The angle and direction is similar to those obtained from Cretaceous rocks around the Caribbean (MacDonald and Opdyke, 1972). The crust in the region of Barbados, both sides of the subduction zone, is likely to be of Cretaceous from various lines of evidence, which are discussed in Chapter 7, mainly the oceanic magnetic anomaly pattern.

A possible variant of the model considered is one in which the

4.14 The magnetic anomaly at latitude 12° 59' N modelled using a magnetised layer 0.4 km thick. The dip of the magnetisation is 4.3°. Dots are the observed values. The continuous curve is the calculated anomaly. S is the standard error. C is the correlation coefficient. B is the background to the anomaly.

4.15 The magnetic anomaly at latitude 13° 24' N modelled using a magnetised layer 0.4 km thick. The dip of the magnetisation is -34.5°.

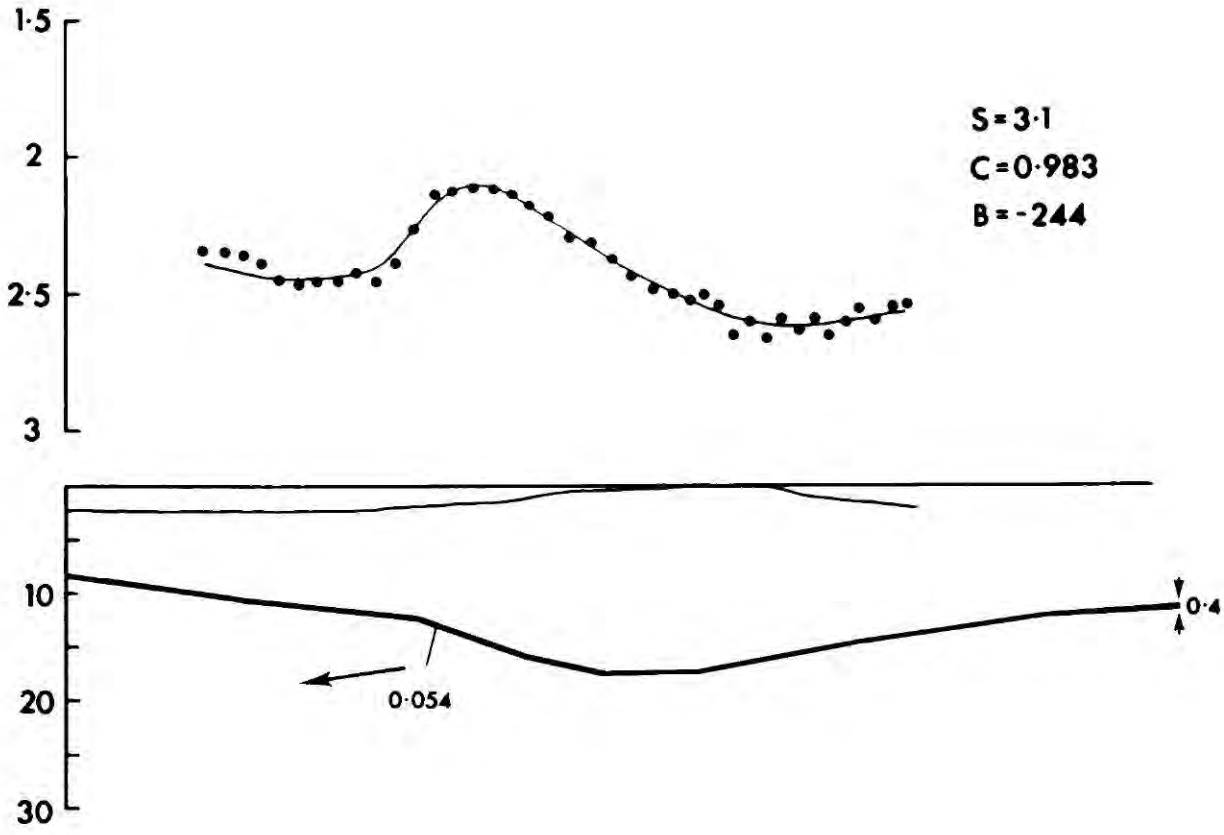
1·5
2
2·5
3
S = 3·1
C = 0·983
B = -244
10
20
30
0·4
0·054

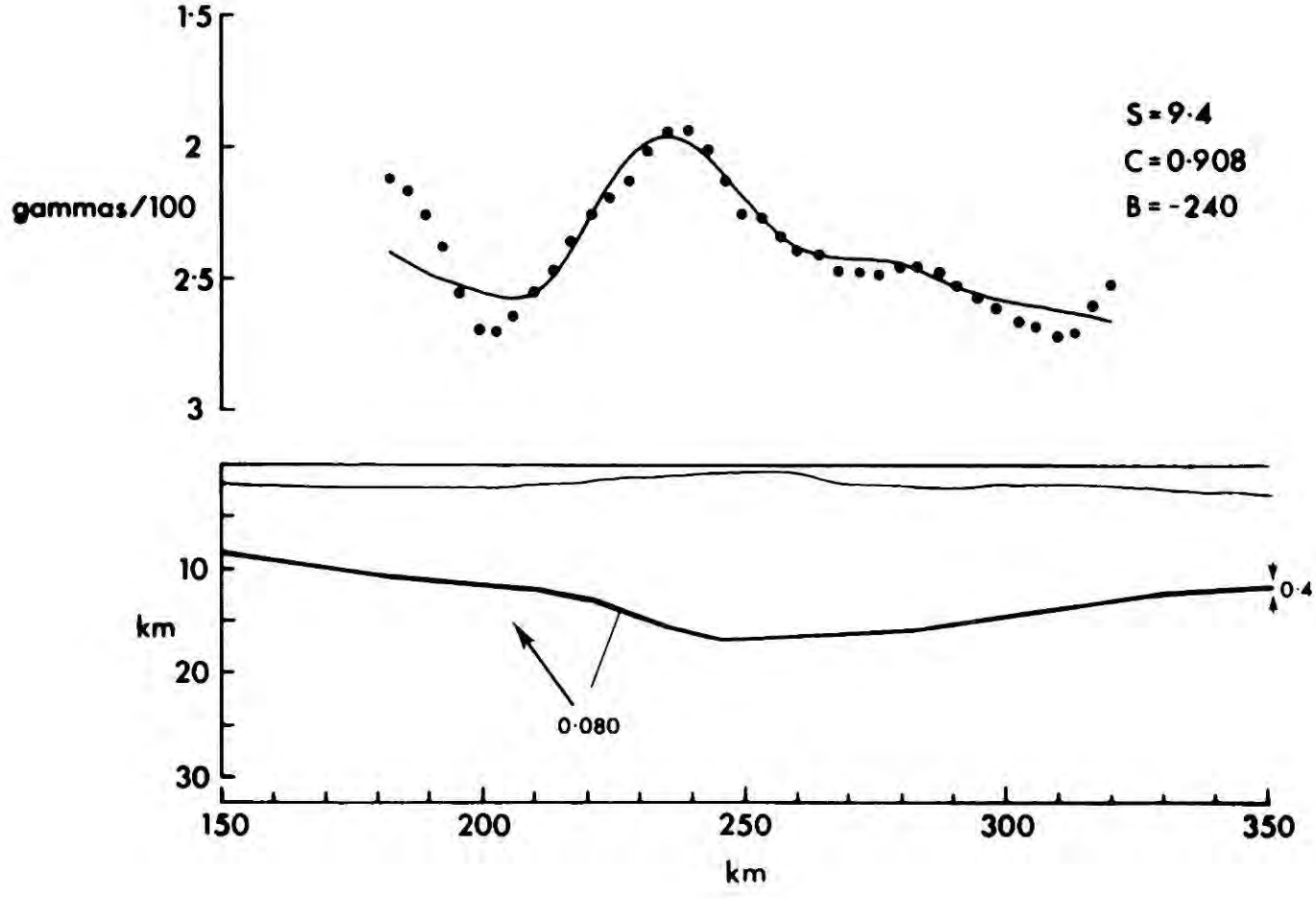
1·5
2
gammas/100
2·5
3
S = 9·4
C = 0·908
B = -240
10
km
20
30
0·4
0·080
150
200
250
300
350
km

anomaly would be due in part to a change in magnetisation across the point of subduction beneath Barbados, if the crust being subducted has a different magnetisation to that opposing it. Although this may not be definitely excluded, it does appear from the earthquake focii (fig 6.7) and the gravity model (fig. 4.20) that the subduction point may be up to 40 km too far east of the anomaly for this to be a significant contributor to it.

The magnetised layer is deep below Barbados and this may raise questions about the stability of the magnetisation. With a normal oceanic geothermal gradient magnetite is stable to about 20 km, and in this region of thick sedimentary cover, temperatures are likely to be depressed. Heat flow measurements in the vicinity of Barbados give values which are half thoseobtained in the Atlantic Ocean basin (Von Herzen, Simmons and Folinsbee, 1970). There is also the effect of low to medium grade metamorpism to be considered, and greenschist facies metamorpism could lower the magnetisation by an order of magnitude (Vine and Moores, 1972). If the temperatures are lowered however, and they may not be more than 250^{o}C, then metamorphism may follow a trend through the prehnite-pumpellyite metagraywacke facies towards the glaucophane schist facies, and magnetite may not be badly altered.

The magnetic anomalies over the island arc are complicated, and indicate the presence of many magnetic bodies. The island arc is a linear magnetic body of a sort, but it is quite clear that many of the magnetic bodies composing it are not linear or planar in shape and are comparatively irregular. Anomalies east of St. Vincent (fig. 2.9) have a relatively circular shape. In between St. Lucia and St. Vincent it

was not possible to contour the magnetic anomalies at the line spacing of the survey, because of the great variability of them.

To obtain some idea of the possible form of magnetic bodies, a two dimensional model was computed for the island arc at the southern end of St. Vincent. This line was chosen because it appeared to be a point on the arc where a two dimensional body would be least likely to be invalid. The calculated anomaly and body shapes were produced by non-linear optimisation (subroutine CB-OPTIMAG, Appendix C 4.3). They are shown in fig. 4.16. It was necessary to use three bodies to obtain a good fit of the calculated to the observed curve. The top surfaces of the bodies were limited in the amount by which they could vary their position, so that they conformed to the shape of the basement obtained from gravity and seismic interpretation. All parameters were optimised non-linearly.

The intensities of magnetisation and the dips of the magnetisation vector obtained for the model are much what one might expect from the measured susceptibilities and remanent magnetisations of lavas from St. Vincent (Khan, 1968). The mean susceptibility measured by Khan on St. Vincent was 0.0016 cgs, and the mean remanent magnetisation was 0.00262 emu cm^{-3}. Masson Smith and Andrew (1965) obtained a mean of in situ measurements of the magnetisation of 0.005 emu cm^{-3}.

The model does not quite match the short wavelength parts of the anomaly, and there must be some near surface changes in magnetisation, or small structures that could arise from intrusions and lava flows. The west side of the model is negatively magnetised and relatively uncomplicated, whereas the east side is negatively and positively

4.16 A model of the magnetised bodies causing the magnetic anomaly over the island arc at latitude 13° 04' N. The angles of dip of the magnetisation vector in the bodies are (from left to right) -55.3°, -113.4° and 78.2°.

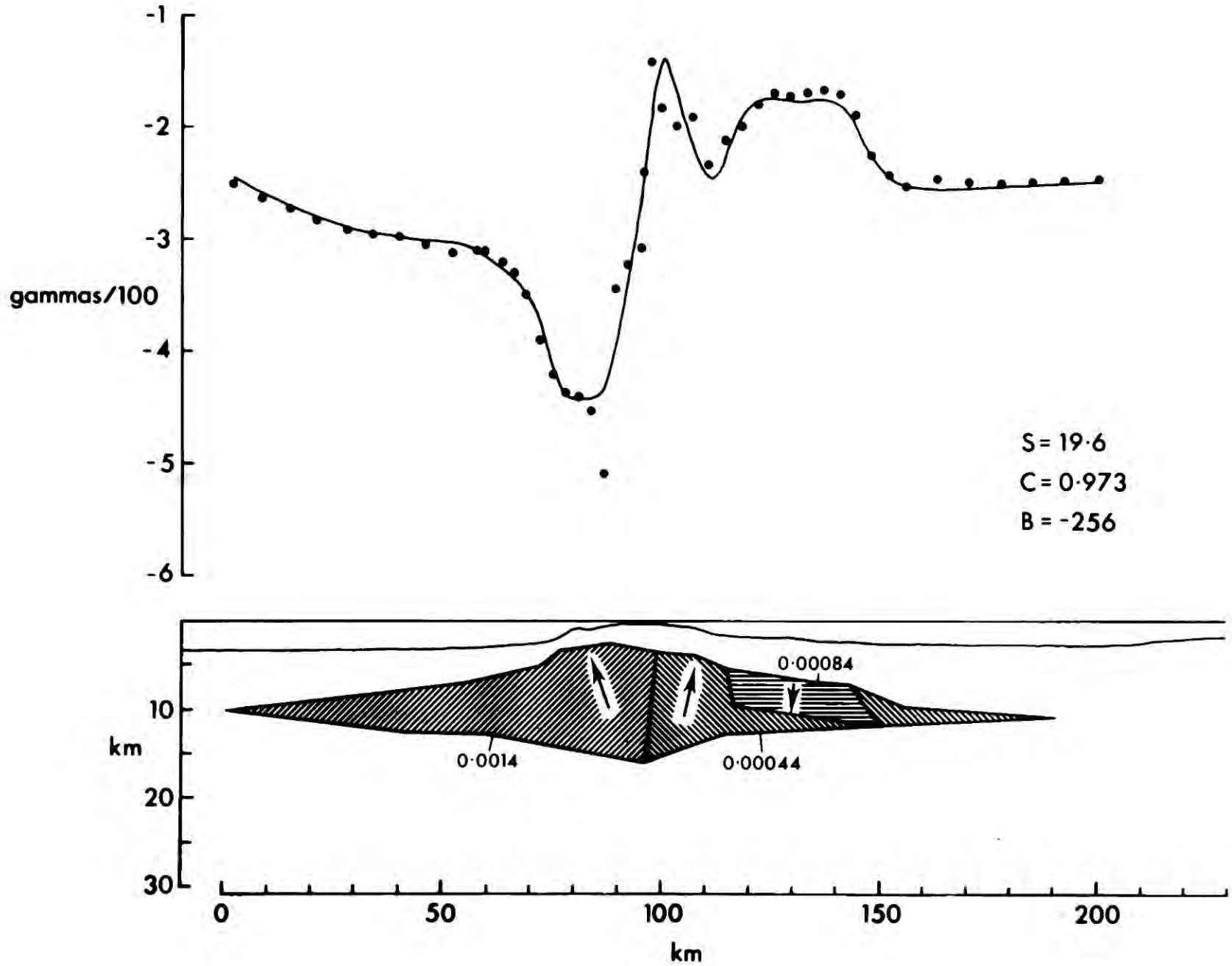
-1
-2
-3
gammas/100
-4
-5
-6
S = 19·6
C = 0·973
B = -256
0·00084
0·0014
0·00044
10
km
20
30
0
50
100
150
200
km

magnetised and fairly complex. The shape of the most strongly magnetised part of the east side of the model is fairly arbitary and as the anomaly to which it is matched is not very linear it can only be taken as a body of different magnetisation without too much significance being placed on its shape.

Along the west side of the island arc the magnetic anomaly is consistently negative, increasing in amplitude from the Grenada Trough towards the centre of the arc, where short wavelength anomalies occur. East of the arc, the anomalies vary, being sometimes positive overall and sometimes negative. Line 10 at lat. 13° 34' N (fig. 4.17) shows an overall negative anomaly produced by the arc disturbed at the centre by a positive anomaly with many short wavelength components. The data of Bunce and others (1971) indicates the persistence of the anomaly on the west side of the arc as far south as lat. 12.7° N, and its absence at lat. 15.6°N.

Magnetics to gravity transformation

Another approach to the interpretation of the magnetic anomalies is to derive a pseudo-gravity anomaly from the magnetic anomaly and use this as an indication of the structure of the magnetised rocks. The transformation was accomplished using a program (TR/MG) written by Ingles (1971). This program first calculates the equivalent layer that will give the observed magnetic anomaly by a matrix solution. The depth to the layer its thickness, the widths of the blocks making it up and the magnetisation direction are specified. The program solves for the intensities of magnetisation in the blocks and the gravity anomaly is calculated by assuming a constant ratio between magnetisation

4.17 Bathymetry and magnetic anomalies on four profiles across the island arc.

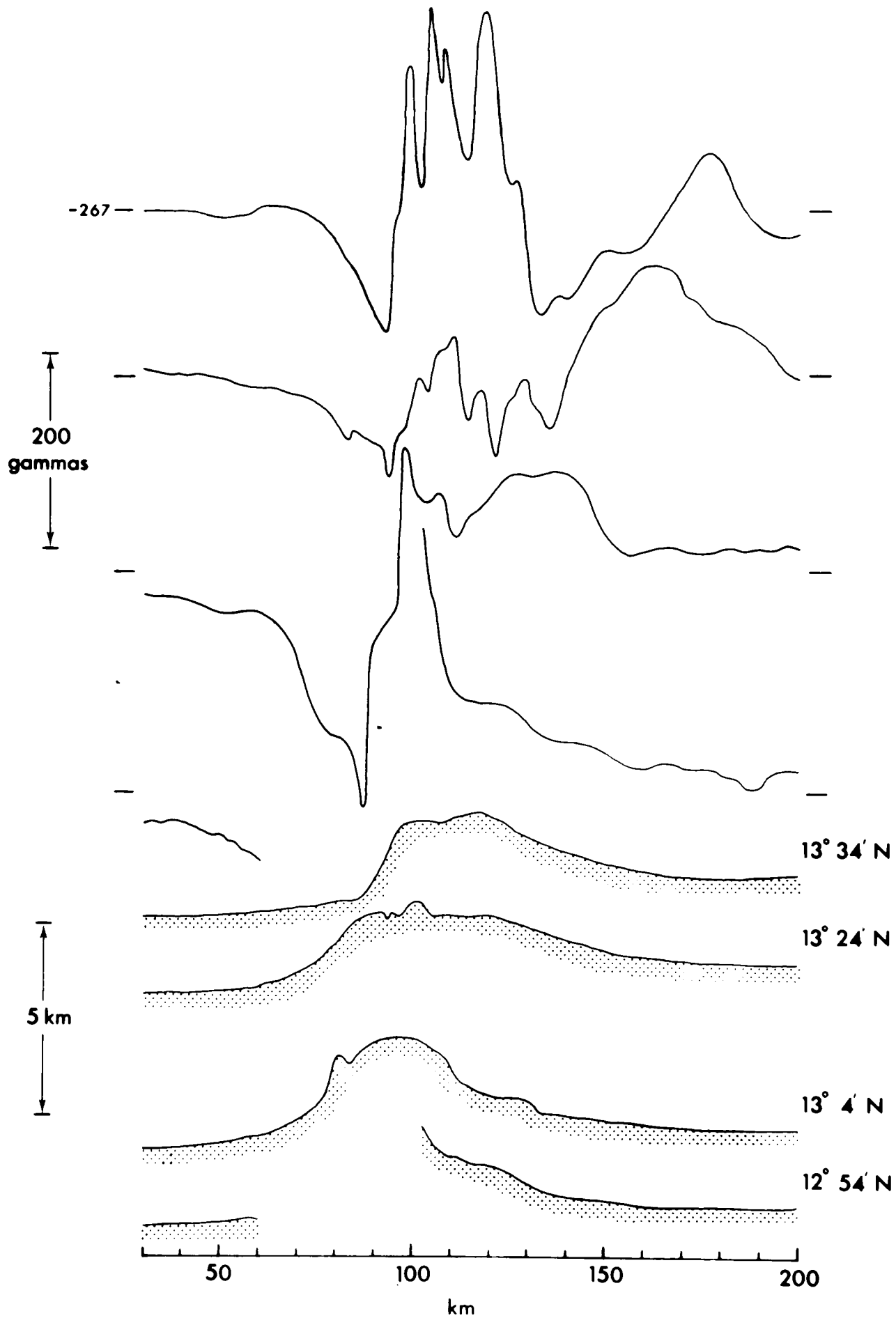
-267
200
gammas
13° 34′ N
13° 24′ N
5 km
13° 4′ N
12° 54′ N
50
100
150
200
km

and density.

The purpose of using the technique here is mainly to determine whether the magnetic anomalies are principally due to variations in the magnetisation of the magnetised rocks or in the shape of bodies of magnetised rock. If the former is the case, then the pseudo-gravity anomalies will be unrelated to the observed gravity anomalies. If the latter is true, then there should be good correlation between the observed and pseudo-gravity anomalies, provided that μ , the angle of inclination of magnetisation vector in the plane of the profile, is known. If the value of μ is known, then the pseudo-gravity anomaly may be used to interpret the shape of the magnetised body with simple gravity interpretation techniques. Conversely μ , the dip of the magnetisation vector in the plane of the magnetic profile, may be estimated by solving to find the value of μ which gives the best correlation between the pseudo and observed gravity anomalies.

The island arc is the only structure in the area of study where the gravity anomaly is caused mainly by rocks which are magnetic. Even so, the relationship between gravity and magnetic anomalies is not a simple one. The gravity anomaly over the arc contains a negative long wavelength component due to the root below the arc, which reduces the apparent amplitude of the anomaly resulting from the upper structure of the magnetic rocks. Also, within the crustal rocks there are igneous cumulates which have a higher density but lower magnetisation than other rocks and consequently a lower ratio of magnetisation to density.

The magnetics to gravity transform was applied to four lines

across the arc at latitudes 13° 04', 24', 34' and 44' N. The top of the equivalent layer was at a depth of 1 km, and the bottom at 6 km. The block widths varied from 2 to 4 km, depending on the spacing of the data points. The pseudo-gravity anomaly was compared with the Bouguer gravity anomaly (density 2.0 gm cm^{-3}) by the program CLTOR (appendix C4.5), which found the correlation coefficient between the two anomalies, and by regressing the pseudo-gravity anomaly on to the Bouguer anomaly found the ratio of magnetisation contrast to density contrast.

Correlations between the pseudo gravity anomaly and the observed gravity anomaly were found to be poor for magnetisation directions in that of the Earth's field. The correlation coefficient was 0.088 for the line at 13° 34' N and -0.090 for the line at 13° 04' N which implies no significant correlation. The angles of μ were varied to find the best correlation, and for the line at 13° 34' N it was found to be -70° with a correlation coefficient of 0.759 which could be taken to indicate a fairly strong connection between the two anomalies. The result is, however, dependent on the number of paired values of the two anomalies included in the correlation. The value of -70° for μ was obtained on 72 points across the arc. A correlation coefficient of 0.771 was obtained for an angle μ of -60° when 93 data points were used, extending the section included in the correlation further east. The length of record used for calculating the pseudo gravity anomaly was longer than the section over which correlation was obtained. Fig. 4.18 shows the gravity, pseudo-gravity, and magnetic anomalies on the lines at latitudes 13° 24', 13° 34', and 13° 44' N for the optimum value of μ . The angle of magnetisation giving the

4.18 Comparisons of the magnetic anomalies, the Bouguer gravity anomalies and the magnetic-gravity transform on three lines across the island arc between St. Lucia and St. Vincent. C is the correlation coefficient between the Bouguer anomaly and the magnetic-gravity transform. D is the dip of the magnetisation Values of the gravity on the left hand scale are indicated by G, magnetics by M.

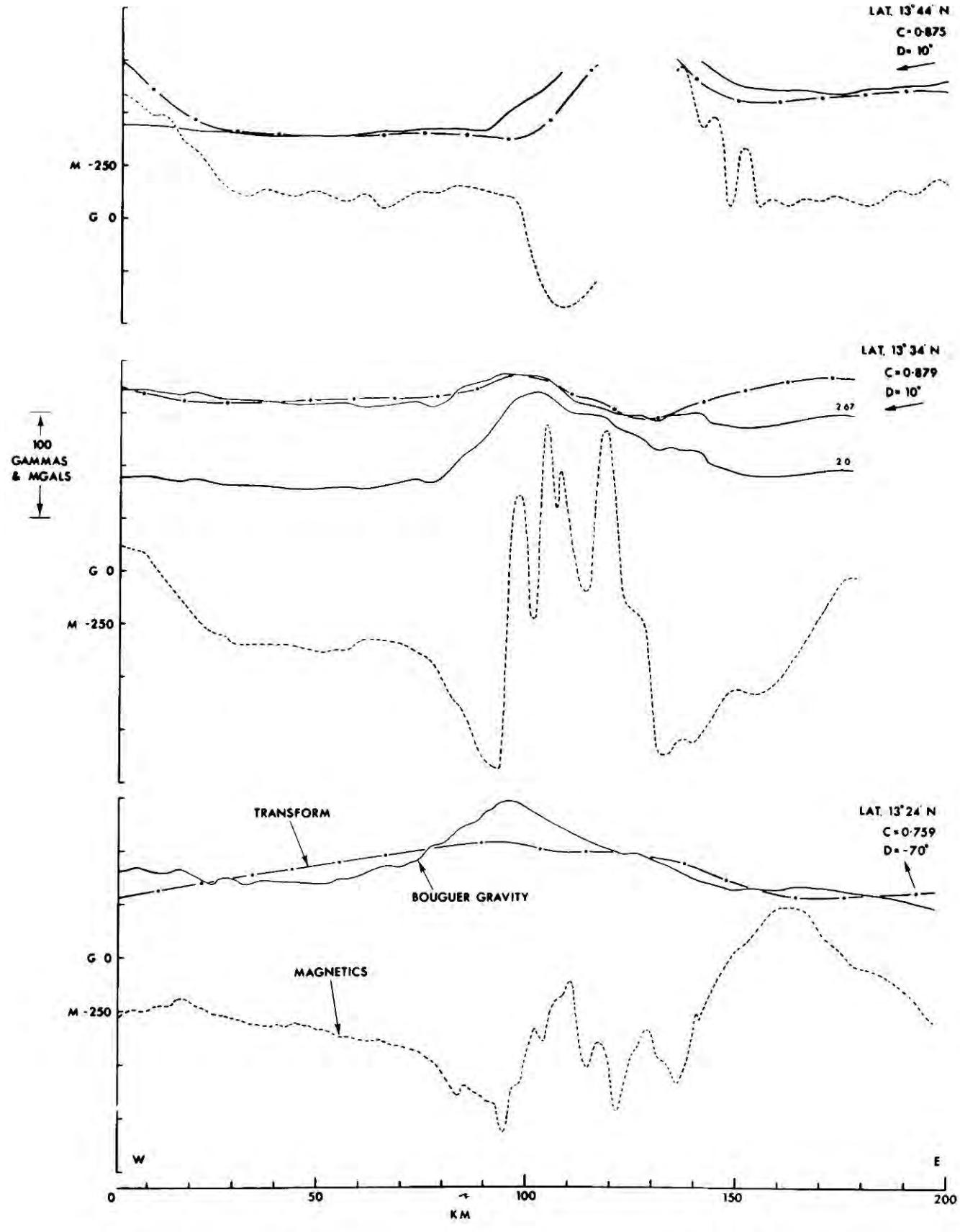
LAT. 13°44' N
C=0·875
D= 10°
M -250
G 0
LAT. 13°34' N
C=0·879
D= 10°
2·67
2·0
100
GAMMAS
& MGALS
G 0
M -250
TRANSFORM
LAT. 13°24' N
C=0·759
D= -70°
BOUGUER GRAVITY
G 0
MAGNETICS
M -250
W
E
0
50
100
150
200
KM

giving the maximum correlation coefficient for line at 13^{o} 34' N and 13^{o} 44' N is 10^{o}. For the line at 13^{o} 34' the maximum value of the correlation coefficient was obtained with the Bouguer anomaly for a density of 2.67 gm cm^{-3}. The correlation coefficient for the 2.0 gm cm^{-3} anomaly is 0.409. This result implies that the magnetic rocks are more dense than 2.67 gm cm^{-3}. This is possible, but the other lines analysed give better correlation with the 2.0 gm cm^{-3} anomaly. The influence of sediment structure and the crust/mantle interface was not included in the analysis and this may be unduly affecting the correlations.

The ratios of magnetisation contrast to density contrast obtained were 0.0043, 0.0200 and 0.0054 for the lines at 13^{o} 24', 13^{o} 34' and 13^{o} 44' N respectively. If we assume that the magnetic anomalies are principally due to basement rocks of density 2.8 gm cm^{-3} (contrasts of 0.8 gm cm^{-3} for the 2.0 gm cm^{-3} Bouguer anomaly and 0.13 gm cm^{-3} for the 2.67 gm cm^{-3} Bouguer anomaly) then the values of magnetisation are 0.0034, 0.0026, and 0.0043 emu cm^{-3}.

These results are reasonable, but the correlations are not very good, and really only show that there is an overall association between the gravity anomaly and magnetic anomaly produced by the arc. Individual anomalies do not show good correlation and it is clear that the structure of the magnetic rocks is not the only cause of the magnetic anomalies. This is brought out by the dependence of the correlation coefficient on the number of data points included in the analysis. Using a different section of record, a different angle of magnetisation can be obtained. Correlation is worst on the east side of the arc, and from this it may be inferred that the anomalies there are mainly due to

variations in the direction and intensity of magnetisation. This could be the result of the multiple intrusion and extrusion of magnetic rocks over a comparatively long period.

The values of μ obtained are probably not of great significance in view of the probably large number of magnetic bodies which are involved, but it does seem likely that many of them have a strong horizontal component. A good correlation may have been obtained on the line at lat. 13^{o} 44' N because the central section was missing and the short wavelength anomalies which are so prominent on the other lines, and clearly from a different source to the anomaly over the west side of the arc, were excluded from the analysis. If the central anomalies are of a comparatively young age, then the older rocks may be those with an almost horizontal magnetisation which may be significant in view of the low angles of magnetisation obtained for the magnetic basement below Barbados. Even so, the form of the magnetised rocks can be modelled quite realistically without recourse to using a horizontal vector, as was shown above for the profile at latitude 13^{o} 04' N (fig. 4.16).

Spectral analysis of the magnetics

In order to overcome the ambiguity between the effects of structure, and magnetisation direction and intensity on magnetic anomalies, a technique which is virtually independent of these effects was applied to the magnetic records. The method used calculates the depth to the magnetic basement from the slope of the one dimensional power spectrum of the magnetic anomaly. This was investigated and developed by M. K. Lee (1972), whose program package was used to

analyse the records. The method will not reveal the shape of the magnetic rocks, but will give an average depth to them over the length of the profile. In theory this profile should be infinitely long, but in practise it need only be several times longer than the longest wavelength component of the sampled anomaly. The choice of profile length needs some care. The length of the lag window must be such that it will sample all the frequencies present, yet it should not be greater than 20% of the total length. Lee showed that the smaller the lag window length is, the closer the calculated estimate of the power spectrum is to the theoretical one.

In the area studied, where the depth to magnetic basement may vary considerably, the shorter the profile is the less ambiguous is the result as to what area of basement is at what depth. If the profile is too short, the method becomes inaccurate. Taking these factors into consideration the method was applied to several profiles, using a Hanning window of length 0.2 of the profile length. The results are shown in fig. 4.19.

Over the island arc the results are satisfactory; the depth estimates being a little greater than the water depth. In the rest of the area they are less encouraging. The north-south line at longitude 57° W yields an estimate of 4.8 km for the basement depth, which is the depth of the water, and seismic evidence shows the probable magnetic basement to be 2 to 3 km deeper. Similarly, in the region of the Tobago Trough, the estimates of the depth to magnetic basement are shallower than might be expected from seismic results, by 3 to 5 km. The most southerly line east of Barbados gives 9.8 km which is probably a good average value, but still likely to be a slight under

4.19 Map showing the depths to the magnetic basement obtained from analysis of the power spectra of the magnetic anomalies along the lines indicated.

DEPTHS TO MAGNETIC BASEMENT FROM SPECTRAL ANALYSIS

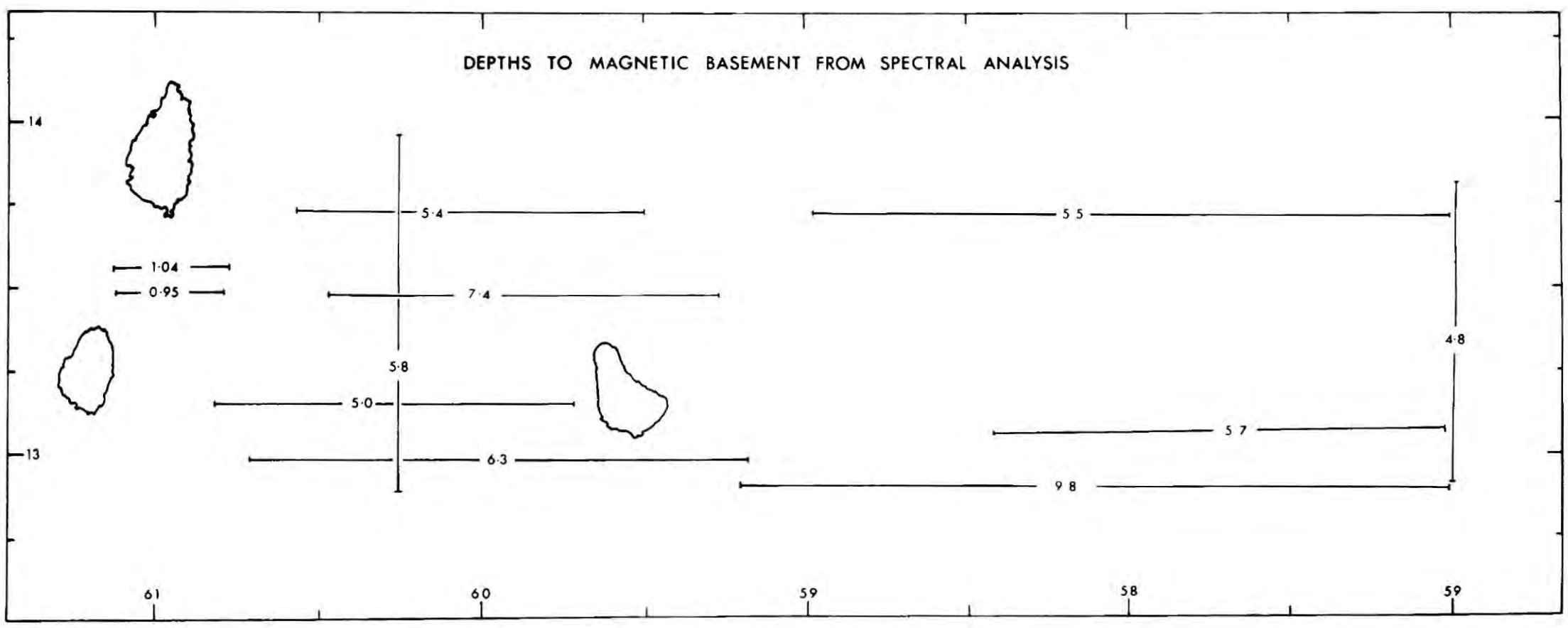

estimate. Lines further north seem far too low.

The underestimation of the depth to magnetic basement is probably due in part to the presence of short period fluctuations in the records caused by solar magnetic disturbances that were not completely removed during the reduction of the magnetic data. Because of this the lines that were used were those which were run on magnetically quieter days, but some disturbances remain. There are a few fluctuations in the horizontal field with periods of 40 to 80 minutes and amplitudes of up to 10 gamma on the magnetograms for the days used. If these remained uncorrected they would appear on the magnetic profiles as anomalies with wavelengths of 14 to 30 km and amplitudes up to 7 gamma, which would effect the power estimate for the first four wave numbers, from which the depth is estimated. A rough estimate of the power in some of the disturbances compared with the power in the first 4 wave numbers shows that there could be a noticeable effect leading to an underestimate of depth of about 10%. This is not as great as the apparent error observed. Taking for example the line at longitude 57°W, from seismic refraction the basement is expected at a depth of 8 km, but the power spectrum of the magnetics puts it at 4.8 km. Lee (1972), however, obtained a depth estimate of 3 km from the power spectrum of a basement model at 5 km. He attributed the discrepancy to an incomplete representation of all the frequencies in his basement model, which should contain all frequencies at equal amplitude. This may be the reason for underestimation here. Also there is the possibility of higher magnetic sources than the igneous basement. A possible high level body in the Barbados Ridge was discussed in the section of sediments.

The spectral analysis has been of some use in giving a rough idea

of the variation of the depth of the magnetic basement. It has not provided an accurate method of estimating the depth, except where the magnetic basement is close to the surface, such as over the island arc.

Combined interpretation.

This took the form of two dimensional modelling to fit the gravity anomaly, in which the parameters of the model were constrained to conform with seismic measurements, and to a lesser degree with the magnetic interpretation. The shape of the body was found by non-linear optimisation using the subroutine OPTIGRAV (appendix C4.4) in conjunction with MINUIT.

Three lines were chosen for study of the structure across the region. These were at latitudes 12° 54' N, 13° 04' N, and 13° 24' N. Lines further north were not used, because east-west structures, which are analysed below, lessen the validity of two dimensional interpretation. In the Tobago Trough lines chosen for interpretation run along or close to the seismic reflection profiles, and the LASP seismic refraction line crosses them diagonally.

The anomaly used for interpretation was a Bouguer anomaly, taking into account the two dimensional effect of the bathymetry, calculated for a sediment density of 2.1 gm cm^{-3}. The model was derived by calculating the departure of the crustal structure from that of the Atlantic Ocean east of the Lesser Antilles, which was taken as the standard section. The Bouguer value over the ocean was subtracted from the Bouguer anomaly over the area studied to give the anomaly

relative to the standard section. In obtaining the Bouguer anomaly over the ocean, use was made of gravity and bathymetry measured across the Atlantic at lat. 13° N by HMS VIDAL on the NAVADO project. The gravitational effect of the low velocity sediments (1.7 km s^{-1}) in the Tobago Trough was removed from the anomaly by calculating the anomaly due to them with GRAVN (Bott, 1969) with body points derived from the seismic reflection lines. The density assigned to the sediments for this calculation was 1.8 gm cm^{-3} (Horn, Horn and Delach, 1968).

The densities used in the model were derived from the seismic velocities using the empirical curves of Ludwig, Nafe and Drake (1970), and Horn, Horn and Delach (1968). The structure was modelled using layers with the densities and velocities as follows:-

layer	velocity (km s^{-1})	density (gm cm^{-3})
water	1.5	1.04
unconsolidated sediment	1.7	1.8
semi-consolidated sediment	2.5	2.1
consolidated sediment	4.0	2.4 or 2.5
igneous crust	6.8	2.9
upper mantle	8.1	3.3

The effect of the interfaces between the first three layers was already incorporated in the anomaly before it was presented to the program. The velocity of 2.5 km s^{-1} for the semi-consolidated layer is a good average of those obtained in the upper sedimentary layers, and the density of 2.1 gm cm^{-3} which corresponds to it on the empirical curve is also that estimated to be the best Bouguer correction density by Nettleton's method. Layer 2 of oceanic crust was omitted from the

analysis, because it was not detected seismically and its fairly constant thickness will give it little anomalous effect on the gravity at the depth which it is at. In the region of the island arc the velocities obtained in the igneous crustal layer were about 6.4 km s^{-1} and a density of 2.8 gm cm^{-3} was used for much of the crust below the arc.

The gravity models are quite complex with many body points. If the number of parameters to be varied for a model is large then the time for computation can become very long (>20 minutes), and because of this, the model computations were done in two parts. First the anomaly from the Lesser Antilles to the Atlantic was fitted, and in this run the shape of the island arc was included as a fixed body estimated from the seismic measurements. In the second part the anomaly across the island arc was fitted with the shape of the structure east of the Tobago Trough determined by the first computation included as a fixed body. The body points in the region of the Tobago Trough were variable in both computations.

The amount by which any body point in a model could vary in the x or z direction was limited so that it would conform to the estimates of the position of the layer of which it was a part, obtained from seismic refraction. East of Barbados, the position of the oceanic crust was controlled by the results of LASP (h1). Between the island arc and Barbados, the top of the igneous crust was bounded so that the dip of it would not be less than that obtained from LASP, assuming an average overburden velocity of 3.5 km s^{-1}. The top of the 4.0 km s^{-1} layer was bounded to conform to the shape observed on the seismic reflection profiles, where it was detected. Over the Barbados Ridge

4.20 Cross sectional model across the area at latitude 13° 04' N, derived from gravity and seismic data. Dots are the observed gravity values. The continuous curve is the calculated anomaly. Bodies of different density are shown by different ornament, with the values indicated. The short bars below letters and figures such as e17w indicate the depths of layers determined from seismic refraction lines by Ewing and others (1957), see fig. 3.1 and appendix 3.1. S is the standard error of the fit. C is the correlation coefficient.

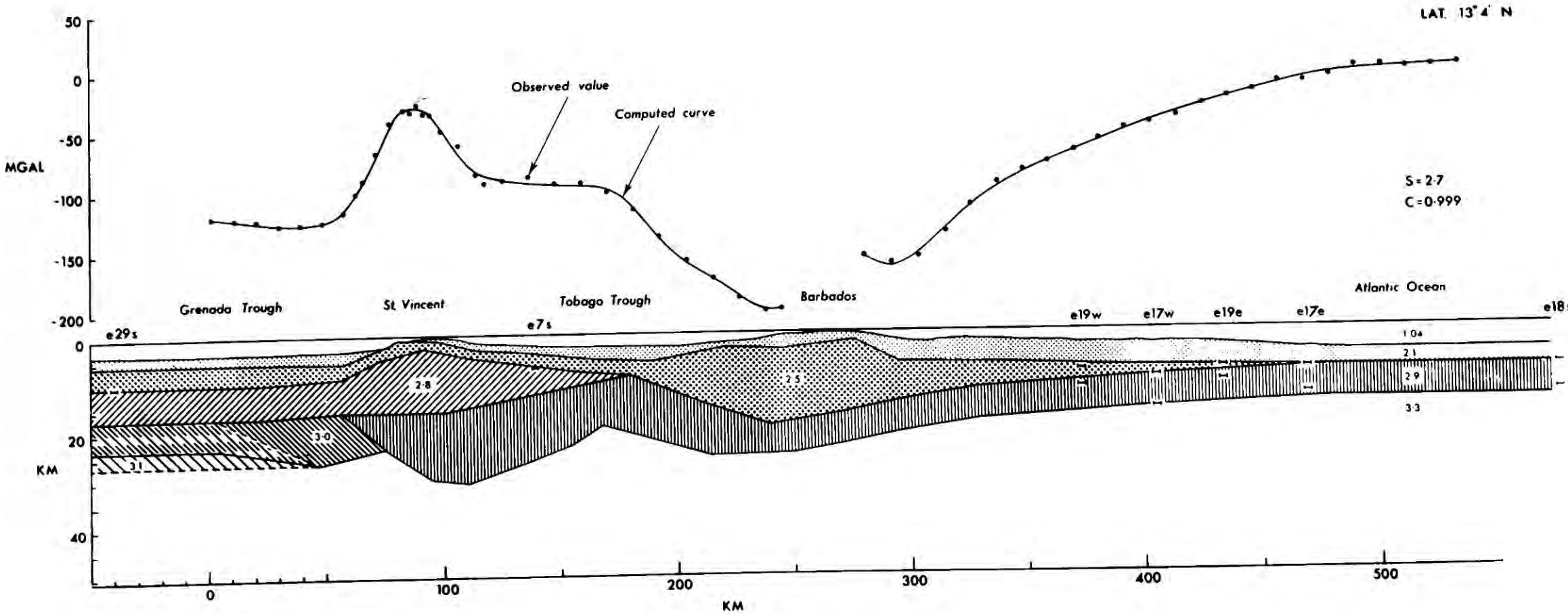
LAT. 13°4' N
Observed value
Computed curve
S = 2·7
C = 0·999
MGAL
50
0
-50
-100
-150
-200
Grenada Trough
St Vincent
Tobago Trough
Barbados
Atlantic Ocean
e29s
e7s
e19w
e17w
e19e
e17e
e18s
1·04
2·1
2·9
3·3
2·8
2·5
3·0
3·1
KM
20
40
0
100
200
300
400
500
KM

the top of the 4.0 km s^{-1} layer was given an upper bound from the refraction data of Ewing and others (1957). Estimates of Moho depths obtained by time term analysis of the refraction data from LASP (C. Boynton, personal communication) were used in the Tobago Trough region. Body points were not constrained too rigidly to these estimates, because the time terms were determined only from stations on the volcanic islands. Except east of Barbados, body points along the Moho were allowed a large variation in position.

The Barbados Ridge area

In modelling this region, with the bounds placed on the structure by seismic data as given above, difficulty was encountered in obtaining a model that would fit the anomaly when a density of 2.4 gm cm^{-3} was used for the 4.0 km s^{-1} layer. The calculated anomaly fell below the observed by about 30 mgal over the ridge, with the basement at a maximum depth of 17.5 km. The intercept time for the seismic refraction station at St. Phillip's on Barbados indicated that the depth to the basement below it was at least 20 km. In order to fit the anomaly it was found to be necessary to increase the density of the 4.0 km s^{-1} layer to 2.5 gm cm^{-3}. Although this no longer falls on the median curve drawn through the points of the empirical curve of Ludwig, Nafe and Drake (1970) it is still well within the scatter of points and does not seem an unreasonable figure.

The models are shown in figs. 4.20 and 4.21. These show the basement depressed below the Barbados Ridge and the consolidated sediment rising up to a high level within the ridge. 45 km south of Barbados a seismic velocity of 4.9 km s^{-1} was detected at a depth of

4.21 Cross sectional model across the area at latitude 13° 24' N, derived from gravity and seismic data.

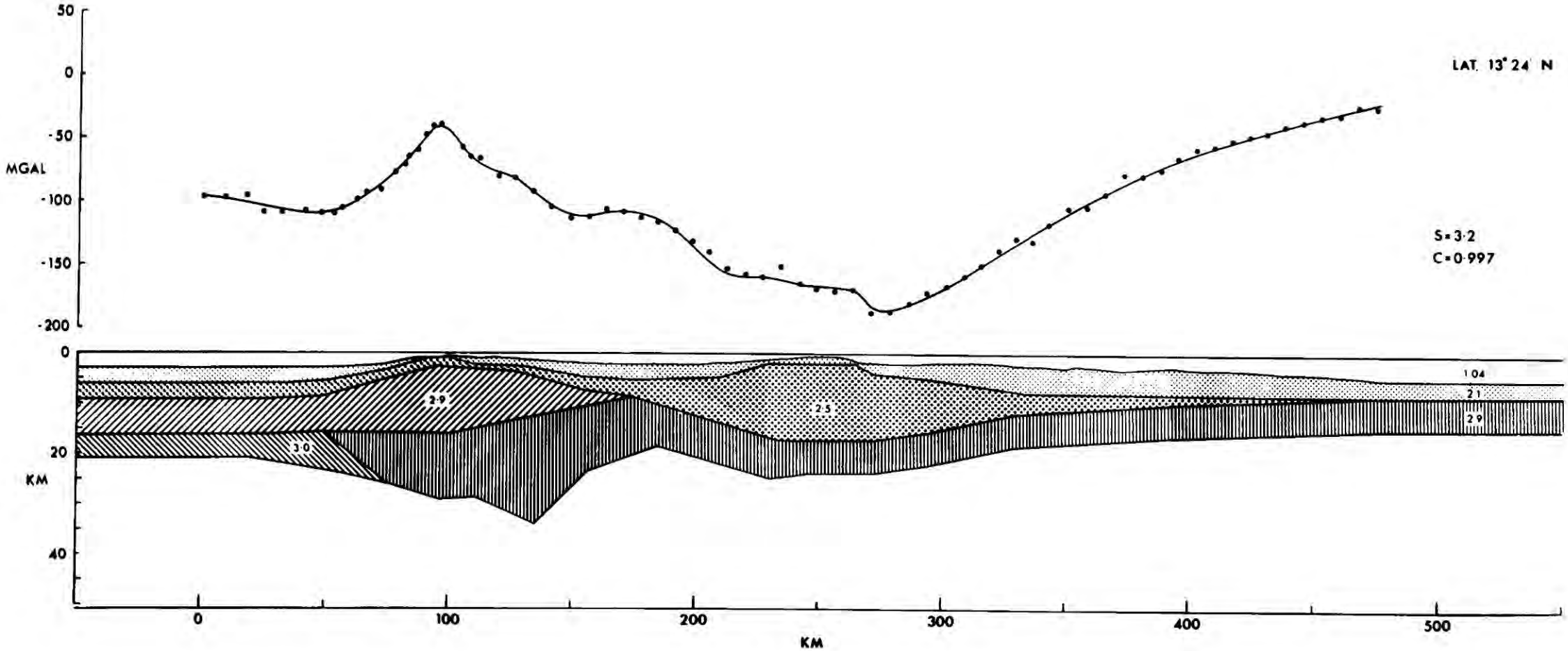
LAT. 13° 24' N
S=3·2
C=0·997
MGAL
50
0
-50
-100
-150
-200
KM
0
20
40
2·9
3·0
2·5
1·04
2·1
2·9
0
100
200
300
400
500
KM

4.7 km (E22). It is not clear whether this occurs beneath Barbados or not. It does not seem to be present further north (E6, fig. 3.1). To find the effect of this layer if it is present, an additional layer of density 2.6 gm cm^{-3} and thickness estimated by extrapolating the seismic refraction results of Ewing and others (1971), was added to the model. This is shown in fig. 4.22, and the layer is accommodated in the structure without any significant change of the model. The Moho is depressed slightly, west of Barbados, and the top of the consolidated sediments is depressed in part, as compared with the model in which the additional layer was not present. The effect of this additional layer of higher density rock was greater when the consolidated sediments had a denisty of 2.4 gm cm^{-3}. If other parameters are held the addition of the extra layer can depress the basement by 1 km to 2 km.

The two models shown in fig. 4.22 are for the line at 12^{o} 54' N and have the basement dipping under Barbados from the Tobago Trough at the lowest dip estimated from seismic refraction. The gravity anomaly for this model also has subtracted from it the gravity effect of subducted crust (but not the effects from the mantle, see Chapter 5).

In the region of the Barbados Ridge there are some short wavelength anomalies which are not completely accounted for by the models. These are caused by the contrast between the unconsolidated and older sediments in minor structures near the surface. There is not sufficient seismic reflection data to calculate the individual effect of these structures, but the amplitudes of the anomalies they cause are unlikely to exceed 15 mgal. The small basin east of

4.22 Gravity derived model across the Barbados Ridge at latitude 12° 54' N. The effect of adding a layer of density 2.6 gm cm^{-3} beneath the ridge is shown by the dashed lines. Figures indicate the densities of the layers. Dots are the observed gravity values (Bouguer anomaly, 2.1 gm cm^{-3}). The continuous curve is the calculated anomaly. Dashed curve is anomaly with 2.6 gm cm^{-3} layer included. S is the standard error of the fit. C is the correlation coefficient.

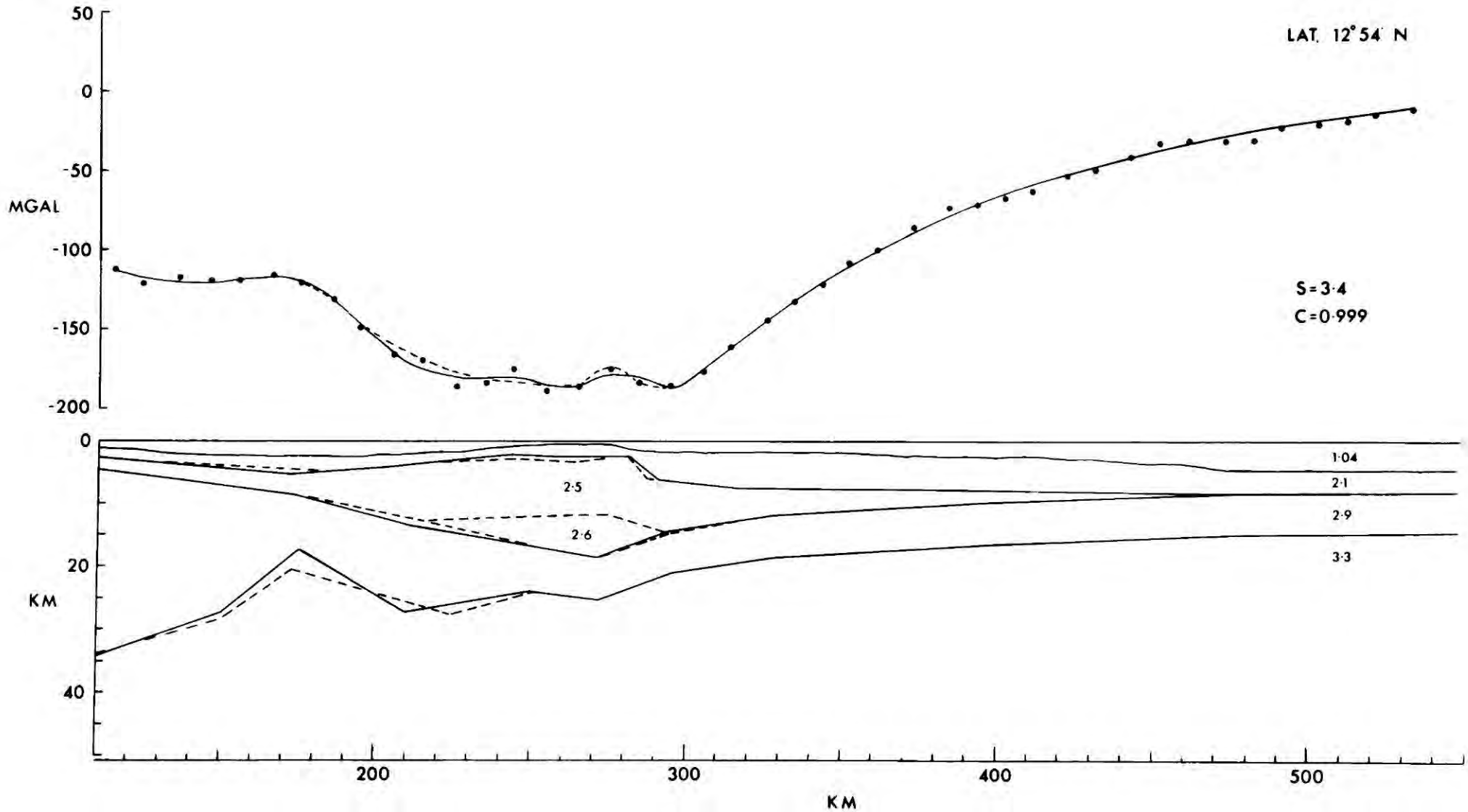
LAT. 12°54' N
S=3·4
C=0·999
MGAL
50
0
-50
-100
-150
-200
KM
0
20
40
2·5
2·6
1·04
2·1
2·9
3·3
200
300
400
500
KM

Barbados produces a negative anomaly which steepens the gradient on the long wavelength anomaly resulting from the whole Barbados Ridge structure.

A common feature of the crustal models is the rise of higher density sediments in the Barbados Ridge. This rise has an asymmetrical shape, with steeper dips of the top surface on the eastern side. The amount by which it is raised above material of the same density either side is about 5 km and this amount of tectonic uplift is about what might be expected from the surface exposure of the Oceanic Formation of Barbados which was probably deposited at normal oceanic depths.

The point of deepest depression of the igneous basement, where from the earthquake activity of the region subduction of the Atlantic Ocean crust is expected (see chapter 6), is situated below the axis of the Barbados Ridge.

The depth to the basement below Barbados appears, from the models and the residual Bouguer anomaly map (fig. 4.25), to lessen from south to north by about two to three kilometres.

The volcanic arc

The crustal models in this region must inevitably be an oversimplification of the true structure. Masson Smith and Andrew (1965) found great variation in the densities measured on the islands and used an average value of 2.5 gm cm^{-3} for their Bouguer correction, except on young volcanic cones where 2.0 gm cm^{-3} was the highest reasonable value. The higher density rocks collected by them had

densities of about 2.8 gm cm^{-3}, which is the value obtained for basement rocks, derived from the seismic refraction velocities (6.3 to 6.4 km s^{-1}). The minimum depth to basement determined by time-term analysis of LASP results was in the range 2.5 to 3.25 km for the two lines considered for modelling. The position of the base of the 2.8 gm cm^{-3} layer is uncertain. It may be at the Moho, but this is unlikely in view of the presence of high density ultrabasic plutonic rocks which are seen at the surface as xenoliths (K. Wills, personal communication) and must form a substantial part of the magma chambers from which the extrusive and hyperbyssal rocks were derived. The lower part of the model was given a density of 2.9 gm cm^{-3}, the same as oceanic layer 3. There is probably no distinct boundary between the 2.8 and 2.9 gm cm^{-3} layers.

The basement in the Grenada Trough has a seismic velocity of 6.4 km s^{-1} (Ewing and others, 1957) and so does the western half of the Tobago Trough (see Chapter 3). The average thickness of the 6.4 layer in the Grenada Trough is 7 km, and this was fixed in the model. The position of the 2.8/2.9 gm cm^{-3} interface is arbitrary, except that the 2.9 gm cm^{-3} layer does not extend into the Grenada Trough, and the 2.8 gm cm^{-3} layer does not occur in the eastern half of the Tobago Trough.

The position of the 2.8/2.9 gm cm^{-3} interface beneath the island arc was varied between models, and the effects of this are shown in figs. 4.23 and 4.24. Depressing the interface has the effect of raising the Moho. The model which is chosen depends on how the development of the island arc is interpreted. If it is considered that the entire volcanic pile lies above the original seafloor and that

4.23 Possible variations in the density model for the island arc at Latitude 13° 04' N.

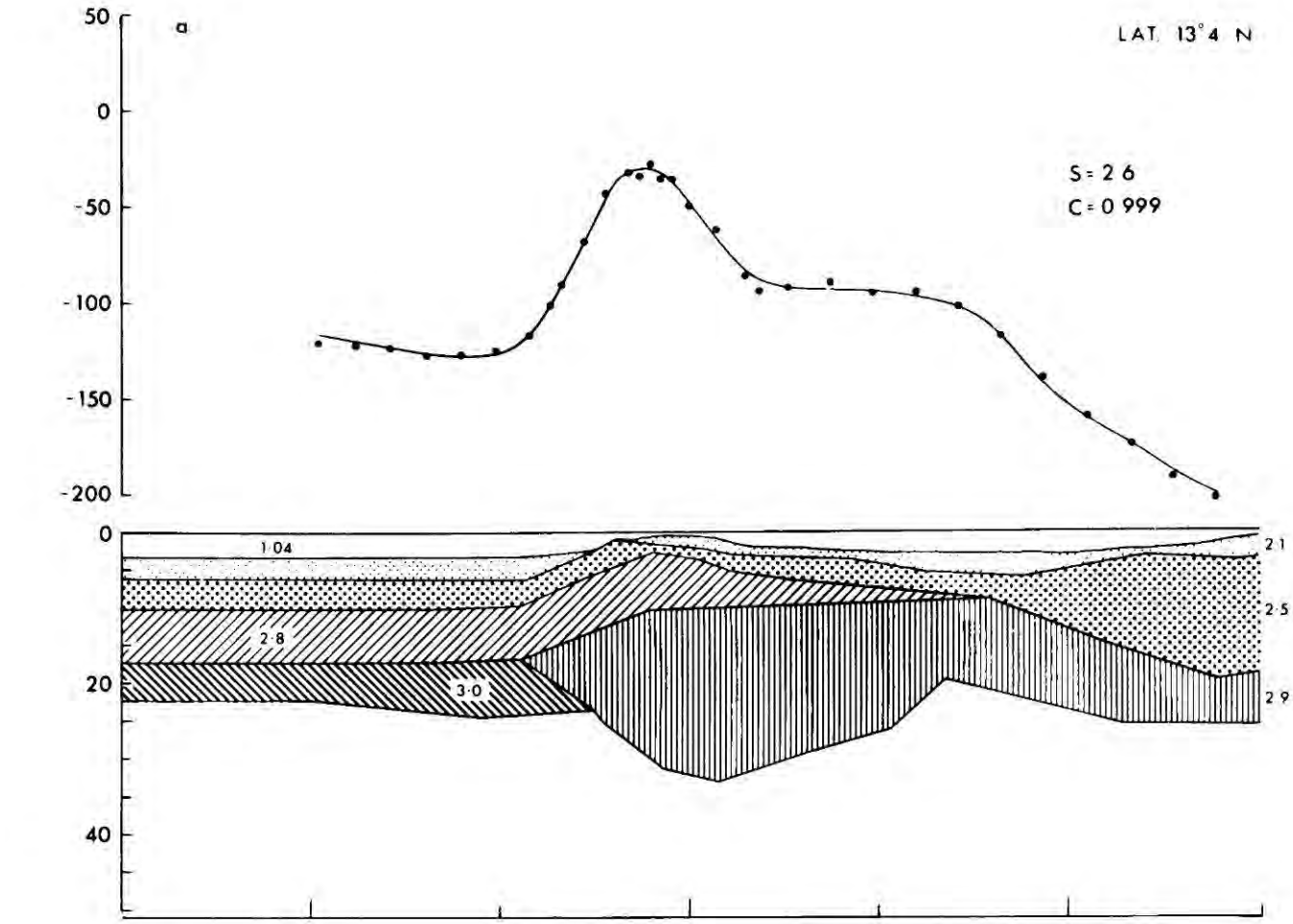
a
LAT. 13°4 N
S = 2 6
C = 0 999
50
0
-50
-100
-150
-200
1·04
2·8
3·0
2·1
2·5
2·9
20
40

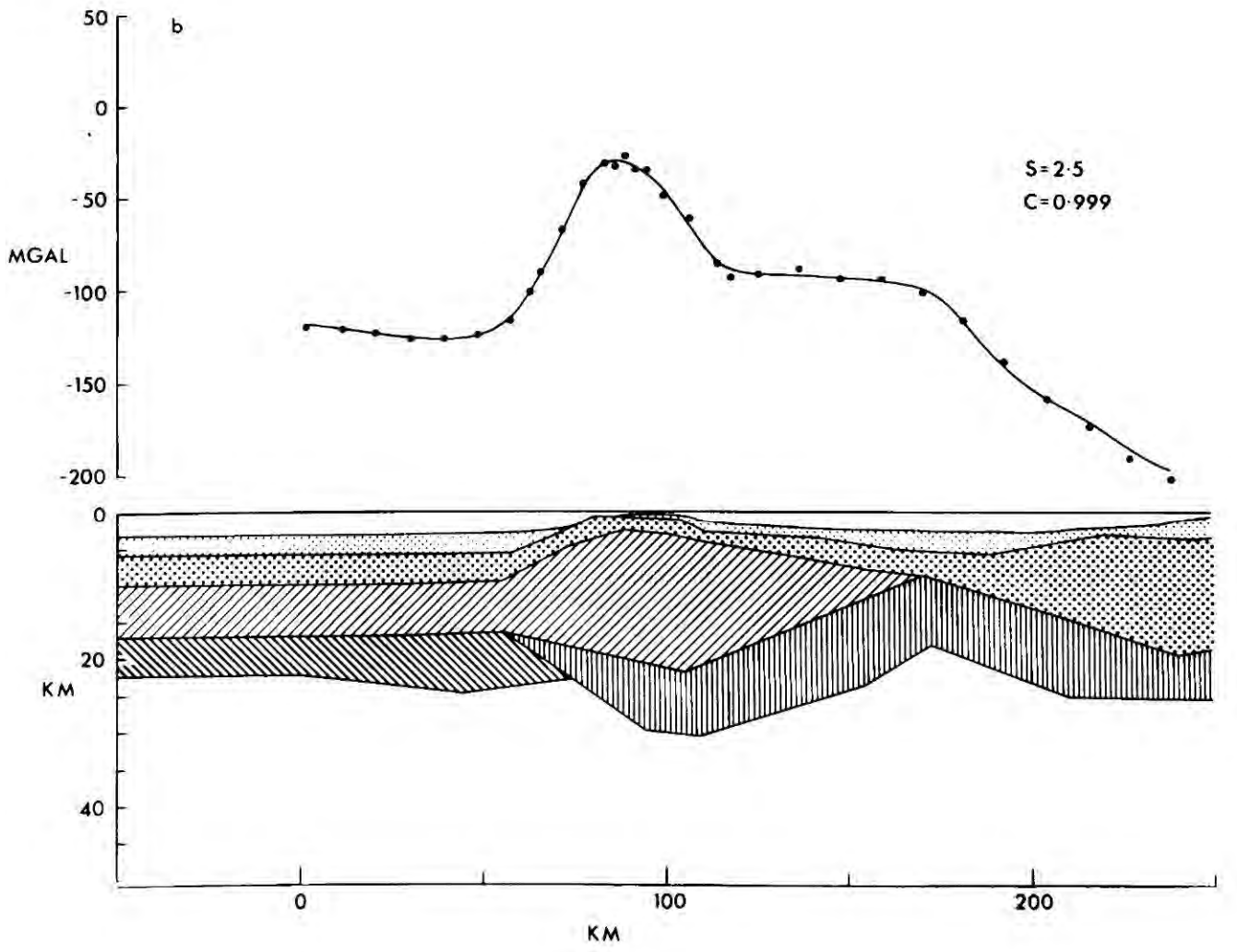
b
S=2·5
C=0·999
MGAL
50
0
-50
-100
-150
-200
20
40
KM
0
100
200
KM

magma chambers exist only within the pile, then an interpretation in which the 2.9 layer is comparatively thin, representing old oceanic crust, and close to the Moho, may be favoured. Alternatively, a hypothesis, in which large volumes of magma were emplaced in and below the original ocean floor and from them the volcanics differentiated, would favour a model in which the 2.9 gm cm^{-3} layer predominated. The deepest point of the Moho calculated by the models ranges from 35 km, in model 4.24a, to 31 km, in model 4.23b. The anomaly is not fitted by model 4.24b as well as the others, and this may imply that model is becoming invalid. The Bouguer anomalies in the centres of the island are 30 mgal higher than over the sea between them and it is possible that the depth to the base of the crust beneath them is greater if they are in approximate isostatic equilibrium.

In the west of the Grenada Trough a layer of seismic velocity 7.4 km s^{-1} exists, which should have a density of about 3.1 gm cm^{-3}. How this layer joins the island arc is not known, but an abrupt change in structure with a marked density contrast is not expected. A density of 3.0 gm cm^{-3} was used for the layer in the east of the Grenada Trough because of this, and consequently in the models the layer is thinner in the west than it probably should be. In fig. 4.21 the effect of giving the western part a density of 3.1 gm cm^{-3} is shown.

Over the arc and on its flanks there are short wavelength anomalies which are not well fitted by the models. These will be due to minor variations in the structure and density of the upper part of the crust. In the islands there are many rocks with densities intermediate to those

4.24 Possible variations in the density model for the island arc at latitude 13° 24' N.

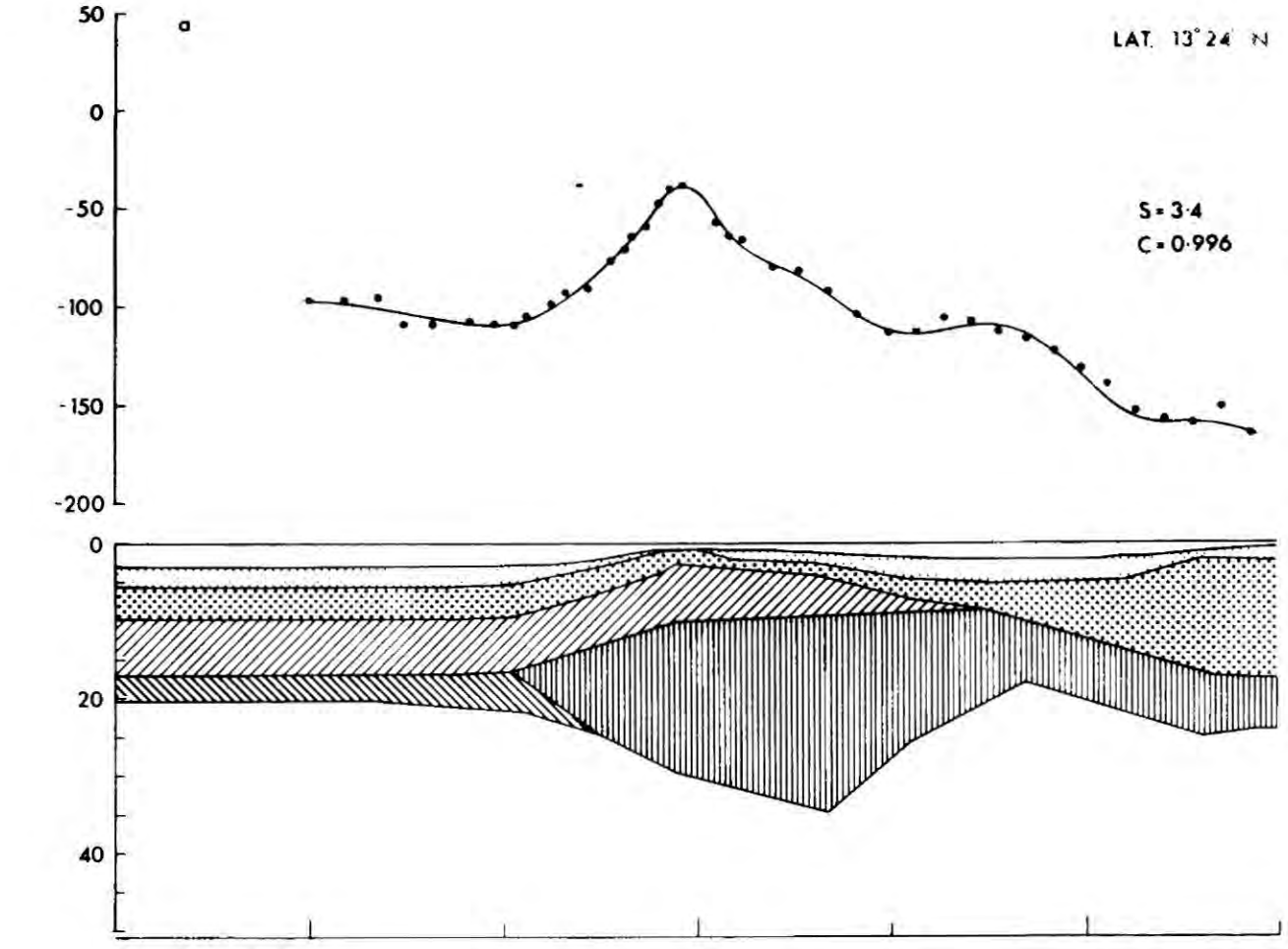
a
LAT. 13° 24' N
S = 3·4
C = 0·996
50
0
-50
-100
-150
-200
0
20
40

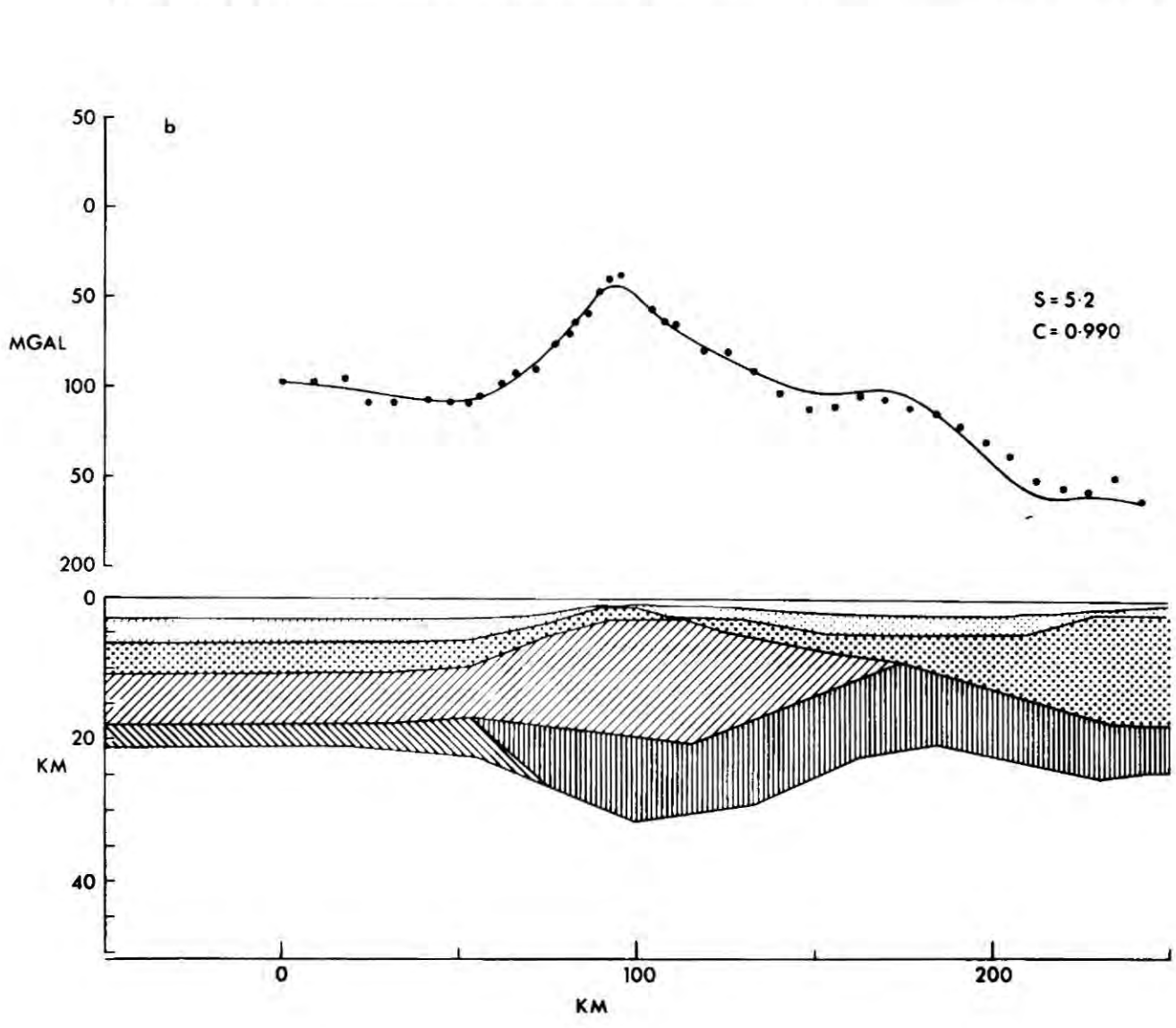
b
S = 5·2
C = 0·990
MGAL
50
0
50
100
50
200
0
20
KM
40
0
100
200
KM

used for the upper two layers of the model. To fit the anomaly on the line at lat. 13° 24' N, the top of the 2.8 gm cm^{-3} layer had to be brought closer to the surface than predicted by the results of LASP (see Chapter 3) at the point where there are acoustic basement rocks in a rise on the west side of the Tobago Trough seen on reflection line H2 (fig. 4.2).

In the Grenada Trough a layer of density 2.6 gm cm^{-3} (velocity 5.3 km s^{-1}) and a layer of density 2.3 gm cm^{-3} (velocity 3.8 km s^{-1}) are represented by a single layer of density 2.5 gm cm^{-3}.

The Tobago Trough

The crustal models show that the Tobago Trough is not formed in a depression of the igneous basement. Its formation is a consequence of the creation and uplift of the Barbados Ridge. The depth to the basement increases from west to east across the Trough. Beneath the centre of the trough the Moho is shallower than beneath the Barbados Ridge or the island arc. The shallowest depth obtained by time-term analysis of the LASP results (C. Boynton, personal communication) was 23 km. The gravity models put it at 19 - 20 km. Nearly all the depths estimated across the trough by time-term analysis are greater than those obtained by modelling to fit the gravity anomaly, though the variation is about the same. This discrepancy may result from the effect of gravity anomalies due to subducted lithosphere on the gravity anomaly used for determining the model. How this may do so is examined in Chapter 5.

The depth of the Moho at the centre of the trough is a little greater than in the Atlantic Ocean and the apparent rise in the Moho

is likely to be the result of the depression of the Moho either side by the Barbados Ridge and the island arc, with centre of the trough most nearly representing the original ocean crust structure prior to subduction and the formation of the Lesser Antilles. The igneous crustal layer east of the centre of the trough is thickened with respect to the Atlantic Ocean crust, but is thin by comparison with that under the island arc.

The St. Lucia East Ridge.

Part of this feature has been described by Bassinger and Keller (1971) under the name Barbados Ridge-St. Lucia Cross Warp. This name is not used here, because the feature is not confined to the region between St. Lucia and the Barbados Ridge, and the term warp has genetic implications.

Between St. Lucia and the northern end of the Barbados Ridge lies a broad saddlelike feature in the bathymetry, which forms the northern margin of the Tobago Trough. The upper sedimentary layers drape gently over the feature in a north-south direction (reflection profile D5 fig. 4.3, and the reflection profiles of Bassinger and Keller, 1971). The depth to a refractor of velocity 5.35 km s^{-1} at the east of refraction line E14, which is a little to the east of the centre of the saddle, is 6.22 km. The Bouguer anomaly maps show that there is a gravity high associated with the feature, which has an amplitude of 50 mgal with respect to the region between St. Vincent and Barbados. The Bouguer anomaly map of Bassinger and Keller confirms that this gravity high is restricted to the East Ridge. The value of the anomaly decreases to the north, but not as steeply as it does

to the south.

A residual Bouguer anomaly map for a density of 2.0 gm cm^{-3} was constructed by subtracting a regional anomaly based on the trend of the contours in the southern half of the 2.0 gm cm^{-3} Bouguer anomaly map from the rest of the map. The resulting map (fig. 4.25) shows well the easterly trend of the anomaly associated with the East Ridge, and what is more it shows that there is an equally pronounced, but smaller amplitude, anomaly east of the Barbados Ridge, with the same trend as that to the west. This can be seen on the ordinary Bouguer anomaly maps, but the residual map brings it out more clearly. The widening of the anomaly over the Barbados Ridge is no doubt the result of a variation in the structure of the Ridge.

In order to determine the nature of the East Ridge several two dimensional gravity models were computed using OPTIGRAV. Two profiles were taken to the east of St. Lucia. One was the north-south line at long. 60° 15' W (fig. 2.1), but this has the disadvantage of crossing diagonally the gradient in the gravity field due to the variations in the east-west structure. To avoid this, another profile was taken at long. 60° 30' W by using the values from the east-west lines at the same longitude. For both profiles the background anomaly was taken as the average value of the two most southerly points, assuming the background over the rest of the Tobago Trough to be comparatively invariant in a north-south direction. The depths to the interfaces between the 2.1 and 2.5 layers and the 2.5 and 2.9 layers were limited by the results of seismic refraction and reflection.

4.25 Map of the residual Bouguer gravity anomaly obtained by removing the regional field, shown by the pecked contours, away from the Bouguer anomaly map with a compensation density of 2.0 gm cm^{-3}.

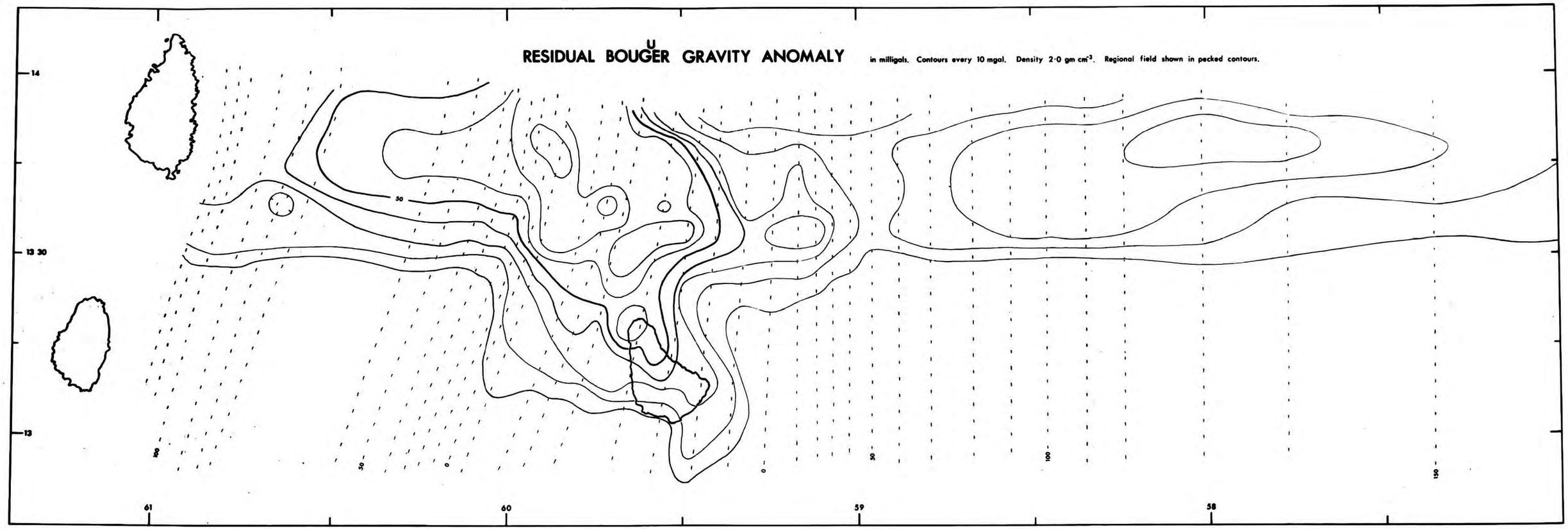
RESIDUAL BOUGUER GRAVITY ANOMALY
in milligals. Contours every 10 mgal. Density 2·0 gm cm⁻³. Regional field shown in packed contours.
14
13 30
13
61
60
59
58
50
0
50
0
50
100
150

The crustal models obtained (fig. 4.26) show a distinct rise in the 2.9 gm cm^{-3} layer overlain by a more gentle flexure of the 2.5 gm cm^{-3} layer. The rise is asymmetrical with its southern faces steeper than its northern ones. The position of the Moho is not defined by seismic work and therefore its influence on the gravity across the structure is not known. Fig. 4.26b shows a model where the Moho is horizontal at its probable minimum depth, estimated from the crustal models across the Tobago Trough further south. When horizontal, the Moho has no effect on the anomaly and is not included in the model. Fig. 4.26a shows the effect of putting a root below the ridge, which is to make the ridge more pronounced. This model does not conform well with the seismically determined depth limits. The comparative body shapes, assuming a root or no root, for the line at long. 60° 30' W are shown in fig. 4.26c. The crustal thickness used for the root models is thinner than expected from seismic data and serves to accentuate the effect of the root. The models in which the Moho was not included as a variable interface give the best fits, but a gentle deepening of the Moho below the East Ridge is quite likely on isostatic grounds.

The shape of the top surface of the igneous part of the ridge might be a little different from that shown in the models because a layer corresponding to the 5.35 km s^{-1} refractor was not included in the model. This was because too little is known about it to do so. The difference in shape would not be significantly large, although it is probable that the surface of the igneous part of the ridge is much more irregular than shown by the model.

The structure of the ridge east of the Barbados Ridge was modelled

4.26 Two dimensional gravity models across the St. Lucia East Ridge at longitudes 60° 15' W and 60° 30' W. Dots are the observed values of the Bouguer anomaly (2.1 gm cm^{-3}). The continuous curve is the computed anomaly. The same ornament indicates the same density throughout the models. S is the standard error of the fit. C is the correlation coefficient.

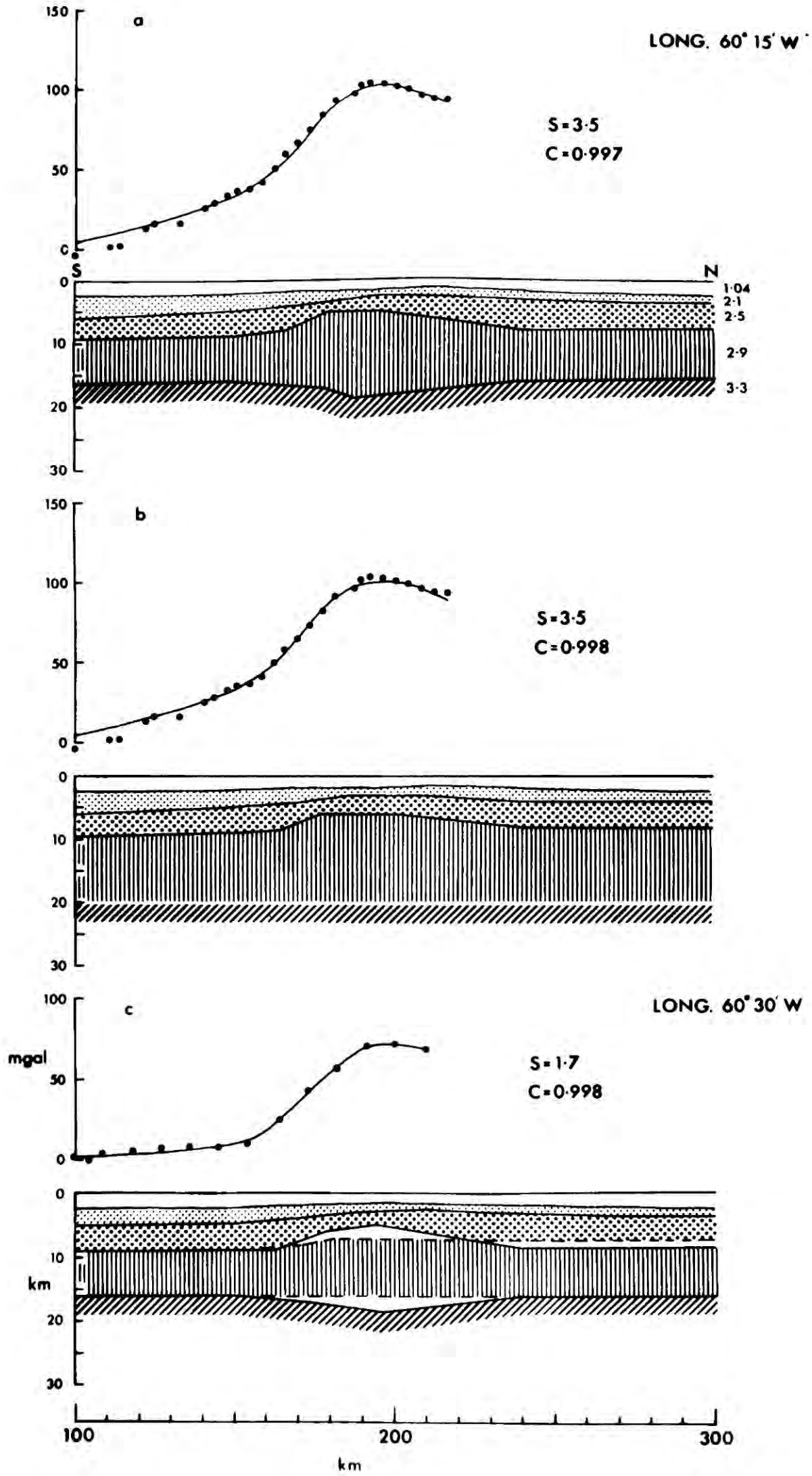
a
LONG. 60° 15' W
S=3·5
C=0·997
S
N
1·04
2·1
2·5
2·9
3·3
b
S=3·5
C=0·998
c
LONG. 60° 30' W
S=1·7
C=0·998
mgal
km
km
150
100
50
0
10
20
30
100
200
300

using the gravity anomaly measured along the north-south line at long. 57° W. This is over flat ocean floor and unaffected by structures in the sediments of the complicated Barbados Slope region. Fig. 4.27a shows a simple model which will satisfy the anomaly, based on seismic refraction results. It is just a rise in Oceanic layer 3. Seismic reflection lines D1 and D2 (fig. 4.3) show what appears to be a rise in the basement 30 km north of the position predicted by the simple gravity model. This is also north of the apparent axis of the residual gravity anomaly. The values of the Bouguer anomaly on the northern edge of the map are, however, probably a little lower then they should be, because the Bouguer anomaly reduction program only took into account the bathymetric relief along the ships tracks which are east-west, whereas there is an appreciable northward deepening of the bathymetry (fig. 1.3) which has a negative effect on the gravity anomaly, that is not corrected for. It is possible, therefore, that the axis of the positive residual anomaly is further north than it appears from the map.

In fig. 4.27b the model used is derived from the structure observed on the seismic reflection line D1 at long. 57° 22' W. The surfaces of the 2.3 gm cm^{-3} and 2.9 gm cm^{-3} layers were fixed at the positions seen on the reflection line, and only the Moho and the top of the 2.9 gm cm^{-3} layer where it was not detected were allowed to vary their shape within the limits set by seismic refraction results. The fit to the anomaly obtained is well within the limits of the accuracy of the measurements, but it is not as good as that in 4.27a. Maybe there is another ridge with smaller relief south of that seen on D1 and not shallow enough to be detected. More gravity data north of lat. 14° N are needed to resolve the structure of the ridge.

4.27 Two dimensional gravity models for the St. Lucia East Ridge extension, east of the Barbados Ridge, at longitude 57^{o} W. Dots are the observed values of the Bouguer anomaly (2.1 gm cm^{-3}). The continuous curve is the computed anomaly. Densities of layers are indicated at the side of the model.

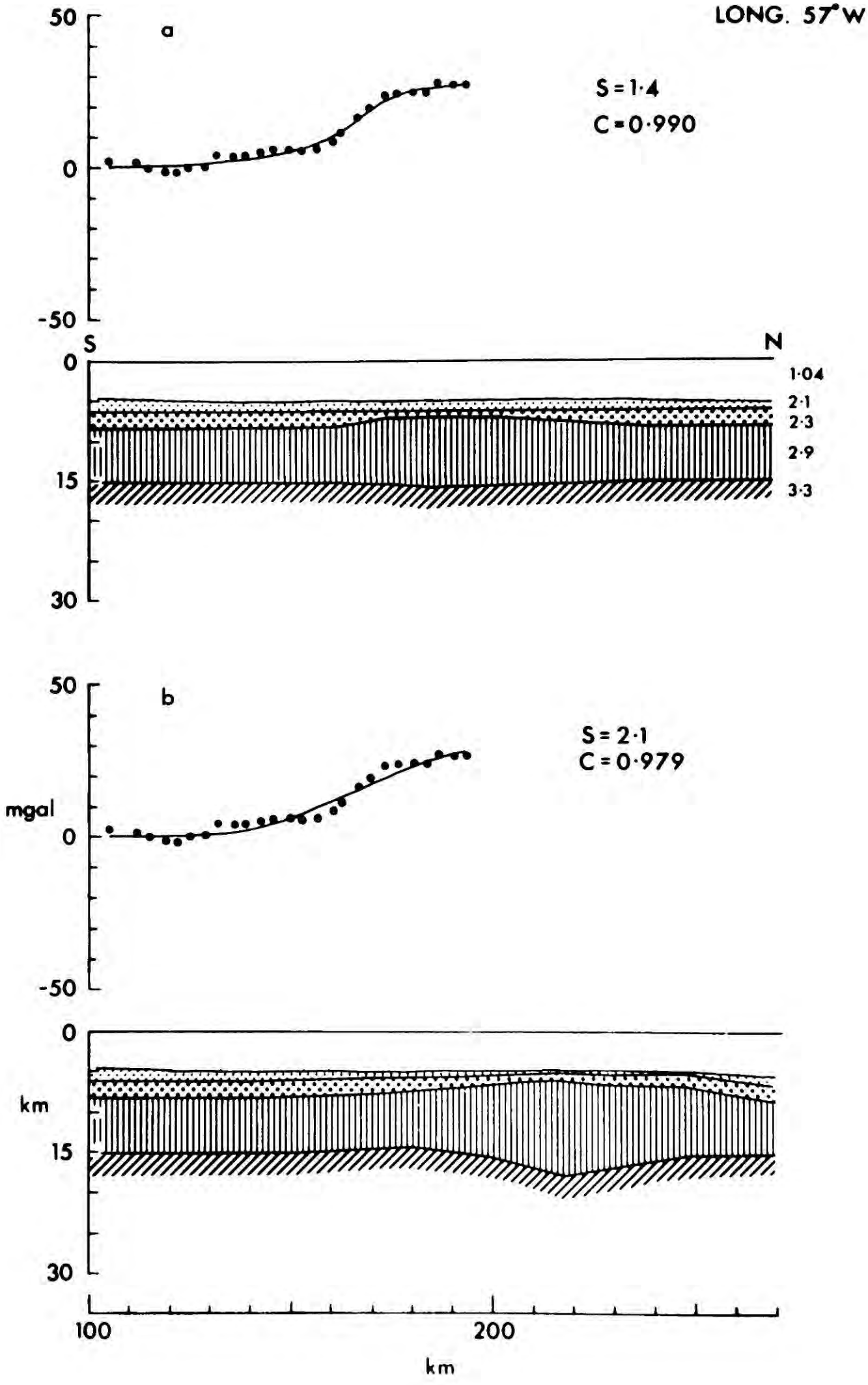
LONG. 57°W
50
a
S = 1·4
C = 0·990
0
-50
S
N
0
1·04
2·1
2·3
2·9
15
3·3
30
50
b
mgal
S = 2·1
C = 0·979
0
-50
0
km
15
30
100
200
km

The St. Lucia East Ridge must post date the volcanic island arc, because there is no trace of a similar feature on the west side of St. Lucia (P. Keary, personal communication). It is strange that it should continue on the east side of the Barbados Ridge, because all the evidence points to the Barbados Ridge being the site of subduction of the Atlantic Ocean crust, and therefore a major tectonic discontinuity.

The most plausible origin for the ridge east of Barbados in the Atlantic Ocean floor is that it is a ridge bordering an old transform fault. By analogy with the present situation at the Mid Atlantic Ridge east of the Lesser Antilles, where the highest ridge bordering a transform fault is on the youngest side even where it is a few hundred kilometres from the Mid Atlantic Ridge crest, the old transform fault should lie to the south of the ridge east of Barbados, because the offsets of the Mid Atlantic Ridge are left handed.

How the subduction of a transform fault could produce a ridge above it in the opposing lithospheric plate is a matter for conjecture. It may be that discontinuity in subducted slab has somehow increased the flow of volatiles into the mantle above it thereby giving increased vulcanicity. As has been noted in Chapter 1, St. Lucia is anomalous with respect to the other volcanic islands in having higher proportion of silicic rocks. The East Ridge is older than the upper sedimentary layers (A, B and C) and may not have been caused purely by subduction of the continuation of the feature now seen east of the Barbados Ridge. A further suggestion for the origin of the East Ridge is that if the Lesser Antilles occupy the site of a former subduction zone that produced the vulcanism which built the Aves Ridge, then

the part of the East Ridge between St. Lucia and the Barbados Ridge was a part of a transform fault feature that was being subducted and was isolated when subduction commenced in its present position, east of the Lesser Antilles. This is speculation, but there are some grounds for considering it (see Chapters 7 and 8).

The East Ridge has influenced the development of the Barbados Ridge. It is clear from the bathymetry that north of the East Ridge the sea bottom slopes downward, whereas south of it the depth of the crest of the Barbados Ridge is fairly constant. It seems that the transform fault ridge, although now buried, once acted as a barrier to turbidite sediment flow across the ocean bottom from South America, damming it so that the amount of sediment accumulated south of the ridge was greater than that north of it. Eventually the feature was buried and more sediment was deposited north of it than previously. The effect of subduction has been to magnify the difference in sediment thickness north and south of the transform fault ridge by piling it into the trench, and building up a ridge south of the transform fault, whereas north of the transform fault, where sediment thicknesses became progressively less, northwards, the ridge of sediment filling the trough sloped down. This would to some extent be a consequence of distance from sediment source, but the marked break in bathymetric profile at the northern end of the Barbados Ridge must certainly be due to the presence of the East Ridge.

Chapter 5

The effects of subducted lithosphere

The subducted lithosphere in the Lesser Antilles could be expected to cause a gravity anomaly contributing to the observed field. Calculations of the likely gravity anomaly have been made for thermal models of subducted plates using published data on phase relationships. The possibility that this anomaly can be observed, and its importance in interpreting the crustal structure are considered.

The thermal model

Thermal models for subducted plates have been published by the following authors: McKenzie (1969), Minear and Toksoz (1970), Oxburgh and Turcotte (1970), Toksoz, Minear and Julian (1971), and Griggs (1972). McKenzie considered a lithospheric slab descending into a mantle maintained at adiabatic temperatures and expressed the temperature inside the slab analytically in dimensionless form. Minear and Toksoz (1970) produced a numerical solution using a finite difference scheme, which was criticised on two counts (McKenzie 1971, Hanks and Whitcomb 1971). Firstly their model did not correctly represent the behaviour of short wavelength temperature disturbances that govern the thermal structure of the sinking slab, because the element size of 20 km was too large particularly at the top surface of the slab and successive errors were conserved. Secondly, some of the physical assumptions were in error, particularly the amount of shear strain heating, which was thought to be far too high. Toksoz, Minear and Julian (1971) produced revised models with a smaller

stepsize in time and distance, and smaller values of shear strain heating, but this was still greater than that of other models (Griggs 1972). The amount of shear strain heating assumed for these models is governed by the assumption of partial melting in the region to which andesitic magmas are thought to be derived, and the normal geothermal gradient used for the models is an important factor in estimating the amount of heating required for this. Minear and Toksoz used the oceanic geothermal gradient of MacDonald (1965) whereas Griggs assumed one which reaches the solidus at 100 km depth requiring very little extra heat to produce partial melting. A matter that is particularly relevant to this argument is whether or not the driving force of subduction is the gravitational instability of the subducted plate or some other force. In the former case the energy available can be estimated giving an upper bound for shear strain heating. Minear and Toksoz do not think that the gravitational mechanism is the sole mechanism and with this McKenzie (1972) agrees.

The thermal model of Toksoz, Minear and Julian (1971) for a subduction rate of 1 cm y^{-1} at an angle of 45^{o} with all heat sources included was used for the purpose of calculating the gravity anomalies that may result from subduction at the Lesser Antilles as this model was closest to the observed situation.

This model does deviate from the Lesser Antilles situation in some respects. The subduction rate there may be slightly smaller than 1 cm y^{-1}, but 1 cm y^{-1} is probably as good an estimate as any (See chapters 6 and 7).

The depth of the subducted plate given by the seismic zone, is

200 km in the Lesser Antilles as opposed to a plate nearly 800 km deep in the model. Using McKenzie's (1969) and Griggs' (1972) criteria for the length to the bottom of the seismic zone in subducted plates, based on temperature anomalies, an estimate can be made of length of the seismic zone that would be given by the model. According to McKenzie this should be 320 km and according to Griggs 185 km (depths of 200 km and 120 km respectively). Thus the depth of subducted lithosphere cannot be estimated from the earthquakes since seismically inactive lithosphere may exist deeper. The subducted lithosphere, however, cannot be as deep as 700 km, because (see chapter 7) there has not been sufficient time (104 my) for this to take place at 1,cm y^{-1}. The maximum time available is 80 my and it is quite likely to be as small as 30 my. The latter estimate is consistent with the present length of the seismic zone and the former would give subducted lithosphere down to a depth of 500 km. If the rate of subduction were increased the length of the seismic zone would increase also. In both the models considered the temperature field below the maximum depth estimated is ignored. This does not introduce as large errors as it might seem because the temperature field is not very time dependent in the region already penetrated by the slab, as demonstrated by Toksoz, Minear and Julian (1971). The geotherms in the region west of the slab may not be raised as far as in the model because there would be no heat source due to the post spinel phase change.

Another slight alteration made to the model was to change the horizontal scale to give a dip of 40° rather than 45°. The difference in the thermal model between 40° and 45° would be quite small, but it

does alter the distances along the gravity anomaly, which is what is considered here. The model used is shown in fig 5.1, and fig. 5.2 shows the temperature anomalies.

The anomalies caused by thermal expansion

The average temperature anomaly over a square was computed, and from it the mass excess or deficiency with respect to the undisturbed mantle was calculated. This mass was taken to be the mass per unit length of a line mass of infinite length passing normally through the centre of the square. The overall anomaly was found by summing those due to all the line masses. The spacing of the squares was such that the top of a square was always at a depth greater than its width. The normal density distribution with depth, and coefficient of thermal expansion necessary for this calculation were taken from Press (1970) and Birch (1952) respectively. The program to do these calculations is listed in appendix C5.1.

The anomaly caused by phase changes in the mantle

The phase changes which are relevant in this situation are those taking place in the first 100 km, involving the transition from pyrolite to garnet pyrolite in the lithospheric mantle (Green and Ringwood, 1966), and those from 350 to 400 km depth, which are the pyroxene - garnet transformation and the olivine - spinel - B.Mg_2SiO_4 transformation (Ringwood, 1970). The Pyrolite III model of Green and Ringwood is assumed for the mantle.

5.1 Thermal model of a subducted slab from Toksoz, Minear and Julian (1971) used for the calculation of gravity anomalies resulting from the subduction of lithosphere. The subduction rate is 1 cm y^{-1}. The position of the base of the olivine - spinel and pyroxene - garnet transition is shown by a pecked line (s). Dots indicate the points used for calculation of the gravity anomaly due to thermal expansion.. The shaded areas in the subducted slab indicate the positions of phase changes considered by Toksoz, Minear and Julian (1971)

5.2 The temperature anomalies arising from the model in fig. 5.1. The scales on the diagram are the same.

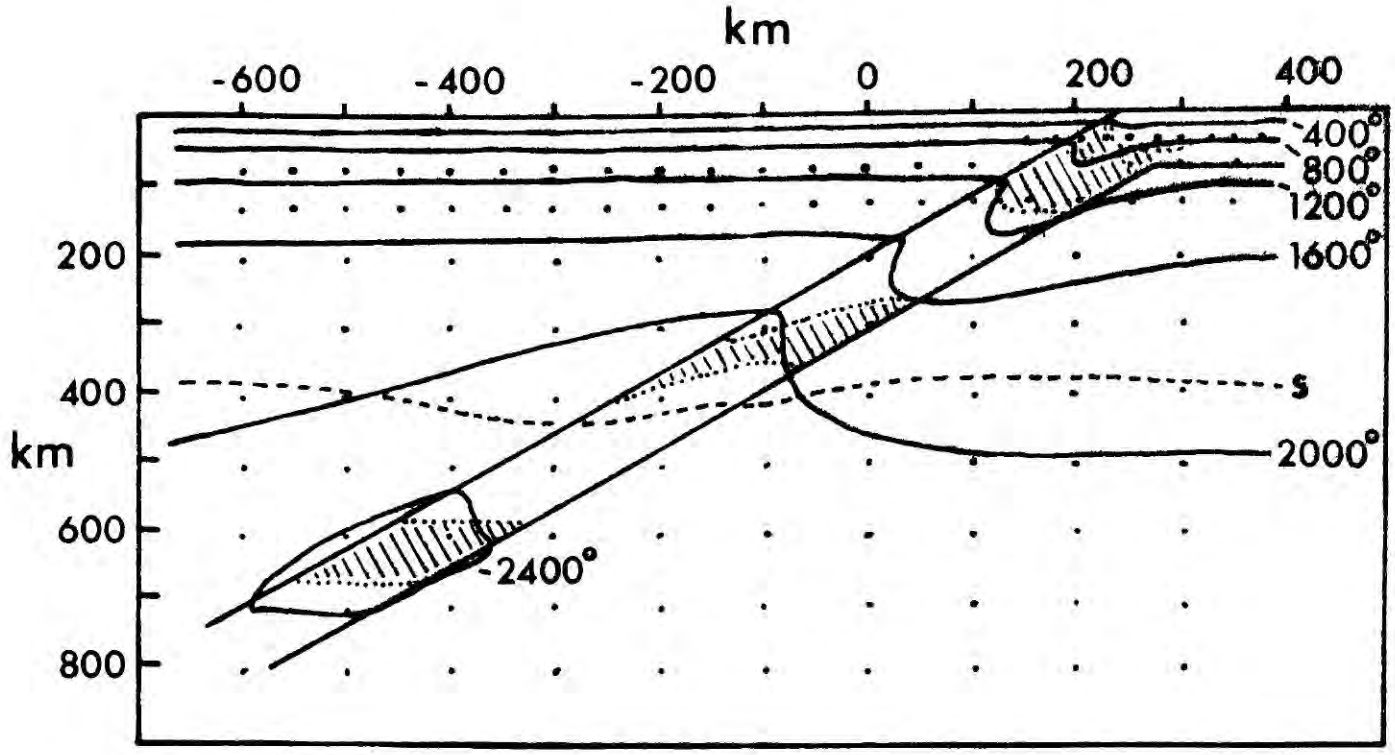
km
-600
-400
-200
0
200
400
200
400
km
600
800
400°
800°
1200°
1600°
S
2000°
2400°

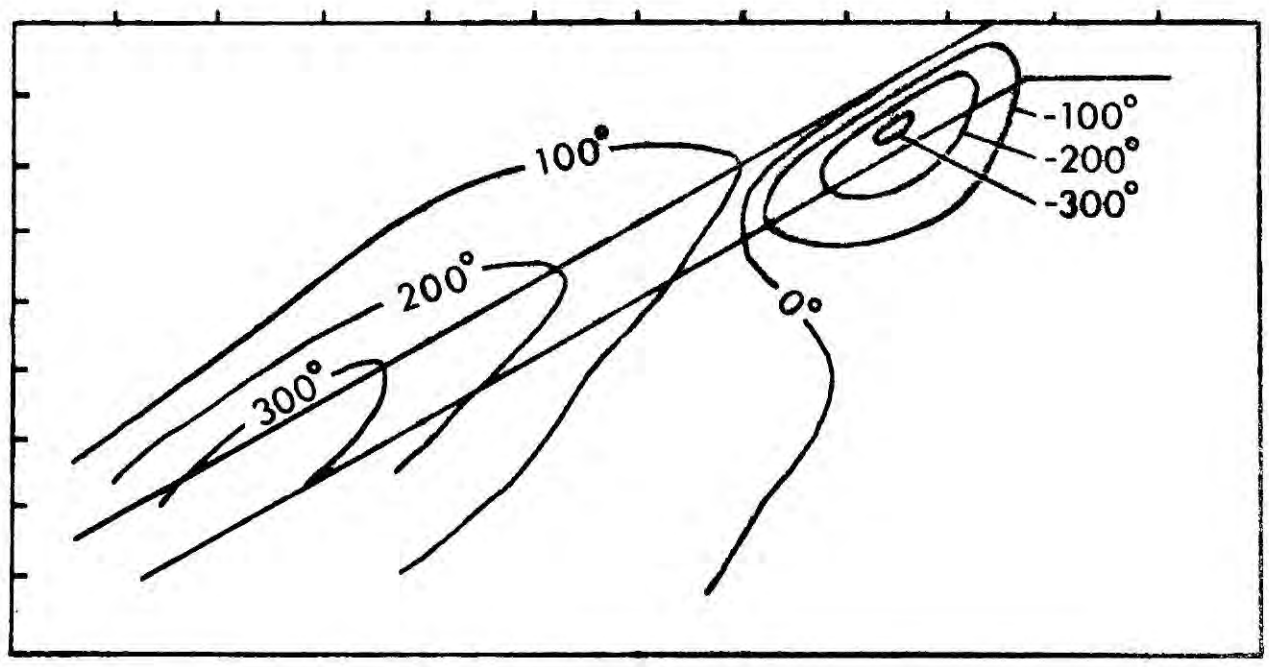
100°
200°
300°
0°
-100°
-200°
-300°

The 350 - 400 km transitions only affect the 500 km deep model, and the density change is about 7% (Ringwood, 1970). The equation used for the position of the transition was that of Griggs (1972), and gives a position somewhat below that of Toksoz, Minear and Julian. This is because Toksoz, Minear and Julian assumed a broader range for the transition (100 km) than do Griggs (35 km) and Ringwood (40 to 60 km). The density contrast used for the transition was 0.24 gm cm^{-3}. The effect of the thermal anomaly of the model is to depress the transition below its normal position over most of the region.

The density contrasts produced by the phase transitions in normal lithospheric mantle are comparatively small. The maximum contrast is 0.05 gm cm^{-3} between ampholite (Olivine + amphibole $\pm$ enstatite) and pyroxene pyrolite (Olivine + aluminous pyroxenes $\pm$ spinel). According to the model of Green and Ringwood (1970), ampholite is the stable phase in the mantle to a depth of 32 km with a normal oceanic geotherm. The presence of this phase is dependent on the presence of water, and plagioclase pyrolite (Olivine + pyroxenes + plagioclase + chromite) would replace it under completely anhydrous conditions. The presence of both amphibole and plagioclase is more dependent on pressure than on temperature. The density contrast arising from the absence of plagioclase would be about 0.06 gm cm^{-3}. The main phases are shown in fig. 5.3 together with the geotherm used. It can be seen that lowering the temperature by 100°C makes little difference to the depth at which plagioclase is stable. Consequently the amplitude of gravity anomalies likely to arise from the effect of temperature anomalies on this phase transition would be

5.3 Phase diagram for a mantle of Pyrolite III composition, from Green and Ringwood (1970). Pl - Plagioclase Pyrolite, Py - Pyroxene Pyrolite, Ga - Garnet Pyrolite. Dashed lines marked from 1 to 5 indicate the percentage of Al_2O_3 in pyroxene in Garnet Pyrolite. Curve o is the normal oceanic geothern used in the thermal model. Dotted lines 1, 2, 3 indicate depression of the geotherm from 100 to 300° C. Curve g is the normal oceanic geotherm used by Griggs (1972)

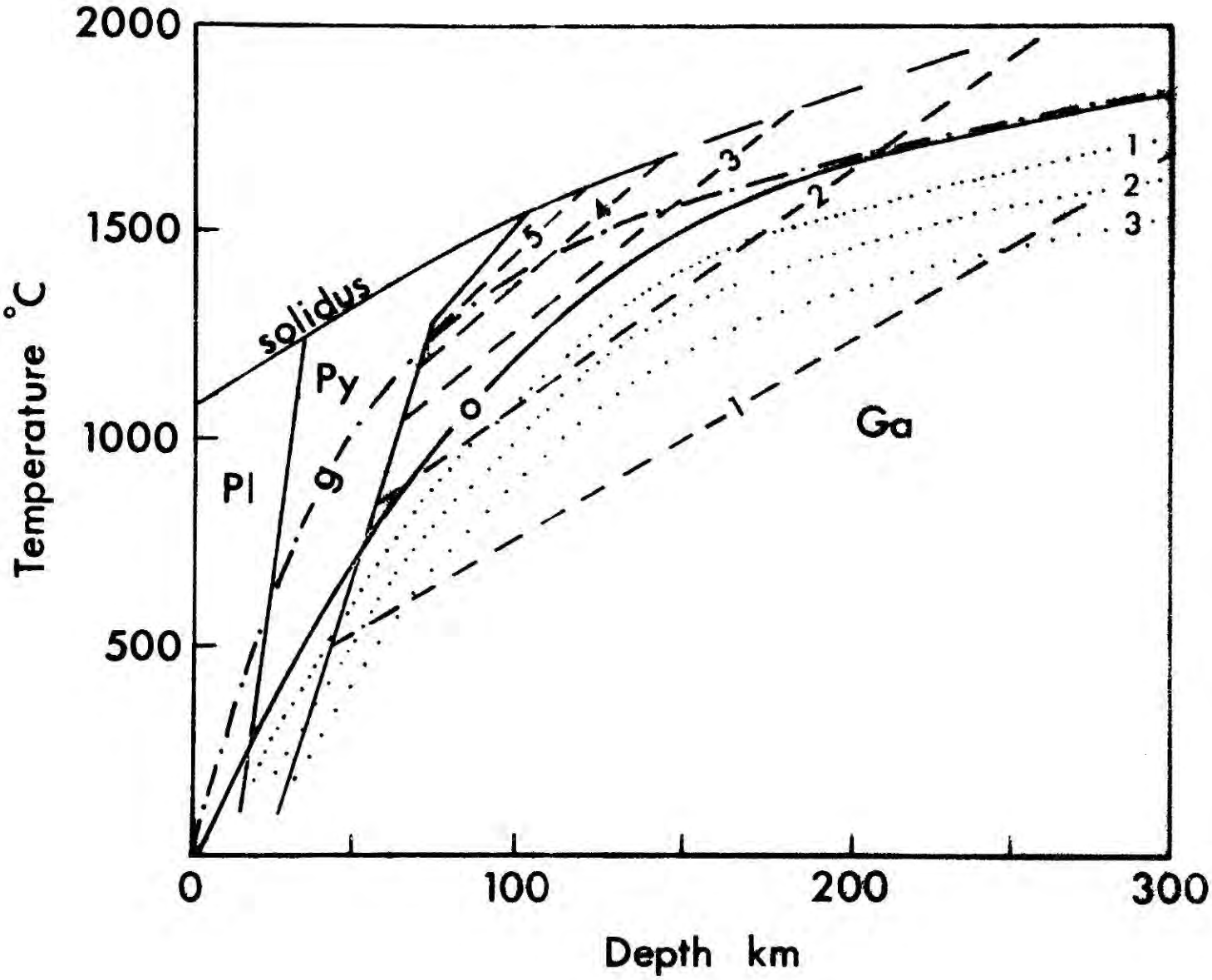
2000
1500
1000
500
Temperature °C
solidus
Py
Pl
Ga
0
1
2
3
4
5
1
2
3
0
100
200
300
Depth km

small and are not considered here.

The main factor influencing density changes below about 60 km is the relative proportion of orthopyroxene to garnet, which is dependent on the percentage of Al_2O_3 in the orthopyroxene. The percentage is strongly temperature and pressure dependent. Lowering the temperature affects the density, because at any fixed pressure it increases the proportion of garnet present, and hence increases the density.

The gravity anomaly arising from phase changes in the mantle caused by subduction (excluding that from the transition at 350 km) was calculated from the effect of the temperature anomaly pattern, (fig. 5.2), on the densities of phases in Green's and Ringwood's Pyrolite III model of the mantle (fig 5.3). The densities of different phases are taken from the values calculated by Haigh (1973) for use in a model of oceanic lithosphere. In the region from 60 to 250 km depth a temperature change of 100°C gives an average density change of 0.05 gm cm^{-3}. Beyond 250 km a temperature anomaly of 300°C is needed to give a density change of 0.05 gm cm^{-3}.

The anomaly caused by phase changes and initial density contrast in the subducted crust

The gravity anomaly due to the phase changes in the subducted oceanic crust results principally from the transformation of gabbro to eclogite. This transformation was investigated by Ringwood and Green (1966), and was considered by them to be a significant factor in subduction by gravitational instability. The reaction they

studied was anhydrous. It does not seem likely, however, that conditions in the oceanic crust are completely anhydrous. It is probable that layer 2 and perhaps layer 3 have some hydrous minerals in them. Greenschists and amphibolites have been dredged from mid ocean ridges, and there is another opportunity for introduction of water to the crust at the site of subduction. It is likely that much of the oceanic crust goes through a change to amphibolite before transforming to eclogite. Essene, Hensen and Green (1970) have investigated the stability of basaltic material under conditions of high temperature and pressure, where $P.H_2O = P.$ Load. They showed that the material went through a phase of garnet amphibolite before finally reaching eclogite at 70 km depth, and that this transformation was almost entirely pressure dependent. Essene, Hensen and Green concluded that amphibolite containing plagioclase feldspar was stable down to depths of about 30 km, and that the transformation from amphibolite to eclogite was a gradual reaction among amphibole, garnet and pyroxene.

A simple model of the density contrast between the subducted crust and the undisturbed mantle was made, using the data of Essene, Hensen and Green (1970) for the crust, and Green and Ringwood (1970) for the mantle. The shape of the upper surface was deduced from the distribution of earthquake hypocentres in the Lesser Antilles, and the top of the model was fixed at the base of the crust as interpreted from gravity and seismic data. The model is shown in fig. 5.4.

The combined effect

The gravity anomalies resulting from the effects given above were

5.4 A density contrast model for the crustal layer of subducted lithosphere. Phase data used was from Essene, Hensen and Green(1970). Density contrasts are in gm cm^{-3}.

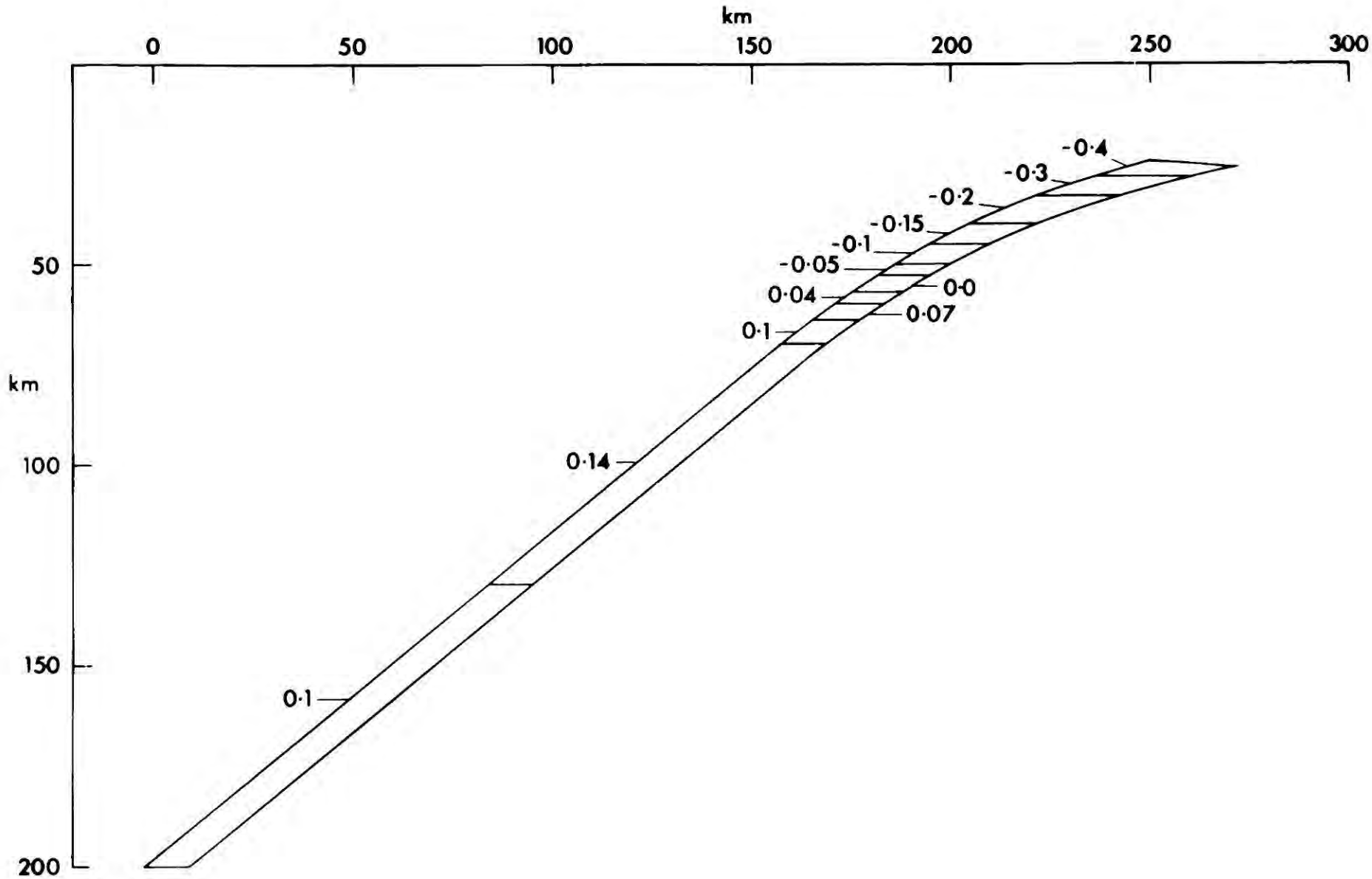
km
0
50
100
150
200
250
300
km
50
100
150
200
-0·4
-0·3
-0·2
-0·15
-0·1
-0·05
0·0
0·04
0·07
0·1
0·14
0·1

computed for models in which the lithosphere was subducted to depths of 200 and 500 km, and shown in figs 5.5 and 5.6. In the 500 km model, the olivine-spinel and pyroxene-garnet transformations produce a large negative anomaly of long wavelength. An anomaly of this size is not observed in the eastern Caribbean. It would occur over much of the Venezuelan Basin, where the crustal structure is of a uniform nature and the anomaly would be noticeable. On the basis of this alone the 500 km model is not applicable. This may be because the thermal model is incorrect, but it is more probable that the subducted lithosphere does not reach a depth of 500 km.

In the 200 km model the negative part of the anomaly is considerably diminished, because of the absence of an anomaly from the transition at 350 km depth. If the model is valid, the positive anomaly of nearly 40 mgal amplitude should be discernible in the observed field. The anomaly is superimposed on that caused by the crustal structure of the island arc, and overlaps into the region of the Tobago Trough. The observed positive free-air anomaly over the arc has an asymmetrical lobe on the east side (fig. 5.7), which may be produced partly by the subducted lithosphere.

The effect of the gravity anomaly caused by subducted lithosphere on the determination of the crustal structure was assessed by subtracting the anomaly calculated for lithosphere subducted to 200 km from the Bouguer (2.1 gm cm^{-3}) gravity anomaly and modelling the structure as described in chapter 4. The subducted plate produces a positive anomaly of 5 mgal in the region of the Atlantic Ocean taken for reference in the modelling of the crustal structure, and accordingly

5.5 The gravity anomalies caused by the subduction of lithosphere to a depth of 200 km at a rate of 1 cm y^{-1}.

Pc - the anomaly from the phase changes in the crust.

Pm - the anomaly from phase changes in the mantle.

Te - the anomaly from thermal expansion and contraction.

C - the combined anomaly. V - the position of St. Vincent

B - the position of Barbados.

5.6 The gravity anomalies caused by subduction of lithosphere to a depth of 500 km at a rate of 1 cm y^{-1}. Pc - the anomaly from phase changes in the crust. Pm-the anomaly from phase changes in the mantle. Po - the anomaly from phase changes in the olivine-spinel transition at 350 km depth. Te - the anomaly from thermal expansion and contraction. C - the combined anomaly. V - the position of St. Vincent. B - the position of Barbados.

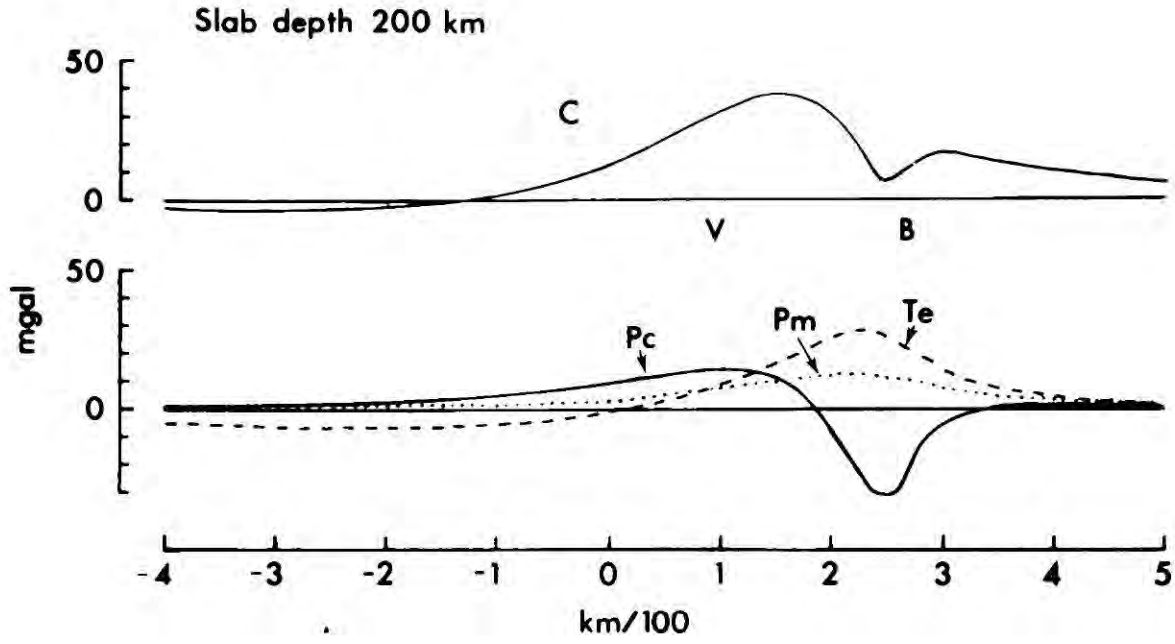
Slab depth 200 km
50
0
C
V
B
50
mgal
0
Pc
Pm
Te
-4
-3
-2
-1
0
1
2
3
4
5
km/100

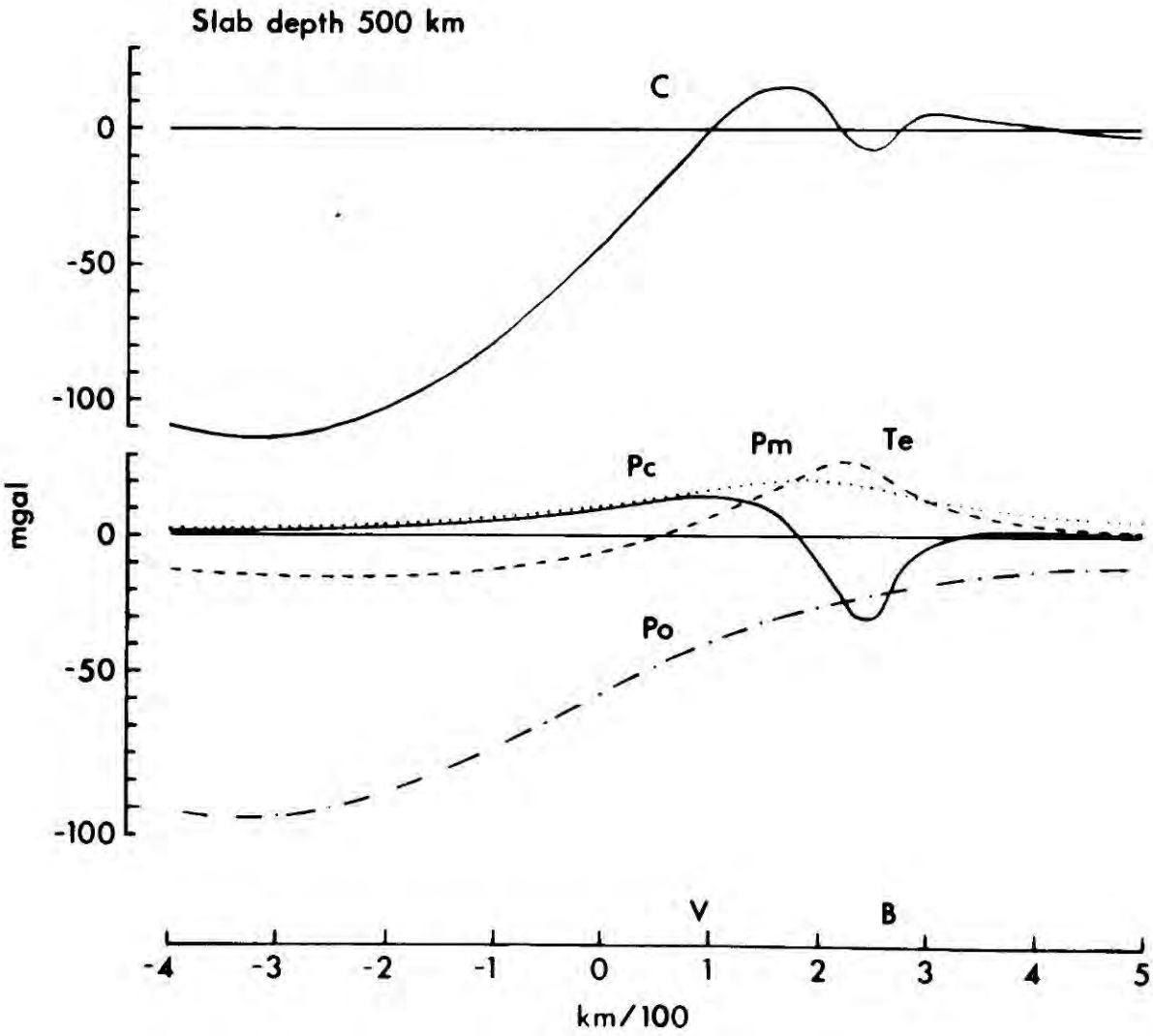
Slab depth 500 km
0
-50
-100
C
Pc
Pm
Te
mgal
0
Po
-50
-100
V
B
-4
-3
-2
-1
0
1
2
3
4
5
km/100

the values subtracted were 5 mgal lower than those in fig. 5.5.

The crustal structure determined is shown in fig. 5.8, and it is worthwhile comparing it with the structure determined directly from the Bouguer anomaly shown in fig. 4.20. A noticeable difference is that the Moho is deeper below the Tobago Trough in the model which takes account of the subducted lithosphere than in that which does not. In particular the minimum calculated depth of the Moho below the Tobago Trough is 24 km. This depth and the sharp increase of depth to the west matches well the shape of the Moho determined from time term analysis of the LASP results (C. Boynton, personal communication). This gave a 23 km minimum depth increasing westerly to 31 km depth over 10 km, and eventually extending to 37 km below the island arc. The velocity layering in the basement used in the time term analysis was approximately the same as that used for the density model, layers of velocity 6.3 km s^{-1} and 6.9 s^{-1} corresponding to the layers of density 2.8 gm cm^{-3} and 2.9 gm cm^{-3}. The base of the 6.3 km s^{-1} layer was put at 20 km below the Lesser Antilles. Subtraction of the gravity anomaly calculated for the subducted lithosphere from the observed gravity anomaly, therefore, improves the congruence between the shapes of the Moho computed from seismic and gravity data. This suggests that there is a noticeable gravity anomaly from the subducted lithosphere and that its amplitude is probably not substantially different from that predicted.

In the foregoing discussion the effects of inhomogeneity in the composition of the mantle beneath the island arc were neglected. This is because, although inhomogeneity may be expected to occur, its nature

5.7 Free air gravity anomalies across the eastern Caribbean at latitudes 13° 24' N and 13° 04' N. The bathymetry on each profile is shown below the anomaly.

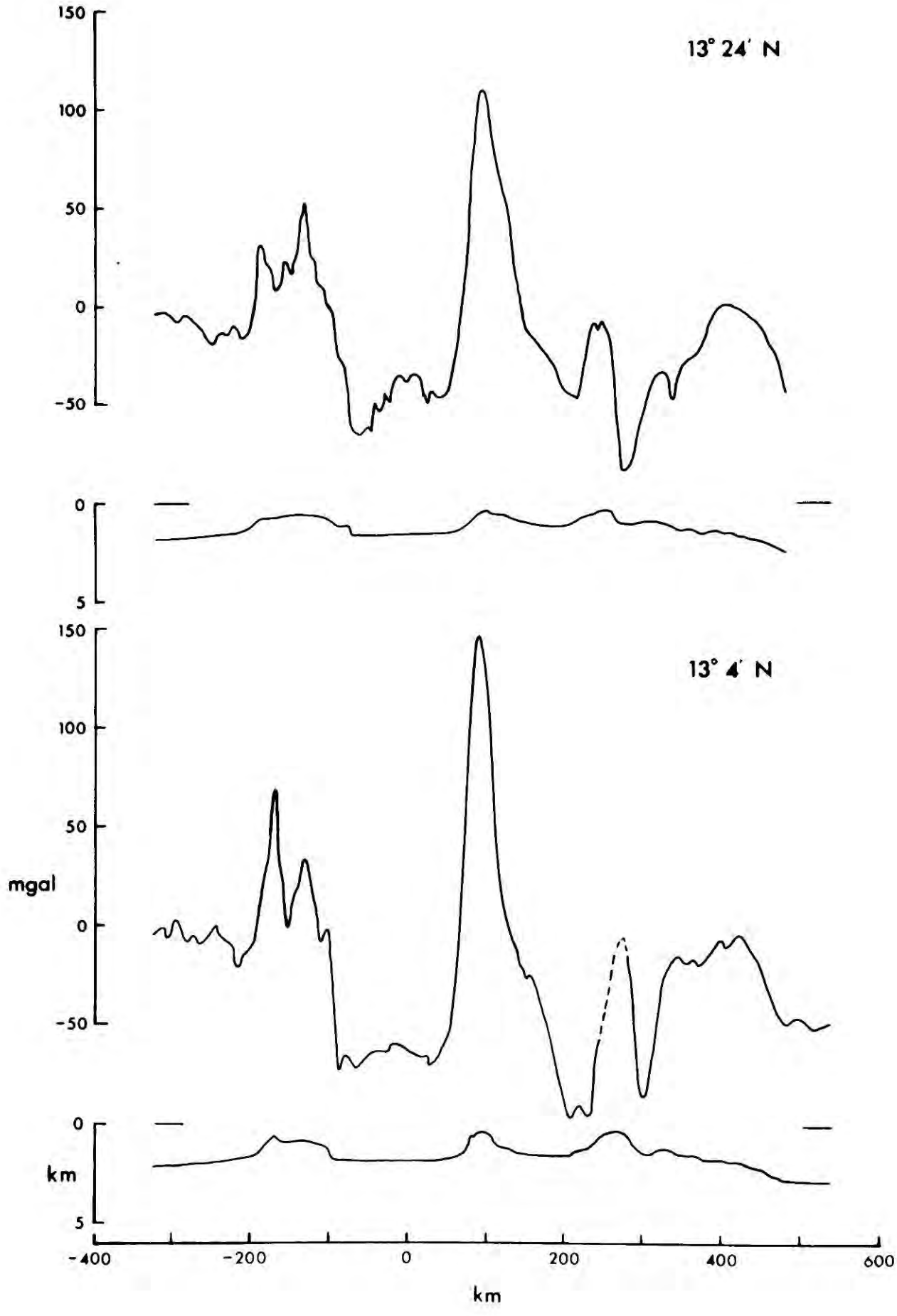
13° 24' N
150
100
50
0
-50
0
5
13° 4' N
150
100
50
mgal
0
-50
0
km
5
-400
-200
0
200
400
600
km

and possible effects can only be guessed at. Depending on the view taken as to the derivation of the rocks forming the island arc, either basaltic material is added to the mantle making it less dense, or basalt is derived from the mantle, depleting it and making it more dense. If basaltic material is derived from the subducted crust, then the former must apply, but if the material is derived from the mantle above the subducted plate through the action of volatiles, mainly water, given off from the subducted crust, then the latter is favoured Only further study of the petrogenesis of calc-alkaline rock suites can resolve this question. Recent work cited by Ringwood (27th William Smith Lecture of the Geological Society, 1973) suggests that derivation from the mantle above the subducted plate is most likely.

Seismic evidence

Barr and Robson (1963) examined the delays of teleseismic arrivals at Barbados with respect to the island arc for the purpose of determining the likely depth of the Moho beneath Barbados. The mean delay was found to be 2.94 $\pm$ 0.34 s. Taking the crustal structure to be that shown in fig. 5.7, the calculated delay time for Barbados relative to St. Vincent is 1.94 s. If these results are reliable then the presence of mantle with a faster seismic velocity below the island arc than Barbados is indicated. However, the result given by Barr and Robson was obtained from 10 observations made in the four years following the installation of seismic stations in the eastern Caribbean. Since then many more observations have been made and the mean delay of arrivals from regional earthquakes at Barbados relative to the island arc is 2.0 s (J. Tomblin, personal communication). This implies no

5.8 Two dimensional density model across the Lesser Antilles region at latitude 13° 04' N. The anomlay is the Bouguer anomaly for a correction density of 2.1 gm cm^{-3} from which the anomaly caused by subducted lithosphere (C of fig. 5.5) has been subtracted. Dots are the observed values of the anomaly. The continuous curve is the calculated anomaly. S is the standard error of the fit. C is the correlation coefficient. Densities in gm cm^{-3} are shown on the layers of the model.

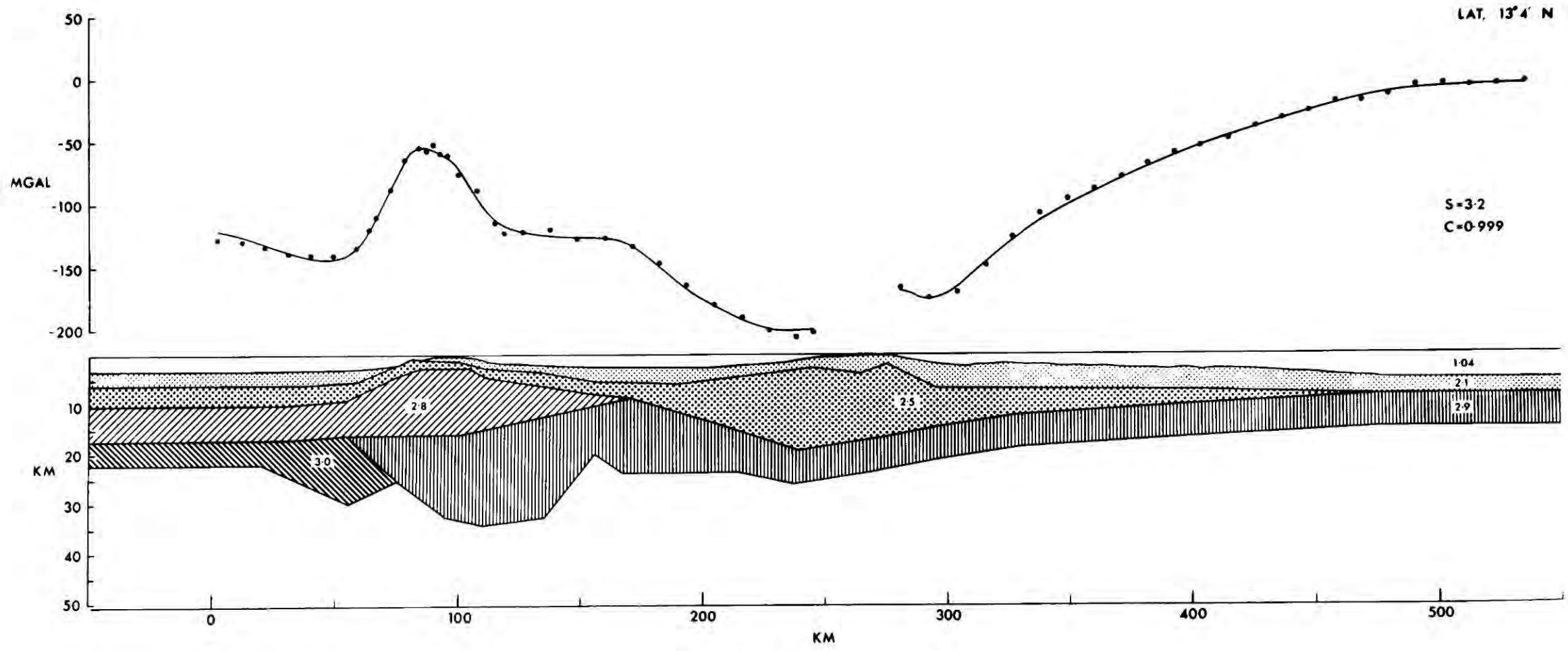
LAT. 13°4′ N
S=3·2
C=0·999
MGAL
50
0
-50
-100
-150
-200
KM
10
20
30
40
50
1·04
2·1
2·9
2·5
2·8
3·0
0
100
200
300
400
500
KM

noticeable difference in the mantle velocity directly below Barbados from that below the island arc. If the delay indicated by the teleseismic arrivals is real then it must indicate an inhomogeneity at a depth greater than that sampled by seismic waves from regional earthquakes.

A consideration of the long wavelength components of the gravity anomaly.

By digitally low pass filtering the observed gravity anomalies, the effects of near surface structures can be diminished and an anomaly more readily comparable with those expected from mainly mantle sources may be obtained. The filtered values for two lines across the eastern Caribbean region are shown in fig. 5.9. These were computed from the free-air anomalies shown in fig. 5.7 using the program described in appendix C2.3. The cutoff wavelengths used were 250, 333 and 500 km. Gravity values from the Venezuelan Basin (Bush and Bush, 1969; U.S.G.S., 1972) and the Atlantic (Navado Project) were used to extend the lines into stable areas. The long wavelength anomaly in the region determined from satellites (Kaula, 1972) is in good agreement with those values.

The dominant wavelength of the anomaly calculated from the model of lithosphere subducted to 200 km (described above) is about 300 km, although there are significant shorter wavelength components which result mainly from the effect of the subducted crust. The 333 km filtered anomaly, however, shows the effects of crustal structure as is evidenced by the anomalies over the Aves Swell, the Lesser Antilles and Barbados Ridge still appearing. Consequently, the anomaly caused by the subducted lithosphere cannot be separated from those caused by variations in the crustal structure.

5.9 Filtered free-air gravity anomalies across the eastern Caribbean region at latitudes 13° 04' N and 13° 24' N. The curves for cutoff wavelengths of 250, 333, and 500 km are shown. The unfiltered free-air gravity anomalies are shown in fig. 5.7.

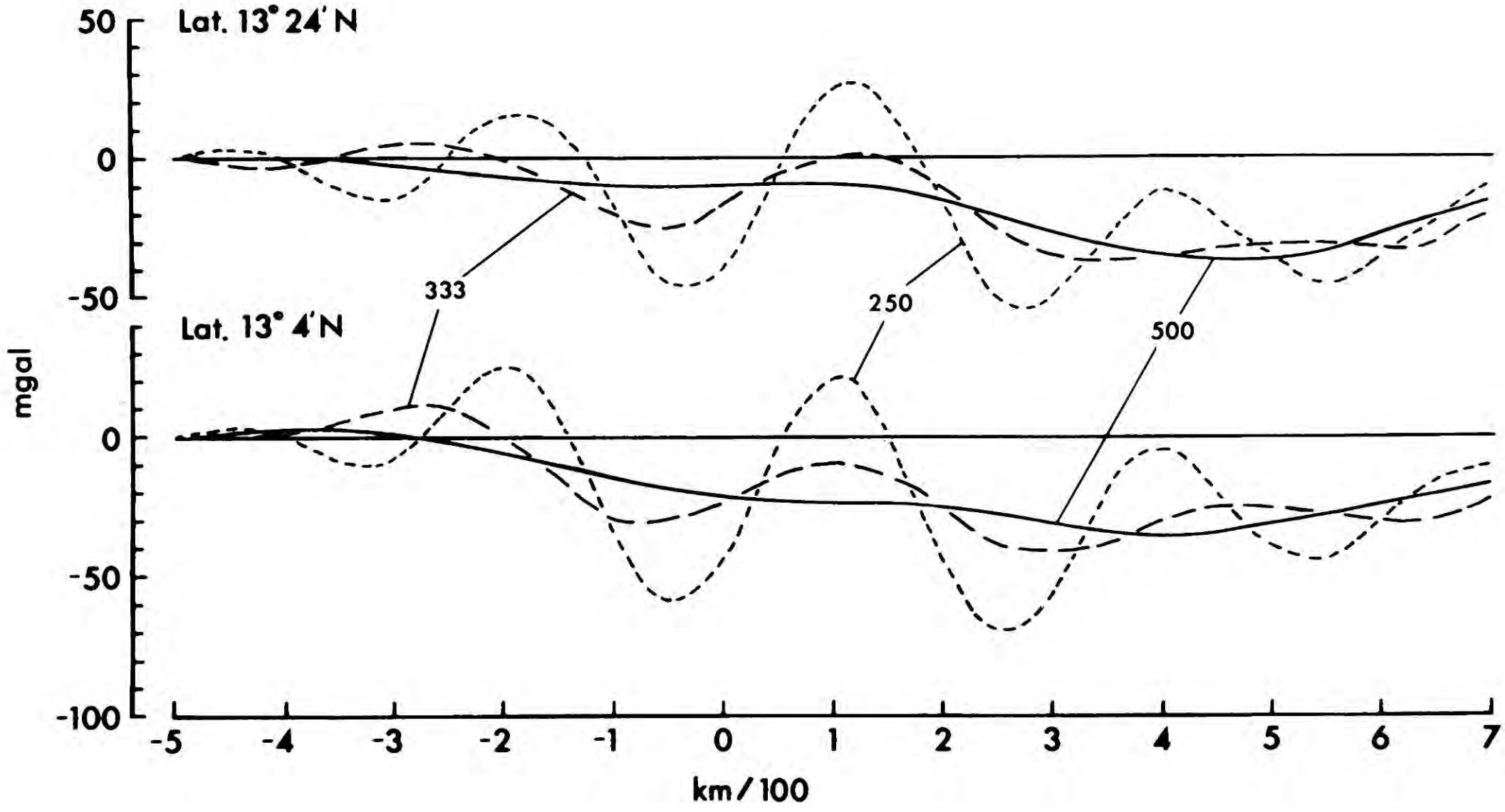
Lat. 13° 24' N
Lat. 13° 4' N
333
250
500
50
0
-50
-50
0
-50
-100
-5
-4
-3
-2
-1
0
1
2
3
4
5
6
7
mgal
km / 100

The 500 km filtered anomaly does not show the effects of individual crustal feature and reflects the overall gravity anomaly of the region. From the satellited determined gravity field (Kaula, 1972) the value of the free-air anomaly decreases steadily from 0 mgal in the Venezuelan Basin to -20 mgal in the Atlantic Basin. The anomaly deviates negatively from a linear regional joining the background fields of the Venezuelan Basin and the Atlantic, by up to 25 mgal.

Integrating the free-air anomaly minus the expected regional along the line at latitude 13° 34' N yields a value of -2.57×10^{9} $cm^{2}s^{-2}$ which could be produced by a total mass deficiency over the area of 6.14×10^{12}gm. It might be thought that this deficiency is due in part to the large volume of sediments in the Barbados Ridge. However a simple calculation, comparing the masses of segments (10 km wide and 30 km deep) of the crustal model derived from the gravity and seismic data across the region east of the Lesser Antilles with the mass of a segment of the Atlantic Ocean crust of the same size, reveals that there is a small mass excess over the region relative to the Atlantic. The crustal downwarp beneath Barbados is deficient in mass with respect to the ocean crust, but the region of the slope east of Barbados has a mass excess which more than balances it. The calculated anomaly resulting from the variation in mass across this region is shown in fig. 5.10. The positive mass anomaly east of Barbados is quite a small isostatic anomaly, because the region of oceanic crust with which it was compared has a free-air anomaly of -40 mgal and is isostatically negative.

5.10 The gravity anomaly caused by the variation of mass across the crustal section east of the Lesser Antilles shown in fig. 5.8. Comparison is made with the mass of a standard section of crust and mantle in the Atlantic Ocean.

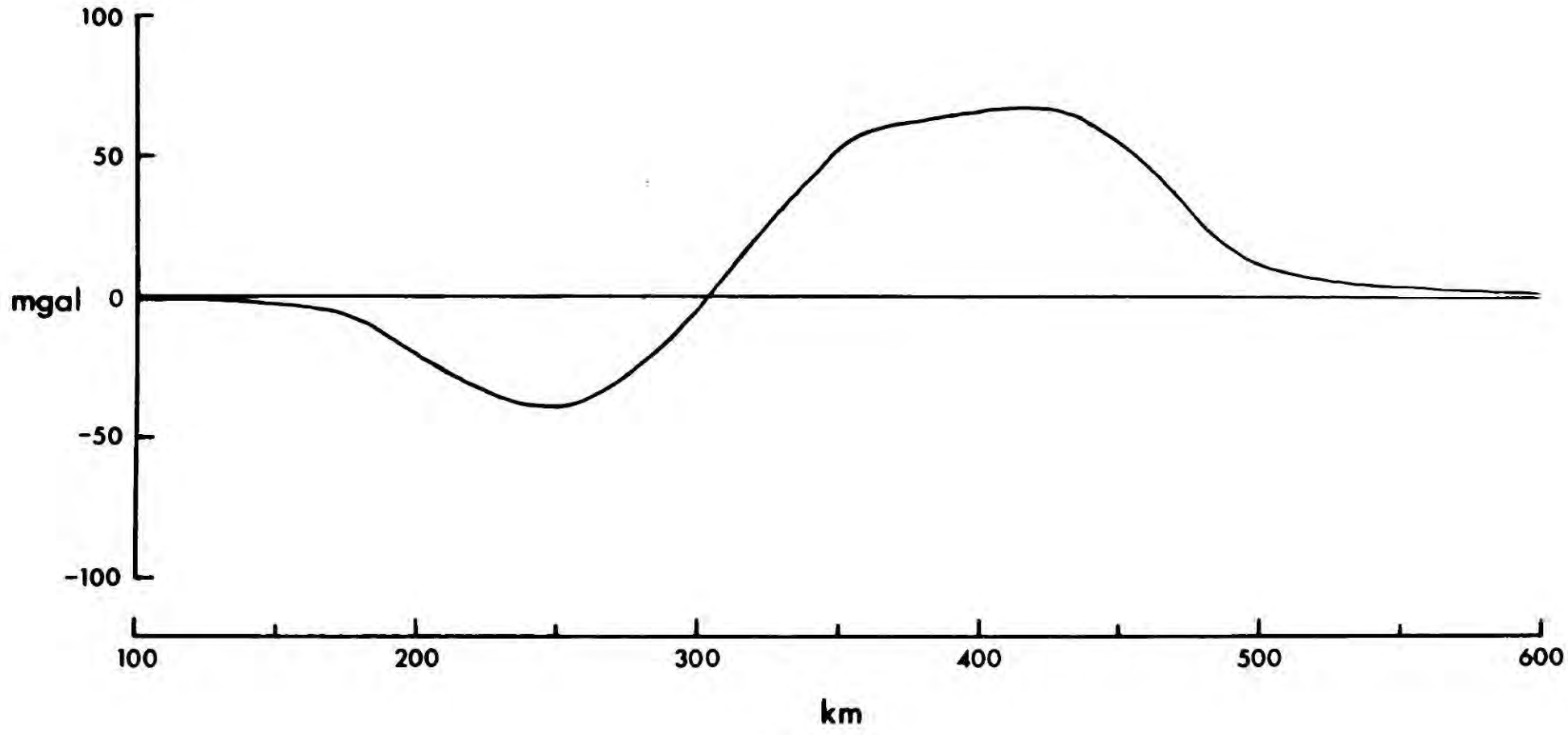
100
50
mgal 0
-50
-100
100
200
300
400
500
600
km

Interpretation of the significance of the overall negative anomaly across the Lesser Antilles is not straightforward. Its amplitude is dependent on the assumed regional between the gravity fields over two areas that are thought to be unaffected by the process of subduction below the Lesser Antilles. How the regional would vary across the region if subduction were not taking place cannot really be determined. Although one takes as a guide the satellite observed global gravity anomalies, which have a longer wavelength than the anomaly considered, one cannot be sure how much the global anomaly has been contributed to by the anomaly considered. Taking into consideration these qualification, the possible causes of the long wavelength anomaly over the Lesser Antilles region may be speculated on.

One cause could be a low density inhomogeneity in the mantle, but another possibility is that the whole of the area east of the Lesser Antilles, including some of the Atlantic Ocean, is out of isostatic equilibrium in a negative sense. The cause of such a major imbalance may be the process which is producing subduction in the Lesser Antilles. The shorter wavelength negative and positive anomalies in the region of Barbados could be an effect of the bending of the lithosphere as it is subducted. It appears to be a common feature of ocean trenches that a positive free-air gravity anomaly of about 40 mgal amplitude occurs on the seaward side of the trench about 120 km from the trench axis (Talwani, 1971) accompanied by a gentle rise in the bathymetry. The negative anomaly is situated over the part of the descending lithosphere that is being bent downward past the non-descending lithosphere which must also be depressed by the stress

induced by the descending lithosphere. The bending of the subducted lithosphere seems to result in the elevation of part of its surface above its isostatic equilibrium position, giving rise to the positive anomaly observed on the oceanward side of the subduction zone.

If subduction is the cause of the overall negative free-air anomaly in the Lesser Antilles region, then the force acting is 4.78×10^{15} dynes per cm along the subduction zone, which is a little in excess of the forces estimated to be acting on plates from the hydrostatic pressure resulting from the elevation of mid ocean ridges above the surrounding sea floor, which is about 1.8×10^{15} dynes. If the average shear stress along the subduction zone to a depth of 200 km is 1 kbar (Wyss, 1970) then the force needed to maintain the stress is 3×10^{16} dynes. Clearly the process causing subduction is of sufficient magnitude to create the isostatic imbalance. The cause of subduction cannot be the negative buoyancy of the subducted lithosphere, which should produce an overall positive gravity anomaly instead of the negative one that is observed.

Chapter 6

Seismicity and the present tectonic state of the Caribbean

The most evident indication of the present day tectonism is the seimic activity of the region. The seismicity, which has been described by Sykes and Ewing (1965), Molnar and Sykes (1969), and Tomblin (1971), is almost wholly confined to the margins of the Caribbean, and focal mechanism solutions from earthquake first motions indicate the nature of tectonic activity on various parts of the Caribbean 'plate' boundary. Fig. 6.1 shows earthquake focal mechanism solutions from Molnar and Sykes (1969), and Tomblin (personal communication). Along the Lesser Antilles there is a large proportion of thrust type faults which are presumably associated with underthrusting of the lithosphere. The axes of principal extensive stress in these earthquakes generally plunge towards the west at about 45°. Not all the solutions show this type of motion, however, and some mechanisms have vertical fault planes with an easterly strike on which there has been either vertical or strike slip motion. These mechanisms may be due to motion on old transcurrent faults in the subducted lithosphere reactivated, though probably not in their original sense, by deformation of the subducted plate. The presence of these faults is supported by the distribution of earthquakes and aftershocks along east-north-easterly trending lines, particularly in the northern part of the Lesser Antilles. Fig. 6.2 shows an example of such a sequence.

At the southern end of the Lesser Antilles in the north of Trinidad and Venezuela earthquake mechanisms are of two types; dextral strike slip with an easterly trend, and vertical fault planes with an easterly

6.1 Current tectonic activity in the Caribbean Region. Showing earthquake focal plane solutions projected into the lower hemisphere, with focal depth indicate alongside; major faults; recent volcanoes, shown by triangles; sites of subduction, indicated by dotted lines.

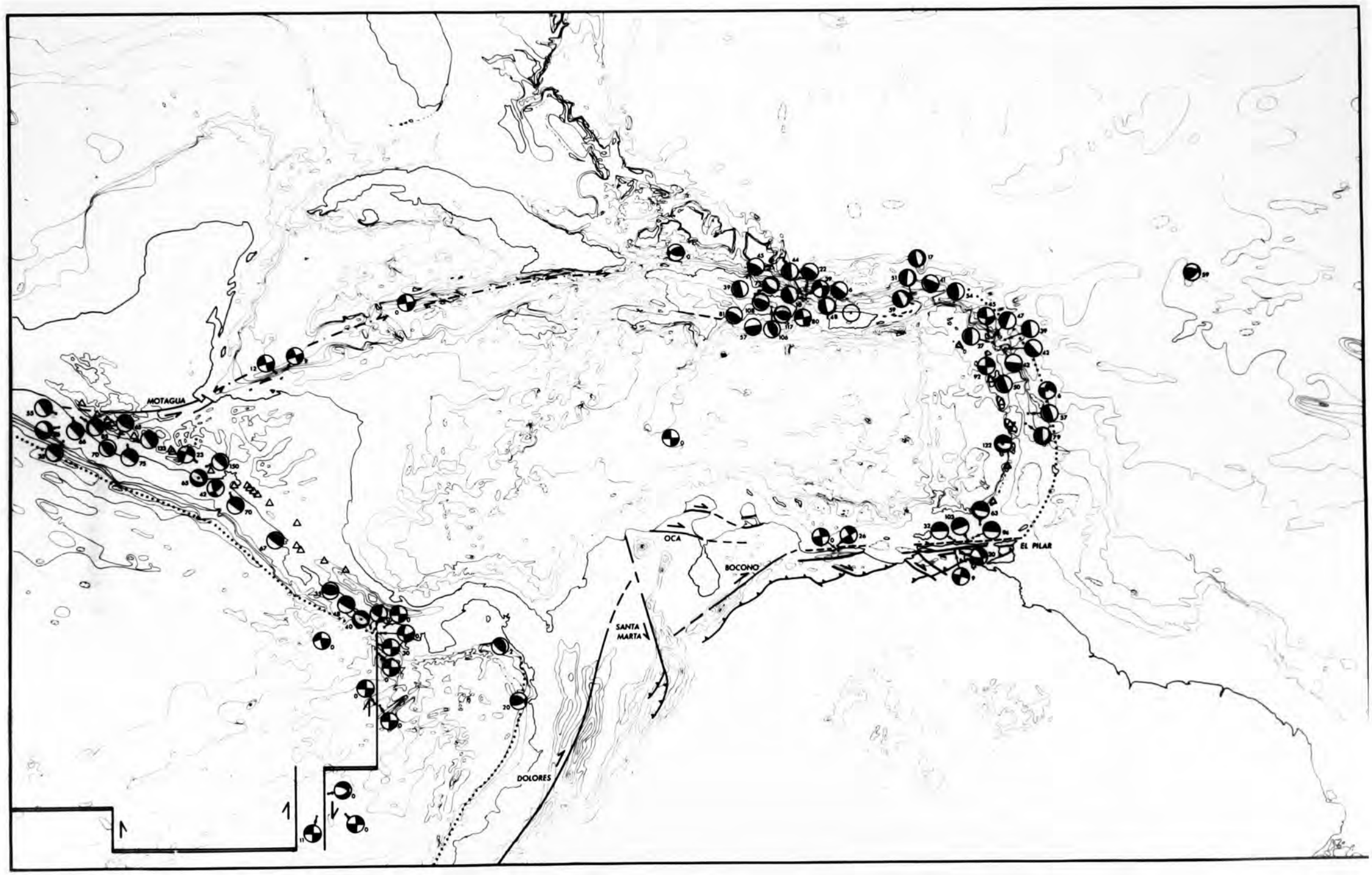
MOTAGUA
OCA
BOCONO
SANTA MARTA
DOLORES
EL PILAR

strike down-throwing to the north which are interpreted as hinge faults by Molnar and Sykes (1969). The hinge faults are thought to be situated on the southern limit of the subduction zone where the edge of the descending plate moves past the adjacent plate. Further west in Venezuela mechanisms are dextral strike slip with a predominantly easterly strike.

The focal mechanisms in the Greater Antilles are mainly of the thrust type with a few sinistral strike slip motions. The orientation of the thrust mechanisms does not fit easily in to any plate tectonic interpretation. The direction of the principal stress axes vary from 180° to 270° and would seem to indicate that the Greater Antilles are being obliquely underthrust and that the mechanisms are caused by internal deformation of the underthrust plate. Some of these mechanisms arise in the Puerto Rico Trench area, where one might expect only strike slip motions. Bracey and Vogt (1970) proposed that the Puerto Rico Trench is essentially a transform fault and that subduction takes place along the northeast coast of Hispaniola. As will be shown later, the distribution of hypocentres does not support a simple subduction zone hypothesis, and the mechanisms of the Puerto Rico Trench region are hardly typical of a straightforward transform fault. This point is discussed by Molnar and Sykes (1971).

In the Cayman Trough, focal mechanisms indicate sinistral strike slip faulting; the strike of the fault is parallel to the trend of the trough. Along the Middle Americas Trench there is underthrusting which terminates at the Panama Fracture Zone. In the region between the Panama Fracture Zone and Colombia there are very few intermediate

6.2 Eastern Caribbean earthquake epicentres determined by the Seismic Research Unit, Trinidad for the period July to September 1966. The east-northeasterly trend of epicentral groups is well shown in the northern half of the Lesser Antilles. From Tomblin (1971).

Fig. 6.2 Eastern Caribbean earthquake epicentres, July-September 1966.

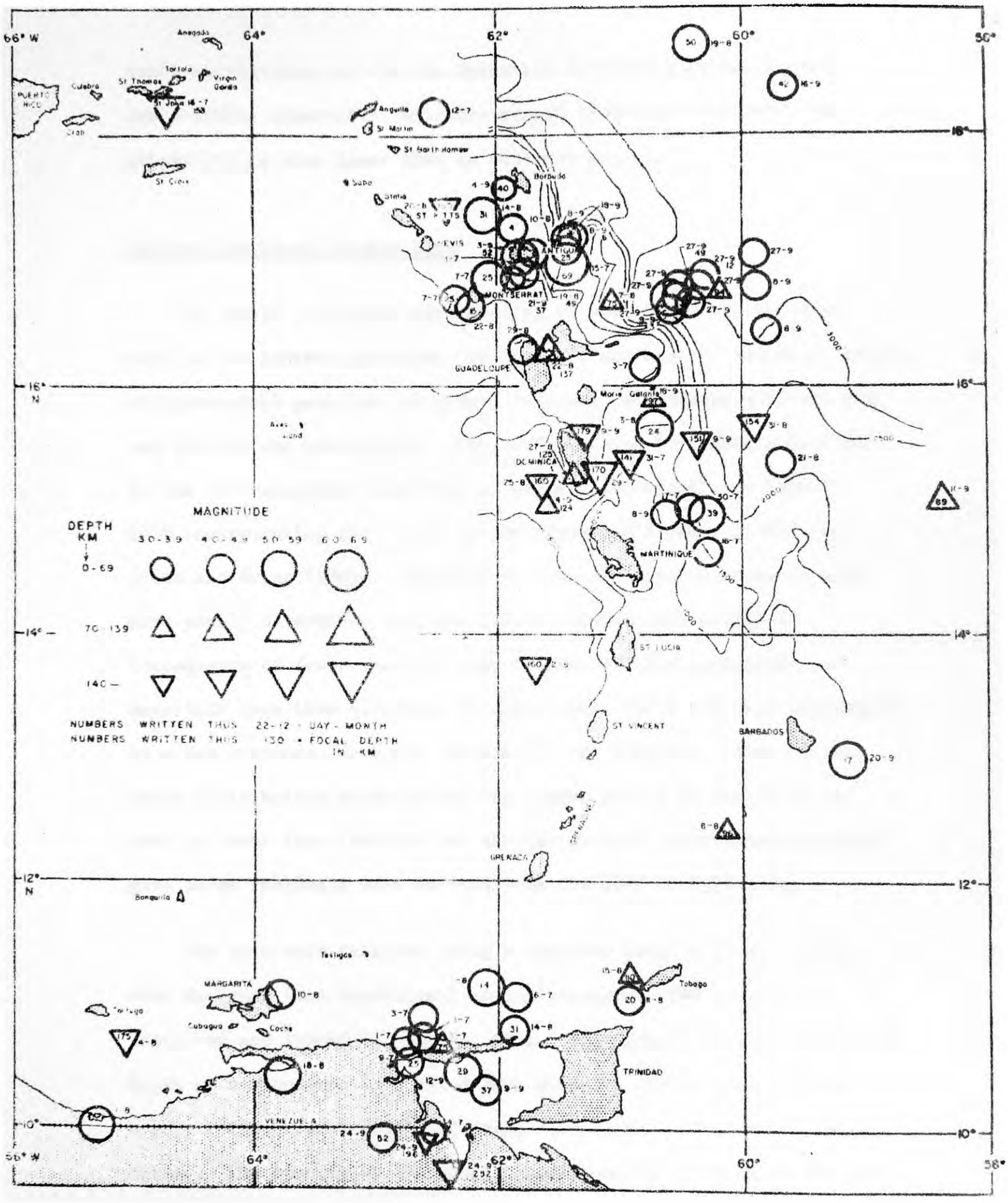

depth earthquakes and the one mechanism determined by Molnar and Sykes (1969) apparently indicates normal faulting. The level of seismicity is also lower than in adjacent regions.

Eastern Caribbean Seismic Zone

To obtain a clearer understanding of the nature of the seismic zone in the eastern Caribbean, an analysis was made of the distribution of hypocentral position and energy release. Earthquake activity over two periods was considered; 1964 to 1970 using positions determined by the International Seismological Centre, Edinburgh, and 1904 to 1970 incorporating data given by Gutenberg and Richter (1954), and Sykes and Ewing (1965). Earthquakes from the last two sources were more poorly determined than the I.S.C. hypocentres, mainly a consequence of fewer stations, and because of this earthquakes of magnitude less than 4.0 from the older data, which are only determined by a few stations, were not included in the analysis. Even so the depth distribution produced for the longer period is likely to be more in error than that for the shorter period. Determinations which gave large residuals were omitted from the 1964 to 1970 data.

The data were analysed using a computer program to do rolling mean analysis (two dimensional moving average). The program is described and listed in appendix C6.1. This produced maps of the mean depth of earthquakes in a one degree diameter circle, and the mean energy release per degree^2 per year, also using a 1° diameter sample circle. The spacing of the sample points was 0.05° which is the error on the better determined earthquakes. The energy was derived from the

6.3 Map of earthquake focal depth in the Antilles for the period 1964 to 1970. Computed as a two dimensional moving average of a one degree diameter sample circle.

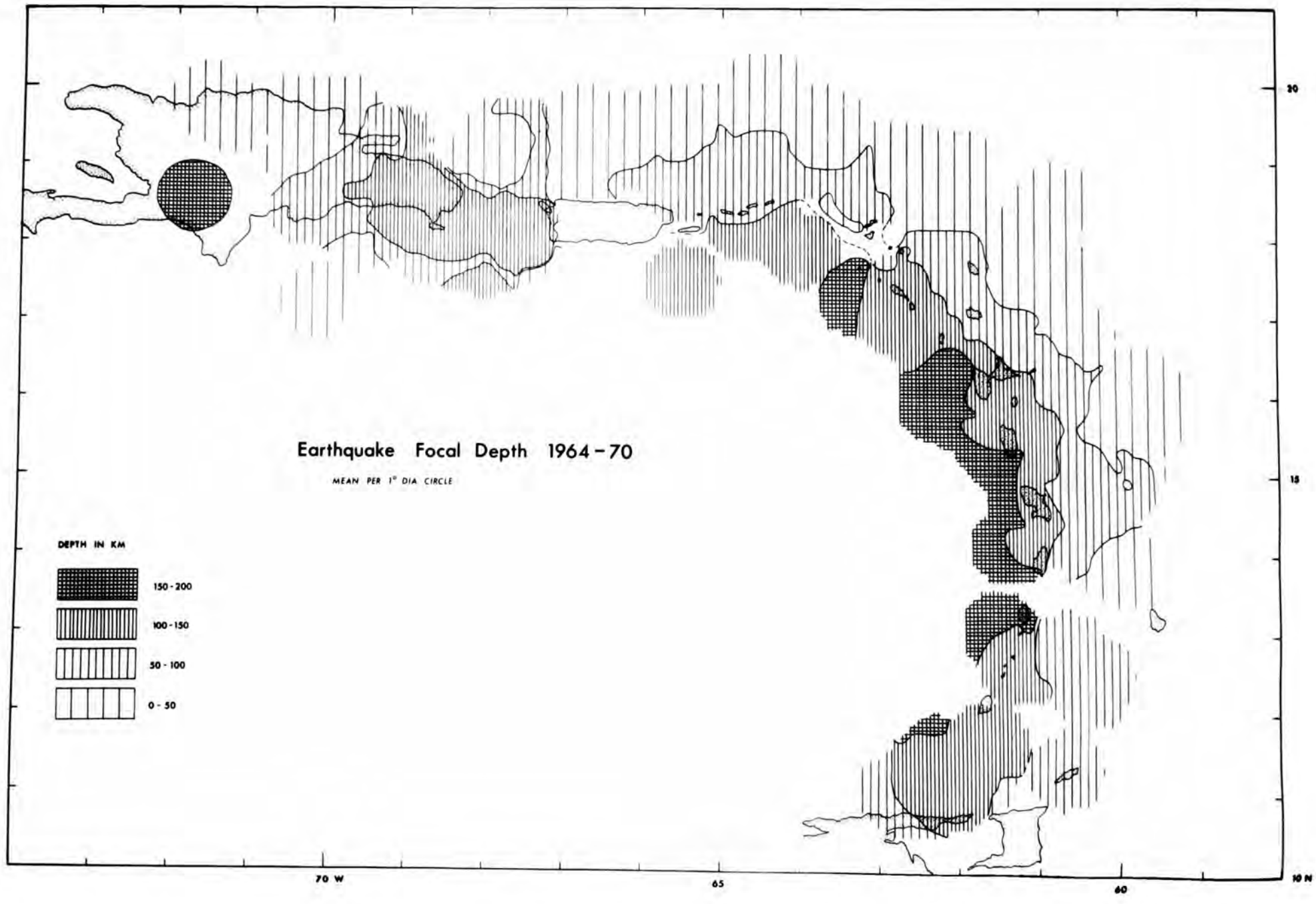
Earthquake Focal Depth 1964 – 70
MEAN PER 1° DIA CIRCLE
DEPTH IN KM
150 - 200
100 - 150
50 - 100
0 - 50
70 W
65
60
20
15
10 N

6.4 Map of earthquake focal depth in the Antilles for the period 1904 to 1970.

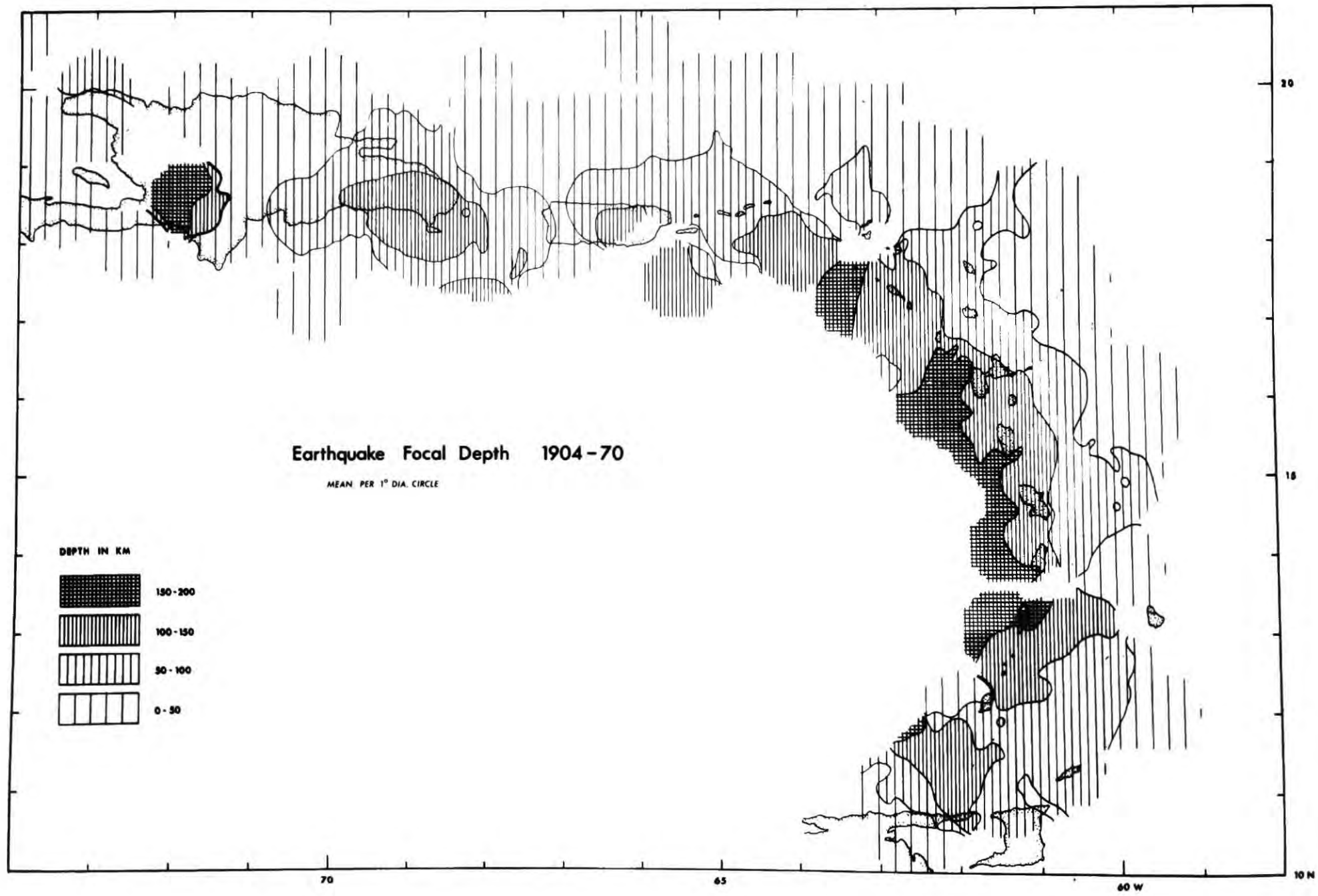
Earthquake Focal Depth 1904 - 70
MEAN PER 1° DIA. CIRCLE
DEPTH IN KM
150 - 200
100 - 150
50 - 100
0 - 50
20
15
10 N
70
65
60 W

6.5 Map of the energy released by earthquakes in the Antilles for the period 1964 to 1970. Computed as a two dimensional moving average using the relationship Log_{10} Energy = 5.8 + 2.4 m_b. Values given in ergs per degree^2 per year.

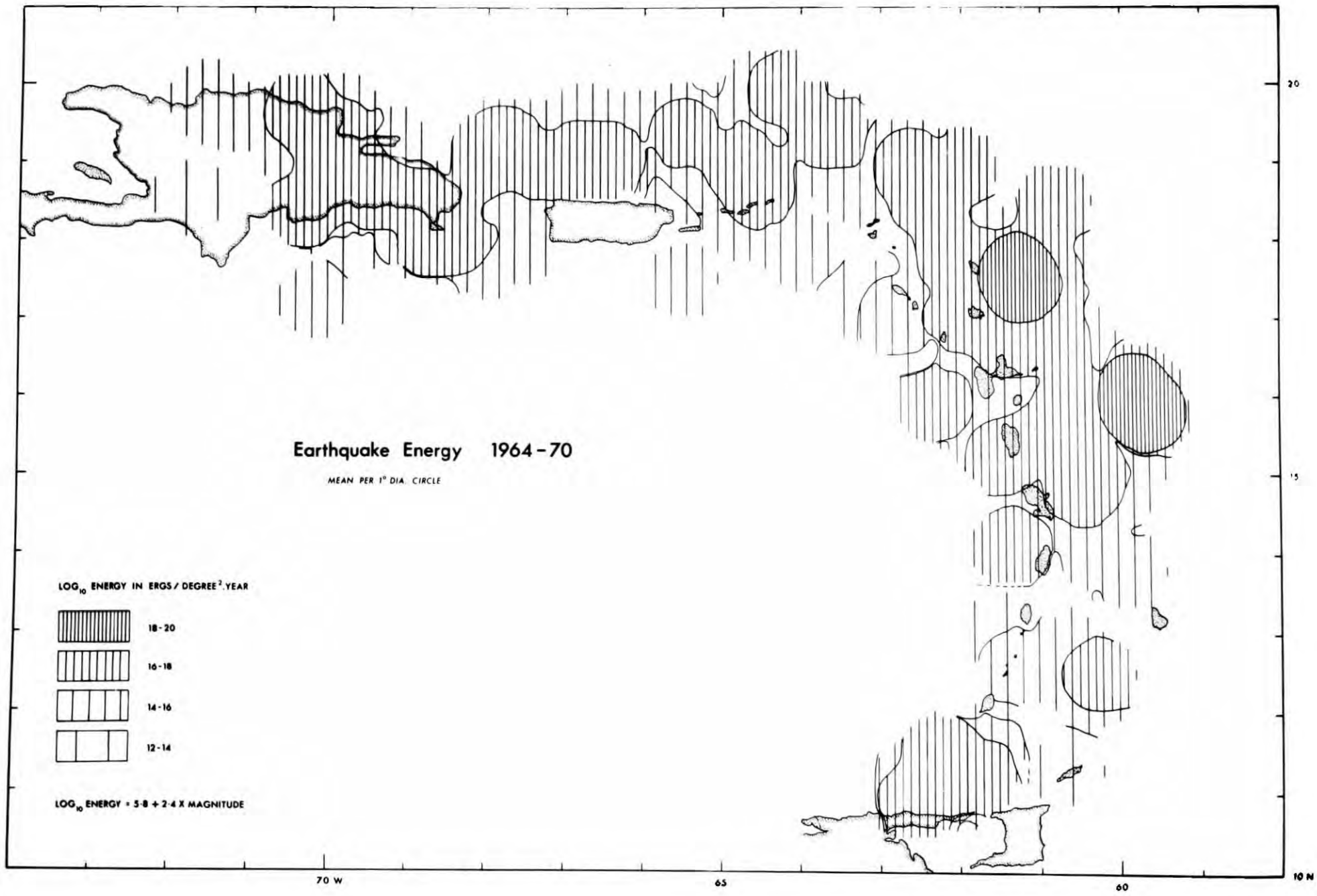
Earthquake Energy 1964 – 70
MEAN PER 1° DIA. CIRCLE
LOG10 ENERGY IN ERGS / DEGREE2 . YEAR
18 - 20
16 - 18
14 - 16
12 - 14
LOG10 ENERGY = 5·8 + 2·4 X MAGNITUDE
20
15
10 N
70 W
65
60

6.6 Map of the energy released by earthquakes in the Antilles for the period 1904 to 1970.

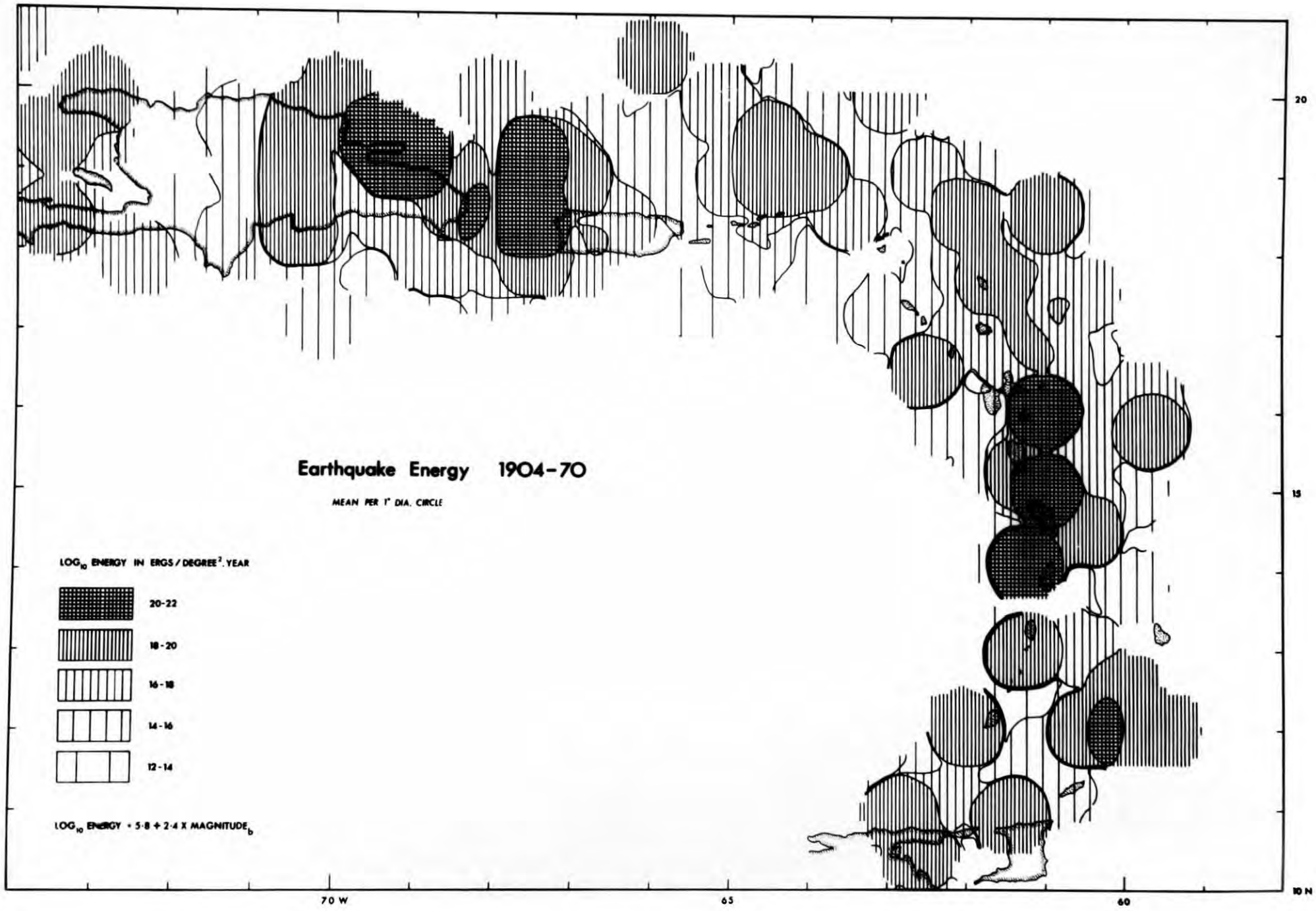
Earthquake Energy 1904-70
MEAN PER 1° DIA. CIRCLE
LOG10 ENERGY IN ERGS / DEGREE². YEAR
20-22
18-20
16-18
14-16
12-14
LOG10 ENERGY = 5·8 + 2·4 X MAGNITUDEb
20
15
10 N
70 W
65
60

magnitude (m_b) using the relationship $\log_{10}$ Energy = 5.8 + 2.4 x Magnitude (Gutenberg and Richter, 1956). The magnitudes of the earlier earthquake data given as M_s and to make these compatible with the other data they were converted to m_b using the relationship $M_s = 1.59m_b - 3.97$ (Gutenberg and Richter, 1956). There are more recent formulae for relating M_s to m_b (Gupta and Rastogi, 1971), but the M_s values in the early set of data were mostly derived originally from m_b using the relationship given. There are also recent estimates for the energy relationship. Bath's (1966) ($\log_{10}$ energy = 4.8 + 2.57 m_b) is a little different and gives greater energy values for magnitudes over 5.9, but only as little as 0.2 at magnitude 7.2 which is the largest in the data set.

The maps produced are shown in figs. 6.3, 6.4, 6.5, and 6.6. The most clearly defined feature on the focal depth maps is the inclined zone of earthquakes beneath the Lesser Antilles, extending to depth of 200 km and dipping at between 40° and 45° to the west. The eastern limit of the earthquakes follows approximately the axis of the negative free-air gravity anomaly. Fig. 6.7 shows a cross section through the Lesser Antilles for the period 1964 to 1970 in which all the focii are projected onto a single plane radial from the arc. This also shows the dipping zone clearly. The deepest earthquakes in the eastern Caribbean occur just west of the Lesser Antilles. Although for clarity on the maps displayed the depths are given in classes of 50 km the class interval for the computed maps was 5 km. The indented pattern of the earthquake depth map, though partly a function of uneven distribution, seems to be related to the north easterly trending faults suspected in the north of the Lesser Antilles. These

6.7 Cross section of earthquakes in the Lesser Antilles over the period 1964 to 1970. Distance is given radially from island arc and depths are indicated by dots with error bars.

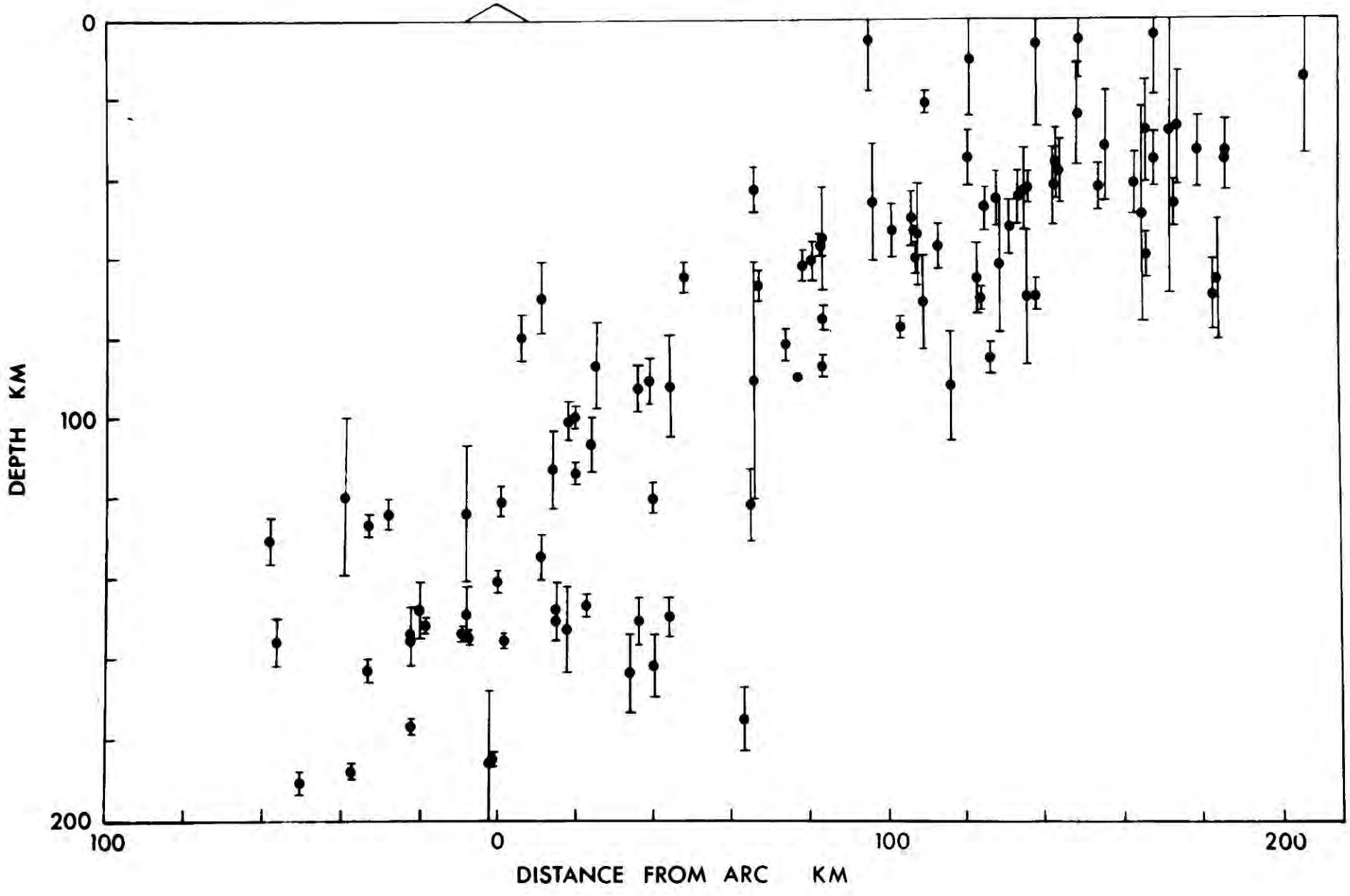
0
100
200
DEPTH KM
100
0
100
200
DISTANCE FROM ARC KM

faults may be reactivated because of distortion of the subducted lithosphere caused by its non-satisfaction of a principle of spherical geometry, postulated by Frank (1968) to be a controlling factor of the curvature of island arcs. This is that if the surface of a sphere with a thin inextensible elastic shell is depressed then the radius of the depression (in this case the radius of curvature of the trench) $r = \frac{1}{2} R\theta$, where R is the radius of the sphere (the Earth) and θ is the angle of depression (the subduction angle). The angle of subduction in the Lesser Antilles is 40° but the radius of curvature is 5.5° which means the angle of subduction should be 11° if the principle is to be satisfied, alternatively the radius of curvature of the trench should be 20°. The subducted plate must therefore undergo some extension across it to achieve a subduction angle of 40°. There are two drawbacks to this analysis; firstly while the thickness of the lithosphere is small in comparison to the radius of the Earth it cannot really be considered of negligible thickness; and secondly the plate cannot be considered to behave truly elastically. If the lithosphere is 80 km thick when subducted most of it must deform plastically, because of the radius of curvature of the top surface is about 210 km the bottom surface must undergo shortening of about 38%, and as 3% is a reasonable value for the elastic limit (Ramsay, 1967) only the top 12 km can deform elastically (if the plane of no strain is 6 km below the top surface). Extension of the top surface due to bending of the plate may be the cause of many of the earthquakes whose axes of principal extensional stress plunge to the west.

Luyendyk (1970) has derived an empirical relationship between the

dip of a subducted plate and the rate of subduction, which neglects the effect of a spherical earth, and has as its basis the premise that the subducted lithosphere sinks vertically at a rate of 4 to 6 cm y^{-1}, regardless of its horizontal velocity. This relationship gives a subduction angle of 45^{o} for a subduction rate of 8 cm y^{-1} and an angle of 90^{o} for a rate of 1 cm y^{-1}. Whilst this is an invalid relationship (It is internally inconsistent since a slab with a subduction rate of 1 cm y^{-1} cannot be sinking at 4 to 6 cm y^{-1}, and totally neglects the resistance of the mantle to horizontal motion), it does draw attention to the effect of the slab's own negative buoyancy arising from its relatively cool interior, which must be a major cause of distortion of the plate from its theoretical shape as predicted by Frank's hypothesis. Also pertinent is the fact that the bottom and sides of a subducted slab are free edges and relatively unrestrained, which is not the case for the depression in the thin inextensible shell. This diversion from the theoretical case is more acute the shorter the length of arc is, and since it is the smaller island arcs of the world which are least satisfactorily accounted for by Frank's hypothesis it seems that free edges of the subducted plate are an influence upon its shape.

In the Greater Antilles the distribution of earthquake focii becomes more complicated. North of Puerto Rico they generally are distributed along an inclined plane dipping southwards. Further west the pattern is more of a very steep V shape in cross-section, but this is not clearly defined. The zone of deeper earthquakes does not continue along the northern coast of Hispaniola. The trend, if anything, is along the southern coast and does not suggest a subduction

zone parallel to the northeast coast.

From the 1964-1970 energy map there appear to be several gaps in the seismicity, but inspection of the 1904-1970 energy map shows that these areas are filled, often by one earthquake of large magnitude. For the period 1904-1952 only data for large magnitude earthquakes was available. It is worth noting that several areas such as Jamaica and central Venezuela appear to have been relatively inactive seismically during the 20th century yet have a history of large destructive earthquakes. It is probable that these places are at points of greater than average resistance on the fault systems bounding the Caribbean and consequently a greater stress needs to build up before fault motion takes place. Also it is possible that much of the relative movement in these places is dissipated in the form of creep. The period over which one could consider movement to have taken place along all the boundary faults is certainly more than a century and this makes our detailed knowledge of the seismicity based on a few years observations very incomplete. This sort of period length for seismicity seems to be characteristic of regions where relative plate motion is fairly slow.

Earthquake focal depth distribution

Another aspect to consider is how the frequency and energy of earthquakes in the Antilles are distributed with depth. The frequency of earthquakes associated with subduction zones seems to decrease exponentially with depth, taking the form frequency = constant x exp (-depth/100) (Isacks and others, 1968), and this is

attributed to an increase in the rate of deformation by ductile flow compared to that by sudden shear failure. Figs. 6.8, 6.9, 6.10, and 6.11 show the distribution with depth of earthquake frequency and energy in the Lesser and Greater Antilles for the periods 1904-1970 and 1964-1970. For the computation of these graphs it was assumed that the errors in the determination of the depth of the focii were normally distributed and that all the determinations had a standard error of 10 km, which is the average standard error. The validity of the graphs would be improved if the individual standard error for each earthquake hypocentral depth were used. Individual values for all the focii were not readily available and brief inspection of the error bars on the focii plotted in fig. 6.7 will show that the use of an average value of 10 km is not unrealistic. (Details of program for computation of the graphs are given in appendix C6.2).

The frequency distribution for the Lesser Antilles over the period 1964-1970 shows a strong maximal peak at 45 km which tails off with increasing depth but gives a secondary maximum at 150 km. The distribution over the period 1904-1970 shows the same characteristics, though the maximum is at about 40 km depth. The energy distributions show the influence of large earthquakes. The Lesser Antilles 1964-1970 period graph shows a peak at zero depth with an exponential decrease with depth, but the 1904-1970 graph shows two large peaks at 100 and 140 km depth. The peak on the first graph is caused by a magnitude 6.4 earthquake at 1 km depth. This fades into insignificance however, when compared with the earthquakes of magnitude 7.0, 7.2 and 7.2 at 100 km, and 7.2 at 134 km which are the major contributors to the maxima on the 1904-1970 graph. The frequency distributions for

6.8 Graphs showing the distribution with depth of earthquake.
6.9 frequency and energy. The standard error of depth of
6.10 hypocentre is taken as 10 km. The graphs are taken
6.11 from the Lesser and Greater Antilles separately for the
periods 1904 to 1970 and 1964 to 1970.

Lesser Antilles 1964 - 1970

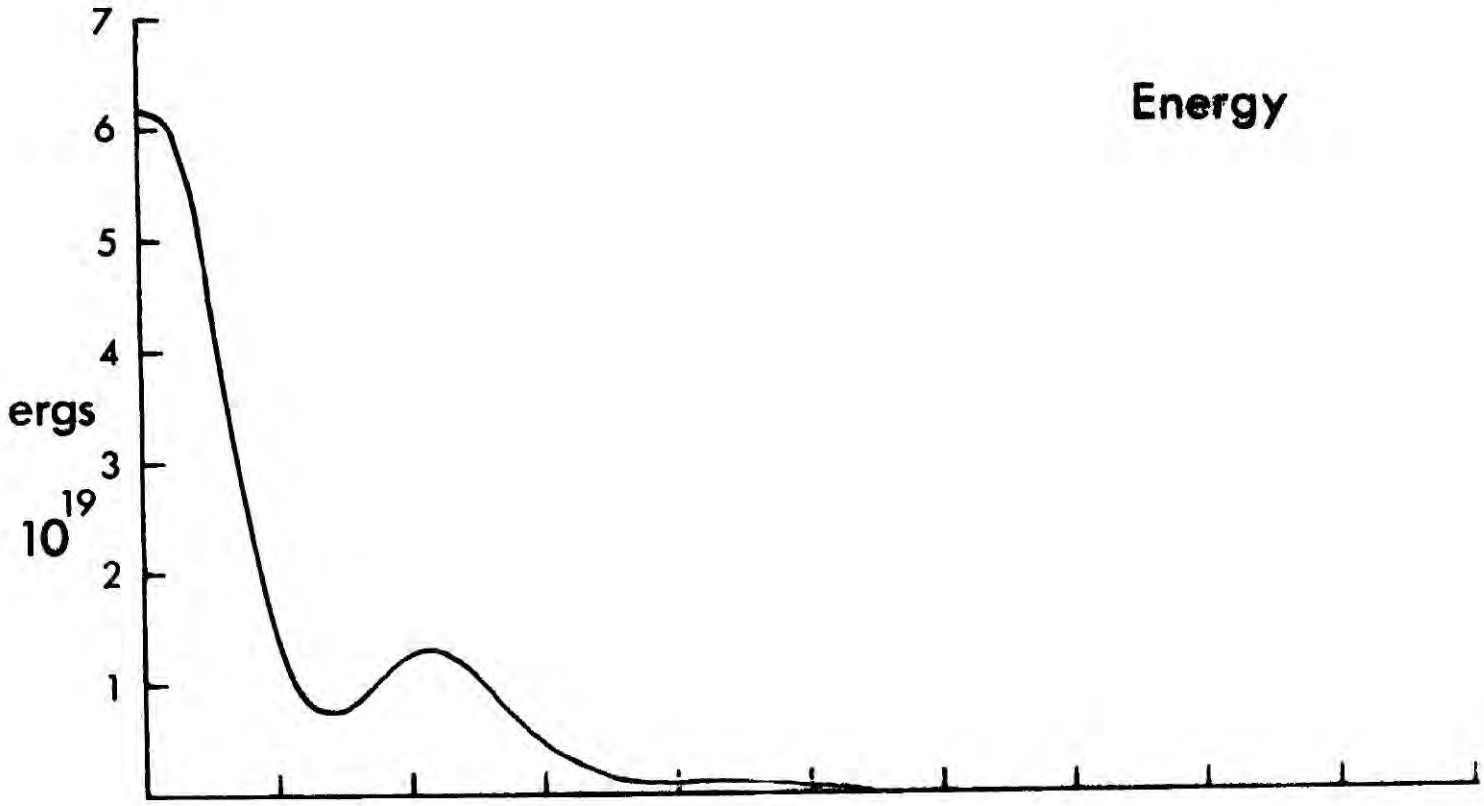

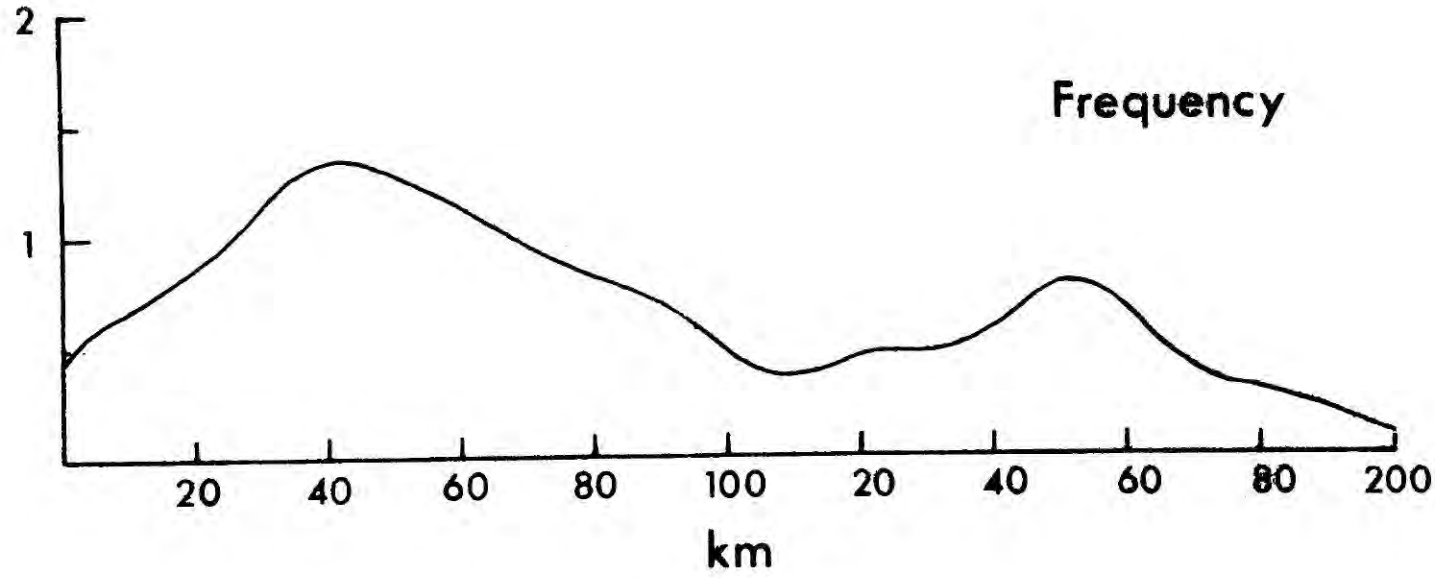

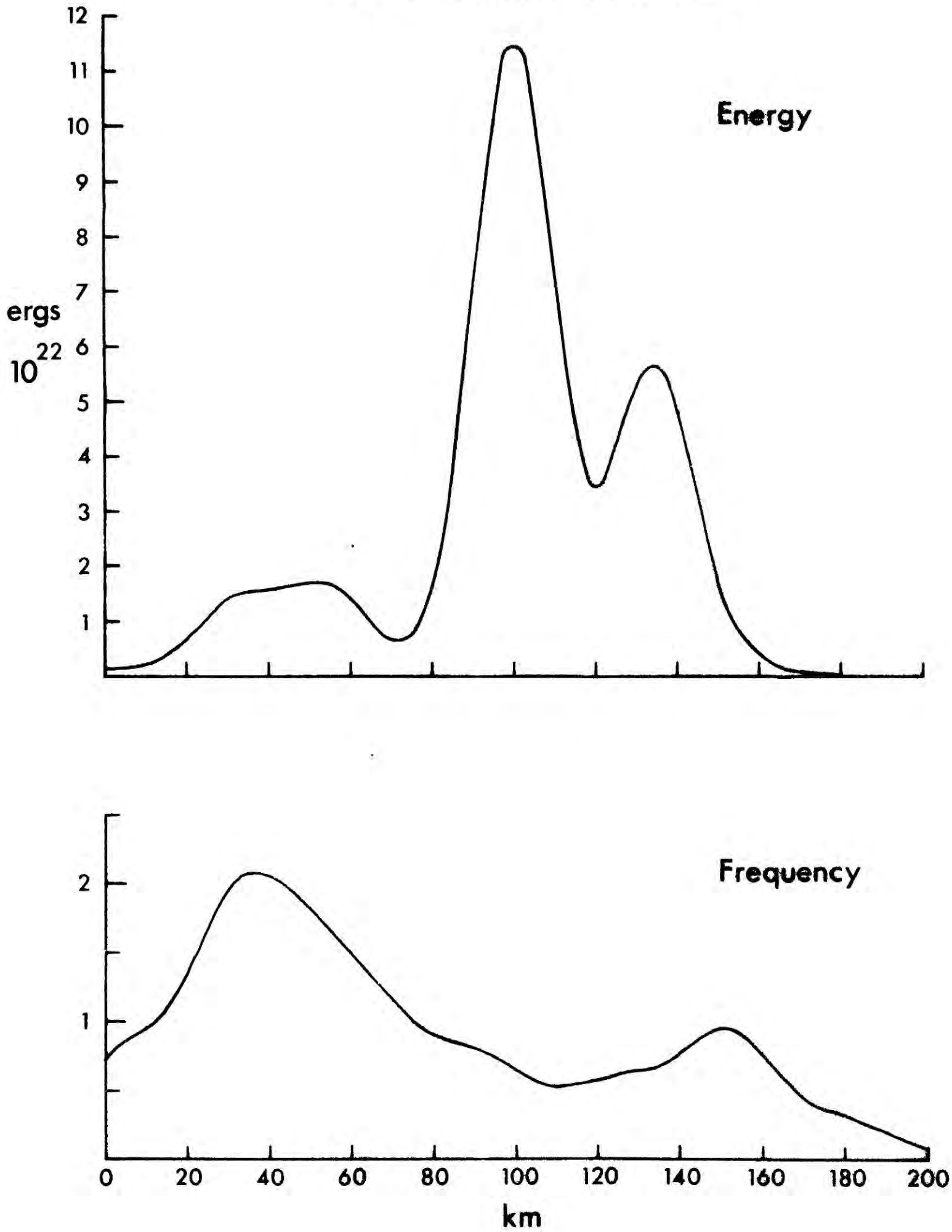
Lesser Antilles 1904 - 1970
Energy
ergs
10^{22}
12
11
10
9
8
7
6
5
4
3
2
1
Frequency
2
1
0
20
40
60
80
100
120
140
160
180
200
km

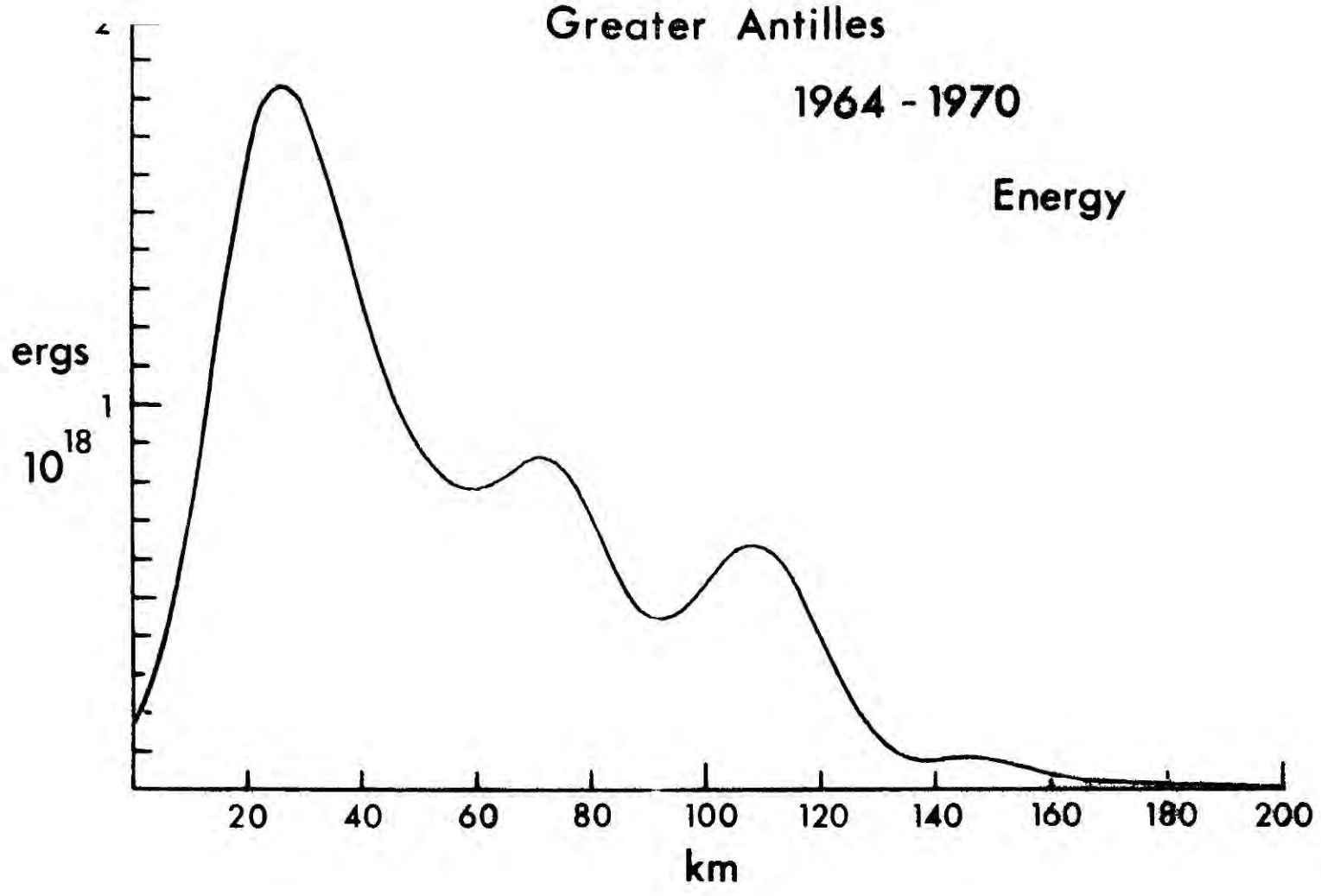
Greater Antilles
1964 - 1970
Energy
ergs
10^{18}
1
20
40
60
80
100
120
140
160
180
200
km

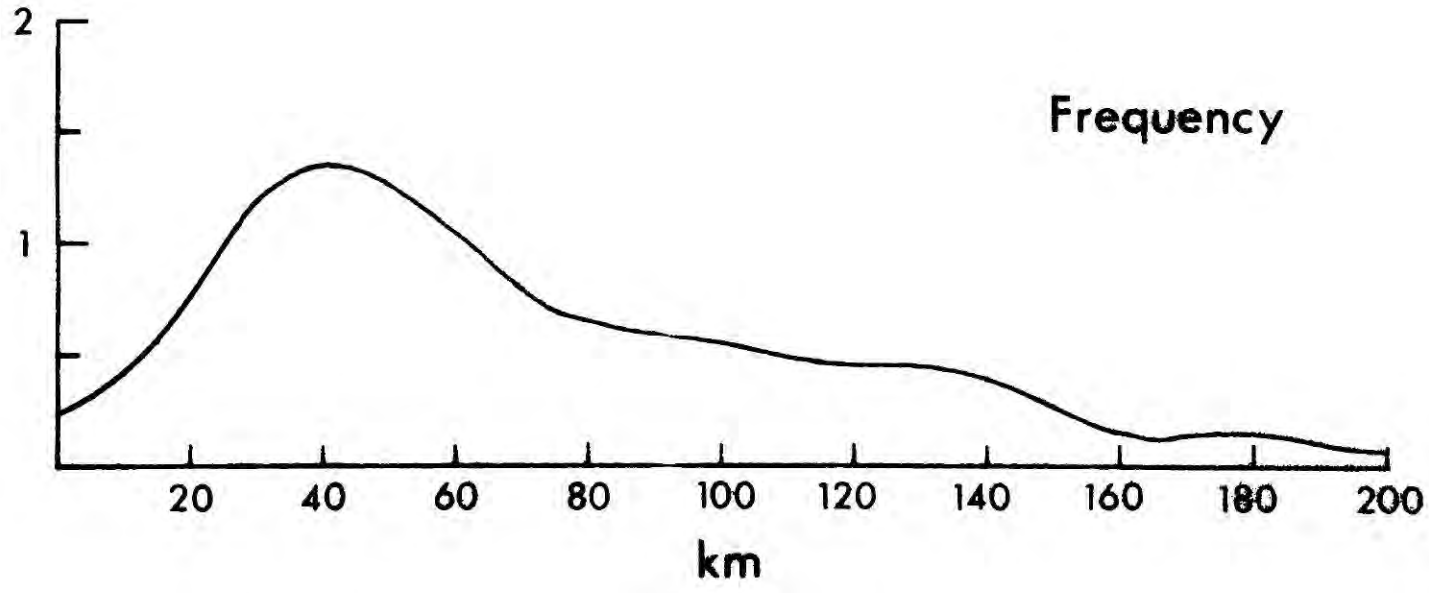
2
1
Frequency
20
40
60
80
100
120
140
160
180
200
km

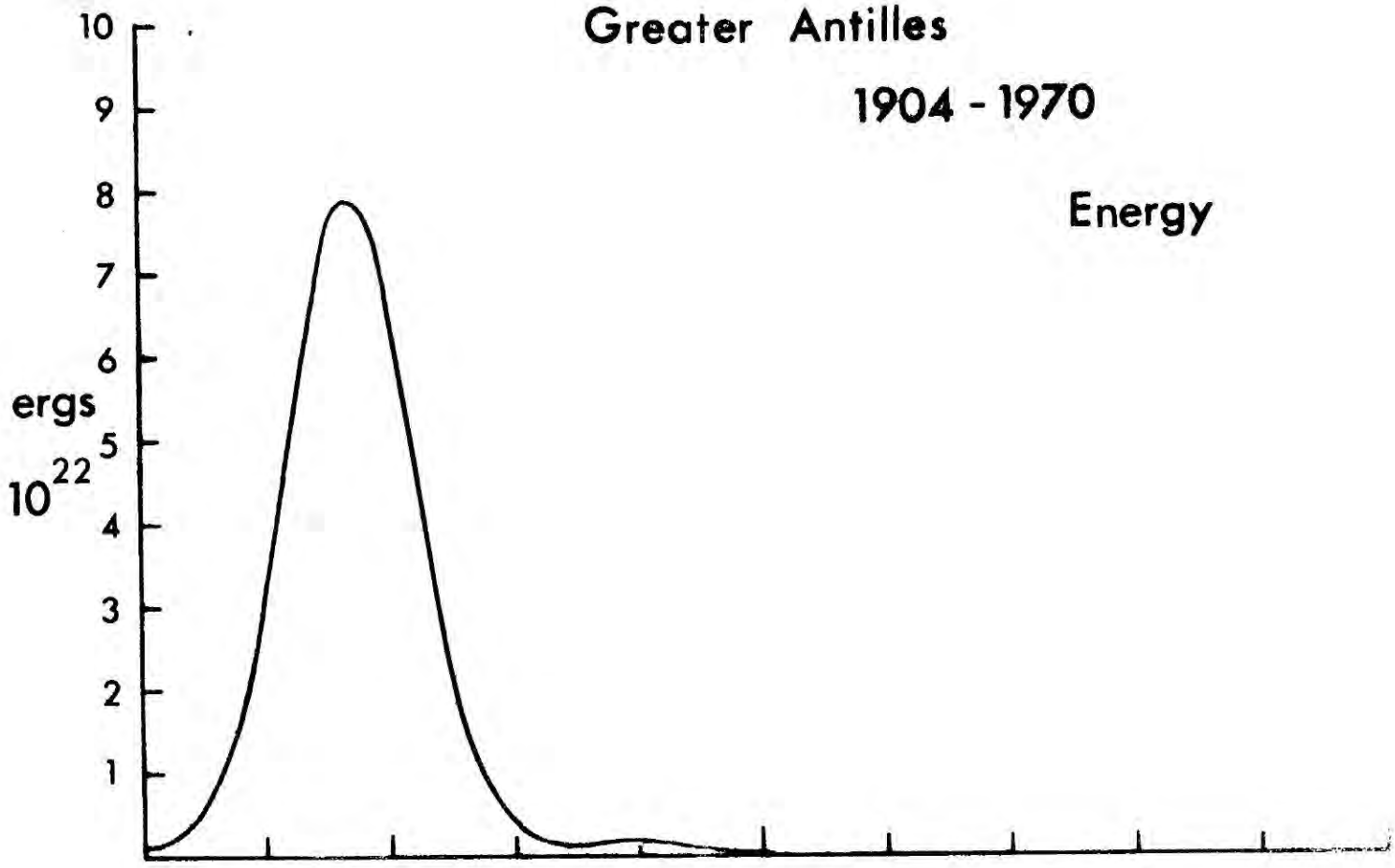
Greater Antilles
1904 - 1970
Energy
ergs
10^{22}
10
9
8
7
6
5
4
3
2
1

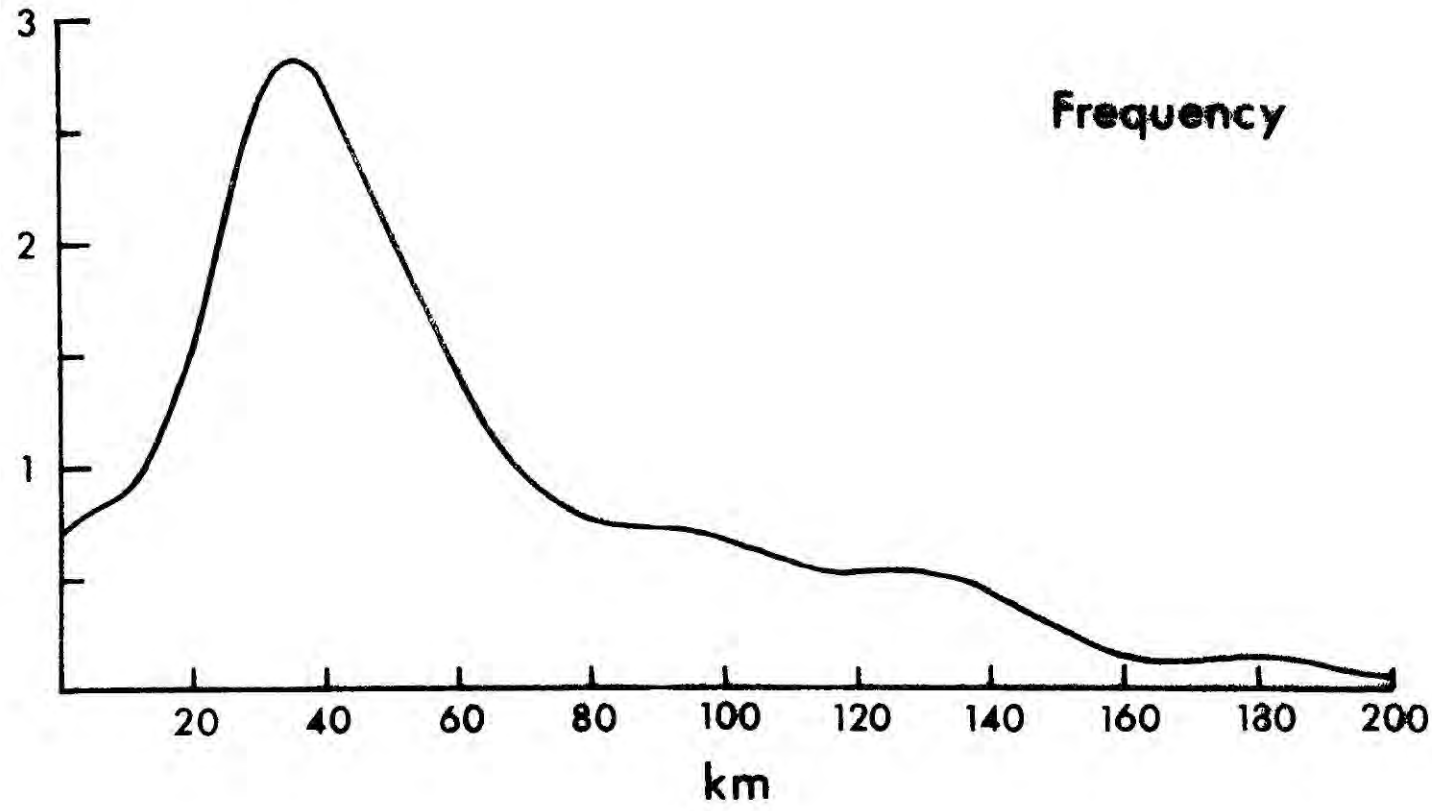
Frequency
3
2
1
20
40
60
80
100
120
140
160
180
200
km

the Greater Antilles show a maximum around 40 km and no pronounced secondary peaks. By contrast with the Lesser Antilles the energy distributions are similar to the frequency distributions. The frequency distributions do not follow the simple exponential decay law given above, except below about 50 km. What are the reasons for this? From interpretation of the crustal structure in the southern part of the Lesser Antilles it seems that the fault plane at the top of the descending lithosphere does not go through crystalline basement until a depth of 20 km and there is also no strong curvature on the subducted lithosphere up to this depth. The majority of earthquakes in the depth range 30 to 70 km occur well below the probable top surface of the subducted plate as interpolated between the crustal structure and the trend of the deeper earthquakes. It seems, therefore, that the maximum frequency peak of earthquakes at about 40 km depth is a result of internal deformation of the lithosphere as it is bent down into the mantle. The energy distribution for the Lesser Antilles 1904-1970 may be poorly defined because the large magnitudes are from the older data and the depth and magnitude determinations are probably not too good. A comparatively small error in the magnitude determination can have a large effect on the apparent energy release. Comparison of magnitude determinations from regional stations with those from world wide stations shows a bias towards values from the world wide stations (J. Tomblin, personal communication).

Subduction rate

Using the energy release values for the period 1904-1970 the rate

of movement down the subduction zone was calculated using the method of Brune (1968). Taking the value of 10^{22} ergs per degree^2 per year and a dip of the seismic zone of 40°, 0.5 cm per year is the rate obtained, which is the same as that estimated by Molnar and Sykes (1969) using the same method. Rates calculated by this method are usually an underestimate; Brune's method applied to the Imperial Valley fault gave a value of 3.2 cm per year whereas the movement measured geodetically was 8.0 cm per year. Brune attributed the discrepancy to displacement by creep in the surrounding rocks, and this is supported by the presence of mylonites in region of the fault. If the rate determined above is valid for the present period of Lesser Antillean vulcanism which started some time near the end of the Miocene, then about 50 to 100 km of lithosphere has been subducted since then.

The maximum depth of the seimic zone is not necessarily directly related to the depth of subducted lithosphere, but may reflect the depth at which a critical ratio between the temperature of the subducted lithosphere and the temperature of the surrounding is passed, and beyond which there is not sufficient physical contrast for earthquakes to occur. McKenzie (1969) using data for the length of seismic zone and subduction rate for most of the world's island arcs from Isacks, Oliver and Sykes (1968) found that for his thermal model of a subduction zone the critical point was reached when the temperature at the centre of the subducted slab reached 85% of his adiabatic mantle temperature. Griggs (1972) believes the critical temperature at the centre of the subducted slab to be two thirds of the melting temperature, and derives a more sophisticated relationship between subduction rate and length of seimic zone than the straight line fit of

Isacks, Oliver and Sykes (1968). According to these relationships the subduction rate at the Lesser Antilles should be 2.8 or 3.1 cm y^{-1}. These rules are empirical and there are several exceptions, most of which, like the Lesser Antilles, have seismic zones deeper than predicted by the subduction rate.

Plate Motions

Considering the evidence for the nature of present day plate motions in the Caribbean region, it can be seen that the Caribbean Plate is almost completely bounded by seismically active zones. Ball and Harrison (1969, 1971) thought that the Caribbean is coupled to South America and took as evidence, the apparent lack of seismicity in central Venezuela, the absence of any obviously continuous fault along the southern boundary of the Caribbean, and the small estimate of displacement (15 km) given by Metz (1968) for the Pilar Fault. This necessitates underthrusting of the Lesser Antilles by the mechanism shown as model 2 in fig. 6.12. The pole positions and rates of rotation for the North and South Atlantic spreading regimes (from analysis described in chapter 7) do indicate relative movement between North and South America of the right sense to drive this model. Set against this, however, is the almost complete absence of seismicity in the region east of the Lesser Antilles where the necessary boundary fault between the North and South American Plates must occur. The few earthquakes that do occur are widely scattered and do not indicate any linear feature. The absence of earthquakes in central Venezuela was only a temporary anomaly, valid for the period over which the data shown in Sykes and Ewing (1969) was gathered. More recent epicentral determinations

6.12 The two alternative mechanisms of plate motion by which underthrusting in the Lesser Antilles could be caused. Model 1 shows the Caribbean Plate moving eastward relative to the North American Plate and South American Plate which are probably joined to form one large American Plate. The Caribbean Plate may have some connection with plates in the Pacific. Model 2 shows the Caribbean as part of the South American Plate which moves eastward with respect to the North American Plate. A transform fault runs from the southern end of the Lesser Antilles to the Mid Atlantic Ridge.

1

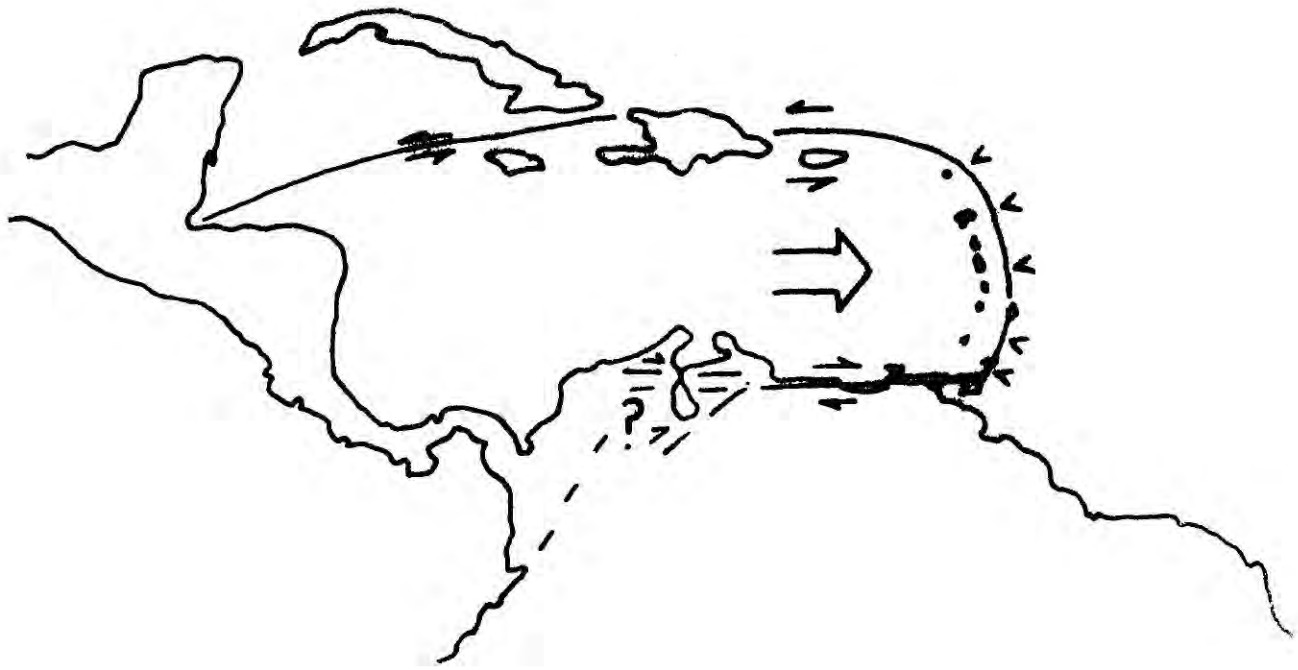

2

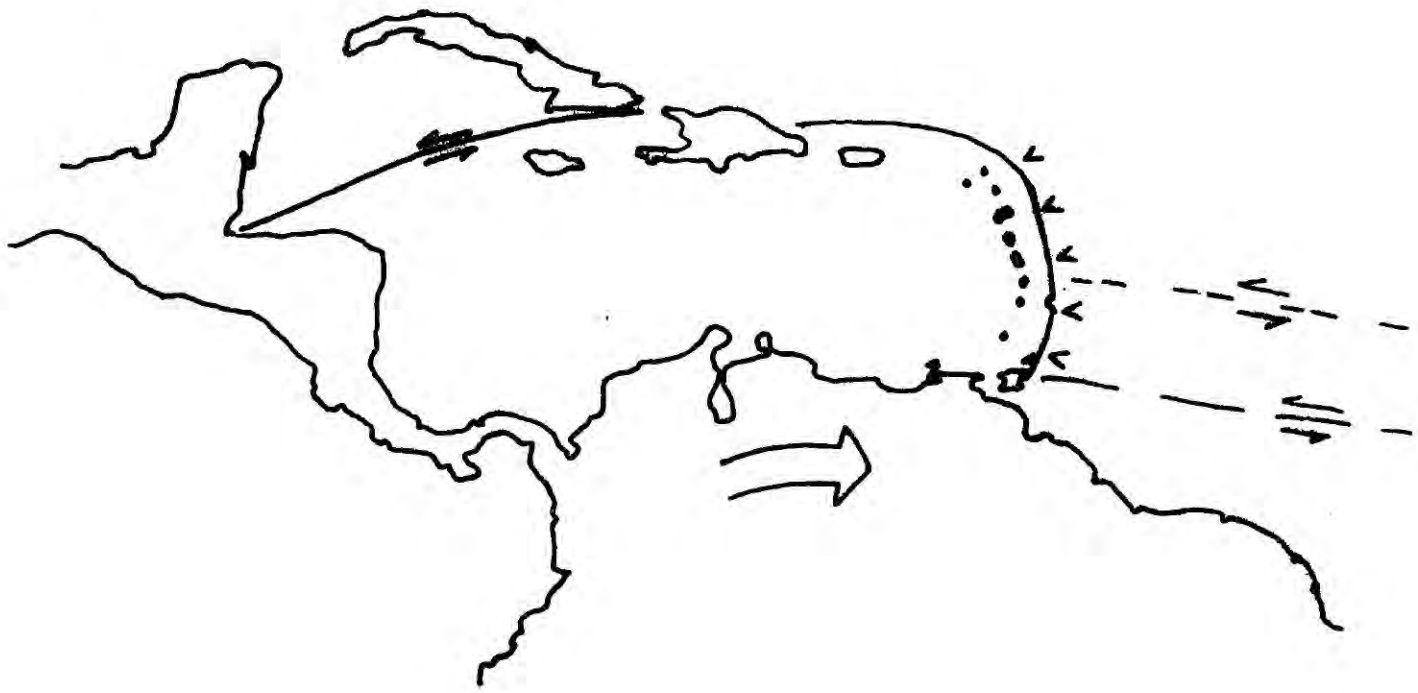

Caribbean Plate Tectonic Models

show earthquakes in this region and as mentioned previously it has been seismically active earlier. Taking this into account it is more likely that model 1 of fig 6.12 is the better representation of present Caribbean plate motions. Displacement at the western end of the Caribbean's southern boundary could be taken up in the folding and overthrusting of the Colombian Andes which commenced 9 my ago (the Andean Orogeny). There is probably partial coupling between the Caribbean Plate and the Nazca Plate in the region of the Panamanian isthmus and its sigmoidal shape may be the result of crustal deformation there. The motions causing the Nazca Plate to underthrust South America also provide a driving force for the Caribbean Plate. The strike slip motion in northern Venezuela is probably taking place along the Pilar fault system and some immediately offshore faults. Although most of the movement measured on the El Pilar fault in eastern Venezuela appears to have taken place in late Eocene times, further west faults in the same system such as the La Victoria fault show displacement of late Miocene to Recent age. The speculative Southern Caribbean Fault postulated to run along the base of the continental slope (Barr, 1955; North, 1965) has been shown not to occur in the region north of Trinidad, where it should exist to connect with the subduction zone (Weeks and others, 1971; Bassinger and others, 1971).

There remains the possibility that the present tectonic situation is a combination of models 1 and 2. If this is the case, then the relative amounts of movement along the mutual boundaries of the plates can be determined if the poles of the relative rotation between the plates are known. The pole which gives a small circle fit

to the Cayman Trough provides an estimate of the Caribbean/N. America pole. The El Pilar Fault gives the Caribbean/S. America pole, and the N. America/S. America comes from the analysis of the North and South Atlantic spreading regimes. These give relative rates of rotation in ratios 0.42:1.0:0.12: for C./N.A.:C./S.A.:S.A./N.A. and taking into account the arc length from pole to fault this means that most of the movement should be taking place along the southern boundary of the Caribbean. The seismicity seems to indicate that the northern boundary is the most active. The analysis does not lend immediate support to the hypothesis of motion between three plate, but this may be due to a poor assessment of the poles of relative rotation. Most suspect in this respect is the Caribbean/S.America pole. The El Pilar fault is likely to be a poor estimator because it is of short length and also a reactivated older fault. Other faults which also show seismicity, such as the Bocono Fault, have a northeast trend and some of the earthquake mechanisms give fault planes with a NNE strike These features are in the west of Venezuela and a rotational pole which accommodates these features most likely lies well to the south in South America. A pole in this area would probably lie near to the pole determined from the Cayman Trough and this would favour model 1 as being the predominant mode of plate motion. The Cayman Trough appears to have undergone some east-west extension during the Pliocene (Bowin, 1968; Gough and Heirtzler, 1969; Ericson and others, 1972) even though fault plane solutions are parallel to the trend of the trough. Another point about the Cayman Trough is that is extension through Central America, commonly assumed to be the Motagua Fault, does not lie on the same small circle as the trough. It is however, on a small

circle with the northern slope of the Nicaraguan Rise and it may be that the fault ran along there earlier in the Tertiary. This still leaves the problem of present day motion and one must appeal to en echelon faulting and crustal deformation to resolve it.

The alignment of the principal axes of extensive stress of earthquakes in the Lesser Antilles down the subducted plate might be interpreted as favouring the concept of subduction due to the gravitational instability of the descending lithosphere, as has been suggested for many of the circum-Pacific arcs. The subducting lithosphere, however, cannot be dragging the whole of the western Atlantic plate towards the Caribbean. It is also unlikely that a plate the size of the Caribbean could have a driving force of its own. It seems, therefore, that some sort of coupling with the Nazca Plate is the most probable cause of the movement giving subduction in the Lesser Antilles.

Chapter 7

Tectonic History of the Caribbean Region

Introduction

The object of this chapter is to assess the probable nature of the tectonic movements which brought the Lesser Antilles arc into being and influenced its development. The tectonic state of the Caribbean area has changed several times since the commencement of movement in this region, when the initial rifting of the Atlantic began 180 my ago. Thus simple extrapolation into the past of the present tectonic regime is certain to lead to erroneous conclusions.

The history of the Caribbean has been interpreted in terms of plate tectonics, either wholly or partly, by several authors, and recently there has been much debate about the implications (Freeland and Dietz, 1971 & 1972; Mattson, 1972; Malfait and Dinkleman, 1972 & 1973; Bell, 1973; Meyerhoff and Meyerhoff, 1973). These reconstructions attempt to provide sequential evolutions relating relative movement between various plates of differing size to the formation of distinctive rock types (eugeosynclinal sediments, calc-alkaline volcanics, evaporites) and structural movements in the Caribbean region during various stages of its history. The interpretations depend critically on the relative positions of the North and South American Plates during the evolution of the Caribbean, but in the above mentioned reconstructions the positions are derived mainly from an internal consideration of the tectonics of the Caribbean, and so are dependent on the interpretation. These reconstructions, appeal to plate tectonics for the license to move portions of the Earth's lithosphere around, but do not always accept the constraints imposed by the geometry

of movement on a sphere.

In order to gain a more objective view of this problem, a semi-quantitative evaluation is made below of how the spreading histories of the North and South Atlantic could have influenced the development of the Caribbean.

Methods of Analysis

Transform faults provide a means of assessing the relative motion between the adjacent two plates, because the fault must lie on a small circle of the pole of relative rotation between the two plates. The determination of relative plate motion using transform faults is one of the principal methods of analysis in plate tectonics (Morgan, 1968; Le Pichon, 1968) and has been used extensively to find poles describing the opening of the Atlantic (Fox and others, 1969; Phillips and Luyendyk, 1970; Le Pichon and Hayes, 1971; Le Pichon and Fox, 1971).

To calculate pole positions from transform faults three computer programs (C7.1, C7.2, C7.3) were written using three different methods; two analytical, and one iterative. In all these calculations a spherical earth was assumed. The first method of calculation finds the mean intersection of the great circles that cut orthogonally chords joining pairs of points situated along the feature or features being used to find the pole, and is similar to that used by Morgan (1968). The second method fits planes through all the combinations of three points out of a group situated along any small circle feature,and finds the mean position of the poles to the planes. These two methods provide a direct estimate of the standard error on the pole in longitude and

latitude or distance from the pole, and one can plot the individual pole positions to give an impression of the shape of the zone in which the poles fall. They are also very rapid and take only a few seconds on the computer.

The third method, which is iterative, finds the pole position that will give the best least squares fit of small circles from the pole to the points situated on one or more transform faults, by minimising the variance of the difference in latitude, with respect to the pole, between the small circle and points along the feature. This method gives the standard error of the fit of the small circles to the points, but not the standard error on the pole position. If the number of points is small the standard error of fit to the small circles can be small but the pole may be very poorly defined.

Le Pichon and Fox using the third type of method (1971) quoted 12 km as a minimum standard deviation for their pole of early opening of the North Atlantic at 58.3 N 21.8 W, which is misleading in two ways. Firstly it appears that the standard deviation quoted is for the pole whereas it is really for the fit of the points to the small circle, and secondly it gives no indication of what the real standard error on the pole is. This apparent weakness in the method can easily be overcome by mapping the function that is being minimised (i.e. the variance) to give the shape of the zone of minimum error in which the pole falls. From this map one can see easily the limits of the valid pole positions and because of this mapping facility the iterative program was that most used. The other programs could be written to produce a similar type of map based on least square distance to the pole. Using the iterative program to recompute the position of the pole from Le Pichon's and Fox's data it

is found that their pole lies in a small 'valley' of minimum standard error, the limiting positions at either end being 59.2 N 19.0 W and 57.9N 22.9 W. This pole position is in fact well defined, and a principal reason for this is that there is a good spread of longitude values which give good definition of the latitude of the pole which is often the most poorly defined parameter.

The best available data on the spreading histories of the North and South Atlantic were employed to find the relative motions of North and South America with respect to Africa during the various phases of opening. These motions were then used to calculate the relative motions between North America and South America. To do these calculations a short program was written to compute composite and simple rotation additions (Pars, 1965). This program is described and listed in appendix C7.4 together with the pole location programs and several other small programs to compute quantities useful in this analysis such as the rotated positions of locations, spreading rates from rotation rates and vice versa, and rotations on poles in three plate problems when pole positions are known from fault boundaries.

The opening of the Atlantic

There has been much work on the opening of the Atlantic since the continental reconstruction of Bullard, Everett and Smith (1965). Morgan (1968) and Le Pichon (1968) used fracture zones to derive pole positions for the present phase of opening of the whole Atlantic. They treated the Atlantic as a single spreading regime because no obvious zone of earthquake activity separates the North and South American plates. The

present positions of North and South America when compared with their pre-drift positions reveal that they must have had different poles of rotation at some time. Le Pichon and Hayes (1971), and Le Pichon and Fox (1971) looked at the manner of early opening of the South and North Atlantic by computing the poles to features thought to be old fracture zones. They considered that the early opening was controlled by marginal offsets of the continents (major faults forming part of the continents' edges). Both contributions find that there was a major change in plate movement about 80 my bp. The pole that describes the relative movement between North and South America over the period 80 my to present is 3.88 N 56.8 W rotation 8^{o}. The probable age of the Caribbean Plate is 80 my (Edgar, Saunders and others, 1971) and plate motions associated with the formation of the Lesser Antilles must consequently be more recent than this.

The geological history of the Caribbean reveals that it has undergone periodic phases of tectonic activity of differing type and orientation, suggesting that the relative motion between N. and S. America has not been constant in its nature, although in this context the effect of plate motions in the Pacific must not be overlooked. Vogt and others (1969) remarked on discontinuities in seafloor spreading in the North Atlantic and Fox and others (1969) presented evidence for at least two poles of rotation during the Tertiary. Phillips and Luyendyk (1970) calculated a pole position for the past 40 my which differs significantly from the present pole position of Morgan. Most recently Pitman and Talwani (1972) have shown by matching magnetic anomalies that the North Atlantic has had several poles of rotation during its opening. To assess the possible influence of these changes, the poles of Talwani and Pitman and

7.1 Bathymetry of the Atlantic Ocean (from Russian chart) with the major fracture zones considered in this analysis emphasised.

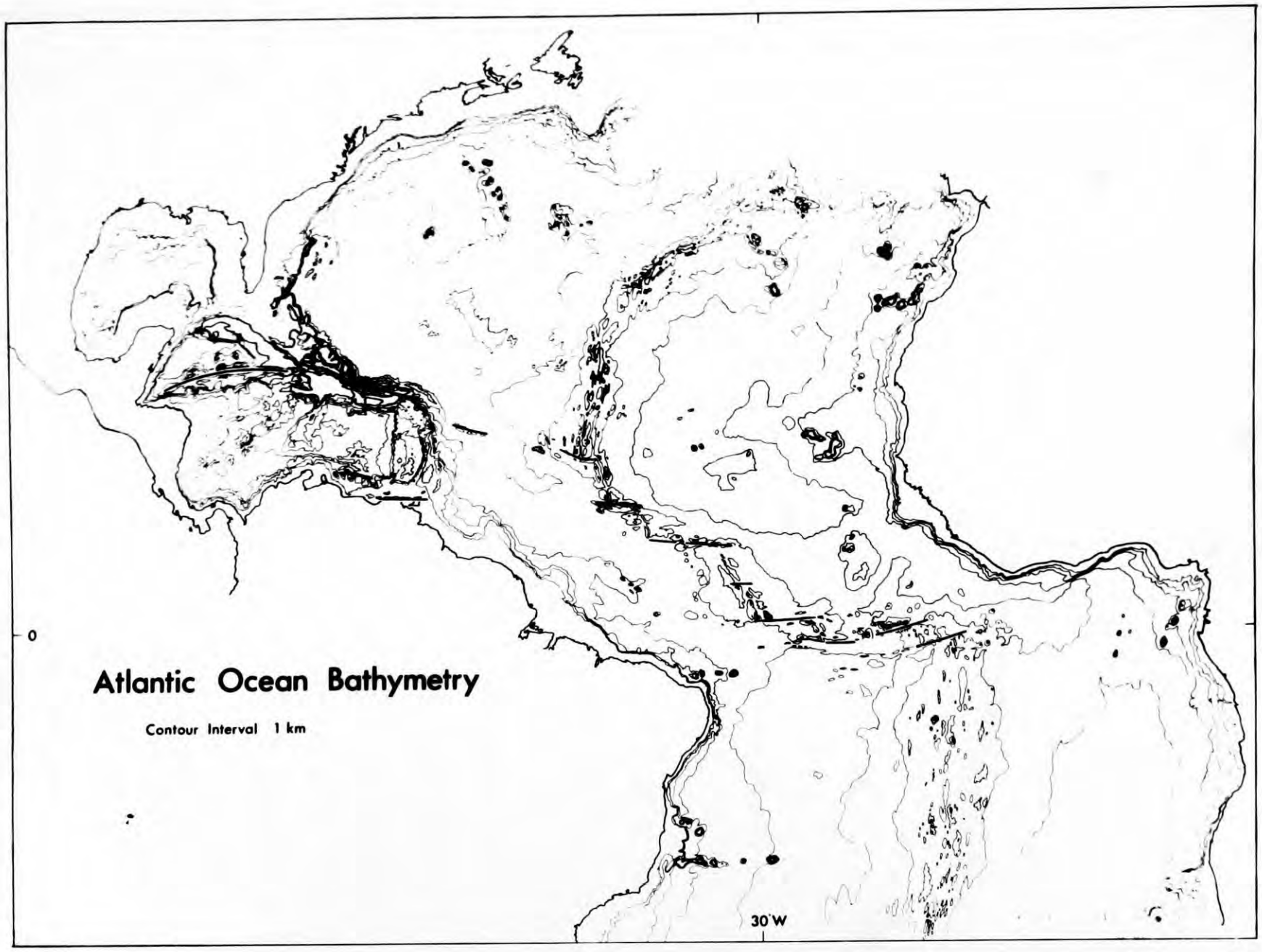
0
Atlantic Ocean Bathymetry
Contour Interval 1 km
30°W

their rates of rotation were used in conjunction with the late pole of opening of the South Atlantic (80 my to present) given by Le Pichon and Hayes. The rate of opening in the South Atlantic was taken to be constant for the calculations. Pitman and Talwani used the time scale of Heirtzler and others (1968), subsequently confirmed by JOIDES results (Maxwell and others, 1970). Therefore any changes in the rate of motion will only produce errors in the rate of relative rotation calculated, not the pole position or total amount of rotation.

Pitman and Talwani produced a pole of rotation to describe the present motion of the North Atlantic, based on four fracture zones, that is substantially different from that given by Morgan for the whole Atlantic. Morgan's pole was based mainly on fracture zones from the Central Atlantic, many of which lie in the area east of the Caribbean where the boundary between the North and South American Plates must lie, and therefore Morgan's pole is possibly calculated from features in separate spreading regimes. A recalculation of the present South Atlantic pole has been made using only fracture zones that can be due to spreading in the South Atlantic (see fig. 7.1). A best pole position at 53.96 N 40.1 W was determined, but it was found that by omitting some fracture zones from the analysis a slightly different position was found. The regions of minimum standard error for three different combinations of fracture zones are shown in fig. 7.2. These data seem to show that at present the North and South Atlantic are opening about different though not widely separated poles. The recent pole determined for the South Atlantic was subtracted from the late pole of Le Pichon and Hayes to give the pole for the period 81 to 9 my bp. An attempt to find the present South Atlantic pole using earthquake data, which indicate the

7.2 Map of the object function, the variance of the fit of a small circle from a pole to points on a transform fault, multiplied by 100, determined in finding the best fit pole for spreading in the South Atlantic using fracture zone data from the equatorial region of it. a, b and c are the pole positions found using different combinations of data and around them are shown the limits of the areas of equal pole validity with the minimum function value indicated. Contours shown are for pole a. m is the Atlantic pole of Morgan (1968).

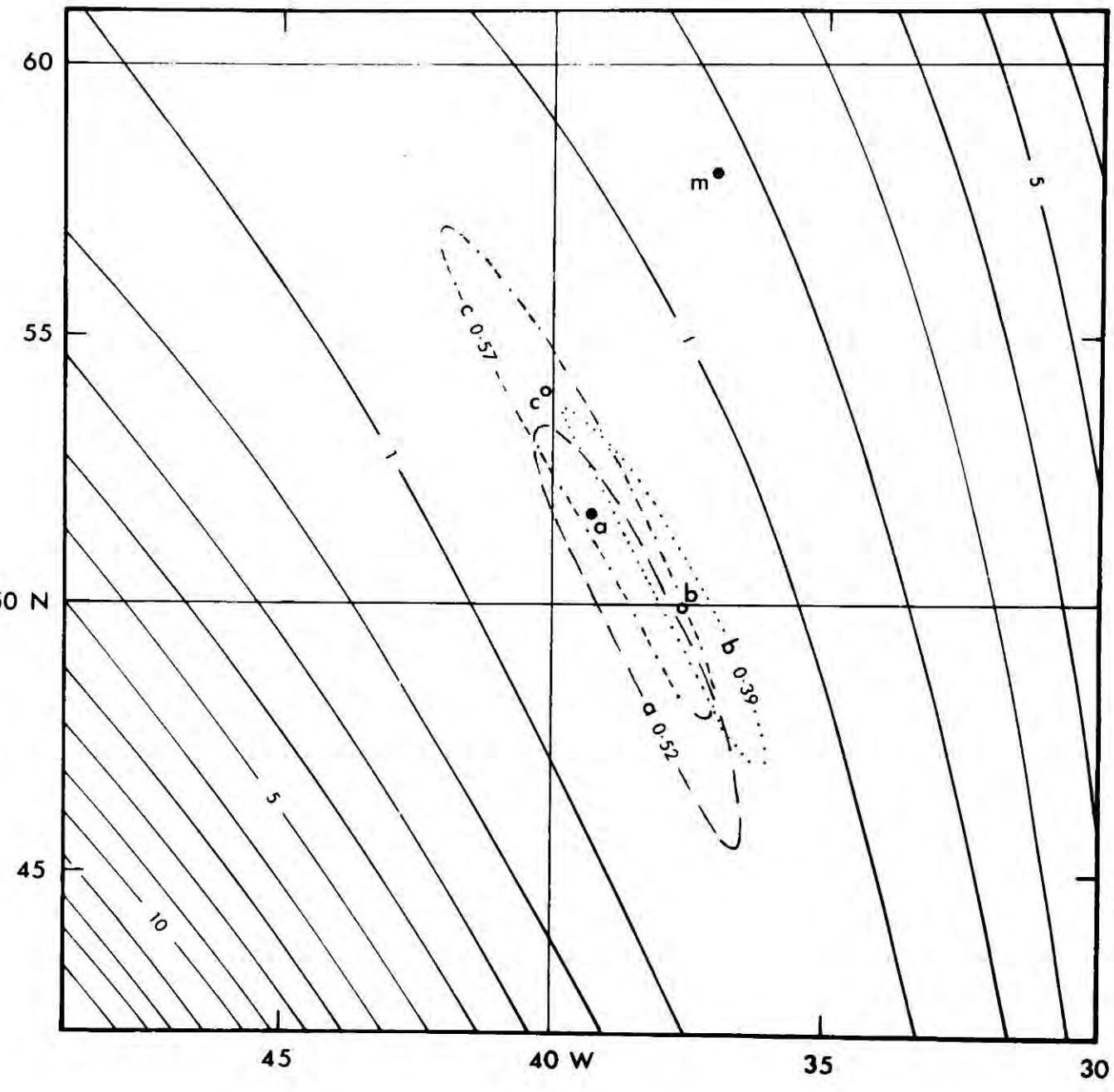
60
55
50 N
45
45
40 W
35
30
m
a
b
c
d
1
5
10
c 0·57
b 0·39
a 0·52

currently active faults, gave a very poorly defined pole. This was due partly to the inaccuracies of epicentral determination and partly to difficulty in correctly identifying those epicentres which fell on fracture zones.

The rotations used in the analysis are given in table 7.1 and from them it can be seen that for most of their history the North and South Atlantic have been opening about different poles of rotation. Before considering the consequences of these rotations in the Caribbean, an outline of the possible causes of underthrusting in the Lesser Antilles will be given.

Table 7.1

Table of rotation poles
used in this analysis.

	Finite rotations					
Age my	North Atlantic			South Atlantic		
	Lat.	Long.	Rot.	Lat.	Long.	Rot.
9	69.7 N	33.4 W	3.6	53.96N	40.1 W	3.6
38	79.0 N	13.0 E	9.75	65.42N	39.62 W	15.31
53	77.0 N	15.0 E	13.9	66.41N	39.56 W	21.35
63	75.0 N	15.0 E	17.0	66.82N	39.53 W	25.4
81	67.83 N	19.14W	31.26	67.3N	39.5 W	32.8
	79.1 N	15.7 W	30.4 *			
140	69.65 N	12.77W	53.49	44.0N	30.6 W	57.0
160	67.95 N	12.51W	61.73		"	
180	66.0 N	12.0 W	74.8		"	

Instantaneous poles

Period	North Atlantic			South Atlantic			N. America/S. America		
	Lat.	Long.	Rot.	Lat.	Long.	Rot.	Lat.	Long.	Rot.
9-0	69.7N	33.4W	3.6	53.96N	40.1W	3.6	27.62S	49.53W	-1.0
38-9	78.4N	56.7E	6.34	68.88N	40.67	11.8	46.35N	56.61W	6.67
53-38	72.4N	19.8E	4.17	68.88N	40.67W	6.05	41.24N	75.79W	2.54
63-53	66.2N	18.2E	3.15	68.88N	40.67W	4.05	33.55N	94.26W	1.62
63-81	54.4N	29.7W	15.14	68.88N	40.67W	7.4	41.13N	25.05W	-8.3
	75.43N	57.9W	13.75*	68.88N	40.67W	7.4	79.36N	98.2W	-6.57*
140-81	58.3N	1.0W	24.0 *	21.5N	14.0W	29.9	30.33S	34.2W	-18.66

* Pole from Le Pichon & Fox

Caribbean plate models

There are two main hypotheses which provide a mechanism for subduction beneath the Lesser Antilles (fig. 6.12). The first is that the Caribbean Plate moves easterly with respect to North and South America, which together form a single large plate. The leading edge of the Caribbean plate overrides the Atlantic lithosphere, and its northern and southern boundaries are transform faults. The second hypothesis is that the Caribbean is attached to South America which moves eastward (rotating clockwise) relative to North America. Along the northern boundary there is a transform fault which runs into the subduction zone along the eastern edge of the Caribbean, and another transform fault separating the North and South American Plates runs from the southern edge of the subduction zone to the Mid-Atlantic Ridge. There may be more than one transform fault opposite the arc, in which case the northern

part of the arc would be underthrust at a faster rate than the southern part.

A major drawback of the first hypothesis (model 1) is that there is no continuous feature along the southern boundary of the Caribbean on which strike slip motion could have taken place. East-west faults in Colombia do not directly join the Pilar and Victoria faults, and neither do they appear to extend any distance offshore (Krause, 1971). On one of the major faults, (El Pilar), a maximum displacement of only 15 km since the Cretaceous has been estimated (Metz, 1968) and recent estimates for the movement on other faults in northern South America (Bell, 1973) are conservative by comparison with the earlier estimates of Rod (1956) and Alberding (1957), giving values of tens of kilometres rather than hundreds. In spite of this, however, the evidence presented in chapter 6, does suggest that model 1 most adequately explains Caribbean tectonics during the present period of subduction and vulcanicity in the Lesser Antilles, which started about 9 my bp.

Any plate tectonic scheme for the evolution of the Caribbean must account for several important features of the geological history of the region. These are:-

underthrusting of northern Venezuela to give the coastal metamorphics;

the igneous Dutch Lesser Antilles and eclogites on Margarita;

east-west dextral faults in Venezuela no earlier than Eocene;

late Cretaceous to mid Eocene vulcanism and geosynclinal deposition in the Greater Antilles;

separation by Middle Americas Trench of the Caribbean from the Pacific in the late Eocene;

the onset of vulcanism in the Lesser Antilles in the Eocene; the possible cessation of vulcanism for the Oligocene and most of the Miocene.

Reconstructions

Figs. 7.3 to 7.13 show a series of reconstructions of the relative positions of the continents in the Caribbean area drawn by computer, using a program described in appendix C7.5 (Maplot) and the data of table 7.1. The first problem encountered in the reconstruction is the difference in the position of North America at 81 my bp determined by the pole of Le Pichon and Fox from that determined by the pole of Pitman and Talwani. The floor of the Caribbean basin is slightly more than 80 my old and unless it has changed in size or position by a very large amount since then the position of Le Pichon and Fox must be preferred to that of Pitman and Talwani as the latter does not allow enough room for the Caribbean Basin. The possibility of large displacements will be discussed again below, but the length of subducted lithosphere under the Lesser Antilles does place limits on this and it is probable that this does not exceed 500 km, which is not sufficient to clear the Caribbean Plate from the area.

Acceptance of the position of Le Pichon and Fox does not invalidate the use of the rest of Pitman and Talwanis' analysis, because their other positions are derived independently. It does, however, make one more careful in the use of the positions when unsupported by other evidence, and it also alters the position of the instantaneous poles for the periods either side of 81 my.

7.3 The positions of North America, South America and Africa at the beginning of rifting in the North Atlantic 180 my bp. The positions are after Bullard, Everett and Smith (1965), with that of North America as modified by Le Pichon and Fox (1971). The positions and all those in succeeding diagrams are given relative to Africa in its present position. The arrow shown leading from a point on the outline of Cuba gives the direction and amount of movement required to move the point to this position on the following reconstruction. The inclusion of the outline of Cuba, and on later diagrams Hispaniola and Puerto Rico, is for the purpose of making more easy comparison of past positions with the present one and do not indicate the actual position or existence of the islands.

7.4 Position at 160 my bp. A small ocean is forming in the North Atlantic but the nature of the development in the Caribbean area is uncertain. Shown as a dotted line is the pre drift position of S. America relative to N. America and as a dashed line the outline of the Gulf of Mexico relative to S. America Dashed-dotted line shows one possible position of the Mid Atlantic Ridge and also shown is a possible transform fault position if spreading is taking place in the Gulf of Mexico.

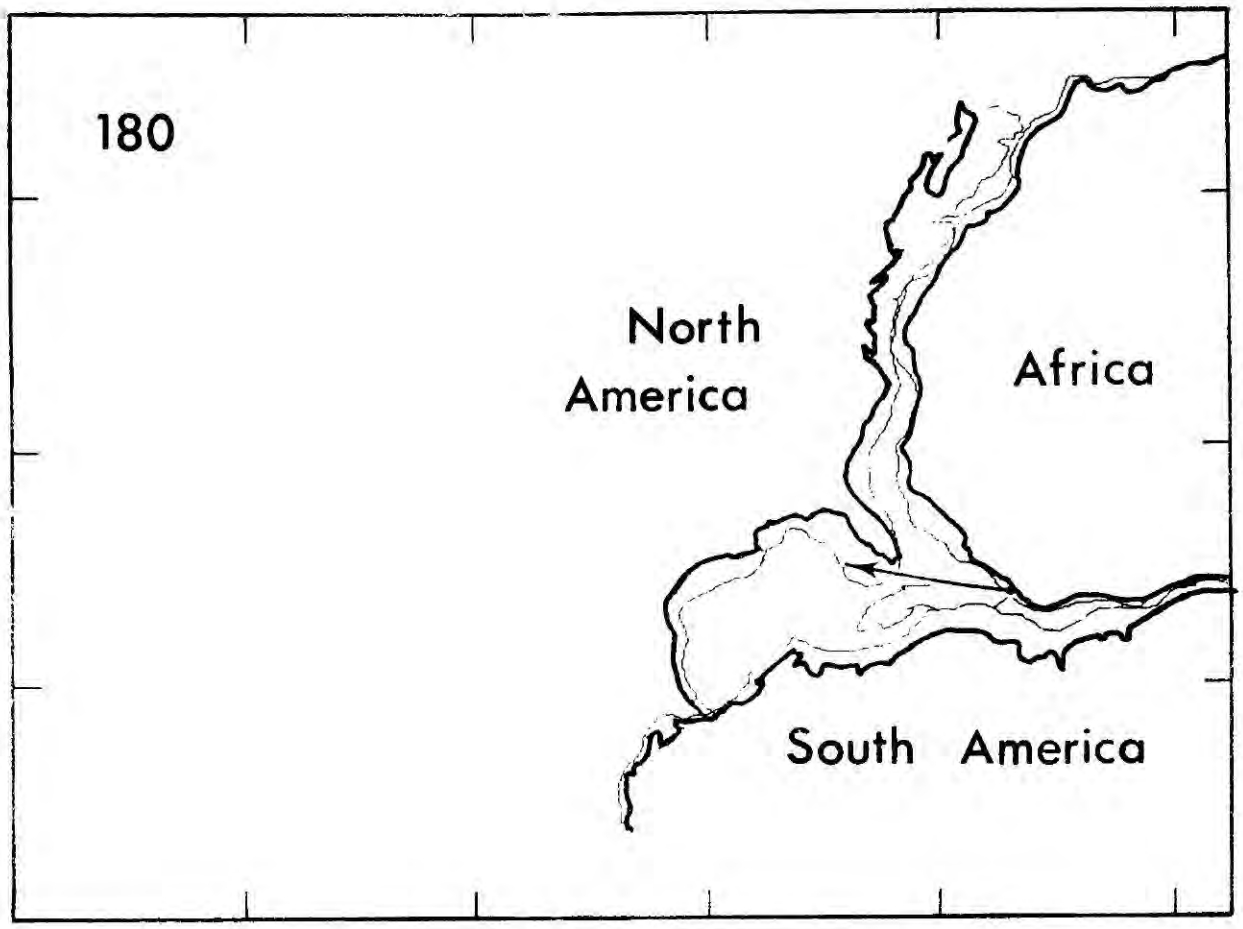
180
North
America
Africa
South America

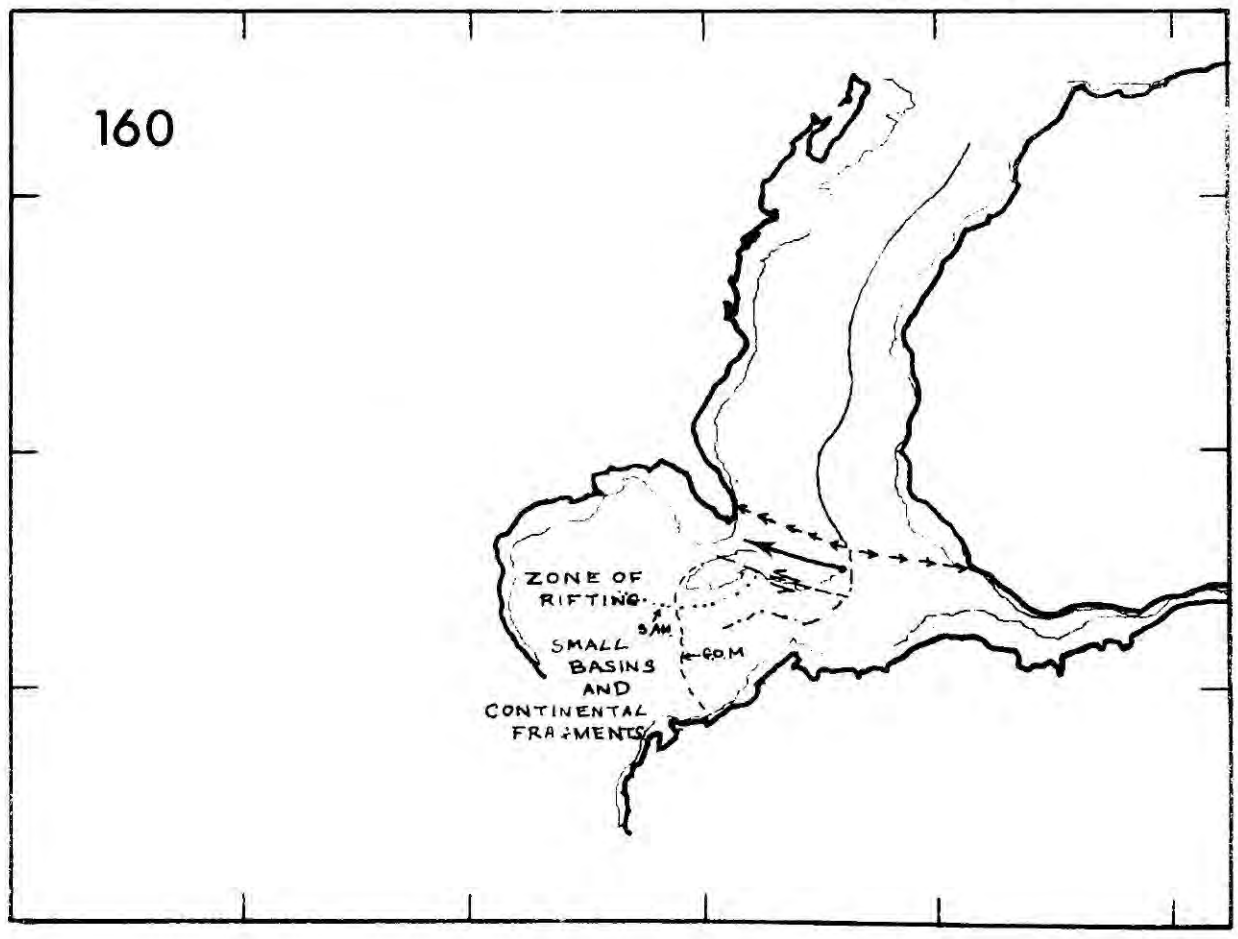
160
ZONE OF
RIFTING
SAM
SMALL
BASINS
AND
CONTINENTAL
FRAGMENTS
GOM

7.5 Position at 140 my bp. At this time the South Atlantic began to open and the rift system is connected to the Mid Atlantic Ridge by a large transform fault. Transform motion of some sort must be occurring in the Caribbean region but this may be complication by interaction with Pacific Plates. Dashed lines show the previous position of the Mid Atlantic Ridge relative to America and Africa.

7.6 Position at 110 my bp. The halfway stage of the early opening of the South Atlantic and transform faulting is the dominant mechanism of separation. At this stage some form of ridge in the Caribbean region may have begun to form the present Caribbean basin.

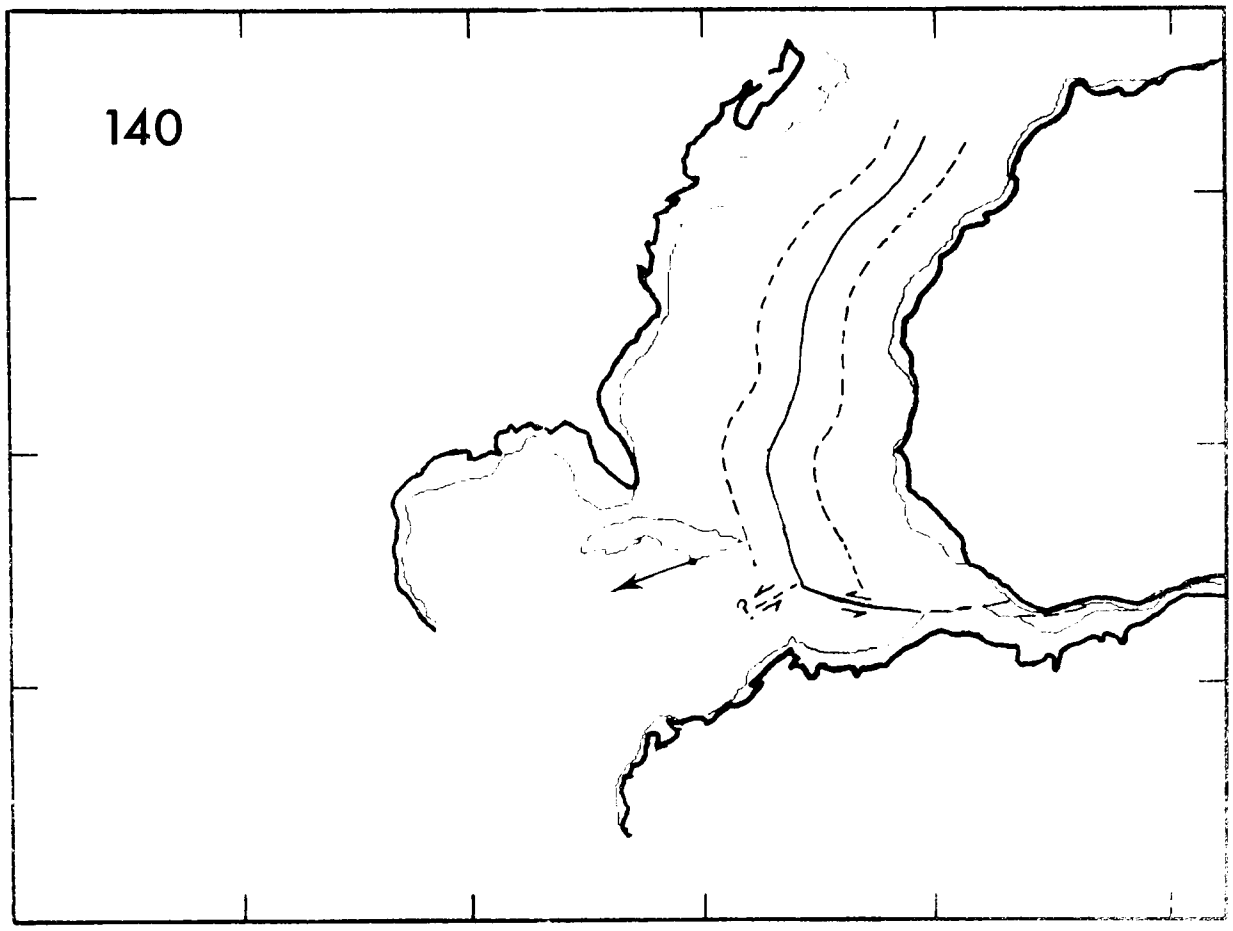
140

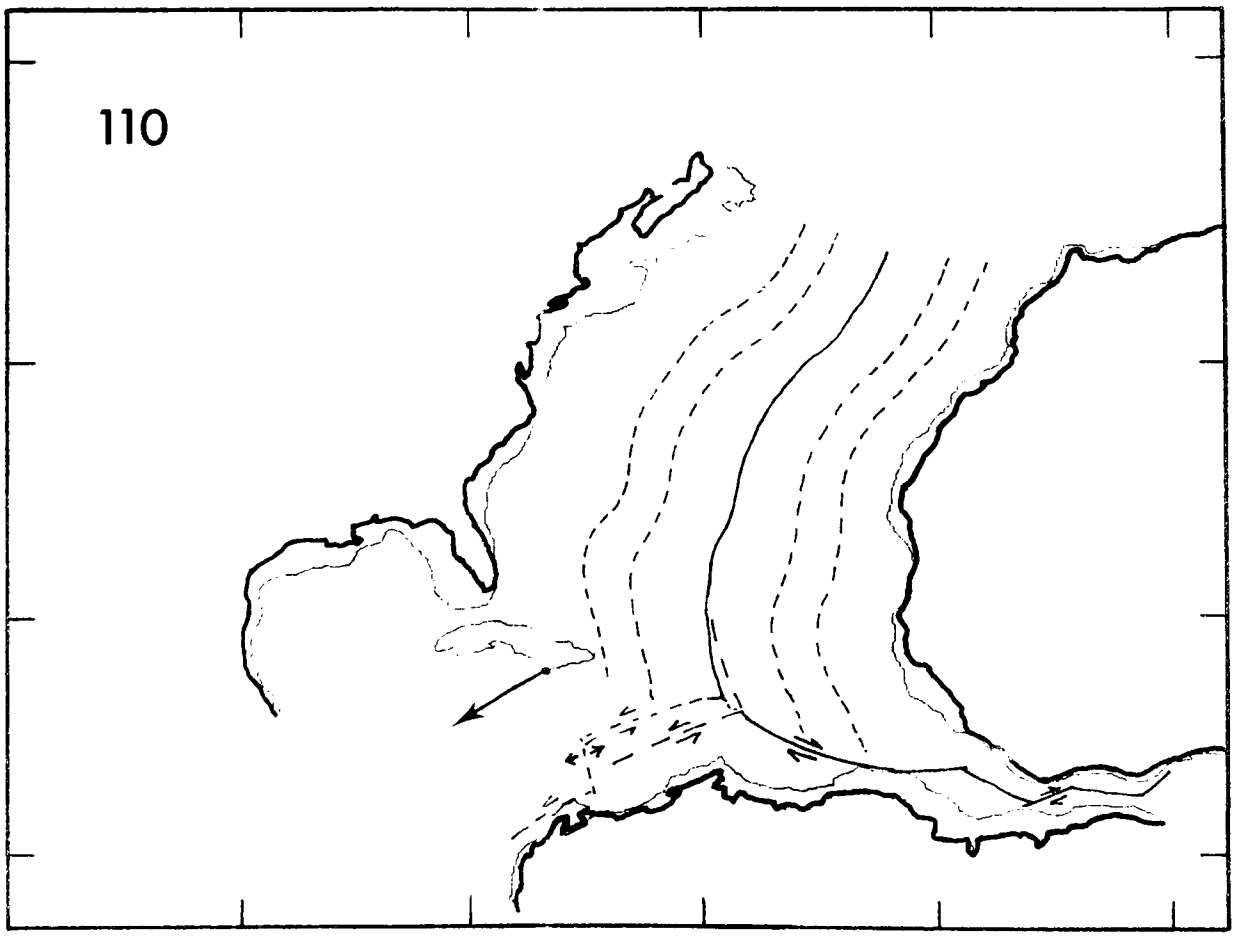
110

7.7 Position at 81 my bp. The Caribbean basin has finished forming and the late period of opening of the South Atlantic begins. Details of how a stable triple point might have developed at the point marked tp are given in fig. 7.14.

7.8 Position at 81 my bp according to Pitman and Talwani. North America is much closer to South America and there is not enough room for the Caribbean basin in its present position relative to South America. If this model is accepted, spreading takes place in the Caribbean over the next 18 my.

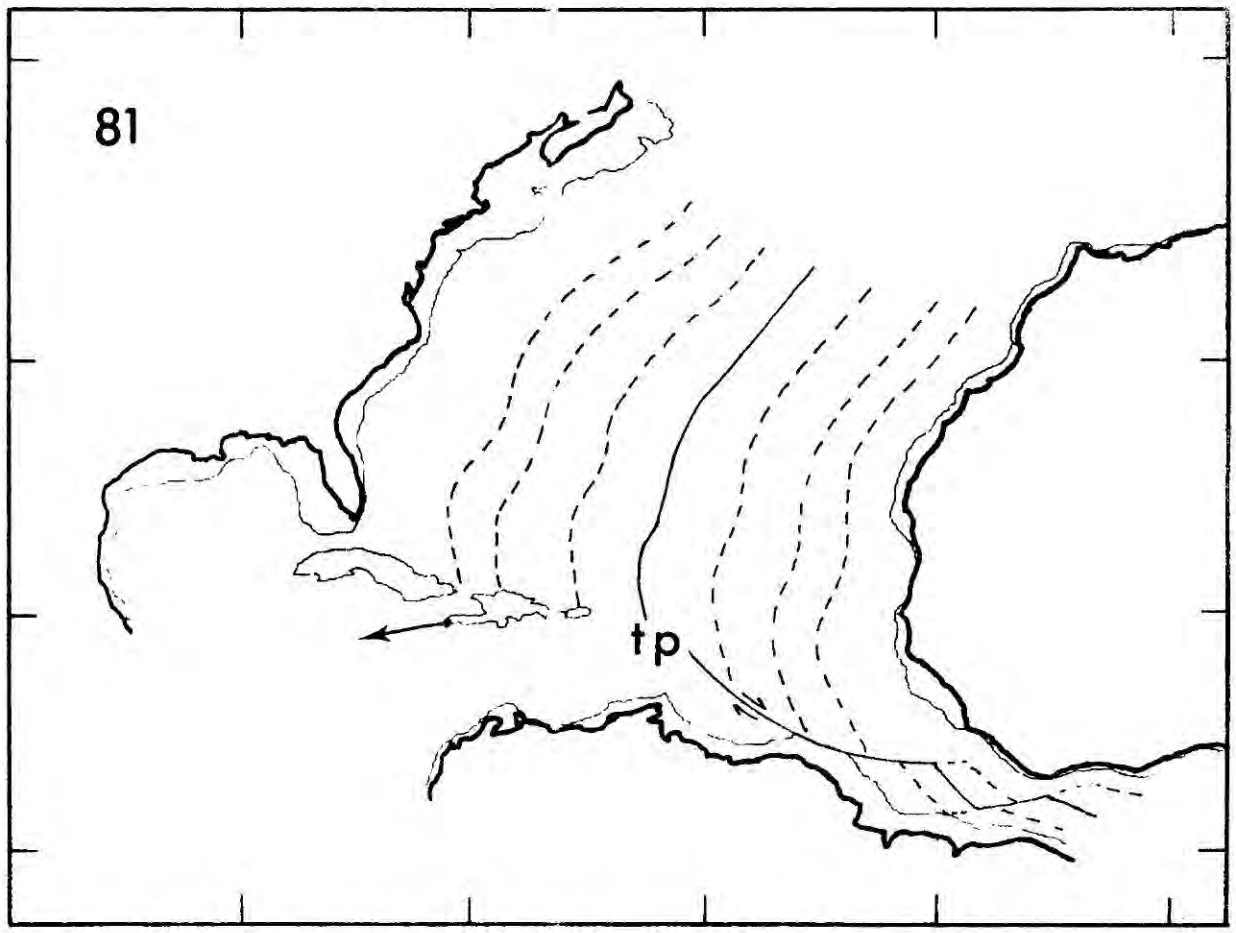
81
tp

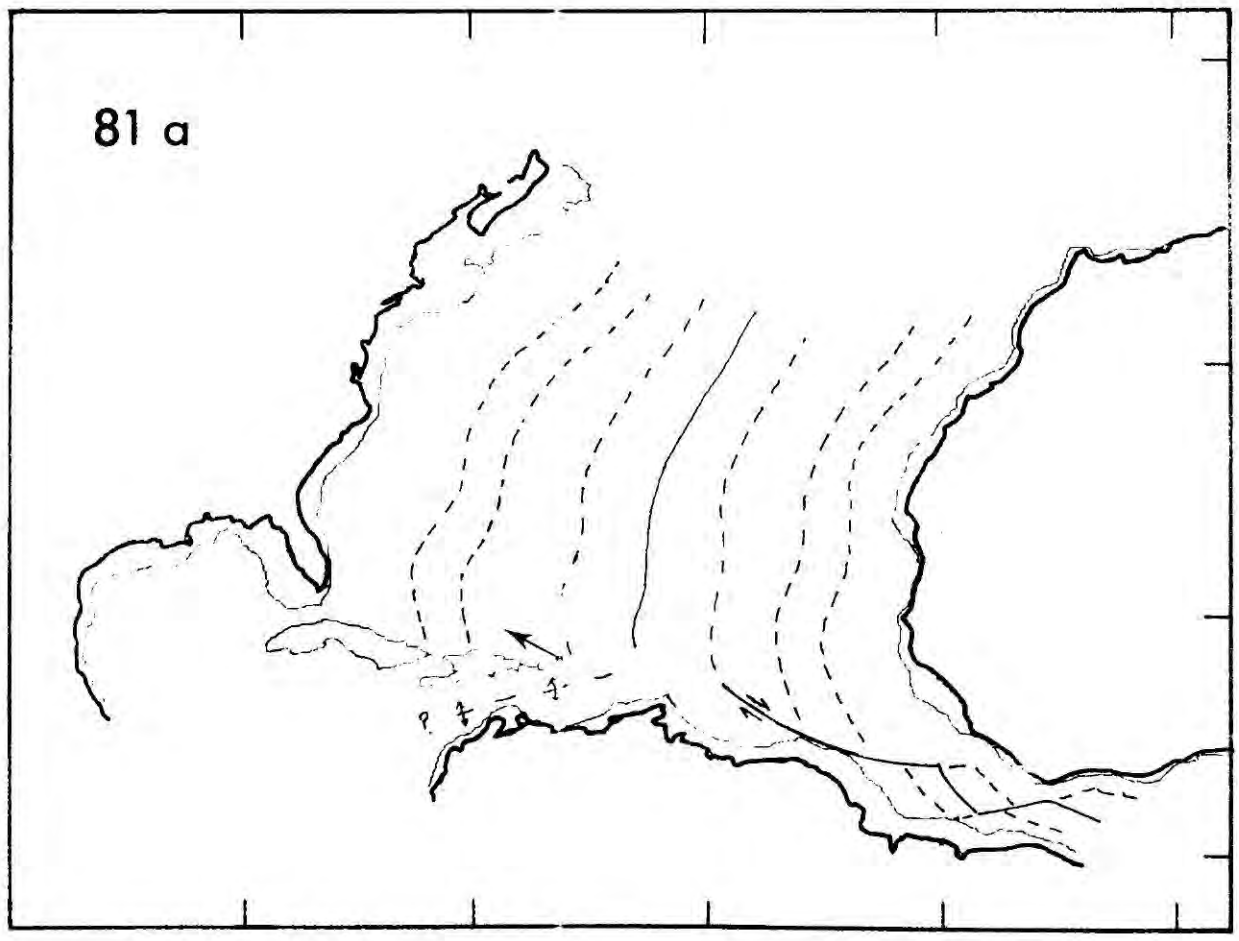
81 a

7.9 Position at 63 my bp. A subduction zone may have formed in the region of the Lesser Antilles, but the plate motions determined directly from the spreading data used do not provide favourable conditions for its continuance. The position of North America relative to South America is possibly too far west.

7.10 Position at 53 my bp. The positions of tectonic features are omitted from this and following diagrams because the motions determined do not appear to satisfy the histroy deduced from the geology very well.

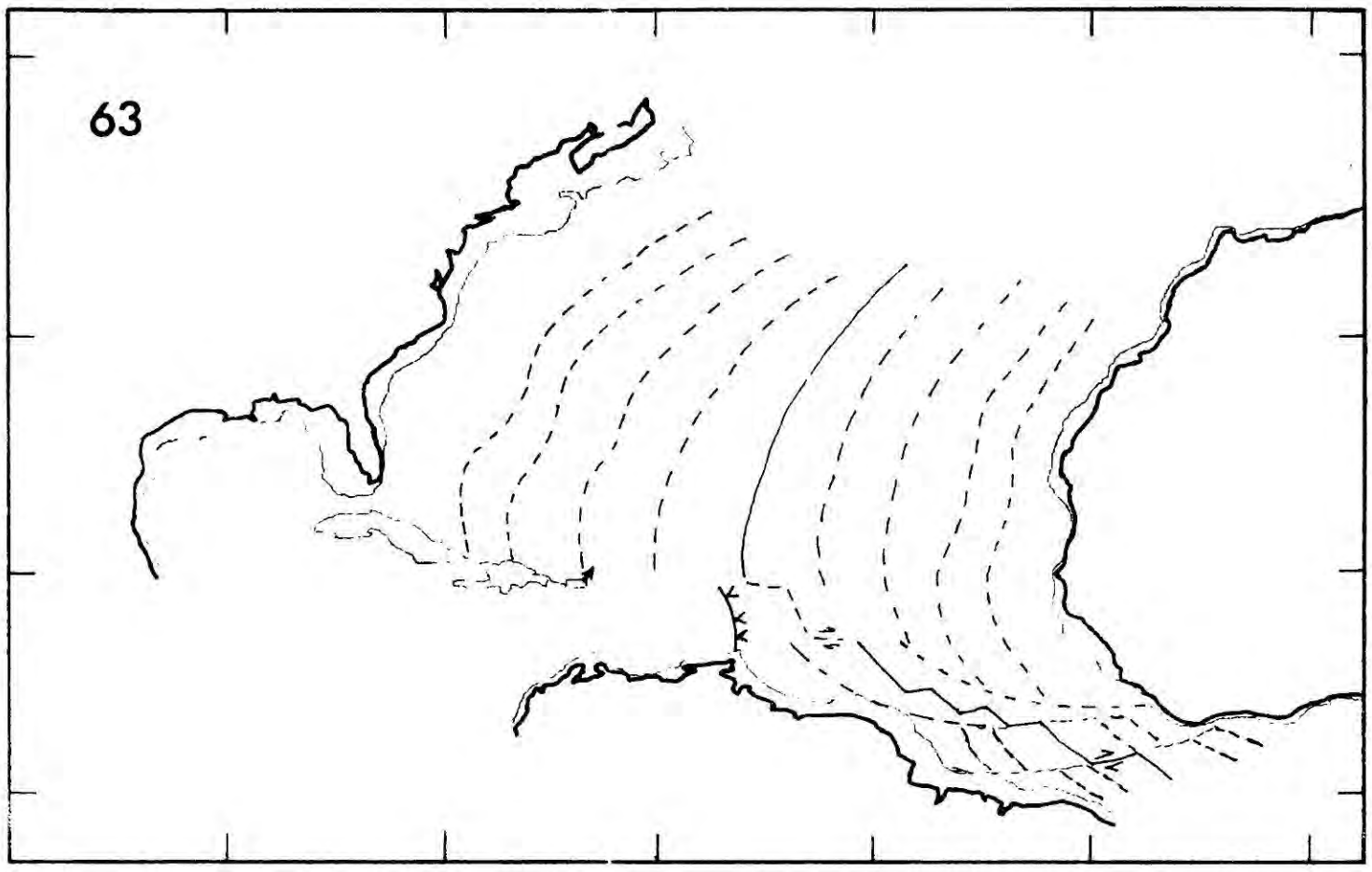
63

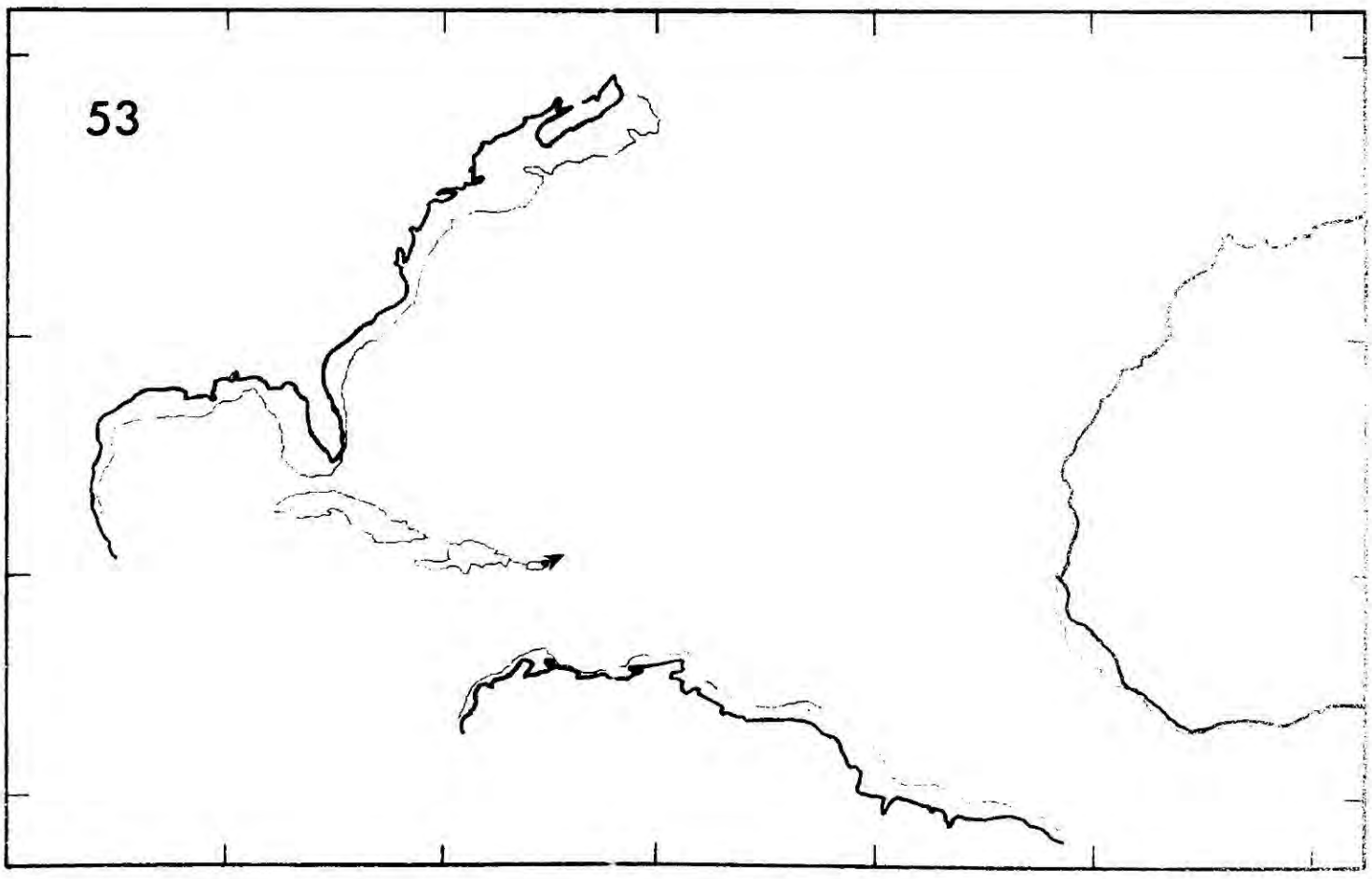
53

7.11 Position at 38 my bp

7.12 Position at 9 my bp.

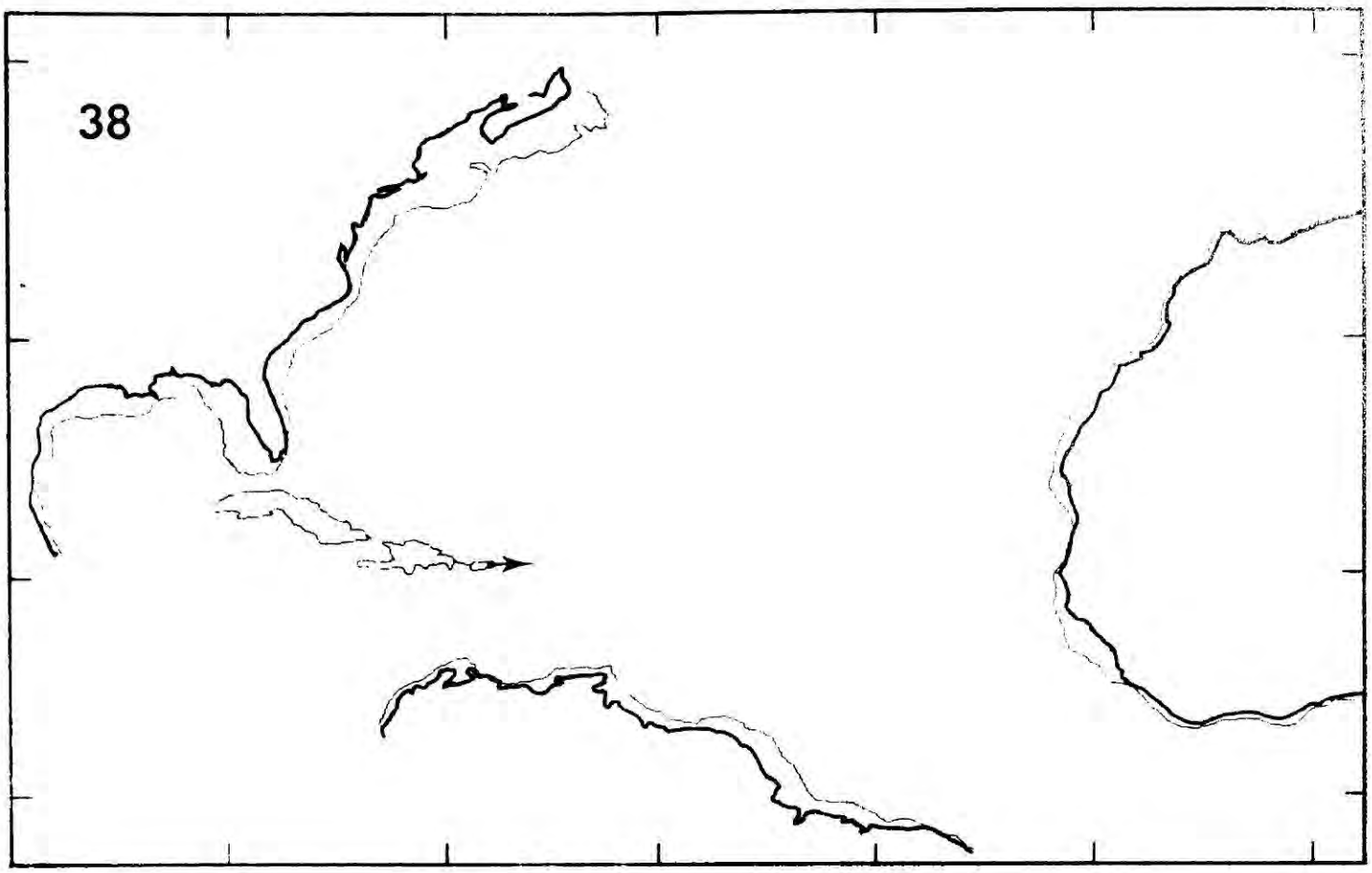
38

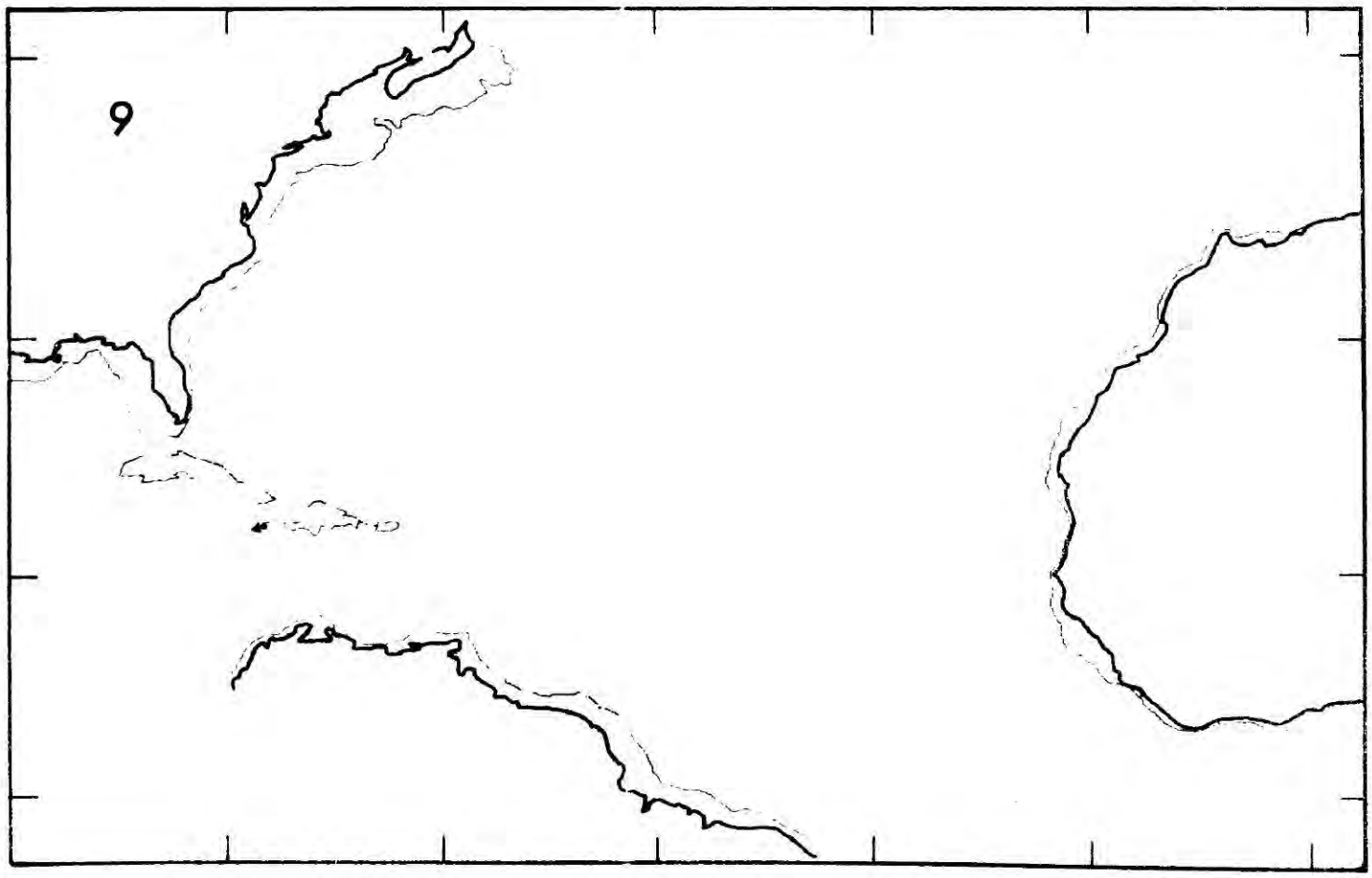
9

7.13 Present position.

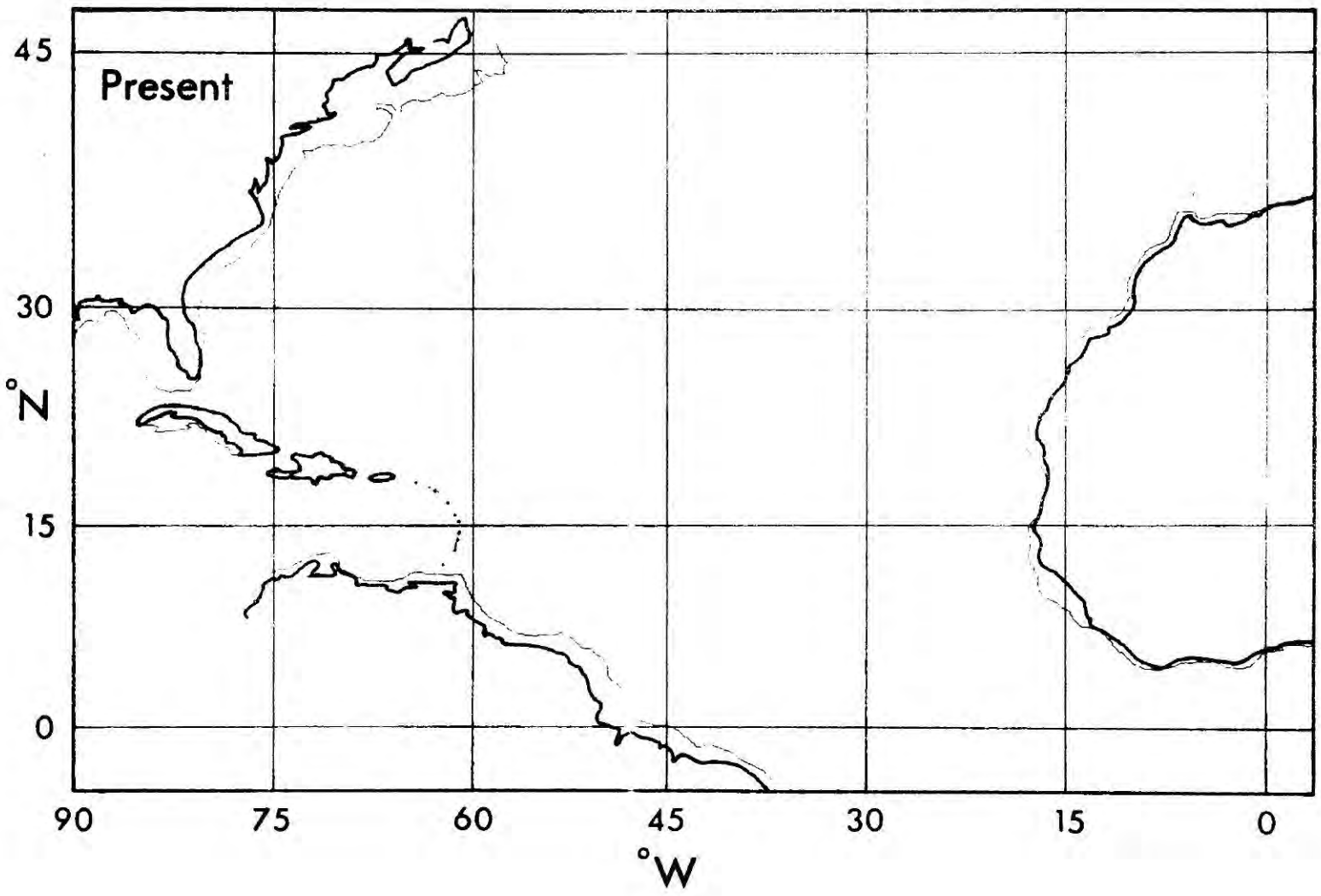
Present
45
30
15
0
°N
90
75
60
45
30
15
0
°W

7.14 Models describing the possible development of a stable triple junction in the Central Atlantic during the early opening of the South Atlantic. The initial configuration is shown at 1 and the sequence 2a to 4a shows the possible development if asymmetrical spreading takes place, the position of the spreading zone being controlled by the corner of the bottom plate. 2b and 3b show a model in which symmetrical spreading takes places, but this leads to a space problem and part of the bottom plate is subducted at s to keep the system functioning. The pecked line shows the amount of plate subducted. This subduction model seems unlikely to occur. 2c and 3c show a model with symmetrical spreading in which the extension of a transform fault to the ridge divides it and allows the top part to spread faster than the bottom part. The bottom plate has material added to it. A possible variant of the a models would seem to be spreading controlled at its southern end by the corner of the bottom plate but symmetrical at its northern end. This would mean a constantly changing azimuth of the spreading zone leading eventually to situations of type b or c.

1

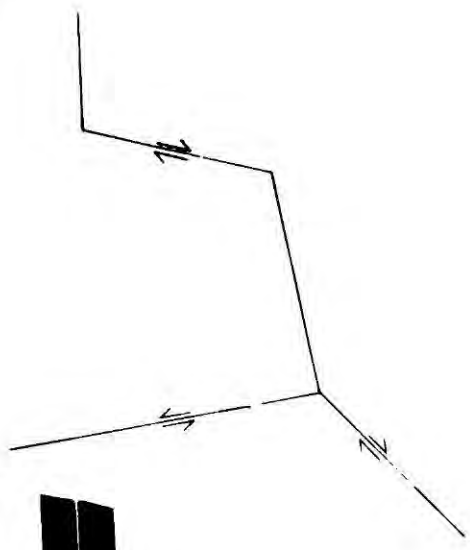

2a

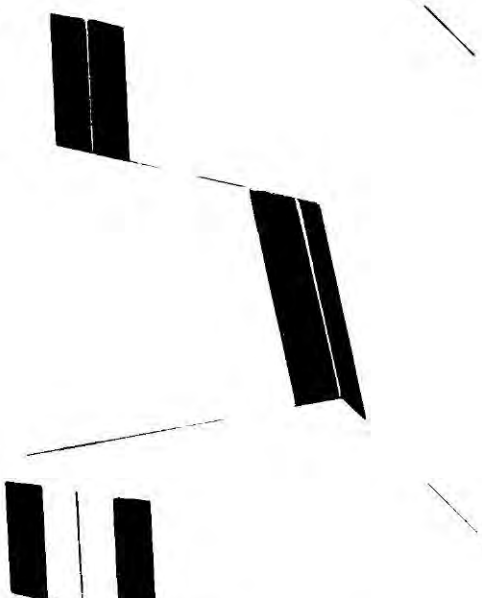

3a

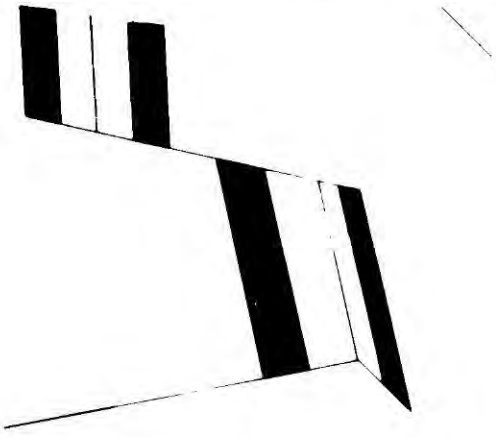

4a

2b

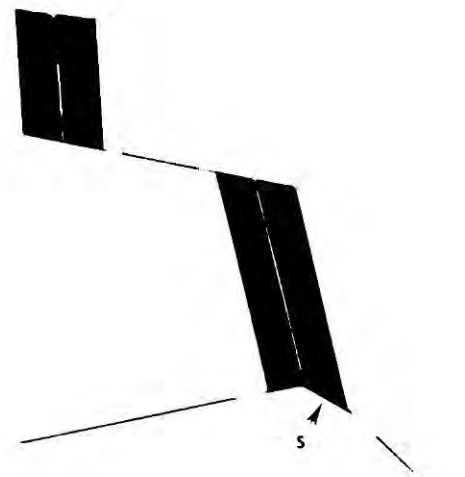

3b

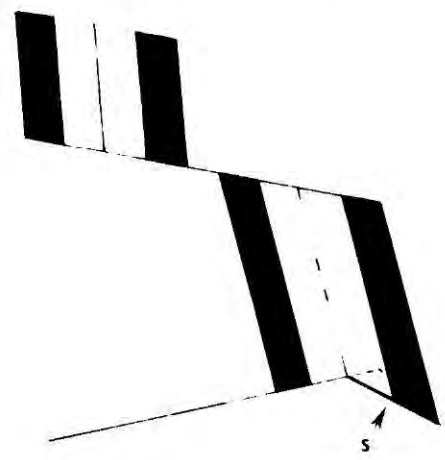

2c

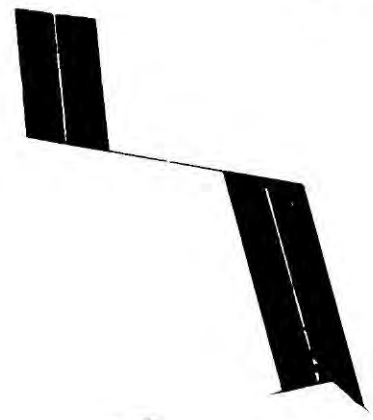

3c

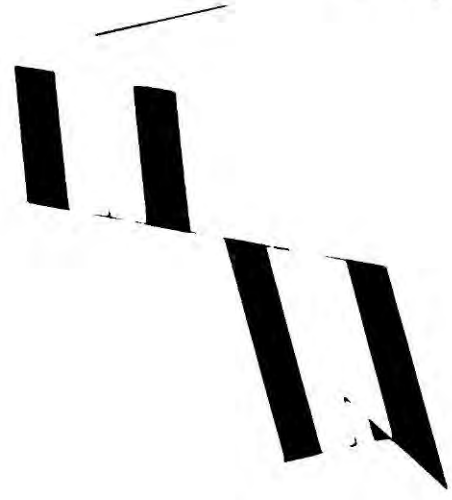

Accepting the 81 my position of Le Pichon and Fox gives a period until 63 my of left lateral movement of North America with respect to South America. This is a situation in which model 2 can be expected to operate, but appears to give too much left lateral movement. The present position of the plates around the Caribbean is such that North America is only 300 km west of its position relative to South America 81 my ago whereas the 63 my position is 600 km west. This indicates either that the intermediate positions are in error or that following the initial sinistral movement, dextral movement has occurred.

The consequences of dextral movement are difficult to guess, but there would have had to have been dextral movement along the southern boundary of the Caribbean or reverse movement along all the faults involved in the previous phase. This latter would have apparently included reverse motion of the subduction zone, which is hardly very likely, but some reversal of the tectonics in the area may have been responsible for a stepping back of the site of subduction from where it had been giving rise to the vulcanism forming the Aves Swell, to its present position giving vulcanism in the Lesser Antilles. The Aves Swell is older than the Lesser Antilles; the youngest age obtained by isotopic dating from a rock dredged from it is 57 my (Fox and others, 1971). The suite of rocks taken from it so far seem to indicate calc-alkaline vulcanicity.

It is equally possible that dextral movement did not take place and that the positions are in error due to ambiguity in the fitting process used by Pitman and Talwani and the invalidity of assuming a constant direction of rotation for the South Atlantic over the period 81 to 9 my.

Anomaly 13 (38 my) is one of the best defined anomalies used by Pitman and Talwani whereas anomalies 21 (53 my) and 25 (63 my) are difficult to correlate. Although the amount of sinistral movement predicted by the model may not be as much as that shown for 63 my, that obtained for 38 my should have occurred if the model is right, and still needs dextral motion to resolve it with its present position. If no dextral movement occurred then the error is likely to be due to an error in the position of South America. If the position of South America was further west at 81 my than given by Le Pichon and Hayes, their temporal definition is not as good in the South Atlantic as in the North Atlantic, then these discrepancies can probably be accounted for and the period from 38 to 9 my instead of being one of dextral movement between North and South America is one of no relative movement.

From the reconstructions prior to 81 my the following points emerge. Firstly, the Caribbean Basin must have been the last to evolve, with the Gulf of Mexico and Yucatan Basin forming before it. The manner of formation of these basins is problematical, even though the cause is clearly the separation of North America from South America. There is no clear evidence of the formation of ocean crust at a mid ocean ridge, with a lack of linear magnetic anomaly patterns, which may be because the crust was formed during one of the long periods of single polarity during the Cretaceous (Irving and Couillard, 1973). There are also no bathymetric features that might be interpreted as a ridge. From the dates of the oceanic basement obtained by JOIDES leg VI (Edgar and others, 1972) the Caribbean basin appears to young towards its northwestern margin, rather than its centre. If there was a mid ocean ridge structure in the Caribbean area there should be a triple junction with the Mid

Atlantic Ridge of an age older than 80 my present somewhere in the area, unless it has been subducted.

The structure of the basin floor though of an oceanic type is not like that of most oceans, with layers of velocity 6.2 and 7.4 km s^{-1} instead of one of velocity 6.8 km s^{-1} as in the North Atlantic. It is similar in form to the marginal basins behind some of the western Pacific island arcs. It has been proposed that the Caribbean is a fragment of older Pacific ocean floor thrust eastward (Edgar, 1971) but its age makes this most unlikely and there is no apparent reason why the Pacific should have had such an unusual layered structure.

A second point arising from the reconstructions is that the Atlantic Ocean floor in the vicinity of the Lesser Antilles must be of a considerable age, particularly off the coast of Guiana, because it was formed in the first period of separation of North America from South America.

The Left Lateral offset hypothesis (Model 2)

Most of the left lateral movement (2000 km) and separation invoked by Ball and Harrison (1969, 1971) for the formation of the Caribbean and the Lesser Antilles occurred before 81 my bp, well before the Lesser Antilles were formed. Ball and Harrison based their idea on a paper by Funnell and Smith (1969) which shows North and South America in successive stages of drift from Africa, but this paper by using the finite rotation poles of Bullard, Everett and Smith (1965) neglects the effect of different instantaneous poles. Attention is also diverted from the effect of the different ages of opening of the North and South

Atlantic. Ball's and Harrison's idea, which is essentially that of model 2, although somewhat misconceived, must be taken seriously when considering the 300 km or more post 81 my sinistral offset.

Transform faults separating North and South American Plates must lie on small circles to the pole of relative rotation between the two plates. Ball and Harrison implicitly assumed that the poles for the North and South Atlantic were coincident since they propose transform faults which lie on the same small circles as those offsetting the Mid Atlantic Ridge, though the spreading in the North Atlantic is faster than that in the South Atlantic, hence giving the differential movement. Freeland and Dietz (1971) propose a similar situation but with a pole of relative rotation between North and South America different from that of the North Atlantic, yet the transform fault shown by them to connect the southern end of the Lesser Antilles to the Mid Atlantic Ridge does not lie on a small circle to their pole of relative rotation, invalidating their model as shown.

Possible triple junctions in the Central Atlantic

An important part of the reconstructions of the model 2 type is the junction between the North America/South America boundary transform fault and the Mid Atlantic Ridge system. This triple junction can initiate as a ridge:ridge:transform or a transform:ridge:transform, but the former is unstable (McKenzie and Morgan, 1969) and must evolve into a ridge:ridge:ridge form or the transform:ridge:transform, and this latter configuration is itself unstable except in two cases. These cases are when the poles to the transform faults are coincident

or when the poles are separate but give small circles with the same azimuth at the triple junction (i.e. when the triple junction and the two poles lie on the same great circle). In all other cases the triple junction evolves into a modified ridge:ridge:ridge situation, and an example of this form of evolution relevant to the case being considered is shown in fig. 7.15. As spreading proceeds after the initiation of the new transform fault the position of the initial triple point migrates away from the spreading axis and a thin zone of spreading develops to keep the system operative by connecting the transform fault to the main spreading ridge. No features of this kind have actually been described in the vicinity of the Mid Atlantic Ridge, but this is not surprising since magnetic zonations produced by the thin spreading zone would probably be too fine to be observed from the sea surface and also very few surveys have been made in sufficient detail to detect any features that could be formed in this situation. Some of the very wide trench features associated with transform faults on the Mid Atlantic Ridge could have been due to a thin spreading zone.

If left lateral motion has occurred between the North and South American Plates then the offsets on the Mid Atlantic Ridge should have increased with time. Examination of the magnetic anomaly pattern east of the Mid Atlantic Ridge would show this most clearly, but the region has not been surveyed in enough detail to delineate it. The magnetic anomaly pattern west of the ridge should also show whether the offsetting has taken place, because, as fig. 7.15 illustrates, the amount of offset should increase away from the ridge. Examination of the magnetic anomaly pattern mapped by G. Peter and others in this region (personal communication) does not show this. The region mapped does not, however, extend far enough

7.15 The evolution of a triple junction that would allow relative strike slip movement between the North and South American Plates. It is likely that the fault would be initiated at a prexisting offset of the ridge and the situation at the initiation of the fault is shown at 1. The azimuths of the offsets are due to the preceeding plate motion. The new azimuths will follow the new relative rotations which are shown in the vector diagram V. The evolution of the system is shown from 2 to 6. The position of the initial triple point on the South American Plate migrates westward with respect to the ridge. The transform fault is connected to the ridge by a narrow spreading zone and the SA/AF ridge transform is also replaced by a thin spreading zone making the triple junction a stable ridge:ridge:ridge type. In practice it seems likely that the thin spreading zone might be modified by strike slip faulting. The transform fault increases the offsets west of the ridge as demonstrated at 6. a is the original offset of the ridge, b is the present offset of the ridge, and c is the offset of the western parts of the original ridge across the transform fault.

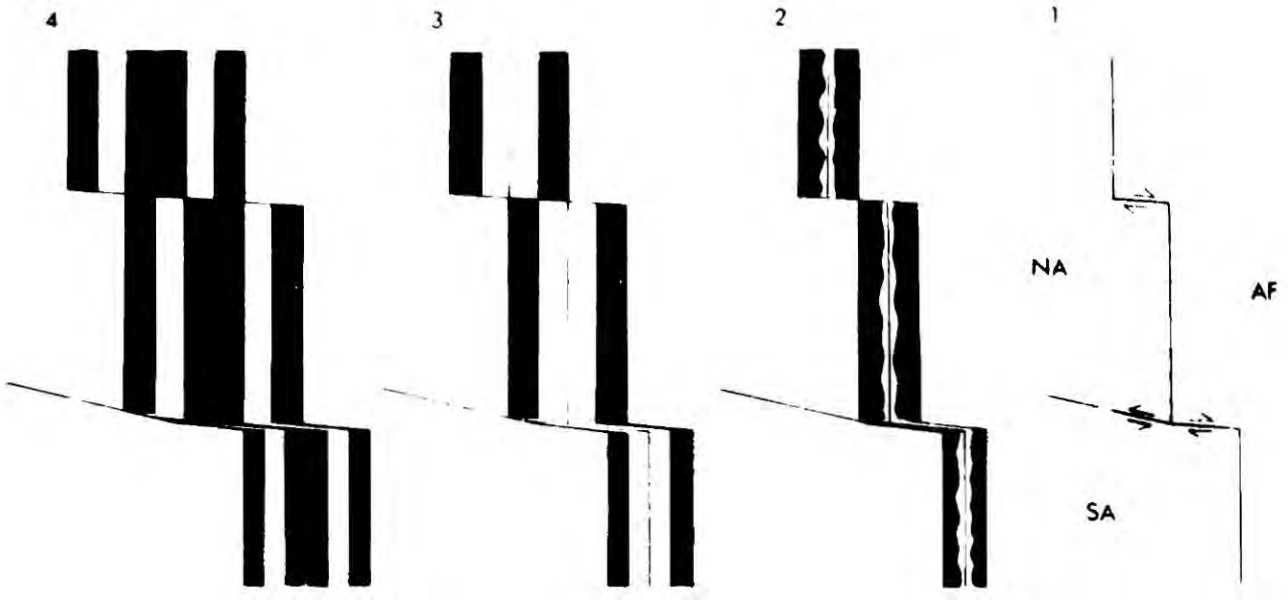
4
3
2
1
NA
AF
SA


V

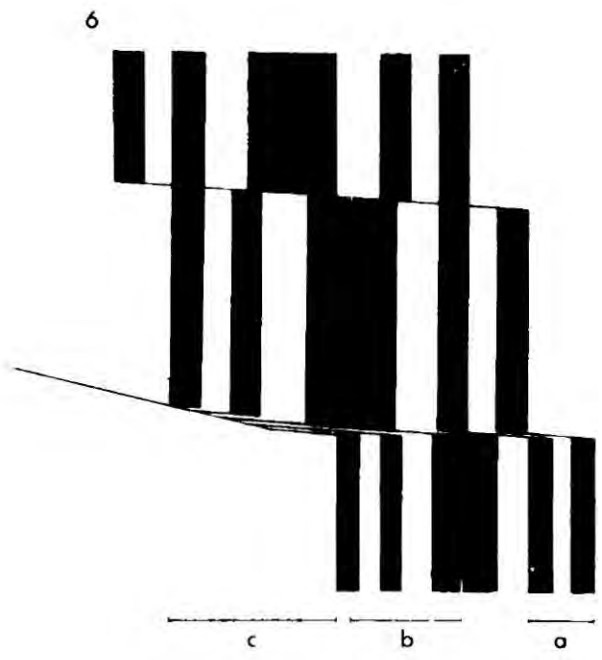
6
c
b
a

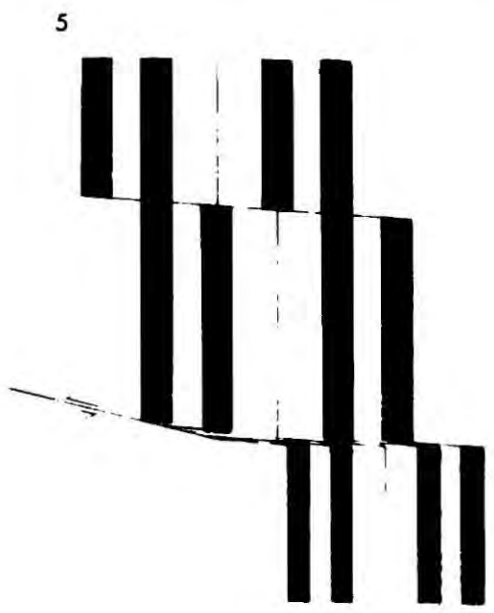
5

south to cover the position of the transform fault that would connect with the southern end of the Lesser Antilles.

Accepting that some offset may have taken place leads to the question of at what time the the transform fault was operative. The conditions of a similar azimuth of transform faults at the triple junction seems likely to have been most nearly satisfied in the period from 81 to 63 my bp. The data of Peter and others shows a marked change in trend of fracture zones around anomaly 20, (49 my),and that from anomaly 13 (38 my) to the present there has been little variation in trend. The bathymetry does show well defined trenches that run into the ridge from the west but terminate at anomaly 5 before reaching the ridge This last feature, which presumably reflects a change in spreading regime, also occurs on the East Pacific Rise. The evidence does favour an early rather than late period of sinistral shear, which is reasonable because the shorter distance over which the transform fault would have had to operate would have made it easier to initiate and accommodate changes in the relative movement of the plates either side. Features such as the Barracuda Ridge may be deformed fracture zones.

Discussion of the relative movements between North and South America although relevant to model 2 does not bear directly on model 1 and it is worth considering at this stage how much of the geological history can be satisfied by the models. While it can be seen that the relative motion of North and South America can have given conditions likely to cause underthrusting in the Lesser Antilles at some time from the late Cretaceous to the Eocene, the necessary motions required to produce underthrusting of Venezuela in the late Cretaceous, and the Late

Cretaceous to mid Eocene vulcanism of the Greater Antilles have not been determined. To produce the latter it is easy to invoke a variant of model 1, as do Malfait and Dinkleman (1972). The former is not so easy to accommodate. The late Cretaceous model of Malfait and Dinkleman does not explain this satisfactorily, and is actually unworkable as shown. For this underthrusting to have occurred, there must have been convergence between North and South America in the late Cretaceous. (It is assumed in this discussion that mid ocean ridges are a consequence and not a cause of spreading, so that seafloor spreading in the Caribbean will not produce underthrusting in Venezuela). This reintroduces the critical subject of the relative separations of North and South America.

Palaeomagnetic evidence

The separation of North and South America shown by Smith, Briden and Drewry (1972) for the Cretaceous (fig. 7.16) is much greater than that in any of the reconstructions considered so far. This separation diminishes to its present size by the Tertiary and only a relatively small amount of left lateral shear is required to transform the Tertiary position to the present one. MacDonald and Opdyke (1972), who include in their analysis the results of Vincenz (1971) and Fink and Harrison (1971), considered the Cretaceous pole positions from sites around the Caribbean Plate. Their reconstructed position shows North and South America almost as close together as in their pre-drift position. (fig. 7.19). The reconstruction is for the Late Cretaceous whereas that of Smith and others is for the early Cretaceous which is the main reason for the difference between them, but MacDonald's and Opdykes' position for the South American Continent is much further north than any of the positions of

7.16 The Cretaceous reconstruction of the Atlantic from Smith, Briden and Drewry (1971).

7.17 The Tertiary reconstruction of the Atlantic from Smith, Briden and Drewry (1971).

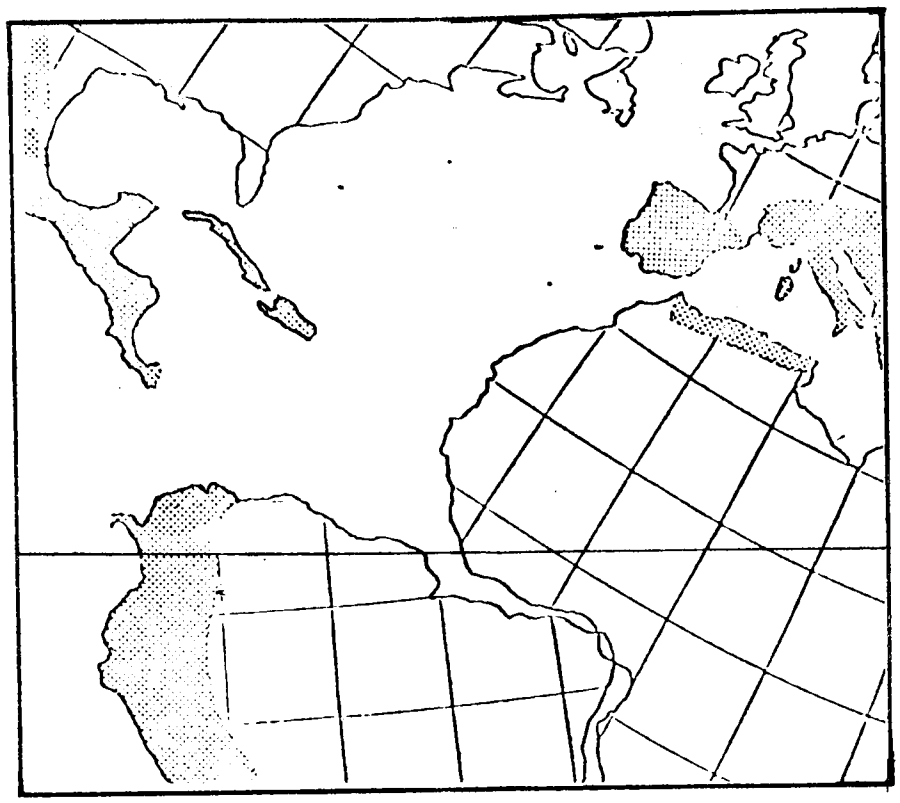

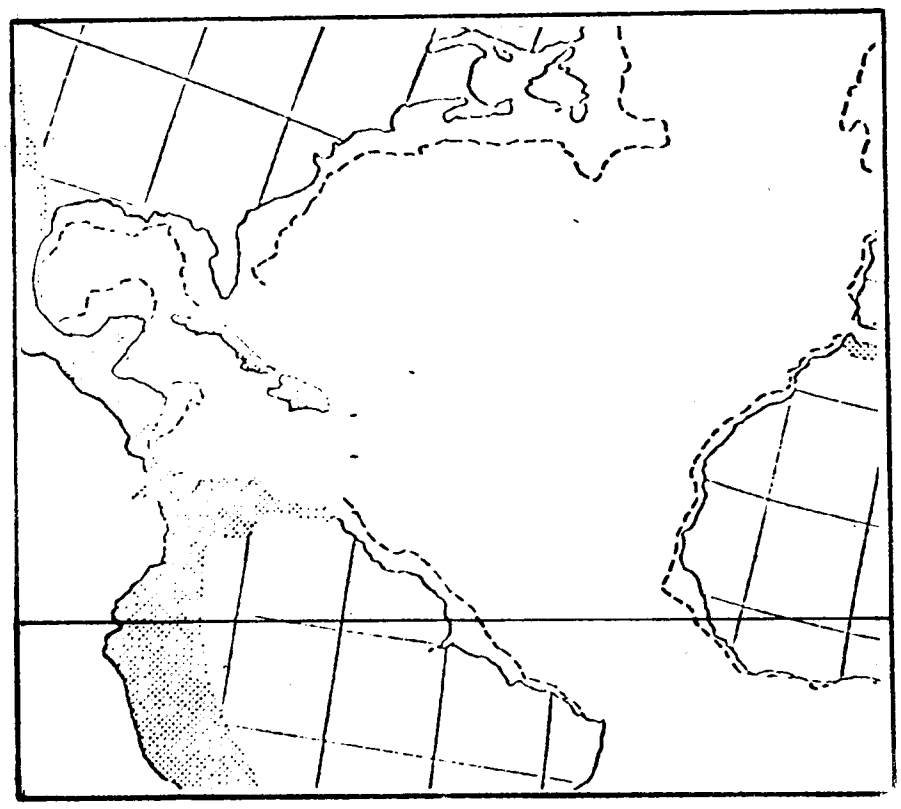

Smith and others and is further north than its present position. The positions of the circum Caribbean poles show quite a spread (fig. 7.18) and they may be due to rotational deformation of the Caribbean Plate boundaries rather than wholesale rotation of the whole plate. In either interpretation, however, the evidence of MacDonald and Opdyke implies motion of model 1 between late Cretaceous and early Tertiary times.

Relation of Caribbean features to tectonic phases

Can some of the transform fault feature in the Caribbean area be related to any of the stages of development as hypothesised from the Atlantic spreading data? The poles of 'rotation' to various features are given in table 7.2 and these were rotated through the finite rotations given in table 7.1 to see if they fell near any of instantaneous poles. The results of this exercise were disappointing in that none of the positions were sufficiently coincident to be worth considering. This may be just a function of poor data or it may be because motion of model 1 type was predominant. In the case of the Cayman Trough it does seem to indicate that its present form is a result of the most recent tectonic phase, although a feature of some kind has been there since Late Cretaceous (Khudoley and Meyerhoff, 1971).

Table 7.2

Feature	Pole giving best small circle fit.	
Cayman Trough	23.3 S	72.0 W
El Pilar Fault	73.3 N	79.5 W
Barracuda Ridge	36.0 N	52.7 W

7.18 Cretaceous circum Caribbean pole positions from MacDonald and Opdyke (1972).

7.19 Late Cretaceous reconstruction of the Caribbean area from MacDonald and Opdyke (1972).

Caribbean Cretaceous paleomagnetic pole positions compared with those of North and South America. Paleomagnetic poles are shown by closed circles, and the corresponding sites are shown by plus signs. Numbers refer to sites in Table 5. Paleomagnetic poles of circum-Caribbean sites (7–13) are greatly displaced from those for North and South America (1 and 2). Circum-Caribbean sites give paleomagnetic poles forming a rough arc around the Caribbean at a distance of 80°–90° This configuration suggests Cretaceous and younger tectonic rotations of the circum-Caribbean sites and Cretaceous latitudes between 0° and 10° for these sites. Equal-area projection.

A paleotectonic reconstruction of the Americas based on Cretaceous paleolatitudes (Table 5). The poles of *Larochelle* [1968] and of *Creer* [1962] for North and South America, respectively, have been superimposed on those for Guajira, Jamaica, and Puerto Rico (see text). The slanted shading indicates the latitude range thought to have been occupied by the Greater Antilles in Cretaceous times. The three plus signs off western South America represent, from south to north, the latitudinal positions of the Guajira peninsula, Jamaica, and Puerto Rico in Cretaceous times. In this reconstruction there is no control on relative longitudes. Equal-area projection with center marked by large plus sign.

Concluding Summary

No attempt will be made here to provide a synthesis of the tectonic history of the Caribbean area. It would undoubtedly suffer the fate of most previous syntheses by being considerably in error, because of lack of sufficient data. Some of the more salient features emerging from this appraisal of presently available data are worth reiterating for their significance in respect of the formation of the Lesser Antilles.

Since its formation 80 my ago the Caribbean Plate has acted rather like a bearing between the North and South American Plates, probably changing its shape slightly as its margins were deformed. During its history there appear to have been at least three major changes in the plate tectonic regime affecting the area at 80, 40 and 9 my bp. Around 40 my bp the Middle Americas Trench cut off the Caribbean from the Pacific (Malfait and Dinkleman, 1972) and this may have been related to the creation of the Galapagos Gore (Holden and Dietz, 1972). It seems that following this change there was a gradual cessation of activity in the Lesser Antilles. There is evidence for some vulcanism early in the Oligocene. About 9 my ago Vulcanism restarted in the Lesser Antilles, along a slightly different location in the north of the arc. The relationship between the early vulcanism in the Lesser Antilles which probably started about 45 my bp and the 80 my plate regime change is not immediate and there may be two reasons for this. Firstly, the calc-alkaline vulcanism of island arcs is thought to be caused by the introduction of melts and/or water released from hydrous minerals, from the oceanic crust of the subducted plate into the mantle above it. This

release of material takes place at about 120 km depth and in the case of the Lesser Antilles the plate at a rate of 1 cm y^{-1} needs to have been subducted for 20 my before vulcanism would have occurred. Secondly, subduction may have produced vulcanism initially along the Aves Swell and only later stepped back to the Lesser Antilles.

A point that needs consideration is why subduction should start at any particular place. Presumably the presence of some discontinuity or inhomogeneity will initiate it and it seems that the northeast corner of South America could very well have provided a starting point for subduction being the first place at which oceanic rather than continental lithosphere could be underthrust. If this were so then relative permanence of the position of the subduction zone would favour model 2 as the dominant plate motion. It appears that the subducted lithosphere beneath the Lesser Antilles does not reach the Transition Zone of the mantle. (This is deduced from the possible thermal effect of the descending slab and resulting gravity anomaly, discussed in chapter 5). The Lesser Antilles subduction zone cannot have migrated more than 500 km if this is so and if the amount of crust subducted in the last 9 my is in the range 50 to 100 km then the subduction rate during the period 80 to 40 my bp would have been about 1 cm y^{-1} or perhaps twice that if there was also subduction beneath the Aves Swell. Pinet (1972) has estimated the movement on the Cayman Trough-Motagua fault to be 300 - 1000 km.

The most critical area for deciding on the validity of models 1 and 2 is the southern boundary of the Caribbean where the apparent absence of movement greater than 50 km favours model 2 as the dominant one,

especially until mid Eocene when the east-west faults were first activated, yet the transform fault necessary for this model, running in from the east to the southern end of the arc, has still to be shown to exist. The palaeo magnetic evidence and geological history of the Greater Antilles, however, appear to require model 1 motion from late Cretaceous to Mid Eocene times. How these apparently conflicting lines of evidence may finally resolve, the writer is still unsure. It may be that some processes of lithospheric formation of the type considered by Karig (1971) and Moberly (1972) to have produced the marginal basins in the western Pacific, have played an important part in the development of the Caribbean.

The analysis does show that some amount of sinistral shear between the North and South American plates has affected the Caribbean and that the amount of shear is about 300 km. Most of this shear may have occurred in Eocene Times. The Caribbean plate has also moved semi-independently of the two major American plates but is unlikely to have moved far enough to be derived from the Pacific.

Chapter 8

Tectonics and history of the area: general conclusions

The major factor influencing the tectonic development of the region east of the Lesser Antilles has been the subduction of the western Atlantic lithospheric plate beneath the Caribbean plate. In some of the preceding chapters this has been assumed, but the evidence warrants this assumption if "plate tectonics" is a valid concept. The well defined inclined zone of earthquakes, the production of a chain of calc-alkaline volcanic islands and the presence of a trench or buried trench all confirm this view.

The mechanism of formation of the sediment pile of the Barbados region, by subduction

The formation of the Barbados Ridge and Slope is directly related to the subduction process, situated as it is over the site of subduction The slope from the ridge to the Atlantic ocean floor is the region of accumulation of sediment tectonically derived from the subducted plate. Chase and Bunce (1969) have drawn an analogy between this situation and the sandbox experiment of Hubbert, which by lateral compression layers of sand produces thrusts in them with a characteristic dip of 30°. The matter of the identification of reflectors in the sediments which might be these thrusts was discussed in chapter 4. The situation here, however, is not strictly one of lateral compression. The moving surface of the oceanic crust is parallel to the sediment layers and carries them passively along. Resistance to the sediments is greatest at the point of subduction and there decollement must occur between the sediments and the basement,

accompanied by subsidiary thrusts and folds allowing the material to be elevated. This decollement with continued movement increases the stress applied to the sediments further away from the subduction point so that the decollement extends away from the subduction zone as the yield strength is exceeded. It is likely that in the sediements failure will occur along bedding planes which present discontinuities subparallel to the probable direction of maximum shearing stress. To accommodate the extra amount of material brought in to the pile overthrusts must develop leading away from the decollement plane towards the surface. The outermost of these low angle thrusts will be the boundary between the disturbed sediments in sedimentary pile of the Barbados Ridge and Slope, and the undisturbed sediments of the Atlantic Ocean floor. This means that at the point of initial deformation the disturbed sediments will overlap undisturbed sediments. This appears to be the case at the foot of the Barbados Slope (figs. 4.9 and 4.10).

The continual addition of sediment to the oceanward base of the sedimentary pile would have the effect of raising the overlying sediments and tilting them back towards the west. This would account for the prevalence of westerly dipping reflectors in Barbados Slope region. There must be a limit to how far any one block of sediment can be raised up along an overthrust without the stress needed to raise it further exceeding that needed to cause a new decollement and overthrust and because of this the zone of deformation will migrate eastwards. The migration of pore fluids under pressure probably aid this process, as in other, well documented, cases of overthrust sequences in sedimentary rocks (Rubey and Hubbert, 1959). With the exception of the sediments that are deposited directly on to the slope region, the

sediments in it must young towards the east, although in any particular section of it between major discontinuities they young towards the top. Summarising briefly, the slope region is composed of many superimposed, overlapping segments of sediment, dipping to the west and being continually added to at their eastern base (fig. 8.1).

The Uplift of the Barbados Ridge

The Barbados Ridge in its present form appears to be something more than just the end result of the process outlined above. The amount of uplift (at least 5 km) that it has undergone since about Pliocene times is difficult to explain easily as it is probably no longer in the zone of significant sediment addition. Bowin (1972) has explained the formation of the ridge by a decrease in the volume of the trench in which the sediments lie. This in itself sounds plausible, and Bowin ascribes the volume decrease to tectonic compression of the trench by eastward movement of the Caribbean Plate, overriding the subducting Atlantic Plate. For this mechanism to produce anything other than faster subduction, the edge of the Caribbean plate in being thrust over the Atlantic plate must be raised above its former position. This would need a constant force to prevent it reverting to its previous state, and would be isostatically imbalanced, producing a large positive gravity anomaly. There is, however, an overall negative anomaly in the area, as shown in chapter 5. It is difficult to see why an increase in the rate of relative eastward motion of the Caribbean should produce overrriding as suggested by Bowin rather than faster subduction. Resistance to plate motion in the mantle and the mechanisms of plate motion and

8.1 A synthetic cross-section across the Lesser Antilles and the Barbados Ridge, summarising the geophysical interpretations.

1. Low density unconsolidated and semi-consolidated sediments.
2. Consolidated sediments and those deformed by subduction.
3. Volcanic and plutonic rocks of the island forming volcanic piles.
4. Plutonic igneous rocks of the oceanic crust and the deep root of the island arc.

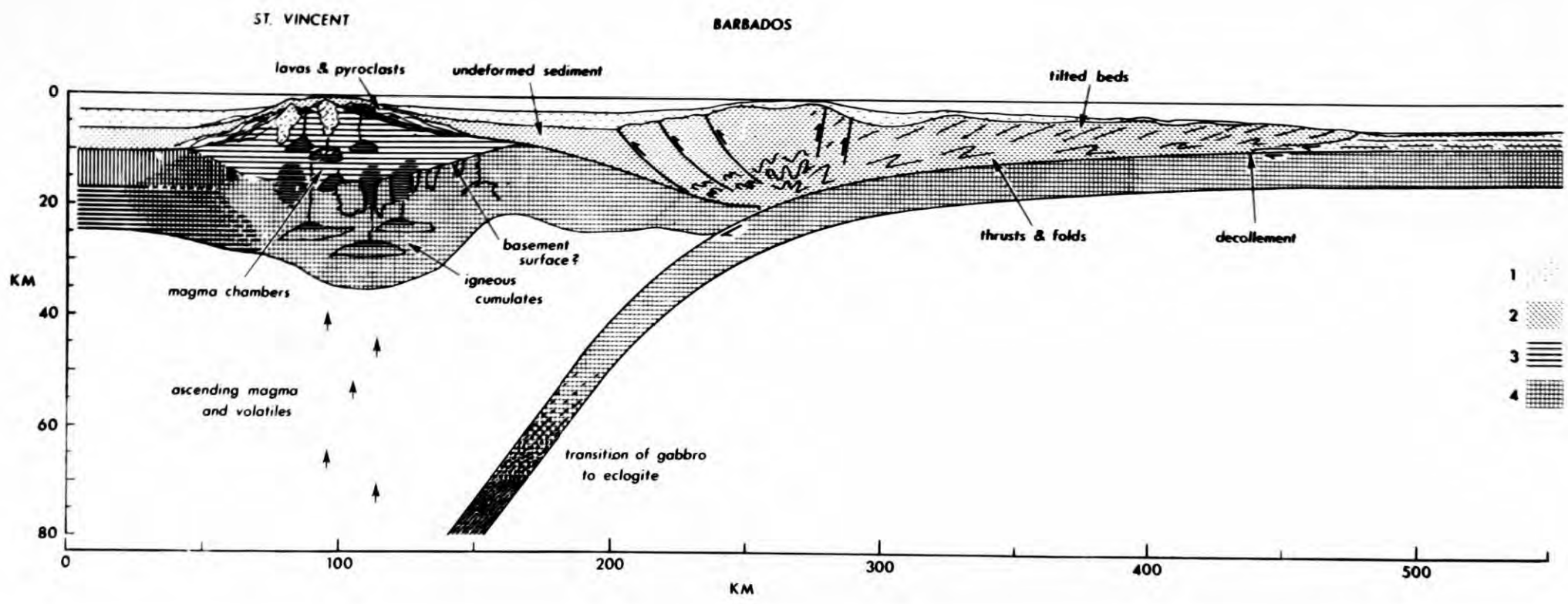
ST. VINCENT
BARBADOS
lavas & pyroclasts
undeformed sediment
tilted beds
0
20
KM
40
60
80
basement surface?
igneous cumulates
magma chambers
thrusts & folds
decollement
1
2
3
4
ascending magma and volatiles
transition of gabbro to eclogite
0
100
200
300
400
500
KM

subduction are important factors, but as their exact nature is at present unknown it is not possible to assess the likelihood of overriding taking place.

Eastward movement of the Caribbean or westward movement of the Atlantic is a thorny point of discussion for several writers on the Lesser Antilles. Some claim to be able to see evidence in the style of deformation of the area for movement in one direction or the other (Meyerhoff and Meyerhoff, 1971). However, as far as material overlying the two plates is concerned, there is no difference between eastward movement of the Caribbean and westward movement of the Atlantic. All that is significant is the relative convergent motion between them.

The uplift of the Barbados Ridge is quite likely to have resulted from a decrease in the cross-sectional area of the crustal depression underlying the ridge, but the mechanisms of a different nature to that of Bowin (1972) are proposed here. The crustal material underlying the eastern half of the Tobago Trough, adjacent to the subducting plate, must be in a state of compression and shearing parallel to the direction of motion of the subducting plate. The crust may, therefore be thickened as a result of creep under horizontal stress (thickened crust is seen on the crustal models), or parts of it may be sheared off and carried down with the subducted plate. Both these processes would lead to crustal shortening beneath the Barbados Ridge and consequently the compression and uplift of the overlying sediments. Another factor is that the region of subduction is depressed below its position of isostatic equilibrium by the forces causing subduction. If there is a relaxation in the subduction process

the region will rise, producing uplift of the ridge.

Structures of the Barbados Ridge, and their possible origin

From the crustal models (figs. 4.20, 4.21 and 4.22) it appears that the eastern margin of the Barbados Ridge may be fault bounded, downthrowing to the east. The western flank of the ridge terminates at an abrubt change in nature of the reflecting horizons that may be underlain by a fault (figs. 4.6 and 4.7). In the western flank of the ridge the upper sedimentary layers are gently buckled above an irregular surface of more disturbed sediment. The buckling could be caused by movement of the underlying material on faults. These faults are thought likely to be thrust faults arising from the slow westward displacement of material caused by subduction, and possibly crustal shortening. The faults on the east side of the ridge are possibly high angle reverse or maybe normal, caused by the uplift of the ridge.

The structures observed in the Scotland Formation of Barbados are not completely explained by the subduction tectonic scheme described above (fig 8.1). Although the presence of several large dislocated sheets (Baadsgard, 1960) and north-south trending faults is compatible, the strike of the axial traces of the folds, at 065°, poses a problem. One would expect the strike to be approximately north-south if they were due solely to subduction. Herrera and Spence (1964), after a detailed study of the Scotland Formation, concluded that the folding was associated with the emplacement of the rocks as thrust sheets by gravity sliding northward from the region of the South American continental margin. The Joes River Formation is

considered by them to be severely sheared and tectonically displaced Lower Scotland Formation sediments. The allocthonous nature of the deposits would explain the presence of some apparently fairly shallow water sediments in what was a deep sea trench. The minimum angle of slope needed for gravity sliding is about 1^{o} (Kuenen, 1956), which would have been the case is the water depth at Barbados at the time of emplacement (Eocene) was greater than 4 km, which is likely. As the folds are penecontemporaneous with deposition, they are probably no younger than Middle Eocene, and predate the island arc and possibly the subduction zone. Consequently they may be completely unrelated to the present tectonic situation.

Daviess (1971) takes the gravity sliding hypothesis one stage further, and envisages the whole area of the Barbados Ridge and Slope as one massive gravity slide. This, however, poses a problem of derivation for such a large amount of material. Daviess was unsure where it came from, but mentioned an uplifted "Caribbean Block" from which the sediments slid. The thickness of sediments involved (up to 20 km) does seem rather too great for the en masse movement of sediment suggested and involves movement up slope on the eastern side of the trough. A massive slide as envisaged by Daviess, therefore, is rather implausible, but the role of gravity sliding on a smaller scale as suggested by Herrera and Spence, does seem to have played an important part in the early development of the area.

The folding in Barbados has been related by several authors (e.g. Martin-Kaye, 1969) to the late Eocene episode of folding in Trinidad and Venezuela, partly on the grounds of the similar strike of the structures. Weeks and others (1971) claim continuity between

the structures of the South American continental shelf and those of the Barbados Ridge. Much of the evidence put forward in support of this is given by Bassinger and others (1971). The only two features that are apparently continuous across the break of the continental shelf are two long period magnetic anomalies, and how these are correlated from survey line to survey line is not demonstrated. The structures seen on the reflection profiles over the Barbados Ridge are completely absent from the shelf.

It seems unlikely that the mechanism causing the deformation continental margin of northern South America would also have affected Barbados. As in most orogenic belts, deformation is confined to a comparatively narrow linear zone. The intervening lithosphere between Barbados and the continetal shelf shows no sign of deformation, and it is improbable that it would be deformed. Barbados, therefore, cannot have been deformed by the process which produced folds in Trinidad and Venezuela unless the zone of deformation curved round to include Barbados, in which case the trend of the folds should be northward. There remains the possibility that underthrusting of the Caribbean Plate beneath the northern margin of South America produced some strike-slip motion along the subduction zone which may have contributed to the deformation of Barbados.

Summary of tectonic features

The main points concerning the structure and tectonics of the Barbados ridge region may be summarised as follows. The presence of the Barbados Ridge is a consequence of subduction, and active deformation is presently taking place at the eastern edge of the

sediment pile and directly above the lithosphere moving into the subduction zone. The upper parts of the sediment pile are no longer affected by subduction, except for some adjustment on faults. The uplift of the Barbados Ridge is probably not simply a consequence of continued subduction, but may be related to a change in shape of the crustal depression created by subduction and isostatic uplift. Fold structures seen in Barbados are primarily related to deformation penecontemporaneous with deposition, in which gravity sliding was important. Structures of the northern margin of South America are unlikely to be directly related to those of Barbados, although they were probably influenced by the same plate motions.

The relationship between ocean trenches and subduction zones

As a general rule, the negative Bouguer gravity anomaly associated with deep sea trenches is situated over the landward wall of the trench (Talwani, 1970). Another widespread feature of trenches is that the inclined zone of earthquakes attributed to subduction appears to intersect the surface on the landward side of the trench as far as 50 km away from the trench axis (Sykes, 1966). An apparent anomaly of many deep sea trenches is that there often appears to be very little sediment in them, and that what there is in them is in many cases undeformed (Scholl and others, 1968; Seyfert, 1968; Von Huene and others, 1969; Scholl and Von Huene, 1970), though not always so (Lister, 1971).

The above mentioned features are almost certainly related. An ocean trench need not necessarily lie directly over the site of subduction, where the site of subduction is taken to mean the point where

igneous crustal material on the subducted plate passes through similar material on the opposing plate. The cross sectional shape of a subduction zone and the region of the trench seems to be controlled by the forces causing subduction, though loading of the crust has some influence. When a subduction zone is young, the trench will be situated over the site of subduction, and will be at its deepest. As sediment is added to the trench area by subduction, the trench itself will migrate away from the point of subduction as sediment is piled up behind it. The Bouguer anomaly will still be situated over the site of subduction where the crust is deepest, as will the top of the seismic zone, and after some time they will appear well to the landward side of the trench, depending on the rate of subduction and the amount of sediment on the subducted plate. Fig. 8.2 illustrates this development.

The trench is situated at the front of the deformed sediment zone, and hence the sediment in its bottom and on its seaward side will always be undisturbed. If the hinterland behind the trench produces any appreciable amount of sediment, the deformed sediments will be overlain by a layer of new sediment, and the deformation may pass unnoticed on reflection profiles across such an area. Burk (1972) in a study of the Aleutian Arc, noted that the trench had migrated seaward and although the landward portions of the trench are now uplifted it is possible that the way in which the trench migrated was similar to the scheme presented above. The Barbados region is a case in which the sediment pile with the trench at its growing margin has migrated completely out of the tectonic depression produced by subduction. If we can use the structure of the Barbados region as

8.2 Schematic diagram illustrating the development of an ocean trench at the top of a subduction zone, its oceanward migration and eventual disappearance.

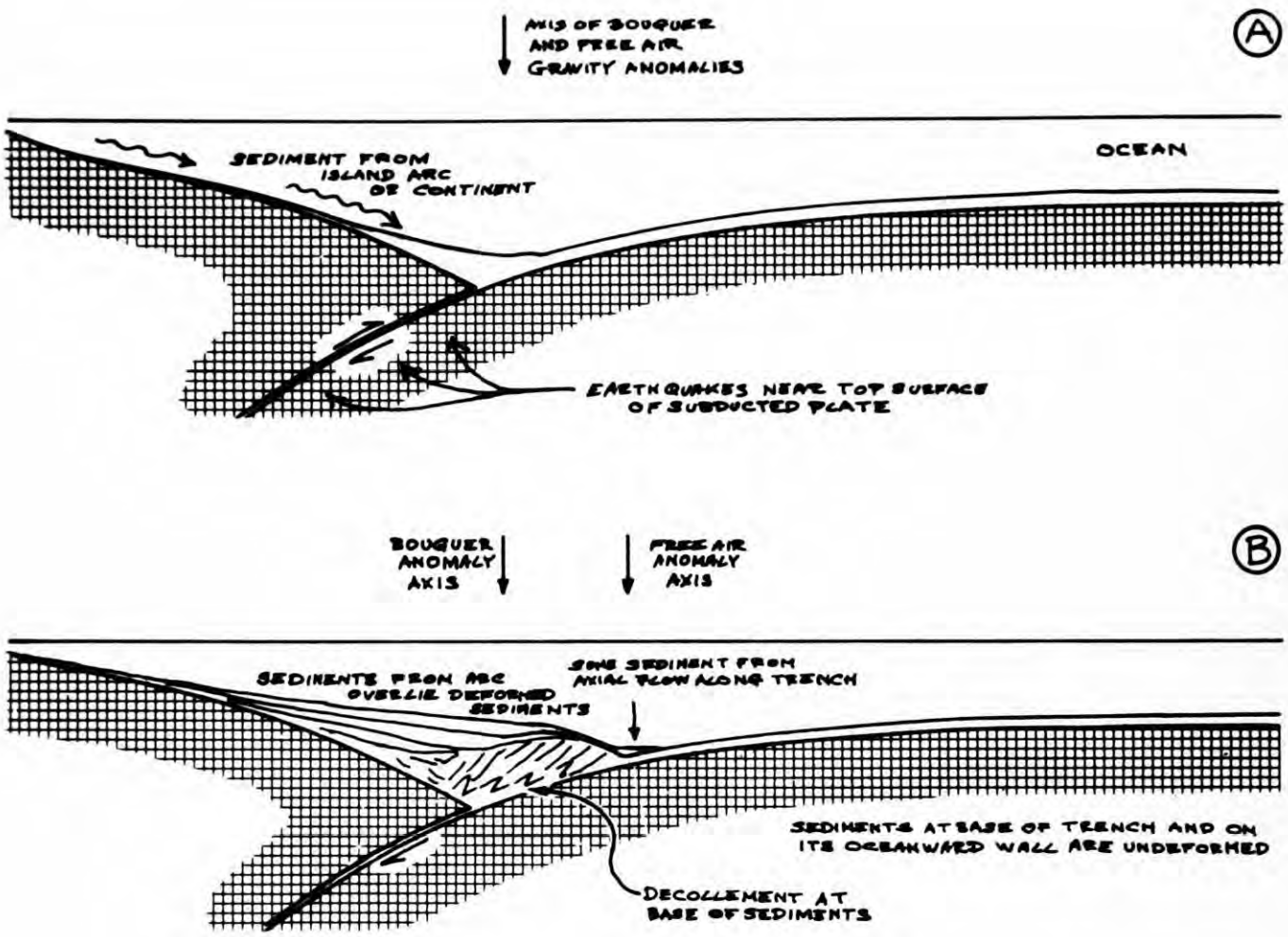
AXIS OF BOUGUER AND FREE AIR GRAVITY ANOMALIES
A
SEDIMENT FROM ISLAND ARC OR CONTINENT
OCEAN
EARTHQUAKES NEAR TOP SURFACE OF SUBDUCTED PLATE
BOUGUER ANOMALY AXIS
FREE AIR ANOMALY AXIS
B
SEDIMENTS FROM ARC OVERLIE DEFORMED SEDIMENTS
SOME SEDIMENT FROM AXIAL FLOW ALONG TRENCH
SEDIMENTS AT BASE OF TRENCH AND ON ITS OCEANWARD WALL ARE UNDEFORMED
DECOLLEMENT AT BASE OF SEDIMENTS
C
TRENCH BEGIN TO DISAPPEAR AS IT MIGRATES FROM POINT OF SUBDUCTION.

a model, then a trench can migrate up to 60 km from the site of subduction and still have a depth of 8 km, or maybe 6 km if the effect of isostatic loading in the Barbados region is allowed for. A faster subduction rate could probably increase these amounts.

Sediment volume as an estimate of subduction rate

In chapters 6 and 7 estimates were made of the subduction rate at the Lesser Antilles from considerations of the present seismicity, the length of the subducted plate, and the possible plate tectonic history. Another estimate of the rate of subduction or the period for which it has occurred is made here from the volume of sediment contained in the region of the Barbados Ridge and Slope.

A simple calculation is obtained from the assumption that the thickness of sediment on the subducted plate is constant. The cross-sectional area of sediment in the pile estimated from the crustal model at latitude 13^{o} 24' N (fig. 4.21) is 2084 km^{2} over a distance of 341 km. The thickness of sediment on undisturbed ocean floor is 3 km. Hence the cross-sectional area of excess sediment is 1061 km^{2}, which means that at a rate of 1 cm y^{-1} it has taken 35 my to accumulate the sediment. Put differently, this means that 350 km of lithosphere has been subducted, which agrees well with the length estimated from the depth of the seismic zone.

A little more realistic estimate may be made by assuming that the rate of sedimentation is constant. Then the thickness of sediment will be linearly related to the age of the crust. The quantities involved are listed below.

t = time

T = total time elapsed since start of subduction

S = sedimentation rate = 0.0348 km my^{-1}

R = single spreading rate at the mid-ocean ridge = 15.3 km my^{-1}

D = distance between ridge and subduction point at start of subduction.

U = subduction rate

P = present distance from ridge to subduction point = 1650 km

l = distance from subduction point to edge of sediment pile = 230 km

d = distance from subduction point to edge of sediments on arc side of zone = 111 km

A = age of crust beneath sediment on non-subducting side of pile = 80 my

R was obtained from the magnetic anomaly data of Peter (personal communication). S was obtained from seismic data given in chapter 4 in conjunction with the magnetic anomaly data.

The rate of sediment accretion in the trench at time t due to subduction is $\frac{US(t(R - U) + D)}{R}$

The amount of sediment accreted in time T is

$$\frac{US}{R} \int_0^T t(R - U) + D \, dt$$

$$= \frac{US}{R}\left(\frac{T^2}{2}(R - U) + DT\right) \qquad D = P - T(R - U)$$

The amount of sediment added to the pile by direct sedimentation is

$$\frac{(2P - l)}{2R} Sl + dSA$$

Cross-sectional area of the sediment in the pile is

$$\frac{S}{R}\frac{2Pl - l^2}{2} + U(PT - \frac{T^2}{2}(R - U)) + dSA = 2084 \text{ km}^2$$

Substituting the values given above for S, R, P, l, d and A in the equation gives

$$U(1650T - \frac{T^2}{2}(15.3 - U)) = 428000$$

If the rates of subduction (U) of 1 cm y^{-1} and 0.5 cm y^{-1} are substitued into the equation (V), then 26.4 and 55.4 my are obtained for values of the period over which subduction has been taking place (T). Alternatively if 40 my and 15 my are given for the periods of subduction rates of 0.72 and 1.72 cm y^{-1} are obtained.

Drawbacks to this analysis are that sedimentation rates may not have been constant, either temporally or areally. There was probably an increased amount of sedimentation in the trench when it existed, compared with that in the ocean, which would lead to an overestimate of the subduction rate. After the sediments had been uplifted above the level of the ocean basin there would have been less sedimentation in the subduction area than in the ocean basin. Also the subduction rate may have varied and even stopped.

The estimates of rate and period of subduction are comparable with those obtained from seismicity and length of subduction zone. The results are compared below.

Estimator	Rate	Period
Seismicity *	0.5 cm y^{-1}	
Length of subduction zone	0.5 cm y^{-1}	62 my
	1.0 cm y^{-1}	31 my
Sediment volume	0.5 cm y^{-1}	55.4 my
	1.0 cm y^{-1}	26.4 my

* using Brune's method (1968) which is known to give an underestimate.

Although individually each method of estimating the subduction rate is fairly inaccurate,the close correspondence between the values obtained by each method does imply that a subduction rate in the range of 0.5 to 1 cm y^{-1} is probably close to the average subduction rate at the Lesser Antilles.

Development of the structure of the island arc

In chapter 4 it was remarked that the choice of velocity/density model (figs. 4.23 and 4.24) for the island arc is dependent in some degree on manner of development of the island arc structure that is favoured. The most commonly assumed evolution of island arcs (eg. Mitchell and Reading, 1971) commences with the outpouring of lavas onto the seafloor, building up a volcanic pile in which all new material is added above the old seafloor. The weight of the new material leads to the depression of the Moho beneath it. The pile grows with the intrusion of more new material, and plutonic bodies are formed within it. Even after the island arc has become well developed, the Moho beneath it is essentially that of the original ocean crust, although it may have become modified in some degree by the passage of material through it. It is interesting to note that

Mitchell and Reading (1971), with no geophysical evidence to guide them, conservatively underestimated the depth of the Moho beneath the island arc, putting it at 15 km.

Ultrabasic xenoliths found in extrusive rocks in the arc indicate the presence of more ultrabasic rocks at depth (K. Wills, personal communication). If the alkali basalts, which are the most basic extrusive rocks found in the arc, are most close to the parental magma, then in order to derive the dominantly andesitic volcanics of the arc there must be a residuum of undersaturated basic rocks at least equal in volume to the extrusive rocks. The question that arises is where do these basic and ultrabasic rocks occur within the arc? Are they all above the original seafloor or do they occur within and below the old ocean crust? If the latter is the case then it is possible that the island arc may develop in the manner illustrated by 'b' of fig. 8.3 rather than 'a' which is the most commonly assumed case. The old seafloor would not be depressed as much as in 'a' and the Moho would be at the base of newer material, not the old oceanic crust. Calcic xenoliths containing wollastonite, grossular garnet, anorthite and a pyroxene, fassaite, are probably the products of reaction between calcic rich sediments and basaltic magma (K. Wills, personal communication). The environmental conditions for the mineral assemblage are not well know, but comparison with similar metamorphic assemblages and experiments (Turner, 1968) indicates conditions of high temperature and fairly low pressure. The depth of formation is not greater than 20 km. This suggests that if the sediments metamorphosed were those lying on the original seafloor then the old basement cannot be too far down in the volcanic

pile; a feature that would favour model 'b'. The predominance of alkali basalts among the oldest rocks of the arc implies that there was relatively little differentiation occurring in the early part of the development of the arc and that consequently large magma chambers only form once a considerable volcanic pile had been built up. This favours model 'a' as 'b' should produce differentiated products early on. It might also be considered that the basaltic magma being less dense than the ocean crust should rise above it, which is also a point in favour of model 'a'.

Comparing the two models (fig. 8.3), it does seem that 'a' is perhaps the most plausible, but it is likely that the original ocean crust may become considerably altered by the passage of material through it and be intruded in the manner shown in 'b' 3. It is not possible with the geophysical information available to be able to differentiate between the two models, but it can be said that there must be a high proportion of basic plutonic rocks in the island arc.

Another feature of the island arc is that the volcanic islands in the region considered are west of the centre of the volcanic pile as derived from the gravity and seismic evidence (figs. 4.20, 4.21, 4.23, and 4.24). It may be that vulcanicity shifted westward in the region of St. Vincent as it did in the northern part of the arc (Martin-Kaye, 1969), only by not so large an amount. If this were the case then the complicated pattern of magnetic anomalies east of the arc might be interpreted as being produced by the multiply intruded older part of the arc, whereas the more uniform anomaly on the western side might be thought to be the result of the more homogeneous newer part.

8.3 Two possible modes of island arc growth.

a.

b.

1

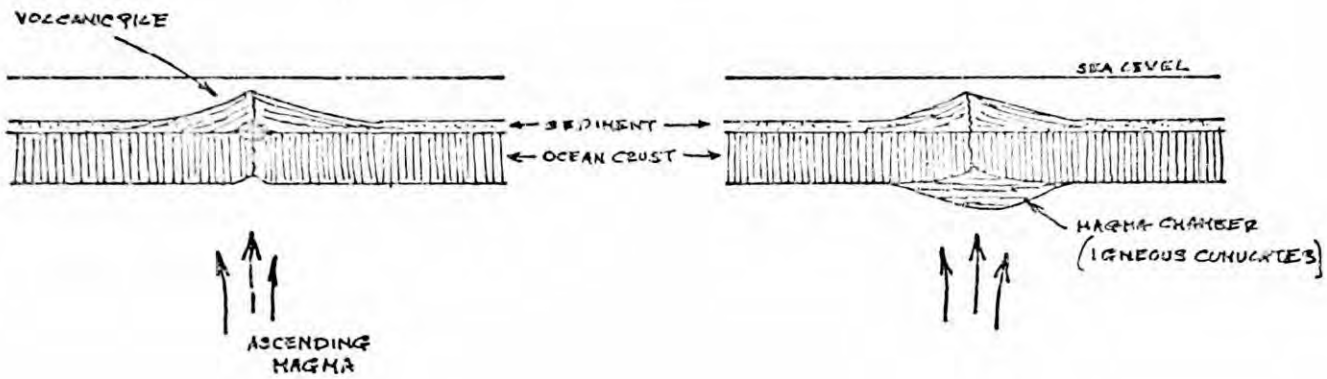
VOLCANIC PILE
SEDIMENT
OCEAN CRUST
SEA LEVEL
MAGMA CHAMBER
(IGNEOUS CONDUITS)
ASCENDING
MAGMA

2

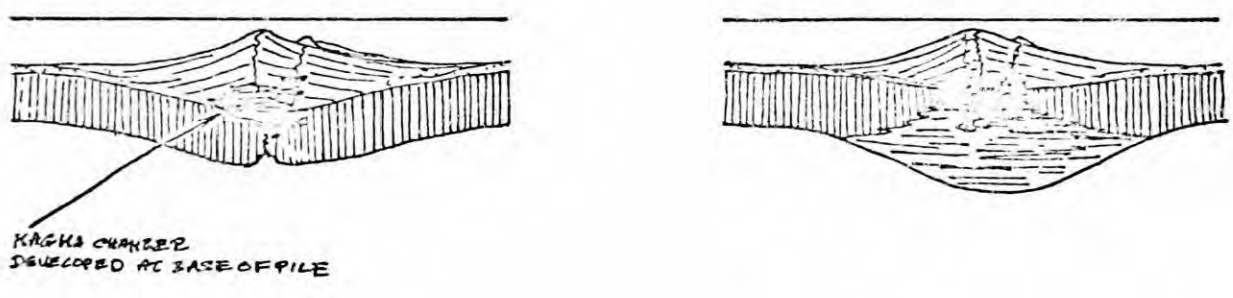
MAGMA CHAMBER
DEVELOPED AT BASE OF PILE

3

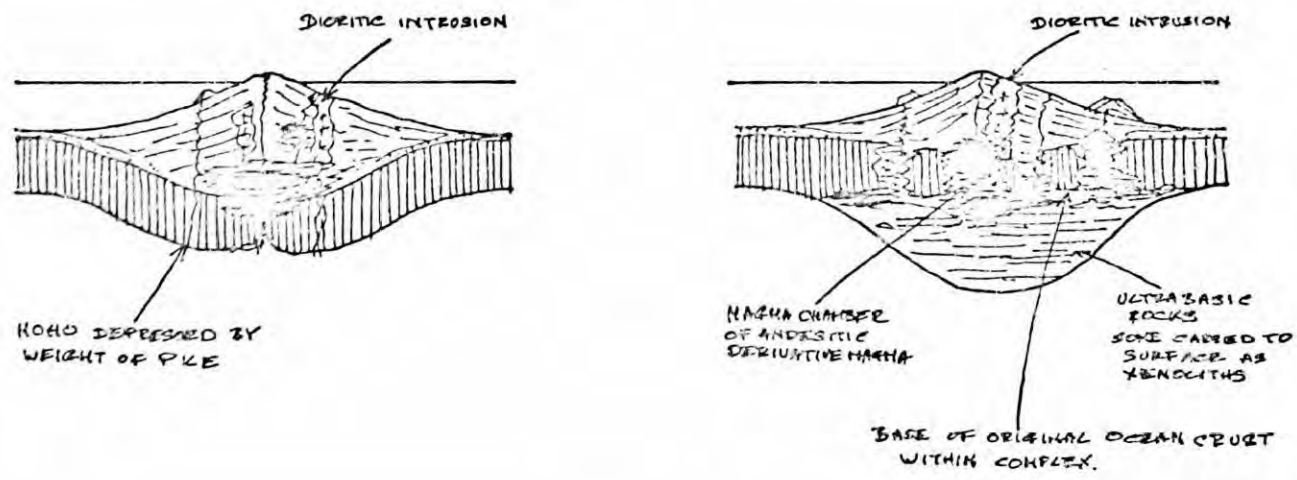
DIORITIC INTRUSION
MOHO DEPRESSED BY
WEIGHT OF PILE
DIORITIC INTRUSION
MAGMA CHAMBER
OF ANDESITIC
DERIVATIVE MAGMA
ULTRABASIC
ROCKS
SOME CARRIED TO
SURFACE AS
XENOLITHS
BASE OF ORIGINAL OCEAN CRUST
WITHIN COMPLEX.

The reason for the remarkable linearity of the Lesser Antilles, even though it is a common feature of island arcs, is not easily understood. Most current hypotheses place the volcanic islands directly above the region of the subducted plate where volatiles or partial melts are derived. The depth from the arc to this zone appears to be related to the subduction rate. Given that the zone of derivation is narrow, and many authors make it very broad, one might expect some divergence of material on its passage to the surface. Instead the reverse appears to be true. How are the products focussed to appear at the same place on the surface? Little is known about the tectonic state of the lithosphere when the subduction zone is formed. Perhaps the fracture system produced initially guides the volcanic products, which once they have established a route always follow it, because removal of material from one end of the system tends to draw more into it.

Was there once a subduction zone at the present site of the Lesser Antilles?

The crustal structure either side of the arc is different. The Grenada Trough in common with the Venezuelan Basin has two layers of seismic velocity 6.3 and 7.4 km s^{-1} in place of the one layer of velocity 6.9 km s^{-1} present under the Atlantic Ocean and the Tobago Trough (fig. 4.20). If the double layer is a feature of the Caribbean Plate and the arc has been formed on the plate then the change in structure would be expected to occur across the subduction zone, not the island arc. It may be that the Aves Swell is a former island arc. The rocks collected from it are of the calc-alkaline type and

are older than any present in the Lesser Antilles (Fox, Schreiber and Heezen, 1971). The eastern side of the Aves Swell has a convex form, suggesting that any subduction that took place would have done so from the east. The most likely site of subduction, therefore, would have been on the eastern side of the Grenada Trough, near where the Lesser Antilles now are. This could have been active from 80 to 50 or 40 my bp. The apparent absence of deformed sediments in the Tobago Trough (P. Keary, personal communication) appears to stand against the hypothesis. However, the position of the Grenada Trough during subduction below the Aves Swell would have been analogous with that of the Tobago Trough now, where all the upper sediments are undeformed, and sedimentation during the following 40 to 50 my will have completely buried any once discernible deformed structures to a depth too deep to be seen by the reflection profiling system. Another point against is that there does not seem to be enough sediment in the Grenada Trough, but there may not have been as much sediment on the subducted lithosphere as there is nowadays and consequently one would not expect a large amount of sediment to be accumulated, as is now seen below the Barbados Ridge. More needs to be known about the crustal structure in the eastern half of the Grenada Trough to be able to establish the plausibility of this early subduction zone hypothesis more certainly.

An alternative method of development for the Grenada Trough and the Venezuelan Basin is some form of "back arc spreading" process, as has been proposed for marginal basins in the western Pacific (Karig, 1971; Moberly, 1972).

The possible association between geochemical variations in the island arc, and the Barbados Ridge and the St. Lucia East Ridge.

Geochemical sampling of the Lesser Antilles has shown that St. Vincent, Grenada and the Grenadines are more undersaturated than the rest of the Lesser Antilles (K. Wills, personal communication). There are also fewer pyroclastic 'glowing avalanche' type deposits on them. It is surely not just coincidence that the Barbados Ridge should be formed opposite these islands, and that the St. Lucia East Ridge should mark the northernmost extent of both the Barbados Ridge and the undersaturated islands.

In chapter 4 the hypothesis was put forward that the eastern part of the St. Lucia East Ridge was an old transform fault and the effect of it damming the sediments derived from South America had been to limit the northward development of the Barbados Ridge. In chapters 6 and 7 a model of plate motion (model 2, fig. 6.12) causing subduction below the Lesser Antilles was discussed, in which transform faults could run into the arc from the east. A feature of this model was that south of each transform fault the rate of subduction would be less than that north of it. If the St. Lucia East Ridge was such a transform fault, then during the period of its activity subduction would have been proceeding at a slower rate beneath St. Vincent, Grenada and the Grenadines than the rest of the arc.

The amount of partial melting that occurs in the mantle to give the magmas that form the island arc is presumably related to the supply of volatiles from the subducted plate, in particular water released from hydrous minerals. The rate of volatile supply is related to

subduction in two ways. Firstly, the rate at which volatiles are taken into the mantle is directly proportional to the rate of subduction. Secondly, the faster the rate of subduction is, the cooler is the subducted lithosphere at any given depth. Consequently the volatiles may be taken down deeper, and fewer will be given off before the main region of magma genesis.

At slow rates of subduction partial melting will be less then at fast rates. When partial melting is small the products of it are undersaturated. Hence there would seem to be a connection between a slower subduction rate and the production of relatively more undersaturated rocks in the southern islands of the arc. This would also explain why the volume of volcanic material is smaller in the southern part of the arc than the northern part. Fig. 8.4 illustrates this. Another consequence of slower subduction in the southern part of the arc is that seismic zone would be expected to be shallower than in the northern part. Fig. 6.3 shows that the deepest earthquakes are generally deeper north of St. Lucia than south of it, but the distinction is not very marked.

An objection to the argument is that the St. Lucia East Ridge is not presently active as a transform fault and was probably only active during the early phase of vulcanicity in the Lesser Antilles, but the geochemical samples were taken from rocks of the present volcanic phase. Judging from earthquake hypocentres, the subducted lithosphere is 140 km deep below the island arc. If subduction for the present phase of volcanic activity has lasted 10 my then the material now in the zone of volatile derivation was at 108 or 76 km depth 10 my ago for rates of 0.5 and 1 cm y^{-1} respectively. At both these depths some

8.4 Hypothetical tectonic scheme producing a difference in volcanic rocks between the northern and southern parts of the island arc. C is a constant related to the resistance to motion either side of the transform fault. V is the rate of subduction.

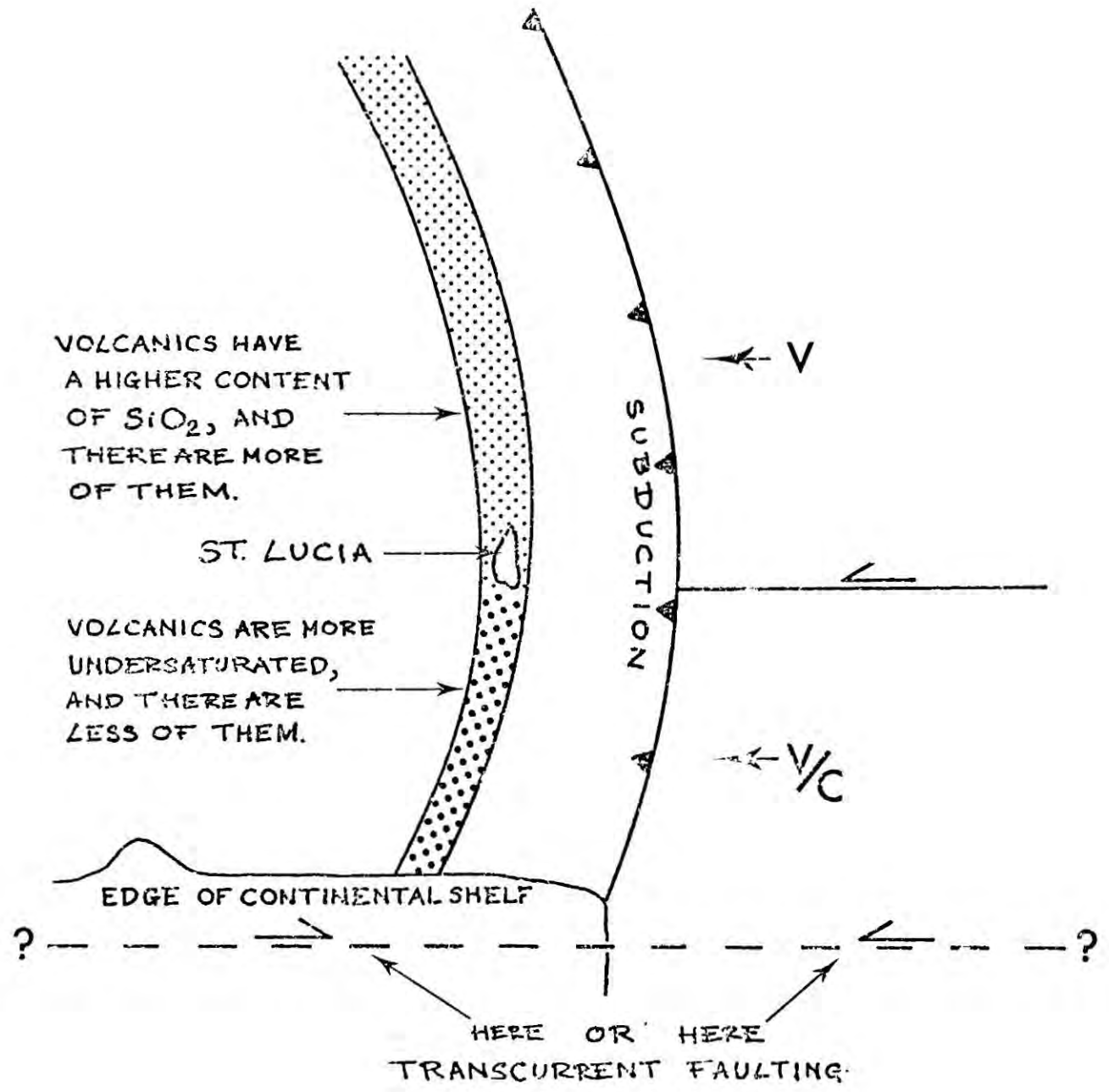
VOLCANICS HAVE A HIGHER CONTENT OF SiO_2, AND THERE ARE MORE OF THEM.
ST. LUCIA
VOLCANICS ARE MORE UNDERSATURATED, AND THERE ARE LESS OF THEM.
SUBDUCTION
V
V/C
EDGE OF CONTINENTAL SHELF
?
?
HERE OR HERE
TRANSCURRENT FAULTING

loss of water from hydrous minerals is expected. Maybe the effects of the earlier situation were still preserved in the mantle because of the slow subduction rate, and during the earlier part of the present phase this influenced the volcanic products of the zone of partial melting.

History of the area

Given below in tabular form (table 8.1) is a summary of the main events of geological significance that have occurred in the area studied. It is compiled from the published sources mentioned in chapter 1, in conjunction with inferences made from the interpretation of the structures determined by the geophysical investigation.

Table 8.1

Age my	Epoch	Event
	Recent	Deposition of layer A* in the Tobago Trough and minor troughs east of the Barbados Ridge
		Formation of Coral Rock on Barbados.
	Pleistocene	Rapid uplift of Barbados.
		Deposition of layers A and B in the Tobago Trough.
	Pliocene	Gentle rise of Barbados Ridge area.
	—	Trench becomes filled.
9		Commencement of the second phase of vulcanism
		in the Lesser Antilles and the westward shift
15		of the axis of vulcanism in the north of
	Miocene	the arc.
		Bissex Hill Formation (Barbados).
		Formation of limestones on volcanic islands.
	—	
	Oligocene	Waning of vulcanism.
		Cessation of subduction?
	—	
		Deposition of Oceanic Formation commences.

Age my	Epoch	Event
40		Deformation of Tufton Hall Formation in Grenada
	Eocene	and Lower Eocene rocks in Trinidad.
		Vulcanism in the Lesser Antilles.
	—	Beginning of subduction opposite the Lesser
		Antilles.
	Palaeocene	Deposition of the Scotland Formation commences.
	—	Formation of Aves Swell begins.
		Deformation of north coast of South America
		due to subduction?
80	Cretaceous	Caribbean Plate formed.

The interval between the initiation of subduction and the start of vulcanism is not known, but it is probably related to subduction rate. Judging from the present situation, about 200 km of lithosphere needs to be subducted before magma is generated, which at 1 cm y^{-1} would take 20 my.

Although Cretaceous sedimentary rocks are not seen on Barbados, it seems very probable that they exist at depth within the Barbados Ridge and are possibly metamorphosed.

Summary and conclusions

Listed below are some of the major features elucidated by this work.

1. The crustal structure across the area has been determined in some detail. The main points of which are:-

   a) The oceanic basement is about 20 km deep below the Barbados Ridge.

b) The Barbados Ridge is composed entirely of sediments, some of which are probably metamorphosed.

c) The Barbados Ridge has been uplifted by about 5 km.

d) The Tobago Trough has a crust similar to that of the Atlantic.

e) Two unconformities are seen in the succession of sediments in the Tobago Trough.

f) There is considerable indirect evidence indicating deformation of the sediments of the Barbados Ridge and Slope by subduction.

g) The upper sedimentary layers are unaffected by subduction.

h) The root beneath the island arc in the region of St. Vincent is about 30 km deep.

i) Magnetic anomalies indicate that the arc has been built up by many igneous bodies intruded over a fairly long period.

2. From various lines of evidence it is estimated that the subduction rate has been about 1 cm y^{-1}.

3. The site of subduction of the Atlantic plate is directly below the Barbados Ridge.

4. A gravity anomaly is produced by the subducted lithosphere which may not be greatly different from that estimated from a model of lithosphere being subducted at 1 cm y^{-1}.

5. The nature of the inclined zone of earthquakes is clearly shown by a simple statistical technique.

6. The amount of sinistral shear produced in the Lesser Antilles region since their formation by relative movement between North America and South America is 300 km.

7. The ocean crust beneath the area is of at least Early Cretaceous age.

8. The present phase of underthrusting at the Lesser Antilles is probably related to plate motions causing mountain building in the Andes, and the Caribbean Plate may have some connection with the Nazca Plate.

9. An eastward running buried ridge has been shown to exist east of St. Lucia, and this ridge which may be part of an old transform fault has limited the development of the Barbados Ridge, and probably has some connection with a variation in vulcanism along the arc.

References

Alberding, H., 1957. Application of principles of wrench-fault tectonics of Moody and Hill to northern South America. Geol. Soc. Am. Bull., 68, p 785-790.

Baadsgaard, P. H., 1960. Barbados, W.I. Exploration results 1950-1958. Int. Geol. Congr. Rept. of 21st Session, 18, p 21 - 27.

Bader, R. G. et al. 1970. Initial Reports of the Deep Sea Drilling Project, Volume IV. Washington (U.S. Government Printing Office) 753 pp.

Ball, M. M., Harrison, C. G. A. and Supko, P. R. 1969. Atlantic opening and the origin of the Caribbean. Nature, 223, p 167 - 168.

Ball, M. M. and Harrison C. G. A., 1970. Crustal plates in the central Atlantic. Science, 167, p 1128 - 1129.

Ball, M. M., Harrison, C. G. A., Supko, P. R., Bock, W. and Maloney, N. J. Marine Geophysical measurements on the southern boundary of the Caribbean Sea. Mem . Geol. Soc. Am., 130, p 1 - 34.

Barr, K. G. and Robson, G. R., 1963. Seismic delays in the eastern Caribbean. Geophys. J. Roy. Astr. Soc., 7, p 342 - 349.

Barr, K. W. and Saunders, J. B., 1968. An outline of the geology of Trinidad. IV Caribbean Geol. Conf. Trans. p 1 - 10.

Bassinger, B. G., Harbison, R. N., Weeks, L. A., Marine geophysical study northeast of Trinidad-Tobago. Am. Assoc. Petr. Geol. Bull., 55, p 1730 - 1740.

Bassinger, B. G. and Keller, G. H., 1971. Marine geophysical observations across the Barbados Ridge - St. Lucia cross warp. Sixth Caribbean Geological Conference Abstracts p 8.

Bath, M., 1966. Earthquake energy and magnitude. Physics Chem. Earth, 7, p 115 - 165.

Bell, J. S., 1973. Geotectonic evolution of the Southern Caribbean. in Studies in Earth and Space Sciences. Geol. Soc. America Mem., 132, (Harry Hess Volume) p 369 - 386.

Bell, J. S., 1971. Tectonic evolution of the central part of the Venezuelan Coast Ranges. in Donnelly T. W., ed., Caribbean, Tectonic and Petrologic studies: Geol. Soc. America Mem., 130, p 107 - 118.

Bomford, G. 1962. Geodesy 2nd Edition. Oxford.

Bowin, C. O. 1968. Geophysical study of the Cayman Trough. J geophys. Res., 73, p 5159 - 5175.

Bowin, C., 1972. Puerto Rico Trench Gravity Anomaly Belt. Geol. Soc. Am. Mem., 132, p 339 - 350.

Bracey, D. R. and Vogt, P. R., 1970. Plate tectonics in the Hispaniola area. Geol. Soc. Am. Bull., 81, p 2855 - 2860.

Brune, J. N. 1968. Seismic moment, seismicity and rate of slip along major fault zones. J. Geophys. Res., 73, p 777 - 784.

Bullard, E. Everett, J. E. and Smith, A. G. 1965. The fit of the continents around the Atlantic. Phil. Trans. Roy. Soc. Lond. Ser. A, 258, p 41.

Bunce, E. T., Phillips, J. D., Chase, R. L. and Bowin, C. O. 1971. The Lesser Antilles Arc and the eastern margin of the Caribbean Sea. in the Sea A. E. Maxwell Editor, Vol 4 pt II, p 359 - 385.

Burk, C. A., 1972. Uplifted eugeosynclines and continental margins. Mem. Geol. Soc. Am., 132, p 75 - 85.

Bush, S. A. and Bush, P. A., 1969. Isostatic gravity map of the eastern Caribbean region. Gulf Coast Assoc. Geol. Socs. Trans., 19, p 281 - 285.

Campbell, C. J., 1965. The Santa Marta Wrench Fault of Colombia and its regional setting. 4th Caribbean Geol. Conf., Trinidad, p 247 - 261.

Chase, R. L. and Bunce, E.T., 1969. Underthrusting of the eastern margin of the Antilles by the floor of the western North Atlantic Ocean, and the origin of the Barbados Ridge. J. geophys. Res, 74, p 1413 - 1420.

Clark, S. P. Jr. (Editor), 1966. Handbook of physical constants. Revised edition. Mem. Geol. Soc. Am., 27, 587 pp.

Collette, J., Ewing, J., Lagaay, R. A. and Trushan, M. Sediment distribution in the oceans: the Atlantic between 10° and 19°N Marine Geol., 7, p 279.

Daviess, S. N., 1971. Barbados: A Major submarine gravity slide. Geol. Soc. Amer. Bull., 82, p 2593 - 2602.

Dickson, G. O., Pitman, W. C. and Heirtzler, J. R., 1968. Magnetic anomalies in the South Atlantic and ocean floor spreading. J. geophys Res., 73, p 2087 - 2100.

Donnelly, T. W., Rogers, J. J. W., Pushkar, P. and Armstrong, R. L. 1971. Chemical evolutions of igneous rocks of the eastern West Indies: an investigation of thorium, uranium and potassium distributions, and lead and strontium isotope rations. Mem. Geol. Soc. Am., 130, p 181.

Edgar, N. T., Ewing, J. I. and Hennion, J. 1971. Seismic refraction and reflection in the Caribbean Sea. Am. Assoc. Petroleum Geologists Bull., 55, p 838 - 870.

Edgar, N. T., Saunders, J. B., et al. 1971. Deep Sea Drilling Project Leg 15. Geotimes, 16, p 12 - 16.

Erickson, A. J., Helsley, C. E., and Simmons. G. 1972. Heat flow and continuous seismic profiles in the Cayman Trough and Yucatan Basin. Geol. Soc. Am. Bull., 83, p 1241 - 1260.

Essene, E. J., Henson, B. J., and Green, D. H., 1970. Experimental study of Amphibolite and eclogite stability. Phys. Earth Planet Interiors, 3, p 378 - 384.

Ewing, J. I., Edgar, N. T. and Antoine, J. W. 1971. 'Structure of the Gulf of Mexico and Caribbean Sea' in The Sea A. E. Maxwell editor Vol 4 pt II.

Ewing, J. I., Officer, C. B., Johnson, H. R., and Edwards, R. D., 1957. Geophysical investigations in the eastern Caribbean: Trinidad shelf, Tobago Trough, Barbados Ridge, Atlantic Ocean. Geol. Soc. America Bull., 68, p 897 - 912.

Ewing, J., M. Talwani & M. Ewing 1968. Sediment distribution in the Caribbean Sea. Caribbean Geol. Conf. Trans. 4th, 1965, Port of Spain, Trinidad.

Ewing, J., Worzel, J. L., Ewing, M. and Windisch, C. 1966. Age of Horizon A and the oldest Atlantic sediments. Science, 154, p 1125.

Ewing, M., Le Pichon, X. and Ewing, J. I., 1966. Crustal structure of the mid-ocean ridges, 4 sediment distribution in the South Atlantic Ocean and the Cenozoic history of the Mid-Atlantic Ridge. J. geophys . Res., 71, p 1611 - 1636.

Fink, L. K. Jr., Harper, C.T., Stipp, J. J. and Nagle, F. 1971. Tectonic significance of La Desirade - possible relict sea-floor crust. Abstracts of the Sixth Caribbean Geological Conference, Margarita, Venezuela. Latecomers p 4.

Fox, P. J., Pitman, W. C., III, and Shepherd, F. 1969. Crustal plates in the Central Atlantic: evidence for at least two poles of rotation. Science, 165, p 487 - 489.

Fox, P. J., Schreiber, E. and Heezen B. C. 1971. The Geology of the Caribbean Crust: Tertiary sediments, granitic and basic rocks from the Aves Ridge. Tectonophysics, 12, p 89 - 109

Frank, F. C. 1968. Curvature of island arcs. Nature, Lond., 220 p 363.

Freeland, G. L. and Dietz, R. S. 1971. Plate tectonic evolution of Caribbean - Gulf of Mexico region. Nature, 232, p 20 - 23.

Freeland, G. L. & Dietz, R. S. 1972. Plate Tectonics in the Caribbean: a reply. Nature, 235, p 156 - 157.

Gansser, A. 1973. Facts and theories on the Andes. Jl. Geol. Soc Lond., 129, p 93 - 131.

Gough, D. I., and Heirtzler, J. R. 1969. Magnetic anomalies and tectonics of the Cayman Trough. Geophys. J. Roy. Astr. Soc., 18, p 33 - 49.

Grant, F. S. and West, G. F. 1965. Interpretation theory in applied geophysics. McGraw Hill New York 584 pp.

Green, D. H., and Ringwood, A. E. 1970. Mineralogy of peridotitic compositions under upper mantle conditions. Phys. Earth Planet. Interiors, 3, 359 - 371.

Griggs, D. T., 1972. The sinking lithosphere and the focal mechanism of deep earthquakes. in the Nature of the Solid Earth, edit. E. C. Robertson., p 361.

Gupta, H. K. and Rastogi, B. K., 1971. Earthquake m_b vs M_s relations and source multiplicity. Geophys. J. R. astr. Soc., 28, p 65 - 89.

Gutenberg, B. and Richter, C. F., 1954. Seismicity of the earth and associated phenomena. Princeton University Press, Princeton, New Jersey. 310 pp.

Gutenberg, B. and Richter, C. F. 1956. Magnitude and energy of earthquakes. Ann. Geofis, 9, p 1 - 15.

Haigh, B.I.R. 1973. Crustal and Mantle structure in oceanic regions. University of Durham, unpublished Ph.D thesis.

Hatherton, T., 1970. Upper mantle inhomogeneity beneath New Zealand: Surface manifestations. J. geophys. Res., 75, 269 - 284.

Heirtzler, J. R., Dickson, G. O., Herron, E. M., Pitman, W. C., and Le Pichon, X. 1968. Marine magnetic anomalies, geomagnetic field reversals and motions of the ocean floor and continents. J. geophys. Res., 73, p 2119 - 2136.

Herrera, R. C., and Spence, J. 1964. The geology and oil prospects of the Scotland Group sediments at Barbados. Sinclair & B. P. explorations Inc. unpublished report.

Hersey, J. B., 1966. Marine geophysical investigations in the West Indies. Canada Geol. Survey Paper 66 - 15 p 151 - 164.

Hess. H. H., 1933. Interpretation of geological and geophysical observations in the Navy - Princeton Gravity Expedition to the West Indies in 1932. Bull. Geol. Soc. Amer. 49.

Hess, H. H., 1938. Gravity anomalies and island arc structure with particular reference to the West Indies. Proc. Amer. Phil. Soc. 79, 71 - 96.

Higgins, G. E., 1959. Seismic velocity data from Trinidad, B.W.I. and comparison with the Caribbean area. Geophysics, 24, p 580 - 597.

Holden, J. C. and Dietz, R. S., 1972. Galapagos Gore, NazCoPac Triple Junction and Carnegie/Cocos Ridges. Nature, 235, p 266 - 269.

Horn, D. R., Horn, B. M., and Delach, M. N. 1968. Correlation between Acoustical and other physical properties of Deep-sea cores. J. geophys Res., 73, p 1939 - 1957.

Houtz, R., Ewing, J. and Le Pichon, X. 1968. Velocity of deep sea sediments from sonobuoy data. J. geophys. Res., 73, p 2615 - 2641.

Hurley, R. J., 1966. Geological studies of the West Indies. Canada Geol. Survey Paper 66 - 15, p 139 - 150.

I.A.G.A., 1969. International geomagnetic reference field 1965 - 0. J. geophys. Res., 74., p 4407 - 4408.

Ingles, A. D., 1971. The interpretation of magnetic anomalies between Iceland and Scotland. Unpublished Ph.D, Thesis, University of Durham.

Irving, E. and Couillard, R. W., 1973. Cretaceous normal polerity interval. Nature Physical Science, 244, p 10 - 11.

Isacks, B and Molnar, P. 1971. Distribution of stress in descending lithosphere from a global survey of focal mechanism solutions of mantle earthquakes. Rev. Geophys. Spaces Phys, 9, p 103 - 114.

James, F. and Roos, M., 1969. Minuit: A program to minimise a function of n variables, compute the covariance matrix, and find the true errors. Unpublished. Long write up, CERN Computer 6000 series Program Library.

Karig, D. E., 1971. Origin and development of marginal basins in the Western Pacific. J. geophys. Res., 76, p 2542 - 2561.

Karig, D. E., 1972. Remnant Arcs. Geol. Soc. Am. Bull., 83, p 1057 - 1068.

Kaula,W. M., 1972. Global gravity and tectonics in'The nature of the solid Earth' E. C. Robertson Ed. p 385 - 405. McGraw-Hill New York.

Keller, G. H., Lambert, D. N., Bennett, R. H., and Rucker, J. B., 1971. Mass physical properties of Tobago Trough sediments. Sixth Caribbean Conference Abstracts p 8.

Khan, M. A., 1965. A note on the magnetic properties of some volcanic rocks from the island of St. Vincent, West Indies. Fourth Caribbean Geological Conference, Trinidad 1965.

Khudoley, K. M. and Meyerhoff, A. A. 1971. Palaeogeography and Geological History of Greater Antilles. Geol. Soc. Am. Mem, 129, 199p.

Krause, D. C., 1971. Bathymetry, geomagnetism and tectonics of the Caribbean Sea north of Colombia. in Caribbean geophysical, tectonic and petrological studies, ed. T. W. Donnelly. Geol. Soc. Am. Mem., 130, p 35 - 54.

Ku. T. L., 1968. Protactinium 231 Method of dating coral from Barbados. J. geophys. Res., 73, p 2271 - 2276.

Kuenen. Ph. H. 1955. The difference between sliding and turbidity flow. Deep Sea Research, 3, p 134 - 138.

Laving, G. J., 1971. Automatic methods for interpretation of gravity and magnetic field anomalies and their application to marine geophysical surveys. Unpublished Ph. D thesis University of Durham.

Lee, M. K., 1972. Use of the one-dimensional power spectrum for depth determination to magnetic structures. Unpublished M. Sc. Dissertation, University of Durham.

Le. Pichon, X., Ewing, J. and Houtz, R. E. 1968. Deep sea sediment velocity determination made while reflection profiling. J. geophys. Res, 73, p 2597 - 2614.

Le Pichon, X. and Fox, P. J., 1971. Marginal offsets, fracture zones and the early opening of the North Atlantic. J. geophys. Res. 76, p 6294 - 6308.

Lister, C. R. B., 1971. Tectonic movement in the Chile Trench. Science, 173, p 719 - 722.

Lowrie, A. and Escowitz, E eds, 1969. Kane 9s. Global ocean floor analysis and research data series - Vol. 1, U. S. Naval Oceanographic office. 971 pp.

Ludwig, W. J., Nafe, J. E. and Drake, C. L., 1970. 'Seismic Refraction' in The Sea ed. A. E. Maxwell 4 pt 1 p 53 - 84.

Luyendyk, B. P., 1970. Dip of the downgoing lithospheric plate beneath island arcs. Geol. Soc. Amer. Bull.

MacDonald, W. D. and Opdyke, N. D. 1972. Tectonic rotations suggested by palaeomagnetic results from Northern Colombia, South America. J. geophys. Res. 77, p 5720.

Macintyre, I. G., 1967. Submerged coral reef off the west coast of Barbados, West Indies. Canadian J. of Earth Sci., 4 , p 461 - 474.

Malfait, B. T. and Dinkleman, M. G., 1972. Circum-Caribbean tectonic and igneous activity and the evolution of the Caribbean Plate. Geol. Soc. Am. bull., 83, p 251 - 272.

Malfait, B. T. and Dinkleman, M. G., 1973. Circum-Caribbean tectonic and igneous activity and the evolution of the Caribbean Plate: Reply. Geol. Soc. Am. Bull., 84, p 1105 - 1108.

Maresch, W. V., 1973. Eclogitic-Amphibolitic Rocks on Isla Margarita, Venezuela: A preliminary account. in studies in Earth and Space Sciences. Geol. Soc. Amer. Mem, 132, (Harry Hess volume), p 429 - 437.

Martin- Keye P.H.A., 1969. A summary of the geology of the Lesser Antilles. Overseas Geology and Mineral Resources. Inst. Geol. Sci. 10 (2) p 172 - 206.

Masson Smith, D. J, and Andrew, E. M., 1965. Gravity and Magnetic measurements in the Lesser Antilles. Overseas Geological Surveys (Geophysical Division) Preliminary Report and Illustrations 16pp.

Masson Smith, D., Andrew, E. M., and Robson, G. R.. 1970. Gravity anomalies in the Lesser Antilles. Inst. Geol. Sci. Geophys Paper 5, 21p.

Matsushita, S., 1967. Solar quiet and lunar daily variation fields in Physics of geomagnetic phenomena. eds Matsushita, S. and Campbell, W. th Vol 1. p 301 - 424 Academic Press Lond.

Matthews, D. J., 1939 Tables of the velocity of sound in pure water and sea water for use in echo sounding and sound ranging, 52 pp Admiralty Office, London.

Mattson, P. H., 1972 Plate Tectonics in the Caribbean. Nature, 235, p 155-156.

Maxwell, A. E. and others. 1970. Deep sea drilling in the South Atlantic. Science, 168, 1047 - 1059.

McKenzie, D. P., 1969. Speculations on the consequences and causes of plate motions. Geophys. J. Roy.Astr. soc., 18, p 1 - 32.

McKenzie, D. P., 1972. "Plate tectonics" in the Nature of the Solid Earth ed. E. C. Robertson McGraw Hill p 323 - 360.

McKenzie, D. P. and Morgan, W. J., 1969. Evolution of triple points. Nature, 224, p 125 - 133.

Metz, H. L., 1965. Geology of the El Pilar fault zone, State of Sucre, Venezuela. Fourth Caribbean Geoligical Conference, Trinidad p 293 - 298.

Meyerhoff, A. A. and Meyerhoff, H. A., 1971. Tectonics of the eastern Caribbean margin. Sixth Caribbean Geological Conference abstracts, p 2.

Meyerhoff, A. A. and Meyerhoff, H. A., 1972. Continental Drift IV. The Caribbean 'Plate'. J. Geol., 80 (1), p 34.

Meyerhoff, H. A., and Meyerhoff, A. A., 1973. Circum-Caribbean Tectonic and igneous activity and the evolution of the Caribbean Plate: Discussion. Geol. Soc. Am. Boll., 84, p 1101 - 1104.

Minear, J. W. & Toksöz, M. N., 1970. Thermal regime of a downgoing slab and new global tectonics. J. geophys. Res., 75, 1397 - 1419.

Mitchell, A. H. and Reading, H. G., 1971. Evolution of island arcs. J. of Geol., 79, p 253 - 284.

Moberly, R., 1972. Origin of Lithosphere behind island arcs, with reference to the Western Pacific. Geol. Soc. Am. Mem, 132, p 35 - 55.

Molnar, P. and Sykes, L. R., 1969. Tectonics of the Caribbean and Middle America regions from focal mechaisms and seismicity. Geol. Soc. Am. Bull., 19,p487 - 494.

Molnar, P. and Sykes, L. R., 1971. Plate tectonics in the Hispaniola area: discussion. Geol. Soc. Am. Bull., 82, p 1123 - 1126.

Monroe, W. H., 1968. The age of the Puerto Rico Trench. Geol. Soc. Am. Bull., 79, p 487 - 494.

Murphy, A. J, L. R. Sykes and T. W. Donelly, 1970. Preliminary survey of the Microseismicity of the North eastern Caribbean. Geol. Soc. Am. Bull., 81, p 2459 - 2464.

Nagle, F., 1971. Rocks from seamounts and escarpments on the Aves Ridge. Sixth Caribbean Geological Conference Abstracts - late arrivals, p 3.

Officer, C. B., Ewing, J. I., Hennion, J. F., Harkrider, D. G. and Mitter, D.E., 1959. Geophysical investigations in the eastern Caribbean: Summary of 1955 and 1956 cruises. Physics and Chemistry of the Earth. Physics and Chemistry of the Earth, 3, 17 - 109.

Oxburgh, E. R., & D. L. Turcotte, 1968. Problem of high heat flow associated with the zones of descending mantle convective flow. Nature, 218, 1041 - 1043.

Oxburgh, E.R., and D. L. Turcotte. 1970. Thermal structure of island arcs. Geol. soc. Am. Bull., 81, p 1665 - 1688.

Pars, L. A., 1965. A Treatise on Analytical Dynamics. Heinemann London.

Peter, G., 1971. Geology and geophysics of the Venezuelan continetal margin between Blanquilla and Orchilla islands. University of Miami, Unpublished Ph. D. thesis, 206 pp.

Phillips, J. D. and Forsyth, D. 1972. Plate tectonics, palaeomagnetism and the opening of the Atlantic. Geol. Soc. Am. Bull., 83p 1579 - 1600.

Phillips, J. D. and Luyendyk, B. P., 1970. Central North Atlantic plate motions over the last 40 million years. Science, 170, p 727 - 729.

Pinet, P. R., 1972. Diapir like features offshore Honduras: implications regarding tectonic evolution of Cayman Trough and Central America Geol. Soc. Am. Bull., 83, p 1911 - 1922.

Pitman, W. C. III, and Talwani, M. 1972. Sea floor spreading in the North Atlantic. Geol. Soc. Am. Bull., 83, p 619 - 646.

Press, F., 1970. Earth models consistent with geophysical data. Phys. Earth Planet. Interiors, 3, p 3 - 22.

Ramsay, A. T. S., 1968. A preliminary study of some Barbados Ridge cores. Maritime Sediments, 4, p 108 - 112.

Ramsay, J. G. 1967. Folding and fracturing of rocks. McGraw Hill New York, 568 pp.

Ringwood, A. E., 1970. Phase transformations and the constitution of the mantle. Phys. Earth Planet. Interiors, 3, p 109 - 155.

Ringwood, A. E. & Green, D. H., 1966. An experimental investigation of the gabbro-eclogite transformation and some geophysical implication. Tectonophysics, 3 (5), p 383 - 427.

Rod, E., 1956. Strike-slip faults of northern Venezuela. Am. Assoc. Petroleum Geologists Bull., 40, p 457 - 476.

Roden, R. B., and Mason, C. S. 1965. The correction of shipboard magnetic observations. Geophys. J. Roy. Astron. Soc. 9, p 9 - 13.

Rubey, W. W. and Hubbert, M. K., 1959. Role of fluid pressure in mechanics of overthrust faulting II. Geol. Soc. Am. Bull., 70, p 167 - 206.

Saunders, J. B., 1968. Fidd trip guide, Barbados. Caribbean Geol. Conf. Trans 4th, 1965, Port of Spain, Trinidad. p 443 - 449.

Saunders, J. B. and Cordey, W. G., 1968. The biostratigraphy of the Oceanic Formation in the Bath Cliff section, Barbados. Caribbean Geol. Conf. Trans. 4th, 1965. Port of Spain,Trinidad. p 170 - 182.

Scholl, D. W., Christensen, M. N., Von Huene, R. and Marlow, M. S., 1970. Peru Chile Trench. Sediments and sea-floor spreading. Bull geol. Soc. Am.., 81, p 1339 - 1360.

Scholl, D. W., von Huene, R. and Ridlon, J. B., 1968. Spreading of the ocean floor: undeformed sediments in the Peru- Chile Trench. Science, 159, p 869 - 871.

Scholl, D. W. and von Huene, R., 1970. Comments on paper by R. L. Chase and E. T. Bunce - underthrusting of the eastern margin of the Antilles by the floor of the western north Atlantic ocean and the origin of the Barbados Ridge. J. Geophys. Res., 75, p 488 - 490.

Senn, A. A., 1940. Palaeogene of Barbados and its bearing on the history and structure of the Antillean Caribbean region. Bull. Am. Assoc. Pet. Geol., 24, 1578 - 1610.

Seyfert, C. K., 1968. Undeformed sediments in oceanic trenches with seafloor spreading. Nature, 222, p 70.

Shor, G. G. Jr., 1963. "Refraction and reflection techniques and procedure". in The Sea 3 M. N. Hill, Ed., Interscience, New York, pp 20 - 38.

Skvor, V., 1969. The Caribbean area: a case of destruction and regeneration of a continent. Geol. Soc. Am. Bull., 80, p 961 - 968.

Smith, A. G., Briden, J. D. and Drewry, G. E., 1972. Phanerozoic world maps, in Palaeontology, Palaentological Association of London in press.

Smith, A. J., and Toksöz, M. N., 1972. Stress distribution beneath island arcs. Geophys. J. Roy. astr. Soc., 29, p 289 - 318.

Sykes, L. R., 1966. The seismicity and deep structure of island arcs, J. geophys. Res., 71, p 2981 - 3006.

Sykes, L. R. and Ewing, M., 1965. The seismicity of the Caribbean region. J. geophys. Res., 70, p 5065 - 5074.

Talwani, M., 1970. "Gravity" in the Sea A. E. Maxwell Ed. vol 4 pt I p 251 - 297. Interscience.

Talwani, M., Sutton, G. M. and Worzel, J. L., 1959. A crustal section across the Puerto Rico Trench. J. geophys. Res., 64, p 1545 - 1555.

Talwani, M., Windish, C. C. and Langseth, M. G., 1971. Reykjanes Ridge crest: A detailed geophysical study. J. geophys. Res., 76, p 473 - 517.

Toksöz, M. N., Minear, J. W. and Julian B. R., 1971. Temperature field and geophysical effects of a downgoing slab. J. geophys. Res., 76, p 1113 - 1138.

Tomblin, J. F., 1968. The volcanic history and petrology of the Soufriere region, St. Lucia. Trans. Fourth Caribbean Geology Conf., Port of Spain. 1965, p 367 - 376.

Tomblin, J. F., 1971. Seismicity and plate tectonics of the eastern Caribbean. Preprint of paper read at Sixth Caribbean Geoligical Conference, Margarite Island, Venezuela.

Tomblin, J. F., Sigurdsson, H. and Aspinall, W. 1972. Activity at the Soufriere Volcano, St. Vincent, West Indies, in October-November 1971. Nature, 235, p 157 - 158.

Tucker, D. G. and Gazey, B. K., 1966. Applied underwater acoustics, Pergamon Press Ltd. London. 244 p..

Turner, F. J., 1968. "Metamorphic Petrology: Mineralogical and Field Aspects." McGraw Hill New York 403 pp.

U. S. Geological Survey, 1972. International Decade of Ocean Exploration. Leg 4, 1971 Cruise, UNITEDGEOI. Regional gravity anomalies, Venezuela continental Border land. U. S. Geological Survey Open file report.

Vine, F. J. and Moores, E. M., 1972. A model for the gross structure petrology, and magnetic properties of oceanic crust. Mem. Geol. Soc. Am., 132, p 195 - 205.

Von Herzen, R. P., Simmons, G. and Folinsbee, A., 1970. Heat flow between the Caribbean Sea and the Mid-Atlantic Ridge. J. geophys. Res., 75, p 1973 - 1984.

Von Huene R., Scholl, D. W., and Ridlon, J. B., 1968. Submarine trenches and deformation. Science, 160, p 1024.

Weeks, L. A., Lattimore, R. K., Harbison, R. N., Bassinger, B. G., and Merrill, G. F., 1971. Structural relationships between Lesser Antilles, Venezuela, and Trinidad-Tobago. Am. Assoc. Petr. Geol. Bull., 55, p 1741 - 1752.

Westbrook, G. K., Bott, M. H. P. and Peacock, J. H., 1973. The Lesser Antilles subduction zone in the region of Barbados. Nature Physical Science, 244, p 18 - 20.

Wyllie, P. J., 1971. Role of water in Magma generation and indication of diapric uprises in the mantle. J. geophys. Res., 76, p 1328 - 1338.

Wyllie, P. J., 1973. Experimental Petrology and global tectonics. Tectonophysics, 17, p 189 - 209.

Wyss, M., 1970. Stress estimates for South American shallow and deep earthquakes. J. geophys. Res. 75, p 1529 - 1544.

Ties to gravity bases. Lesser Antilles April-May 1971

Place	Day	Base sta.	Quay base	Meter ht. ft	Gravity at mtr.	Eno	Z	Spr	Eff. Eno	Meter grav. difference
Bridgetown 12 bollard	104	978294.0	978294.4	1	978294.3	288	C	26	-212	0.0
Kingstown 11 bollard	114	978486.2	978490.6	1	978490.5	740	C	29	+240	199.92
	116					239	L	29	+239	
Castries Geest wharf	117	978528.2	978528.9	4	978528.5	635	L	29	+635	238.12
	117					595	C	30	+095	237.86
Kingstown 3bollard	122		978491.5	1	978491.4	760	C	29	+260	201.82
	123								"	
Bridgetown 28 bollard	126		978294.9	2	978294.7	326	C	26	-174	3.68
	132					835	C	25	+335	2.16
Kingstown 11 bollard	142		978490.6	1	978490.5	203	C	30	-297	199.74
	142								"	
Castries North wharf	146		978528.9	7	978528.2	581	C	30	+081	237.16

Meter: Askania Sea Gravimeter Gss-2 no. 18
1 spring turn = 537 units on the Enograph = 52.04 mgal.
Gravimeter is 7 ft 5 ins above the waterline and 10 ins below the bottom of the scuttle on 3 Deck, HMS HECLA.

Appendix 3.1

Summary of the seismic refraction data of Ewing and other (1957)

	Velocities					Thicknesses			
E6	1.5	(1.74)	2.73*	3.35*	6.17*	3.14	0.86	2.67	3.8
					6.88				5.09
E7	1.5	(1.72)	2.86	4.0	6.84	N1.72	1.24	1.57	4.8
						S2.09	0.95	1.98	2.72
E8	1.5	1.68	2.64	4.07	6.62	N2.12	1.06	2.12	3.12
						S1.58	0.27	1.70	1.96
E13	1.5	(1.7)	4.33	5.3		N1.1	1.3	3.48	
						S0.82	1.3	2.96	
E14	1.5	(1.7)	4.19	5.35		E1.54	1.48	3.2	
						W0.82	1.31	2.63	
E15	1.5	1.81*	2.5*	3.38*		0.73	0.78	2.18	
E16	1.5	(1.72)	2.22	3.21	4.27	N0.37	0.38	2.0	5.2
						S1.09	0.27	0.51	3.32
E17	1.5	(1.7)	2.58	6.74	8.32	E4.07	1.2	2.62	5.79
						W2.85	0.54	6.21	6.79
E18	1.51	(1.7)	2.23	6.64	8.09	N5.05	0.25	1.99	7.07
						S4.73	0.11	2.99	3.62
E19	1.5	(1.7) + 1.91	2.41	4.31	6.77	E2.37	2.38	2.87	3.1
						W2.01	0.67	5.37	3.92
E20	1.5	(1.7)	2.95*	/3.7/		N1.27	/5.63/	/2.23/	
						S2.10	0.87	2.23	
E21	1.5	(1.7) + 1.93	3.81	5.31		N2.19	3.48	4.7	
						S2.19	2.17	3.39	
E22	1.5	(1.7)	3.97	4.91	(6.74)	N1.1	1.07	2.56	
						S1.23	0.32	2.82	
E29	1.5	2.0	3.82	5.29	6.34 7.47	N2.93	0.66	2.05	1.94 5.64
						S2.93	1.37	2.88	2.69 8.7
B	1.5	1.71*	2.75*	3.38*		0.05	0.75	0.95	

Appendix B

In this appendix are computer drawn graphs of the bathymetry, magnetic anomaly, free-air gravity anomaly, and Bouguer gravity anomalies for 2.0 and 2.67 gm cm^{-3} measured along each of the major survey lines run by HMS HECLA east of the Lesser Antilles in 1971. The distances along the x axis are kilometres east of Longitude $62^{o}W$. On lines 17 and 19 the distances are north of $12^{o}N$.

DGL 39

DEPTH METRES (X10^{-2})

-100.13 -50.13 -.13 49.87 99.87 149.87 199.87 249.87 299.87 349.87 399.87

MAG. GAMMAS (X10^{-1})

180.00 -160.00 -140.00 -120.00 -100.00 -80.00 -60.00 -40.00 -20.00 -.00 20.00

F.A.A. MGAL (X10^{-1})

40.00 -30.00 -20.00 -10.00 .00 10.00 20.00 30.00 40.00 50.00 60.00

BA 2.0 MGAL (X10^{-1})

40.00 -30.00 -20.00 -10.00 .00 10.00 20.00 30.00 40.00 50.00 60.00

BA 2.67 MGAL (X10^{-1})

40.00 -30.00 -20.00 -10.00 .00 10.00 20.00 30.00 40.00 50.00 60.00

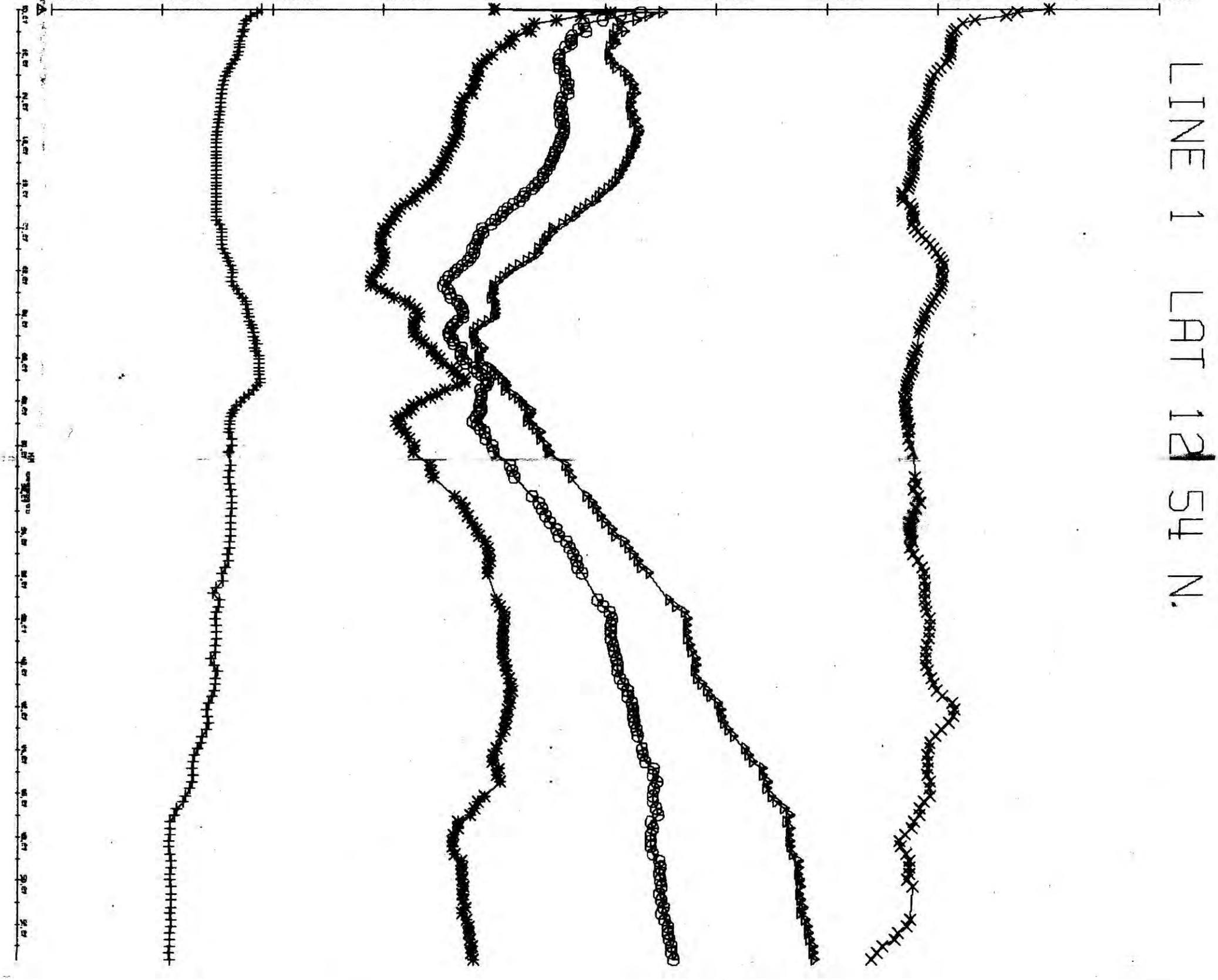

LINE 1 LAT 12 54 N.

LINE 2 LAT. 12 57 N
DEPTH METRES (X10-2)
-100.13 -50.13 -.13 49.87 99.87 149.87 199.87 249.87 299.87 349.87 399.87
MAG. GAMMAS (X10-1)
-180.00 -160.00 -140.00 -120.00 -100.00 -80.00 -60.00 -40.00 -20.00 -.00 20.00
F.A.A. MGAL (X10-1)
-40.00 -30.00 -20.00 -10.00 .00 10.00 20.00 30.00 40.00 50.00 60.00
BA 2.0 MGAL (X10-1)
-40.00 -30.00 -20.00 -10.00 .00 10.00 20.00 30.00 40.00 50.00 60.00
BA 2.67 MGAL (X10-1)
-40.00 -30.00 -20.00 -10.00 .00 10.00 20.00 30.00 40.00 50.00 60.00
DGL36

DGL36

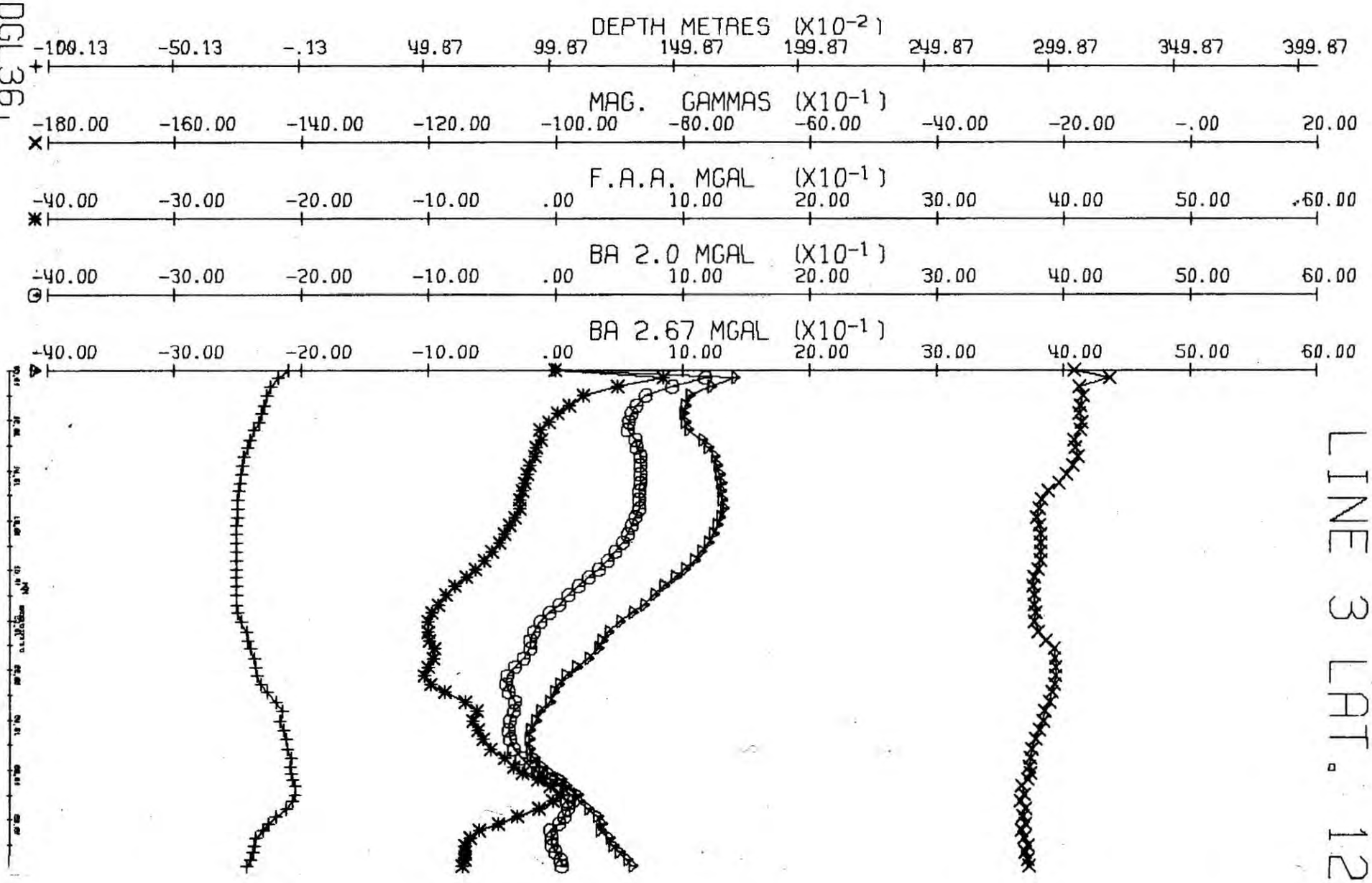

LINE 3 LAT. 12 59 N

DGL36

DEPTH METRES (X10^{-2})

-100.13 -50.13 -.13 49.87 99.87 149.87 199.87 249.87 299.87 349.87 399.87

MAG. GAMMAS (X10^{-1})

-180.00 -160.00 -140.00 -120.00 -100.00 -80.00 -60.00 -40.00 -20.00 -.00 20.00

F.A.A. MGAL (X10^{-1})

-40.00 -30.00 -20.00 -10.00 .00 10.00 20.00 30.00 40.00 50.00 60.00

BA 2.0 MGAL (X10^{-1})

-40.00 -30.00 -20.00 -10.00 .00 10.00 20.00 30.00 40.00 50.00 60.00

BA 2.67 MGAL (X10^{-1})

-40.00 -30.00 -20.00 -10.00 .00 10.00 20.00 30.00 40.00 50.00 60.00

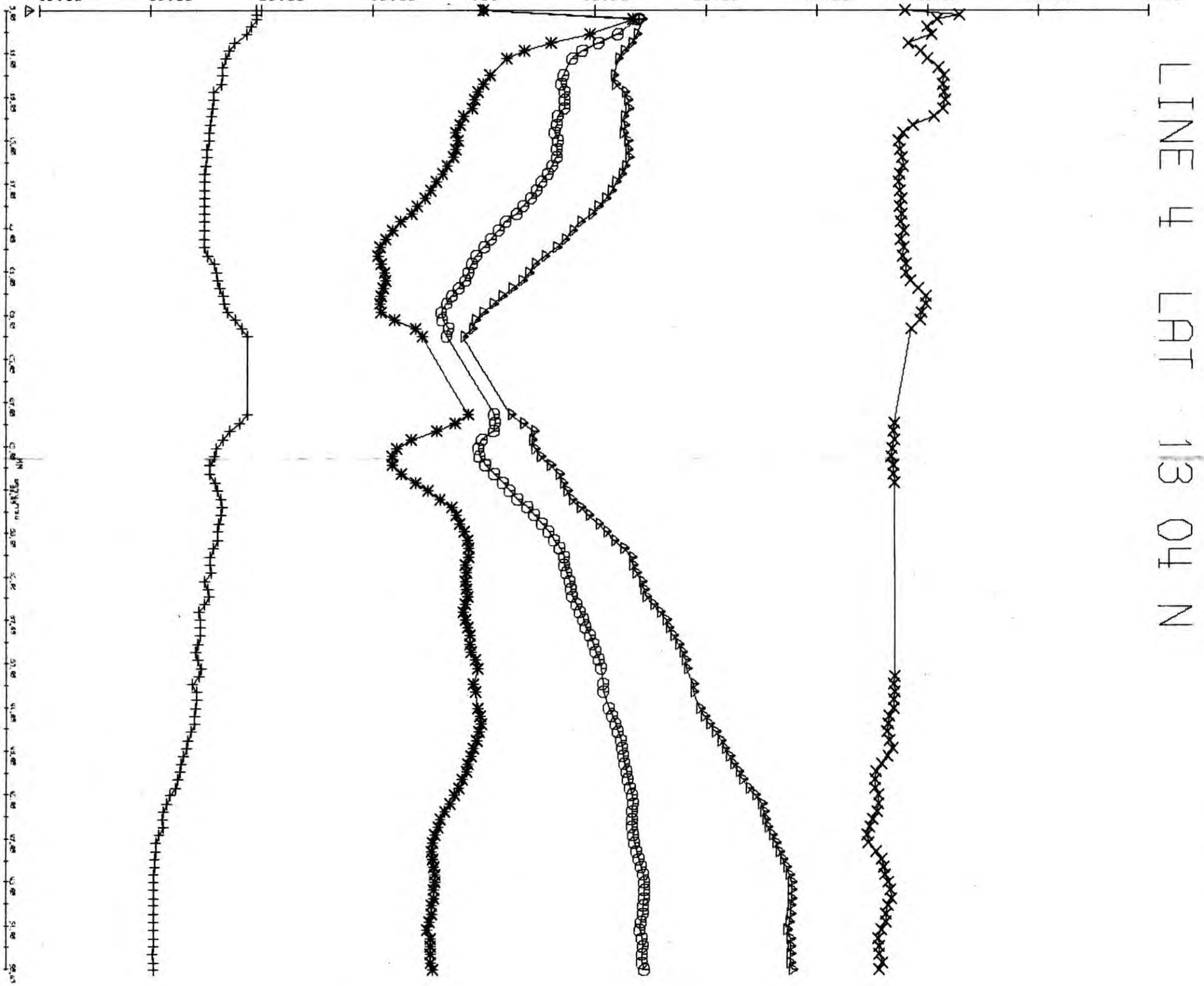

LINE 4 LAT 13 04 N

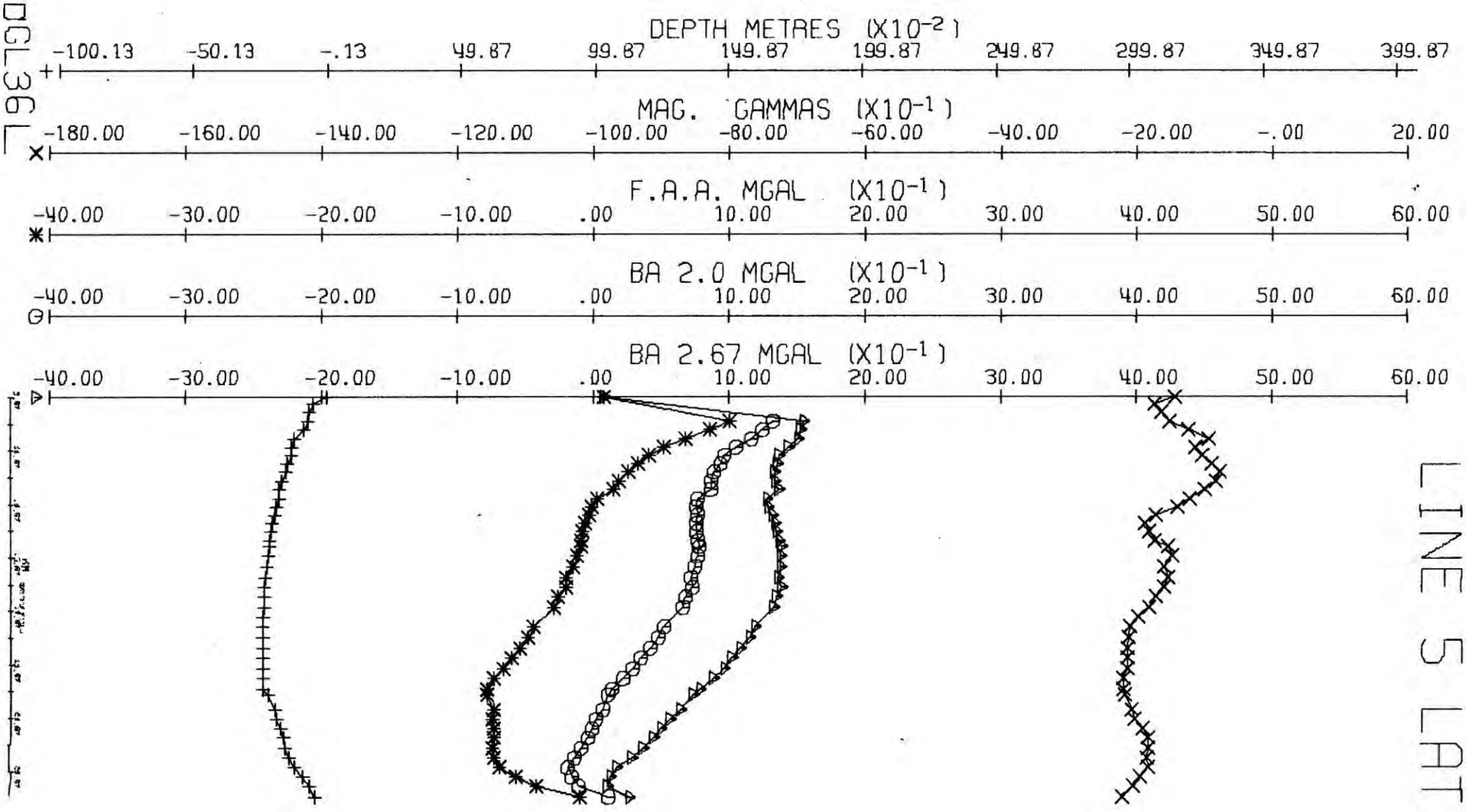

DGL36

LINE 5 LAT. 13 09 N

DGL36

DEPTH METRES (X10^{-2})
-100.13 -50.13 -.13 49.87 99.87 149.87 199.87 249.87 299.87 349.87 399.87

MAG. GAMMAS (X10^{-1})
-180.00 -160.00 -140.00 -120.00 -100.00 -80.00 -60.00 -40.00 -20.00 -.00 20.00

F.A.A. MGAL (X10^{-1})
-40.00 -30.00 -20.00 -10.00 .00 10.00 20.00 30.00 40.00 50.00 60.00

BA 2.0 MGAL (X10^{-1})
-40.00 -30.00 -20.00 -10.00 .00 10.00 20.00 30.00 40.00 50.00 60.00

BA 2.67 MGAL (X10^{-1})
-40.00 -30.00 -20.00 -10.00 .00 10.00 20.00 30.00 40.00 50.00 60.00

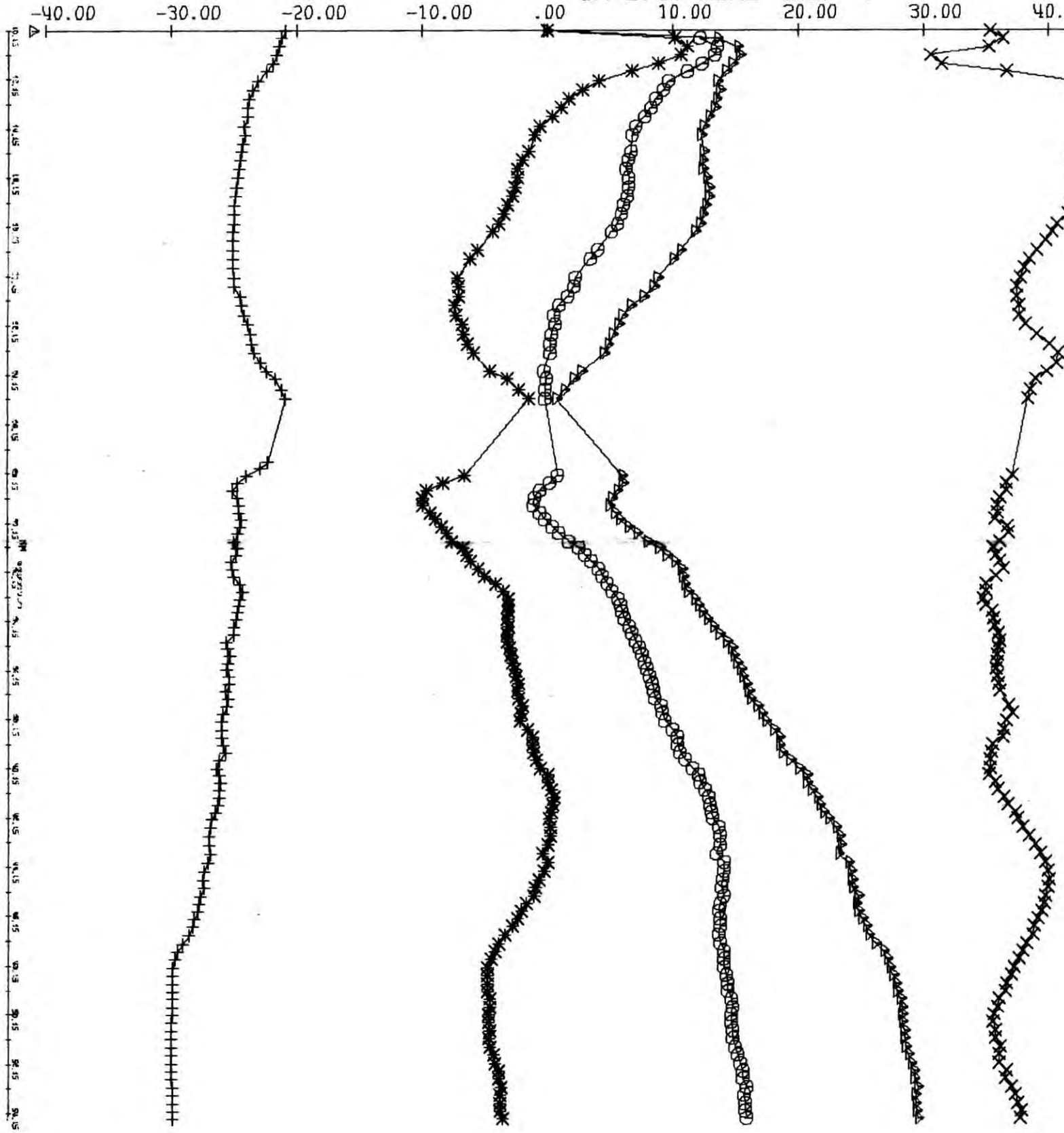

LINE 6 LAT. 13 14 N

LINE 7 LAT. 13 19 N

DGL361

DEPTH METRES ($X10^{-2}$)
-100.13 -50.13 -.13 49.87 99.87 149.87 199.87 249.87 299.87 349.87 399.87

MAG. GAMMAS ($X10^{-1}$)
-180.00 -160.00 -140.00 -120.00 -100.00 -80.00 -60.00 -40.00 -20.00 -.00 20.00

F.A.A. MGAL ($X10^{-1}$)
-40.00 -30.00 -20.00 -10.00 .00 10.00 20.00 30.00 40.00 50.00 60.00

BA 2.0 MGAL ($X10^{-1}$)
-40.00 -30.00 -20.00 -10.00 .00 10.00 20.00 30.00 40.00 50.00 60.00

BA 2.67 MGAL ($X10^{-1}$)
-40.00 -30.00 -20.00 -10.00 .00 10.00 20.00 30.00 40.00 50.00 60.00

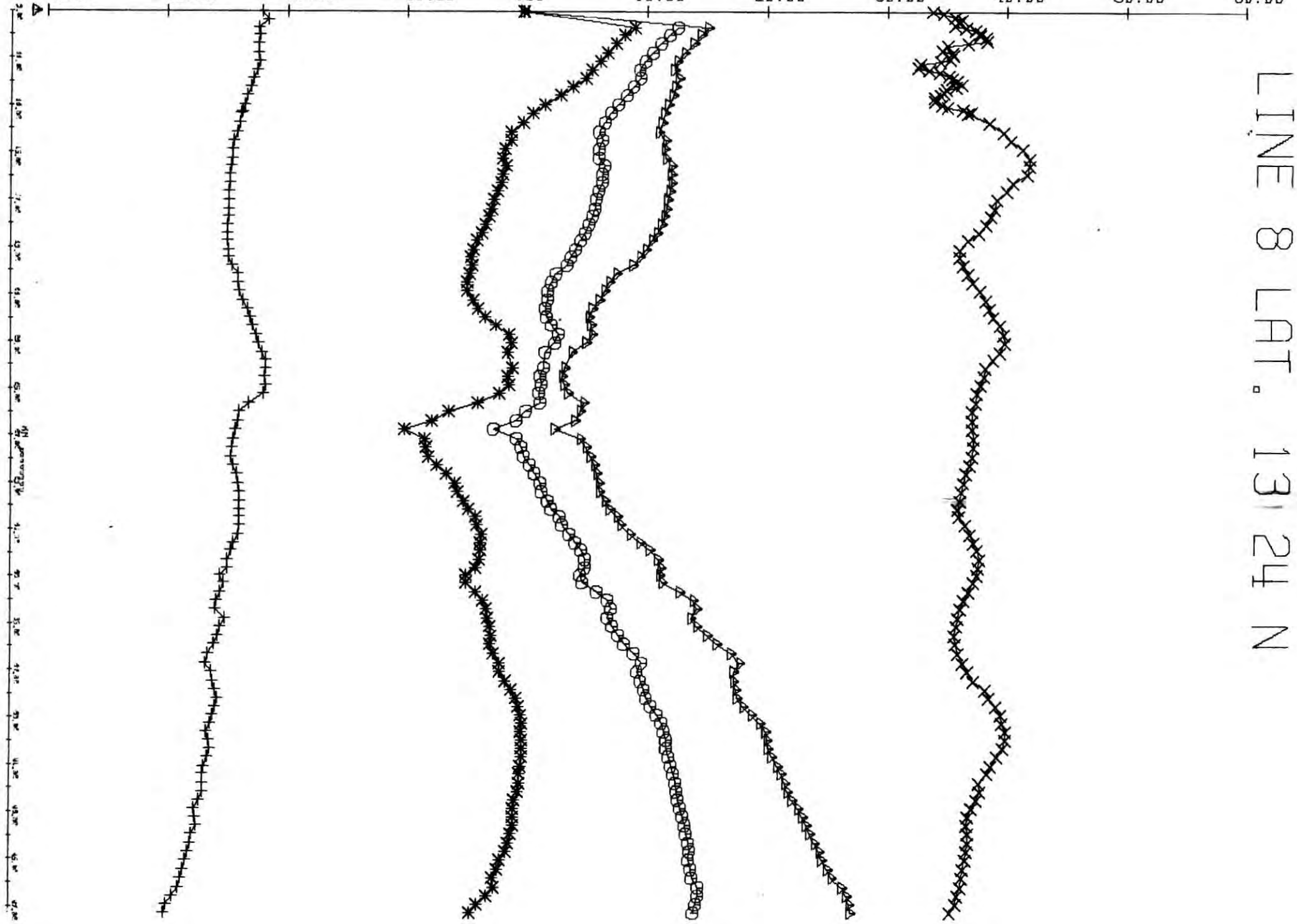

LINE 8 LAT. 13 24 N

DGL36

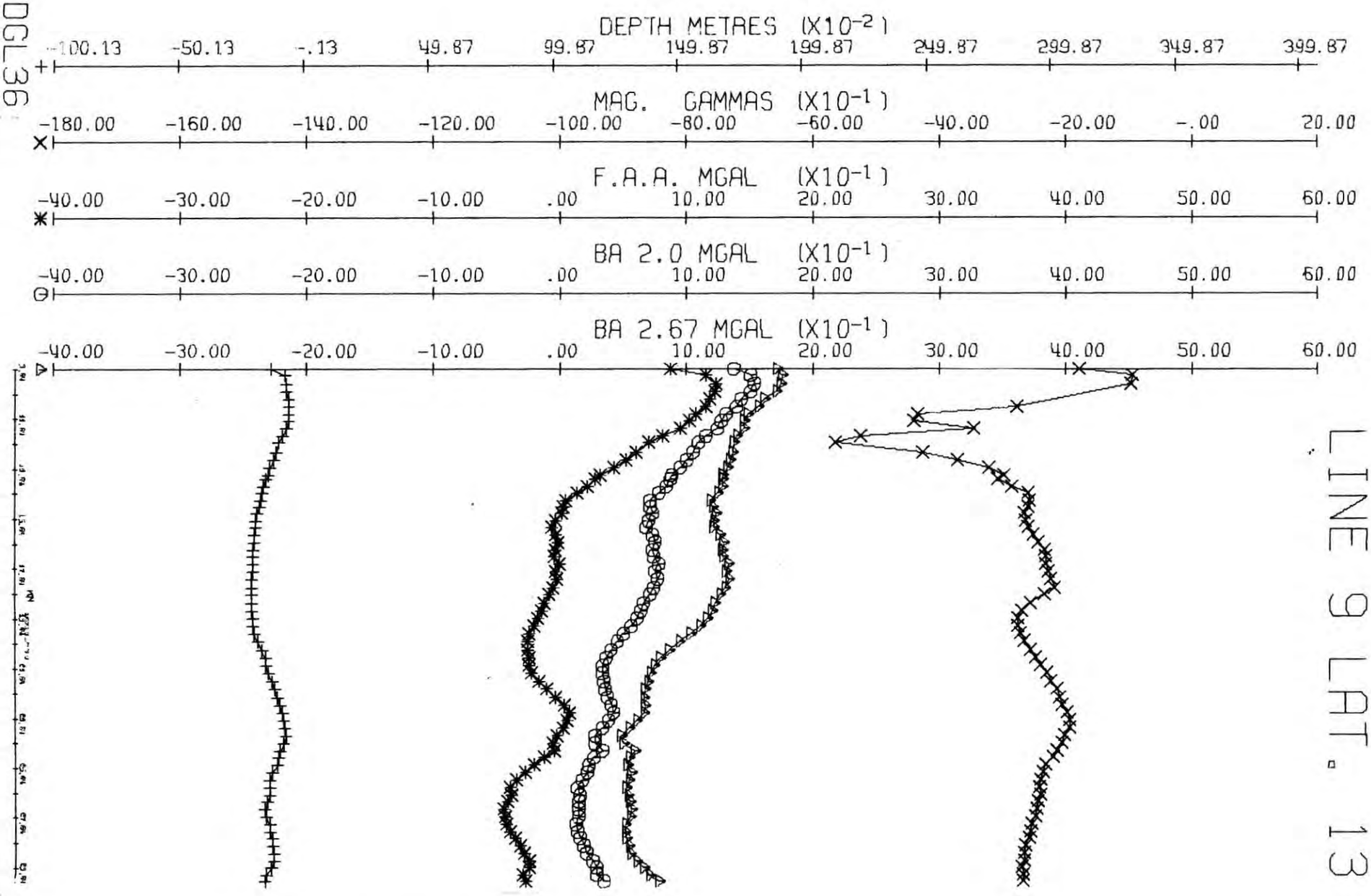

LINE 9 LAT. 13 29 N

DGL36_L

DEPTH METRES (X10^{-2})
-100.13 -50.13 -.13 49.87 99.87 149.87 199.87 249.87 299.87 349.87 399.87

MAG. GAMMAS (X10^{-1})
-180.00 -160.00 -140.00 -120.00 -100.00 -80.00 -60.00 -40.00 -20.00 -.00 20.00

F.A.A. MGAL (X10^{-1})
-40.00 -30.00 -20.00 -10.00 .00 10.00 20.00 30.00 40.00 50.00 60.00

BA 2.0 MGAL (X10^{-1})
-40.00 -30.00 -20.00 -10.00 .00 10.00 20.00 30.00 40.00 50.00 60.00

BA 2.67 MGAL (X10^{-1})
-40.00 -30.00 -20.00 -10.00 .00 10.00 20.00 30.00 40.00 50.00 60.00

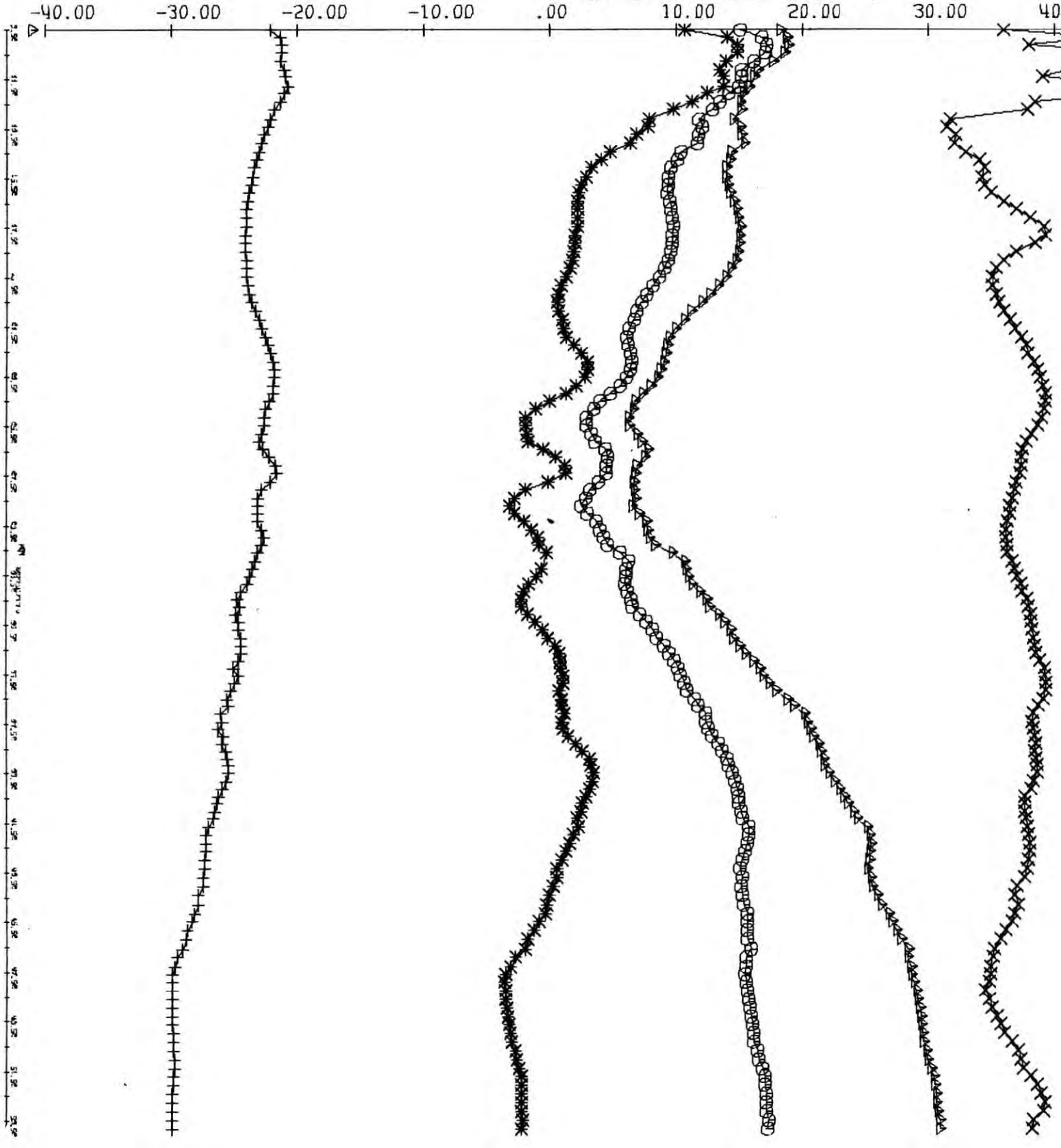

LINE 10 LAT. 13 34 N

LINE 11 LAT. 13 39 N

DGL36

DGL 361

DEPTH METRES (X10^{-2})
-100.13 -50.13 -.13 49.87 99.87 149.87 199.87 249.87 299.87 349.87 399.87

MAG. GAMMAS (X10^{-1})
-180.00 -160.00 -140.00 -120.00 -100.00 -80.00 -60.00 -40.00 -20.00 -.00 20.00

F.A.A. MGAL (X10^{-1})
-40.00 -30.00 -20.00 -10.00 .00 10.00 20.00 30.00 40.00 50.00 60.00

BA 2.0 MGAL (X10^{-1})
-40.00 -30.00 -20.00 -10.00 .00 10.00 20.00 30.00 40.00 50.00 60.00

BA 2.67 MGAL (X10^{-1})
-40.00 -30.00 -20.00 -10.00 .00 10.00 20.00 30.00 40.00 50.00 60.00

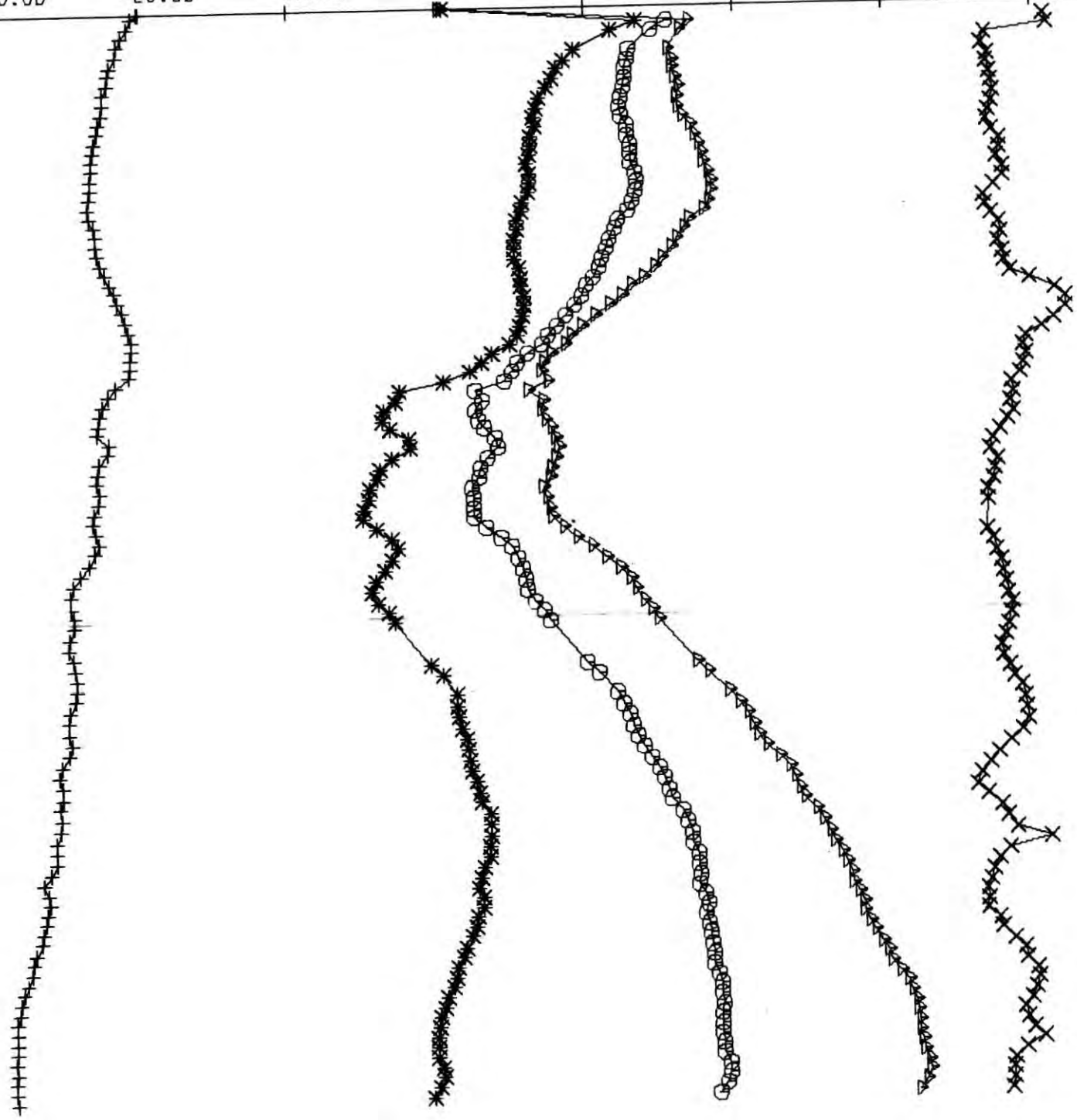

LINE 12 LAT. 13 HH N

DGL 39

DEPTH METRES (X10^{-2})
-100.13 -50.13 -.13 49.87 99.87 149.87 199.87 249.87 299.87 349.87 399.87

MAG. GAMMAS (X10^{-1})
-180.00 -160.00 -140.00 -120.00 -100.00 -80.00 -60.00 -40.00 -20.00 -.00 20.00

F.A.A. MGAL (X10^{-1})
-40.00 -30.00 -20.00 -10.00 .00 10.00 20.00 30.00 40.00 50.00 60.00

BA 2.0 MGAL (X10^{-1})
-40.00 -30.00 -20.00 -10.00 .00 10.00 20.00 30.00 40.00 50.00 60.00

BA 2.67 MGAL (X10^{-1})
-40.00 -30.00 -20.00 -10.00 .00 10.00 20.00 30.00 40.00 50.00 60.00

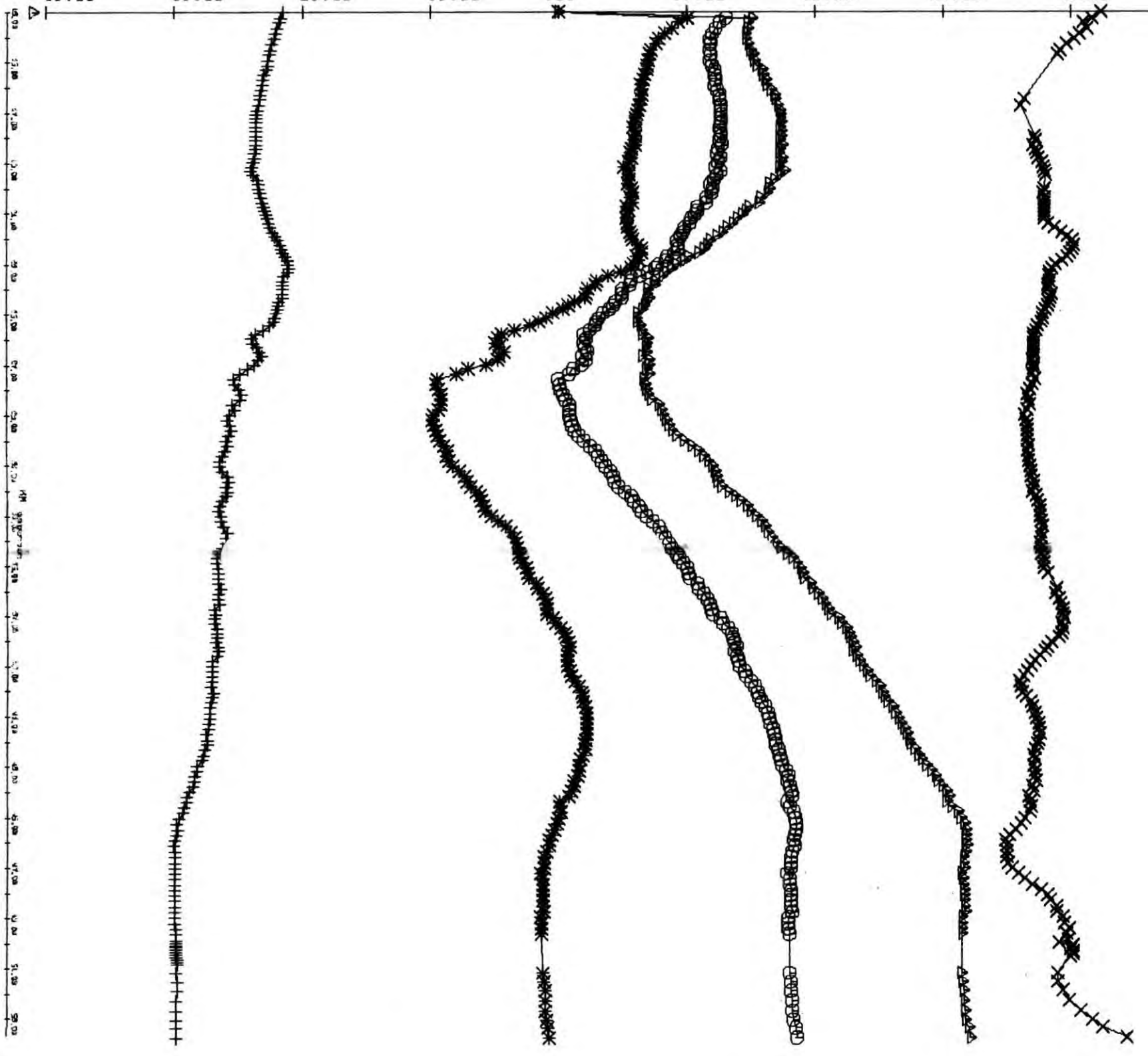

LINE 13 LAT. 13 49 N

DGL 36L

DEPTH METRES (X10^{-2})
-100.13 -50.13 -.13 49.87 99.87 149.87 199.87 249.87 299.87 349.87 399.87

MAG. GAMMAS (X10^{-1})
-180.00 -160.00 -140.00 -120.00 -100.00 -80.00 -60.00 -40.00 -20.00 -.00 20.00

F.A.A. MGAL (X10^{-1})
-40.00 -30.00 -20.00 -10.00 .00 10.00 20.00 30.00 40.00 50.00 60.00

BA 2.0 MGAL (X10^{-1})
-40.00 -30.00 -20.00 -10.00 .00 10.00 20.00 30.00 40.00 50.00 60.00

BA 2.67 MGAL (X10^{-1})
-40.00 -30.00 -20.00 -10.00 .00 10.00 20.00 30.00 40.00 50.00 60.00

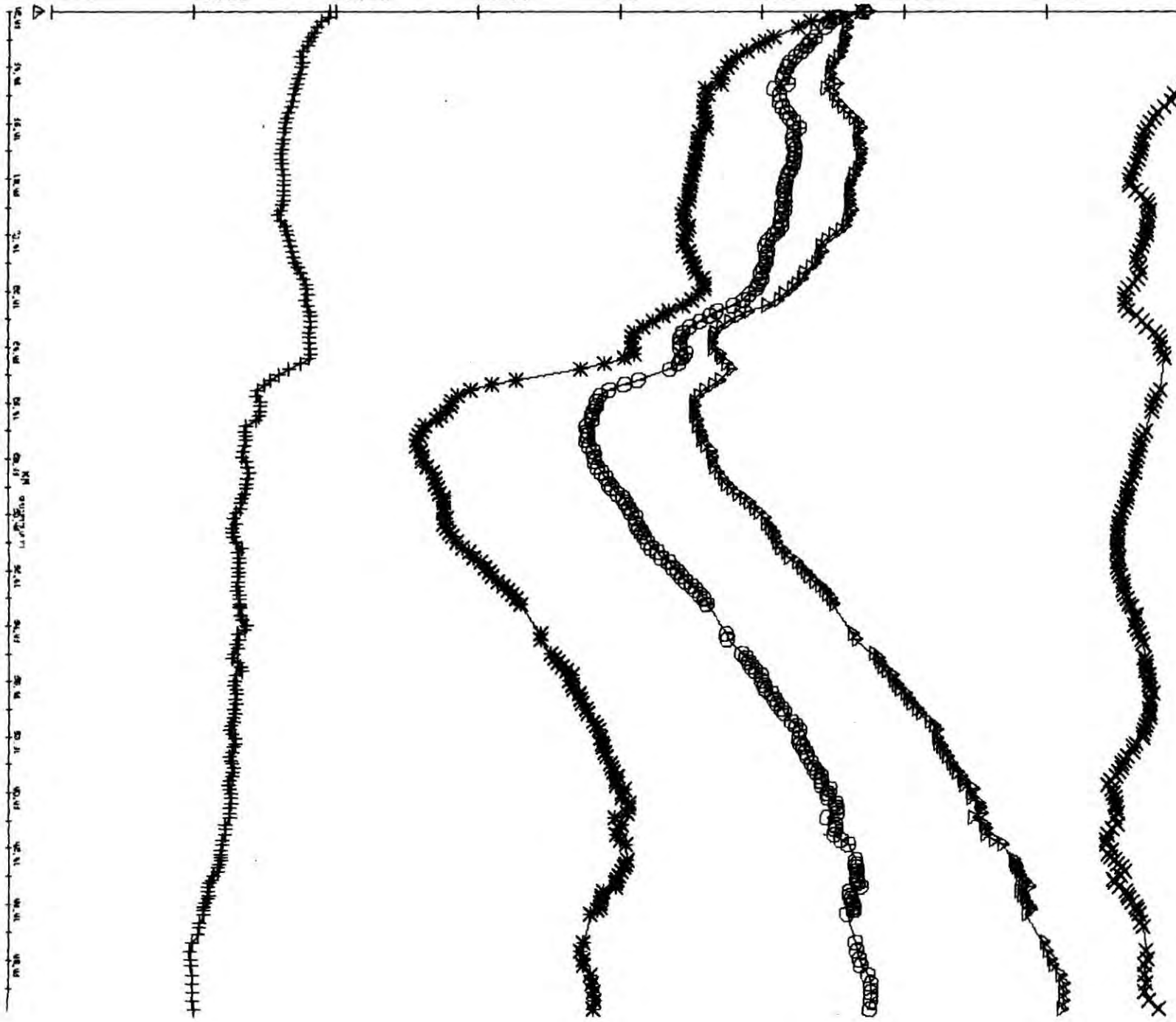

LINE 1H LAT. 13 54 N

DGL36-1

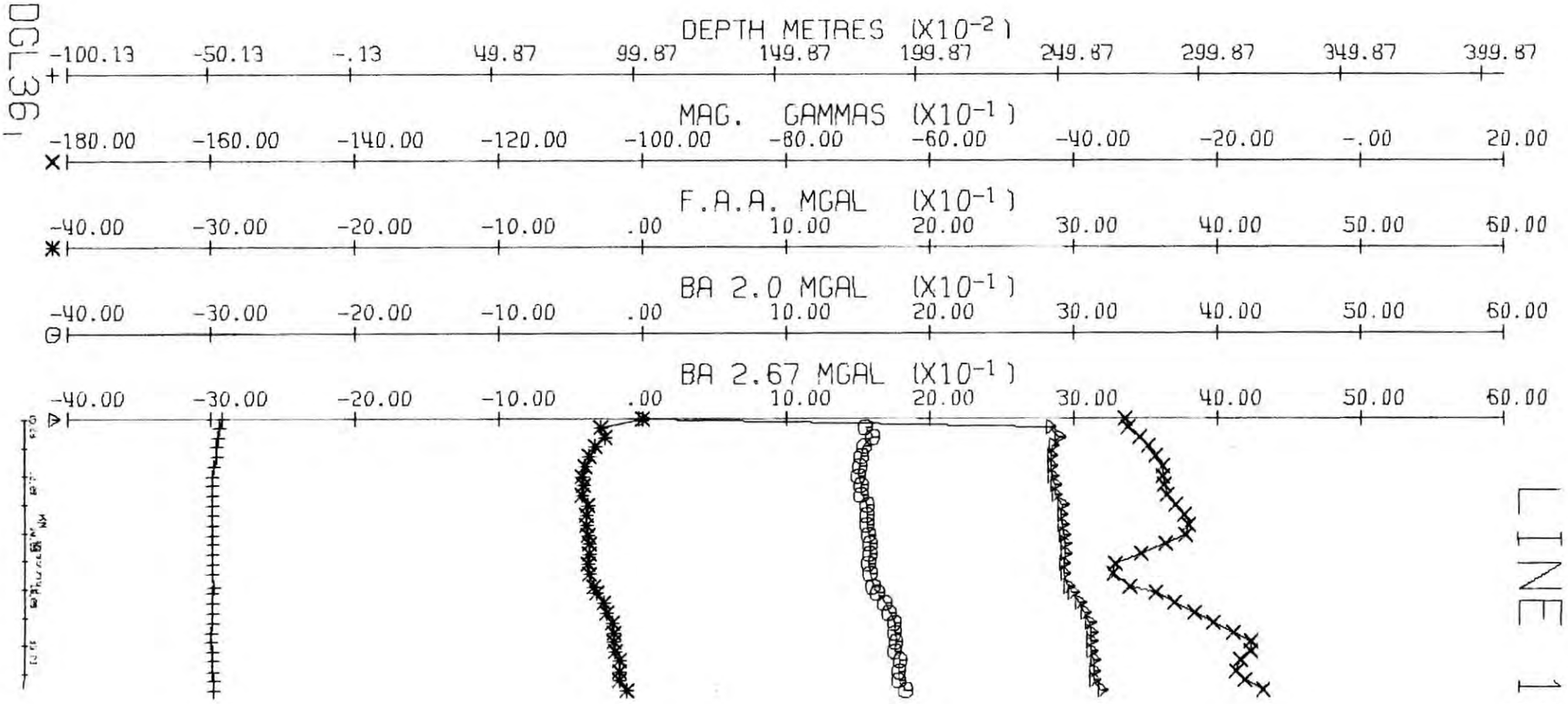

LINE 19 SOUTH TO NORTH AT LONG 57 W

DGL36

DEPTH METRES (X10^{-2})

-100.13 -50.13 -.13 49.87 99.87 149.87 199.87 249.87 299.87 349.87 399.87

MAG. GAMMAS (X10^{-1})

-180.00 -160.00 -140.00 -120.00 -100.00 -80.00 -60.00 -40.00 -20.00 -.00 20.00

F.A.A. MGAL (X10^{-1})

-40.00 -30.00 -20.00 -10.00 .00 10.00 20.00 30.00 40.00 50.00 60.00

BA 2.0 MGAL (X10^{-1})

-40.00 -30.00 -20.00 -10.00 .00 10.00 20.00 30.00 40.00 50.00 60.00

BA 2.67 MGAL (X10^{-1})

-40.00 -30.00 -20.00 -10.00 .00 10.00 20.00 30.00 40.00 50.00 60.00

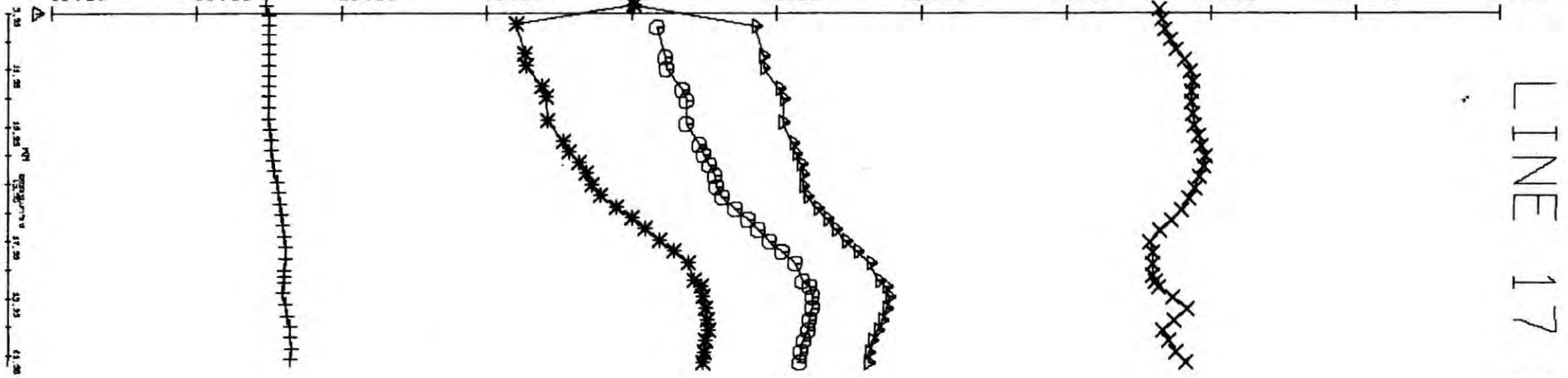

LINE 17 LONG 60 15 W

Appendix C

Computer program descriptions and listings

In this appendix are given descriptions and listings of most of the computer programs written to reduce and interpret the data considered in this thesis. They are presented so that the manner of derivation of quantities used in the interpretation may be checked if so desired. Not included are several short programs and those which perform operations that are straightforward but tedious to do manually. In this category are several plotting subroutines that are called by the programs listed. PLOTX and PLOTV are routines that will plot up to seven curves on one graph on the line printer. In PLOTX the curves all have the same Y axis. In PLOTV each curve has a different scale on the Y axis. GPLOTV performs a similar function to PLOTV, only the graph is plotted on the plotter. GPLOT draws the body shapes and observed and computed curves from two dimensional gravity and magnetic interpretation. Another program plots the output from the two dimensional averaging program. A subroutine that is used by several programs is SPLINE (obtained from P. J. Gunn) which is a monocubic interpolation routine that produces an array of regularly spaced values from irregularly spaced data. For use of the plotting routines in MTS on the NUMAC IBM 360/67 reference should be made to "A brief guide to some of the facilities available to produce plots on the Durham 1130 plotter under MTS" by P. Shelton.

The word program is used here in its shortened form to describe specifically a computer program. Programme is used in its normal sense as list of actions or items.

Appendix C2.1

A program written in PL1 to translate the paper tape output of the free air gravity reduction program MANGRA MK3 of the Hydrographic Branch of the Royal Navy.

Input:

Eight hole paper tape punched in HYTIP code.

Output:

Card images on FILE YY which must be assigned to a device when running the program. The following items are put out:-

IA Setting of Upper Spring on Askania Sea Gravimeter.

IB Reading on Enograph.

IC Zero setting on Enograph

D Distance run in ten minutes. i.e. between fixes.

IE Course over ten minutes.

IF Latitude: degrees.

G Latitude: minutes

R Eotvos correction.

S Measured gravity

T Free-air gravity anomaly

IU Time of fix.

FILE XX is a temporary storage file and must be assigned filespace when running the program.

```
/* GRAVITY TAPE TRANSLATOR.   TRANSLATES THE PAPER TAPE
  OUTPUT FROM THE GRAVITY REDUCTION PROGRAM MANGRA MK3
  OF THE HYDROGRAPHIC BRANCH OF THE NAVY.  PUTS OUT DATA
  IN FORM SUITABLE FOR CARDS ON FILE (YY).  FILE (XX) IS
  A TEMPORARY STORAGE FILE AND MUST BE ASSIGNED
  FILESPACE ON THE RUN CARD. */
WESTDEC:PROC OPTIONS(MAIN);
      DCL Y(0:255) CHAR(1) INIT (
  ' ',' ',' ',' ',' ',' ',' ',' ',' ',' ',' ',' ',' ','
                                          ',' ',' ',
  ' ',' ',' ',' ',' ',' ',' ',' ',' ',' ',' ',' ',' ','
                                          ',' ',' ',
 ' ',' ','"',' ',' ',' ',' ','''','(',' ',' ','+',' ','-
                                          ','.',' ',
  '0',' ',' ','3',' ','5','6',' ',' ','9',':',' ','<','
                                          ',' ','?',
  ' ','A','B',' ','D',' ',' ','G','H',' ',' ','K',' ','M
                                          ','N',' ',
  'P',' ',' ','S',' ','U','V',' ',' ','Y','Z',' ',' ','
                                          ',' ',' ',
  ' ',' ',' ',' ',' ',' ',' ',' ',' ',' ',' ',' ',' ','
                                          ',' ',' ',
  ' ',' ',' ',' ',' ',' ',' ',' ',' ',' ',' ',' ',' ','
                                          ',' ',' ',
  ' ',' ',' ',' ',' ',' ',' ',' ',' ',' ',' ',' ',' ','
                                          ',' ',' ',
  ' ',' ',' ',' ',' ',' ',' ',' ',' ',' ',' ',' ',' ','
                                          ',' ',' ',
  ' ',' ',' ','#',' ',' ','%','&',' ',' ',')','*',' ',',','
                                          ',' ','/',
  ' ','1','2',' ','4',' ',' ','7','8',' ',' ',':',' ','=
                                          ','>',' ',
  'D',' ',' ','C',' ','F','E',' ',' ','I','J',' ','L','
                                          ',' ','?',
  ' ','Q','R',' ','T',' ',' ','W','X',' ',' ','(',' ',')
                                          ',' ',' ',
  ' ',' ',' ',' ',' ',' ',' ',' ',' ',' ',' ',' ',' ','
                                          ',' ',' ',
  ' ',' ',' ',' ',' ',' ',' ',' ',' ',' ',' ',' ',' ','
                                          ',' ',' ') ;
DCL B BIT(1) INIT ('0'B);
   DCL XX FILE STREAM, CARD  CHAR(80), CH CHAR(1);
DCL YY FILE OUTPUT STREAM,WRD CHAR(1);
     ON ENDFILE (SCARDS) GOTO P;
    CARD=' ':
     K=1;
   L1:GET EDIT (CH)(A(1));
     IN = UNSPEC(CH):
   SUBSTR(CARD,K,1)=Y(IN);
   K=K+1:
   IF K>80 THEN DO;
     PUT FILE(XX) EDIT(CARD)(A(80)); K=1;
          CARD=' ':      END:
   GOTO L1;
P:CLOSE FILE(XX):
OPEN FILE(XX) INPUT;
R1:GET FILE(XX) EDIT (WRD) (A(1));
IF WRD ¬= 'T' THEN GO TO R1;
GET FILE(XX) EDIT (WRD) (A(1));
```

```
IF WRD ¬= 'I' THEN GO TO R1;
GET FILE(XX) EDIT (WRD) (A(1));
IF WRD ¬= 'M' THEN GO TO R1;
GET FILE(XX) EDIT (WRD) (A(1));
IF WRD ¬= 'E' THEN GO TO R1;
H:GET FILE(XX) LIST (IA,IB,IC,D,IE,IF,G,R,S,T,IU);
ON ENDFILE (SYSIN) GO TO Z ;
PUT FILE(YY) EDIT (IA,IB,IC,D,IE,IF,G,R,S,T,IU) (SKIP,F(2)
                                                 ,X(2),F(3),
X(2),F(4),X(2),F(3,1),X(2),F(3),X(2),F(2),X(1),F(6,2),X(2)
                                                 ,F(5,1),X(2)
,F(3,1),X(2),F(4,1),X(2),F(4));
GO TO H;
Z:END;
```

Appendix C2.2

Data Reduction Programs

A. Input Program. Written in FORTRAM IV, this program accepts data and organises it into a form ready for calculation of the Bouguer anomaly. This is to be followed by a run of GRAVN and a run of the output program (B). The input for the program, as formatted, is designed to take the output of a data program which gives the magnetic anomaly (C) uncorrected for diurnal variations. The data should be presented as survey lines.

Input:

Read on 5 from cards or any other file.

NAME	Identification.
OFFSET	Difference between meter gravity and true gravity at start of line as estimated from drift between base stations.
HDDRIF	Meter drift in half a day.
DC	Density contrast for Bouguer correction

Output of gravity tape translator

AG	Free air gravity value.
JTIM(K)	Time of Kth gravity value. If JTIM(K) = 2500 the program stops reading gravity values. If JTIM(K) = 2400 the program inputs new values of OFFSET and HDDRIF.

Output of (C)

ITIM	Time of fix.
LATDEG	Latitude: degrees.
ATMIN	Latitude: minutes.
LONDEG	Longitude: degrees.
ONMIN	Longitude: minutes

DISTE Distance east in km on arbitary grid system.

DISTN Distance north in km on arbitary grid system.

IBATH Bathymetry in metres.

MAG Total intensity magnetic field.

MANOM Total intensity magnetic anomaly.

Output:

Written on 8 the data items taken in form (C).

Written on 9 to be read by GRAVN:-

DIST(K) Distance along line to Kth point.

DEPTH Depth below Kth point in km.

DC Density Contrast.

NO Number of station points, at which Bouguer anomaly is calculated.

In defining the seabed for calculation of the Bouguer anomaly it may be necessary to include a few points a great distance from the end of the line, with one at the sea surface. These should be entered with the output from (C) in the same format. They will not be used for station points, because they will have no gravity values associated with them.

Note that in this program distance to points are taken directly from easterly distances, because the program as listed was used only for east west lines. The statement which assigns this value can easily be changed to use northerly values for north-south lines or both east and north for lines with different courses.

eg. DIST(K) = SQRT ((DISTE - SDE)**2 + (DISTN - SDN)**2)

where SDE and SDN are the values of DISTE and DISTN on the first point

of the line, and are assigned before statement no 11.

B Output Program. Written in FORTRAN IV, this program combines the outputs of (A) and GRAVN and produces a data card for each point along the survey line, which contains the values for all the parameters measured or calculated.

Input:

Read in on 3:-

NO	The number of free-air gravity values.
FAG(I)	The Ith free-air gravity value.

Read in on 7:-

DISTG	Distance to a point for which the Bouguer gravity correction has been calculated.
BOUG	The Bouguer gravity correction.

Read in on 8 is the output of (A) on 8.

Output:

Written on 6:-

ITIM	Time of fix.
LATDEG	Latitude: degrees.
ATMIN	Latitude: minutes
LONDEG	Longitude: degrees.
ONMIN	Longitude: minutes
DISTE	Distance east in km.
DISTN	Distance north in km.
IBATH	Bathymetry in metres.
MAG	Total intensity magnetic field.

MANOM	Total intensity magnetic anomaly.
FAG(K)	Free-air gravity anomaly.
GRAV	Bouguer gravity anomaly.

Written on 4 are the same items as on 6, but without headings and spaced suitably for putting on cards.

A note on GRAVN. Slight alterations are necessary to use this program to calculate the Bouguer correction. The array sizes will probably need to be increased. UNITS needs to be set permanently to KM within the program. An output file needs to be created to put out the values of distance and correction in F(8,3) and F(8,2) respectively.

```
C       INPUT PROGRAM FOR DATA CARDS.
C       NAME = IDENTIFYING CHARACTERS.  OFFSET = DIFFERENCE IN
C       VALUE AT BEGINNING OF DAY BETWEEN METER GRAVITY AND
C       GRAVITY EXPECTED FROM BASE STATIONS.  HDDRIF = AMOUNT
C       OF DRIFT IN HALF A DAY.  DC = DENSITY CONTRAST FOR BOU
C
C       GUER CORRECTION.  AG = FREE AIR GRAVITY ON NAVY TAPE.
C       JTIM(K) = TIME OF KTH VALUE ON NAVY TAPE.  ITIM = TIME
C       ON POSITION CARD.  LATDEG & ATMIN = LATITUDE IN DEGREE
C       S AND MINUTES.  LONDEG & ONMIN = LONGITUDE IN DEGREES
C       AND MINUTES.  DISTE = DISTANCE EAST OF 42 W IN KM.
C       DISTN = DISTANCE NORTH OF 12 N IN KM.  IBATH = BATHYME
C       TRY IN METRES.  MAG = MEASURED MAGNETIC FIELD.  ANOM
C       = MAGNETIC ANOMALY
        DIMENSION DIST(300),FAG(300),JTIM(300),NAME(6)
        READ(5,2) NAME,OFFSET,HDDRIF,DC
      2 FORMAT(6A4,1X,F5.0,1X,F5.0,1X,F5.0)
        COR=OFFSET
        K=1
      3 K=K+1
        READ(5,4) AG,JTIM(K)
      4 FORMAT(53X,F6.1,2X,I4)
        IF(JTIM(K).EQ.2500) GO TO 7
        IF(JTIM(K).EQ.2400) GO TO 9
        FAG(K)=AG+COR
        IF(JTIM(K).EQ.2350) COR=COR-HDDRIF
        IF(JTIM(K).EQ.1150) COR=COR-HDDRIF
        GO TO 3
      9 READ(5,91) OFFSET,HDDRIF
     91 FORMAT(F5.0,F5.0)
        COR=OFFSET
        K=K-1
        GO TO 3
      7 K=1
        READ(5,8) ITIM,LATDEG,ATMIN,LONDEG,ONMIN,DISTE,DISTN,I
                                                  BATH,MAG,
       1MANOM
      8 FORMAT(I4,1X,I2,1X,F4.1,1X,I2,1X,F4.1,1X,F5.1,1X,F6.1,
                                                  1X,I4,1X,
       1I5,1X,I4)
        WRITE(8,8) ITIM,LATDEG,ATMIN,LONDEG,ONMIN,DISTE,DISTN,
                                                  IBATH,MAG,
       1MANOM
        BATH=IBATH
        DEPTH=BATH/1000.
        DIST(K)=DISTE
        WRITE(9,10) NAME,DIST(K),DEPTH,DC
     10 FORMAT(6A4,'     :  ',F6.1,1X,F6.3,1X,F4.2,1X)
     11 K=K+1
     12 READ(5,8) ITIM,LATDEG,ATMIN,LONDEG,ONMIN,DISTE,DISTN,I
                                                  BATH,MAG,
       1MANOM
        BATH=IBATH
        DEPTH=BATH/1000.
        DIST(K)=DISTE
        IF(ITIM-2500)17,15,17
     17 WRITE(8,8) ITIM,LATDEG,ATMIN,LONDEG,ONMIN,DISTE,DISTN,
                                                  IBATH,MAG,
       1MANOM
```

```
      IF(JTIM(K)-TTIM)30,13,30
   13 WRITE(9,14) DIST(K),DEPTH,DC
   14 FORMAT(1H ,F6.1,1X,F6.3,1X,F4.2,1X)
      GO TO 11
   30 WRITE(9,14) DIST(K),DEPTH,DC
      GO TO 12
   15 WRITE(9,16) DIST(K),DEPTH
   16 FORMAT(1H ,F6.1,1X,F6.3,1X,'5.0  0',1X)
      K=K-1
      WRITE(3,18) (DIST(I),I=2,K)
   18 FORMAT(6(1X,F6.1,1X, '0.0 '))
      WRITE(9,20) DIST(K)
   20 FORMAT(1H ,F6.1,1X,'1000000 '/' 0')
      WRITE(3,50)
   50 FORMAT('  0  ')
      NO=K-1
      WRITE(3,19) NO
   19 FORMAT(I3/)
      WRITE(3,22) (FAG(I),I=2,K)
   22 FORMAT(10(F4.1))
      END
```

```
C       OUTPUT PROGRAM FOR DATA CARDS.
C       INPUT ON 3: NO = NO. OF FREE AIR GRAVITY VALUES
C       FAG(I) = ITH FREE AIR GRAVITY VALUE.
C       INPUT ON 7: DISTG= DISTANCE ALONG LINE TO GRAVITY POIN
C       .    BOUG = BOUGUER CORRECTION.
C       INPUT ON 8:  ITIM = TIME.  LATDEG & ATMIN = LATITUDE
C       IN DEGREES AND MINUTES.  LONDEG & ONMIN = LONGITUDE IN
C       DEGREES AND MINUTES.  DISTE = DISTANCE EAST OF LONG.
C       52 W IN KM.  DISTN = DISTANCE NORTH LAT. 12 N IN KM.
C       IBATH = BATHYMETRY IN METRES.  MAG = MEASURED MAGNETIC
C       VALUE.  MANOM = MAGNETIC ANOMALY.
        DIMENSION FAG(300)
        READ(3,2) NO
      2 FORMAT(I3)
        READ(3,3) (FAG(I),I=1,NO)
      3 FORMAT(10(F6.1))
        WRITE(6,5)
      5 FORMAT(1H1,'TIME LAT      LONG     KMEAST KMNOR  BATH AB
                                                 MAG  M.ANOM

     1F.A.G.  B.GRAV'/)
        READ(7,6) DISTG,BOUG
        DO 30 K=1,NO
     11 READ(8,4) ITIM,LATDEG,ATMIN,LONDEG,ONMIN,DISTE,DISTN,I
                                                 BATH,MAG,

     1 MANOM
      4 FORMAT(I4,1X,I2,1X,F4.1,1X,I2,1X,F4.1,1X,F6.1,1X,F6.1,
                                                 1X,I4,1X,

     1IF,1X,I6)
        READ(7,6) DISTG,BOUG
      6 FORMAT(F8.3,F8.2)
      7 IF(DISTG-DISTE) 9,10,8
      8 WRITE(4,4) ITIM,LATDEG,ATMIN,LONDEG,ONMIN,DISTE,DISTN,
                                                 IBATH,MAG,

     1MANOM
        WRITE(6,40) ITIM,LATDEG,ATMIN,LONDEG,ONMIN,DISTE,DISTN
                                                 ,IBATH,MAG,

     1MANOM
     40 FORMAT(1H ,I4,1X,I2,1X,F4.1,1X,I2,1X,F4.1,1X,F6.1,1X,F
                                                 6.1,1X,I4,1X

     1,I5,1X,I6)
        READ(8,4) ITIM,LATDEG,ATMIN,LONDEG,ONMIN,DISTE,DISTN,I
                                                 BATH,MAG,

     1MANOM
        GO TO 7
      9 READ(7,6) DISTG,BOUG
        GO TO 7
     10 GRAV=FAG(K)+BOUG
        WRITE(6,20) ITIM,LATDEG,ATMIN,LONDEG,ONMIN,DISTE,DISTN
                                                 ,IBATH,MAG,

     1 MANOM,FAG(K),GRAV
     20 FORMAT(1H ,I4,1X,I2,1X,F4.1,1X,I2,1X,F4.1,1X,F6.1,1X,F
                                                 6.1,1X,I4,

     11X,I5,1X,I6,1X,F6.1,1X,F6.1)
        WRITE(4,22) ITIM,LATDEG,ATMIN,LONDEG,ONMIN,DISTE,DISTN
                                                 ,IBATH,MAG,

     1MANOM,FAG(K),GRAV
     22 FORMAT(I4,1X,I2,1X,F4.1,1X,I2,1X,F4.1,1X,F6.1,1X,F6.1,
                                                 1X,I4,1X,

     1I6,1X,I6,1X,F6.1,1X,F6.1)
```

```
   5 CONTINUE
  80 STOP
     END
```

C Simple Magnetic Program. Written in FORTRAN IV, this program reads cards containing the latitude and longitude of each data point, the bathymetry and the total intensity magnetic field. It puts out the magnetic anomaly, calculated using REGMAG, and the position of the data point on a kilometric grid in longitude 61° W and latitude 12°N are the baselines for eastings and northings. Data should be fed in as days.

Input:

Read in on 5:-

IDAY	The scientific day no. (on separate card).
ITIM	The time of fix.
LATDEG	Latitude: degrees.
ATMIN	Latitude: minutes.
LONDEG	Longitude: degrees.
ONMIN	Longitude: minutes.
IBATH	Bathymetry in metres.
MAG	Total intensity magnetic field.

Output:

Written on 6 (Line printer) and 9 (Punch cards or any other file):-

ITIM

LATDEG

ATMIN

LONDEG

ONMIN

DISTE	Distance east of 61°W in km.
DISTN	Distance north of 12°N in km.
MAG	
ANOM	Predicted value of Earth's field at fix.
MANOM	Total field magnetic anomaly.

ANOM is not put out on 9. This program should be run with the subroutine REGMAG.

```
C       ORIGINAL MAGNETIC ANOMALY PROGRAM.
C       IDAY = DAY NO..  ITIM = TIME.  LATDEG & ATMIN = LATITU
C       DE IN DEGREES AND MINUTES.  LONDEG & ONMIN = LONGITUDE
C       IN DEGREES AND MINUTES.  IBATH = BATHYMETRY IN METRES.
C       MAG = MEASURED MAGNETIC VALUE.
      1 READ(5,2)IDAY
      2 FORMAT(3X,I3)
        WRITE(6,21) IDAY
     21 FORMAT(1H1,'DAY',I3)
        WRITE(6,22)
     22 FORMAT(1H ,'TIME',2X,'LATDE',4X,'LONGDE',3X,'KMEAST',2
                                              X,'KMNORT',
       12X,'MAGVAL',2X,'EARTHF',2X,'RESID')
        DAY=IDAY
        DATE=1971+DAY/365
      3 READ(5,4) ITIM,LATDEG,ATMIN,LONDEG,ONMIN,IBATH,MAG
      4 FORMAT(I4,2X,I2,1X,F4.0,2X,I2,1X,F4.0,2X,I4,2X,I4)
        IF(2500-ITIM)20,1,5
      5 YLAT=LATDEG+ATMIN/60
        YLON=-(LONDEG+ONMIN/60)
        CALL REGMAG(YLAT,YLON,DATE,ANOM)
        DISTE=(62+YLON)*COS(YLAT*0.01745)*6.08*0.3048*60.
        DISTN=(YLAT-12)*6.08*0.3048*60.
        IF(MAG.EQ.0.) GO TO 15
        MAG=MAG+10
        MANOM=MAG-ANOM
        WRITE(6,10) ITIM,LATDEG,ATMIN,LONDEG,ONMIN,DISTE,DISTN
                                              ,MAG,ANOM,
       1MANOM
     10 FORMAT(1H ,I4,2X,I2,1X,F4.1,2X,I2,1X,F4.1,2X,F6.1,2X,F
                                              6.1,2X,I5,
       13X,F6.0,2X,I6)
        WRITE(9,11) ITIM,LATDEG,ATMIN,LONDEG,ONMIN,DISTE,DISTN
                                              ,IBATH,MAG,
       1MANOM
     11 FORMAT(I4,1X,I2,1X,F4.1,1X,I2,1X,F4.1,1X,F6.1,1X,F6.1,
                                              1X,I4,
       11X,I5,1X,I6)
        GO TO 3
     15 WRITE(6,16) ITIM,LATDEG,ATMIN,LONDEG,ONMIN,DISTE,DISTN
                                              ,ANOM
     16 FORMAT(1H ,I4,2X,I2,1X,F4.1,2X,I2,1X,F4.1,2X,F4.1,2X,F
                                              6.1,2X,'*****
       1**',2X,F6.0,2X,'*******')
        WRITE(9,18) ITIM,LATDEG,ATMIN,LONDEG,ONMIN,DISTE,DISTN
                                              ,IBATH
     18 FORMAT(I4,1X,I2,1X,F4.1,1X,I2,1X,F4.1,1X,F4.1,1X,F4.1,
                                              1X,I4)
        GO TO 3
     20 CALL EXIT
        END
```

Appendix C2.3

A program written in FORTRAN IV to do low pass filtering using a SINC function window. Window length is ten times the cutoff frequency The filtered function produced ends half the window length from each end of the record, unless the record is artificially extended by that amount. As listed the program is adapted to filter long wavelength anomalies and distances are divided by 10 in the statement following statement no. 4. Input data need not be evenly spaced.

Input:

Read on 5:-

TITLE	Up to 40 identifying characters.
XD(I)	Distance to Ith data point. If XD(I) is less than -9000 data input ends.
YV	The value of the function to be filtered.
VV	The value of another function which may be used to modify YV.
F	Cutoff frequency.

Output:

Written on 6:-

O(I)	Ith filter parameter.
SIM	Value of integration along filtered record.

The record, the filtered record, and the residuals are plotted on the lineprinter by PLOTX, and on the plotter by GPLOTV. The program must be run with subroutine SPLINE.

```
C      A PROGRAM TO DO LOW PASS FILTERING.
C      TITLE IS A NAME OF UP TO 40 CHARACTERS:  XD IS AN ARRA
                                               Y HOLDING
C      THE X VALUES OF THE INPUT DATA : YV IS THE VALUE OF TH
                                               E VARIABLE
C      AT EACH POINT: VV IS THE VALUE OF ANOTHER VARIABLE OR
                                               CONSTANT
C      USED TO MODIFY YV IN ANY RELATION SHIP WHICH MAY BE WR
                                               ITTEN AT
C      STATEMENT NO 4. :  DATA IS ENDED BY A VALUE LESS THAN
                                              -9000 IN
C      THE XD POSITION :  F IS THE CUTOFF FREQUENCY.
C      THIS PROGRAM NEEDS TO BE RUN WITH SUBROUTINES SPLINE,
                                               PLOTX, AND
C      GPLOTV.  SPLINE IS ESSENTIAL BUT PLOTX OR GPLOTV MAY B
                                               E OMITTED
C      DEPENDING ON THE FORM OF OUTPUT DATA REQUIRED.
       DIMENSION O(500),XD(500),YD(500),Y(700),D(700),Z(3,700
                                               ),TITLE(10),
      1FAY(3),B(3),XUN(3),YUN(3,3)
       DATA XUN/'TENS OF KM'/,YUN/'MEASURED    FILTERED    RE
                                               SIDUAL    '/
       READ(5,101) TITLE
  101  FORMAT(10A4)
       I=1
    1  READ(5,2) XD(I),YV,VV
    2  FORMAT(33X,F6.0,25X,F6.0,1X,F6.0)
       IF(XD(I)+9000) 5,5,3
    3  IF(YV) 4,1,4
    4  YD(I)=YV
       XD(I)=XD(I)/10.0+1000.0
       I=I+1
       GO TO 1
    5  I=I-1
       CALL SPLINE(XD,YD,Y,I,NP,IY,IZ,1.0)
       READ(5,6) F
    6  FORMAT(F8.0)
       SIM=0.
       WL=10/F
       KH=5/F
       K=2*KH+1
       C=3.14159/KH
       CV=-3.14159
       DO 10 I=1,K
       J=I-KH-1
       IF(J) 11,12,11
   12  O(I)=2*F
       GO TO 9
   11  O(I)=(0.45*COS(CV)+0.55)*SIN(2*3.14159*F*J)/(3.14159*J
                                               )
    9  CV=CV+C
   10  CONTINUE
       NO=NP-KH*2
       DO 50 I=1,NO
       L=I+IY-1
       SUM=0.
       DO 40 J=1,K
       SUM=SUM+Y(L)*O(J)
   40  L=L+1
```

```
      Z(2,I)=SUM
      SIM=SIM+SUM
   50 CONTINUE
      DO 60 I=1,NO
      J=I+IY+KH-1
      D(I)=J
      Z(3,I)=Y(J)-Z(2,I)
   60 Z(1,I)=Y(J)
      WRITE(6,65) (D(I),I=1,K)
   65 FORMAT(1H1,'FILTER PARAMETERS'/1H0,(10F10.4))
      WRITE(6,64) SIM
   64 FORMAT(1H0,'INTEGRATION =',E13.6)
      CALL PLOTX(D,Z,3,NO,1.0,0.2,-1.0)
      FAX=0.19685
      FAY(1)=0.01
      FAY(2)=0.01
      FAY(3)=0.01
      B(1)=400.0
      B(2)=400.0
      B(3)=100.0
      CALL GPLOTV(D,Z,3,NO,FAX,FAY,B,TITLE,XUN,YUN)
      STOP
      END
```

Appendix C2. 4

A program written in PL1 to translate paper tape containing magnetic data abstracted from the output tapes of the automatic data logging system of HMS HECLA, 1971. The values on the tapes are at one minute intervals and the program puts them out on file, five to a line so that each line begins with a ten minute or five minute value. The program is written to detect and correct for errors or absence of data.

Input:

Eight hole tape punched in HYTIP code. Tape contains time, latitude and longitude, and total intensity magnetic field. Latitude and longitude can be in error and are not used.

Output:

On FILE YY which must be assigned to a device or storage when running the program:-

ITIM	Day number and time, in a field of eight. Last four spaces contain the time. The first four give the day every hour.
MAG	Total intensity magnetic field value.

FILE XX is a temporary storage file and must be assigned filespace when running the program.

```
/* MAGNETICS TAPE TRANSLATOR.  TRANSLATES PAPER TAPE
   WITH MAGNETICS DATA ON PRODUCED FROM THE AUTOMATIC
   DATA LOGGING SYSTEM TAPES FROM HMS HECLA.  PUTS OUT
   TIME AND MAGNETIC VALUES AT TEN MINUTE INTERVALS ON
   FILE (YY). (XX) IS A TEMPORARY STORAGEFILE.  */
WESTDEC:PROC OPTIONS(MAIN);
        DCL Y(0:255) CHAR(1) INIT (
     ' ',' ',' ',' ',' ',' ',' ',' ',' ',' ',' ',' ',' ',
                                           ' ',' ',' ',
     ' ',' ',' ',' ',' ',' ',' ',' ',' ',' ',' ',' ',' ',
                                           ' ',' ',' ',
   ' ',' ',' ','"',' ',' ',' ',' ','''','(',' ',' ','+',' ',' ','-
                                           ','.',' ',' ',
     '0',' ',' ','3',' ',' ','5','6',' ',' ','¬',':',' ',' ','<',
                                           ' ',' ','?',
     ' ',' ','A','B',' ',' ','D',' ',' ',' ','G','H',' ',' ',' ','K',' ',' ','M
                                           ','N',' ',' ',
     'R',' ',' ',' ','S',' ',' ','U','V',' ',' ',' ','Y','Z',' ',' ',' ',
                                           ' ',' ',' ',
     ' ',' ',' ',' ',' ',' ',' ',' ',' ',' ',' ',' ',' ',
                                           ' ',' ',' ',
     ' ',' ',' ',' ',' ',' ',' ',' ',' ',' ',' ',' ',' ',
                                           ' ',' ',' ',
     ' ',' ',' ',' ',' ',' ',' ',' ',' ',' ',' ',' ',' ',
                                           ' ',' ',' ',
     ' ',' ',' ',' ',' ',' ',' ',' ',' ',' ',' ',' ',' ',
                                           ' ',' ',' ',
     ' ',' ',' ',' ','#',' ',' ','%','&',' ',' ',' ',')','*',' ',' ',',',
                                           ' ',' ','/',
     ' ',' ','1','2',' ',' ','4',' ',' ',' ',' ','7','8',' ',' ',' ',';',' ',' ','=
                                           ','>',' ',' ',
     '@',' ',' ',' ','C',' ',' ','E','F',' ',' ',' ','I','J',' ',' ','L',
                                           ' ',' ','O',
     ' ',' ','Q','R',' ',' ','T',' ',' ',' ','W','X',' ',' ',' ','(',' ',' ',')
                                           ',' ',' ',' ',
     ' ',' ',' ',' ',' ',' ',' ',' ',' ',' ',' ',' ',' ',
                                           ' ',' ',' ',
     ' ',' ',' ',' ',' ',' ',' ',' ',' ',' ',' ',' ',' ',
                                           ' ',' ',' ') ;
DCL B BIT(1) INIT ('0'B);
   DCL XX FILE STREAM, CARD  CHAR(8 ), CH CHAR(1);
DCL YY FILE OUTPUT STREAM,WRD CHAR(1);
DCL (ITIM,MAG,ID,IJ) FIXED BIN (31) ;
      ON ENDFILE (SCARDS) GOTO P;
     GET EDIT (CARD) (A(80)) ;
     CARD=' ';
      K=1;
   L1:GET EDIT (CH)(A(1));
     IN = UNSPEC(CH);
   SUBSTR(CARD,K,1)=Y(IN);
   K=K+1;
   IF K>80 THEN DO;
     PUT FILE(XX) EDIT(CARD)(A(80)); K=1;
            CARD=' ';     END;
   GOTO L1;
P:CLOSE FILE(XX);
OPEN FILE(YY) INPUT;
ON ENDFILE (XX) GO TO Z;
J=1 ;
```

```
L=1 ;
 DO I=1 TO 10 ;
GET FILE(XX) LIST(ITIM,AD,AM,OD,OM,MAG) ;
IF MOD(ITIM,10) = 0 THEN GO TO G ;
 END ;
F:GET FILE(XX) LIST(ITIM,AD,AM,OD,OM,MAG) ;
G:IF MOD(ITIM,10000) = 2000 DO I=1 TO 4 ;
ITIM=ITIM+8000 ;
IF MAG < 30000 THEN DO ;
CALL DBD(ITIM,MAG) ;
J=J+1 ;
END ;
PUT FILE(YY) EDIT(ITIM,MAG) (X(2),F(8),X(1),F(5)) ;
DO WHILE(J<60) ;
GET FILE(XX) LIST(ITIM,AD,AM,OD,OM,MAG) ;
IF MAG < 30000 THEN DO :
CALL DBD(ITIM,MAG) :
J=J+1 ;
END ;
ITIM=ITIM-2000 ;
PUT FILE(YY) EDIT(ITIM,MAG) (X(2),F(8),X(1),F(5)) ;
J=J+1 ;
END;
J=1 ;
GET FILE(XX) LIST(ITIM,AD,AM,OD,OM,MAG) ;
END;
IF MAG < 30000 THEN DO ;
CALL DBD(ITIM,MAG) ;
L=L+1 ;
END ;
ITIM=ITIM+4000 ;
PUT FILE(YY) EDIT(ITIM,MAG) (X(2),F(8),X(1),F(5)) ;
DO WHILE(L<10) ;
GET FILE(XX) LIST(ITIM,AD,AM,OD,OM,MAG) ;
IF MAG < 30000 THEN DO ;
CALL DBD(ITIM,MAG) :
L=L+1 ;
END ;
ITIM=ITIM+4000 ;
PUT FILE(YY) EDIT(ITIM,MAG) (X(2),F(8),X(1),F(5)) ;
L=L+1 ;
END ;
L=1 ;
GO TO F;
DBD:PROCEDURE(ITIM,MAG) ;
DCL (ITIM,MAG) FIXED BIN(31) ;
MAG=0 ; ITIM=0 ;
PUT FILE(YY) EDIT(ITIM,MAG) (X(2),F(8),X(1),F(5)) ;
GET FILE(XX) LIST(PUB,BISH) ;
DO K=1 TO 12 ;
GET FILE(XX) LIST(VAL) ;
IF VAL > 30000 THEN GO TO T ;
END;
T: MAG=VAL ;
END ;
Z:END;
```

Appendix C2.5

A program written in PL1 to read digitised magnetograms and put out values of the vertical and horizontal magnetic field at ten minute intervals for the two stations used. Each magnetogram was digitised using the DMAC table and a transparent plastic overlay was used to align each magnetogram with fixed marks giving the distances between known values.

Input:

From FILE XX after five hole paper tape in Elliot code has been translated by program CLT9:DCL99SPL.

PBZ	Base value of vertical field at first station.
PAZ	Value to which the vertical variations are to be referred as a zero.
PFZ	Number of gammas between two points YP and BP on the scale of the vertical field.
PBH	Base value of horizontal field.
PAH	Value to which the horizontal variations are to be referred as a zero.
PFH	Number of gammas between points YP and BP on the scale of the horizontal field.
XP, YP	The coordinates of a point at 0 hours on the bottom of the magnetogram.
AP, BP	The coordinates of a point at 24 hrs on the top of the magnetogram.
XZP,YZP	Coordinates of a point on the baseline for the vertical field.

XHP, YHP — Coordinates of a point on the baseline for the horizontal field.

SBZ, SAZ, SFZ, SBH, SAH, SFH, XS, YS, AS, BS, XZS, YZS, XHS, YHS are the corresponding quantities to thoseabove for the second station.

IDAY — The day number of the two magnetograms (one for each station) that follow. If IDAY = 500 the program ends.

XD,YD — Points along the curve being digitised. They need not be regularly spaced, but should adequately define all the maxima and minima and points of inflection. If XD is set to a value greater than 10000 the program proceeds to the next curve.

Output:

On FILE ZZ:- the day no. followed by the values of vertical and horizontal deviation from normal every ten minutes, spaced alternately vertical before horizontal in 16F(5,0), for the first station.

On FILE YY the output for the second station as above.

This program must be run with subroutine SPLINE, which is a cubic interpolation routine producing values at regularly spaced points.

```
/* READS DIGITISED MAGNETOGRAMS AND PRODUCES VALUES OF
VERTICAL AND HORIZONTAL FIELDS AT TEN MINUTE INTERVALS
   PBZ = BASE TO WHICH VERTICAL VALUES ARE REFERRED ON
FIRST MAGNETOGRAM.  PAZ  MEAN VALUE AT STATION OR BASE
TO WHICH OUTPUT VALUES WILL BE REFERRED.  PFZ  FACTOR
TO CONVERT DISTANCES ON MAGNETOGRAM TO GAMMAS.
PBH, PAH, PFH  ARE SIMILAR QUANTITIES FOR HORIZONTAL

FIELD.   SBZ, SAZ, SFZ, SBH, SAH, SFH, SIMILARLY FOR
SECOND GEOMAGNETIC STATION.  OTHER INPUT PARAMETERS
REFER TO POINTS ON DIGITISING OVERLAY SHEET.  */
PRCMAG:PROC OPTIONS(MAIN);
   DCL PZ(150)FLOAT,PD(150)FLOAT,PH(150)FLOAT,PE(150)FLOA
                                        T,SZ(150)
   FLOAT,SD(150) FLOAT,SH(150) FLOAT,SE(150) FLOAT,ZP(150
                                        ) FLOAT,
   HP(150) FLOAT,ZS(150) FLOAT,HS(150) FLOAT,V(150) FLOAT
                                       ,
   U(150) FLOAT,VH(150) FLOAT,UH(150) FLOAT ;
   DCL (I,IY,IZ,NC) FIXED BIN (31) :
   DCL XX FILE  INPUT STREAM ;
   DCL YY FILE OUTPUT STREAM ;
   DCL ZZ FILE OUTPUT STREAM ;
   GET FILE(XX) LIST(PBZ,PAZ,PFZ,PBH,PAH,PFH,SBZ,SAZ,SFZ,
                                        SBH,SAH,SFH,
   XP,YP,AP,BP,YZP,YZP,XHP,YHP,XS,YS,AS,BS,YZS,YZS,XHS,YH
                                        S) ;
   PFP=144/(AP-XP) ;
   ZFP=PFZ/(BP-YP) ;
   HFP=PFH/(BP-YP) ;
   DFS=144/(AS-XS) ;
   ZFS=SFZ/(BS-YS) ;
   HFS=SFH/(BS-YS) :
 A:GET FILE(XX) LIST(IDAY) ;
   IF IDAY = 999 THEN GO TO C :
   I=0 ;
B1:GET FILE(XX) LIST(XD) ;
   IF XD > 10000 THEN GO TO B2 :
   GET FILE(XX) LIST(YD) ;
   IF XD=XT THEN GO TO B1 ;
   XT=XD ;
   I=I+1 ;
   PUT LIST (I,XD,YD) ;
   PZ(I)=ZFP*(YD-YZP)+PBZ ;
   PD(I)=DFP*(XD-XP)+1 ;
   GO TO B1 ;
B2:IF PD(1) > 1.0 THEN DO :
   PZ(1)=PZ(1)-(PZ(2)-PZ(1))*(PD(1)-1.0)/(PD(2)-PD(1)) :
   PD(1)=1.0 ;
   END ;
   CALL SPLINE(PD(1),PZ(1),ZP(1),I,NC,IY,IZ,1.0E0) ;
   I=0 ;
B3:GET FILE(XX) LIST(XD) ;
   IF XD > 10000 THEN GO TO B4 :
   GET FILE(XX) LIST(YD) ;
   IF XD=XT THEN GO TO B3 ;
   XT=XD ;
   I=I+1 ;
   PUT LIST (I,XD,YD) ;
```

```
   PH(I)=HFP*(YD-YHP)+PPH ;
   PE(I)=DFP*(XD-XP)+1.0 ;
   GO TO B3;
B4:IF PE(1) > 1.0 THEN DO ;
   PH(1)=PH(1)-(PH(2)-PH(1))*(PE(1)-1.0)/(PE(2)-PE(1)) ;
   PE(1)=1.0 ;
   END ;
   CALL SPLINE(PE(1),PH(1),HP(1),I,NC,IY,IZ,1.E6) ;
   I=0 ;
B5:GET FILE(XX) LIST(XD) ;
   IF XD > 10000 THEN GO TO B6 ;
   GET FILE(XX) LIST(YD) ;
   IF XD=XT THEN GO TO B5 ;
   XT=XD ;
   I=I+1 ;
   PUT LIST (I,XD,YD) ;
   SZ(I)=ZFS*(YD-YZS)+SPZ ;
   SD(I)=DFS*(XD-XS)+1.0 ;
   GO TO B5;
B6:IF SD(1) > 1.0 THEN DO ;
   SZ(1)=SZ(1)-(SZ(2)-SZ(1))*(SD(1)-1.0)/(SD(2)-SD(1)) ;
   SD(1)=1.0 ;
   END ;
   NC=0 ; IY=0 ; IZ=0 ;
   CALL SPLINE(SD(1),SZ(1),ZS(1),I,NC,IY,IZ,1.0E6) ;
   I=0 ;
B7:GET FILE(XX) LIST(XD) ;
   IF XD > 10000 THEN GO TO B8 ;
   GET FILE(XX) LIST(YD) ;
   IF XD=XT THEN GO TO B7 ;
   XT=XD ;
   I=I+1 ;
   PUT LIST (I,XD,YD) ;
   SH(I)=HFS*(YD-YHS)+SPH ;
   SE(I)=DFS*(XD-XS)+1.0 ;
   GO TO B7 ;
B8:IF SE(1) > 1.0 THEN DO ;
   SH(1)=SH(1)-(SH(2)-SH(1))*(SE(1)-1.0)/(SE(2)-SE(1)) ;
   SE(1)=1.0 ;
   END ;
   CALL SPLINE(SE(1),SH(1),HS(1),I,NC,IY,IZ,1.0E6) ;
   PUT FILE(YY) EDIT(IDAY) (F(3)) ;
   PUT FILE(YY) SKIP(1) ;
   PUT FILE(ZZ) EDIT(IDAY) (F(3)) ;
   PUT FILE(ZZ) SKIP(1) ;
   DO I=1 TO 144 ;
   V(I)=ZS(I)-SAZ ;
   VH(I)=HS(I)-SAH ;
   U(I)=ZP(I)-PAZ ;
   UH(I)=HP(I)-PAH ;
   PUT FILE(YY) EDIT(V(I),VH(I)) (F(5,0),F(5,0)) ;
   PUT FILE(ZZ) EDIT(U(I),UH(I)) (F(5,0),F(5,0)) ;
   END;
   GO TO A ;
 C:END ;
```

Appendix C2.6

A program written in FORTRAN IV to compute the magnetic anomaly from the measured magnetic field and the predicted magnetic field from the IGRF and the variation in field measured at two geomagnetic observatories.

Input:

Read on 5:-

NDAY	Number of days of measurements.
PLAT	Latitude of first geomagnetic observatory.
PLON	Longitude of first geomagnetic observatory.
SLAT	Latitude of second geomagnetic observatory.
SLON	Longitude of second geomagnetic observatory.
DIP	Inclination of Earth's magnetic field in area of survey.

(These parameters appear at the front of the deck.)

MDAY	The Scientific day number of the following data. If MDAY = 500 the program ends.
ITIM	Time of measurement.
LATD	Latitude: degrees.
ATM	Latitude: minutes.
LOND	Longitude: degrees.
ONM	Longitude: minutes.
IBATH	Bathymetry in metres.

Read on 2:-

IE(J)	Scientific day number of Jth set of data from the second geomagnetic observatory.
EV(I,J)	Value of the variation in the vertical field at the second geomagnetic observatory on day IE(J) at 1 x 10 minutes.

EH(I,J) Value of the variation in the horizontal field at the second observatory on day IE(J) at I x 10 minutes.

Read on 3 are ID(J), DV(I,J) and DH(I,J), which are the corresponding values for the first geomagnetic observatory.

Read on 4:-

JTIM Time of measurement of magnetic field.

IMAG Measurement of total intensity magnetic field.

2 reads the output on FILE YY of C2.5. 3 reads the output on FILE ZZ of C2.5. 4 reads the output of C2.4.

Output:

Written on 6 are the inputs on 2 and 3.

Written on 6 (lineprinter) and 7 (punch or other file):-

ITIM

LATD

ATM

LOND

ONM

IBATH

IMAG Total intensity magnetic field.

MAG Total intensity magnetic anomaly.

```
C       COMPUTES MAGNETIC ANOMALY FROM TOTAL FIELD MAGNETIC ME
C       ASUREMENTS.  INPUT ON  :  NDAY - NO. OF DAYS.  PLAT &
C       PLON ARE THE LATITUDE AND LONGITUDE OF THE 1ST GEOMAGN
C       ETIC STATION.  SLAT & SLON ARE LAT. AND LONG. OF 2ND
C       GEOMAGNETIC STATION.  DIP = INCLINATION OF EARTH'S
C       FIELD IN REGION OF MEASUREMENT.. MDAY IS THE SCIENTIFI
C       C DAY NO. ON WHICH THE MAGNETIC VALUES WERE MEASURED.
C       ITIM = TIME.  LATD & ATM ARE DEGREES AND MINUTES OF L
C       ATITUDE AT THE POSITION OF MEASUREMENT. LOND & ONM ARE
C       DEGREES & MINUTES OF LONGITUDE. IBATH IS THE BATHYMETR
C       Y.  INPUT ON 2:  IE = DAY NO. OF 1ST GEOMAGNETIC STATI
C       ON.  EV(I,J) = ITH VALUE AT TEN MINUTE INTERVALS OF TH
C       E VERTICAL FIELD ON THE JTH DAY.  EH(I,J) SIMILARLY FO
C       R HORIZONTAL FIELD.  INPUT ON      ID, DV, DH ARE THE S
C       AME QUANTITIES AS IE, EV, EH ONLY FOR  2ND GEOMAGNETIC
C       STATION.  INPUT ON4:  JTIM = TIME.  IMAG   MEASURED
C       MAGNETIC VALUE.
        DIMENSION ID(9),DV(150,9),DH(150,9),IE(9),EV(150,9),EH
                                              (150,9)
        READ(5,2) NDAY,PLAT,PLON,SLAT,SLON,DIP
     2  FORMAT(I2/5F10.0)
        DIP=DIP*0.01745
        COD=COS(DIP)
        SID=SIN(DIP)
        DO 3  J=1,NDAY
        READ(2,4)  IE(J),(EV(I,J),EH(I,J),I=1,144)
        READ(3,4)  ID(J),(DV(I,J),DH(I,J),I=1,144)
     4  FORMAT(I3/(16F5.0))
        WRITE(6,112)  ID(J),(DV(I,J),DH(I,J),I=1,144)
        WRITE(6,112)  IE(J),(EV(I,J),EH(I,J),I=1,144)
   112  FORMAT(1H1,I3/(16F5.0))
     3  CONTINUE
     5  READ(5,6) MDAY
     6  FORMAT(3X,I3)
        IF(MDAY.EQ.500) GO TO 30
        MINC=(MDAY-100)*0.25
        DAY=MDAY
        DATE=1971+DAY/365
        DO 8  I=1,9
        IF(MDAY.EQ.ID(I)) GO TO 9
     8  CONTINUE
        GO TO 30
     9  READ(5,10) ITIM,LATD,ATM,LOND,ONM,IBATH
    10  FORMAT(I4,1X,I3,1X,F4.0,1X,I3,1X,F4.0,2X,I4)
    11  READ(4.12)  JTIM,IMAG
    12  FORMAT(6X,I4,1X,I5)
    13  IF(JTIM-ITIM) 11,20,28
    20  YLAT=LATD+ATM/60
        YLON=-(LOND+ONM/60)
        DE=SQRT((YLON-PLON)**2+(YLAT-PLAT)**2)
        F=DE/(DE+SQRT((YLON-SLON)**2+(YLAT-SLAT)**2))
        IK=ITIM/100
        K=IK*6+(ITIM-IK*100)/10+1
        CALL  REGMAG(YLAT,YLON,DATE,ANOM)
        MAG=IMAG-ANOM-(DV(K,I)*F+(1-F)*EV(K,I))*SID-(DH(K,I)*F
                                              +(1-F)*EH(K,
      1I))*COD+MINC
        WRITE(7,24) ITIM,LATD,ATM,LOND,ONM,IBATH,IMAG,MAG
    24  FORMAT(I4,1X,I3,1X,F4.1,1X,I3,1X,F4.1,2X,I4,1X,I5,1X,I
```

```
                                                          5)
      WRITE(6,25) ITIM,LATD,ATM,LOND,ONM,IRATH,IMAG,MAG
   25 FORMAT(1H ,I4,1X,I3,1X,F4.1,1X,I3,1X,F4.1,2X,I4,1X,I5,
                                                          1X,I5)
      IF(ITIM-2350) 5,5,30
   23 WRITE(6,29) ITIM
   29 FORMAT(1HC,'MAG VAL MISSING AT ',I4)
      READ(5,10) ITIM,LATD,ATM,LOND,ONM,IRATH
      GO TO 10
   30 STOP
      END
```

DATA CARDS

The outputs of the reduction programs were combined to give a set of data cards giving on one card all the geophysical data for each fix position. The format of these cards is given below.

```
YEAR, DAY,  TIME, LATITUDE (DEGREES),LATITUDE(MINUTES), LONGITUDE(DEGREES)
 I4,1X,I3,1X,I4,1X,    I3,          1X,     F4.1,    1X,      I4,       1X,

LONGITUDE(MINUTES),EASTING(KM),NORTHING(KM),BATHYMETRY(METRES),
     F4.1,      1X,   F6.1, 1X,   F6.1,  1X,   I4,          1X,

TOTAL INTENSITY MAGNETIC FIELD, TOTAL INTENSITY MAGNETIC ANOMALY,
            I5,           1X,              I5,              1X,

FREE-AIR GRAVITY ANOMALY, BOUGUER GRAVITY ANOMALY(2.0 gm cm^-3)
         F6.1        1X,           F6.1
```

A listing of the program which compiles the data cards follows.

Input:

IYEAR	The year of the survey.
IDAY	The scientific day number.
CLAT	The central latitude of the survey area.
IT	The time which will signify a change of day.

Other input variable names have the same meaning as in the data reduction programs.

```
      READ(4,1) IYEAR,IDAY,CLAT,IT
    1 FORMAT(2I4,F6.0,I4)
      ER=6356.775**2
      ER=6378.16**2
      E2=(ER-PR)/ER
      CLAT=CLAT*0.017453
      FLA=6378.16*(1-E2)*0.017453/(1-E2*SIN(CLAT)**2)**1.5
      FLC=SQRT(ER/(PR*TAN(CLAT)**2/ER+1))*0.017453
      WRITE(6,5)
    5 FORMAT(1H1,'YEAR DAY TIME LATITUDE LONGITUDE KM E.  KM
                                                  N.  BATH T.
     1MAG A.MAG F.GRAV B.GRAV')
    9 READ(3,3) JTIM,MAGT,MANOM
    3 FORMAT(I4,25X,I5,1X,I5)
   10 READ(4,2) ITIM,LATD,ATMN,LOND,CNMN,IBATH,FGR,BGR
    2 FORMAT(I4,1X,I2,1X,F4.1,1X,I2,1X,F4.1,15X,I4,14X,F6.1,
                                                  1X,F6.1)
      IF(ITIM.EQ.IT) READ(4,101) IDAY
  101 FORMAT(I4)
      IF(ITIM-5000) 11,50,50
   11 IF(ITIM-JTIM) 40,12,40
   12 IND=0
   13 DE=(62-LOND-CNMN/60)*FLC
      DN=(LATD+ATMN/60-12)*FLA
      LOND=-LOND
      WRITE(6,20) IYEAR,IDAY,ITIM,LATD,ATMN,LOND,CNMN,DE,DN,
                                                  IBATH,MAGT,
     1MANOM,FGR,BGR
   20 FORMAT(1H ,I4,1X,I3,1X,I4,1X,I3,1X,F4.1,1X,I4,1X,F4.1,
                                                  1X,F6.1,1X,
     1F6.1,1X,I4,1X,I5,1X,I5,1X,F6.1,1X,F6.1)
      WRITE(7,22) IYEAR,IDAY,ITIM,LATD,ATMN,LOND,CNMN,DE,DN,
                                                  IBATH,MAGT,
     1MANOM,FGR,BGR
   22 FORMAT(I4,1X,I3,1X,I4,1X,I3,1X,F4.1,1X,I4,1X,F4.1,1X,F
                                                  6.1,1X,F6.1,
     11X,I4,1X,I5,1X,I5,1X,F6.1,1X,F6.1)
      IF(IND) 10,9,10
   40 MANOM=0
      MAGT=0
      IND=1
      GO TO 13
   50 STOP
      END
```

Appendix C3.1

A program written in PL1, to make line drawings of seismic reflection profiles from digitised reflection records. The records are digitised using the DMAC table. The record must be aligned horizontally with the table before starting. This is best achieved by using a straight edge (not metallic) on the bottom of the record. The record is digitised by the following each reflecting horizon with position indicator.

Input:

On FILE XX after five hole tape in Elliot code has been translated by CLT9:DCL99SPL

BEC	Reflection time in seconds at the top left hand corner of the record.
BX,BY	The coordinates of the top left hand corner.
CX,CY	The coordinates of a point 3 seconds down from the top left hand corner.
DIST	The distance between the top left hand corner and any point near the top right hand corner i.e. the distance travelled by the ship.
ZX,ZY	The coordinates of the point near the top right hand corner.
X, Y	The coordinates of a point on a reflecting horizon. If X = 11111 and Y = 0 the plotter will move with the pen up to the next point. Used when one is changing from one reflector to another.

If X = 11111 and Y = 1 then a change in the delay time on the record is indicated and the next time read DEC is the amount of change in the delay time.

DEC

If X = 11111 and Y = 11111 then a horizontal shift of the record is indicated, and the x value of the last point read is taken to be the new zero value and should, therefore, be moved to the position of zero. i.e. the same value as BX.

If X = 11111 and Y = 55555 the program is directed to read in a new initial data list. (BEC,BX,BY,CX,CY,DIST, ZX,ZY). To be used when digitising more than one record on the same line.

If X = 11111 and Y = 22222 or any other value not previously used, then the program ends.

Read on FILE SCARDS:-

NAME	Up to 80 identifying characters.
IL	The number of characters in NAME.
FAX	The scaling in the x direction on the plot, in inches per user unit.
FAY	The scaling on the plot in the y direction, in inches per second.
DTM	The amount of seconds delay at the top of the plot.
DS	The distance at the beginning of the plot.
XLM	The maximum length of the plot, in inches.

Output:

A line drawing on plain or graph paper from the plotter.

The program must be run with *PLOTSYS followed by a run of *DURPLOT.

```
/* READS DIGITISED SEISMIC REFLECTION RECORDS AND PLOT
S THEM AT ANY SCALE DESIRED. .
NAME IS ANY SET OF IDENTIFYING CHARACTERS, AND IL IS
THE NO. OF CHARACTERS IN NAME, INCLUDING BLANKS.
FAX IS A SCALING FACTOR IN THE X DIRECTION, INCHES PER
UNIT. FAY IS SIMILARLY A FACTOR FOR THE Y DIRECTION.
DTM IS THE NO. OF SECONDS REFLECTION TIME AT WHICH THE
ZERO LINE IS SET.  DS IS THE DISTANCE VALUE AT THE
START OF THE PROFILE..  XLM IS THE MAXIMUM LENGTH OF
THE GRAPH PLOT IN INCHES..
FILE (XX) IS THE INPUT FILE FOR THE DIGITISED DATA.
REC = REFLECTION TIME AT THE TOP LEFT HAND CORNER.
BX, BY ARE X, Y COORDINATES AT TLHC
CX, CY ARE X, Y COORDINATES AT BLHC.
DIST = DISTANCE BETWEEN POSITIONS AT THLC AND TRHC
ZX, ZY ARE X, Y COORDINATES OF TRHC
X AND Y ARE COORDINATES OF POINTS ALONG A REFLECTOR.
11111 1 D INDICATES A CHANGE IN THE DELAY TIME OF THE
RECORD, WHERE D IS THE AMOUNT OF CHANGE.
11111 11111 INDICATES A HORIZONTAL SHIFT OF THE RECORD
11111 55555 DIRECTS PROGRAM TO A NEW INPUT DATA LIST.
11111 22222 ENDS PROGRAM. */
SDRW:PROC OPTIONS(MAIN);
     DCL XX FILE INPUT STREAM;
     DCL NAME CHAR(80) VAR, IL FIXED BIN(31);
     DCL 1 DUM,2(N FIXED BIN(31), CHPAR CHAR(80) VAR),
     FPAR DEFINED CHPAR;
     GET LIST(NAME,IL,FAX,FAY,DTM,DS,XLM);
     RAY=1/FAY; COX=2.0;
     RAX=1/FAX;
     GET FILE(XX) LIST(REC,BX,BY,CX,CY,DIST,ZX,ZY);
     FS=3.0/(CY-BY);
     FX=DIST/(ZY-BX);
     XFAC=FX*FAX;
     TX=FAX*10.0 ;
     CALL PLOTXMX(XLM);
     CHPAR='TWO WAY TIME. SECS': N=-18;
     CALL RAXIS(2.0E0,10.0E0,FPAR,N,0.0E0,-90.0E0,DTM,RAY,F
                                                  AY);
     N=0;
     CALL RAXIS(2.0E0,10.0E0,FPAR,N,XLM,0.0E0,DS,FAX,TX) ;
     CHPAR='NAME'; N=IL;
     CALL PSYMB(0.0E0,10.2E0,-0.3E0,FPAR,0.0E0,N);
     CHPAR='DGL36'; N=5;
     CALL PSYMB(0.0E0,0.5E0,-0.2E0,FPAR,0.0E0,N);
2:   GET FILE(XX) LIST(X,Y);
     IF X=11111 THEN DO;
     IF Y=1 THEN DO;
     GET FILE(XX) LIST(DEC);
     REC=REC+DEC;
     GO TO 2;
     END;
     ELSE IF Y=0 THEN DO;
     GET FILE(XX) LIST(X,Y);
     XO=(X-BX)*XFAC+COX;
     YO=10.0-((Y-BY)*FS+REC-DTM)*RAY;
     CALL PENUP(XO,YO) ;
     GO TO 2;
     END;
```

```
   ELSE IF Y=11111 THEN DO;
   COX=XO;
   GO TO 3;
   END;
   ELSE IF Y=55555 THEN DO;
   COX=XO ;
   GET FILE(XX) LIST(BEC,BX,BY,CX,CY,DIST,ZX,ZY) ;
   FS=3.0/(CY-BY) ;
   FX=DIST/(ZX-BX) ;
   XFAC=FX*FAX ;
   END;
   ELSE GO TO E;
   END;
   ELSE DO;
   XO=(X-BX)*XFAC+COX;
   YO=10.0-((Y-BY)*FS+BEC-BTM)*FAY;
   CALL PENDN(XO,YO);
   END;
   GO TO 3;
E: CALL PLTEND ;
   END;
```

Appendix C3.2

A subroutine written in FORTRAN IV, to find the optimum values of depth, dip, and velocity of overlying layer for a series of reflectors appearing on a wide angle reflection record. To be run with MINUIT (see appendix C4.1). The initial values of the dip, and velocity for each of the reflectors are entered in the MINUIT prescribed format. (Velocity: first variable and dip:second variable for each reflector in order of increasing depth.) The values of velocity and dip can be fixed or limited within desired bounds. The program first optimises the layers sequentially in order of increasing depth and then optimises the solution as a whole to reduce the effect of a poorly determined layer. Layers are entered to the program by CALL FCN 5.

Input:

Read on 5:-

NL — The number of reflectors.

NP — The number of data points for which the reflection times are known. These should be regularly spaced.

DX — The distance between data points.

FO — The format of the times of reflection from reflectors for each of the data points.

Read on 7 are the reflection times for each the data points in the format defined in FO. A(J,I) is the time for the Jth layer at the Ith point.

Output:

Written on 6:-

I	The number of the reflector.
X(J1)	The velocity in the Ith layer.
B(I)	The depth to the Ith reflector.
X(J2)	The dip of the Ith reflector.
CA(I)	The critical angle for the Ith reflector.
CD(I)	The critical distance for the Ith reflector.
SE	The standard error of the fit for the Ith reflector.
IT(I)	The number of calculated points on the Ith reflector.

Output is obtained with the command CALL FCN 3.

Refer to Appendix C4.1 for a description of the use of MINUIT with subroutines.

```
C     OPTIMISATION SUBROUTINE FOR WIDE ANGLE REFLECTION DATA
C      NL= NO. OF LAYERS.    NP = NO. OF REFLECTION TIMES
C      DX = DISTANCE BETWEEN UNIFORMLY SPACED REFLECTION POIN
                                                      TS.
C      FO IS THE FORMAT OF THE INPUT DATA FOR REFLECTION TIME
                                                     S.
       SUBROUTINE FCN(NPAR,G,F,X,IFLAG)
       DIMENSION A(5,200),CA(5),CD(5),X(15),G(15),FO(6),IT(5)
                                                    ,SU(5),B(5),
      1SM(5)
       DATA CA/5*0./,CD/5*0./,SM/5*1.0/
       RAD=1/57.296
       GO TO(10,20,30,40,50),IFLAG
   10  READ(5,12) NL,NP,DX,FO
   12  FORMAT(I1,1X,I3,1X,F6.4,1X,4A4)
       READ(7,FO) ((A(J,I),J=1,NL),I=1,NP)
       NT=1
   20  CONTINUE
   40  SUM=0.
       DEN=-NT
       NN=NT
       V1=X(1)
       D1=X(2)*RAD
       OD1=A(1,1)*V1*0.5
       COD1=COS(D1)
       SID1=SIN(D1)
       B(1)=OD1/COD1
       SU(1)=0.
       IT(1)=0
       IF(2-NN)411,411,410
  411  V2=X(3)
       D2=X(4)*RAD
       DD1=D2-D1
       OD2=(A(2,1)*0.5-OD1/(V1*COS(DD1)))*V2+OD1/COS(DD1)
       B(2)=OD2/COS(D2)
       SU(2)=0.
       IT(2)=0
       IF(3-NN)412,412,410
  412  V3=X(5)
       D3=X(6)*RAD
       DD2=D3-D2
       OD3=(A(3,1)*0.5-OD1*(1/V1-1/V2)/COS(D3-D1)-OD2/(V2*COS
                                                    (DD2)))*V3+O
      1D2/COS(DD2)
       B(3)=OD3/COS(D3)
       SU(3)=0.
       IT(3)=0
       IF(4-NN)413,413,410
  413  V4=X(7)
       D4=X(8)*RAD
       DD3=D4-D3
       OD4=(A(4,1)*0.5-OD1*(1/V1-1/V2)/COS(D4-D1)-OD2*(1/V2-1
                                                   /V3)/COS(D4-
      1D2)-OD3/(V3*COS(DD3)))*V4+OD3/COS(DD3)
       B(4)=OD4/COS(D4)
       SU(4)=0.
       IT(4)=0
       IF(5-NN)414,414,410
  414  V5=X(9)
```

```
      D5=X(10)*RAD
      DD4=D5-D4
      OD5=(A(5,1)*0.5-OD1*(1/V1-1/V2)/COS(D5-D1)-OD2*(1/V2-1
                                                  /V3)/COS(D5-
     1D2)-OD3*(1/V3-1/V4)/COS(D5-D3)-OD4/(V4*COS(DD4)))*V5+O
                                                  D4/COS(DD4)
      B(5)=OD5/COS(D5)
      IT(5)=0
      SU(5)=0.
  410 DO 48 ID=1,150
      AID=(ID*0.005)**0.5
      AINC=ARCOS(AID)
      SAINC=SIN(AINC)
      CAINC=AID
      AR=1.5708-AINC+D1
      PD1=OD1/COS(AR)
      SEA=SIN(3.14159-AINC-2*AR)
      PU1=PD1*SAINC/SEA
      XD1=PD1*SIN(2*AR)/SEA
      T1=(PD1+PU1)/V1
      K=XD1/DX
      J=K+1
      L=K+2
      IF(J.LT.1) GO TO 48
      IF(L.GT.NP) GO TO 48
      SU(1)=SU(1)+((XD1-DX*K)*(A(1,L)-A(1,J))/DX+A(1,J)-T1)*
                                                  *2
      IT(1)=IT(1)+1
      IF(2-NN)402,402,48
  402 RE1=(V2*SIN(AR)/V1)
      IF(ABS(RE1).GE.1) GO TO 492
      R1=ARSIN(RE1)
      AR2=R1+DD1
      IF(AR2-1.5708) 422,48,48
  422 PD2=(OD2-PD1*COS(AR+DD1))/COS(AR2)
      RR1=AR2+DD1
      COR1=COS(R1)
      CORR1=COS(RR1)
      PU2=PD2*COR1/CORR1
      HD=PD2*SIN(2*AR2)/CORR1
      AA1=ARSIN(V1*SIN(RR1)/V2)
      PU1=(PD1*SAINC+HD*SID1)/COS(D1+AA1)
      T2=(PD1+PU1)/V1+(PD2+PU2)/V2
      XD2=PD1*CAINC+HD*COD1+PU1*SIN(D1+AA1)
      K=XD2/DX
      J=K+1
      L=K+2
      IF(J.LT.1) GO TO 48
      IF(L.GT.NP) GO TO 48
      SU(2)=SU(2)+((XD2-K*DX)*(A(2,L)-A(2,J))/DX+A(2,J)-T2)*
                                                  *2
      IT(2)=IT(2)+1
      IF(3-NN)403,403,48
  403 RE2=V3*SIN(AR2)/V2
      IF(ABS(RE2).GE.1) GO TO 493
      R2=ARSIN(RE2)
      AR3=R2+DD2
      IF(AR3-1.5708) 423,48,48
  423 PD3=(OD3-PD1*COS(AR+D3-D1)-PD2*COS(AR2+DD2))/COS(AR3)
      RR2=AR3+DD2
```

```
      COR2=COS(R2)
      CORR2=COS(RR2)
      PU3=PD3*COR2/CORR2
      HD2=PD3*SIN(2*AR3)/CORR2
      AA2=ARSIN(V2*SIN(RR2)/V3)
      SDD1=SIN(DD1)
      CDD1=COS(DD1)
      PU2=(PD2*COR1+HD2*SDD1)/COS(DD1+AA2)
      S2=SIN(DD1+AA2)
      HD1=PD2*RE1+HD2*CDD1+PU2*S2
      AA1=ARSIN(V1*S2/V2)
      PU1=(PD1*SAINC+HD1*SID1)/COS(D1+AA1)
      XD3=PD1*CAINC+HD1*COD1+PU1*SIN(AA1+D1)
      T3=(PD1+PU1)/V1+(PD2+PU2)/V2+(PD3+PU3)/V3
      K=XD3/DX
      J=K+1
      L=K+2
      IF(J.LT.1) GO TO 48
      IF(L.GT.NP) GO TO 48
      SU(3)=SU(3)+((XD3-K*DX)*(A(3,L)-A(3,J))/DX+A(3,J)-T3)*
                                              *2
      IT(3)=IT(3)+1
      IF(4-NN)404,404,48
  404 RE3=V4*SIN(AR3)/V3
      IF(ABS(RE3).GE.1) GO TO 494
      R3=ARSIN(RE3)
      AR4=R3+DD3
      IF(AR4-1.5708) 424,48,48
  424 PD4=(OD4-PD1*COS(AR+D4-D1)-PD2*COS(AR2+D4-D2)-PD3*COS(
                                                  AR3+DD3))/CO
     1S(AR4)
      RR3=AR4+DD3
      COR3=COS(R3)
      CORR3=COS(RR3)
      PU4=PD4*COR3/CORR3
      HD3=PD4*SIN(2*AR4)/CORR3
      AA3=ARSIN(V3*SIN(RR3)/V4)
      S3=SIN(DD2+AA3)
      SDD2=SIN(DD2)
      CDD2=COS(DD2)
      PU3=(PD3*COR2+HD3*SDD2)/COS(DD2+AA3)
      HD2=PD3*RE2+HD3*CDD2+PU3*S3
      AA2=ARSIN(V2*S3/V3)
      PU2=(PD2*COR1+HD2*SDD1)/COS(DD1+AA2)
      S2=SIN(DD1+AA2)
      HD1=PD2*RE1+HD2*CDD1+PU2*S2
      AA1=ARSIN(V1*S2/V2)
      PU1=(PD1*SAINC+HD1*SID1)/COS(AA1+D1)
      T4=(PD1+PU1)/V1+(PD2+PU2)/V2+(PD3+PU3)/V3+(PD4+PU4)/V4
      XD4=PD1*CAINC+HD1*COD1+PU1*SIN(AA1+D1)
      K=XD4/DX
      J=K+1
      L=K+2
      IF(J.LT.1) GO TO 48
      IF(L.GT.NP) GO TO 48
      SU(4)=SU(4)+((XD4-K*DX)*(A(4,L)-A(4,J))/DX+A(4,J)-T4)*
                                              *2
      IT(4)=IT(4)+1
      IF(5-NN)405,405,48
  405 RE4=V5*SIN(AR4)/V4
```

```
      IF(ABS(RE4).GE.1) GO TO 495
      R4=ARSIN(RE4)
      AR5=R4+DD4
      IF(AR5-1.5708) 425,48,48
  425 PD5=(OD5-PD1*COS(AR+D5-D1)-PD2*COS(AR2+D5-D2)-PD3*COS(
                                                  AR3+D5-D3)-
     1PD4*COS(AR4+DD4))/COS(AR5)
      RR4=AR5+DD4
      COR4=COS(R4)
      CORR4=COS(RR4)
      PU5=PD5*COR4/CORR4
      HD4=PD5*SIN(2*AR5)/CORR4
      AA4=ARSIN(V4*SIN(RR4)/V5)
      PU4=(PD4*COR3+HD4*SIN(DD3))/COS(DD3+AA4)
      S4=SIN(DD3+AA4)
      HD3=PD4*RE3+HD4*COS(DD3)+PU4*S4
      AA3=ARSIN(V3*S4/V4)
      PU3=(PD3*COR2+HD3*SDD2)/COS(DD2+AA3)
      S3=SIN(DD2+AA3)
      HD2=PD3*RE2+HD3*CDD2+PU3*S3
      AA2=ARSIN(V2*S3/V3)
      PU2=(PD2*COR1+HD2*SDD1)/COS(DD1+AA2)
      S2=SIN(DD1+AA2)
      HD1=PD2*RE1+HD2*CDD1+PU2*S2
      AA1=ARSIN(V1*S2/V2)
      PU1=(PD1*SAINC+HD1*SID1)/COS(D1+AA1)
      T5=(PD1+PU1)/V1+(PD2+PU2)/V2+(PD3+PU3)/V3+(PD4+PU4)/V4
                                                  +(PD5+PU5)/V
     15
      XD5=PD1*CAINC+HD1*COD1+PU1*SIN(AA1+D1)
      K=XD5/DX
      J=K+1
      L=K+2
      IF(J.LT.1) GO TO 48
      IF(L.GT.NP) GO TO 48
      SU(5)=SU(5)+((XD5-K*DX)*(A(5,L)-A(5,J))/DX+A(5,J)-T5)*
                                                  *2
      IT(5)=IT(5)+1
   48 CONTINUE
      DO 490 L=1,NT
      IF(IT(L)) 491,491,489
  489 SM(L)=SU(L)
  491 SUM=SUM+SM(L)
      DEN=DEN+IT(L)
  490 CONTINUE
      FUN=SUM*100.0/DEN
      F=FUN-NT
      WRITE(6,448) F
  448 FORMAT(1H ,E13.6)
      RETURN
  492 CA(1)=AR/RAD
      CD(1)=XD1
      NN=1
      GO TO 48
  493 CA(2)=AR2/RAD
      CD(2)=XD2
      NN=2
      GO TO 48
  494 CA(3)=AR3/RAD
      CD(3)=XD3
```

```
      NN=3
      GO TO 48
  495 CA(4)=AR4/RAD
      CD(4)=XD4
      NN=4
      GO TO 48
   30 WRITE(6,31)
   31 FORMAT(1H1,30X,'OPTIMISATION ANALYSIS OF WIDE ANGLE RE
                                                 FLECTION DAT
     1A'/30X,53(1H*)///)
      DO 32 I=1,NT
      J1=2*I-1
      J2=2*I
      SE=SQRT(SU(I)/(IT(I)-1))
      WRITE(6,33) I,X(J1),B(I),X(J2),CA(I),CD(I),SE,IT(I)
   33 FORMAT(1HO,'LAYER'I1/1H ,2X,'VELOCITY =',F7.4,/2X,'DEP
                                                 TH =',F7.3/2
     1X,'DIP ='F6.2/2X,'CRITICAL ANGLE =',F6.2/2X,'CRITICAL
                                                 DISTANCE =',
     2F8.3/2X,'STANDARD ERROR OF FIT =',F7.4/2X,'NUMBER OF F
                                                 IT POINTS ='
     3,I3)
   32 CONTINUE
      WRITE(6,34) FUN
   34 FORMAT(1HO,'FUNCTION VALUE =',1PE13.6)
      RETURN
   50 NT=NT+1
      IF(NT.GT.NL) NT=NL
   54 WRITE(6,55) NT
   55 FORMAT(1HO,'LAYER ',I1,' IN COMPUTATION'//)
      RETURN
      END
```

Appendix C3.3

A program written in FORTRAN IV, to calculate distances between sources and receivers in seismic refraction experiments, and the azimuths of incoming arrivals at receivers. The formula used is from Robbins, A.R. 1962. Long lines on the spheroid. Emp. Svy. Rev. 125. Its accuracy is 1 in 10^7 at 1600 km range.

Input:

Read on 5:-

NLP	The number of receivers.	First card.
NSP	The number of sources.	
NL(I)	The identification no. of the Ith receiver	NLP cards.
AL	Latitude: degrees of the Ith receiver.	
AM	Latitude: minutes of the Ith receiver.	
OL	Longitude: degrees of the Ith receiver.	
OM	Longitude: minutes of the Ith receiver	
NS(I)	The identification no of the Ith source.	NSP cards.
AL, AM, OL, OM as above for the source.		

Output:

Written on 6:-

NL(I)	Identification no. of the Ith receiver.
NL(J)	Identification no. of Jth receiver.
DIST	Distance between Ith and Jth receivers.
DAZ	The azimuth of the Jth receiver from the Ith receiver.
NS(I)	Identification of the Ith source.
NS(J)	Identification of the Jth source.

DIST	Distance between the Ith and Jth sources.
DAZ	Azimuth of the Jth source from the Ith source.
NL(I)	Identification no. of the Ith receiver.
NS(J)	Identification no. of the Jth source.
DIST	Distance between the Ith receiver and the Jth source.
DAZ	Azimuth of the Jth source from the Ith receiver.

NLP can be made zero.

```
C                                DISTAZ
C      DISTANCE CALCULATOR ACCURATE TO 1 IN 10**7 AT 1600 KM
C     USES FORMULA OF ROBBINS, A.R. 'LONG LINES ON THE
C     SPHEROID' EMP. SVY. REV. 125 1962. WRITTEN FOR
C     FINDING DISTANCES BETWEEN RECEIVING STATIONS AND SHOT
C     POINTS IN SEISMIC EXPERIMENTS, BUT CAN BE USED FOR ANY
C     DISTANCE CALCULATION. NLP = NO. OF STATIONS.  NSP = NO
C     OF SHOTS.  NL(I) = IDENTIFICATION NO. OF ITH RECEIVING
C     STATION.  AL= DEGREES OF LATITUDE.  AM = MINUTES OF LA
C     TITUDE.  OL = DEGREES OF LONGITUDE.  OM = MINUTES OF L
C
C     LONGITUDE.  NS(I) = IDENTIFICATION NO. OF ITH SHOT.
      DOUBLE PRECISION AL,OL,ERQ,PRQ,A,B,SS,VS,SI,V,CO,S,SDL
                                          ,CDL,DIF,S1,
     1C1,G,GA,EC,EL,TA
      DIMENSION NL(50),A(2,50),NS(300),B(2,300),SI(50),CO(50
     1                                    ),V(50),VS(3
     100),SS(300),GA(50),TA(300)
      DTR=0.01745328
      ER=6378.160
      PR=6356.775
      ERQ=ER**2
      PRQ=PR**2
      EC=(ERQ-PRQ)/ERQ
      EL=(ERQ-PRQ)/PRQ
      READ(5,2) NLP,NSP
    2 FORMAT(2I5)
      IF(NLP) 21,21,9
    9 DO 10 I=1,NLP
      READ(5,4) NL(I),AL,AM,OL,OM
    4 FORMAT(I5,4F10.0)
      AL=(AL+AM/60.0)*DTR
      OL=(OL+OM/60.0)*DTR
      S=DSIN(AL)
      V(I)=ER/DSQRT(1-EC*S**2)
      GA(I)=DSQRT(EL*S**2)
      SI(I)=S
      CO(I)=DCOS(AL)
      A(1,I)=AL
      A(2,I)=OL
   10 CONTINUE
      WRITE(6,14)
   14 FORMAT(1H1,20X,'DISTANCES IN KM AND AZIMUTHS BETWEEN P
                                          OINTS OF GIV
     1EN LATITUDE AND LONGITUDE'/21X,73(1H-)///'DISTANCES BE
                                          TWEEN STATIO
     2NS'/)
      INDEX=1
      L=NLP-1
      IF(L) 21,21,19
   19 DO 20 I=1,L
      K=I+1
      S1=SI(I)
      C1=CO(I)
      V1=V(I)
      DO 20 J=K,NLP
      DIF=A(2,J)-A(2,I)
      CDL=DCOS(DIF)
      SDL=DSIN(DIF)
```

```
      G=GA(I)
      T=(1.0-EC+EC*V1*S1/(V(J)*SI(J)))*DTAN(A(I,J))
      GO TO 50
   20 WRITE(6,22) NL(I),NL(J),DIST,DAZ
   22 FORMAT(1H ,I5,' TO',I5,' =',2F10.3)
   20 CONTINUE
   21 READ(5,4) NS(1),AL,AM,OL,OM
      AL=(AL+AM/60.0)*DTR
      OL=(OL+OM/60.0)*DTR
      B(1,1)=AL
      B(2,1)=OL
      SS(1)=DSIN(AL)
      TA(1)=DTAN(AL)
      VS(1)=EP/DSQRT(1-EC*SS(1)**2)
      WRITE(6,28)
   28 FORMAT(1H1,'DISTANCES BETWEEN CONSECUTIVE SHOT POINTS
                                                 WITH AZIMUTH
     1S OF PREVIOUS POINT'//)
      INDEX=2
      DO 30 I=2,NSP
      J=I-1
      READ(5,4) NS(I),AL,AM,OL,OM
      AL=(AL+AM/60.0)*DTR
      OL=(OL+OM/60.0)*DTR
      B(1,I)=AL
      B(2,I)=OL
      S1=DSIN(AL)
      C1=DCOS(AL)
      V1=EP/DSQRT(1-EC*S1**2)
      DIF=B(2,J)-OL
      COL=DCOS(DIF)
      SOL=DSIN(DIF)
      SS(I)=S1
      VS(I)=V1
      TA(I)=DTAN(AL)
      T=(1.0-EC+EC*V1*S1/(VS(J)*SS(J)))*TA(J)
      GO TO 50
   39 WRITE(6,22) NS(I),NS(J),DIST,DAZ
   30 CONTINUE
      INDEX=3
      DO 40 I=1,NLP
      WRITE(6,42) NL(I)
   42 FORMAT(1H1,'DISTANCES AND AZIMUTHS OF SHOTS FROM STATI
                                                 ON',I5//)
      S1=SI(I)
      C1=CO(I)
      V1=V(I)
      OL=A(2,I)
      DO 40 J=1,NSP
      DIF=B(2,J)-OL
      COL=DCOS(DIF)
      SOL=DSIN(DIF)
      T=(1.0-EC+EC*V1*S1/(VS(J)*SS(J)))*TA(J)
      GO TO 50
   49 WRITE(6,46) NS(J),DIST,DAZ
   46 FORMAT(1H ,I5,2X,2F10.3)
   40 CONTINUE
      STOP
   50 AT=ATAN(T)
      PAZ=C1*T-S1*COL
```

```
      SL=SOL
      AZ=ATAN2(SL,PAZ)
      HQ=EI*C1**2*COS(AZ)**2
      H=SQRT(HQ)
      RAZ=ABS(AZ)-3.14159
      IF(RAZ.GT.-1.0.OR.RAZ.LT.-2.14159) GO TO 57
      ED=SOL*COS(AT)/SIN(AZ)
      D=ARSIN(ED)
      GO TO 58
   57 D=ARSIN(COS(AT)*PAZ/COS(AZ))
   58 DIST=V1*D*(1.0-D**2*HQ*(1.0-HQ)/6.0+D**3*G*H*(1.0-2.*
                                                  HQ)/8.0+D**4
     1*(HQ*(4.0-7.0*HQ)-3.0*G**2*(1.0-7.0*HQ))/120.0-D**5*G*
                                                  H/48.0)
      DAZ=AZ/DTR
      GO TO (29,39,49),INDEX
      END
```

Appendix C3.4

A program written in FORTRAN IV, to find the velocity of a refractor from the distances and arrival times of shots. The effect of the varying thicknesses of layers overlying the refractor (such as water) may be corrected for by adding the thickness and velocity of the layer for each shot, as indicated below. The velocity is first determined by linear regression without any of the overlying layers included. The effects of the overlying layers are then included, added in one after another with a solution after each addition.

Input:

Read on 5:-

ND	The number of shot points.
NL	The number of overlying layers.
WV(I)	The velocity of the Ith overlying layer.
X(I)	Distance to the Ith shot.
T(I)	Time from the Ith shot.
W(I,J)	The thickness of the Jth layer at the Ith shot.

Output:

Written on 6:-

ND, X(I), T(I), W(I,J)

VT	The slope of the regression of time on to distance.
DT	The intercept time.
STE	The standard error of the regression.
VX	The velocity. (Slope of regression of distance on to time.)
DX	The constant of the regression of distance on to time.

SXE	The standard error of the regression of distance on to time.
RVT	The velocity from the reciprocal of the slope of the first regression.
RDT	The constant from RVT.
SRTE	Standard error of fit to RVT.
EV	Standard error on the velocity.
EI	Standard error on the intercept time.
R(I)	The time residual for the Ith shot.

```
C      REFRACTION VELOCITY STATISTICS FOR ONE LAYER WITH
C      CORRECTIONS FOR OVERLYING LAYERS. LINEAR REGRESSION TO
C      ARRIVAL TIMES.  ND = NO. OF ARRIVAL TIMES.  NL = NO. O
C      F OVERLYING LAYERS.  WV(I) = VELOCITY OF ITH OVERLYING
C      LAYER.  X(I) = DISTANCE TO ITH DATA POINT.  T(I) =
C      ARRIVAL TIME AT ITH POINT.  W(I,J) = THICKNESS OF JTH
C      OVERLYING LAYER AT ITH POINT.
C     REFRACTION  VELOCITY STATISTICS FOR ONE LAYER + CORRECT
                                                      IONS
      DIMENSION X(100),T(100),A(100),W(100,5),WV(5),R(100),S
                                                      (100)
      READ(5,2) ND,NL
    2 FORMAT(I3,I2)
      READ(5,3) (WV(I),I=1,NL)
    3 FORMAT(5F10.0)
      IND=1+NL
      JI=1
      SX=0.
      ST=0.
      WRITE(6,12) ND
   12 FORMAT(1H1,20X,'ANALYSIS OF REFRACTION VELOCITY FOR ON
                                                      E LAYER WITH
     1 CORRECTIONS FOR OVERLYING LAYERS'/21X,83(1H-)///'NO.
                                                      OF DATA POIN
     2TS =',I3/'DIST.    TIME.    LAYER THICKNESSES'/)
      DO 10 I=1,ND
      READ(5,4) X(I),T(I),(W(I,J),J=1,NL)
    4 FORMAT(8F10.0)
      WRITE(6,5) X(I),T(I),(W(I,J),J=1,NL)
    5 FORMAT(1H ,8F8.2)
      SX=SX+X(I)
      ST=ST+T(I)
      A(I)=T(I)
   10 CONTINUE
      STM=ST/ND
      SXM=SX/ND
   15 SV=0.
      STQ=0.
      SXQ=0.
      DO 20 I=1,ND
      ET=A(I)-STM
      EX=X(I)-SXM
      SV=SV+ET*EX
      STQ=STQ+ET**2
      SXQ=SXQ+EX**2
   20 CONTINUE
      VT=SV/SXQ
      VX=SV/STQ
      OT=STM-VT*SXM
      OX=SXM-VX*STM
      RVT=1/VT
      ROT=SXM-RVT*STM
      TE=0.
      XE=0.
      RTQ=0.
      DO 30 I=1,ND
      U=X(I)
      V=A(I)
      RES=(V-OT-VT*U)
```

```
      TE=TE+RES**2
      R(I)=RES
      XE=XE+(U-DX-VX*V)**2
      RTE=RTE+(U-RDT-RVT*V)**2
   30 CONTINUE
      STE=SQRT(TE/(ND-2))
      SXE=SQRT(XE/(ND-2))
      SRTE=SQRT(RTE/(ND-2))
      EV=SXE/SQRT(STQ)
      EI=SQRT(STE*STE/ND+STE*STE*SXM*SXM/SXQ)
      GO TO(32,45,45,32),JIM
   32 WRITE(6,36) VT,DT,STE,VX,DX,SXE,RVT,RDT,SRTE,EV,EI
   36 FORMAT(1H0,'REGRESSION OF TIME ON TO DISTANCE'//'SLOPE
                                              =',F6.3/'IN
     1TERCEPT =',F6.2/'STANDARD ERROR =',F5.2//'REGRESSION O
                                              F DISTANCE O
     2N TO TIME'//'VELOCITY =',F5.2/'INTERCEPT =',F6.2/'STAN
                                              DARD ERROR =
     3',F5.2//'REGRESSION OF RECIPROCAL T ON TO D FOR V'//'V
                                              ELOCITY =',
     4F5.2/'INTERCEPT =',F6.2/'STANDARD ERROR =',F5.2/'S.E.
                                              ON VELOCITY
     5=',F6.3/'S.E. ON INTERCEPT =',F6.3///)
      WRITE(6,37) (R(I),I=1,ND)
   37 FORMAT(1H0,'TIME RESIDUALS'/(10F8.3))
      GO TO (90,40,40,40,40,40),IND
   40 IND=IND-1
      JIM=1
      IT=NL+1-IND
      WRITE(6,42) IT,WV(IT)
   42 FORMAT(1H0,'VELOCITIES WITH CORRECTION FOR LAYER',I2,'
                                              WITH VELOCI
     1TY',F5.2/)
      DO 44 I=1,ND
   44 B(I)=A(I)
   45 ANG=ARSIN(WV(IT)/VX)
      FAC=1/(COS(ANG)*WV(IT))-TAN(ANG)/VX
      ST=0.
      DO 50 I=1,ND
      A(I)=B(I)-W(I,IT)*FAC
   50 ST=ST+A(I)
      STM=ST/ND
      JIM=JIM+1
      GO TO 15
   90 STOP
      END
```

Appendix C4.1

Non-linear optimisation in geophysical interpretation.

An analysis of the use of non-linear optimisation in geophysics is given by M. Al-Chalabi 1970. (The application of non-linear optimisation techniques in geophysics. Unpublished Ph.D. thesis. University of Durham). Use has been made of this technique by the writer for the interpretation of wide angle reflection data (C3.2), magnetic anomalies (C4.2, C4.3), gravity anomalies (C4.4), and rotation pole positions for plate motions (C7.1).

The program package MINUIT (James and Roos, 1969) minimises a function of n variables presented to it by a subroutine which performs the calculations or operations desired by the user (eg. finding the model that will give the best fit to a gravity anomaly). The three methods of minimisation used by MINUIT are SEEK a random search method using the Monte Carlo technique. TAUROS is a rotating coordinate system technique devised by Rosenbrock. MIGRAD makes use of the Davidon variable matrix algorithm, and is basically a method of steepest descent.

SEEK is not strictly a minimisation routine, but successive calls to it will produce some sore to slow convergence on a minimum. It is however very useful for obtaining good estimates of the initial values of the variable parameters if they are not well known. TAUROS is a stable routine which converges quickly toward the region of the minimum. In the region of the minimum, however, it is relatively slow, stepping around the actual minimum. MIGRAD is rapid in the region of a well defined minimum, but is slow when far from the minimum or if

the function is badly defined. For most of the problems considered in geophysical interpretation the function to be minimised does not usually have a well defined minimum, and accordingly TAUROS is the most useful routine, although MIGRAD can be used to find the final minimum after several runs of TAUROS.

The method of entering data to, and running MINUIT is described in the Long Write-up of the program, copies of which are available in the Department of Geological Sciences at Durham. A brief and incomplete summary of the method of use is given below.

Data on the parameters to be varied are entered in a list as specified by MINUIT. Following this is a list of data to be read by the user's subroutine in the format specified by the subroutine. The user's subroutine must be called FCN. After the data come the commands which tell the program what minimisation routine to use and how many calls to make to the subroutine. CALL FCN 3 will obtain an output of results. CALL FCN 5 will make the subroutine perform any other desired operation which may be written in to it. Parameters may have their values fixed by using FIX. An example of the input for a run of MINUIT is given on the following pages.

The first card of the user subroutine is as follows:-

SUBROUTINE FCN (NPAR,G,F,X,IFLAG)

NPAR* = The number of variable parameters.

G is a vector containing the values of the derivatives.

F * The function value calculated by FCN.

X* is a vector containing the parameter values.

IFLAG* is an indicator which specifies the section of FCN that will operate.

The arguments marked * are input to FCN.

In writing FCN care needs to be taken to ensure that F, the value of the function to be minimised is only dependent on the variable parameters. Also the value of F and the convergence criteria for the minimisation routines must be compatible so that apparent convergence is not too easily reached, or alternatively that the possibility that convergence is never reached is avoided.

Appendix C4.2

A subroutine written in FORTRAN IV, for use with MINUIT, to find the two dimensional body-model that will give the best fit between the observed magnetic anomaly and the magnetic anomaly produced by the model. The body may have only one magnetisation contrast which is the first parameter on the variable parameter list. The angle of dip of the magnetisation vector is the second variable parameter, and the background value of the magnetic anomaly is the third parameter. The fourth and fifth variable parameters are the x and z coordinates of the first variable body point. The sixth and seventh are x and z for the second variable point, and so on up to the last point. As well as variable body points there are fixed body points, the x and z coordinates of which remain unaltered and do not appear in the variable parameter list. There are also related body points, which have a constant relationship in x and z to a variable body point. ($X_r = X_v + C_x$, $Y_r = Y_v + C_y$). Related points are very useful for layers of constant thickness.

For any particular body shape and angle of magnetisation, the magnetisation and background value are linearly related to the amplitude of the anomaly, and these will be found by linear regression in the subroutine if the magnetisation is set to 1.0 and the background is set to 0.0.

The subroutine uses as its base the magnetic anomaly due to a semi-infinite magnetised slab with a sloping face, where the slab goes to infinity on the right hand side of the model. If it is desired that the body should be closed, the last point should be a related

point at the same position as the first point. The order of points should be anticlockwise or the magnetisation should be of the opposite polarity.

Input:

Read by the subroutine on 5:-

EI	Inclination of the Earth's magnetic field.
D	The declination of magnetic north with respect to the positive end of the magnetic profile.
NFP	The number of fixed body points.
NRP	The number of related body points.
NBP	The total number of body points.
NSP	The number of station points at which the magnetic anomaly has been measured.
N	The number of a fixed body point.
XD	The x coordinate of a fixed body point.
ZD	The z coordinate of a fixed body point.
IRP(I)	The number of the Ith related body point.
KP(I)	The number of the body point to which the Ith related point has a constant relationship.
RX(I)	The constant which when added to the x coordinate of the KP(I)th body point will give the x coordinate of the IRP(I)th related point.
RY(I)	The constant which will give the z coordinate of the related point when added to that of KP(I)th body point. (z is positive downwards)
SP(1,L)	The x coordinate of the Lth station point.
SP(2,L)	The height of the Lth station point. (height positive upwards)

AN(L) The value of the magnetic anomaly at the Lth station point.

Output:

Written on 5 when CALL FCN 3 is commanded:-

X(1) The magnetisation contrast.

X(2) The dip of the magnetisation vector.

B The background value of the field.

SP(1,I)

SP(2,I)

AN(I)

CAN(I) Calculated anomaly.

RESID The residual between the calculated and observed anomalies.

BP(1,J) The x coordinate of the Jth body point.

BP(2,J) The z coordination of the Jth body point.

COR The correlation coefficient of the observed and calculated curves.

SD The standard error of the fit.

Written on 7 when CALL FCN 5 is commanded is a list of body point and station point data which can be plotted by GPLOT.

The derivation of a reasonable body shape is aided if the x coordinates of the body points are fixed during the first run of the minimisation routine. This prevents individual points being moved a large amount to try and satisfy the anomaly while the body is still poorly defined.

```
C                              'OPTIMAG'
C
C      EI = INCLINATION OF THE EARTH'S FIELD, D = DECLINATION
C      OF EARTH'S FIELD WITH RESPECT TO THE LINE OF THE
C      PROFILE, NFP = NO OF FIXED POINTS, NRP = NO OF RELATED
C      POINTS, NBP = NO OF BODY POINTS, NSP = NO OF STATION
C      POINTS.
C      N = ID NO OF ITH FIXED POINT, XD = DISTANCE TO POINT,
C      ZD = DEPTH TO POINT.
C      IRP(I) = ID NO OF ITH RELATED POINT, KP( ) = ID NO OF
C      POINT TO WHICH IT IS RELATED, RX(I) = X DISTANCE FROM
C      KP TO IRP, RZ(I) = Z DISTANCE FROM KP TO IRP.
C      SP(1,L) = DISTANCE TO LTH STATION POINT, SP(2,L) =
C      HEIGHT OF LTH STATION POINT, AN(L) = MEASURED ANOMALY
C      AT STATION POINT.
       SUBROUTINE FCN(NPAR,G,F,X,IFLAG)
       DIMENSION G(40),X(40),BP(2,40),NP(40),M(40),SP(2,100),
                                              AN(100),CAN(
     1100),HYP(40),SINT(40),COST(40),RX(20),RY(20),IRP(20),K
                                              P(20)
       DATA BP/40*0./,NP/40*0/
       GO TO (10,20,30,40,50),IFLAG
    10 CONTINUE
       READ(5,12) EI,D,NFP,NRP,NBP,NSP
    12 FORMAT(2F7.2,3I2,I3)
       RAD=1/57.296
       EI=EI*RAD
       D=D*RAD
       SEI=SIN(EI)
       CID=COS(EI)*COS(D)
       NI=NBP-NFP-NRP
       IF(NFP)17,17,13
    13 DO 14 I=1,NFP
       READ(5,16) N,XD,ZD
    16 FORMAT(I2,F8.0,F8.0)
       BP(1,N)=XD
       BP(2,N)=ZD
       NP(N)=N
    14 CONTINUE
    17 IF(NRP.EQ.0) GO TO 117
       DO 114 I=1,NRP
       READ(5,116) IRP(I),KP(I),RX(I),RY(I)
   116 FORMAT(2I2,2F8.0)
       N=IRP(I)
       NP(N)=N
   114 CONTINUE
   117 J=1
       DO 18 I=1,40
       IF(NP(I).EQ.I) GO TO 18
       M(J)=I
       IF(J.EQ.NI) GO TO 19
       J=J+1
    18 CONTINUE
    19 READ(5,15) ((SP(K,L),K=1,2),AN(L),L=1,NSP)
    15 FORMAT(3(F8.0))
       AM=0.
       DO 180 I=1,NSP
   180 AM=AM+AN(I)
       AMM=AM/NSP
```

```
20 CONTINUE
40 CONTINUE
   DO 42 J=1,NI
   K1=2*J+2
   K2=2*J+3
   MI=M(J)
   BP(1,MI)=X(K1)
   BP(2,MI)=X(K2)
42 CONTINUE
   IF(NRP.EQ.0) GO TO 43
   DO 43 I=1,NRP
   J=IRP(I)
   K=KP(I)
   BP(1,J)=BP(1,K)+RX(I)
   BP(2,J)=BP(2,K)+RY(I)
43 CONTINUE
   DIP=X(2)*RAD
   VM=X(1)*SIN(DIP)
   HM=X(1)*COS(DIP)
   B=X(3)
   SUM=0.
   SM=0.
   NO=NBP-1
   DO 44 J=1,NO
   K=J+1
   HYP(J)=SQRT((BP(1,J)-BP(1,K))**2+(BP(2,J)-BP(2,K))**2)
   SINT(J)=(BP(2,K)-BP(2,J))/HYP(J)
   COST(J)=(BP(1,J)-BP(1,K))/HYP(J)
44 CONTINUE
   DO 46 I=1,NSP
   CSUM=0.
   DO 47 J=1,NO
   K=J+1
   ZA=BP(2,J)+SP(2,I)
   XA=BP(1,J)-SP(1,I)
   ZB=BP(2,K)+SP(2,I)
   XB=BP(1,K)-SP(1,I)
   RA=XA**2+ZA**2
   RB=XB**2+ZB**2
   TA=XA/ZA
   TB=XB/ZB
   TD=TA-TB
   TS=1+TA*TB
   PH=ATAN2(TD,TS)
   PLOG=0.5*ALOG(RB/RA)
   CO=COST(J)
   SI=SINT(J)
   E1=PH*CO+PLOG*SI
   E2=PH*SI-PLOG*CO
   CSUM=CSUM+2000CO*SI*(VM*(E1*CID-E2*SEI)+HM*(E2*CID+E1*
                                              SEI))
47 CONTINUE
   SUM=SUM+(CSUM+B-AN(I))**2
   CAN(I)=CSUM+B
   SM=SM+CSUM
46 CONTINUE
   IF(X(1)-1) 49,48,48
49 CM=SM/NSP
   TOP=0.
   BOT=0.
```

```
      DO 480 I=1,NSP
      CA=(CAN(I)-CM)
      TOP=TOP+CA*(AN(I)-AMM)
  480 BOT=BOT+CA**2
      FAC=TOP/BOT
      B=AMM-FAC*CM
      SUM=0.
      DO 481 I=1,NSP
      CAN(I)=FAC*CAN(I)+B
  481 SUM=SUM+(CAN(I)-AN(I))**2
   49 F=SUM/(NSP-1)
      RETURN
   30 CONTINUE
      IF(X(1).EQ.1) X(1)=FAC
      WRITE(6,32) X(1),X(2),B
   32 FORMAT(1H1,'MAGNETISATION CONTRAST = ',F8.6/1H ,'ANGLE
                                                 OF MAGNETIS
     1ATION = ',F7.2/1H ,'BACKGROUND VALUE = ',F8.2///1HO,'S
                                                 TATION POINT
     2S'/1H ,'    X          Z       OBSERVED  COMPUTED  RESIDU
                                                 AL'/)
      SUB=0.
      SUC=0.
      CHI=0.
      DO 36 I=1,NSP
      RESID=CAN(I)-AN(I)
      SUB=SUB+AN(I)
      CHI=CHI+RESID**2/ABS(CAN(I)-B)
      SUC=SUC+CAN(I)
      WRITE(6,34) SP(1,I),SP(2,I),AN(I),CAN(I),RESID
   34 FORMAT(1H ,4(F8.3,2X),F7.3)
   36 CONTINUE
      WRITE(6,39)
   39 FORMAT(1HO,'BODY POINTS'/ 1H ,'    X          Z     '/)
      WRITE(6,38) ((BP(I,J),I=1,2),J=1,NBP)
   38 FORMAT(2(F8.3,2X))
      SUB=SUB/NSP
      SUC=SUC/NSP
      CD1=0.
      CD2=0.
      CN=0.
      DO 37 J=1,NSP
      ACB=AN(J)-SUB
      ACC=CAN(J)-SUC
      CN=CN+ACB*ACC
      CD1=CD1+ACB**2
      CD2=CD2+ACC**2
   37 CONTINUE
      COR=CN/(CD1*CD2)**0.5
      SD=SQRT(SUM/(NSP-1))
      WRITE(6,70) COR,CHI,SD
   70 FORMAT(1HO,'CORRELATION COEFFICIENT =',F6.3/1H ,'CHI S
                                                 QUARE VALUE
     1=',F8.3/1H ,'STANDARD DEVIATION =',F8.3)
      RETURN
   50 WRITE(7,52) NSP
   52 FORMAT(I3)
      WRITE(7,54) (SP(1,I),AN(I),CAN(I),I=1,NSP)
   54 FORMAT(3F8.3)
      WRITE(7,56) NBP
```

```
56 FORMAT(I3)
   WRITE(7,58) ((BP(I,J),I=1,2),J=1,NBP)
58 FORMAT(2F8.3)
   RETURN
   END
```

Appendix C4.3

A subroutine written in FORTRAN IV, for use with MINUIT, to find the shapes of n two dimensional body-models that will give the best fit of the calculated magnetic anomaly to the observed magnetic anomaly. (Total intensity anomaly). This is similar to the program described in appendix C4.2, only it is written to compute the magnetic anomaly caused by n closed (discrete) magnetised bodies. As written the program will handle up to 5 bodies. The program automatically closes the body, so the first point does not need to be respecified as the last point, but the number of points specified for each body must be one larger than the number of body point positions. This program is useful for calculating the effect of several nearby bodies or a large multiple body of several differently magnetised parts. The input for variable parameters is the same as for C4.2 except that magnetisation and dip for the bodies take up the first n x 2 variables and the background occupies the n x 2 + 1 th variable.

Input:

Read by the subroutine on 5, is the same as for C4.2 with the following additions:-

NB — The number of bodies.

LP(I) — The number of the last point on the Ith body. The body points should be numbered sequentially through all the bodies (ie. not a separate list for each body) and the last numbered point on each body should be at the first point on it (i.e. the first point will have two numbers).

Output:

Written on 6 and 7, is the same as for C4.2 with the addition of the magnetisation value and dip of the magnetisation vector for each of the bodies.

```
C                              'CB-OPTIMAG'
C
C     EI = INCLINATION OF THE EARTH'S FIELD, D = DECLINATION
C     OF EARTH'S FIELD WITH RESPECT TO THE LINE OF THE
C     PROFILE, NFP = NO OF FIXED POINTS, NRP = NO OF RELATED
C     POINTS, NBP = NO OF BODY POINTS, NSP = NO OF STATION
C     POINTS.
C     NB = NO OF BODY POINTS
C     LP(I) = ID NO OF LAST POINT OF ITH BODY.
C     N = ID NO OF ITH FIXED POINT, XD = DISTANCE TO POINT,
C     ZD = DEPTH TO POINT.
C     IRP(I) = ID NO OF ITH RELATED POINT, KP( ) = ID NO OF
C     POINT TO WHICH IT IS RELATED, RX(I) = X DISTANCE FROM
C     KP TO IRP, RZ(I) = Z DISTANCE FROM KP TO IRP.
C     SP(1,L) = DISTANCE TO LTH STATION POINT, SP(2,L) =
C     HEIGHT OF LTH STATION POINT, AN(L) = MEASURED ANOMALY
C     AT STATION POINT.
      SUBROUTINE FCN(NPAR,G,F,X,IFLAG)
      DIMENSION G(60),X(60),BP(2,30),NP(30),N(30),SP(2,100),
                                            AN(100),CAN(
     1100),RYP(30),SINT(30),COST(30),LP(5),NLP(5),IRP(20),KP
                                            (20),RX(20),
     2RY(20)
      DATA BP/60*0./,NP/30*0/,CAN/100*0./,NLP/5*0/
      GO TO (10,20,30,40,50),IFLAG
   10 CONTINUE
      READ(5,12) EI,D,NB,NFP,NRP,NBP,NSP
   12 FORMAT(2F7.2,4I2,I3)
      RAD=1/57.296
      EI=EI*RAD
      D=D*RAD
      SEI=SIN(EI)
      CID=COS(EI)*COS(D)
      NI=NBP-NFP-NRP
      READ(5,11) (LP(I),I=1,NB)
   11 FORMAT(5I2)
      IF(NFP)17,17,13
   13 DO 14 I=1,NFP
      READ(5,16) N,XD,ZD
   16 FORMAT(I2,F8.0,F8.0)
      BP(1,N)=XD
      BP(2,N)=ZD
      NP(N)=N
      DO 114 K=1,NB
      IF(N-LP(K)) 115,115,114
  115 NLP(K)=NLP(K)+1
      GO TO 14
  114 CONTINUE
   14 CONTINUE
   17 IF(NRP.EQ.0) GO TO 118
      DO 117 I=1,NRP
      READ(5,116) IRP(I),KP(I),RX(I),RY(I)
  116 FORMAT(2I2,2F8.0)
      N=IRP(I)
      NP(N)=N
      DO 119 K=1,NB
      IF(N.GT.LP(K)) GO TO 119
      NLP(K)=NLP(K)+1
      GO TO 117
```

```
119 CONTINUE
117 CONTINUE
118 J=1
    DO 18 I=1,30
    IF(NP(I).EQ.I) GO TO 19
    M(J)=I
    J=J+1
 18 CONTINUE
 19 READ(5,15) ((SP(K,L),K=1,2),AN(L),L=1,NSP)
 15 FORMAT(3(F8.0))
    KP=NB*2+1
 20 CONTINUE
 40 CONTINUE
    B=X(KP)
    SUM=0.0
    L1=1
    LB=1
    IB=0
    DO 41 IT=1,NB
    IB=IB+NLP(IT)
    J2=IT*2
    J1=J2-1
    LT=LP(IT)-IB
    DO 42 J=LB,LT
    JI=J
    IF(J.EQ.LT) JI=LP
    K1=2*JI+2*NB+2-2*IT
    K2=K1+1
    MI=M(J)
    BP(1,MI)=X(K1)
    BP(2,MI)=X(K2)
 42 CONTINUE
    LB=LT+1
 41 CONTINUE
    IF(NPP.EQ.0) GO TO  435
    DO 43 I=1,NPP
    I1=IRP(I)
    I2=KP(I)
    BP(1,I1)=BP(1,I2)+RX(I)
    BP(2,I1)=BP(2,I2)+RY(I)
 43 CONTINUE
435 DO 45 IT=1,NB
    J2=IT*2
    J1=J2-1
    NC=LP(IT)-1
    DIP=X(J2)*RAD
    VM=X(J1)*SIN(DIP)
    HM=X(J1)*COS(DIP)
    DO 44 J=L1,NC
    K=J+1
    HYP(J)=SQRT((BP(1,J)-BP(1,K))**2+(BP(2,J)-BP(2,K))**2)
    SINT(J)=(BP(2,K)-BP(2,J))/HYP(J)
    COST(J)=(BP(1,J)-BP(1,K))/HYP(J)
 44 CONTINUE
    DO 46 I=1,NSP
    IF(IT.EQ.1) CAN(I)=0.
    CSUM=0.
    DO 47 J=L1,NC
    K=J+1
    ZA=BP(2,J)+SP(2,I)
```

```
      XA=BP(1,J)-SP(1,I)
      ZB=BP(2,K)+SP(2,I)
      XB=BP(1,K)-SP(1,I)
      RA=XA**2+ZA**2
      RB=XB**2+ZB**2
      TA=XA/ZA
      TB=XB/ZB
      TD=TA-TB
      TS=1+TA*TB
      PH=ATAN2(TD,TS)
      PLOG=0.5*ALOG(RB/RA)
      CC=COST(J)
      SI=SINT(J)
      E1=PH*CC+PLOG*SI
      E2=PH*SI-PLOG*CO
      CSUM=CSUM+200000*SI*(VM*(E1*CIC-E2*SEI)+HM*(E2*CIC+E1*
                                                 SEI))
   47 CONTINUE
      CAN(I)=CSUM+CAN(I)
   46 CONTINUE
      L1=NO+2
   45 CONTINUE
      DO 48 I=1,NSP
      CAN(I)=CAN(I)+B
      SUM=SUM+(CAN(I)-AN(I))**2
   48 CONTINUE
      F=SUM/(NSP-1)
      RETURN
   30 CONTINUE
      DO 33 K=1,NB
      L1=2*K-1
      L2=2*K
      WRITE(6,31) K,X(L1),X(L2)
   31 FORMAT(1HO,'BODY',I2/1H ,'MAGNETISATION CONTRAST = ',F
                                                 8.6/1H ,'ANG
     1LE OF MAGNETISATION = ',F7.2/)
   33 CONTINUE
      WRITE(6,32) B
   32 FORMAT(1HC/,'BACKGROUND VALUE = ',F8.3///'STATION POIN
                                                 TS'/1H ,'
     1 X          Z       OBSERVED  CALCULATED  RESIDUAL'/)
      SUB=0.
      SUC=0.
      CHI=0.
      DO 36 I=1,NSP
      RESID=CAN(I)-AN(I)
      SUB=SUB+AN(I)
      SUC=SUC+CAN(I)
      CHI=CHI+RESID**2/(ABS(AN(I))+1)
      WRITE(6,34) SP(1,I),SP(2,I),AN(I),CAN(I),RESID
   34 FORMAT(1H ,4(F8.3,2X),F7.3)
   36 CONTINUE
      WRITE(6,39)
   39 FORMAT(1HO,'BODY POINTS'/ 1H ,'    X          Z     '/)
      WRITE(6,38) ((BP(I,J),I=1,2),J=1,NBP)
   38 FORMAT(2(F8.3,2X))
      SUB=SUB/NSP
      SUC=SUC/NSP
      CD1=0.
      CD2=0.
```

```
      CN=0.
      DO 37 J=1,NSP
      ACB=AN(J)-SLB
      ACC=CAN(J)-SUC
      CN=CN+ACB*ACC
      CD1=CD1+ACB**2
      CD2=CD2+ACC**2
   37 CONTINUE
      COR=CN/(CD1*CD2)**0.5
      SD=SQRT(SUM/(NSP-1))
      WRITE(6,70) COR,CHI,SD
   70 FORMAT(1HO,'CORRELATION COEFFICIENT =',F6.3/1H ,'CHI S
                                                  QUARE VALUE
     1=',F8.3/1H ,'STANDARD DEVIATION =',F8.3)
      GO TO 40
   50 WRITE(7,52) NSP
   52 FORMAT(I3)
      WRITE(7,54) (SP(1,I),AN(I),CAN(I),I=1,NSP)
   54 FORMAT(3F8.3)
      WRITE(7,56) NBP
   56 FORMAT(I3)
      WRITE(7,58) ((BP(I,J),I=1,2),J=1,NBP)
   58 FORMAT(2F8.3)
      RETURN
      END
```

Appendix C4.4

A subroutine written in FORTRAN IV, using MINUIT, to find the best fit between the computed gravity anomaly due to one or more body-models and the observed gravity anomaly. The program uses as its base the gravitational effect of a semi-infinite slab with a sloping end going to infinity towards the right hand side of the model (i.e. positively).

The first n variables in the variable parameter list are the density contrasts of the n bodies. The x and y coordinates of the body points then follow, but they need not start from the n + 1th variable parameter. A space may be left to insert the density contrasts for additional bodies should they be required. When defining bodies the last point of the body should be in the same position or at the same depth as the first one, unless the addition of the effect of a semi-infinite slab, the thickness of which is the difference in depth, is desired. Body-points should be numbered sequentially through the total number of bodies.

Input:

Read by the subroutine on 5:-

NL	The number of bodies.
NFP	The number of fixed points. (Those which can never vary).
NRP	The number of related points. (Those which have a constant relationship to a variable point.)
NBP	The total number of body-points.
NSP	The number of station points.

LP(I)	The number of the last point of the Ith body.
N	The number of a fixed point.
XD	The x coordinate of a fixed point.
ZD	The z coordinate of a fixed point.
INP(I)	The number of the Ith related point.
IRP(I)	The number of the point with which the related point has a constant relationship.
RX(I)	The relationship in x between the related point and the point to which it is related. ($X_{INP(I)} = X_{IRP(I)} + RX(I)$)
RZ(I)	The contrast in z relating the INP(I)th point to the IRP(I)th point. ($Z_{INP(I)} = Z_{IRP(I)} + RZ(I)$) (x is positive to the right, z is positive downwards)
NP(I)	The number of the Ith variable point.
NX(I)	The variable parameter number which gives the value of the x coordinate for the Ith variable point. (i.e. the NP(I)th point.)
NZ(I)	The variable parameter number which gives the z coordinate of the Ith variable point.
D(I)	The distance to the Ith station point.
Z(I)	The height of the Ith station point. (height positive up)
A(I)	The value of the measured gravity anomaly at the Ith point.

Output:

Written on 6 when CALL FCN 3 is commanded:-

D(J)

Z(J)

A(J)

C(J)	Computed gravity anomaly at the Jth station point.
RESID	The residual between the computed and the observed gravity anomalies at the Jth station point.
J	Number of body.
X(J)	The density contrast of the Jth body.
J	Body-point number.
BX(J)	The x coordinate of the Jth body-point.
BX(J)	The z coordinate of the Jth body-point.
J	Number of body.
LP(J)	The number of the last point on the Jth body.
SE	The standard error of the fit of the computed anomaly to the observed anomaly.
COR	The coefficient of correlation between the observed and computed curves.

Written on 7 is a list of the above data which can be plotted by GPLOT.

A listing of the input data for a run of

OPTIGRAV with MINUIT.

PARAMETER NUMBERS

NAME | INITIAL VALUE | ESTIMATED ERROR OR STEP SIZE | LOWER LIMIT | UPPER LIMIT

VARIABLE PARAMETER LIST

	NAME	INITIAL VALUE	ESTIMATED ERROR OR STEP SIZE	LOWER LIMIT	UPPER LIMIT
1	EC1				
2	EC2				
3	EC3				
4	X1				
5	Z1				
6	X2				
7	Z2				
8	X3				
9	Z3				
10	X4				
11	Z4				
12	X5				
13	Z5				
14	X7				
15	Z7				
16	X8				
17	Z8				
18	X9				
19	Z9				
20	X10				
21	Z10				
22	X12				
23	Z12				
24	X13				
25	Z13				
26	X14				
27	Z14				
28	X15				
29	Z15				
30	X16				
31	Z16				

NB NFP NRP NBP NTP

LAST POINTS OF BODIES

FIXED POINTS

RELATED POINT

VARIABLE POINTS

STATION POINTS

57	13[illegible]	[illegible].7	STATION POINTS
58	14[illegible]	[illegible].2	
59	15[illegible]	1[illegible].2	
60	164.[illegible]	[illegible].2	
61	17[illegible]	[illegible]3.[illegible]	
62	181.[illegible]	57.[illegible]	
63	191.3	[illegible]	
64	2[illegible]	7[illegible].1	
65	2[illegible]	[illegible]	
66			
67	CALL FCN	3	COMMANDS
68	FIX	4	PARAMETER FIXED
69	FIX	6	
70	FIX	[illegible]	
71	FIX	10	
72	FIX	14	
73	FIX	18	
74	FIX	24	
75	FIX	26	
76	TAURCS	[illegible]	MINIMISATION ROUTINE
77	CALL FCN	[illegible]	
78	RESTORE		FIXED PARAMETERS RELEASED
79	TAURCS	[illegible]	
80	CALL FCN	[illegible]	OUTPUT LIST
81	CALL FCN	5	GRAPH OUTPUT
82	EXIT		

END OF FILE

```
C                              'OPTIGRAV'
C
C     NL = NO OF LAYERS.  NFP = NO OF FIXED POINTS.
C     NRP = NO OF RELATED POINTS.  NO OF BODY POINTS.
C     NSP = NO OF STATION POINTS.
C     LP(I) = ID NO OF LAST POINT OF ITH BODY.
C     N = ID NO OF ITH FIXED POINT, XD= X VALUE,.ZD=Z VALUE
C     INP(I) = ID NO OF ITH RELATED POINT. IRP(I) = ID NO OF
C     POINT TO WHICH IT IS RELATED. RX(I) = RELATION IN X
C     DIRECTION. RZ(I) = RELATION IN Z DIRECTION.
C     NP(I) = ID NO OF ITH VARIABLE POINT, NX(I) = ARRAY
C     INDEX OF X VALUE, NZ(I) = ARRAY INDEX OF Z VALUE.
C     D(I) = DISTANCE TO ITH STATION POINT, Z(I) = HEIGHT OF
C     STATION POINT, A(I) = MEASURED ANOMALY.
      SUBROUTINE FCN(NPAR,G,F,X,IFLAG)
      DIMENSION G(60),X(60),D(100),Z(100),A(100),C(100),BX(8
                                                  0),BZ(80),
     1LP(10),NP(80),NX(80),NZ(80),INP(60),IRP(60),RX(60),RZ(
                                                  60),SB(80),
     2CB(80)
      GO TO (10,20,30,40,50),IFLAG
   10 READ(5,11)NL,NFP,NRP,NBP,NSP
   11 FORMAT(4I2,I3)
      READ(5,12),(LP(I),I=1,NL)
   12 FORMAT(10I2)
      IF (NFP)111,111,110
  110 DO 14 I=1,NFP
      READ(5,15) N,XD,ZD
   15 FORMAT(I2,F8.0,F8.0)
      BX(N)=XD
      BZ(N)=ZD
   14 CONTINUE
  111 IF(NRP) 113,113,112
  112 READ(5,17) (INP(I),IRP(I),RX(I),RZ(I),I=1,NRP)
   17 FORMAT(2I2,2F8.0)
  113 K=NBP-NFP-NRP
      READ(5,16) (NP(I),NX(I),NZ(I),I=1,K)
   16 FORMAT(3I2)
      READ(5,18) (D(I),Z(I),A(I),I=1,NSP)
   18 FORMAT(3F8.0)
   20 CONTINUE
   40 F=0.
      DO 401 IN=1,K
      IP=NP(IN)
      IX=NX(IN)
      IZ=NZ(IN)
      BX(IP)=X(IX)
      BZ(IP)=X(IZ)
  401 CONTINUE
      IF(NRP) 411,411,412
  412 DO 402 IN=1,NRP
      IP=INP(IN)
      IR=IRP(IN)
      BX(IP)=BX(IR)+RX(IN)
      BZ(IP)=BZ(IR)+RZ(IN)
  402 CONTINUE
  411 DO 451 IB=1,NL
      IL=IB-1.
      IF(IL) 452,452,453
```

```
452 L1=1
    GO TO 454
453 L1=LP(IL)+1
454 L2=LP(IB)-1
    DO 451 JB=L1,L2
    JL=JB+1
    BZB=BZ(JL)-BZ(JB)
    BXB=BX(JB)-BX(JL)
    H=SQRT(BXB*BXB+BZB*BZB)
    SB(JB)=BZB/H
    CB(JB)=BXB/H
451 CONTINUE
    DO 41 I=1,NSP
    DS=D(I)
    ZS=Z(I)
    SUM=0.
    L1=1
    DO 42 KI=1,NL
    DC=X(KI)
    L2=LP(KI)-1
    U1=BX(L1)-DS
    V1=BZ(L1)-ZS
    R1=SQRT(U1*U1+V1*V1)
    A1=ATAN2(V1,U1)
    DO 43 J=L1,L2
    J1=J+1
    U2=BX(J1)-D(I)
    V2=BZ(J1)-Z(I)
    R2=SQRT(V2*V2+U2*U2)
    A2=ATAN2(V2,U2)
    SI=SB(J)
    CO=CB(J)
    SUM=SUM+DC*(A2*V2-A1*V1-(U1*SI+V1*CO)*(SI*ALOG(R2/R1)+
                                          CO*(A2-A1)))
    V1=V2
    U1=U2
    A1=A2
    R1=R2
43  CONTINUE
    L1=L2+2
42  CONTINUE
    DG=SUM*13.334
    C(I)=DG
    F=F+(DG-A(I))**2
41  CONTINUE
    F=F/(NSP-1)
    RETURN
30  WRITE(6,31)
31  FORMAT(1H1,4X,'X',9X,'Z',7X,'ANOM',7X,'CALC',7X,'RESID
                                                    '/)
    RQ=0
    SA=0
    SC=0
    DO 300 J=1,NSP
    RESID=A(J)-C(J)
    SA=SA+A(J)
    SC=SC+C(J)
    RQ=RQ+RESID*RESID
    WRITE(6,32) D(J),Z(J),A(J),C(J),RESID
32  FORMAT(1H ,1X,F8.3,2X,F8.3,2X,F8.2,2X,F8.2,2X,F8.2)
```

```
300 CONTINUE
    WRITE(6,33) (J,X(J),J=1,NL)
 33 FORMAT(1HO/5X,'DENSITY CONTRAST  LAYER',I2,' =',F6.3)
    WRITE(6,34)
 34 FORMAT(1HO//5X,'BODY POINTS',/4X,'X',9X,'Z'/)
    WRITE(6,36) (J,BX(J),BZ(J),J=1,NBP)
 36 FORMAT(1H ,I2,2X,F8.3,2X,F8.3)
    WRITE(6,38)
 38 FORMAT(1HO/5X,'LAST POINT OF EACH LAYER'/)
    WRITE(6,39) (J,LP(J),J=1,NL)
 39 FORMAT(1H ,I2,' = ',I2)
    SAM=SA/NSP
    SCM=SC/NSP
    SE=SQRT(RQ/(NSP-1))
    AC=0
    A2=0
    C2=0
    DO 350 J=1,NSP
    DA=A(J)-SAM
    DC=C(J)-SCM
    AC=AC+DA*DC
    A2=A2+DA*DA
    C2=C2+DC*DC
350 CONTINUE
    COR=AC/SQRT(A2*C2)
    WRITE(6,37) SE,COR
 37 FORMAT(1HO/'STANDARD ERROR =',F8.3/'CORRELATION COEFFI
                                       CIENT =',F7.
   14)
    RETURN
 50 WRITE(7,52) NSP,(D(I),A(I),C(I),I=1,NSP)
 52 FORMAT(I3/(F8.3,2F8.2))
    NNBP=NBP+NL
    WRITE(7,54) NNBP
 54 FORMAT(I3)
    K=1
    DO 60 I=1,NL
    L=LP(I)
    DO 59 J=K,L
    WRITE(7,56) BX(J),BZ(J)
 56 FORMAT(2F8.3)
 59 CONTINUE
    WRITE(7,56) BX(K),BZ(K)
    K=LP(I)+1
 60 CONTINUE
    RETURN
    END
```

Appendix C4.5

A program to calculate the coefficient of correlation between the pseudo-gravity anomaly, derived from the magnetic anoamly and the Bouguer gravity anomalies for densities of 2.0 and 2.67 gm cm^{-3}. The pseudo anomaly is also regressed on to the Bouguer anomaly to find the ratio of magnetisation contrast to density contrast.

Input:

Read on 5:-

NF	The number of the first data point to be included in the calculation of the correlation coefficient.
NL	The number of the last point included in the calculation.
NP	The number of data points read in.
Y(4,J)	The magnetic value of the Jth point. (J = NP - I +1)
FG	The free-gravity value.
YG	The Bouguer gravity value (2.0 gm cm^{-3}).

Read on 7 the output of TR/MG:-

X(I)	The distance to the Ith point.
Y(1,I)	The value of the pseudo gravity anomaly at the Ith point.

Output:

Written on 6:-

CORB	The correlation coefficient for the 2.0 Bouguer anomaly.
CORC	The correlation coefficient for the 2.67 Bouguer anomaly.
FB	Ratio density contrast: magnetisation contrast (2.0 anomaly).
FC	Ratio density contrast: magnetisation contrast (2.67 anomaly).
BF	Ratio magnetisation contrast: density contrast (2.0 anomaly).

CF	Ratio magnetisation contrast: density contrast (2.67 anomaly).
DB	The constant for factor FB.
DC	The constant for factor FC.
BD	The constant for factor BF.
CD	The constant for factor CF.

The subroutine GPLOTV gives a computer drawn graph. If PLOTV is used a graph on the lineprinter can be obtained.

```
C       COMPUTES CORRELATION COEFFICIENT AND DOES LINEAR
C       REGRESSION. BETWEEN GRAVITY AND MAGNETICS TRANSFORM.
C       INPUT ON 5: NF = NO OF FIRST DATA POINT TO BE COMPARED
C       NL = NO OF LAST POINT TO BE COMPARED. NP = TOTAL NO OF
C       POINTS. Y(4,J) = MAGNETIC ANOMALY VALUE AT JTH POINT,
C       FG = FREE AIR GRAVITY ANOMALY, YG = BOUGUER ANOMALY.
C       FOR DENSITY 2.0.
C       INPUT ON 7: X(I) = DISTANCE TO JTH POINT ,Y(1,I) =
C       MAGNETICS-GRAVITY  TRANSFORM VALUE.
        DIMENSION X(300),Y(4,300),FY(4),B(4),TITLE(10),XUN(3),
                                              YUN(3,4)
        DATA TITLE/'MAGNETICS-GRAVITY TRANSFORM COMPARISON '/,
                                              XUN/'TENS OF
       1 KM   '/,YUN/'TRANSFM MGALMAG.  GAMMASBA 2.0 MGAL BA 2.
                                              67 MGAL'/
        DATA AM,BM,CM,BS,CS,ASQ,BSQ,CSQ,SAB,SAC,SAQ,SBQ,SCQ/13
                                              *0.0/
       1FY(1)=0.02
        FY(2)=0.02
        FY(3)=0.02
        FY(4)=0.02
        B(1)=300.0
        B(2)=300.0
        B(3)=300.0
        B(4)=100.0
        READ(5,2) NF,NL,NP
      2 FORMAT(3I3)
        READ(7,4) (X(I),Y(1,I),I=1,NP)
      4 FORMAT(F10.4,2X,F10.4)
        NC=0
        DO 10 I=1,NP
        X(I)=X(I)/10.0
        J=NP-I+1
        READ(5,6) Y(4,J),FG,YG
      6 FORMAT(58X,F5.0,2F7.0)
        IF(YG.EQ.0) NC=NC-1
        Y(2,J)=YG
        Y(3,J)=FG+(YG-FG)*1.63/0.96
     10 CONTINUE
        DO 15 J=NF,NL
        AM=AM+Y(1,J)
        BM=BM+Y(2,J)
        CM=CM+Y(3,J)
     15 CONTINUE
        NO=NL-NF+1
        AMM=AM/NO
        BMM=BM/(NC+NC)
        CMM=CM/(NC+NC)
        DO 20 I=NF,NL
        R=Y(1,I)
        S=Y(2,I)
        T=Y(3,I)
        IF(S) 12,20,12
     12 BS=BS+(R-AMM)*(S-BMM)
        CS=CS+(R-AMM)*(T-CMM)
        ASQ=ASQ+(R-AMM)**2
        BSQ=BSQ+(S-BMM)**2
        CSQ=CSQ+(T-CMM)**2
        SAB=SAB+R*S
```

```
      SAC=SAC+R*T
      SAQ=SAQ+R**2
      SBQ=SBQ+S**2
      SCQ=SCQ+T**2
   20 CONTINUE
      CORB=BS/SQRT(ASQ*BSQ)
      CORC=CS/SQRT(ASQ*CSQ)
      FB=BS/ASQ
      FC=CS/ASQ
      BF=BS/BSQ
      CF=CS/CSQ
      DB=BMM-FB*AMM
      DC=CMM-FC*AMM
      BD=AMM-BF*BMM
      CD=AMM-CF*CMM
      WRITE(6,30) CORB,CORC,FB,FC,BF,CF,DB,DC,BD,CD
   30 FORMAT(1H1,'CORRELATION COEFFICIENT B =',F7.4/1H ,'CORRELATION COE
     1FFICIENT C =',F7.4/1H ,'FACTORS B/A,C/A,A/B,A/C ',4F10.4/1H ,'CONS
     2TANTS                  ',4F10.4)
      J=2
      D=DB
      F=FB
      IF(CORB-CORC) 38,39,39
   38 D=DC
      F=FC
      J=3
   39 DO 40 I=1,NP
   40 Y(1,I)=Y(1,I)*F+D
      CHI=0.
      DO 50 I=NF,NL
      IF(Y(J,I)) 51,50,51
   51 CHI=CHI+(Y(J,I)-Y(1,I))**2/ABS(Y(1,I)-AMM)
   50 CONTINUE
      NDF=NO+NC-1
      WRITE(6,45) CHI,NDF
   45 FORMAT(1HO,'CHI SQUARE VALUE =',F8.3/1H ,'DEGREES OF FREEDOM =',I3
     1)
      CALL GPLOTV(X,Y,4,NP,0.7876,FY,B,TITLE,XUN,YUN)
      STOP
      END
```

Appendix C5.1

A program written in FORTRAN IV, to compute the gravity anomalies resulting from the thermal expansion of rock in the region of a temperature anomaly. From the average temperature over a square area the change in the mass of the area is calculated from density and coefficient of thermal expansion data. The mass difference is taken as the mass per unit length of an infinitely long line mass. From the effect of all the line masses the gravity anomaly is calculated.

Input:

Read on 5:-

TITLE	Up to 40 identifying characters.
LOP	An indicator which if set to 0 will cause the graph output to be omitted. Otherwise a graph is drawn.
NP	The number of square areas over which the average temperature anomaly has been determined.
XS	The distance to the first point at which the anomaly is to be calculated.
XE	The distance to the last point at which the anomaly is to be calculated.
DX	The distance between points at which the anomaly is to be calculated.
X(I)	The x coordinate of the centre of the Ith square.
Z(I)	The z coordinate of the centre of the Ith square.
A(I)	The area of the Ith square.
P(I)	The density of the Ith square before heating.
T(I)	The average temperature anomaly over the Ith square.

Output:

Written on 6:-

X(I)

Z(I)

A(I)

P(I)

T(I)

XO Distance to a point at which the value of the anomaly has been calculated.

AG The gravity anomaly at the point at XO.

GPLOTV plots the graph of the gravity anomaly.

```
C     THIS PROGRAM COMPUTES THE GRAVITY ANOMALIES DUE TO THE
                                                RMAL
C     EXPANSION.
C     TITLE IS A NAME OF UP TO 40 CHARACTERS :  LOP IS AN IN
                                                DICATOR IF
C     SET TO 1 A GRAPH IS IS PLOTTED AND THE PROGRAM MUST BE
                                                 RUN WITH
C     GPLOTV, IF LOP IS SET TO 0 NO GRAPH IS PLOTTED : NP IS
                                                 THE NUMBER
C     OF DATA INPUT POINTS : XS IS THE FIRST X VALUE OF THE
                                                 POINTS AT
C     WHICH THE GRAVITY ANOMALY IS TO BE COMPUTED, AND XE IS
                                                 THE LAST.
C     DX IS THE SPACING BETWEEN POINTS :
C     INPUT DATA :-  X(I) X VALUE OF POINT,  Y(I) Y VALUE,
                                                A(I)  AREA
C     ABOUT POINT OVER WHICH THE ANOMALY IS AVERAGED,  P(I)
                                                AVERAGE
C     DENSITY AT POINT BEFORE HEATING,  T(I) TEMPERATURE ANO
                                                MALY.
      DIMENSION X(300),Z(300),A(300),P(300),T(300),D(200),G(
                                                200),TITLE(1
     10),YUN(3,1),XUN(3),B(1),YF(1)
      DATA XUN/'TENS OF KM  '/,YUN/'ANOMALY MGAL'/
      READ(5,1) TITLE
    1 FORMAT(10A4)
      READ(5,2) LOP,NP,XS,XE,DX
    2 FORMAT(I1,1X,I3,3F10.0)
      READ(5,4) (X(I),Z(I),A(I),P(I),T(I),I=1,NP)
    4 FORMAT(5F10.0)
      WRITE(6,6) (X(I),Z(I),A(I),P(I),T(I),I=1,NP)
    6 FORMAT(1H1,'TEMPERATURE ANOMALY MODEL'/'      X
                                                  Z     BLOCK
     1AREA  DENSITY  D TEMP.'/(2F10.3,F10.1,2F10.3))
      WRITE(6,7)
    7 FORMAT(1H1,'      X       ANOM.'/)
      L=(XE-XS)/DX+1
      XO=XS
      DO 10 I=1,L
      AG=0.
      DO 20 J=1,NP
      ZD=Z(J)
      C=(3.6-ZD*0.0018)*0.00001
      AG=AG+13334.*P(J)*ZD*(1/(1+C*T(J))-1)/((ZD*ZD)+(X(J)-X
                                                 O)**2)
   20 CONTINUE
      WRITE(6,16) XO,AG
   16 FORMAT(F10.3,F8.2)
      D(I)=XO*0.1
      G(I)=AG
      XO=XO+DX
   10 CONTINUE
      IF(LOP.EQ.0) GO TO 40
      XF=0.07874
      YF(1)=0.02
      B(1)=300.0
      CALL GPLOTV(D,G,1,L,XF,YF,B,TITLE,XUN,YUN)
   40 STOP
      END
```

Appendix C6.1

A program written in FORTRAN IV, to do rolling mean (two dimensional moving average) analysis and produce a map of the magnitude of the quantities analysed. A circle of chosen radius is moved over the area with its centre located at a regular grid of points. The values falling within the circle are meaned and the mean value assigned to the grid point at the circle centre. The program as listed is adapted specifically to give maps of average earthquake depth and average energy release. A line printer map is produced as output, but this is over elongated down the page because of the character spacing. Output on another file can be read by a plotter program (not listed here) to produce a true scale map and superimpose it on to geographic features.

Input:

Read on 5:-

GX	The x coordinate of the bottom left hand corner of the map.
GY	The y coordinate of the bottom left hand corner of the map.
XM	The maximum x value.
YM	The maximum y value.
GS	The distance between the grid points at which values of the map function will be calculated.
CR	The radius of the sample circle.
CI(I)	The contour interval for the Ith quantity.
NF	The number of quantities to be mapped (up to 3). (2 in this case)
YN	The number of years over which the data has been collected.

X The x coordinate of a data point. If x is greater than 999999, the end of the data input is signified.

Y The y coordinate of a data point.

F The value of the first quantity at a data point. In this case the focal depth of an earthquake.

G The value of the second quantity at a data point. In this case the body wave magnitude of an earthquake.

H The value of the third quantity at a data point. Not used here.

Ouput:

Written on 6:-

FM The mean value of the first quantity.

DF The standard error of the first quantity.

GM The mean of the second quantity.

DF The standard error of the second quantity.

HM The mean of the third quantity.

DH The standard error of the third quantity.

A line printed map for the first quantity (Average hypocentral depth).

A line printed map for the second quantity (Log of the average energy release per unit area square per year).

A map for the third quantity is not produced when the program is run for earthquakes.

A line printed map showing the sample density divided by 10.

MX The number of x coordinates across the map.

MY The number of y coordinates.

GS

CR

Written on 8 are the maps, which can be read for plotting on a plotter to true relative scale.

```
      DIMENSION A(3,200,100),IX(200,100),P(110),CHAR(44),IS(
     1                                                100),CI(3)
      DATA A/60000*0./,IX/20000*0/,P/110*'    '/,CHAR/'A   '
     1                                              ,'A   ','B
     1 ','B   ','C   ','C   ','D   ','D   ','E   ','E   ','F
     2                                              ','F   ',
     2'G   ','G   ','H   ','I   ','J   ','K   ','L   ','M
     3                                              ','N   ','O
     3  ','P   ','Q   ','R   ','S   ','T   ','T   ','U   ','
     4                                            U   ','V   '
     4,'V   ','W   ','W   ','X   ','X   ','Y   ','Y   ','Z
     5                                              ','Z   ','Z
     5   ','    ','-   ','+   '/
      DATA SF,SG,SH,SSF,SSG,SSH/6*0.0/
      READ(5,2) GX,GY,XM,YM,GS,CR,CI,NF,YN
    2 FORMAT(5F8.0,I1,F3.0)
      SCR=CR**2
      NP=CR/GS
      N=0
    4 READ(5,6) X,Y,F,G,H
    6 FORMAT(5F10.0)
      IF(X.GT.999999) GO TO 20
      X=(X-GX)
      Y=(Y-GY)
      I=X/GS+1+NP
      J=Y/GS+1+NP
      K1=I-NP
      K2=I+NP+1
      L1=J-NP
      L2=J+NP+1
      IF(J1.LT.1) J1=1
      IF(L1.LT.1) L1=1
      DO 10 I=K1,K2
      DO 10 J=L1,L2
      SR=(X-GS*(I-1-NP))**2+(Y-GS*(J-1-NP))**2
      IF(SR-SCR)11,11,10
   11 A(1,I,J)=A(1,I,J)+F
      A(2,I,J)=A(2,I,J)+10.0**(5.8+2.4*G)
      A(3,I,J)=A(3,I,J)+H
      IX(I,J)=IX(I,J)+1
   10 CONTINUE
      SF=SF+F
      SG=SG+G
      SH=SH+H
      SSF=SSF+F**2
      SSG=SSG+G**2
      SSH=SSH+H**2
      N=N+1
      GO TO 4
   20 FM=SF/N
      GM=SG/N
      HM=SH/N
      DF=SQRT((SSF-SF**2/N)/(N-1))
      DG=SQRT((SSG-SG**2/N)/(N-1))
      DH=SQRT((SSH-SH**2/N)/(N-1))
      WRITE(6,16) FM,DF,GM,DG,HM,DH
   16 FORMAT(1H1,'MEAN 1 =',F8.3,4X,'S.D. 1 =',F8.3/1H ,'MEA
                                                  N 2 =',F8.3,
     14X,'S.D. 2 =',F8.3/1H ,'MEAN 3 =',F8.3,4X,'S.D. 3 =',F
```

```
      MX=(XM-GX)/GS+1
      MY=(YM-GY)/GS+1
      AUC=ALOG10(3.14159*CR*CR*YN)
      DO 70 L=1,NF
      RCI=1.0/CI(L)
      WRITE(6,25) L
   25 FORMAT(1H1,'ROLLING MEAN MAP FOR FACTOR',I1///)
      DO 50 J=1,MY
      K=MY-J+1+NP
      DO 30 I=1,MX
      IT=I+NP
      ID=IX(IT,K)
      IF(ID)32,32,34
   32 P(I)=CHAR(42)
      GO TO 30
   34 IF(L-2) 334,333,334
  333 IR=ALOG10(A(2,IT,K))-ALC
      GO TO 335
  334 IR=(A(L,IT,K)/ID)*RCI+1
  335 IF(IR) 35,35,36
   35 P(I)=CHAR(43)
      GO TO 30
   36 IF(41-IR)37,38,38
   37 P(I)=CHAR(44)
      GO TO 30
   38 P(I)=CHAR(IR)
   30 CONTINUE
   40 WRITE(6,43) P
   43 FORMAT(1H ,10X,110A1)
      WRITE(6,44) P
   44 FORMAT(110A1)
   50 CONTINUE
      WRITE(6,60) GX,GY
   60 FORMAT(1H+,5X,F5.1,'+'/1H ,10X,F5.1)
   70 CONTINUE
      WRITE(6,78)
   78 FORMAT(1H1,'SAMPLE DENSITY MAP'///)
      ASC=3.14159*CR*CR*YN/10.0
SD    DO 80 J=1,MY
      K=MY-J+1+NP
      DO 90 I=1,MX
      IT=I+NP
      IS(I)=IX(IT,K)/ASC
   90 CONTINUE
      WRITE(6,82) IS
   82  FORMAT(1H ,10X,110I1)
   80 CONTINUE
      WRITE(6,60) GX,GY
      WRITE(6,52) MX,MY,GS,CR
   52 FORMAT(1HC,///,'NO. OF X CO-ORDS =',I3,'   NO. OF Y CO
                                        -ORDS =',I3,
     1'   GRID SPACING =',F6.2,'   SAMPLE CIRCLE RADIUS =',F
                                        6.2/)
      STOP
TIN   END
```

Appendix C6.2

A program written in FORTRAN IV, to find the distribution with depth of earthquake frequency and energy. Three methods are used. The first is a simple histogram. The second is a one dimensional moving average using a binomial sample taken from the histogram which is the first part of the program. The third method assumes that the errors on the depth determination are normally distributed and given the standard deviation finds the probability of each earthquake occurring at the depths sampled and hence the total probability of an earthquake occurring at these depths to give the distribution with depth of the earthquakes.

Input:

Read on 5:-

NC	The number of classes.
CL	The class width.
NI	The number of degrees of smoothing in the second method. (i.e. the number of times adjacent classes are added.)
SD	The standard deviation of the depth determination.
D	Depth of earthquake. (If D greater than 999999, end of data.)
G	The magnitude of earthquake.

Output:

Written on 6:-

First method

TIN	Lower limit of class.

AC Frequency of earthquakes in the class.

AE Energy of the earthquakes in the class.

Second method

X Sample depth.

AC Frequency.

AE Energy release.

Third method

VC The probable number of earthquakes occurring at the sample depth during the time of the data.

VE The probable energy release at the sample depth.

The normal distribution sample method is likely to give the most realistic description of the distribution with depth of the earthquakes.

```
      DIMENSION C(100),E(100),P(500),Q(500)
      DATA C/100*0./,E/100*0./
      READ(5,2) NC,CL,NI,SD
    2 FORMAT(I3,F7.0,I2,F8.0)
      SD2=2.0*SD**2.0
      IT=0
    5 READ(5,6) D,G
    6 FORMAT(20X,2F10.0)
      IF(D.GE.999999) GO TO 10
      IT=IT+1
      P(IT)=D
      I=D/CL+1
      C(I)=C(I)+1.0
      EN=10.0**(5.8+2.4*G)
      E(I)=E(I)+EN
      Q(IT)=EN
      GO TO 5
   10 F=100.0/(IT*CL)
      WRITE(6,8)
    8 FORMAT(1H1,'CLASS FREQ.      ENERGY')
      DO 20 I=1,NC
      AC=C(I)*F
      AE=E(I)*F
      TIN=(I-1)*CL
      WRITE(6,12) TIN,AC,AE
   12 FORMAT(1H ,F6.2,F6.3,E13.6)
   20 CONTINUE
      WRITE(6,22)
   22 FORMAT(1HO,'ROLLING MEAN ANALYSIS, BINOMIAL SAMPLE')
      DO 30 I=1,NI
      NL=NC-I
      X=(I-1)*CL*0.5
      WRITE(6,32)
   32 FORMAT(1HO,'    X    FREQ.     ENERGY')
      DO 30 J=1,NL
      K=J+1
      X=X+CL
      C(J)=(C(J)+C(K))*0.5
      E(J)=(E(J)+E(K))*0.5
      AC=C(J)*F
      AE=E(J)*F
      WRITE(6,34) X,AC,AE
   34 FORMAT(1H ,F6.2,F6.3,E13.6)
   30 CONTINUE
      WRITE(6,38)
   38 FORMAT(1HO,//'NORMAL DISTRIBUTION SAMPLE'//'DEPTH FREQ
                                                .   ENERGY')
      NK=NC+1
      DO 40 I=1,NK
      AM=(I-1)*CL
      VC=0
      VE=0
      DO 45 J=1,IT
      EX=(P(J)-AM)**2/SD2
      IF(EX.GT.15) GO TO 47
      FN=(1/(SD*2.50663))/2.7183**EX
      GO TO 49
   47 FN=0.
   49 VC=VC+FN
```

```
      VE=VE+FN*G(J)
   45 CONTINUE
      WRITE(6,46) AM,VC,VE
   46 FORMAT(1H ,F6.2,F6.3,E13.6)
   40 CONTINUE
      STOP
      END
```

Appendix C7.1

A program written in FORTRAN IV, to find the pole of rotation that will best fit one or more geological features such as fracture zones which are thought to have been formed by relative movement about it. The program calculates the equations of planes that are normal to the lines joining pairs of points along the features and finds the mean position of intersection of the planes, which is the best fit pole position.

Input:

Read on 5:-

NDS	The number of pairs of points.
AL1	Latitude of the first point.
OL1	Longitude of the first point.
AL2	Latitude of the second point.
OL2	Longitude of the second point.

Output:

Written on 6:

SLA	Mean latitude of pole. (obtained by summing the x,y,z coordinates before converting to latitude).
SLO	Mean longitude of the pole.
AM	The mean of the latitudes of the plane intersections.
OM	The mean of the longitudes of the plane intersections.
SE	The standard error of the pole, in degrees.
SAM	The standard error on the latitude.
SOM	The standard error on the longitude.

A list of the intersection positions. EPA latitude, EPO longitude.

```
C      PROGRAM TO FIND THE  POLE OF ROTATIONFOR ONE OR MORE S
                                                    MALL
C      CIRCLE FEATURES BY FINDING THE MEAN INTERSECTION OF GR
                                                    EAT
C      CIRCLES WHICH ARE ORTHOGONAL TO LINES JOINING GIVEN PA
                                                    IRS POINTS
C      SITUATED ALONG THE SMALL FEATURES.
C      NDS=NUMBER OF POINT PAIRS.
C      AL1 & AL2 ARE LATITUDES OF POINTS, OL1 & OL2 ARE LONGI
                                                    TUDES.
       DIMENSION P(20,3),Q(200,3),PLA(200),PLO(200)
       RAD=1/57.296
       READ(5,1) NDS
     1 FORMAT(I2)
     4 DO 20 I=1,NDS
       READ(5,2) AL1,OL1,AL2,OL2
     2 FORMAT(4F7.0)
       XP=SIN(RAD*OL1)*COS(AL1*RAD)
       YP=COS(RAD*OL1)*COS(AL1*RAD)
       ZP=SIN(RAD*AL1)
       XQ=SIN(RAD*OL2)*COS(AL2*RAD)
       YQ=COS(RAD*OL2)*COS(AL2*RAD)
       ZQ=SIN(RAD*AL2)
       P(I,1)=XP-XQ
       P(I,2)=YP-YQ
       P(I,3)=ZP-ZQ
    20 CONTINUE
       NP=NDS-1
       L=0
       DO 40 I=1,NP
       J=I+1
       DO 40 K=J,NDS
       L=L+1
       Q(L,1)=P(I,2)*P(K,3)-P(I,3)*P(K,2)
       Q(L,2)=P(I,3)*P(K,1)-P(I,1)*P(K,3)
       Q(L,3)=P(I,1)*P(K,2)-P(I,2)*P(K,1)
    40 CONTINUE  Q(I
       SX=0.    =PLA(I))**
       SY=0.  *+(  -PLO(I))*
       SZ=0.    *  COS(
       WRITE(6,46)/(
    46 FORMAT(1H1,' LATITUDE  LONGITUDE'/)
       DO 50 I=1,L    AND
    52 PM=SQRT(Q(I,1)**2+Q(I,2)**2+Q(I,3)**2)
       Q(I,1)=Q(I,1)/PM
       Q(I,2)=Q(I,2)/PM
       Q(I,3)=Q(I,3)/PM
       SX=SX+Q(I,1)
       SY=SY+Q(I,2)
       SZ=SZ+Q(I,3)
    50 CONTINUE
       SX=SX/L
       SY=SY/L
       SZ=SZ/L
       XM=0.
       YM=0.
       ZM=0.
       AM=0.  *EY
       OM=0.  *EZ
```

```
      DO 45 I=1,L
      AN=ARCOS(Q(I,1)*SX+Q(I,2)*SY+Q(I,3)*SZ)/RAD
      IF(AN-90) 47,47,48
   48 Q(I,1)=-Q(I,1)
   77 Q(I,2)=-Q(I,2)
      Q(I,3)=-Q(I,3)
   47 XM=XM+Q(I,1)
      YM=YM+Q(I,2)
      ZM=ZM+Q(I,3)
      PLA(I)=ARSIN(Q(I,3))/RAD
      PLO(I)=ATAN2(Q(I,1),Q(I,2))/RAD
      WRITE(6,56) PLA(I),PLO(I)
   56 FORMAT(1H ,2(3X,F7.2))
      AM=AM+PLA(I)
      OM=OM+PLO(I)
   45 CONTINUE
      XM=XM/L
      YM=YM/L
      ZM=ZM/L
      AM=AM/L
      OM=OM/L
      SLO=ATAN2(XM,YM)/RAD
      SLA=ARSIN(ZM)/RAD
      WRITE(6,58) SLA,SLO
   58 FORMAT(1HO,'LATITUDE OF MEAN POLE =',F7.2,'  LONGITUDE
                                                 OF MEAN POL
     1E =',F7.2/)
      WRITE(6,58) AM,OM
      VAM=0.
      VOM=0.
      ANG=0
      EX=0.
      EY=0.
      EZ=0.
      DO 60 I=1,L
      EX=EX+(XM-Q(I,1))**2
      EY=EY+(YM-Q(I,2))**2
      EZ=EZ+(ZM-Q(I,3))**2
      VAM=VAM+(AM-PLA(I))**2
      VOM=VOM+(OM-PLO(I))**2
   60 ANG=ANG+(ARCOS(XM*Q(I,1)+YM*Q(I,2)+ZM*Q(I,3))/RAD)**2
      SE=SQRT(ANG/(L-1))
      WRITE(6,66) SE
   66 FORMAT(1HO,'STANDARD ERROR OF POLE =',F7.2,'DEGREES')
      SAM=SQRT(VAM/(L-1))
      SOM=SQRT(VOM/(L-1))
      WRITE(6,68) SAM,SOM
   68 FORMAT(1HO,'S.E. LAT.=',F7.2,'  S.E. LONG.=',F7.2)
      EX=SQRT(EX/(L-1))
      EY=SQRT(EY/(L-1))
      EZ=SQRT(EZ/(L-1))
      DO 70 I=1,2
      T1=(-1)**I
      DO 70 J=1,2
      T2=(-1)**J
      DO 70 K=1,2
      T3=(-1)**K
      A=XM+T1*EX
      B=YM+T2*EY
      C=ZM+T3*EZ
```

```
      ES=SQRT(A**2+B**2+C**2)
      EPA=ARSIN(C/ES)/RAD
      EPO=ATAN2(A,B)/RAD
      WRITE(6,77) EPA,EPO
77    FORMAT(1H ,F7.2,2X,F7.2)
70    CONTINUE
      END
```

Appendix C7.2

A program written in FORTRAN IV, to find the pole of rotation for a small circle feature, such as a fracture zone. The program finds the equations of the planes that fit all the combinations of three points from the points situated along the feature. The mean position of the poles to these planes is taken as the pole of rotation.

Input:

Read on 5:-

NP	The number of points on the feature.
Al	The latitude of a point.
OL	The longitude of a point.

Output:

Written on 6:-

SLAT	The latitude of the pole derived from the mean of the x, y, z coordinates of the poles.
SLONG	The longitude of the pole.
AM	The mean of the latitudes of the poles to the planes.
OM	The mean of the longitudes of the poles to the planes.
PLAT(I)	The latitude of the pole to the Ith plane.
PLONG(I)	The longitude of the pole to the Ith plane.
SE	The standard error of the pole.
SA	The standard error on the latitude.
SO	The standard error on the longitude.
AM	The colatitude of the feature with resepct to the pole.
AE	The standard error on the colatitude.

```
C      PROGRAM TO CALCULATE A POLE OF ROTATION FROM POINTS AL
                                                    ONG A
C      SMALL CIRCLE FEATURE BY FITTING PLANES THROUGH COMBINA
                                                    TIONS
C      OF THREE POINTS AND FINDING THE MEAN POSITION OF THE P
                                                    OLES TO THE
C      PLANES.
C      NP=NUMBR
C      NP=NUMBER OF POINTS
C      AL=LATITUDE OF PCINT.     OL=LONGITUDE OF POINT.
       DIMENSION P(3,20),Q(3,600),PLAT(600),PLONG(600),AR(20)
       RAD=1/57.296
       READ(5,2) NP
     2 FORMAT(I2)
       DO 10 I=1,NP
       READ(5,3) AL,OL
     3 FORMAT(2F7.0)
       P(1,I)=SIN(OL*RAD)*COS(AL*RAD)
       P(2,I)=COS(OL*RAD)*COS(AL*RAD)
       P(3,I)=SIN(AL*RAD)
    10 CONTINUE
       SX=0.
       SY=0.
       SZ=0.
       L=0
       K1=NP-1
       K2=NP-2
       DO 20 I=1,K2
       I1=I+1
       DO 20 J=I1,K1
       J1=J+1
       DO 20 K=J1,NP
       L=L+1
       X=P(2,I)*(P(3,J)-P(3,K))+P(3,I)*(P(2,K)-P(2,J))+P(2,J)
                                                    *P(3,K)-P(2,
      1K)*P(3,J)
       Y=P(3,I)*(P(1,J)-P(1,K))-P(3,K)*P(1,J)+P(3,J)*P(1,K)-P
                                                    (1,I)*(P(3,J
      1)-P(3,K))
       Z=P(1,J)*P(2,K)-P(2,J)*P(1,K)+P(1,I)*(P(2,J)-P(2,K))+P
                                                    (2,I)*(P(1,K
      1)-P(1,J))
       QS=SQRT(X**2+Y**2+Z**2)
       Q(1,L)=X/QS
       Q(2,L)=Y/QS
       Q(3,L)=Z/QS
       SX=SX+X
       SY=SY+Y
       SZ=SZ+Z
    20 CONTINUE
       WRITE(6,8)
     8 FORMAT(1H1,'POLES OF ROTATION USING PLANE FITTING METH
                                                    OD')
       SX=SX/L
       SY=SY/L
       SZ=SZ/L
       SM=SQRT(SX**2+SY**2+SZ**2)
       SX=SX/SM
       SY=SY/SM
```

```
      SZ=SZ/SM
      XM=0.
      YM=0.
      ZM=0.
      AM=0.
      OM=0.
      DO 40 I=1,L
      AN=(ARCOS(Q(1,I)*SX+Q(2,I)*SY+Q(3,I)*SZ)/RAD)
      IF(AN-90) 45,45,46
   46 Q(1,I)=-Q(1,I)
      Q(2,I)=-Q(2,I)
      Q(3,I)=-Q(3,I)
   45 XM=XM+Q(1,I)
      YM=YM+Q(2,I)
      ZM=ZM+Q(3,I)
      IF(Q(1,I).EQ.0.AND.Q(2,I).EQ.0) GO TO 39
      PLAT(I)=ARSIN(Q(3,I))/RAD
      PLONG(I)=ATAN2(Q(1,I),Q(2,I))/RAD
      GO TO 41
   39 PLAT(I)=90
      PLONG(I)=0
   41 AM=AM+PLAT(I)
      OM=OM+PLONG(I)
   40 CONTINUE
      WRITE(6,6) (PLAT(I),PLONG(I),I=1,L)
    6 FORMAT(1H ,4(F7.2,4X,F7.2,5X))
      AM=AM/L
      OM=OM/L
      XM=XM/L
      YM=YM/L
      ZM=ZM/L
      SLAT=ARSIN(ZM)/RAD
      SLONG=ATAN2(XM,YM)/RAD
      WRITE(6,16) SLAT,SLONG
      WRITE(6,16) AM,OM
   16 FORMAT(1H1,'MEAN POLE.     LAT.=',F7.2,'    LONG.=',F7.2
     )
      VA=0.
      VO=0.
      EX=0.
      EY=0.
      EZ=0.
      ANG=0.
      DO 50 I=1,L
      X=Q(1,I)
      Y=Q(2,I)
      Z=Q(3,I)
      EX=EX+(XM-X)**2
      EY=EY+(YM-Y)**2
      EZ=EZ+(ZM-Z)**2
      VA=VA+(AM-PLAT(I))**2
      VO=VO+(OM-PLONG(I))**2
      ANG=ANG+(ARCOS(X*XM+Y*YM+Z*ZM)/RAD)**2
   50 CONTINUE
      EX=SQRT(EX/(L-1))
      EY=SQRT(EY/(L-1))
      EZ=SQRT(EZ/(L-1))
      SE=SQRT(ANG/(L-1))
      SA=SQRT(VA/(L-1))
      SO=SQRT(VO/(L-1))
```

```
      WRITE(6,56) SE,SA,SO
   56 FORMAT(1HO,'STANDARD ERROR OF POLE =',F7.2,' DEGREES'/
                                                  1H ,'STANDAR
     1D ERROR LAT.=',F7.2,'  LONG.=',F7.2/)
      DO 60 I=1,2
      T1=(-1)**I
      DO 60 J=1,2
      T2=(-1)**J
      DO 60 K=1,2
      T3=(-1)**K
      A=XM+T1*EX
      B=YM+T1*EY
      C=ZM+T3*EZ
      ES=SQRT(A**2+B**2+C**2)
      EPA=ARSIN(C/ES)/RAD
      EPO=ATAN2(A,B)/RAD
      WRITE(6,66) EPA,EPO
   66 FORMAT(1H ,F7.2,2X,F7.2)
   60 CONTINUE
      AM=0.
      DO 70 I=1,NP
      AR(I)=ARCOS(XM*P(1,I)+YM*P(2,I)+ZM*P(3,I))/RAD
   70 AM=AM+AR(I)
      AM=AM/NP
      DO 71 I=1,NP
   71 AV=AV+(AM-AR(I))**2
      AE=SQRT(AV/(NP-1))
      WRITE(6,77) AM,AE
   77 FORMAT(1HO,'LAT. OF SMALL CIRCLE THROUGH POINTS =',F7.
                                                  2/'STANDARD
     1ERROR =',F7.2)
      STOP
      END
```

Appendix C7.3

A subroutine written in FORTRAN IV, using MINUIT, to find the pole giving the best small circle fit to one or more transform faults or other features due to plate motion, which are not actually contructive or destructive margins. The program minimises the variance between small circles from the pole and points along the features considered.

Input:

Read on 5:-

ND	The number of features in the fit.
NP(J)	The number of points along the Jth feature.
P(I,J)	The latitude of the Ith point on the Jth feature.
Q(I,J)	The longitude of the Ith point on the Jth feature.

Output:

Written on 6 when CALL FCN 3 is commanded:-

X(1)	The latitude of the pole.
X(2)	The longitude of the pole.
SE	The standard error of the fit. (Not the error on the pole).
P(I,J)	
Q(I,J)	
R(I,J)	The residual between the Ith point on the Jth feature and the small circle through the Jth feature.

Written on 6 when CALL FCN 5 is commanded is a map of the object function around the pole position. This gives an estimate of area of error of the pole position.

The first estimate of the pole latitude should be entered as the first variable parameter in MINUIT. the longitude should be the second variable parameter.

```
      DO 36 J=1,
C     OPTIMISATION ROUTINE FOR CALCULATING POLES OF ROTATION
      WRI 16,                          FROM DATA
C  36 POINTS ON ONE OR MORE SMALL CIRCLES.
C     ND=NUMBER OF DATA SETS.
C     NP(J)= NUMBER OF POINTS IN JTH DATA SET.
C     PEIS ARRAY HOLDING POINT LATITUDES
C  50 Q IS ARRAY HOLDING POINT LONGITUDES
C     X(1) IS POLE LATITUDE    X(2) IS POLE LONGITUDE
C     CALL FCN  3  GIVES OUTPUT.
C     CALL FCN  5  GIVES OBJECT FUNCTION MAP (VARIANCE)
      SUBROUTINE FCN(NPAR,G,F,X,IFLAG)
      RAD=1/57.296
      DIMENSION P(40,10),Q(40,10),A(40),X(15),NP(10),VM(20),
     0                                        R(40,10)
      GO TO (10,20,30,40,50),IFLAG
   10 READ(5,11) ND
   11 FORMAT(I2)
      DO 15 J=1,ND
      READ(5,11) NP(J)
      N=NP(J)
      READ(5,12) (P(I,J),Q(I,J),I=1,N)
   12 FORMAT(2F7.0)
   15 CONTINUE
      INB=1
   20 CONTINUE
   40 PO=X(2)*RAD
      PA=X(1)*RAD
   41 AX=SIN(PO)*COS(PA)
      AY=COS(PO)*COS(PA)
      AZ=SIN(PA)
      AN=0.
      K=0
      DO 43 J=1,ND
      SUM=0.
      N=NP(J)
      DO 42 I=1,N
      RA=P(I,J)*RAD
      RB=Q(I,J)*RAD
      RX=SIN(RB)*COS(RA)
      RY=COS(RB)*COS(RA)
      RZ=SIN(RA)
      A(I)=ARCOS(AX*RX+AY*RY+AZ*RZ)/RAD
      SUM=SUM+A(I)
   42 CONTINUE
      ANG=SUM/N
      DO 44 I=1,N
      K=K+1
      DIF=ANG-A(I)
      R(I,J)=DIF
   44 AN=AN+DIF**2
   43 CONTINUE
      SE=SQRT(AN/(K-ND))
      F=AN*100/(K-ND)
      IF(IND) 55,45,45
   45 RETURN
   30 WRITE(6,32) X(1),X(2),SE
   32 FORMAT(1H1,'POLE LATITUDE =',F7.2/'POLE LONGITUDE =',F
                                          7.2/'STANDAR
     2D ERROR OF FIT =',F7.2)
```

```
      DO 36 J=1,ND
      N=NP(J)
      WRITE(6,34) (P(I,J),Q(I,J),R(I,J),I=1,N)
   34 FORMAT(1HO,'INPUT DATA'//'  LAT.   LONG.  RESID.'//(3F
                                          7.2))
   36 CONTINUE
      RETURN
   50 M1=X(1)-9
      M2=X(1)+10
      L1=X(2)-9
      L2=X(2)+10
      WRITE(6,52) (L,L=L1,L2)
   52 FORMAT(1H1,'OBJECT FUNCTION MAP'/10X,20I5/)
      IND=-1
      DO 58 M=M1,M2
      PA=M*RAD
      IL=1
      DO 56 L=L1,L2
      PO=L*RAD
      GO TO 41
   55 VM(IL)=F
      IL=IL+1
   56 CONTINUE
      WRITE(6,57) M,(VM(IL),IL=1,20)
   57 FORMAT(1H ,I10,20F5.1//)
   58 CONTINUE
      RETURN
      END
```

Appendix C7.4

A program written in FORTRAN IV, to add rotations vectorially to give instantaneous poles, or add rotations compositely to give the rotation equivalent to two sequential rotations.

Input:

Read on 5:-

NDS	The number of data sets.
PLA	Latitude of first rotation pole.
PLO	Longitude of first rotation pole.
PRO	The amount of rotation about the first pole.
QLA	The latitude of the second pole.
QLO	The longitude of the second pole.
QRO	The amount of rotation about the second pole.

Written on 6:-

PLA, PLO, PRO, QLA, QLO, QRO,

FLA	Latitude of the instantaneous pole.
FLO	Longitude of the instantaneous pole.
FRO	Rotation about the instantaneous pole.
VLA	Latitude of the composite pole.
VLO	Longitude about the composite pole.
VRO	Rotation about the composite pole.

```
C      PROGRAM TO DO COMPOSITE AND SIMPLE (VECTOR) ROTATION A
                                                    DDITION.
C      PLA,PLO & PRO ARE THE LATITUDE AND LONGITUDE OF THE FI
                                                    RST POLE
C      OF ROTATION AND THE AMOUNT OF ROTATION IN DEGREES.
C      QLA,QLO & QRO ARE THE CORRESPONDING VALUES FOR THE SEC
                                                    OND
C      ROTATION.
C      NDS = THE NUMBER DATA SETS.
       READ(5,1) NDS
     1 FORMAT(I3)
       WRITE(6,3)
     3 FORMAT(1H1,'ROTATION PROGRAM RESULTS'/'CONVENTION: LAT
                                                    ITUDE NORTH,
      1 LONGITUDE WEST & ROTATION ANTICLOCKWISE ARE POSITIVE'
                                                    /'ALTERNATIV
      2ELY: LATITUDE NORTH, LONGITUDE EAST & ROTATION CLOCKWI
                                                    SE ARE POSIT
      3IVE.')
       RAD=1/57.296
       DO 50 I=1,NDS
       READ(5,2) PLA,PLO,PRO,QLA,QLO,QRO
     2 FORMAT(6F7.0)
       PM=TAN(0.5*PRO*RAD)
       QM=TAN(0.5*QRO*RAD)
       XP=SIN(PLO*RAD)*PM*COS(RAD*PLA)
       YP=COS(PLO*RAD)*PM*COS(RAD*PLA)
       ZP=SIN(PLA*RAD)*PM
       XQ=SIN(QLO*RAD)*QM*COS(RAD*QLA)
       YQ=COS(QLO*RAD)*QM*COS(RAD*QLA)
       ZQ=SIN(QLA*RAD)*QM
       SX=XP+XQ
       SY=YP+YQ
       SZ=ZP+ZQ
       FM=SQRT(SZ**2+SY**2+SX**2)
       FLO=ATAN2(SX,SY)/RAD
       FLA=ARSIN(SZ/FM)/RAD
       FRO=2*ATAN(FM)/RAD
       SP=XP*XQ+YP*YQ+ZP*ZQ
       SD=1-SP
       VX=(SX-YP*ZQ+ZP*YQ)/SD
       VY=(SY-ZP*XQ+XP*ZQ)/SD
       VZ=(SZ-XP*YQ+YP*XQ)/SD
       VM=SQRT(VZ**2+VY**2+VX**2)
       VLO=ATAN2(VX,VY)/RAD
       VLA=ARSIN(VZ/VM)/RAD
       VRO=2*ATAN(VM)/RAD
       WRITE(6,6) PLA,PLO,PRO,QLA,QLO,QRO,FLA,FLO,FRO,VLA,VLO
                                                    ,VRO
     6 FORMAT(1HO,'ROTATION LAT.',F7.2,'  LONG.',F7.2,'  ROT.
                                                    ',F7.2,'  +
      1ROTATION LAT.',F7.2,'  LONG.',F7.2,'  ROT.',F7.2//1HO,
                                                    'SIMPLE ROT
      2ATION ADDITION'/'LAT.=',F7.2,'  LONG.=',F7.2,'  ROT.='
                                                    ,F7.2/1HO,'C
      3OMPOSITE ROTATION'//'LAT.=',F7.2,'  LONG.=',F7.2,'  ROT
                                                    .=',F7.2///)
    50 CONTINUE
       END
```

Appendix C7.5

A program written in PL1, to read coordinates from a map, convert them to latitude and longitude and plot them at a new scale and/or in a different projection and rotated to new positions if desired. The program reads the coordinates from a digitised Mercator Projection map. The map is digitised using the DMAC table and the paper tape from it is translated by CLT9:DCL99SPL. The coordinates may be rotated about a given pole through a given angle, and the resultant position may be given with respect to the pole of rotation or the original reference frame. A map can be plotted either as a Mercator projection or a polar equal area projection.

Input:

Read from SCARDS:-

NAME — Up to 25 identifying characters. If NAME = 'END' program stops.

IND — If IND = 0 then the coordinates are given with respect to the pole of rotation.

PLAT — Latitude of the pole of rotation.

PLONG — Longitude of the pole of rotation.

ROT — Rotation about the pole.

Read from SCARDS:-

OP — An indicator. If OP = 'POLAR' a polar projection map is drawn. If OP = 'DEGREE' a list of the latitude and longitude of the points is given. If OP = 'SCALED' a Mercator projection map is drawn. If OP = 'anything else' list given in radians.

SCALE	The scale of the map drawn. In inches per degree.
CX	Constant added to x coordinates of map to put coordinates in the field of the plotter.
CY	Constant for y direction of map. Coordinates of bottom left hand corner of map are -CX, -CY.

Read from FILE MAP:-

TRCO	Longitude of top right hand corner of the digitised map.
TRCA	Latitude of the top right hand corner of the map.
TRCX	X coordinate of the top right hand corner.
TRCY	Y coordinate of the top right hand corner.
BLCO	Longitude of the bottom left hand corner.
BLCA	Latitude of the bottom left hand corner.
BLCX	X coordinate of the bottom left hand corner.
BLCY	Y coordinate of the bottom left hand corner.
AX	X coordinate of the digitised point. If AX =1111 data from first set of coordinates ends.
AY	Y coordinate of the digitised point. If AY = 22222 the data from a new map are read.

Output:

Written on SPRINT and FILE PLOT:-

DLAT	Latitude of point in degrees.
DLONG	Longitude of point in degrees.
SLAT	X coordinate of point on output Mercator map.
SLONG	Y coordinate of point on output Mercator map.
TLAT(K)	Latitude of Kth point in radians.
TLONG(K)	Longitude of Kth point in radians.
X	X coordinate of point on polar projection map.

Y Y coordinate of point on polar projection map.

To obtain the map output the program must be run with *PLOTSYS, followed by a run of *DURPLOT. Files MAP and PLOT must be assigned to files on the run card. When digitising the map care should be taken to keep the lines of latitude horizontal with the DMAC table.

```
/* A PROGRAM TO READ IN COORDINATES FROM A MAP AND CONVERT
                                                    THEM TO
 LATITUDE AND LONGITUDE, AND IF DESIRED ROTATE THEM TO NEW
                                                    POSITIONS ABOUT
 GIVEN POLES OF ROTATION AND GIVE THE NEW POSITIONS EITHER
                                                    WITH RESPECT
 TO THE POLE OF ROTATION OR THE ORIGINAL REFERENCE FRAME. T
                                                    HE RESULTS
 CAN BE PLOTTED AS A MERCATOR PROJECTION TO ANY SCALE OR AS
                                                     A POLAR
 EQUAL AREA PROJECTION. THE COORDINATES ARE ALSO OUTPUT AS
                                                     FIGURES.
 FILE (MAP) IS THE FILE CONTAINING THE MAP COORDINATES IN
                                                    X & Y VALUES.
 USUALLY FROM DIGITISING TABLE.  TRCC & BLCC ARE THE LONGIT
                                                    UDES OF THE
 TOP RIGHT HAND CORNER AND BOTTOM LEFT HAND CORNERS OF THE
                                                    MAP.
 TRCA & BLCA ARE THE LATITUDES OF THESE POINTS. TRCX, TRCY,
                                                    BLCX &
 BLCY ARE THE X AND Y COORDINATES OF THE MAP CORNERS.
 NAME IS THE IDENTIFIER OF ONE SET OF POINTS
 IND IS AN INDICATOR. IF IND=1 OUPUT IS IN ORIGINAL REFEREN
                                                    CE FRAME
 IF IND=0 OUPUT IS GIVEN WITH RESPECT TO THE POLE OF ROTATI
                                                    ON
 11111 11111 MARKS THE END OF ONE SET OF POINTS IN FILE MAP
 (1111 22222 INDICATE THAT AT THE END OF THE SET OF POINTS
                                                    NEW POSITIONS
 FOR THE MAP CORNERS ARE TO BE READ IN.
 IF NAME = 'END' THEN THE PROGRAM STOPS
 OP IS THE OPTION TO BE EXECUTED WHEN PUTTING OUT THE POINT
                                                    S.
 IF OP = 'DEGREE'   THEN THE POINTS ARE OUT PUT AS LATITUDE
                                                     AND LONGITUDE
 IN DEGREES. (NO MAP IS PLOTTED).
 IF OP = SCALED
 IF OP = 'SCALED'  THEN A MAP IS DRAWN IN MERCATOR PROJECTI
                                                    ON TO THE
 SCALE SPECIFIED. ALSO POINTS ARE PUT OUT ON FILE IN THE VA
                                                    LUES GIVEN
 BY THE SCALE FACTOR.  SCALE = THE FACTOR BY WHICH THE POIN
                                                    TS WHOSE
 POSITIONS ARE IN RADIANS ARE MULTIPLIED. CX & CY ARE CONST
                                                    ANTS ADDED
 TO THE SCALED POINTS TO GIVE THE ORIGIN OF THE MAP IN ANY
                                                    DESIRED POSITION.
 IF OP = 'POLAR' A MAP IS DRAWN IN AN EQUAL AREA POLAR PROJ
                                                    ECTION .
 POINTS IN THEIR NEW VALUES ARE ALSO PUT ONTO FILE.
 SCALE = THE FACTOR BY WHICH THE POINT VALUES IN RADIANS AR
                                                    E MULTIPLIED.
 CX & CY ARE THE X AND Y COORDINATE OF THE POLE OF PROJECTI
                                                    ON IN THE
 UNITS OF THE MAP.
 TO GAIN PLOTTED MAP OUTPUT THIS PROGRAM MUST BE RUN WITH A
                                                    PLOTSYS. */
MAPLOT:PROCEDURE OPTIONS(MAIN);
DECLARE OP CHAR(6),TLONG(900) FLOAT,TLAT(900) FLOAT :
```

```
      DECLARE NAME CHAR(25) ;
      DECLARE (MAP)FILE INPUT STREAM ;
      DECLARE (PLOT)FILE OUTPUT STREAM ;
      RAD=1/57.296 ;
  L0:GET FILE(MAP) LIST(TRCO,TRCA,TRCX,TRCY,BLCO,BLCA,BLCX,
                                                BLCY) ;
      SCALEX=(BLCO-TRCO)/(BLCX-TRCX) ;
      XZERO=BLCX-BLCO/SCALEX ;
 SCALEY=57.296*(LOG(TAN((45+TRCA/2)*RAD))-LOG(TAN((45+BLCA/
                                                2)*RAD)))/
          (TRCY-BLCY) ;
 YZERO=BLCY-57.296*LOG(TAN((45+BLCA/2)*RAD))/SCALEY ;
  L1:GET LIST (NAME,IND) ;
      IF NAME='END' THEN GO TO L10 ;      I=0  ;
      PUT EDIT (NAME) (PAGE,A(25)) ;
      GET LIST (PLAT,PLONG,ROT) ;
      IF (PLAT=90) & (PLONG=0) THEN GO TO L5 ;
      RROT=ROT*RAD ;
      AP=(90-PLAT)*RAD ;
      AZ=PLONG*RAD ;
  L2:GET FILE(MAP) LIST(AX,AY) ;
      IF AX=11111 THEN GO TO L6 ;
      I=I+1 ;
      PX=AZ-(AX-XZERO)*SCALEX*RAD ;
 AR=AY-YZERO ;
 IF AR < 0 THEN DO;
AR=-AR ;
      AT=-(ATAN(EXP(AR*SCALEY*RAD))-0.785)*2 ;
 END ;
 ELSE  AT=(ATAN(EXP(AR*SCALEY*RAD))-0.785)*2 ;
      CX=COS(PX)*COS(AT) ;
      CY=SIN(PX)*COS(AT) ;
      CZ=SIN(AT) ;
      AXZ=ATAN(CZ,CX)+AP ;
      SCY=SQRT(1-CY**2) ;
      CX=COS(AXZ)*SCY ;
      CZ=SIN(AXZ)*SCY ;
      AXY=ATAN(CY,CX)-RROT ;
      SCZ=SQRT(1-CZ**2) ;
      CX=COS(AXY)*SCZ ;
      CY=SIN(AXY)*SCZ ;
      IF IND=0 THEN GO TO L3;
      AZX=ATAN(CZ,CX)-AP ;
      SCY=SQRT(1-CY**2) ;
      CX=COS(AZX)*SCY ;
      CZ=SIN(AZX)*SCY ;
      SCZ=SQRT(1-CZ**2) ;
  L3:TLAT(I)=ATAN(CZ,SCZ) ;
      TLONG(I)=-ATAN(CY,CX)+AZ ;
      GO TO L2 ;
  L5:GET FILE(MAP) LIST(AX,AY) ;
      IF AX=11111 THEN GO TO L6 ;
      I=I+1;
      TLONG(I)=((AX-XZERO)*SCALEX+ROT)*RAD ;
 AR=AY-YZERO ;
 IF AR < 0 THEN DO;
AR=-AR ;
      TLAT(I)=-(ATAN(EXP(AR*SCALEY*RAD))-0.785)*2.0 ;
 END ;
 ELSE  TLAT(I)=(ATAN(EXP(AR*SCALEY*RAD))-0.785)*2.0 ;
```

```
    GO TO L5 ;
L5:PUT EDIT ('NO OF POINTS = ',I) (SKIP,A,F(3)) ;
    PUT FILE(PLOT) SKIP :
    GET LIST (OP) ;
    IF OP='POLAR' THEN GO TO L8;
    IF OP='DEGREE' THEN DO K=1 TO I ;
    DLONG=TLONG(K)/RAD ;
    DLAT=TLAT(K)/RAD ;
    PUT EDIT (DLAT,DLONG) (SKIP,F(7,2),X(2),F(7,2)) ;
    PUT FILE(PLOT) EDIT (DLAT,DLONG) (X(1),F(7,2),X(1),F(7
                                        ,2)) ;
    END ;
    ELSE DO ;
    IF OP='SCALED' THEN DO ;
    GET LIST (SCALE,CX,CY) ;
    DO K=1 TO I ;
    SLAT=LOG(TAN(0.785+TLAT(K)/2.0))*SCALE+CY ;
    SLONG=TLONG(K)*SCALE+CX ;
    IF K=1 THEN CALL PENUP(SLONG,SLAT) ;
    ELSE CALL PENDN(SLONG,SLAT) ;
    PUT EDIT (SLAT,SLONG) (SKIP,F(7,2),X(2),F(7,2)) ;
    PUT FILE(PLOT) EDIT (SLAT,SLONG) (X(1),F(7,2),X(1),F(7
                                        ,2)) ;
    END ;
    END ;
    ELSE DO K=1 TO I ;
    PUT EDIT (TLAT(K),TLONG(K)) (SKIP,F(7,3),X(2),F(7,3))
                                        ;
    PUT FILE(PLOT) EDIT (TLAT(K),TLONG(K)) (X(1),F(7,3),X(
                                        1),F(7,3)) ;
    END ;
    END ;
    GO TO L9;
 L8:GET LIST (SCALE,CX,CY) ;
    PUT SKIP ;
    DO K=1 TO I;
    Z=SCALE*(1-SIN(TLAT(K)))**0.5;
    X=Z*SIN(TLONG(K))+CX ;
    Y=Z*COS(TLONG(K))+CY ;
    IF K=1 THEN CALL PENUP(X,Y) ;
    ELSE CALL PENDN(X,Y) ;
    PUT EDIT (X,Y) (F(7,3),X(2),F(7,3),X(4)) ;
    PUT FILE(PLOT) EDIT (X,Y) (X(1),F(7,3),X(1),F(7,3)) ;
    END;
 L9:IF MY=22222 THEN GO TO L0;
    ELSE GO TO L1 ;
L10:CALL PLTEND ;
    END;
```

Appendix C7.6

A program written in FORTRAN IV, to calculate spreading rates from rotation rates and vice versa.

Input:

Read on 5:-

NC	The number of calculations.
ALAT	Latitude of pole of rotation.
ALON	Longitude of pole of rotation.
BLAT	Latitude of point at which spreading rate is known or to be calculated.
BLON	Longitude of point.
IND	Indicator. If IND = -1 the spreading rate is calculated If IND = 0 only the arclength is calculated. If IND = 1 the rotation rate is calculated.
ROT	Input spreading rate or rotation rate. (cm y^{-1} or degrees my^{-1})

Output:-

Written on 6:-

SR	Spreading rate.
AR	Rotation rate.
I	Number of calculation.
ALAT	
ALON	
BLAT	
BLON	
D	Arclength.

```
C       PROGRAM TO CALCULATE SPREADING RATE FROM ROTATION RATE
                                                AND VICE
C       VERSA & CALCULATE ARC LENGTH FROM POLE TO POINT AT WHI
                                                CH RATES
C       ARE TO BE CALCULATED.
C       NC=NUMBER OF CALCULATIONS.
C       ALAT,ALON=LATITUDE & LONGITUDE OF POLE.
C       BLAT,BLON=LAT. & LONG OF POINT.
C       IND IS AN INDICATOR FOR TYPE OF CALCULATION.
C        IND=-1  SPREADING RATE CALCULATED.
C       IND=0  ONLY ARCLENGTH CALCULATED.
C       IND=1  ROTATION RATE CALCULATED.
C       ROT= INPUT SPREADING RATE OR ROTATION RATE IN CM PER Y
                                                EAR OR
C       DEGREES PER M.Y.
        RAD=0.017453
        READ(5,2) NC
      2 FORMAT(I3)
        DO 10 I=1,NC
        READ(5,4) ALAT,ALON,BLAT,BLON,IND,ROT
      4 FORMAT(4F10.0,I2,F8.0)
        AL=ALAT*RAD
        BL=BLAT*RAD
        D=ARCOS(SIN(AL)*SIN(BL)+COS(AL)*COS(BL)*COS((BLON-ALON
                                                )*RAD))
        IF (D.GT.1.57079) D=3.14159-D
        IF(IND) 11,12,13
     11 SR=40011.29*ROT*SIN(D)/360.
        WRITE(6,112) SR
    112 FORMAT(1HO,'SPREADING RATE =',F7.3,'CM/YR')
        GO TO 12
     13 AR=3600*ROT/(40022.29*SIN(D))
        WRITE(6,113) AR
    113 FORMAT(1HO,'ANGLE OF ROTATION =',F7.3,'PER MY')
     12 D=D/RAD
        WRITE(6,122) I,ALAT,ALON,BLAT,BLON,D
    122 FORMAT(1HO,I3,' ARCLENGTH',2F9.3,' TO',2F9.3,' =',F8.3
                                                ///)
     10 CONTINUE
        STOP
        END
```

Appendix C7.7

A program written in FORTRAN IV, to calculate the positions of points after a given amount of rotation about a given pole.

Input:

Read on 5:-

ND	The number of initial points.
PLAT	Latitude of the pole.
PLONG	Longitude of the pole.
SLAT	Latitude of the point.
SLONG	Longitude of the point.
NS	Number of rotated positions for each point.
ROT	Rotation between each position.

Output:

Written on 6:-

PLAT, PLONG, SLAT, SLONG,

TLAT(I)	Latitude of Ith rotated position.
TLONG(I)	Longitude of Ith rotated position.

```
C     PROGRAM TO CALCULATE ROTATED POSITIONS OF POINTS FROM
                                                AN INITIAL
C     GIVEN POINT ABOUT A GIVEN POLE OF ROTATION.
C     ND = NUMBER OF DATA SETS TO BE CALCULATED.
C     PLAT & PLONG  ARE THE LAT. AND LONG. OF THE POLE OF RO
                                                TATION
C     SLAT & SLONG ARE THE LAT. AND LONG. OF THE INITIAL POI
                                                NT.
C     NS= THE NUMBER OF STEPS TO BE MADE ALONG ARC OF ROTATI
                                                ON.
C     ROT= ANGULAR INCREMENT OF EACH STEP IN DEGREES.
      DIMENSION TLAT(90),TLONG(90)
      READ(5,1) ND
    1 FORMAT(I3)
      WRITE(6,6)
    6 FORMAT(1H1,'ARCS ABOUT POLES OF ROTATION')
      DO 50 IN=1,ND
      READ(5,2) PLAT,PLONG,SLAT,SLONG,NS,ROT
    2 FORMAT(2F10.0/2F10.0,I2,F8.0)
      F=1
      RAD=0.01745
      IF(NS) 3,40,5
    3 F=-1
      NS=-NS
    5 AP=(90-PLAT)*RAD
      AZ=PLONG*RAD
      PX=AZ-SLONG*RAD
      AT=SLAT*RAD

      DO 10 I=1,NS
      RROT=F*I*RAD*ROT
      CX=COS(PX)*COS(AT)
      CY=SIN(PX)*COS(AT)
      CZ=SIN(AT)
      AXZ=ATAN2(CZ,CX)+AP
      SCY=SQRT(1.-CY**2)
      CX=COS(AXZ)*SCY
      CZ=SIN(AXZ)*SCY
      AXY=ATAN2(CY,CX)-RROT
      SCZ=SQRT(1.-CZ**2)
      CX=COS(AXY)*SCZ
      CY=SIN(AXY)*SCZ
      AZX=ATAN2(CZ,CX)-AP
      SCY=SQRT(1.-CY**2)
      CX=COS(AZX)*SCY
      CZ=SIN(AZX)*SCY
      SCZ=SQRT(1.-CZ**2)
      TLAT(I)=ATAN2(CZ,SCZ)/RAD
      TLONG(I)=(-ATAN2(CY,CX)+AZ)/RAD
   10 CONTINUE
      WRITE(6,20) PLAT,PLONG,SLAT,SLONG,(TLAT(I),TLONG(I),I=
                                                1,NS)
   20 FORMAT(1HO,'POLE',2F10.2/'INITIAL POINT',2F10.2/'ROTAT
                                                ED POINTS'/
     1'LAT.      LONG.'/(F7.2,2X,F7.2))
   50 CONTINUE
   40 STOP
      END
```